EMERGING INFECTIOUS DISEASES®

CDC
Centers for Disease Control and Prevention

High-Consequence Pathogens

April 2024

Rembrandt van Rijn (1606–1669), *The Night Watch* (1642). Oil on canvas, 149 in × 171 in /379.5 cm × 453.5 cm. Digital image courtesy of Rijksmuseum, Amsterdam, the Netherlands.

EMERGING INFECTIOUS DISEASES®

Emerging Infectious Diseases is published monthly by the Centers for Disease Control and Prevention, 1600 Clifton Rd NE, Mailstop H16-2, Atlanta, GA 30329-4018, USA. Telephone 404-639-1960; email, eideditor@cdc.gov

EMERGING INFECTIOUS DISEASES®

High-Consequence Pathogens

April 2024

On the Cover

Rembrandt van Rijn (1606–1669), *The Night Watch* (1642). Oil on canvas, 149 in × 171 in/379.5 cm × 453.5 cm. Digital image courtesy of Rijksmuseum, Amsterdam, the Netherlands.

About the Cover p. 840

Synopsis

Medscape EDUCATION ACTIVITY

Research

Medscape EDUCATION ACTIVITY

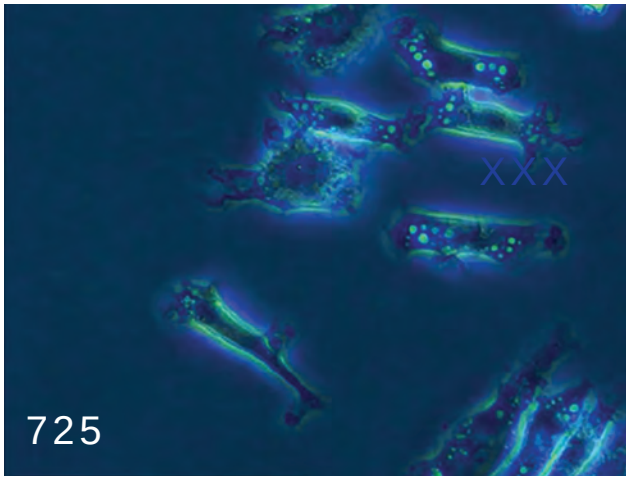

EMERGING INFECTIOUS DISEASES®
April 2024

Historical Review

Dispatches

Commentary

Research Letters

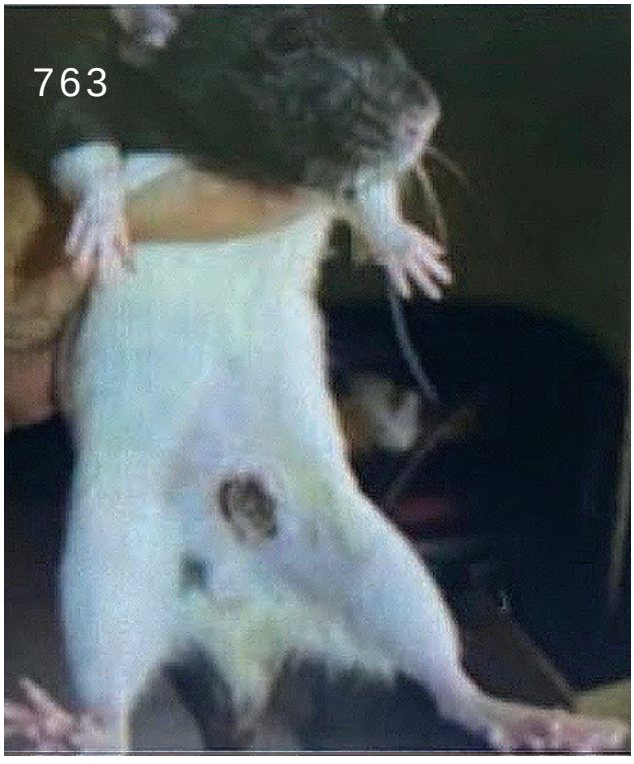

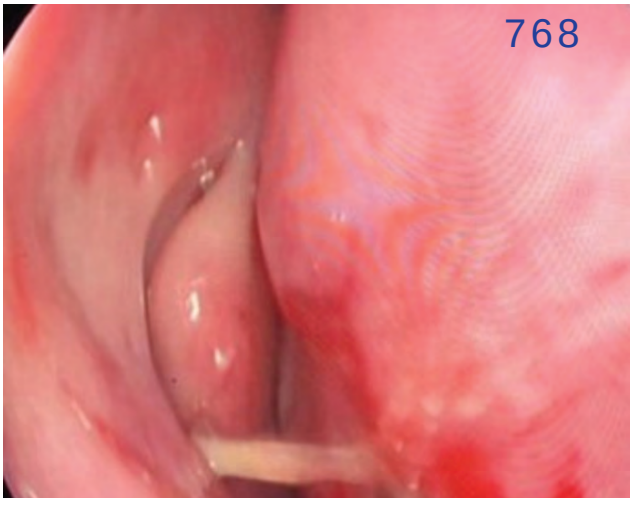

EMERGING INFECTIOUS DISEASES®
April 2024

Books and Media

About the Cover

Online Report

Corrections

Emerging Infectious Diseases
Photo Quiz Articles

Volume 14, Number 9
September 2008

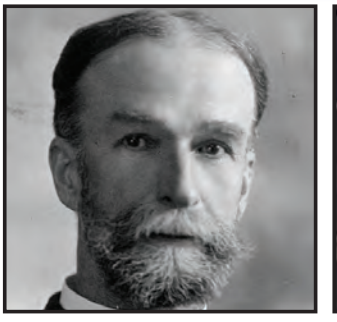

Volume 14, Number 12
December 2008

Volume 15, Number 9
September 2009

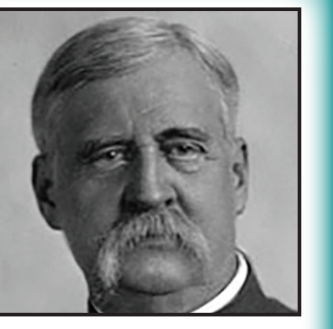

Volume 15, Number 10
October 2009

Volume 16, Number 6
June 2010

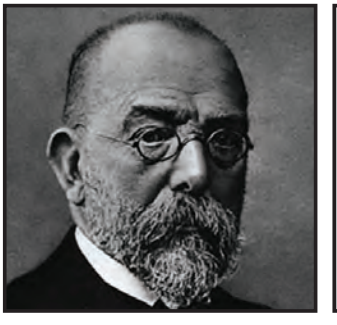

Volume 17, Number 3
March 2011

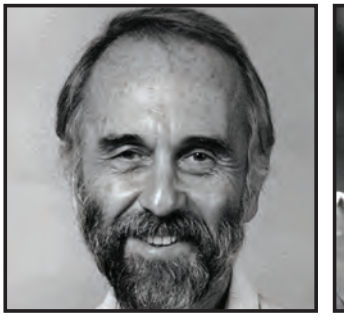

Volume 17, Number 12
December 2011

Volume 19, Number 4
April 2013

Volume 20, Number 5
May 2014

Volume 21, Number 9
September 2015

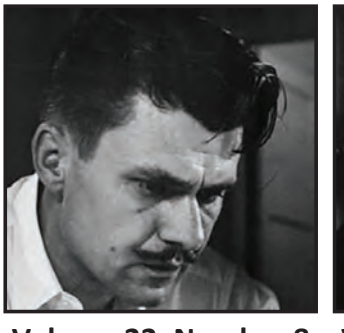

Volume 22, Number 8
August 2016

Volume 28, Number 3
March 2022

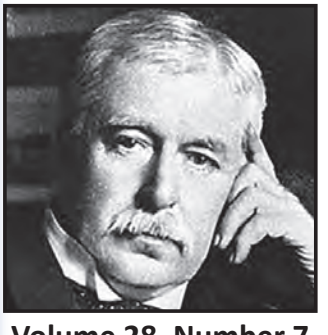

Volume 28, Number 7
July 2022

Click on the link below to read about the people behind the science.

https://bit.ly/3LN02tr

See requirements for submitting a photo quiz to EID.

https://bit.ly/3VUPqfj

EID Journal

Concurrent Outbreaks of Hepatitis A, Invasive Meningococcal Disease, and Mpox, Florida, USA, 2021–2022

Timothy J. Doyle, Megan Gumke, Danielle Stanek, Joshua Moore, Brian Buck, Timothy Locksmith, Kelly Tomson, Sarah Schmedes, George Churchwell, Shan Justin Hubsmith, Baskar Krishnamoorthy, Karalee Poschman, Brandi Danforth, Daniel Chacreton; the outbreak investigation team[1]

Medscape CME Activity

In support of improving patient care, this activity has been planned and implemented by Medscape, LLC and Emerging Infectious Diseases. Medscape, LLC is jointly accredited with commendation by the Accreditation Council for Continuing Medical Education (ACCME), the Accreditation Council for Pharmacy Education (ACPE), and the American Nurses Credentialing Center (ANCC), to provide continuing education for the healthcare team.

Medscape, LLC designates this Journal-based CME activity for a maximum of 1.00 ***AMA PRA Category 1 Credit(s)™***. Physicians should claim only the credit commensurate with the extent of their participation in the activity.

Successful completion of this CME activity, which includes participation in the evaluation component, enables the participant to earn up to 1.0 MOC points in the American Board of Internal Medicine's (ABIM) Maintenance of Certification (MOC) program. Participants will earn MOC points equivalent to the amount of CME credits claimed for the activity. It is the CME activity provider's responsibility to submit participant completion information to ACCME for the purpose of granting ABIM MOC credit.

All other clinicians completing this activity will be issued a certificate of participation. To participate in this journal CME activity: (1) review the learning objectives and author disclosures; (2) study the education content; (3) take the post-test with a 75% minimum passing score and complete the evaluation at https://www.medscape.org/qna/processor/71268?showStandAlone=true&src=prt_jcme_eid_mscpedu; and (4) view/print certificate. For CME questions, see page 844.

NOTE: It is Medscape's policy to avoid the use of brand names in accredited activities. However, in an effort to be as clear as possible, the use of brand names should not be viewed as a promotion of any brand or as an endorsement by Medscape of specific products.

Release date: March 18, 2024; Expiration date: March 18, 2025

Learning Objectives

Upon completion of this activity, participants will be able to:

- Analyze the epidemiology of outbreaks of hepatitis A virus infection, invasive meningococcal disease, and mpox in Florida in 2022
- Assess how these outbreaks particularly affected the community of men who have sex with men
- Distinguish clinical outcomes of these outbreaks of infection

CME Editor

Amy J. Guinn, BA, MA, Technical Writer/Editor, Emerging Infectious Diseases. *Disclosure: Amy J. Guinn, BA, MA, has no relevant financial relationships.*

CME Author

Charles P. Vega, MD, Health Sciences Clinical Professor of Family Medicine, University of California, Irvine School of Medicine, Irvine, California. *Disclosure: Charles P. Vega, MD, has the following relevant financial relationships: consultant or advisor for Boehringer Ingelheim; GlaxoSmithKline; Johnson & Johnson.*

Authors

Timothy J. Doyle, PhD, MPH; Megan Gumke, MPH, CPH; Danielle Stanek, DVM, DACVPM; Joshua Moore, MPH; Brian Buck, DrPH, MPH; Timothy Locksmith, MS; Kelly Tomson, MS, BS; Sarah Schmedes, PhD; George Churchwell, MPH; Shan Justin Hubsmith, MPH.

Author affiliations: Florida Department of Health, Tallahassee, Florida, USA (T.J. Doyle, M. Gumke, D. Stanek, J. Moore, B. Buck, T. Locksmith, K. Thomson, S. Schmedes, G. Churchwell, S.J. Hubsmith, B. Krishnamoorthy, K. Poschman, B. Danforth, D. Chacreton); Centers for Disease Control and Prevention, Atlanta, Georgia, USA (T.J. Doyle, K. Poschman)

DOI: https://doi.org/10.3201/eid3004.231392

[1]Members of the team are listed at the end of the article.

In 2022, concurrent outbreaks of hepatitis A, invasive meningococcal disease (IMD), and mpox were identified in Florida, USA, primarily among men who have sex with men. The hepatitis A outbreak (153 cases) was associated with hepatitis A virus genotype IA. The IMD outbreak (44 cases) was associated with *Neisseria meningitidis* serogroup C, sequence type 11, clonal complex 11. The mpox outbreak in Florida (2,845 cases) was part of a global epidemic. The hepatitis A and IMD outbreaks were concentrated in Central Florida and peaked during March–June, whereas mpox cases were more heavily concentrated in South Florida and had peak incidence in August. HIV infection was more common (52%) among mpox cases than among hepatitis A (21%) or IMD (34%) cases. Where feasible, vaccination against hepatitis A, meningococcal disease, and mpox should be encouraged among at-risk groups and offered along with program services that target those groups.

Outbreaks of hepatitis A have been previously reported among gay, bisexual, and other men who have sex with men (MSM) (*1*). Numerous outbreaks of hepatitis A among MSM were reported in Europe during 1997–2005 (*2*) and 2016–2017 (*3*–*5*). In the United States, hepatitis A outbreaks among MSM were reported in several locations during 2017–2018 (*6*,*7*). Outbreaks of invasive meningococcal disease (IMD) have also been previously reported among MSM (*8*–*10*). In late 2021, increases of hepatitis A and IMD were observed in Central Florida, primarily among MSM, prompting an investigation to guide the implementation of disease control measures.

During the period those 2 concurrent outbreaks were ongoing in Florida, a global epidemic of mpox emerged, in which sexual and intimate contact, particularly among MSM, was the primary mode of recognized transmission (*11*,*12*). In May 2022, a case of mpox associated with the global epidemic was identified in the United States. By November 30, 2022, the United States had >29,600 reported mpox cases and Florida had the fourth highest number of cases in the country (*13*).

We provide a descriptive, cross-sectional analysis of the concurrent outbreaks of hepatitis A and IMD in Florida in the context of an ongoing global mpox epidemic that also is disproportionally affecting MSM. Through this analysis, we attempted to identify common and distinct features of each outbreak and synergistic factors that might have affected disease progression and control.

Methods

Hepatitis A and IMD are designated as reportable conditions in Florida; in 2022, mpox was reportable in Florida under the broader category of a disease of urgent public health importance (*14*). Cases for all 3 diseases are investigated by local staff of the Florida Department of Health (FDOH); investigations involve patient interviews to identify risk factors for illness and close contacts for possible prophylaxis or other needed follow-up actions. Interview questionnaires for each disease are standardized statewide; however, some questions differ between diseases. After recognition of an increased number of case reports, we created outbreak case definitions for hepatitis A and IMD (Table 1). We considered all mpox cases in Florida that met the national surveillance case definition to be outbreak related. The analysis period for this investigation included outbreak-associated cases for any of the 3 diseases that had illness onset during November 1, 2021–November 30, 2022.

Hepatitis A Case Investigation

For all persons clinically diagnosed with hepatitis A, hospital and commercial laboratories were asked to forward available specimens to the FDOH Bureau of Public Health Laboratories (BPHL) for hepatitis A virus (HAV) genotyping based on the VP1-P2B junction region (*17*). Next-generation sequencing was performed on the MiSeq (Illumina) platform, and bioinformatics data processing used the Centers for Disease Control and Prevention (CDC) Global Hepatitis Outbreak Surveillance Technology (GHOST) platform (*18*). Investigation guidelines in Florida require that a case of hepatitis A in a food employee be further investigated to assess risk for possible food item or food preparation system contamination, which might also involve an environmental assessment. FDOH considered patron notification or suspension orders for food establishments, dependent upon the outcome of the risk assessments conducted.

IMD Case Investigation

For persons with diagnosed IMD, isolates of *Neisseria meningitidis* were forwarded to BPHL for serogrouping by slide agglutination, and further characterization by whole-genome sequencing on MiSeq or NextSeq550 (Illumina) systems. Select specimens were also forwarded to CDC laboratories for additional characterization or confirmation. We analyzed sequencing data by using BPHL's FLAQ-AMR pipeline (https://github.com/BPHL-Molecular/flaq_amr) to assess sequence quality and identify the sequence type (ST) and submitted data to CDC's Bacterial Meningitis Genome Analysis Platform (BMGAP; https://github.com/CDCgov/BMGAP) to identify the clonal complex (CC) and to verify serogroup for each isolate (*19*). We identified outbreak-associated cases by serogroup, ST, and CC, and constructed phylogenetic trees.

Table 1. Case definitions used in the investigation of concurrent outbreaks of hepatitis A, invasive meningococcal disease, and mpox, Florida, USA, 2021–2022*

Disease	Definition
Hepatitis A	
Inclusion criteria	Florida residents meeting the surveillance case definition for hepatitis A† with symptom onset during November 1, 2021–November 30, 2022
Confirmed case	A hepatitis A case with laboratory evidence of infection with HAV genotype IA, A17 cluster 21, or epidemiologically linked to a case with HAV A17 cluster 21 infection
Probable case	A hepatitis A case who identified as transgender or MSM or had sexual contact with MSM, irrespective of other risk factors for hepatitis A
Suspected case	A male hepatitis A case with unknown sexual history, and absence of other risk factors for hepatitis A (e.g., foreign travel, drug use, homelessness, incarceration)
Epidemiologically linked	Household or sexual contact during the 15–50 d before symptom onset
Exclusions	Cases with sequencing results indicating infection with HAV other than genotype IA, A17 cluster 21
Invasive meningococcal disease	
Inclusion criteria	Florida residents meeting the surveillance case definition for invasive meningococcal disease† with symptom onset during November 1, 2021–November 30, 2022
Confirmed case	An invasive meningococcal disease case who identifies as MSM or had sexual contact with MSM and evidence of serogroup C infection; or laboratory evidence of infection with ST11 CC11 serogroup C, with <100 SNPs difference to the outbreak strain, irrespective of sexual history
Probable case	An invasive meningococcal disease case who identifies as MSM or had sexual contact with MSM and for whom no additional serogroup, ST, or CC typing is available; or who had evidence of serogroup C infection regardless of sexual history
Exclusions	Cases with sequencing results indicating infection with *Neisseria meningitides* other than ST11 CC11 serogroup C or with >100 SNP differences to the outbreak strain
Mpox	
Inclusion criteria	Florida residents meeting the surveillance case definition for confirmed or probable mpox‡ with symptom onset during May 1–November 30, 2022

*CC, clonal complex; HAV, hepatitis A virus; MSM, men who have sex with men; SNP, single-nucleotide polymorphism; ST, sequence type; STI, sexually transmitted infection.
†Per Florida Department of Health definition (*15*).
‡Per Centers for Disease Control and Prevention definition (*16*).

Mpox Case Investigation

In May 2022, FDOH notified healthcare providers and laboratories that mpox was considered reportable under existing rules. FDOH adopted the national surveillance case definition. That definition initially included clinical manifestations as a criterion, but on July 22, 2022, was modified to focus on laboratory results and epidemiologic risk factors for probable and confirmed cases (*20*).

Initially, all testing for orthopoxvirus and mpox virus infections was conducted at BPHL and CDC using previously described procedures (*21*,*22*). In July 2022, use of the nonvariola orthopoxvirus assay expanded to commercial laboratories (*23*). Molecular subtyping of isolates from mpox patients in Florida was not routinely done for surveillance purposes during the study period; however, CDC performed partial or full sequencing for a subset of samples (*24*,*25*).

Epidemiology and Analyses

FDOH Bureau of Epidemiology operates an electronic patient-based reportable disease surveillance system known as Merlin. Using data from Merlin, we identified persons meeting the outbreak case definition for ≥1 disease in the 3 concurrent outbreaks. We used data from other surveillance systems operated by the Bureau of Communicable Diseases for sexually transmitted infections (STIs) and HIV to ascertain history and risk factors for reportable STIs (e.g., chlamydia, gonorrhea, or syphilis) and HIV infection. We matched patient profiles between systems by using name, sex, date of birth, and address information.

We calculated descriptive statistics to characterize outbreak-related cases by person, place, and time. We assessed pairwise differences in median age via Dunn test and conducted χ^2 tests to compare cases of each disease by HIV infection, history of recent STI, and Orange County residency. We used 2-sided tests in all statistical analyses and considered $p<0.05$ statistically significant.

To assess the role of the public health response in controlling the concurrent outbreaks, we analyzed data from the statewide immunization registry by vaccine antigen and month of first dose administered. To distinguish outbreak response efforts from routine childhood or adolescent immunization, we limited data to vaccines administered to adults ≥18 years of age. We stratified data by persons receiving vaccine from a county health department (CHD) provider. To further characterize synergies in outbreak response efforts, we identified instances of vaccine administration to the same person, on the same day, against >1 of the diseases in the concurrent outbreaks. This activity was reviewed by the Ethics and Human Research

Protection Program of FDOH and by CDC and was determined by both institutions to be public health practice, outbreak investigation, not requiring review and approval by an institutional review board.

Results

Hepatitis A Cases

During the analysis period, a total of 322 hepatitis A cases among Florida residents were reported to FDOH; 153 (48%) met the outbreak case definition. Of nonoutbreak cases during that period, ≈50% had an identifiable risk factor for hepatitis A, among which 60% were associated with recent international travel. Among the 153 outbreak-associated cases, 95% were in male persons and 5% in female persons, 74% were in MSM, and 21% were in persons with HIV; 1 death occurred (Table 2). Among persons for whom sexual history was obtained, 25% reported no sexual contacts in the previous 3 months; 8% reported >5 sexual partners, and 22% reported recent sexual contact with a person whose identity was not known. Seventeen cases were identified among food employees, but no foodborne transmission was documented. Environmental assessments performed at food establishments where exposure might have occurred did not necessitate FDOH orders for patron notification or suspension of service.

Among outbreak-associated cases, 67 (44%) met the confirmed case classification, among which 60 cases had matching HAV genotype IA, GHOST cluster A17 cluster 21 (a.k.a. SC076 US-Mexican); the remaining 7 confirmed cases had an epidemiologic link to a laboratory-confirmed case. We excluded 4 cases from the outbreak that otherwise met the probable or suspected outbreak case classification because HAV sequencing results did not match the outbreak

Table 2. Description of outbreak-related cases during concurrent outbreaks of hepatitis A, invasive meningococcal disease, and mpox, Florida, USA, 2021–2022*

Characteristics	Value		
	Hepatitis A	Invasive meningococcal disease	Mpox†
Total no.	153	44	2,845
Median age, y (range)	35 (9–75)	32 (8–77)	36 (0–81)
Race or ethnicity			
White	102/153 (67)	29/44 (66)	1,957/2,845 (69)
Hispanic	53/150 (35)	22/44 (50)	1,270/2,845 (45)
Sex			
M	145/153 (95)	36/44 (82)	2,786/2,845 (98)
F	8/153 (5)	8/44 (18)	59/2,845 (2)
Transgender	4/153 (3)	1/44 (2)	22/2,845 (1)
MSM‡	113/152 (74)	31/43 (72)	2,507/2,836 (88)
No. sexual partners during past 3 mo‡			
0	25/100 (25)	4/31 (13)	27/1,680 (2)§
1	44/100 (44)	17/31 (55)	914/1,680 (54)§
2–5	23/100 (23)	8/31 (26)	631/1,680 (38)§
>5	8/100 (8)	2/31 (6)	108/1,680 (6)§
Sex with unknown person in previous 3 mo‡	22/101 (22)	6/30 (20)	225/956 (23)§
HIV positive	32/153 (21)	14/44 (34)	1,473/2,836 (52)
Taking HIV preexposure prophylaxis	20/130 (15)	5/44 (11)	Unknown
STI in previous 2 y	42/153 (27)	9/44 (20)	1,567/2,836 (55)
Mpox virus infection in 2022	4	3	All
Recent international travel	12/153 (8)	1/44 (2)	199/2,845 (7)
Recent homelessness	8/153 (5)	2/44 (5)	25/928 (3)
Recent incarceration	1/153 (<1)	0/44 (0)	1/928 (<1)
Recent injection drug use	3/153 (2)	2/44 (5)	Unknown
Orange County resident	53/153 (35)	15/44 (34)	295/2,845 (10)
Food employee	17/121 (15)	7/44 (16)	Unknown
Hospitalized	119/153 (78)	41/44 (93)	162/2,845 (6)
Died	1/153 (<1)	9/44 (20)	3/2,845 (<1)
Outbreak case classification			
Confirmed	67/153 (44)	40/44 (91)	1,720/2,845 (60)
Probable	73/153 (48)	4/44 (9)	1,125/2,845 (40)
Suspect	13/153 (8)	NA	NA
Laboratory evidence of infection with outbreak genotype/sequence	60/153 (39)	34/44 (77)	NA

*Values are no. cases/no. reported (%) except as indicated. All risk factor questions relate to exposures in the 3 mo before symptom onset, except sexual history for mpox cases, which refers to the 3 weeks before symptom onset. Denominators vary based on available data for each variable. Percentages may not add to 100 due to rounding. MSM, men who have sex with men.
†Outbreak ongoing, data through November 30, 2022.
‡Minors age <18 y excluded from numerator and denominator.
§Number of sexual partners in 3 weeks before onset (mpox incubation period).

cluster type. Of the 60 cases with the matching HAV outbreak cluster type, 2 patients appear to be outliers and had no identifiable risk factors or recognized exposures to HAV. One case was in a 74-year-old heterosexual female person and the other was in a 9-year-old male child. Of the 7 confirmed cases not genotyped but confirmed through epidemiologic linkage, 2 were linked to the 9-year-old patient, his parents, who later became ill, likely because of secondary household transmission; the remaining 5 cases were sexual or household contacts of persons who identified as MSM.

IMD Cases

During the analysis period, 71 IMD cases among Florida residents were reported to FDOH. Of those, 44 (62%) cases were classified as outbreak associated. Among the outbreak cases, 72% were in persons who identified as MSM, 34% were in persons with HIV, and 20% of cases resulted in death (Table 2). The distribution of outbreak-associated cases by type of infection was 55% bacteremia, 20% meningitis, 5% septic arthritis, and 20% with >1 clinical syndrome. Case-fatality was highest (33%) among patients with bacteremia.

Among outbreak-associated cases, 40 (91%) met the confirmed case classification. Of those, 33 were caused by the ST11 CC11 outbreak strain; the other 7 confirmed cases were in persons who identified as MSM and had a serogroup C infection, but further strain characterization was not possible. Ten confirmed cases of the outbreak strain were in persons who did not identify as MSM, including a 77-year-old heterosexual woman with no known epidemiologic link to any other cases and 3 women who had no direct connection to one another but who were sexually active with the same male partner. Those 3 cases represent the only identified epidemiologic linkages among all the IMD cases in this outbreak.

Mpox Cases

During May 10–November 30, 2022, Florida reported 2,845 confirmed or probable mpox cases among residents. Most cases were locally acquired, but 14% of patients reported out-of-state travel during the 3-week incubation period. Most cases were among adult (>99%) and male (98%) persons. Among cases in adults, 88% were in persons who identified as MSM, but transmission through sexual contact between heterosexual persons was also identified. Among Florida cases, uncommon transmission routes were identified and have been previously reported by FDOH (*26*–*28*), including nonsexual household contact (n = 8) and occupational exposure among healthcare workers (n = 2).

Among mpox cases, 52% were in persons living with HIV and 55% in persons who had a history of ≥1 STI in the previous 2 years (Table 2). For the 1,414 cases with information available regarding previous HIV diagnoses, 10% were diagnosed within the previous year; 93% of cases were in persons who received HIV care within the previous year, 81% were in persons whose HIV infections were virally suppressed, and 6% were in persons who had a recent CD4 count of <200 cells/μL. Few (6%) cases were hospitalized because of mpox; 3 deaths occurred for which mpox was considered a causative or contributing factor. All 3 deaths were in persons who had a previous AIDS diagnosis, and 2 were unhoused.

CDC sequenced 17 mpox virus isolates and identified 16 as clade IIb subclade B.1 (*25*). One isolate collected early in the outbreak, from a patient with exposure in the United Arab Emirates, was identified as clade IIb subclade A.2 (*24*).

Outbreak Overlap

We observed temporal overlap for the 3 outbreaks; hepatitis A cases occurred somewhat earlier, and peak incidence was during late March and early April 2022 (Figure 1). Peak incidence for IMD occurred a few weeks later, and 13 cases were reported over a 6-week period during May–June. The number of hepatitis A and IMD cases declined as mpox cases rapidly increased; mpox incidence peaked during late July to early August, then rapidly declined. We did not identify any instances of the same person being part of both the hepatitis A and IMD outbreaks. However, among mpox cases, 4 patients were also part of the hepatitis A outbreak, and 3 others were part of the IMD outbreak (Appendix Table 1, https://wwwnc.cdc.gov/EID/article/30/4/23-1392-App1.pdf).

The greatest concentration of outbreak-associated hepatitis A and IMD cases occurred in the central region of Florida (Figure 2). Orange County had the highest number of cases for both diseases: 53 (35%) cases of hepatitis A and 15 (34%) cases of IMD. On the basis of patient residence, we identified 12 postal (ZIP) codes with ≥1 case of both hepatitis A and IMD, 3 of which had ≥2 cases of each disease (Figure 2). For hepatitis A, several cases occurred in west-central Florida (Hillsborough and Pinellas Counties), where IMD was not observed. Several IMD cases occurred in southeastern Florida (Miami-Dade, Broward, and Palm Beach Counties), where outbreak-associated hepatitis A was not frequently observed.

Mpox cases in Florida were more widely dispersed; cases were reported in 45 of 67 counties. The highest concentration was observed in the southeast

region, and 56% of all cases were reported in Broward and Miami-Dade Counties (Figure 3). Orange County reported the third highest (295; 10%) number of mpox cases. The 7 most populated counties in Florida accounted for 87% of mpox cases reported in the state. Exposure occurred exclusively outside the United States for 5% of Florida mpox cases, and an additional 2% of cases reported multiple exposure locations that included ≥1 location outside the United States.

Comparing cases by disease, the median age of IMD case-patients was 32 years, which was significantly younger than for hepatitis A (35 years; p = 0.0145) and mpox (36 years; p = 0.0043) case-patients. We detected statistically significant differences when comparing cases of each disease by HIV infection, history of recent STI, and Orange County residence (p<0.0001). HIV infection was more prevalent among mpox (52%) cases than among IMD (34%) or hepatitis A (21%) cases. In addition, STI in the previous 2 years was more prevalent among mpox (55%) cases than among hepatitis A (27%) or IMD (20%) cases. A lower percentage (10%) of mpox cases were among Orange County residents than were IMD (34%) and hepatitis A (35%) cases.

Control Measures

JYNNEOS (Bavarian Nordic) vaccine for preventing mpox became available in limited supplies in Florida in late May and June 2022. As the vaccine supply increased, persons vaccinated with their first dose increased markedly; in July and August, >53,000

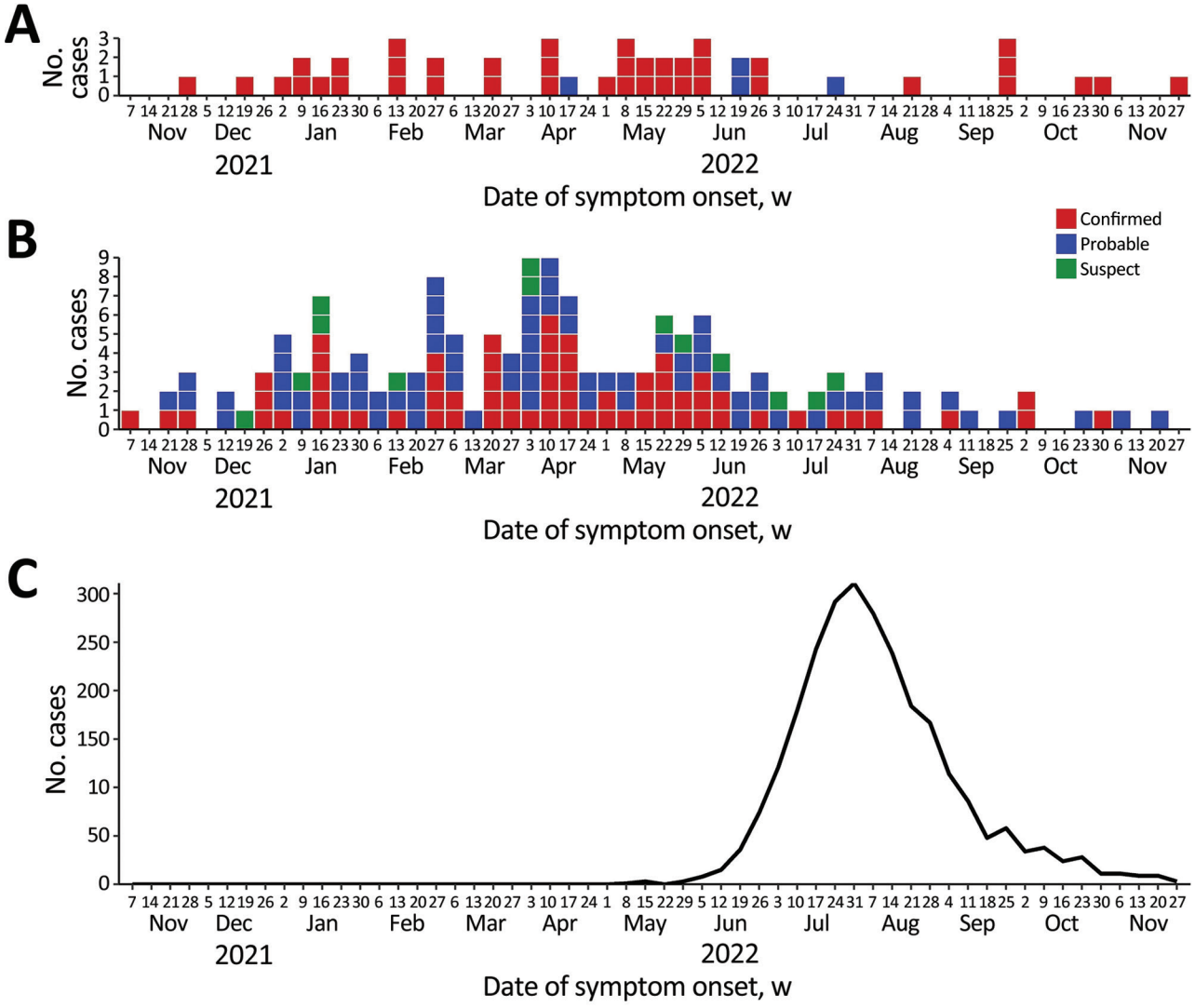

Figure 1. Epidemiologic curve of concurrent outbreaks of hepatitis A, invasive meningococcal disease, and mpox, by week of symptom onset, Florida, USA, November 1, 2021—November 30, 2022. A) Invasive meningococcal disease; B) hepatitis A; C) mpox. The case definition for invasive meningococcal disease cases had 2 categories: confirmed and probable. The case definition for hepatitis A cases had 3 categories: confirmed, probable, and suspect. The graph for mpox includes all confirmed and probable cases.

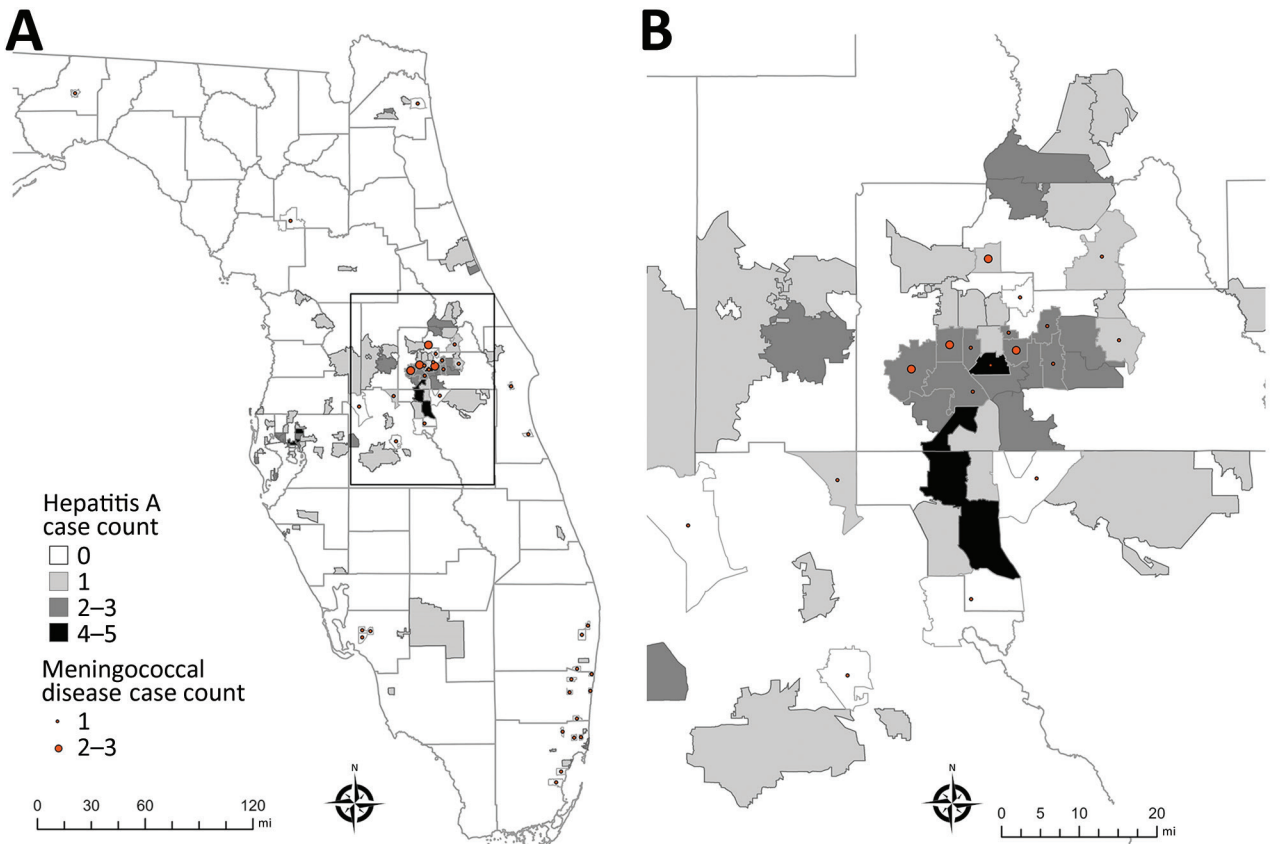

Figure 2. Spatial distribution of outbreak-associated cases of hepatitis A and invasive meningococcal disease in an investigation of concurrent outbreaks of hepatitis A, invasive meningococcal disease, and mpox, Florida, USA, 2021–2022. A) Locations of cases by postal (ZIP) code of patient residence; B) detail of box from central Florida in panel A, in which ≥1 case of each disease were reported in the same postal code. Outside the area represented in that panel, no instances of both diseases were identified in the same postal code. Invasive meningococcal disease cases were georeferenced by postal code centroid. Small polygons are outlines of postal code areas. Light gray lines indicate county borders; dark gray lines indicate postal areas where cases were identified.

adults in Florida received ≥1 dose (Appendix Table 2). Immunization against hepatitis A and IMD also increased markedly among adults during that timeframe (Figure 4). In August 2022, of the 28,592 persons receiving a first dose of JYNNEOS vaccine, 7,305 (26%) received ≥1 other vaccine against either hepatitis A or IMD on the same day; 2,979 (10%) received vaccines against all 3 diseases on the same day. More than half of adult immunizations for hepatitis A and IMD in August were administered by CHD providers. In contrast, during months outside the August–October period, <38% of adults receiving a vaccine for either disease received that dose from a CHD provider.

The hepatitis A and IMD outbreaks concluded by the end of 2022, but mpox cases continued to be reported in Florida as of January 2024. By that time, a total of 2,957 mpox cases had been reported since the start of the outbreak, which is considered ongoing.

Discussion

Outbreaks of hepatitis A and IMD among MSM were ongoing in Florida when the emerging mpox outbreak added further complexity and urgency to the public health response. In addition, the introduction of mpox might have hastened the decline of cases in the hepatitis A and IMD outbreaks, possibly due to multiple factors. First, the negative perceptions and fear of acquiring mpox might have led to changes in sexual behaviors among MSM, particularly persons outside of monogamous relationships. In a national survey of 703 MSM and transgender women conducted in August 2022, more than half reported a change in their sexual behavior because of the mpox outbreak; 40% reported limiting the number of sexual partners, and 24% avoided having any type of sex (*29*). Similarly, in another survey of MSM conducted in August 2022, a total of 50% of respondents reported reducing 1-time sexual encounters and 50% reported reducing sex with partners met on dating apps or at sex venues (*30*).

The response to mpox might also have hastened the end of the hepatitis A and IMD outbreaks through coordinated immunization outreach efforts targeting overlapping risk groups. Before August 2022, demand for JYNNEOS vaccine was strong, but supplies were limited (*31*,*32*). As the vaccine became more readily available (*33*), CHDs in Florida conducted outreach activities to provide mpox vaccination to gay, bisexual, and other MSM, which also helped provide vaccination against hepatitis A or IMD to the same persons, where indicated (*34*,*35*). The strong interest and demand for JYNNEOS vaccine among MSM likely led some persons to get vaccinated against hepatitis A and IMD who might not otherwise have been vaccinated. Vaccines administered by CHDs were provided free of charge to the client and, in some counties, made available outside nightclubs and at social venues or community events. That strategy leveraged lessons learned from HIV prevention programs, including making services available to persons who would most benefit, where they most likely would be, and when they would most likely be comfortable (*36*).

We observed a high percentage of concurrent HIV infection among hepatitis A, IMD, and most notably, mpox case-patients. We observed a similar pattern regarding history of an STI in the previous 2 years. The duration of HAV viremia and stool shedding might be longer in persons with HIV (*37*), and persons with HIV who have low CD4 cell counts are also more susceptible to invasive disease when exposed to *N. meningitidis* (*8*,*10*). Some researchers have proposed the concept of syndemics to refer to multiple diseases occurring in the same population that have a synergistic effect on the progression or outcome of each disease (*38*,*39*). HIV and STIs are frequently cited examples of infectious disease syndemics. We observed current or recent infections in the same person, including HIV, ≥1 STI, mpox, and hepatitis A or IMD, in a setting of concurrent outbreaks. A single case report involving a similar combination with severe hepatitis A was previously reported (*40*).

Of note, 25% of adult hepatitis A case-patients in the outbreak reported no sexual activity in the previous 3 months. That might be the result of unreliable information regarding sexual history provided by case-patients. However, it also might be explained by possible undetected spillover into foodborne transmission or environmental surface contamination at venues that cater to an exclusively or predominantly lesbian, gay, bisexual, and transgender clientele, a possibility that has been noted in similar outbreaks (*41*). No common venues were identified in our outbreaks but interviewed case-patients frequently declined to identify specific venues. Moreover, some

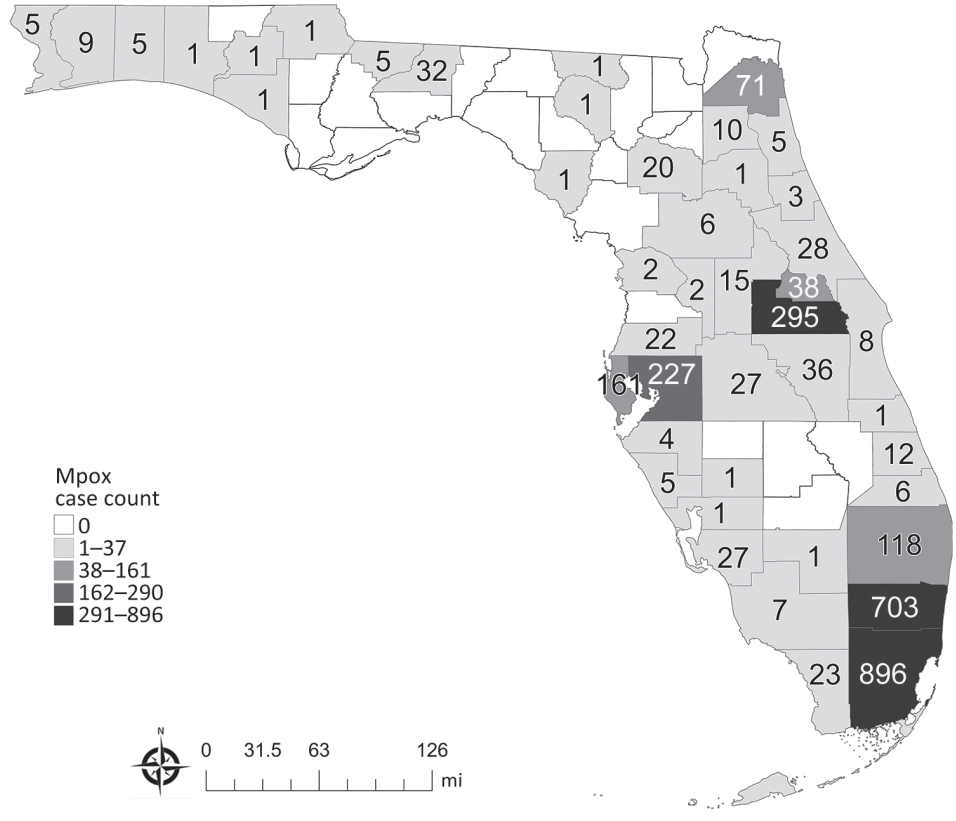

Figure 3. Distribution of mpox cases by county of residence in an investigation of concurrent outbreaks of hepatitis A, invasive meningococcal disease, and mpox, Florida, USA, 2021–2022. Numbers on map indicate numbers of persons with mpox reported to Florida Department of Health, by the person's county of residence. Florida consists of 67 counties, and mpox cases were reported in residents of 45 of 67 counties.

confirmed cases in the hepatitis A outbreak in persons who were not sexually active, such as the elderly woman and young boy, might be explained by limitations of HAV subgenomic sequencing to detect variations in phylogenetic relationships (*42*).

Simultaneous response to these 3 concurrent outbreaks highlighted differences in public health surveillance, investigation, and response activities for diseases considered sexually transmitted compared with other communicable diseases, such as hepatitis A or IMD, that have multiple transmission modes that also can include sexual contact. Many US public health departments, including FDOH, are organizationally separated between general communicable diseases and control programs related to STIs and HIV. Barriers often exist for integration of staff and surveillance information resources across those program areas. Nevertheless, we found added value in close collaboration and integration of case-related data in response to these concurrent outbreaks. Further integration across program areas could provide added benefit in disease control efforts, particularly those involving overlapping risk groups.

When the global mpox epidemic emerged in 2022, and transmission among MSM was quickly recognized, investigation methods in the United States (e.g., questionnaires and case interviews) rapidly aligned to methods typically used for STIs and HIV (*36*). In Florida, methods included using experienced disease intervention specialists (DISs) who have advanced skills in eliciting sensitive details regarding sexual history. In contrast, case investigations for most reportable diseases in Florida, including hepatitis A and IMD, do not routinely include detailed information on gender identity, sexual orientation, or sexual history, nor are those investigations routinely conducted by trained DIS staff with specialized interviewing skills. Thus, data collected during these concurrent outbreak investigations were not standardized nor consistently gathered across diseases, limiting direct comparisons. Furthermore, we did not directly compare MSM status across the diseases because MSM was a criterion within the outbreak case definitions for hepatitis A and IMD but not for mpox. Nor did we compare race or ethnicity across the 3 diseases because population demographics differ by region in Florida and mpox was much more heavily concentrated in southern Florida than the other 2 diseases.

This investigation was also limited by an inability in many instances to identify close contacts, particularly known or anonymous sexual contacts. Thus, epidemiologic linkages between cases were often difficult or impossible to establish. The lack of available specimens from all patients also limited efforts to fully use molecular and genomic analyses to identify connections between cases or to rule out probable or suspected cases that might not have been truly related to the hepatitis A or IMD outbreaks.

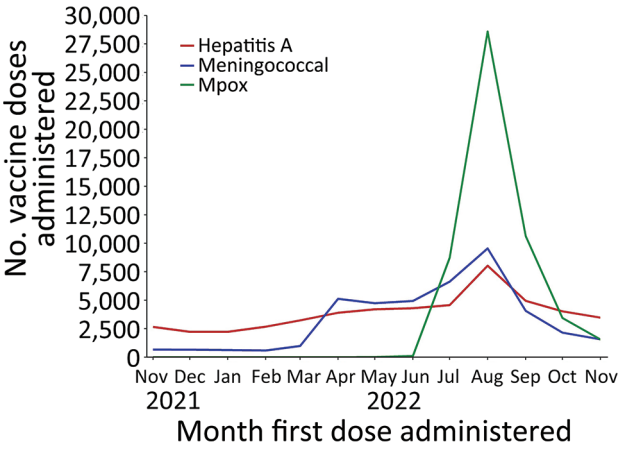

Figure 4. Persons vaccinated by month and antigen during concurrent outbreaks of hepatitis A, invasive meningococcal disease, and mpox, Florida, USA, 2021–2022. The figure shows the number of adult persons (≥18 years of age) vaccinated with their first dose, by month the first dose was administered. For hepatitis A, the number includes persons vaccinated with any Food and Drug Administration (FDA)–approved vaccine against hepatitis A virus. For meningococcal disease, the number includes persons vaccinated with any FDA-approved serogroup ACWY vaccine (Menveo [GlaxoSmithKline], Menactra [Sanofi Pasteur, Inc.], MenQuadfi [Sanofi Pasteur, Inc.]). For mpox, the number includes persons vaccinated with JYNNEOS (Bavarian Nordic). FDA, Food and Drug Administration.

Recognition of factors associated with an emerging syndemic early in its course facilitated improved data sharing and leveraged limited resources among public health programs responsible for disease control in Florida. In addition, combined vaccination efforts targeting overlapping at-risk populations likely contributed to the control of these outbreaks.

In conclusion, we found that cross-training between DIS and general communicable disease surveillance investigators might improve the quality of information collected through case interviews, particularly information related to sexual history. Disease prevention opportunities, also provided by DIS, might be enhanced through an integrated approach to screening, education, and linkage to care for multiple infectious diseases across program areas. Finally, vaccination against hepatitis A, meningococcal disease, and mpox should be encouraged among MSM, consistent with national guidelines (*33*–*35*) and, where feasible, offered with other program services to the same at-risk population.

Outbreak investigation team members: Alvina Chu, Michelle Persaud, Alvaro Mejia-Echeverry, Edhelene Rico, Shannon Patelsky, Jenniffer Rivas, Chelsea Kendrick, Maria Tarnoi, Rebecca Bohinc, Alissa Brown, Dell Walters, Purva Patel, Muniba McCabe, Patricia Kirkland.

Acknowledgments

We gratefully acknowledge the assistance of patients and medical providers in Florida for providing information for this investigation. We also acknowledge the assistance of numerous staff of county health departments and public health laboratories in Florida, as well as Jeremy Adams, Labake Ajayi, Tom Bendle, Tricia Foster, Lorene Maddox, Ann Schmitz, Craig Wilson, Namratha Tarigopula, Omer Tekin, Brenna McGruder Rawson, Ronique Bain, Candiss Ducksworth, Andres Echeverri, Alexandria Fletcher, Jackie Pho, Mariella Rivera, Antonisha Seay, Celia Vickery, Anne Barrera, Reynald Jean, Diana Paladino, Julio Pelaez, Johanna Segura, Nicholas DelVecchio, Jeanete Figueroa, Patrick Jenkins, Rafael Mendoza, Ryan Oms, Jonathan Pope, Chelsee Rose, Maria Diaz, Erin Bates, Ulyee Choe, Shelly Geisler, Gayle Guidash, Colin Hilliard, Rachel Ilic, JoAnne Lamb, Russell Kopit, Karen Thomas, Chowdhury Bari, Jacob Crosby. We also acknowledge CDC's Bacterial Meningitis Laboratory (National Center for Immunization and Respiratory Diseases) and Viral Hepatitis Laboratory (Division of Viral Hepatitis, National Center for HIV, Viral Hepatitis, STD, and TB Prevention) for assistance with genomic analysis used to categorize outbreak associated cases.

About the Author

Dr. Doyle is a CDC Career Epidemiology Field Officer assigned to the Florida Department of Health. His primary research interests include applied infectious disease epidemiology, disease surveillance, and public health workforce development.

References

1. Cotter SM, Sansom S, Long T, Koch E, Kellerman S, Smith F, et al. Outbreak of hepatitis A among men who have sex with men: implications for hepatitis A vaccination strategies. J Infect Dis. 2003;187:1235–40. https://doi.org/10.1086/374057
2. Stene-Johansen K, Tjon G, Schreier E, Bremer V, Bruisten S, Ngui SL, et al. Molecular epidemiological studies show that hepatitis A virus is endemic among active homosexual men in Europe. J Med Virol. 2007;79:356–65. https://doi.org/10.1002/jmv.20781
3. Ndumbi P, Freidl GS, Williams CJ, Mårdh O, Varela C, Avellón A, et al.; Members of the European Hepatitis A Outbreak Investigation Team. Hepatitis A outbreak disproportionately affecting men who have sex with men (MSM) in the European Union and European Economic Area, June 2016 to May 2017. Euro Surveill. 2018;23:1700641. https://doi.org/10.2807/1560-7917.ES.2018.23.33.1700641
4. Beebeejaun K, Degala S, Balogun K, Simms I, Woodhall SC, Heinsbroek E, et al. Outbreak of hepatitis A associated with men who have sex with men (MSM), England, July 2016 to January 2017. Euro Surveill. 2017;22:5. https://doi.org/10.2807/1560-7917.ES.2017.22.5.30454
5. Werber D, Michaelis K, Hausner M, Sissolak D, Wenzel J, Bitzegeio J, et al. Ongoing outbreaks of hepatitis A among men who have sex with men (MSM), Berlin, November 2016 to January 2017—linked to other German cities and European countries. Euro Surveill. 2017;22:30457. https://doi.org/10.2807/1560-7917.ES.2017.22.5.30457
6. Foster MA, Hofmeister MG, Albertson JP, Brown KB, Burakoff AW, Gandhi AP, et al. Hepatitis A virus infections among men who have sex with men—eight U.S. states, 2017–2018. MMWR Morb Mortal Wkly Rep. 2021;70:875–8. https://doi.org/10.15585/mmwr.mm7024a2
7. Latash J, Dorsinville M, Del Rosso P, Antwi M, Reddy V, Waechter H, et al. Notes from the field: increase in reported hepatitis A infections among men who have sex with men—New York City, January–August 2017. MMWR Morb Mortal Wkly Rep. 2017;66:999–1000. https://doi.org/10.15585/mmwr.mm6637a7
8. Bozio CH, Blain A, MacNeil J, Retchless A, Weil LM, Wang X, et al. Meningococcal disease surveillance in men who have sex with men—United States, 2015–2016. MMWR Morb Mortal Wkly Rep. 2018;67:1060–3. https://doi.org/10.15585/mmwr.mm6738a4
9. Taha MK, Claus H, Lappann M, Veyrier FJ, Otto A, Becher D, et al. Evolutionary events associated with an outbreak of meningococcal disease in men who have sex with men. PLoS One. 2016;11:e0154047. https://doi.org/10.1371/journal.pone.0154047
10. Folaranmi TA, Kretz CB, Kamiya H, MacNeil JR, Whaley MJ, Blain A, et al. Increased risk for meningococcal disease among men who have sex with men in the United States, 2012–2015. Clin Infect Dis. 2017;65:756–63. https://doi.org/10.1093/cid/cix438
11. Kava CM, Rohraff DM, Wallace B, Mendoza-Alonzo JL, Currie DW, Munsey AE, et al. Epidemiologic features of the monkeypox outbreak and the public health response—United States, May 17–October 6, 2022. MMWR Morb Mortal Wkly Rep. 2022;71:1449–56. https://doi.org/10.15585/mmwr.mm7145a4
12. Blackburn D, Roth NM, Gold JAW, Pao LZ, Olansky E, Torrone EA, et al. Epidemiologic and clinical features of mpox in transgender and gender-diverse adults—United States, May–November 2022. MMWR Morb Mortal Wkly Rep. 2022;71:1605–9. https://doi.org/10.15585/mmwr.mm715152a1
13. Centers for Disease Control and Prevention. Mpox: 2022 U.S. map & case count [cited 2022 Dec 27]. https://www.cdc.gov/poxvirus/mpox/response/2022/us-map.html
14. Florida Department of Health. Disease reporting and surveillance [cited 2022 Nov 10]. https://www.floridahealth.gov/diseases-and-conditions/disease-reporting-and-management/disease-reporting-and-surveillance/index.html
15. Florida Department of Health. Surveillance case definitions for reportable diseases in Florida [cited 2022 Nov 10]. https://www.floridahealth.gov/diseases-and-conditions/disease-reporting-and-management/disease-reporting-and-surveillance/_documents/surveillance-case-def-select-rd-fl.pdf
16. Centers for Disease Control and Prevention. Case definitions for use in the 2022 monkeypox response [cited 2022 Nov 10]. https://www.cdc.gov/poxvirus/monkeypox/clinicians/case-definition.html
17. Probert WS, Gonzalez C, Espinosa A, Hacker JK. Molecular genotyping of hepatitis A virus, California, USA, 2017–2018.

Emerg Infect Dis. 2019;25:1594–6. https://doi.org/10.3201/eid2508.181489
18. Ramachandran S, Xia GL, Dimitrova Z, Lin Y, Montgomery M, Augustine R, et al. Changing molecular epidemiology of hepatitis A virus infection, United States, 1996–2019. Emerg Infect Dis. 2021;27:1742–5. https://doi.org/10.3201/eid2706.203036
19. Buono SA, Kelly RJ, Topaz N, Retchless AC, Silva H, Chen A, et al. Web-based genome analysis of bacterial meningitis pathogens for public health applications using the Bacterial Meningitis Genomic Analysis Platform (BMGAP). Front Genet. 2020;11:601870. https://doi.org/10.3389/fgene.2020.601870
20. Minhaj FS, Ogale YP, Whitehill F, Schultz J, Foote M, Davidson W, et al.; Monkeypox Response Team 2022. Monkeypox outbreak—nine states, May 2022. MMWR Morb Mortal Wkly Rep. 2022;71:764–9. https://doi.org/10.15585/mmwr.mm7123e1
21. Li Y, Olson VA, Laue T, Laker MT, Damon IK. Detection of monkeypox virus with real-time PCR assays. J Clin Virol. 2006;36:194–203. https://doi.org/10.1016/j.jcv.2006.03.012
22. Li Y, Zhao H, Wilkins K, Hughes C, Damon IK. Real-time PCR assays for the specific detection of monkeypox virus West African and Congo Basin strain DNA. J Virol Methods. 2010;169:223–7. https://doi.org/10.1016/j.jviromet.2010.07.012
23. US Health and Human Services. HHS expanding monkeypox testing capacity to five commercial laboratory companies [cited 2022 Dec 27]. https://www.hhs.gov/about/news/2022/06/22/hhs-expanding-monkeypox-testing-capacity-five-commercial-laboratory-companies.html
24. Gigante CM, Korber B, Seabolt MH, Wilkins K, Davidson W, Rao AK, et al. Multiple lineages of monkeypox virus detected in the United States, 2021-2022. Science. 2022;378:560–5. https://doi.org/10.1126/science.add4153
25. Centers for Disease Control and Prevention. Update on managing monkeypox in patients receiving therapeutics [cited 2022 Nov 17]. https://emergency.cdc.gov/han/2022/han00481.asp
26. Saunders KE, Van Horn AN, Medlin HK, Carpenter A, Lee PA, Gutierrez L, et al. Monkeypox in a young infant—Florida, 2022. MMWR Morb Mortal Wkly Rep. 2022;71:1220–1. https://doi.org/10.15585/mmwr.mm7138e3
27. Hennessee I, Shelus V, McArdle CE, Wolf M, Schatzman S, Carpenter A, et al.; California Department of Public Health Monkeypox Pediat=ric Working Group; CDC Monkeypox Pediatric Working Group. Epidemiologic and clinical features of children and adolescents aged <18 years with monkeypox—United States, May 17–September 24, 2022. MMWR Morb Mortal Wkly Rep. 2022;71:1407–11. https://doi.org/10.15585/mmwr.mm7144a4
28. Mendoza R, Petras JK, Jenkins P, Gorensek MJ, Mableson S, Lee PA, et al. Monkeypox virus infection resulting from an occupational needlestick—Florida, 2022. MMWR Morb Mortal Wkly Rep. 2022;71:1348–9. https://doi.org/10.15585/mmwr.mm7142e2
29. Hubach RD, Owens C. Findings on the monkeypox exposure mitigation strategies employed by men who have sex with men and transgender women in the United States. Arch Sex Behav. 2022;51:3653–8. https://doi.org/10.1007/s10508-022-02423-3
30. Delaney KP, Sanchez T, Hannah M, Edwards OW, Carpino T, Agnew-Brune C, et al. Strategies adopted by gay, bisexual, and other men who have sex with men to prevent monkeypox virus transmission—United States, August 2022. MMWR Morb Mortal Wkly Rep. 2022;71:1126–30. https://doi.org/10.15585/mmwr.mm7135e1
31. Kriss JL, Boersma PM, Martin E, Reed K, Adjemian J, Smith N, et al. Receipt of first and second doses of JYNNEOS vaccine for prevention of monkeypox—United States, May 22–October 10, 2022. MMWR Morb Mortal Wkly Rep. 2022;71:1374–8. https://doi.org/10.15585/mmwr.mm7143e2
32. Millman AJ, Denson DJ, Allen ML, Malone JA, Daskalakis DC, Durrence D, et al.; Atlanta Black Gay Pride Festival Monkeypox Response Team. A health equity approach for implementation of JYNNEOS vaccination at large, community-based LGBTQIA+ events—Georgia, August 27–September 5, 2022. MMWR Morb Mortal Wkly Rep. 2022;71:1382–883. https://doi.org/10.15585/mmwr.mm7143e4
33. Owens LE, Currie DW, Kramarow EA, Siddique S, Swanson M, Carter RJ, et al. JYNNEOS vaccination coverage among persons at risk for mpox—United States, May 22, 2022–January 31, 2023. MMWR Morb Mortal Wkly Rep. 2023;72:342–7. https://doi.org/10.15585/mmwr.mm7213a4
34. Mbaeyi SA, Bozio CH, Duffy J, Rubin LG, Hariri S, Stephens DS, et al. Meningococcal vaccination: recommendations of the Advisory Committee on Immunization Practices, United States, 2020. MMWR Recomm Rep. 2020;69:1–41. https://doi.org/10.15585/mmwr.rr6909a1
35. Nelson NP, Weng MK, Hofmeister MG, Moore KL, Doshani M, Kamili S, et al. Prevention of hepatitis A virus infection in the United States: recommendations of the Advisory Committee on Immunization Practices, 2020. MMWR Recomm Rep. 2020;69:1–38. https://doi.org/10.15585/mmwr.rr6905a1
36. Daskalakis D, Romanik N, Jha AK. Lessons from the mpox response. JAMA. 2024 Jan 8 [Epub ahead of print]. https://doi.org/10.1001/jama.2023.27868
37. Lin KY, Chen GJ, Lee YL, Huang YC, Cheng A, Sun HY, et al. Hepatitis A virus infection and hepatitis A vaccination in human immunodeficiency virus-positive patients: a review. World J Gastroenterol. 2017;23:3589–606. https://doi.org/10.3748/wjg.v23.i20.3589
38. Singer M, Bulled N, Ostrach B, Mendenhall E. Syndemics and the biosocial conception of health. Lancet. 2017;389:941–50. https://doi.org/10.1016/S0140-6736(17)30003-X
39. Tsai AC, Mendenhall E, Trostle JA, Kawachi I. Co-occurring epidemics, syndemics, and population health. Lancet. 2017;389:978–82. https://doi.org/10.1016/S0140-6736(17)30403-8
40. Oprea C, Popa I, Ianache I, Păun A, Vasile S, Grațiela Țârdei, et al. Monkeypox, severe hepatitis A, and syphilis in an HIV returning traveler from Spain to Romania. Travel Med Infect Dis. 2022;50:102455. https://doi.org/10.1016/j.tmaid.2022.102455
41. Friesema IH, Sonder GJ, Petrignani MW, Meiberg AE, van Rijckevorsel GG, Ruijs WL, et al. Spillover of a hepatitis A outbreak among men who have sex with men (MSM) to the general population, the Netherlands, 2017. Euro Surveill. 2018;23:1800265. https://doi.org/10.2807/1560-7917.ES.2018.23.23.1800265
42. Vaughan G, Goncalves Rossi LM, Forbi JC, de Paula VS, Purdy MA, Xia G, et al. Hepatitis A virus: host interactions, molecular epidemiology and evolution. Infect Genet Evol. 2014;21:227–43. https://doi.org/10.1016/j.meegid.2013.10.023

Address for correspondence: Timothy Doyle, Florida Department of Health, 4052 Bald Cypress Way, Bin A-12, Tallahassee, FL 32399, USA; email: tdoyle@cdc.gov

Deaths Associated with Pediatric Hepatitis of Unknown Etiology, United States, October 2021–June 2023

Olivia Almendares,[1] Julia M. Baker,[1] David E. Sugerman, Umesh D. Parashar, Sarah Reagan-Steiner, Hannah L. Kirking, Paul A. Gastañaduy, Jacqueline E. Tate; Hepatitis of Unknown Etiology Group[2]

Medscape CME Activity

In support of improving patient care, this activity has been planned and implemented by Medscape, LLC and Emerging Infectious Diseases. Medscape, LLC is jointly accredited with commendation by the Accreditation Council for Continuing Medical Education (ACCME), the Accreditation Council for Pharmacy Education (ACPE), and the American Nurses Credentialing Center (ANCC), to provide continuing education for the healthcare team.

Medscape, LLC designates this Journal-based CME activity for a maximum of 1.00 ***AMA PRA Category 1 Credit(s)™***. Physicians should claim only the credit commensurate with the extent of their participation in the activity.

Successful completion of this CME activity, which includes participation in the evaluation component, enables the participant to earn up to 1.0 MOC points in the American Board of Internal Medicine's (ABIM) Maintenance of Certification (MOC) program. Participants will earn MOC points equivalent to the amount of CME credits claimed for the activity. It is the CME activity provider's responsibility to submit participant completion information to ACCME for the purpose of granting ABIM MOC credit.

All other clinicians completing this activity will be issued a certificate of participation. To participate in this journal CME activity: (1) review the learning objectives and author disclosures; (2) study the education content; (3) take the post-test with a 75% minimum passing score and complete the evaluation at https://www.medscape.org/qna/processor/71283?showStandAlone=true&src=prt_jcme_eid_mscpedu; and (4) view/print certificate. For CME questions, see page 846.

NOTE: It is Medscape's policy to avoid the use of Brand names in accredited activities. However, in an effort to be as clear as possible, the use of brand names should not be viewed as a promotion of any brand or as an endorsement by Medscape of specific products.

Release date: March 19, 2024; Expiration date: March 19, 2025

Learning Objectives

Upon completion of this activity, participants will be able to:

- Assess the epidemiology of a global outbreak of acute hepatitis among children between 2021 and 2023
- Evaluate the demographic data of children who died during this outbreak of acute hepatitis
- Analyze the clinical presentation of children who died during this outbreak of acute hepatitis
- Distinguish the rate of positive polymerase chain reaction testing for adenovirus among children who died during this outbreak of acute hepatitis

CME Editor

Dana C. Dolan, BS, Technical Writer/Editor, Emerging Infectious Diseases. *Disclosure: Dana C. Dolan, BS, has no relevant financial relationships.*

CME Author

Charles P. Vega, MD, Health Sciences Clinical Professor of Family Medicine, University of California, Irvine School of Medicine, Irvine, California. *Disclosure: Charles P. Vega, MD, has the following relevant financial relationships: served as a consultant or advisor for Boehringer Ingelheim; GlaxoSmithKline.*

Authors

Olivia Almendares, MSPH; Julia M. Baker, PhD; David Sugerman, MD; Umesh D. Parashar, MD, MBBS; Sarah Reagan-Steiner, MD; Hannah L. Kirking, MD; Paul Gastanaduy, MD; Jacqueline E. Tate, PhD.

Author affiliation: Centers for Disease Control and Prevention, Atlanta, Georgia, USA

[1]These authors contributed equally to this article.

[2]Members of the group are listed at the end of this article.

DOI: https://doi.org/10.3201/eid3004.231140

During October 2021–June 2023, a total of 392 cases of acute hepatitis of unknown etiology in children in the United States were reported to Centers for Disease Control and Prevention as part of national surveillance. We describe demographic and clinical characteristics, including potential involvement of adenovirus in development of acute hepatitis, of 8 fatally ill children who met reporting criteria. The children had diverse courses of illness. Two children were immunocompromised when initially brought for care. Four children tested positive for adenovirus in multiple specimen types, including 2 for whom typing was completed. One adenovirus-positive child had no known underlying conditions, supporting a potential relationship between adenovirus and acute hepatitis in previously healthy children. Our findings emphasize the importance of continued investigation to determine the mechanism of liver injury and appropriate treatment. Testing for adenovirus in similar cases could elucidate the role of the virus.

During October–November 2021, clinicians at a single children's hospital in Alabama, USA, identified 5 previously healthy children with acute hepatitis of unknown etiology who tested positive for adenovirus species F, type 41 (*1*); that pathogen was not previously considered a common cause of severe acute hepatitis in immunocompetent persons. In subsequent months, similar cases were identified internationally (*2*), prompting the launch of a nationwide public health investigation into pediatric acute hepatitis of unknown etiology in the United States. On April 21, 2022, the Centers for Disease Control and Prevention (CDC) issued a health advisory recommending that clinicians consider adenovirus testing in pediatric patients with hepatitis of unknown etiology and that patients meeting the following criteria be reported to jurisdictional health departments: <10 years of age with hepatitis manifested by elevated (>500 U/L) aspartate aminotransferase (AST) or alanine aminotransferase (ALT) and onset since October 1, 2021 (*3*).

As of June 6, 2023, health departments reported to CDC a total of 392 children meeting the hepatitis of unknown etiology case criteria. Worldwide, as of July 8, 2022, a total of 1,010 probable cases were reported to the World Health Organization on the basis of a closely aligned case criterion: children ≤16 years experiencing acute, non–A-E hepatitis with AST or ALT >500 IU/L since October 1, 2021. Despite similar case definitions, the United States was one of the few countries to report fatalities (*2*).

Severe acute hepatitis is known to have several potential etiologies, including drug-induced, genetic, metabolic, infectious, or immune-mediated causes (*4*). Adenovirus is a well-known cause of severe hepatitis in immunocompromised persons; it often has a direct pathologic effect on the liver (*4*–*7*). Conversely, few reported cases describe a potential association between adenovirus and severe acute hepatitis in immunocompetent children; the mechanism of liver injury in immunocompetent children is poorly understood (*8*–*11*). Previous studies estimate that 30%–50% of acute liver failure occurring in children without prior liver disease was of undetermined cause (*7*,*12*). However, adenovirus was commonly detected among children tested for the virus in recent investigations in the United States (116/275, 42%) (*13*) and United Kingdom (*14*) (170/258, 66%), raising the question of whether adenovirus may be an underrecognized cause of pediatric acute hepatitis.

We describe the characteristics of children who died after hepatitis of unknown etiology and were reported to CDC as part of the national-level investigation. Second, we describe the potential involvement of adenovirus and other pathogens in the development of severe acute hepatitis among these children. Last, we contextualize the deaths within the broader national-level investigation, describing similarities and differences between this subset of patients with the most severe outcomes and the overall patient population.

Methods

Study Population and Data Collection

This study includes all deaths reported to CDC among US children with acute hepatitis of unknown etiology with onset of October 1, 2021–June 6, 2023. A child was reported if they initially met the criteria defined in the CDC health advisory and if the child's death was related to their hepatitis episode, regardless of the time between hepatitis onset and death. Reported cases underwent further investigation including medical chart abstractions, caregiver interviews, laboratory testing, and, when possible, pathologic evaluation of liver tissue specimens. Health departments or clinicians completed medical chart abstractions using a standardized case report form to collect demographics, medical and illness history, laboratory test results, treatment received, and outcomes. Interviews were conducted with a parent or caregiver at the discretion of the health department to obtain additional information on each patient's symptoms; healthcare use; ill contacts at home, school, or daycare; and other potential exposures such as diet and travel. In addition, autopsy reports, discharge summaries, death certificates, and

other available medical records were requested for further review to better understand the course of illness and elucidate the possible role of adenovirus or other pathogens in development of severe acute hepatitis and death.

Specimen Collection and Testing

Laboratory testing for clinical management was not standardized; testing varied by individual patient and by clinical judgment. Most respiratory and fecal specimens were tested locally by multiplex PCR panel. In addition, testing for adenovirus by nucleic acid amplification testing (e.g., PCR or quantitative PCR) of blood, respiratory, or stool samples was requested at the discretion of the treating clinician and conducted at a clinical or reference laboratory. Available residual adenovirus-positive blood, stool, respiratory, and tissue specimens were sent to select reference laboratories or CDC for adenovirus typing using Sanger sequencing of the 6 hypervariable regions of the hexon gene (*15*). Formalin-fixed, paraffin-embedded (FFPE) tissues from liver biopsy, explant, or autopsy underwent routine evaluation at the clinical institutions or medical examiner's office; available specimens were submitted to CDC. CDC's evaluation of specimens included histopathology, immunohistochemistry (IHC), and conventional PCR and sequencing for adenovirus, as well as IHC and PCR for other infectious etiologies, as indicated based on the pathologic findings and clinical and epidemiologic history.

Record Review

All deaths reported to CDC as part of the hepatitis of unknown etiology investigation through June 6, 2023, are noted in this report. Some children were excluded as cases by the reporting jurisdiction as additional clinical information became available and an etiology was identified. For the remaining children, clinical and epidemiology teams at CDC reviewed all available medical records and related laboratory and pathological evaluations to develop consensus opinions on possible etiologies and confirm each child met the reporting criteria. Two pediatricians (P.A.G. and H.L.K.) independently evaluated reported underlying medical conditions to determine whether those conditions may have contributed to development of or increased risk for acute hepatitis. We excluded children with an etiology for their hepatitis from further investigation and analysis. We describe here in detail the children with no known or suspected etiology after review of all available records.

Statistical Analysis

We used descriptive statistics to summarize the data and results. We analyzed all data in R version 4.2.1 (The R Foundation for Statistical Computing, https://www.r-project.org). CDC reviewed the investigation protocol and confirmed that it was conducted consistent with applicable federal law and CDC policy (45 C.F.R. part 46.102(l)(2), 21 C.F.R. part 56; 42 U.S.C. §241(d); 5 U.S.C. §552a; 44 U.S.C. §3501 et seq.).

Results

Eligibility and Record Availability

During the national investigation, a total of 23 pediatric deaths with hepatitis onset occurring during October 1, 2021–June 6, 2023, were reported to CDC from 13 US jurisdictions: Florida, Georgia, Indiana, Michigan, Missouri, Nebraska, New York City, Pennsylvania, Puerto Rico, South Carolina, Tennessee, Texas, and Wisconsin (Table 1). Fourteen (60.9%) of the 23 children did not meet the reporting criteria defined in the health advisory on the basis of detailed medical record and laboratory testing review by the reporting jurisdiction or CDC. The most common reason for exclusion was identification of an alternative etiology for the hepatitis (n = 12). Alternative etiologies were complications of sepsis from pathogens other than adenovirus (n = 6), congenital conditions (n = 3), and unintentional injury (n = 3) (Table 1). After review of all information provided to CDC, 8 (34.8%) children were confirmed to meet the reporting criteria and are further described in this report. One child's eligibility could not be determined because records were unavailable.

Record availability differed by child (Table 2). A case report form was completed for all children, whereas an exposure questionnaire was available for 5 (62.5%). An autopsy had been conducted for 4 children; all those reports were available for review. A discharge summary was available for all 8 children and a death certificate was available for 6. Other available records included emergency department visit notes, admission history and physical notes, progress and consultation notes, and additional laboratory and radiologic testing results. FFPE autopsy tissue specimens from 3 children were submitted to CDC for evaluation; of those 3 children, 1 also had native liver explant submitted, and 1 a liver biopsy.

Demographics and Clinical Characteristics at Initial Visit

The median age at acute hepatitis onset was 2.4 (range 0.2–6.3) years (Table 3). Five patients (62.5%) were male and 3 (37.5%) female; 5 (5/8, 62.5%) identified as Hispanic or Latino ethnicity. At initial visit, 2 children

were immunocompromised and receiving immunosuppressive therapy (1 for ongoing cancer treatment and 1 after liver transplant), 2 other children had conditions that may have increased their risk of developing hepatitis or complications of adenovirus infection in the right clinical circumstance (1 was small for gestational age; 1 had history of poor weight gain and possible gastrointestinal disorder), and 4 children had no known underlying conditions (Table 3; Appendix Table 1). Children with underlying conditions that may have increased their risk and those with no known underlying conditions are henceforth called previously healthy.

All children manifested hepatitis signs and symptoms (i.e., dark colored urine, pale stool, jaundice, or scleral icterus); most also reported other systemic symptoms (87.5%), gastrointestinal symptoms (87.5%), and respiratory symptoms (75.0%) during their illness course (Table 3; Appendix Table 2). The median duration of symptoms before emergency department or inpatient admission was 7 (range 1–36) days (Figure). Laboratory evaluations showed elevated transaminases; median peak ALT was 4,852 (range 219–5,648) U/L and AST 7,500 (range 786–10,000) U/L. Median peak total bilirubin level was 13.7 (range 1.3–19.4) mg/dL and INR was 8.0 (range 1.4–13.0) (Table 3). Before the hepatitis episode, all but 1 child had received ≥2 doses of hepatitis B vaccine ≥3 weeks before their hepatitis episode (62.5% had 3 or 4 doses) and 5 children had received 1 or 2 doses of hepatitis A vaccine ≥3 months before their hepatitis episode. One child had received COVID-19 vaccine >3 months before the episode.

Table 1. Eligibility and exclusions among fatally ill children reported to the pediatric acute hepatitis of unknown etiology investigation, United States, October 1, 2021–June 6, 2023

Description	No. (%)
Total reported	23 (100.0)
Meets reporting criteria*	8 (34.8)
Does not meet reporting criteria	14 (60.9)
Unknown	1 (4.3)
Reason for exclusion	
Age ≥10 y	1 (7.1)
Onset date before October 1, 2021	1 (7.1)
Alternative etiology†	12 (85.7)
Complications of sepsis, pathogens other than adenovirus	6 (50.0)
Congenital conditions	3 (25.0)
Unintentional injury‡	3 (25.0)

*Child <10 y of age with elevated (>500 U/L) aspartate aminotransferase or alanine aminotransferase and hepatitis of unknown etiology with onset since October 1, 2021.
†Some children presented with complex clinical courses. The cause of hepatitis was not conclusive, but an alternative etiology or etiologies were considered likely. Categorizations were based upon available records.
‡Unintentional injuries include suffocation and acetaminophen toxicity.

Adenovirus and Other Pathogen Testing

For every child, ≥2 specimen types were tested for adenovirus by multiplex PCR panel (using respiratory or stool specimens) or by quantitative PCR (using blood specimens); the most common specimen types tested were blood (n = 7), respiratory (nasopharyngeal, n = 6), FFPE liver tissue (n = 6), and stool/rectal swab (n = 3) (Table 4). Four of the 8 children tested positive for adenovirus; each was positive in both respiratory specimens and whole blood. One child also tested positive in stool and another in both serum and liver tissue. Blood specimens had the highest adenovirus detection rate (4/7, 57.1%), particularly whole blood (4/5, 80%). Adenovirus typing data were available for 2 children.

Of the 4 children who tested positive for adenovirus, 2 (patients 1 and 2) had immunocompromising conditions before hepatitis onset; 1 was positive for adenovirus species B, type 7 (respiratory and stool samples), and 1 was positive for species C, type 1, in whole blood and species C in liver tissue. The third child (patient 3), initially immunocompetent, tested positive for adenovirus (type unknown) after becoming immunocompromised after a liver transplant received during the initial hospital stay; before the liver transplant, the child had tested negative for

Table 2. Record availability for 8 children with hepatitis of unknown etiology, United States, October 1, 2021–June 6, 2023*

Patient ID	Case report form	Exposure questionnaire	Autopsy conducted	Autopsy report	Discharge summary	Death certificate/ cause of death	Other records	Pathology specimen(s) evaluated at CDC†
1	Y	N	N	NA	Y	Y	N	N
2	Y	N	Y	Y	Y	N	Y	Y
3	Y	Y	N	NA	Y	Y	N	N
4	Y	Y	Unknown	N	Y	Y	N	N
5	Y	Y	Y	Y	Y	Y	N	Y
6	Y	Y	Y	Y	Y	Y	N	N
7	Y	Y	Y	Y	Y	Y	Y	Y
8	Y	N	N	NA	Y	N	Y	N
Total no. (%)	8 (100.0)	5 (62.5)	4 (50.0)	4 (50.0)	8 (100.0)	6 (75.0)	3 (37.5)	3 (37.5)

*Y indicates the record was available to CDC; N indicates the record was not available to CDC. CDC, Centers for Disease Control and Prevention; NA, not applicable.
†Available pathology specimens were sent to CDC for evaluation and further characterization. Tissue analyses conducted at the treating facility are not included here.

adenovirus in respiratory, whole blood, and liver specimens. The fourth child (patient 4) who tested positive for adenovirus (type unknown) had no underlying conditions but was <1 year of age. Of the 4 children who were negative for adenovirus (patients 5–8), all were considered previously healthy (Table 4; Figure; Appendix Table 1).

All children tested positive for ≥1 viral or bacterial pathogen (Table 5). After adenovirus, the most commonly detected pathogens were bacterial pathogens isolated in culture from normally sterile sites (blood or joint fluid, n = 4), followed by *Clostridium difficile* (stool specimens, n = 2), rhinovirus/enterovirus (respiratory specimens, n = 2), and respiratory

Table 3. Clinical and demographic characteristics of 8 children with hepatitis of unknown etiology, United States, October 1, 2021–June 6, 2023 *

Characteristic	Value
Demographic characteristics	
Age	
Median age (range)	2.4 (0.2–6.3)
0–11 mo	2 (25.0)
1–2 y	4 (50.0)
3–9 y	2 (25.0)
Sex	
F	3 (37.5)
M	5 (62.5)
Race/ethnicity	
Hispanic or Latino	5 (62.5)
Black, non-Hispanic	2 (25.0)
White, non-Hispanic	1 (12.5)
Clinical characteristics	
Underlying conditions at initial visit	
Immunocompromised†	2 (25.0)
Comorbidities that may have increased risk for hepatitis‡	2 (25.0)
No underlying conditions	4 (50.0)
Reported signs and symptoms§	
Respiratory	6/8 (75.0)
Gastrointestinal	7/8 (87.5)
Hepatic	8/8 (100.0)
Systemic	7/8 (87.5)
Laboratory findings	
Highest alanine transaminase, median (range), U/L	4,852 (219–5,648)
Highest aspartate aminotransferase, median (range), U/L	7,500 (786–10,000)
Highest total bilirubin, median (range), mg/dL	13.7 (1.3–19.4)
Highest international normalized ratio, median (range)	8.0 (1.4–13.0)
Highest ammonia, median (range), μmol/L	126.0 (60.3–801.0)
Duration of symptoms before admission, d	
Median (range)	7 (1–36)
0–7	5 (62.5)
8–14	1 (12.5)
≥15	2 (25.0)
Duration of hospital stay, d	
Median (range)	14.5 (<1– 18)
0–2	2 (25.0)
3–14	2 (25.0)
≥15	4 (50.0)
Physical findings	
Hepatomegaly	5/8 (62.5)
Hepatic encephalopathy	4/8 (50.0)
Splenomegaly	2/7 (28.6)
Ascites	3/7 (42.9)
Outcomes¶	
Acute liver failure	7 (87.5)
Liver transplant	2 (25.0)

*Values are no. (%) except as indicated.
†Immunocompromised at the time of initial presentation. One child immunosuppressed due to ongoing cancer treatment. One child immunocompromised due to a liver transplant.
‡One child was small for gestational age and 1 child had a history of poor weight gain and possible gastrointestinal disorder.
§Symptoms are not mutually exclusive; all children reported multiple symptoms. Respiratory signs/symptoms include cough, congestion, runny nose, shortness of breath, conjunctivitis, sore throat, or wheezing. Gastrointestinal signs/symptoms include diarrhea, nausea, vomiting, or abdominal pain. Hepatitis signs/symptoms include dark colored urine, pale stool, jaundice, or scleral icterus. Systemic signs/symptoms include fatigue, decreased appetite, or fever. See Appendix Table 2 (https://wwwnc.cdc.gov/EID/article/30/4/23-1140-App1.pdf) for data by patient.
¶Not mutually exclusive. Acute liver failure was defined based on documentation written in the medical chart or medical chart abstraction indicating acute liver failure occurred.

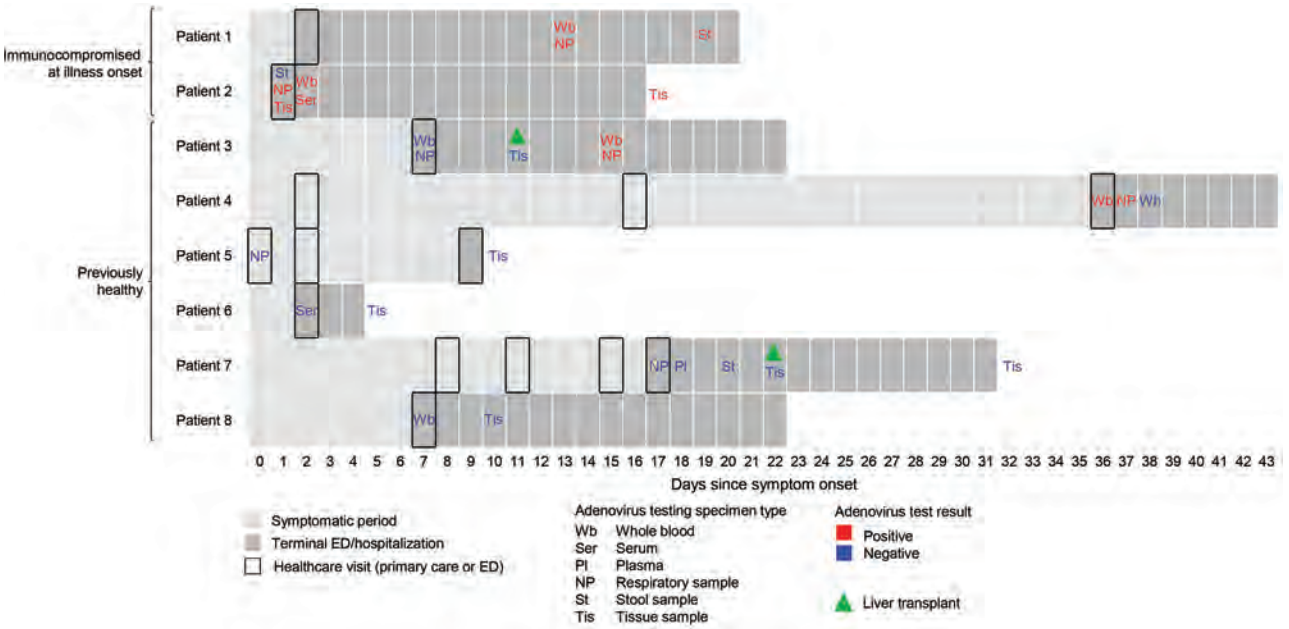

Figure. Health status at initial visit and timeline of clinical course for 8 children fatally ill with hepatitis of unknown etiology, United States, October 1, 2021–June 6, 2023. Symptom onset refers to the first symptom reported for the child including respiratory, gastrointestinal, hepatic, or systemic symptoms. Patients 1 and 2 were immunocompromised at the time of initial visit to emergency department or inpatient admission. Patient 3, initially immunocompetent, tested positive only after receiving a liver transplant during initial admission; before the transplant, the child had tested negative for adenovirus in respiratory, whole blood, and liver specimens. ED, emergency department.

syncytial virus (respiratory specimens, n = 2). In addition, 1 child had serologic evidence of acute Epstein-Barr virus infection. Of note, none of the children had evidence of acute SARS-CoV-2 infection; 2 children were reported to have had previous SARS-CoV-2 infection on the basis of serologic results in their medical records.

Liver specimens from 6 children underwent routine pathological examination at the clinical institution or medical examiner's office; 3 children had FFPE liver tissue specimens submitted to CDC. In 3 children (patients 3, 6, and 8), FFPE liver tissue specimens were negative for adenovirus by IHC at the clinical institution. Of the 3 children for whom FFPE liver tissue specimens were submitted to CDC, 2 (patients 5 and 7) were negative for adenovirus by IHC and PCR at CDC. FFPE liver tissue from 1 child (patient 2) was positive by IHC and PCR at the clinical institution and CDC, and adenovirus species C was detected by PCR at CDC. In addition, adenovirus species C was detected in whole blood and respiratory samples (Table 4). In the same child (patient 2), liver tissue pathology was consistent with classic adenovirus hepatitis including smudge cells. Pathologic findings seen in liver varied in the other 5 children (e.g., acute hepatitis, massive necrosis, interface hepatitis).

Outcomes

The median duration of hospitalization was 14 days (range <1–18 days). Seven (87.5%) children had acute liver failure as noted on the medical abstraction form; 2 of those underwent liver transplantation during acute hospitalization (Table 3; Figure). Seven children had a death certificate or autopsy report available that described the cause of death, including liver-related causes (viral hepatitis, acute cholestatic hepatitis, acute liver failure, hepatic encephalopathy, acute liver transplant rejection), cardiopulmonary causes (acute respiratory distress syndrome, cardiopulmonary arrest), cerebral herniation, or multiorgan failure. Among the 4 children who tested positive for adenovirus, 3 had adenovirus noted in the death certificate or autopsy report. Adenovirus was not mentioned on the death certificate for the fourth adenovirus-positive child (patient 3), who tested positive only after receiving a liver transplant.

Discussion

The deaths reported during the national investigation of pediatric acute hepatitis of unknown etiology represent a group of young children with diverse medical histories and courses of illness, likely reflecting the medical and etiologic complexity of pediatric hepatitis and the broad case criteria used

for the US investigation. Multiple children tested positive for adenovirus and other pathogens. Adenovirus typing data was available for 2 adenovirus-positive children. Of the 4 children who tested positive for adenovirus, most had underlying medical conditions at the time of adenovirus detection that likely put them at greater risk for severe infection and death. The death of 1 previously healthy child with adenoviremia demonstrates the continued importance of adenovirus testing and investigating the potential association between adenovirus and hepatitis in healthy children.

The United States is one of the few countries to report fatalities associated with pediatric acute hepatitis of unknown etiology (*2*), which may reflect minor differences in the case definitions implemented by countries (*16*,*17*), variation in application of those definitions for case finding, or the large size of the US population, enabling identification of rare outcomes. Of note, more than half of the initially reported fatalities in young children with hepatitis were later determined not to meet the case definition, most commonly because an etiology for their hepatitis was ultimately identified.

The diversity and complexities of illness among the children precluded identification of many commonalities; however, we were able to group the children into 3 broad categories. The first category describes a rare but recognized relationship between adenovirus infection and hepatitis: severe hepatitis or acute liver failure in an immunocompromised patient. Three of the 4 children who tested positive for adenovirus fall into this category because they were immunocompromised from immunosuppressive treatment or immunodeficiency at the time of adenovirus detection. The second category of children, of which 4 children were identified in this investigation, encompasses those who were previously healthy and tested negative for adenovirus. Hepatitis among those children may have a wide range of possible etiologies. As previously mentioned, pediatric acute liver failure can have several potential etiologies (*4*); earlier studies estimate that 30%–50% may be of undetermined cause (*7*,*12*). The findings among the fatally ill children reported here and previous studies on pediatric acute liver failure underscore the importance of standardized and comprehensive testing to identify underlying etiologies in children with indeterminate acute liver failure.

The third category encompasses the 1 previously healthy child in this study whose hepatitis appeared to be related to adenovirus, as evidenced by adenoviremia. Although age (<1 year) may be considered a potential risk factor, the child had no known

Table 4. Individual patient adenovirus testing for children with hepatitis of unknown etiology, United States, October 1, 2021–June 6, 2023*

	Result and day of testing								
Patient ID	Any specimen	Respiratory †	Stool‡	Blood (any§)	Whole blood	Serum	Plasma	FFPE tissue tested at clinical institution¶	FFPE tissue tested at CDC#
Patient 1**	P, day 13	P (B7), day 13	P (B7), day 19	P (NT), day 13	P (NT), day 13				
Patient 2**	P, day 1	P (NT), day 1	N†† day 1	P (NT), day 2	P (C1), day 2	P (NT), day 2		P (NT), day 1	P (C), day 1
Patient 3	P, day 15	P‡‡ (NT), day 15		P‡‡ (NT), day 15	P‡‡ (NT), day 15			N, day 11	
Patient 4	P, day 36	P (NT), day 37		P (NT), day 36	P (NT), day 36				
Patient 5	N, day 0	N, day 0							N, postmortem
Patient 6	N, day 2			N, day 2		N, day 2		N, postmortem	
Patient 7	N, day 17	N, day 17	N, day 20	N, day 18			N, day 18		N, day 22
Patient 8	N, day 7			N, day 7	N, day 7			N, day 10	
Total no. positive/no. tested (%)	4/8 (50.0%)	4/6 (66.7%)	1/3 (33.3%)	4/7 (57.1%)	4/5 (80.0%)	1/2 (50.0%)	0/1 (0.0%)	1/4 (25.0%)	1/3 (33.0%)

*Blank cells indicate not tested. P, positive; N, negative; NT, not typed; B7, adenovirus species B, type 7; C1, adenovirus species C, type 1; C, adenovirus species C; FFPE, formalin-fixed, paraffin-embedded.
†Respiratory specimens were tested by multiplex PCR panel. Specific panel type used may have varied based on manufacturer used by the diagnostic or reference laboratory.
‡Stool specimens were tested by nucleic acid amplification testing (e.g., PCR).
§Includes any blood specimen type (whole blood, serum, plasma). Blood specimens were tested by real-time PCR or quantitative RT-PCR.
¶Specimens were tested for adenovirus by immunohistochemistry (IHC) at the clinical institution. Tissue from Patient 2 additionally underwent testing by PCR at the clinical institution.
#Specimens were tested for adenovirus by IHC and PCR at CDC.
**Child considered to be immunocompromised at the time of hepatitis onset.
††Stool was tested by PCR for adenovirus type 40/41 and was negative.
‡‡Adenovirus test was negative before patient's liver transplant and positive after transplant.

Table 5. Positive pathogen detections in children with hepatitis of unknown etiology, United States, October 1, 2021–June 6, 2023*

Patient ID	Respiratory specimen	Stool specimen	Normally sterile site (blood or joint)†	Total no. pathogens detected
1	Adenovirus	Adenovirus	Adenovirus; *Streptococcus pneumoniae*	2
2	Adenovirus; respiratory syncytial virus		Adenovirus	2
3	Adenovirus; rhinovirus/enterovirus		Adenovirus	2
4	Adenovirus; rhinovirus/enterovirus		Adenovirus	2
5			*Staphylococcus hominis*; *Corynebacterium*; *Moraxella* non-liquefaciens‡	3
6	Respiratory syncytial virus		Epstein-Barr virus	2
7		*Clostridioides difficile*		1
8		*Clostridioides difficile*		1

*Table includes all pathogens for which a positive result was detected; it does not include other testing performed for which there were no positive results (e.g., respiratory and/or gastrointestinal panels, other viral testing). Other infections may have been present, but testing was not performed or results were inconclusive. Most respiratory and GI specimens were tested as part of a multiplex PCR panel, but panels used by clinical laboratory varied. All testing was performed at the discretion of treating clinicians.
† Bacterial pathogens were isolated on culture from a normally sterile site such as blood or joint fluid. Testing for viral pathogens was conducted using real-time PCR or quantitative real-time PCR testing, or by serologic assay to detect recent viral antibodies (e.g., IgM).
‡*Staphylococcus hominis*, Corynebacterium, and *Moraxella* non-liquefaciens may reflect contamination of specimen collection and not necessarily infection.

underlying medical conditions or immunodeficiency that would predispose to severe illness or complications from adenovirus infection. Detection of rhinovirus/enterovirus in a respiratory sample was the only other notable laboratory finding. The child had neither an acute nor prior history of SARS-CoV-2 infection. No liver tissue was available for analysis; the relationship between adenovirus infection and liver injury, if any, remains unclear. However, the presence of adenoviremia in conjunction with hepatitis of unknown etiology in this child bears similarity to the original cluster of children in Alabama (*1*) and to other case reports described elsewhere (*18*). The findings from this child and previous literature (*8*–*11*) emphasize the importance of considering adenovirus in the differential diagnosis for pediatric acute hepatitis, despite uncertainty regarding the pathologic mechanism.

The children described in this article are a unique subset of the overall patient population identified in the investigation of acute hepatitis of unknown etiology. Similar to members of the overall patient population, the fatally ill children illustrate a diverse range of possible hepatitis etiologies. The fatally ill children were more likely to have underlying conditions and differed in adenovirus testing results (*13*). Underlying conditions were rare (6%) in the overall patient population, whereas 2 of the 8 fatally ill children had significant underlying medical conditions that increased their risk for hepatitis. Several adenoviruses were detected among the overall patient population, including species B (type 7), C (types 1, 2, 6), and F (types 40, 41). Although adenovirus type 41 is a main focus in the national-level investigation and the most commonly detected type among the nonfatal cases (20/30, 67%), it was not detected in the 2 adenovirus-positive fatal cases that had typing results. Rather, those children were infected with adenovirus types typically seen in severe illness (species B, type 7) or upper respiratory illness (species C, type 1) and reported to be associated with hepatitis in immunocompromised patients (*19*,*20*). Typing was not available for the remaining 2 adenovirus-positive children; however, adenovirus was detected both in respiratory (nasopharyngeal swabs) and whole-blood specimens, suggesting possible infection with an adenovirus other than type 41. Adenovirus 41, which is typically associated with gastrointestinal infections (*20*,*21*), is rarely identified in respiratory specimens (*22*). Last, a high proportion of children in the overall patient population and the fatalities are Hispanic/Latino. Investigation into whether Hispanic/Latino children are at higher risk for diseases and death is needed.

The first limitation of this investigation is that we attempted to construct the clinical context of each child's illness via a secondary analysis of available medical and laboratory data, but we did not have full access to comprehensive medical records. Limited record availability, complexity and heterogeneity in illness course, and differences in clinical evaluations (e.g., laboratory testing) complicated summarization and full comparison of hepatitis cases. Although we detected multiple pathogens among the children, determining their contribution to hepatitis or death was not possible. Similarly, interpreting the role of adenovirus in the clinical course of illness was constrained by variations in specimen type, timing, and frequency of adenovirus testing. Reports from a related, previously published investigation in Alabama (*1*) suggested differences in the sensitivity of detection by specimen type (highest sensitivity in whole blood) that could add further uncertainty to the

interpretation of adenovirus testing results. However, all children were tested for the virus in multiple specimen types, often including blood. Although evaluation was not available at the time of this report, investigation is warranted into the potential role of adeno-associated virus type 2, a parvovirus hypothesized to have either a causal relationship or lead to more severe liver disease in co-infection with adenovirus (*23*,*24*). Last, we could not assess multiple potentially relevant host-related factors that may have affected the risk of illness, clinical course, or treatment, among them genetic or autoimmune predisposition (*24*), socioeconomic status, or behavioral factors (e.g., healthcare-seeking behavior).

The deaths reported during the US investigation of pediatric hepatitis of unknown etiology likely represent a diverse range of etiologies in both the cause of hepatitis and cause of death. This report describes 3 children who demonstrated a recognized relationship between adenovirus and acute hepatitis in immunocompromised persons; it also contributes to the growing evidence suggestive of a potential relationship between adenovirus and acute hepatitis in previously healthy children and the importance of testing for adenovirus early in the course of illness. Further investigation of adeno-associated virus type 2, adenovirus, and other potential helper viruses (e.g., human herpesvirus 6 and 7) (*23*) will contribute to understanding the mechanism of liver injury, if any, and the role of any cofactors or co-infections, particularly among a diverse population of children with no known underlying conditions. If adenovirus or other viral pathogens are contributing to the development of hepatitis, discovery of this relationship may enable clinicians to identify the cause of hepatitis in some future cases in which the etiology and appropriate treatment would have otherwise been unknown.

Additional members of the Hepatitis of Unknown Etiology Group: Jordan Cates, Anita K. Kambhampati, Erin R. McKeever, Melissa M. Coughlin, Caelin Cubenas (Centers for Disease Control and Prevention, Atlanta, Georgia, USA); Neha Balachandran (Centers for Disease Control and Prevention, Atlanta, Georgia, USA; Cherokee Nation Assurance, Arlington, Virginia, USA); Ashley Gent, Dalton Dessi (Florida Department of Health, Tallahassee, Florida, USA); Melissa Tobin-D'Angelo, Ami Gandhi (Georgia Department of Public Health, Atlanta, Georgia, USA); Nicole Stone (Indiana Department of Health, I ndianapolis, Indiana, USA); Geoff Brousseau, Macey Ladisky (Michigan Department of Health and Human Services, Lansing, Michigan, USA); Alexandra Berkley (Missouri Department of Health and Senior Services, St. Louis, Missouri, USA); Matthew Donahue, Derek Julian (Nebraska Department of Health and Human Services, Lincoln, Nebraska, USA); Dominique Balan, Mike Antwi (New York City Department of Health and Mental Hygiene, Long Island City, New York, USA); Lauren Torso Orkis (Pennsylvania Department of Health, Pittsburgh, Pennsylvania, USA); Melissa Marzán Rodríguez, Iris R Cardona Gerena (Puerto Rico Department of Health, San Juan, Puerto Rico, USA); Chelsea Campbell (South Carolina Department of Health and Environmental Control, Columbia, South Carolina, USA); Jessica Schultz (Tennessee Department of Health, Nashville, Tennessee, USA); Jantel Lewis, Ryan Wallace (Texas Department of State Health Services, Austin, Texas, USA); Thomas Haupt ((Wisconsin Department of Health Services, Madison, Wisconsin, USA).

Acknowledgments

We thank Bettina Bankamp, Julu Bhatnagar, Xiaoyan Lu, Roosecelis B. Martines, Jana M. Ritter, Jan Vinjé, Jennifer L. Cannon, Judy Chen, Tingting Gu-Templin, Page Keating, Ramona Lall, Joel Ackelsberg, Carmen J. Rodríguez Caquías, and Whitney Tillman.

About the Author

Ms. Almendares is an epidemiologist within the Epidemiology Branch, Coronavirus and Other Respiratory Viruses Division, National Center for Immunization and Respiratory Diseases, Centers for Disease Control and Prevention, Atlanta, Georgia, USA. Her research interests include vaccine-preventable diseases, respiratory virus epidemiology in children and community surveillance for health risks. Dr. Baker is an epidemiologist in the Viral Gastroenteritis Branch, Division of Viral Diseases, National Center for Immunization and Respiratory Diseases, Centers for Disease Control and Prevention, Atlanta, Georgia, USA. Her research focus is global child health, vaccine-preventable diseases, and viral gastroenteritis.

References

1. Baker JM, Buchfellner M, Britt W, Sanchez V, Potter JL, Ingram LA, et al. Acute hepatitis and adenovirus infection among children—Alabama, October 2021–February 2022. MMWR Morb Mortal Wkly Rep. 2022;71:638–40. https://doi.org/10.15585/mmwr.mm7118e1
2. World Health Organization. Disease outbreak news. Severe acute hepatitis of unknown aetiology in children—multi-country. 2022 [cited 2023 May 23]. https://www.who.int/emergencies/disease-outbreak-news/item/2022-DON400
3. CDC Health Alert Network. Recommendations for adenovirus testing and reporting of children with acute hepatitis of unknown etiology. 2022 [cited 2023 May 23]. https://emergency.cdc.gov/han/2022/pdf/CDC_HAN_462.pdf

4. Squires JE, McKiernan P, Squires RH. Acute liver failure: an update. Clin Liver Dis. 2018;22:773–805. https://doi.org/10.1016/j.cld.2018.06.009
5. Schaberg KB, Kambham N, Sibley RK, Higgins JPT. Adenovirus hepatitis. Am J Surg Pathol. 2017;41:810–9. https://doi.org/10.1097/PAS.0000000000000834
6. Ronan BA, Agrwal N, Carey EJ, De Petris G, Kusne S, Seville MT, et al. Fulminant hepatitis due to human adenovirus. Infection. 2014;42:105–11. https://doi.org/10.1007/s15010-013-0527-7
7. Squires RH Jr, Shneider BL, Bucuvalas J, Alonso E, Sokol RJ, Narkewicz MR, et al. Acute liver failure in children: the first 348 patients in the pediatric acute liver failure study group. J Pediatr. 2006;148:652–8. https://doi.org/10.1016/j.jpeds.2005.12.051
8. Ozbay Hoşnut F, Canan O, Ozçay F, Bilezikçi B. Adenovirus infection as possible cause of acute liver failure in a healthy child: a case report. Turk J Gastroenterol. 2008;19:281–3.
9. Munoz FM, Piedra PA, Demmler GJ. Disseminated adenovirus disease in immunocompromised and immunocompetent children. Clin Infect Dis. 1998;27:1194–200. https://doi.org/10.1086/514978
10. Matoq A, Salahuddin A. Acute hepatitis and pancytopenia in healthy infant with adenovirus. Case Rep Pediatr. 2016;2016:8648190. https://doi.org/10.1155/2016/8648190
11. Rocholl C, Gerber K, Daly J, Pavia AT, Byington CL. Adenoviral infections in children: the impact of rapid diagnosis. Pediatrics. 2004;113:e51–6. https://doi.org/10.1542/peds.113.1.e51
12. Narkewicz MR, Horslen S, Hardison RM, Shneider BL, Rodriguez-Baez N, Alonso EM, et al.; Pediatric Acute Liver Failure Study Group. A learning collaborative approach increases specificity of diagnosis of acute liver failure in pediatric patients. Clin Gastroenterol Hepatol. 2018;16:1801–1810.e3. https://doi.org/10.1016/j.cgh.2018.04.050
13. Cates J, Baker JM, Almendares O, Balachandran N, McKeever ER, Kambhampati AK, et al.; Hepatitis of Unknown Etiology Group. Paediatric acute hepatitis of unknown aetiology: a national surveillance investigation in the USA during 2021 and 2022. Lancet Child Adolesc Health. 2023;7:773–85. https://doi.org/10.1016/S2352-4642(23)00192-X
14. UK Health Security Agency. Investigation into acute hepatitis of unknown aetiology in children in England: Technical briefing 4. 2022 Jul 26 [cited 2023 Mar 1]. https://assets.publishing.service.gov.uk/government/uploads/system/uploads/attachment_data/file/1094573/acute-hepatitis-technical-briefing-4.pdf
15. Lu X, Erdman DD. Molecular typing of human adenoviruses by PCR and sequencing of a partial region of the hexon gene. Arch Virol. 2006;151:1587–602. https://doi.org/10.1007/s00705-005-0722-7
16. Centers for Disease Control and Prevention. Recommendations for adenovirus testing and reporting of children with acute hepatitis of unknown etiology. 2022 Apr 21 [cited 2022 Apr 21]. https://emergency.cdc.gov/han/2022/pdf/CDC_HAN_462.pdf
17. Zhang LY, Huang LS, Yue YH, Fawaz R, Lim JK, Fan JG. Acute hepatitis of unknown origin in children: early observations from the 2022 outbreak. J Clin Transl Hepatol. 2022;10:522–30. https://doi.org/10.14218/JCTH.2022.00281
18. UK Health Security Agency. Investigation into acute hepatitis of unknown aetiology in children in England. Technical briefing 3. 2022 May 19 [cited 2023 Jan 10]. https://assets.publishing.service.gov.uk/government/uploads/system/uploads/attachment_data/file/1077027/acute-hepatitis-technical-briefing_3.pdf
19. Centers for Disease Control and Prevention. Adenoviruses. Outbreaks [cited 2023 Mar 21]. https://www.cdc.gov/adenovirus/outbreaks.html
20. Lynch JP III, Kajon AE. Adenovirus: epidemiology, global spread of novel serotypes, and advances in treatment and prevention. Semin Respir Crit Care Med. 2016;37:586–602. https://doi.org/10.1055/s-0036-1584923
21. Bányai K, Estes MK, Martella V, Parashar UD. Viral gastroenteritis. Lancet. 2018;392:175–86. https://doi.org/10.1016/S0140-6736(18)31128-0
22. Echavarria M, Maldonado D, Elbert G, Videla C, Rappaport R, Carballal G. Use of PCR to demonstrate presence of adenovirus species B, C, or F as well as coinfection with two adenovirus species in children with flu-like symptoms. J Clin Microbiol. 2006;44:625–7. https://doi.org/10.1128/JCM.44.2.625-627.2006
23. Servellita V, Sotomayor Gonzalez A, Lamson DM, Foresythe A, Huh HJ, Bazinet AL, et al.; Pediatric Hepatitis of Unknown Etiology Working Group. Adeno-associated virus type 2 in US children with acute severe hepatitis. Nature. 2023;617:574–80. https://doi.org/10.1038/s41586-023-05949-1
24. Ho A, Orton R, Tayler R, Asamaphan P, Herder V, Davis C, et al.; DIAMONDS Consortium; ISARIC4C Investigators. Adeno-associated virus 2 infection in children with non-A–E hepatitis. Nature. 2023;617:555–63. https://doi.org/10.1038/s41586-023-05948-2

Address for correspondence: Olivia Almendares, Centers for Disease Control and Prevention, 1600 Clifton Rd NE, Mailstop H24-9, Atlanta, GA 30329-4018, USA; email: ncirddvdgast@cdc.gov

Crimean-Congo Hemorrhagic Fever Virus Diversity and Reassortment, Pakistan, 2017–2020

Massab Umair,[1] Zaira Rehman,[1] Shannon Whitmer, Melissa Mobley, Ammad Fahim, Aamer Ikram, Muhammad Salman, Joel M. Montgomery, John D. Klena

Sporadic cases and outbreaks of Crimean-Congo hemorrhagic fever (CCHF) have been documented across Pakistan since 1976; however, data regarding the diversity of CCHF virus (CCHFV) in Pakistan is sparse. We whole-genome sequenced 36 CCHFV samples collected from persons infected in Pakistan during 2017–2020. Most CCHF cases were from Rawalpindi (n = 10), followed by Peshawar (n = 7) and Islamabad (n = 4). Phylogenetic analysis revealed the Asia-1 genotype was dominant, but 4 reassorted strains were identified. Strains with reassorted medium gene segments clustered with Asia-2 (n = 2) and Africa-2 (n = 1) genotypes; small segment reassortments clustered with the Asia-2 genotype (n = 2). Reassorted viruses showed close identity with isolates from India, Iran, and Tajikistan, suggesting potential crossborder movement of CCHFV. Improved and continuous human, tick, and animal surveillance is needed to define the diversity of circulating CCHFV strains in Pakistan and prevent transmission.

Crimean-Congo hemorrhagic fever (CCHF) is a tickborne hemorrhagic disease caused by CCHF virus (CCHFV) and has a 30% fatality rate (*1*). CCHF was initially reported in 1940 in Crimea; identical disease manifestations were reported in the Democratic Republic of the Congo during the late 1960s (*2*,*3*). The virus comprises a tripartite RNA genome with large (L), medium (M), and small (S) segments and noncoding regions at the 5′ and 3′ termini. The coding regions are critical for virus polymerase activity, transcription, replication, and packaging. The L segment encodes an RNA-dependent RNA polymerase, the M segment encodes a glycoprotein precursor, and the S segments encode a nucleocapsid protein (*4*). The primary vectors for CCHFV transmission are *Hyalomma* ticks; domestic ruminant livestock and wild animals are amplifying hosts (*5*).

CCHF is considered a serious global public health threat because of its widespread geographic distribution in Asia, Africa, Europe, and the Middle East and because no reliable treatment options or vaccines are available. Increased CCHF incidence has been observed in some CCHF-endemic regions in Asia over the past decade (*6*). In Africa, southern and eastern Europe, the Middle East, India, and Asia, ≈10,000–15,000 CCHFV infections occur each year. Most infections are subclinical or unrecognized sporadic cases or epidemics in CCHF-endemic regions; however, subclinical infections are frequently not reported and are thought to be a source of disease transmission (*7*). Hospital-acquired infections are another transmission route and are typically symptomatic (*8*). Factors resulting in severe CCHFV infections are unknown, but polymorphisms in toll-like receptors 8, 9, and 10 of the innate immune system correlate with disease severity (*9*–*11*).

In Asia, Pakistan reports the fourth highest number of human CCHF cases, preceded by Turkey, Russia, and Iran (*12*). Pakistan witnessed its first CCHF outbreak in 1976; since then, consistent sporadic outbreaks have occurred (*13*). Livestock maintenance practices in rural regions of the country, as well as the nomadic lifestyle on the border of Pakistan and Afghanistan, have likely favored the spread of CCHFV via infected ticks. Cattle herd movement is unrestricted in the border areas of Pakistan, warranting careful surveillance measures. Analysis of virus phylogeny is crucial for identifying novel treatment

Author affiliations: National Institutes of Health Pakistan, Islamabad, Pakistan (M. Umair, Z. Rehman, A. Ikram, M. Salman); Centers for Disease Control and Prevention, Atlanta, Georgia, USA (S. Whitmer, M. Mobley, J.M. Montgomery, J.D. Klena); The Indus Hospital and Health Networks, Karachi, Pakistan (A. Fahim)

DOI: https://doi.org/10.3201/eid3004.231155

[1]These authors contributed equally to this article.

options and new vaccines and determining the broad extent of CCHFV genetic recombination and reassortment (*14*,*15*). We conducted phylogenetic analyses of whole-genome sequences of CCHFV isolated from patients in Pakistan and evaluated the genomic diversity of circulating CCHFV.

Material and Methods

The National Institutes of Health Pakistan (NIHP) in Islamabad collected CCHFV samples from suspected CCHF cases across the country that were sent for confirmation. During January 2017–December 2020, a total of 795 samples (289 samples in 2017, 224 in 2018, 280 in 2019, and 2 in 2020) from suspected CCHFV cases were tested at NIHP. Virus RNA was extracted from blood samples by using the QIAamp Viral RNA Mini Kit (QIAGEN, https://www.qiagen.com), and real-time PCR was performed by using a RealStar CCHFV RT-PCR Kit (altona Diagnostics, https://www.altona-diagnostics.com) according to manufacturers' instructions. We selected a subset of CCHFV-positive samples that had a cycle threshold (Ct) <26 for whole-genome sequencing. The study was approved by the NIHP Institutional Review Board.

Whole-Genome Sequencing of CCHFV

We treated extracted RNA with RNase-free DNase (Roche, https://www.roche.com) and prepared next-generation sequencing libraries by using a TruSeq RNA Access Library Prep Kit (Illumina, https://www.illumina.com) with CCHFV-specific enrichment oligonucleotides for samples that had Cts >26 or for samples that yielded a partial genome without CCHFV enrichment. For all other samples, we prepared libraries using the NEBNext Ultra II Directional RNA Library Prep Kit (New England Biolabs, https://www.neb.com). We sequenced libraries by using either an Illumina MiSeq or MiniSeq (high output 2 × 150 cycles) instrument. We de novo assembled CCHFV genomes by using SPAdes version 3.14.0 (parameter -k auto; https://github.com/ablab/spades). To improve genome coverage, we analyzed contigs by using BLAST (https://blast.ncbi.nlm.nih.gov) to identify the most closely related reference sequences. We mapped reads 3 times to the most closely related CCHFV genomes by using in-house scripts consisting of quality trimming (parameters: printseq-lite -min_qual_mean 25 -trim_qual_right 20 -min_len 50), read mapping (bwa-mem2 software, https://github.com/bwa-mem2), and PCR deduplication (Picard MarkDuplicates, http://picard.sourceforge.net). We called consensus genomes by using Geneious version 10 (https://www.geneious.com) (threshold = 0%, assign quality = total, minimum coverage >2). We inferred evolutionary history by using all available full-length CCHFV genomes from GenBank and RAxML software (https://github.com/amkozlov/raxml-ng) (parameters for tree generation: -m GTRGAMMA -p $RANDOM -f a -x $RANDOM -N 1000); bootstrap support was provided by 1,000 replicates. We deposited CCHFV genomes from this study into GenBank (accession nos. OM162027–130).

Phylogenetic Analysis

We downloaded reference genomes of all known CCHFV genotypes from GenBank. We conducted BLAST searches of the complete S, M, and L segment sequences and downloaded closely related sequences from GenBank. We performed multiple sequence alignment by using MAFFT (https://mafft.cbrc.jp) and maximum-likelihood analyses for each segment by using IQ-TREE (http://www.iqtree.org) with 1,000 bootstrap replicates. We visualized and annotated the phylogenetic tree by using FigTree v1.4.4 (https://github.com/rambaut/figtree/releases).

Results

During 2017–2020, a total of 795 samples were referred to NIHP for CCHFV laboratory diagnosis; 75 samples were CCHFV positive by using quantitative reverse transcription PCR (25 samples collected in 2017, 20 in 2018, 28 in 2019, and 2 in 2020). A Ct <26 was observed in 36 (47%) of those samples, which were then successfully sequenced. The sequenced samples were collected from patients residing in 14 districts; most (n = 21) resided in Punjab Province, followed by Khyber Pakhtunkhwa Province (n = 8), Islamabad (n = 4), and Sindh Province (n = 3) (Figure 1). Demographic and clinical data for 34 (94%) cases were available; 22 (82%) case-patients were male and 6 (18%) female. The mean age of CCHF patients was 35 (SD ±15; range 5–60) years (Figure 2). The most common clinical signs and symptoms were fever (34/34 [100%]), hemorrhage (22/34 [65%]) and myalgia (14/34 [41%]). Among hemorrhagic patients, most had hematemesis (9/22 [41%]), followed by gum bleeding (06/22 [27%]), melena (4/22 [18%]), hematuria (2/22 [9%]), and vaginal bleeding (1/22 [5%]). Of the 34 CCHF cases, 12 patients died (35% case-fatality rate) (Table 1).

Among the 36 sequenced CCHFV samples, we obtained complete sequences for all S segments, 35 L segments, and 33 M segments. Phylogenetic analysis of all 3 segments indicated the Asia-1 genotype (n = 29/33) was dominant. Moreover, we detected reassortment in 4 samples (Table 2). When phylogenetic

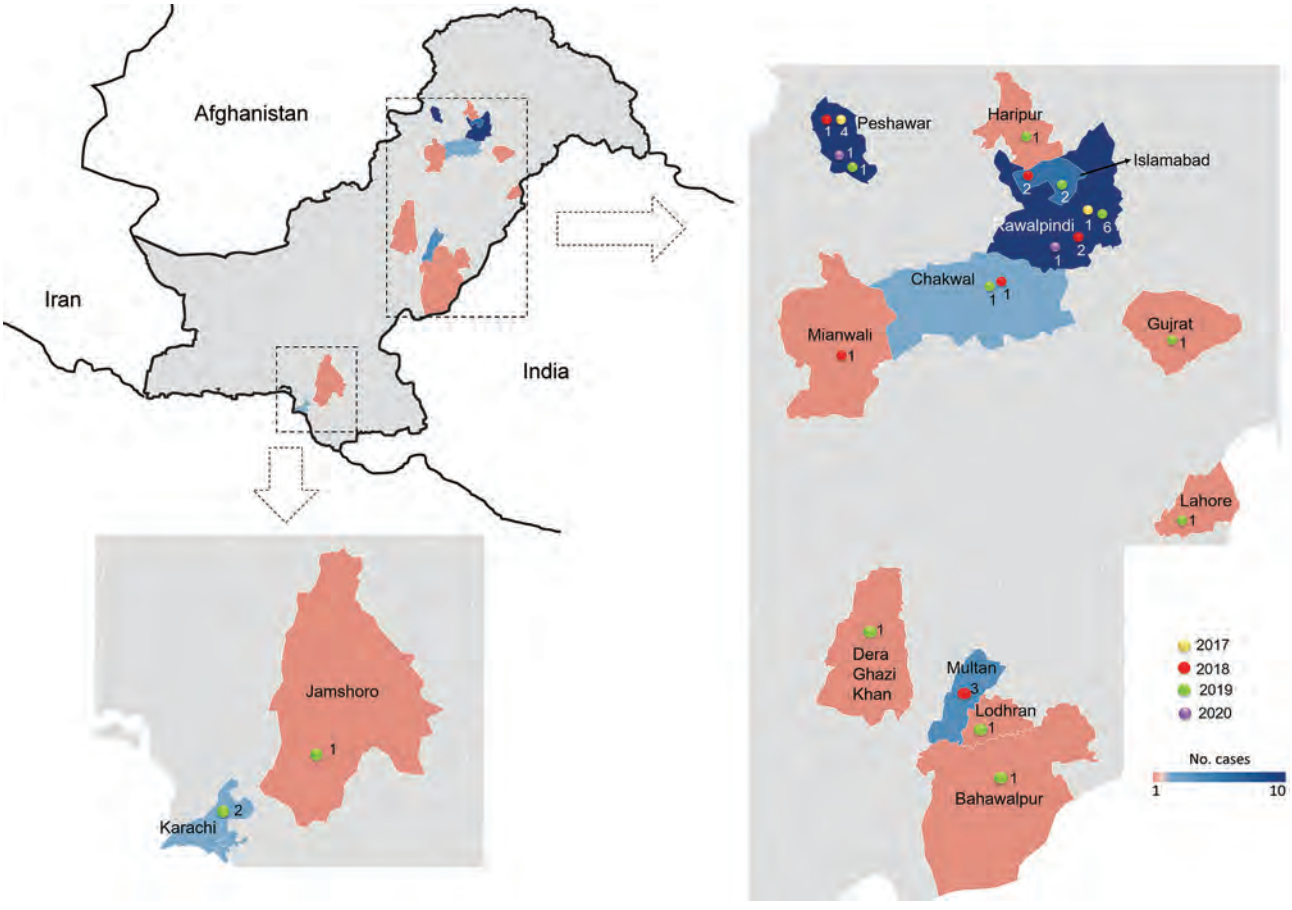

Figure 1. Locations of Crimean-Congo hemorrhagic fever cases in study of virus diversity and reassortment, Pakistan, 2017–2020. Main maps indicate the 2 regions in Pakistan with positive cases. Shading indicates provinces that had 1–10 cases. Inset map shows Pakistan and borders with Afghanistan, India, and Iran.

analysis of individual genomic segments included additional samples, a similar picture emerged. Analysis of S segments revealed that most (n = 33) CCHFV sequences from this study clustered into the Asia-1 genetic lineage along with strains previously reported from humans (GenBank accession nos. AJ538198 [in 2000] and AF527810 [in 1976]) and ticks (accession nos. MN135942 [in 2017] and KY484037 [in 1965]) in Pakistan and other regional countries, such as Iran, India, Afghanistan, China, Oman, and United Arab Emirates. Three sequences clustered with the Asia-2 genotype, along with strains from India, Tajikistan, Uzbekistan, Turkmenistan, and China (Figure 3). The M segment sequences showed the greatest diversity with most samples clustering into the Asia-1 lineage along with strains from India (2015–2016), Iran (2007 and 2017), Afghanistan (2009), United Arab Emirates (1995 and 1998), and Pakistan (2004 and 2017)

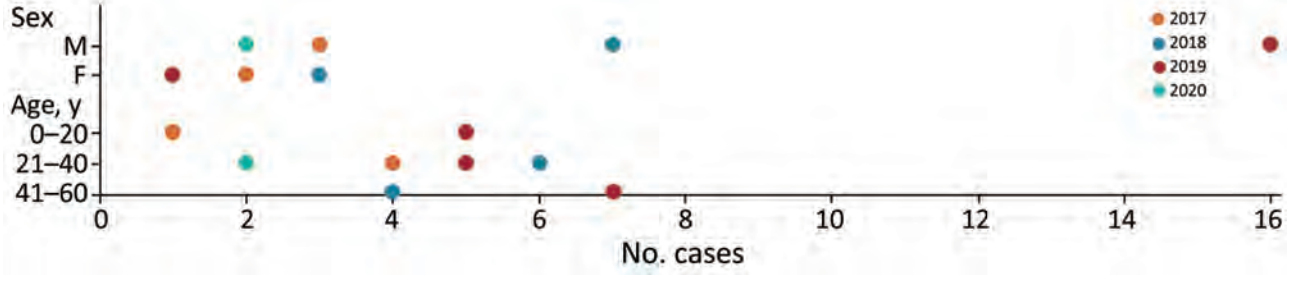

Figure 2. Sex and age distribution of patients with Crimean-Congo hemorrhagic fever in study of virus diversity and reassortment, Pakistan, 2017–2020. Colored dots indicate the number of Crimean-Congo hemorrhagic fever cases each year according to patient sex and age groups.

Table 1. Characteristics of confirmed cases of Crimean-Congo hemorrhagic fever in Pakistan, 2017–2020

Characteristics	No. (%) cases			
	2017, n = 5	2018, n = 10	2019, n = 17	2020, n = 2
Clinical signs				
Fever	5 (100)	10 (100)	17 (100)	2 (100)
Hemorrhage	4 (80)	6 (60)	11 (65)	1 (50)
Myalgia	3 (60)	4 (40)	7 (41)	0
Nausea	0	2 (20)	3 (18)	0
Vomiting	0	2 (20)	3 (18)	1 (50)
Headache	0	2 (20)	2 (12)	0
Hemorrhage types				
Melena	1 (20)	1 (10)	1 (6)	1 (50)
Gum bleeding	1 (20)	1 (10)	4 (24)	0
Hematemesis	2 (40)	2 (20)	5 (29)	0
Hematuria	0	1 (10)	1 (6)	0
Vaginal bleeding	0	1 (10)	0	0
Patient outcome				
Survived	4 (80)	8 (80)	9 (53)	1 (50)
Died	1 (20)	2 (20)	8 (47)	1 (50)

(Figure 4). The 2 Asia-2 isolates grouped with strains from China, Oman, and the Matin strain from Pakistan (GenBank accession no. AF467769). An M segment sequence from Rawalpindi (Gujrat state) in 2019 clustered with the Africa-2 lineage along with viruses reported from India during 2016–2019 (accession nos. MN866218, MH396665, and MN930411) (Figure 4). Phylogenetic reconstructions of the L segment revealed clustering with the Asia-1 lineage; closest matches were from India (2015–2019), Iran, China, Oman, Afghanistan, and previously reported strains from Pakistan isolated from ticks (accession nos. MN135944 [in 2017] and KY484039 [in 1965]) and a human (accession no. AY422208 [in 1976]) (Figure 5). According to analyses of L segments, all CCHFVs from this study shared 98%–100% identity at the nucleotide and amino acid levels.

The L and S segments from the Africa-2 isolate from Pakistan in this study (NIH-PAK-CCHF-233_2019) belonged to the Asia-1 lineage, suggesting reassortment. In addition, 3 other isolates showed reassortment. The S and M segments of NIH-PAK-CCHF-84_2018 clustered with the Asia-2 genotype, and the L segment clustered with Asia-1. The L and M segments of NIH-PAK-CCHF-43_2018 had Asia-1 genotypes, whereas the S segment had an Asia-2 genotype. Similarly, the S and L segments of NIH-PAK-CCHF-20_2019 had Asia-1 genotypes, and the M segment clustered with the Asia-2 genotype.

Discussion

CCHF is endemic in Pakistan, and data reported since 2010 indicate an increase in human CCHF cases. The first human CCHF case was reported in 1976, and several sporadic outbreaks have been reported since then from different parts of the country (*13*,*16*). Human CCHF-positive case counts have increased during 2011–2020; a total of 605 confirmed CCHF cases have been reported (*17*–*19*). The increase in cases can be attributed to multiple factors, including the country's underdeveloped healthcare system that has insufficiently trained healthcare professionals and lacks equipment to manage CCHF, as well as an insufficient number of healthcare facilities that offer CCHF management. Furthermore, the general public is relatively uninformed about CCHFV vector control and risks for transmission to healthy persons while handling livestock and conducting animal husbandry. CCHFV transmission risk becomes higher in urban areas during the Eid ul Azha festival, which includes ritual animal slaughter.

The porous border between Pakistan and Afghanistan has large refugee and nomadic tribal movements, often accompanied by their cattle, across Balochistan Province and Khyber Pakhtunkhwa Province, which also contribute to CCHFV transmission; Afghanistan is also a CCHF-endemic country (*20*). According to the NIHP, 296 cases of CCHF were reported during 2015–2020; most infections were from Balochistan Province (39%), then Punjab (24%), Khyber Pakhtunkhwa (14%), Sindh (12%), and Islamabad (5%) (*18*). Balochistan and Punjab Provinces contributed most of the CCHF cases. Khyber Pakhtunkhwa and Balochistan Provinces border CCHF-endemic countries; Khyber Pakhtunkhwa Province shares a border with Afghanistan, and Balochistan Province shares a border with Iran, where livestock movement takes place routinely and, thus, potentially contributes to reported CCHF case numbers (*13*,*21*). Animal surveillance studies from Pakistan have reported CCHFV from all over Pakistan but primarily from the Balochistan region. Less CCHFV cases have been reported from Punjab Province, although it harbors the largest animal population because of greater

agricultural land mass (*13*,*22*,*23*), which could potentially favor the tick–vertebrate–tick life cycle.

Hyalomma and *Rhipicephalus* spp. (Ixodidae family) ticks, reported as the most prevalent tick species in southern, western, and northern Punjab (*24*,*25*), are the main spreaders of CCHFV in different regions of Pakistan and increase the risk for CCHF outbreaks. Regions of upper Punjab, such as Chakwal, Mianwali, Rawalpindi and Attock, have >20% prevalence of ticks with CCHFV, compared with the lower Punjab regions of Rajanpur and Lahore, which have <10% prevalence. *Hyalomma* and *Rhipicephalus* ticks infesting livestock have been reported from Balochistan Province, where the district of Kalat has the largest percentage of CCHFV-positive ticks (60%), followed by Quetta (30%) and Qilla Abdullah (10%). The semiarid climate comprising shrub rangelands in Balochistan Province appears to favor tick growth (*13*,*23*). Furthermore, Punjab Province, particularly in the upper region, has large rangelands for animal grazing, a semiarid climate with high precipitation, and abundant livestock, which also provide a thriving tick habitat and can subsequently increase CCHFV prevalence (*26*). Previous studies have reported high CCHFV IgG seroprevalence in humans from Upper Punjab (*27*,*28*), which suggests effective control measures are especially needed in this area to inhibit tick infestation of livestock and prevent CCHF outbreaks.

Table 2. Genotypes of Crimean-Congo hemorrhagic fever viruses isolated from patients in Pakistan, 2017–2020*

Sample nos.	Strain name	District	Province/region	Collection date	Genotype			GenBank accession nos.
					L	M	S	
1	NIH-PAK-CCHF-257_2017	Peshawar	Khyber Pakhtunkhwa	2017	Asia-1	Asia-1	Asia-1	OM162030–2
2	NIH-PAK-CCHF-272_2017	Peshawar	Khyber Pakhtunkhwa	2017	Asia-1	Asia-1	Asia-1	OM162033–5
3	NIH-PAK-CCHF-273_2017	Peshawar	Khyber Pakhtunkhwa	2017	Asia-1	Asia-1	Asia-1	OM162036–8
4	NIH-PAK-CCHF-274_2017	Peshawar	Khyber Pakhtunkhwa	2017	Asia-1	Asia-1	Asia-1	OM162039–41
5	NIH-PAK-CCHF-275_2017	Rawalpindi	Punjab	2017	Asia-1	Asia-1	Asia-1	OM162042–4
6	NIH-PAK-CCHF-104_2018	Khyber Agency	Khyber Pakhtunkhwa	2018	Asia-1	Asia-1	Asia-1	OM162096–8
7	NIH-PAK-CCHF-86_2018	Rawalpindi	Punjab	2018	Asia-1	Asia-1	Asia-1	OM162099–101
8	NIH-PAK-CCHF-84_2018	Islamabad	Islamabad	2018	Asia-1	Asia-2	Asia-2	OM162102–4
9	NIH-PAK-CCHF-119_2018	Islamabad	Islamabad	2018	Asia-1	Asia-1	Asia-1	OM162105–7
10	NIH-PAK-CCHF-65_2018	Multan	Punjab	2018	Asia-1	Asia-1	Asia-1	OM162108–10
11	NIH-PAK-CCHF-73_2018	Multan	Punjab	2018	Asia-1	NA	Asia-1	OM162111–2
12	NIH-PAK-CCHF-56_2018	Chakwal	Punjab	2018	Asia-1	Asia-1	Asia-1	OM162113–5
13	NIH-PAK-CCHF-43_2018	Rawalpindi	Punjab	2018	Asia-1	Asia-1	Asia-2	OM162116–8
14	NIH-PAK-CCHF-44_2018	Mianwali	Punjab	2018	Asia-1	Asia-1	Asia-1	OM162119–21
15	NIH-PAK-CCHF-19_2018	Multan	Punjab	2018	Asia-1	Asia-1	Asia-1	OM162122–4
16	NIH-PAK-CCHF-18_2019	Rawalpindi	Punjab	2019	Asia-1	Asia-1	Asia-1	OM162027–9
17	NIH-PAK-CCHF-20_2019	Jamshoro	Sindh	2019	Asia-1	Asia-2	Asia-1	OM162045–7
18	NIH-PAK-CCHF-27_2019	Lodhran	Punjab	2019	Asia-1	Asia-1	Asia-1	OM162048–50
19	NIH-PAK-CCHF-28_2019	DG Khan	Punjab	2019	Asia-1	Asia-1	Asia-1	OM162051–3
20	NIH-PAK-CCHF-80_2019	Rawalpindi	Punjab	2019	Asia-1	Asia-1	Asia-1	OM162054–6
21	NIH-PAK-CCHF-61_2019	Peshawar	Khyber Pakhtunkhwa	2019	Asia-1	Asia-1	Asia-1	OM162057–9
22	NIH-PAK-CCHF-65_2019	Gujrat	Punjab	2019	Asia-1	Asia-1	Asia-1	OM162060–2
23	NIH-PAK-CCHF-97_2019	Karachi	Sindh	2019	Asia-1	Asia-1	Asia-1	OM162063–5
24	NIH-PAK-CCHF-86_2019	Rawalpindi	Punjab	2019	Asia-1	Asia-1	Asia-1	OM162066–8
25	NIH-PAK-CCHF-95_2019	Lahore	Punjab	2019	Asia-1	Asia-1	Asia-1	OM162069–71
26	NIH-PAK-CCHF-156_2019	Chakwal	Punjab	2019	Asia-1	Asia-1	Asia-1	OM162072–4
27	NIH-PAK-CCHF-92_2019	DG Khan	Punjab	2019	NA	NA	Asia-1	OM162075
28	NIH-PAK-CCHF-159_2019	Bahawalpur	Punjab	2019	Asia-1	Asia-1	Asia-1	OM162076–8
29	NIH-PAK-CCHF-168_2019	Islamabad	Islamabad	2019	Asia-1	Asia-1	Asia-1	OM162079–81
30	NIH-PAK-CCHF-190_2019	Haripur	Khyber Pakhtunkhwa	2019	Asia-1	Asia-1	Asia-1	OM162082–4
31	NIH-PAK-CCHF-222_2019	Rawalpindi	Punjab	2019	Asia-1	Asia-1	Asia-1	OM162085–7
32	NIH-PAK-CCHF-233_2019	Rawalpindi	Punjab	2019	Asia-1	Africa-2	Asia-1	OM162088–90
33	NIH-PAK-CCHF-279_2019	Islamabad	Islamabad	2019	Asia-1	NA	Asia-2	OM162091–2
34	NIH-PAK-CCHF-14_2019	Karachi	Sindh	2019	Asia-1	Asia-1	Asia-1	OM162093–5
35	NIH-PAK-CCHF-509_2020	Rawalpindi	Punjab	2020	Asia-1	Asia-1	Asia-1	OM162125–7
36	NIH-PAK-CCHF-510_2020	Peshawar	Khyber Pakhtunkhwa	2020	Asia-1	Asia-1	Asia-1	OM162128–30

*Genotypes were determined by whole-genome sequencing of L, M, and S virus segments. L, large; M, medium; NA, not applicable; S, small.

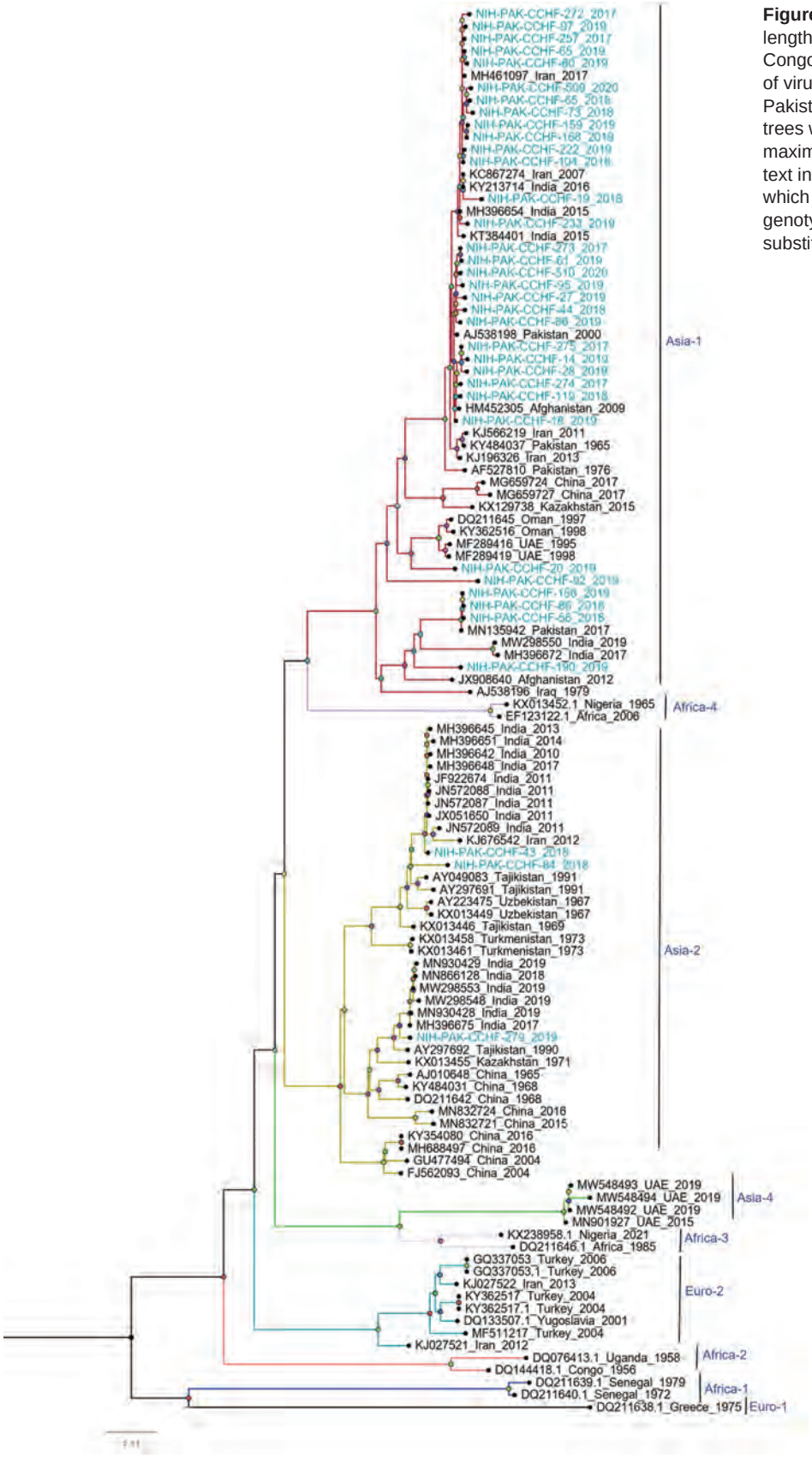

Figure 3. Phylogenetic analysis of full-length small gene segments of Crimean-Congo hemorrhagic fever virus in study of virus diversity and reassortment, Pakistan, 2017–2020. Midpoint-rooted trees were generated by using the maximum-likelihood method. Blue-green text indicates sequences from this study, which clustered with the Asia-1 and Asia-2 genotypes. Scale bar indicates nucleotide substitutions per site.

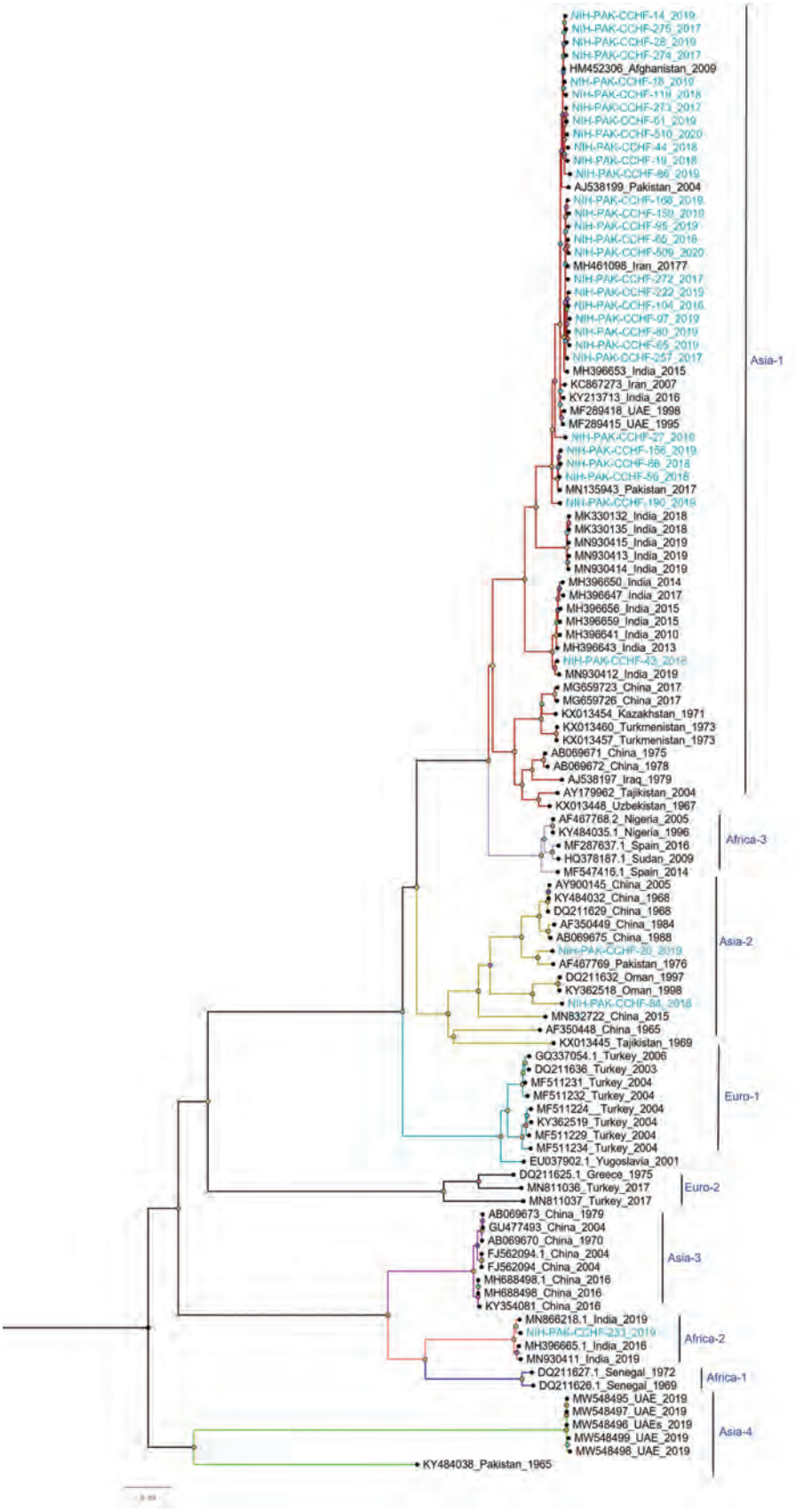

Figure 4. Phylogenetic analysis of full-length medium gene segments of Crimean-Congo hemorrhagic fever virus in study of virus diversity and reassortment, Pakistan, 2017–2020. Midpoint-rooted trees were generated by using the maximum-likelihood method. Blue-green text indicates sequences from this study. Most M segments from Pakistan clustered with the Asia-1 genotype/clade, but 3 reassorted sequences clustered with the Asia-2 clade, and 1 reassorted sequence clustered with the Africa-2 clade. Scale bar indicates nucleotide substitutions per site.

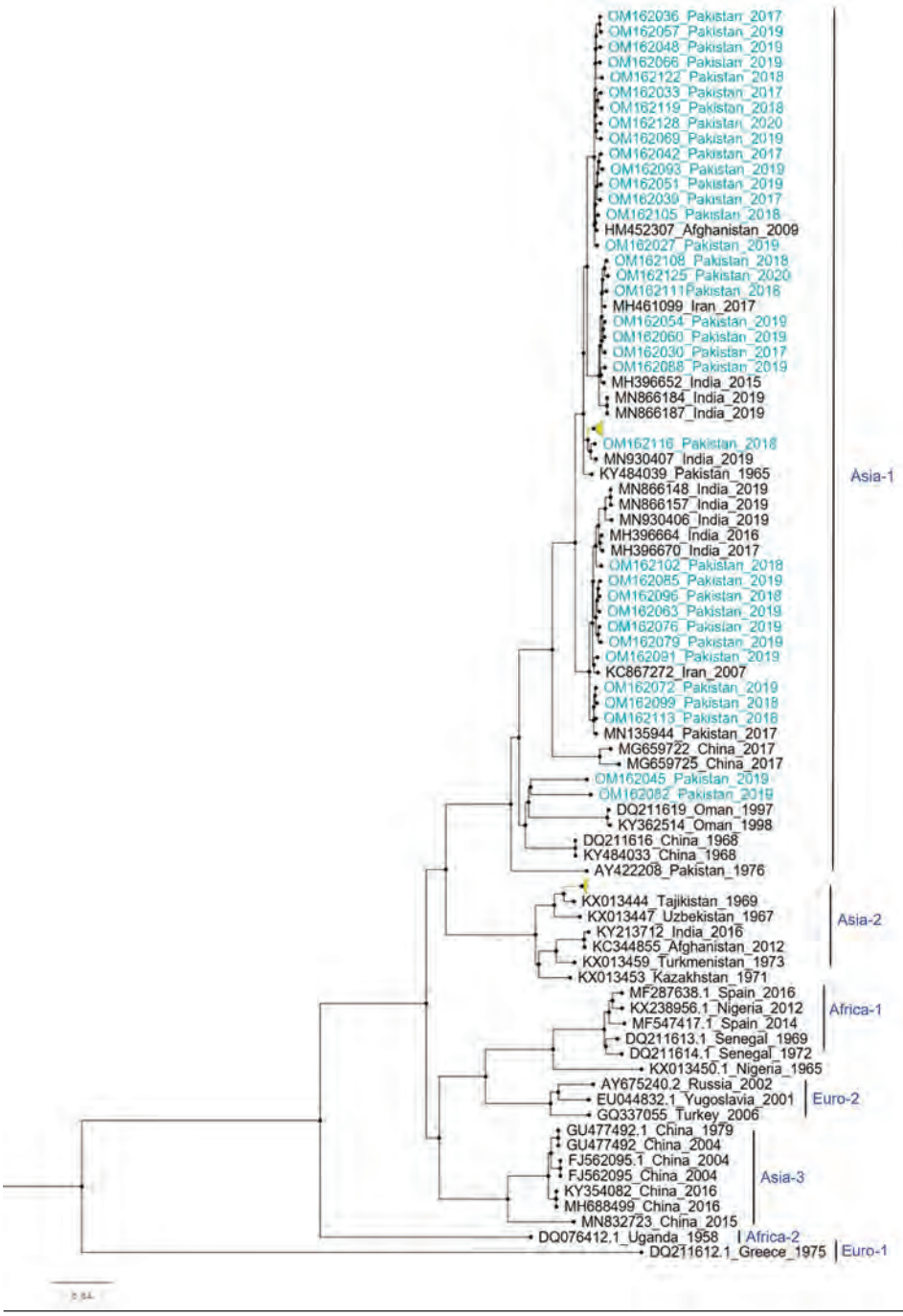

Figure 5. Phylogenetic analysis of full-length large gene segments of Crimean-Congo hemorrhagic fever virus in study of virus diversity and reassortment, Pakistan, 2017–2020. Midpoint-rooted trees were generated by using the maximum-likelihood method. Blue-green font indicates sequences from this study, which clustered only with the Asia-1 genotype. Scale bar indicates nucleotide substitutions per site.

The lack of next-generation sequencing capabilities in Pakistan has been a major limitation for determining the genomic diversity of circulating CCHFV. Previously, partial sequencing of the S gene segment was used for classification and phylogenetic analysis of CCHFV (*13*,*16*,*29*–*31*). Because the S segment is conserved and relatively short compared with L and M segments, it was used as a surrogate for performing phylogenetic analysis. Evidence of reassortment (*31*–*34*) among CCHFV genomes confirmed the need for whole-genome or partial sequencing of all 3 gene segments (*35*). CCHFV samples collected from infected patients intermittently during 1965, 1976, and 2000–2002 in Pakistan showed the prevalence of the Asia-1 genotype and phylogenetic association with viruses from the neighboring countries of Iran, Afghanistan, and United Arab Emirates (*31*). During 2008–2011, the Asia-1 genotype was the most prevalent lineage circulating in the southwest region of Pakistan, specifically Balochistan Province, which

borders the CCHF-endemic countries of Iran and Afghanistan (*13*,*17*). Moreover, in 2008, a single case of Asia-2 genotype was also reported from Quetta in Balochistan Province, which was phylogenetically related to viruses from Uzbekistan, Tajikistan, and Kazakhstan (*29*). According to S segment sequencing, another study on CCHFV in Pakistan during 2019 involved 14 districts and further corroborated the endemicity of the Asia-1 genotype (*30*). In this study, most (80.5%, n = 29) CCHFVs circulating in Pakistan clustered with the Asia-1 (S, M, and L segments) clade alongside strains from neighboring (Iran, India, Afghanistan, and China) and regional (Oman and United Arab Emirates) countries, indicating CCHFV transmission between those countries. Circulation of genetically similar CCHFV strains has been reported in Iran, where frequent animal trade has been hypothesized to cause CCHFV movement between Pakistan and neighboring countries (*13*,*36*–*39*).

In this study, we observed 4 (11%) reassortment events among the 36 whole-genome sequences. Although frequent reassortment events have been reported in the M segment, rendering high virus fitness, we observed reassortment in the S segment as well. The Matin strain isolated from Pakistan has been a good example of CCHFV reassortment events in this region (*15*). Segmental reassortment in RNA viruses has been associated with emergence of pandemic virus strains and antigenic shifts (*33*). The Africa-2 reassorted virus (NIH-PAK-CCHF-233_2019) shared a common clade with sequences from India isolated from pooled tick specimens. Two of the sequences from India (GenBank accession nos. MN866218 and MN930411) were isolated from ticks from Rajasthan and Gujarat state in 2019, showing 98% homology at the nucleotide and amino acid levels with the Africa-2 isolate from Pakistan. Rajasthan state in India shares a border with Punjab and Sindh Provinces of Pakistan, but Gujarat state is more centrally located and does not share a border with Pakistan. M segments of the Asia-2 genotype also clustered with sequences isolated from ticks from China (GenBank accession no. MN832722.1). In China, the virus has been isolated from *Hyalomma asiaticum* ticks. However, in Pakistan, Iran, Turkmenistan, and Tajikistan, *H. anatolicum* is the main CCHFV vector (*40*). Furthermore, both *H. anatolicum* and *Rhipicephalus* ticks have been reported as the primary vectors of CCHFV in Pakistan and Iran (*41*). Because of the diversity of ticks in different regions, further investigation of CCHFV prevalence in various tick species in Pakistan is needed.

Surveillance of CCHFV reassortment, although difficult, is crucial for health authorities. Whether reassortments can be linked to increased virus pathogenicity or disease severity requires further study. Variations in antigenicity among CCHFV isolates have not been reported but need to be considered for future vaccines (*32*). Rapid diagnostics for identifying and managing outbreaks are pivotal; however, considering the evolutionary dynamics of CCHFV strains, immunological assays should be used in conjunction with PCR to achieve high diagnostic sensitivity. A concurrent need exists for better understanding of CCHFV antibody kinetics in clinically diverse samples, and next-generation sequencing can help identify mutant viruses.

In conclusion, we identified CCHFV sequences with verifiable genomic reassortments and highlight the importance of sequencing all 3 virus segments. Our results suggest diversification of circulating strains of CCHFV in Pakistan and warrant rigorous surveillance and follow-up of CCHF cases, particularly in disease-endemic regions of the country. The CCHFV Asia-1 genotype has been prevalent in Pakistan, but the Africa-2 genotype might also be emerging. CCHFV sequences from this study are from humans; however, sequences from other host vertebrates, particularly from ticks, will also be required to identify CCHFV mutations and evolutionary dynamics in different regions of the world. Because CCHFV reassortment is a continual evolutionary phenomenon, which can genetically shift virus genomes enhancing pathogenicity, careful application of routine and effective control measures that reduce overall tick abundance in the environment can likely bring substantial reduction in risk for CCHFV transmission to humans. Furthermore, genomic surveillance of CCHFV is needed to identify the major circulating genotypes in Pakistan and elsewhere, which will further aid in containment of disease.

About the Author

Dr. Umair is a senior scientific officer and head of the virology department at the National Institute of Health, Islamabad, Pakistan. His primary research focuses on emerging and reemerging virus infections.

References

1. Whitehouse CA. Crimean-Congo hemorrhagic fever. Antiviral Res. 2004;64:145–60. https://doi.org/10.1016/j.antiviral.2004.08.001
2. Hoogstraal H. The epidemiology of tick-borne Crimean-Congo hemorrhagic fever in Asia, Europe, and Africa. J Med Entomol. 1979;15:307–417. https://doi.org/10.1093/jmedent/15.4.307
3. Casals J. Antigenic similarity between the virus causing Crimean hemorrhagic fever and Congo virus. Proc Soc Exp

Biol Med. 1969;131:233–6. https://doi.org/10.3181/00379727-131-33847
4. Zivcec M, Scholte FEM, Spiropoulou CF, Spengler JR, Bergeron É. Molecular insights into Crimean-Congo hemorrhagic fever virus. Viruses. 2016;8:106. https://doi.org/10.3390/v8040106
5. Gargili A, Estrada-Peña A, Spengler JR, Lukashev A, Nuttall PA, Bente DA. The role of ticks in the maintenance and transmission of Crimean-Congo hemorrhagic fever virus: a review of published field and laboratory studies. Antiviral Res. 2017;144:93–119. https://doi.org/10.1016/j.antiviral.2017.05.010
6. Estrada-Peña A, Vatansever Z, Gargili A, Ergönul O. The trend towards habitat fragmentation is the key factor driving the spread of Crimean-Congo haemorrhagic fever. Epidemiol Infect. 2010;138:1194–203. https://doi.org/10.1017/S0950268809991026
7. Hawman DW, Feldmann H. Recent advances in understanding Crimean-Congo hemorrhagic fever virus. F1000Res. 2018;7:1715. https://doi.org/10.12688/f1000research.16189.1
8. Tsergouli K, Karampatakis T, Haidich AB, Metallidis S, Papa A. Nosocomial infections caused by Crimean-Congo haemorrhagic fever virus. J Hosp Infect. 2020;105:43–52. https://doi.org/10.1016/j.jhin.2019.12.001
9. Arslan S, Engin A, Özbilüm N, Bakır M. Toll-like receptor 7 Gln11Leu, c.4-151A/G, and +1817G/T polymorphisms in Crimean Congo hemorrhagic fever. J Med Virol. 2015;87:1090–5. https://doi.org/10.1002/jmv.24174
10. Engin A, Arslan S, Kizildag S, Oztürk H, Elaldi N, Dökmetas I, et al. Toll-like receptor 8 and 9 polymorphisms in Crimean-Congo hemorrhagic fever. Microbes Infect. 2010;12:1071–8. https://doi.org/10.1016/j.micinf.2010.07.012
11. Kızıldağ S, Arslan S, Özbilüm N, Engin A, Bakır M. Effect of TLR10 (2322A/G, 720A/C, and 992T/A) polymorphisms on the pathogenesis of Crimean Congo hemorrhagic fever disease. J Med Virol. 2018;90:19–25. https://doi.org/10.1002/jmv.24924
12. Ince Y, Yasa C, Metin M, Sonmez M, Meram E, Benkli B, et al. Crimean-Congo hemorrhagic fever infections reported by ProMED. Int J Infect Dis. 2014;26:44–6. https://doi.org/10.1016/j.ijid.2014.04.005
13. Alam MM, Khurshid A, Sharif S, Shaukat S, Rana MS, Angez M, et al. Genetic analysis and epidemiology of Crimean Congo hemorrhagic fever viruses in Baluchistan province of Pakistan. BMC Infect Dis. 2013;13:201. https://doi.org/10.1186/1471-2334-13-201
14. Lukashev AN. Evidence for recombination in Crimean-Congo hemorrhagic fever virus. J Gen Virol. 2005;86:2333–8. https://doi.org/10.1099/vir.0.80974-0
15. Hewson R, Gmyl A, Gmyl L, Smirnova SE, Karganova G, Jamil B, et al. Evidence of segment reassortment in Crimean-Congo haemorrhagic fever virus. J Gen Virol. 2004;85:3059–70. https://doi.org/10.1099/vir.0.80121-0
16. Khurshid A, Hassan M, Alam MM, Aamir UB, Rehman L, Sharif S, et al. CCHF virus variants in Pakistan and Afghanistan: emerging diversity and epidemiology. J Clin Virol. 2015;67:25–30. https://doi.org/10.1016/j.jcv.2015.03.021
17. National Institute of Health, Pakistan. Seasonal awareness and alert letter, 36th issue, June–September 2016 [cited 2024 Feb 13]. https://www.nih.org.pk/wp-content/uploads/2018/03/Seasoanl-Awareness-and-Alert-Letter-SAAL-36th-Issue.pdf
18. National Institute of Health Pakistan. Seasonal awareness and alert letter. For epidemic-prone infectious diseases in Pakistan, 51st issue, June–September 2021 [cited 2024 Feb 13]. https://www.nih.org.pk/wp-content/uploads/2021/07/51st-Issue-SAAL-print-3.pdf
19. National Institute of Health Pakistan. Seasonal awareness and alert letter. For epidemic-prone infectious diseases in Pakistan, 48th issue, June–September 2020 [cited 2022 Mar 9]. https://www.nih.org.pk/wp-content/uploads/2020/07/48th-Issue-SAAL-final-for-Printing.pdf
20. Sahak MN, Arifi F, Saeedzai SA. Descriptive epidemiology of Crimean-Congo hemorrhagic fever (CCHF) in Afghanistan: reported cases to National Surveillance System, 2016–2018. Int J Infect Dis. 2019;88:135–40. https://doi.org/10.1016/j.ijid.2019.08.016
21. Tabassum S, Naeem A, Khan MZ, Mumtaz N, Gill S, Ohadi L. Crimean-Congo hemorrhagic fever outbreak in Pakistan, 2022: a warning bell amidst unprecedented floods and COVID 19 pandemic. Health Sci Rep. 2023;6:e1055. https://doi.org/10.1002/hsr2.1055
22. Abbas T, Younus M, Muhammad SA. Spatial cluster analysis of human cases of Crimean Congo hemorrhagic fever reported in Pakistan. Infect Dis Poverty. 2015;4:9. https://doi.org/10.1186/2049-9957-4-9
23. Kasi KK, von Arnim F, Schulz A, Rehman A, Chudhary A, Oneeb M, et al. Crimean-Congo haemorrhagic fever virus in ticks collected from livestock in Balochistan, Pakistan. Transbound Emerg Dis. 2020;67:1543–52. https://doi.org/10.1111/tbed.13488
24. Durrani AZ, Shakoori AR, Kamal N. Bionomics of *Hyalomma* ticks in three districts of Punjab, Pakistan. J Anim Plant Sci. 2008;18:17–23.
25. Alam MM, Khurshid A, Rana MS, Aamir UB, Salman M, Ahmad M. Surveillance of Crimean-Congo haemorrhagic fever in Pakistan. Lancet Infect Dis. 2017;17:806. https://doi.org/10.1016/S1473-3099(17)30403-6
26. Shahid MF, Yaqub T, Ali M, Ul-Rahman A, Bente DA. Prevalence and phylogenetic analysis of Crimean-Congo hemorrhagic fever virus in ticks collected from Punjab province of Pakistan. Acta Trop. 2021;218:105892. https://doi.org/10.1016/j.actatropica.2021.105892
27. Shahid MF, Shabbir MZ, Ashraf K, Ali M, Yaqub S, Mukhtar N, et al. Seroprevalence of Crimean-Congo haemorrhagic fever among three selected risk human groups in disease-endemic region of Pakistan. Zoonoses Public Health. 2020;67:755–9. https://doi.org/10.1111/zph.12704
28. Shahid MF, Shabbir MZ, Ashraf K, Ali M, Yaqub S, Ul-Rahman A, et al. Sero-epidemiological survey of Crimean-Congo hemorrhagic fever among the human population of the Punjab Province in Pakistan. Virol Sin. 2020;35:486–9. https://doi.org/10.1007/s12250-020-00195-5
29. Alam MM, Khurshid A, Sharif S, Shaukat S, Suleman RM, Angez M, et al. Crimean-Congo hemorrhagic fever Asia-2 genotype, Pakistan. Emerg Infect Dis. 2013;19:1017–9. https://doi.org/10.3201/eid1906.120771
30. Umair M, Khurshid A, Alam MM, Akhtar R, Salman M, Ikram A. Genetic diversity and phylogenetic analysis of Crimean-Congo hemorrhagic fever viruses circulating in Pakistan during 2019. PLoS Negl Trop Dis. 2020;14:e0008238. https://doi.org/10.1371/journal.pntd.0008238
31. Burt FJ, Swanepoel R. Molecular epidemiology of African and Asian Crimean-Congo haemorrhagic fever isolates. Epidemiol Infect. 2005;133:659–66. https://doi.org/10.1017/s0950268805003730
32. Burt FJ, Paweska JT, Ashkettle B, Swanepoel R. Genetic relationship in southern African Crimean-Congo haemorrhagic fever virus isolates: evidence for occurrence

of reassortment. Epidemiol Infect. 2009;137:1302–8. https://doi.org/10.1017/S0950268808001878
33. Deyde VM, Khristova ML, Rollin PE, Ksiazek TG, Nichol ST. Crimean-Congo hemorrhagic fever virus genomics and global diversity. J Virol. 2006;80:8834–42. https://doi.org/10.1128/JVI.00752-06
34. Grard G, Drexler JF, Fair J, Muyembe JJ, Wolfe ND, Drosten C, et al. Re-emergence of Crimean-Congo hemorrhagic fever virus in Central Africa. PLoS Negl Trop Dis. 2011;5:e1350. https://doi.org/10.1371/journal.pntd.0001350
35. Goedhals D, Bester PA, Paweska JT, Swanepoel R, Burt FJ. Next-generation sequencing of southern African Crimean-Congo haemorrhagic fever virus isolates reveals a high frequency of M segment reassortment. Epidemiol Infect. 2014;142:1952–62. https://doi.org/10.1017/S0950268814000818
36. Tahmasebi F, Ghiasi SM, Mostafavi E, Moradi M, Piazak N, Mozafari A, et al. Molecular epidemiology of Crimean-Congo hemorrhagic fever virus genome isolated from ticks of Hamadan province of Iran. J Vector Borne Dis. 2010;47:211–6.
37. Mild M, Simon M, Albert J, Mirazimi A. Towards an understanding of the migration of Crimean-Congo hemorrhagic fever virus. J Gen Virol. 2010;91:199–207. https://doi.org/10.1099/vir.0.014878-0
38. Chinikar S, Ghiasi SM, Hewson R, Moradi M, Haeri A. Crimean-Congo hemorrhagic fever in Iran and neighboring countries. J Clin Virol. 2010;47:110–4. https://doi.org/10.1016/j.jcv.2009.10.014
39. Al-Abri SS, Abaidani IA, Fazlalipour M, Mostafavi E, Leblebicioglu H, Pshenichnaya N, et al. Current status of Crimean-Congo haemorrhagic fever in the World Health Organization Eastern Mediterranean Region: issues, challenges, and future directions. Int J Infect Dis. 2017;58:82–9. https://doi.org/10.1016/j.ijid.2017.02.018
40. Papa A, Weber F, Hewson R, Weidmann M, Koksal I, Korukluoglu G, et al. Meeting report: First International Conference on Crimean-Congo hemorrhagic fever. Antiviral Res. 2015;120:57–65. https://doi.org/10.1016/j.antiviral.2015.05.005
41. Zohaib A, Saqib M, Athar MA, Hussain MH, Sial AU, Tayyab MH, et al. Crimean-Congo hemorrhagic fever virus in humans and livestock, Pakistan, 2015–2017. Emerg Infect Dis. 2020;26:773–7. https://doi.org/10.3201/eid2604.191154

Address for correspondence: Massab Umair, Department of Virology, National Institute of Health, 45500 Park Rd, Chak Shahzad, Islamabad, Pakistan; email: m.umair@nih.org.pk

etymologia revisited

Influenza

[in"floo-en'zə]

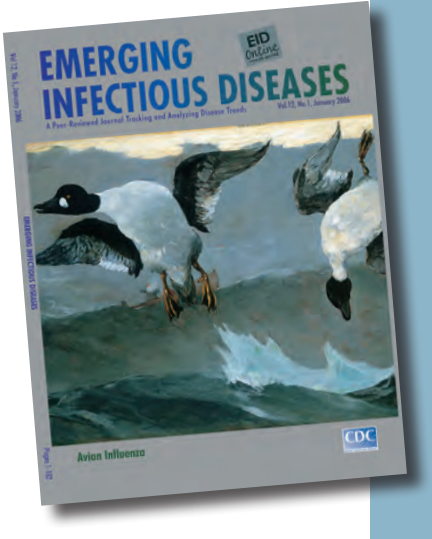

Originally published in January 2006

An acute viral infection of the respiratory tract. From Latin influentia,"to flow into"; in medieval times, intangible fluid given off by stars was believed to affect humans. The Italian influenza referred to any disease outbreak thought to be influenced by stars. In 1743, what Italians called an influenza di catarro ("epidemic of catarrh") spread across Europe, and the disease came to be known in English as simply "influenza."

Reference:

Dorland's illustrated medical dictionary. 30th ed. Philadelphia: Saunders; 2003 and Quinion M. World wide words. 1998 Jan 3 [cited 2005 Dec 5]. Available from http://www.worldwidewords.org/topicalwords/tw-inf1.htm

Clostridium butyricum Bacteremia Associated with Probiotic Use, Japan

Ryuichi Minoda Sada, Hiroo Matsuo, Daisuke Motooka, Satoshi Kutsuna, Shigeto Hamaguchi, Go Yamamoto, Akiko Ueda

Clostridium butyricum, a probiotic commonly prescribed in Asia, most notably as MIYA-BM (Miyarisan Pharmaceutical Co., Ltd.; https://www.miyarisan.com), occasionally leads to bacteremia. The prevalence and characteristics of *C. butyricum* bacteremia and its bacteriologic and genetic underpinnings remain unknown. We retrospectively investigated patients admitted to Osaka University Hospital during September 2011–February 2023. Whole-genome sequencing revealed 5 (0.08%) cases of *C. butyricum* bacteremia among 6,576 case-patients who had blood cultures positive for any bacteria. Four patients consumed MIYA-BM, and 1 patient consumed a different *C. butyricum*-containing probiotic. Most patients had compromised immune systems, and common symptoms included fever and abdominal distress. One patient died of nonocclusive mesenteric ischemia. Sequencing results confirmed that all identified *C. butyricum* bacteremia strains were probiotic derivatives. Our findings underscore the risk for bacteremia resulting from probiotic use, especially in hospitalized patients, necessitating judicious prescription practices.

Probiotics have emerged as agents that improve a wide range of conditions and provide essential ingredients for potential health benefits. Probiotics exhibit a diverse array of effects by engaging in competitive interactions with pathogenic microbial communities, competing for binding sites, helping exclude pathogens, and triggering activation of specific genes within and beyond the host's intestinal tract. This process, in turn, stimulates, regulates, and controls the immune response (*1*). Probiotics have been found to be effective not only in managing conditions such as acute gastroenteritis (*2*) and irritable bowel syndrome (*3*) but also in preventing antibiotic-associated diarrhea (*4*) and even in alleviating symptoms associated with COVID-19 (*5*).

Clostridium butyricum is a strictly anaerobic, gram-positive, spore-forming bacillus named for its capacity to produce high amounts of butyric acid. *C. butyricum* was first isolated from the intestines of pigs by Prazmowski in 1880 (*6*), and several strains of *C. butyricum* have been reported from various environments in humans (*7*) and animals (*8*). *C. butyricum* has been detected in the gut of ≈20% of human adults (*9*). Moreover, *C. butyricum* strains were detected in >30% of environmental samples tested (*10*). Some strains of *C. butyricum* are currently used as probiotics and have beneficial effects on humans and animals. One strain of *C. butyricum*, known as *C. butyricum* MIYAIRI 588 (CBM 588), can be found in pharmaceutical probiotics, such as MIYA-BM (Miyarisan Pharmaceutical Co., Ltd., https://www.miyarisan.com), one of the most commonly prescribed probiotics in Japan. CBM 588 has been described as a unique, nongenetically modified strain that does not naturally produce toxins (*11*) or cause disease owing to its susceptibility to the KM1 bacteriophage (*12*). Several confirmatory factors underpin this characterization: it exhibits no propensity for antibiotic resistance transfer, it is devoid of plasmids bearing mobile genetic elements, and it does not possess genes or produce substances related to clostridial toxins, including botulinum neurotoxins A, B, E, and F, or the *Clostridium perfringens* toxins α, β, and ε. Genomic scrutiny of CBM 588 revealed no indicators of pathogenic traits or hemolytic capabilities (*13*). Numerous studies have substantiated the effectiveness of CBM 588, and various animal model experiments have demonstrated its capacity to inhibit the colonization of *Clostridioides difficile* (*14*) and prevent enterohemorrhagic *Escherichia coli* O157 infection (*15*). Human studies have confirmed that

Author affiliations: Osaka University Graduate School of Medicine, Osaka, Japan (R.M. Sada, H. Matsuo, S. Kutsuna, S. Hamaguchi, G. Yamamoto); Osaka University Research Institute for Microbial Diseases, Osaka (D. Motooka); Osaka University Hospital, Suita, Osaka (A. Ueda)

DOI: http://doi.org/10.3201/eid3004.231633

CBM 588 prevents antibiotic-associated diarrhea (*16*). In the medical context in Japan, CBM 588 has been prescribed not only for its expected effectiveness as a conventional probiotic but also for the prophylaxis of the diseases we have listed.

There are, however, other strains of *C. butyricum* that are involved in infectious diseases (*17*–*21*). A few case reports have noted the development of *C. butyricum* bacteremia in patients taking probiotics, although strain definition tests using whole-genome sequencing were not conducted (*22*,*23*). Bacteremia caused by *C. butyricum* is a rare condition, and the prevalence, clinical features, and bacteriologic and genetic origins of the strains are unknown. We conducted a single-center, retrospective study of cases of bacteremia caused by *C. butyricum* in Japan to shed light on this clinical event.

Patients and Methods

Study Design

We conducted a retrospective cohort study at Osaka University Hospital, a 1,086-bed facility in Osaka, Japan. Our study followed the Strengthening the Reporting of Observational Studies in Epidemiology statement for reporting observational studies (*24*). The Institutional Review Board of Osaka University Hospital approved the study protocol (number 22584(T1)).

Patients and Baseline Characteristics

To identify cases of *C. butyricum* bacteremia, we reviewed all cases of positive blood culture results for any bacteria that occurred during September 19, 2011–February 5, 2023, from the Laboratory for Clinical Investigation database at Osaka University Hospital. We defined *C. butyricum* bacteremia as cases in which *C. butyricum* was detected in ≥1 sets of blood cultures. We used MALDI Biotyper (Bruker, https://www.bruker.com/en) to identify *C. butyricum* (*25*). The data we extracted from medical records encompassed such parameters as age; sex; conditions necessitating hospitalization; underlying diseases; placement of a central venous catheter or a peripherally inserted central catheter; presence of polymicrobial bacteremia, including identification of microorganisms other than *C. butyricum*; symptoms at onset; and the updated Charlson Comorbidity Index at the time of bacteremia diagnosis, which was evaluated for every patient (*26*). In addition, for patients who were prescribed MIYA-BM, we checked the MIYA-BM consumption at the point of diagnosis and confirmed the duration of MIYA-BM prescription. We also identified whether MIYA-BM was used for specific reasons in these patients. We defined specific reasons for use of MIYA-BM as treatment for diarrhea, concurrent antibiotic use, or medical history of *C. difficile* infection (CDI), ulcerative colitis, hepatic encephalopathy, or a combination of those conditions. Our investigation involved a detailed evaluation of electronic medical records, which included symptoms of diarrhea occurring ≥3 times/day, concurrent antibiotic use, and medical history of CDI, ulcerative colitis, or hepatic encephalopathy. Finally, we extracted data on the etiology of bacteremia, antibiotic treatment regimens, and mortality within 90 days.

Microbiologic Information

We determined the MICs for penicillin, ampicillin, cefotaxime, ceftriaxone, cefmetazole, imipenem, meropenem, sulbactam/ampicillin, clavulanic acid/amoxicillin, tazobactam/piperacillin, clindamycin, moxifloxacin, and metronidazole for *C. butyricum* by using the agar dilution method on Brucella agar medium supplemented with 0.5% sheep's blood. Assays to gauge susceptibility followed the guidelines set by the Clinical Laboratory Standards Institute, tailored for anaerobes (*28*). We assessed the homogeneity of antibiotic susceptibility between the clinical strains and 3 medicinal strains from different lot numbers to evaluate the comparability of their antibiotic susceptibility.

Whole-Genome Sequencing Analysis

We conducted whole-genome analysis of all strains of *C. butyricum* obtained from blood cultures. In addition, we analyzed *C. butyricum* extracted from MIYA-BM tablets. We then investigated the genetic homology between those strains by evaluating the number of single-nucleotide polymorphisms (SNPs) or insertion/deletion genetic variants between clinical strains and the strain from the MIYA-BM tablets. Finally, we conducted a genomic comparison between clinical isolates of *C. butyricum*, the CBM 588 strain, and other strains of the same species. For the comparison, in addition to the reference strain CDC 51208, we selected 7 strains with fully sequenced genomes that are stored in a bioresource repository.

Results

We detected 5 blood culture–positive *C. butyricum* bacteremia cases (0.08%) (Table 1) from a total of 6,576 persons who had blood cultures positive for any bacteria (7,484 total clinical strains, including bacteria other than *C. butyricum*). Bacteremia developed in all 5 patients during hospitalization; 3 patients were

Table 1. Detailed clinical information on 5 patients with bacteremia caused by *Clostridium butyricum* based on a single-institute, retrospective study, Osaka University Hospital, Japan*

Category	Patient no.				
	1	2	3	4	5
Age, y/sex	68/F	81/F	77/M	53/M	19/F
Onset during hospitalization	Yes	Yes	Yes	Yes	Yes
Diseases requiring hospitalization	Chemotherapy	Immunosuppressive treatment	Post–aortic valve replacement	Simultaneous pancreas and kidney transplant	Double lung transplant
Underlying disease	Esophageal cancer; gastric cancer	Dermatomyositis	Aortic valve regurgitation; end-stage kidney disease	End-stage kidney disease; type 1 diabetes	Idiopathic pulmonary arterial hypertension
Immunosuppression	Yes	Yes	No	Yes	Yes
Charlson Comorbidity Index score	2	1	4	6	1
Central venous catheter insertion	Yes	No	Yes	No	Yes
Concurrent MIYA-BM use	Yes	No, but previously administered another probiotic with *C. butyricum*	Yes	Yes	Yes
Appropriate reason for the prescription of probiotics	Yes (concomitant antibiotic use)	NA	Yes (concomitant antibiotic use)	No	No
Duration of use of probiotics, d	8	NA	12	91	30
Polymicrobial bacteremia, microorganisms other than *C. butyricum*	Yes (MSSA)	Yes (*Enterococcus faecium*/MRCNS)	None	None	None
Symptoms of onset	Fever and diarrhea	Fever and diarrhea	Fever and abdominal pain, septic shock	Fever and abdominal pain	Fever and diarrhea
Diagnosis	Enterocolitis	Enterocolitis	NOMI	Duodenal perforation	Enterocolitis
Antibiotics	CMZ	CTR	MEM	MEM	VCM
90-d mortality	Alive	Alive	Died	Alive	Alive

*CMZ, cefmetazole; CTR, ceftriaxone; MEM, meropenem; MRCNS, methicillin-resistant coagulase-negative staphylococci; MSSA, methicillin-resistant *Staphylococcus aureus*; NA, not applicable; NOMI, nonocclusive mesenteric ischemia; VCM, vancomycin.

women and 2 were men. Four patients were immunocompromised: 2 had undergone transplantation, 1 was undergoing chemotherapy for esophageal and gastric cancers, and 1 was receiving multiple immunosuppressive treatments for dermatomyositis. Two of the 5 patients also had end-stage kidney disease and were on dialysis. The Charlson Comorbidity Index scores ranged from 1 to 6 points for each patient. Three patients underwent catheterization with either a central venous catheter or a peripherally inserted central catheter. Four patients were taking prescribed MIYA-BM at the time of bacteremia diagnosis, and 1 patient (no. 2) had been prescribed a different probiotic containing *C. butyricum* 1 month before the diagnosis of bacteremia. All 4 patients taking MIYA-BM were prescribed it >1 week prior to hospitalization, and MIYA-BM was discontinued following the diagnosis of bacteremia in all these patients. Despite a detailed review of the medical records, we were unable to identify the specific reason for prescribing probiotics in 2 patients. All 5 patients had fever and abdominal symptoms, such as diarrhea and pain. One patient (no. 3) with nonocclusive mesenteric ischemia died within 90 days.

A consistent pattern of antibiotic susceptibility was observed in all clinical strains (Table 2). Moreover, those results were consistent with those of previous reports on the antibiotic susceptibility of *C. butyricum*. *C. butyricum* has been reported to be susceptible to penicillin, ampicillin, cefmetazole, imipenem, meropenem, clavulanic acid/amoxicillin, tazobactam/piperacillin, clindamycin, moxifloxacin, and metronidazole but resistant to cefotaxime and ceftriaxone (*11*,*29*,*30*).

Whole-genome analysis of all 5 patient clinical strains revealed that they either exhibited complete homology or had a maximum divergence of only 19 mutations relative to CBM 588, which was extracted from the MIYA-BM tablets. This result indicates that all clinical strains had the same clone as the CBM 588 extracted from MIYA-BM (Table 3) (*31*–*34*). We performed genetic annotation of the detected mutations (Appendix Table, https://wwwnc.cdc.gov/EID/article/30/4/23-1633-App1.pdf). We performed phylogenetic analysis of

Table 2. Antimicrobial drug susceptibility of clinical bacterial strains from 5 patients who tested positive for *Clostridium butyricum* in a single-institute, retrospective study, Osaka University Hospital, Japan, and 3 medicinal strains from different lot numbers of *C. butyricum* MIYAIRI 588 strain

Category	Patient strains					Medicinal strains of CBM 588		
Patient no.	1	2	3	4	5			
Strain no.	114–4	129–32	180–11	181–16	216–41	No. 1	No. 2	No. 3
Antimicrobial drug								
Penicillin	0.25	0.25	0.5	0.5	0.25	0.25	0.25	0.25
Ampicillin	0.25	0.25	0.25	0.25	0.25	0.12	0.25	0.25
Cefotaxime	32	32	32	32	32	32	32	32
Ceftriaxone	8	8	16	8	16	8	16	8
Cefmetazole	≤4	≤4	8	≤4	≤4	≤4	≤4	≤4
Imipenem	1	1	2	1	1	1	1	1
Meropenem	≤0.12	≤0.12	0.5	≤0.12	≤0.12	≤0.12	≤0.12	≤0.12
Sulbactam/ampicillin	≤2	≤2	≤2	≤2	≤2	≤2	≤2	≤2
Clavulanic acid/amoxicillin	0.25	0.25	0.5	0.25	0.25	0.12	0.25	0.12
Tazobactam/piperacillin	≤8	≤8	≤8	≤8	≤8	≤8	≤8	≤8
Clindamycin	0.5	0.25	0.5	0.5	0.25	0.25	0.5	0.25
Moxifloxacin	≤0.5	≤0.5	≤0.5	≤0.5	≤0.5	≤0.5	≤0.5	≤0.5
Metronidazole	≤2	≤2	≤2	≤2	≤2	≤2	≤2	≤2

C. butyricum by using the Type (Strain) Genome Server (*35*). All clinical isolates and probiotics strain were clustered on the same branches (Figure). Average nucleotide identity scores of clinical isolates against those of the probiotics strain were higher than against those of reference strains. This analysis further corroborated the genetic homology between all the clinical strains and the CBM 588 strain.

Discussion

Our single-center, retrospective study determined that the prevalence of *C. butyricum* bacteremia was 0.08% among all cases with bacteria-positive whole-blood cultures and that all clinical strains were derived from the CBM 588 strain. Bacteremia developed in all patients during hospitalization. Out of 5 cases, 4 had received immunosuppressive treatment and 2 had intra-abdominal issues (1 case of esophageal and gastric cancer and 1 case of post–pancreas and kidney transplantation).

Ishikawa et al. reported a case series of 11 cases of *C. butyricum* bacteremia, including 3 self-experienced cases and 8 cases from a literature review (*23*). The study revealed that at least 8 cases developed bacteremia during their hospitalization for conditions unrelated to the bacteremia itself. Furthermore, most patients had intra-abdominal issues at the time of developing bacteremia. In 3 cases, *C. butyricum* bacteremia developed after intra-abdominal surgery. Among the 8 cases without intra-abdominal surgery, 6 cases occurred after various intra-abdominal conditions (2 cases of Crohn's disease, 2 cases of gastrointestinal ulcers, 1 case of biliary tract infection, and 1 case of non-obstructive mesenteric ischemia). Our study results align with previous findings, emphasizing the need for vigilant monitoring of bacteremia development associated with probiotic use in patients with intra-abdominal issues or those undergoing immunosuppressive therapy during their hospitalization.

Our study revealed a high degree of genetic similarity between the strains of *C. butyricum* extracted from MIYA-BM tablets and clinical strains identified through genetic analysis, strongly supporting the definition of probiotic-related bacteremia in all our cases. Reports on probiotic-related bacteremia are scarce. Although systematic reviews of cases of bacteremia after probiotic use have been reported (*36*), to the best of our knowledge, no studies have evaluated the genetic similarities among these reports. Our study offers evidence supporting a direct causal relationship between probiotic prescription and bacteremia. Nonetheless, the patients we identified as nos. 1 and

Table 3. Results of whole-genome sequencing of *Clostridium butyricum* obtained from blood culture from 5 patients who tested positive for *Clostridium butyricum* in a single-institute, retrospective study, Osaka University Hospital, Japan

Category	Patient strains				
Patient no.	1	2	3	4	5
Strain no.	114–4	129–32	180–11	181–16	216–41
Average nucleotide identity* against CBM 588 strains	99.986	99.947	99.949	99.943	99.946
All variants†	50	40	63	65	81
Variants not on rRNA region‡	19	1	2	1	0

*Calculated using FastANI (*31*).
†Number of all variants in coding genes, which were called and annotated by GATK HaplotypeCaller (*32*) and snpEff (*33*) with annotation information from DFAST (*34*).
‡Number of variants after excluding variants on rRNA region.

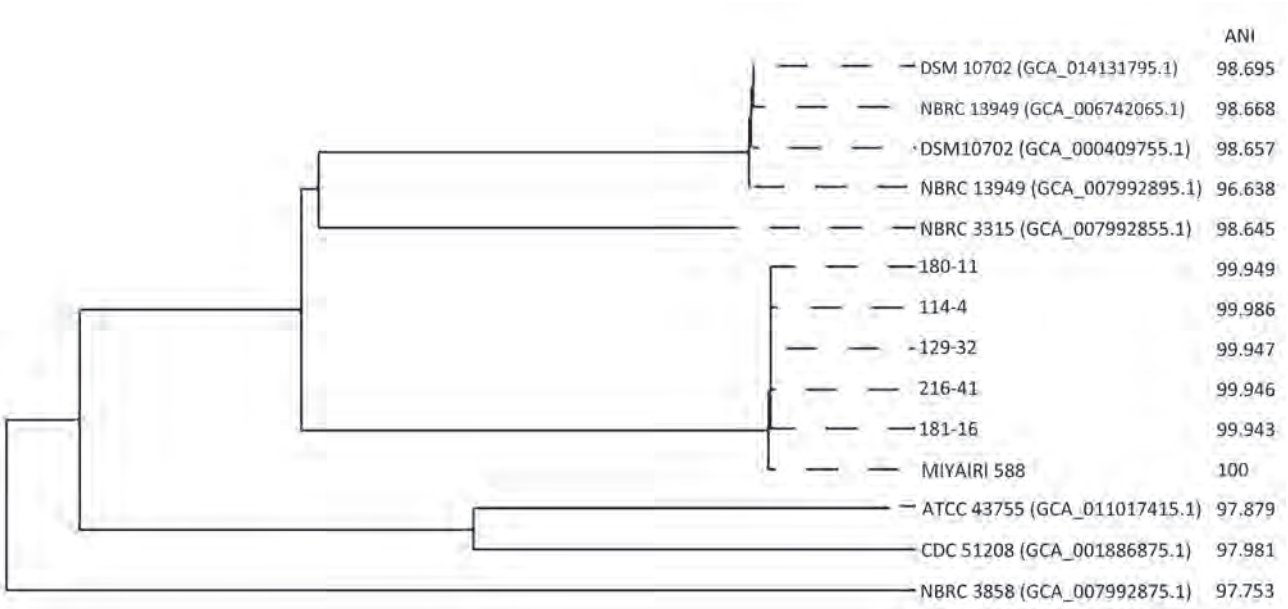

Figure. Phylogenetic tree reflecting the relationship between *Clostridium butyricum* MIYAIRI 588, clinical isolates of *C. butyricum*, and 8 reference strains based on data from a single-institute, retrospective study, Osaka University Hospital, Japan. Note: 114-4, 129-32, 180-11, 181-16, and 216-41 represent strain numbers of clinical isolates of *C. butyricum*. MIYAIRI 588 indicates *C. butyricum* MIYAIRI 588. DSM10702 (GCA_014131795.1), NBRC 13949 (GCA_006742065.1), DSM 10702 (GCA_000409755.1), NBRC 13949 (GCA_007992895.1), NBRC 3315 (GCA_007992895.1), ATCC 43755 (GCA_011017415.1), CDC 51208 (GCA_001886875.1), and NBRC 3858 (GCA_007992875.1) represent 8 reference strains. ANI was calculated using FastANI (*31*). ANI, average nucleotide identity.

2 present lingering challenges. We observed 19 differences in terms of SNPs between the strains found in the blood culture of patient 1 and the CBM 588 strain, which was relatively higher than that of the other patients. However, it is common to evaluate strain dissimilarity using fewer than 100 SNPs. Notably, rapidly growing bacteria, such as *Helicobacter pylori*, can accumulate ≈30 SNPs within 6 months of acute infection (*37*). In fact, some studies have established a genetic similarity cutoff of 80 for carbapenem-resistant *Klebsiella pneumoniae* (*38*), suggesting that the genetic dissimilarity observed in this case could be reasonably acceptable. We also considered the possibility that long-term oral administration of probiotics in the past could have led to genetic mutations in the CBM 588 strain within the bodies of patients we examined. Patient 2, who had been prescribed a different probiotic containing *C. butyricum* 1 month before the diagnosis of bacteremia, developed bacteremia caused by the CBM 588 strain. We considered 2 possibilities for this observation: the patient had previously taken MIYA-BM and it had colonized in the patient's gastrointestinal tract, leading to an infection; or the *C. butyricum* present in the probiotics the patient was taking had genetic similarities to the CBM 588 strain.

Our findings also bring to light the potential adverse effects related to the inappropriate prescribing of probiotics. In all cases where MIYA-BM was prescribed, probiotics were administered for >1 week. However, after a comprehensive review of the detailed medical records, we were unable to identify the appropriate reasons for prescribing probiotics in half of the cases. Probiotics exhibit various therapeutic and preventive effects in different medical conditions, such as averting antibiotic-associated diarrhea (*39*) and CDI (*40*), preventing hepatic encephalopathy in patients with liver cirrhosis (*41*), and managing symptoms in patients with ulcerative colitis (*42*). Although probiotics may demonstrate effectiveness in such specialized clinical scenarios, those scenarios were not observed in the cases we studied, in which probiotics appeared to have been prescribed indiscriminately over an extended period.

One limitation of our study was that it was a single-center, retrospective investigation. Multicenter studies are needed to elucidate the prevalence of *C. butyricum* bacteremia and the genetic origin of the strains. Another limitation was that patient 1 showed improvement with ceftriaxone use, although *C. butyricum* is resistant to it. There is a possibility of contamination resulting from such factors as polymicrobial bacteremia and the absence of central venous catheterization. However, it cannot be ruled out that patients with concurrent sacral pressure ulcers are at risk of developing polymicrobial bacteremia, including *C. butyricum* bacteremia. Also, the duration

of probiotic use for each case patient was based on information documented in their medical records, and the precise prescription durations were not always clear. However, the actual prescription periods must exceed the durations documented in the medical records, because the recorded periods represent at least the minimum assessable timeframe. Moreover, although specific reasons for probiotic prescription were not evident in the medical records, unique justifications may have existed. Nevertheless, it is crucial to note that none of the patients had a history of prior antibiotic use, CDI, irritable bowel syndrome, or liver cirrhosis. Hence, the need for prolonged administration exceeding 2 weeks for therapeutic purposes seems unlikely.

In conclusion, our study demonstrates that all clinical strains of *C. butyricum* identified in the positive blood cultures of the 5 cases we analyzed were derived from the strain found in probiotics. Although this type of bacteremia is rare, careful monitoring is essential when bacteremia is caused by probiotics. Clinicians must avoid long-term, inappropriate prescription of probiotics for hospitalized patients with multiple comorbidities, including immunosuppressive treatment and intraabdominal problems, to prevent bacteremia caused by probiotics.

This research was conducted as part of the All-Osaka U Research in "The Nippon Foundation– Osaka University Infectious Disease Response Project."

About the Author

Dr Sada is an endowed chair associate professor of the Department of Transformative Protection to Infectious Disease, Graduate School of Medicine, Osaka University, Osaka, Japan. His research interests include the epidemiology of bacteremia, infections caused by rare bacteria, and immunodeficiency-related infections.

References

1. Kerry RG, Patra JK, Gouda S, Park Y, Shin HS, Das G. Benefaction of probiotics for human health: A review. Yao Wu Shi Pin Fen Xi. 2018;26:927–39. https://doi.org/10.1016/j.jfda.2018.01.002
2. Collinson S, Deans A, Padua-Zamora A, Gregorio GV, Li C, Dans LF, et al. Probiotics for treating acute infectious diarrhoea. Cochrane Database Syst Rev. 2020;12:CD003048.
3. Zhang T, Zhang C, Zhang J, Sun F, Duan L. Efficacy of probiotics for irritable bowel syndrome: a systematic review and network meta-analysis. Front Cell Infect Microbiol. 2022;12:859967. https://doi.org/10.3389/fcimb.2022.859967
4. Hempel S, Newberry SJ, Maher AR, Wang Z, Miles JN, Shanman R, et al. Probiotics for the prevention and treatment of antibiotic-associated diarrhea: a systematic review and meta-analysis. JAMA. 2012;307:1959–69. https://doi.org/10.1001/jama.2012.3507
5. Zhu J, Pitre T, Ching C, Zeraatkar D, Gruchy S. Safety and efficacy of probiotic supplements as adjunctive therapies in patients with COVID-19: A systematic review and meta-analysis. PLoS One. 2023;18:e0278356. https://doi.org/10.1371/journal.pone.0278356
6. Kerry RG, Patra JK, Gouda S, Park Y, Shin HS, Das G. Benefaction of probiotics for human health: A review. J Food Drug Anal. 2018;26:927–939.
7. Mountzouris KC, McCartney AL, Gibson GR. Intestinal microflora of human infants and current trends for its nutritional modulation. Br J Nutr. 2002;87:405–20. https://doi.org/10.1079/BJN2002563
8. Tran NT, Li Z, Ma H, Zhang Y, Zheng H, Gong Y, et al. *Clostridium butyricum*: a promising probiotic confers positive health benefits in aquatic animals. Rev Aquacult. 2020;12:2573–89. https://doi.org/10.1111/raq.12459
9. Finegold SM, Sutter VL, Mathisen GE. Normal indigenous intestinal flora. In: Hentges DJ, editor. Human Intestinal Microflora in Health and Disease. New York: Elsevier Inc. 1983. p. 1:3–31. https://doi.org/10.1016/C2012-0-01555-4
10. Ghoddusi HB, Sherburn R. Preliminary study on the isolation of *Clostridium butyricum* strains from natural sources in the UK and screening the isolates for presence of the type E botulinal toxin gene. Int J Food Microbiol. 2010;142:202–6. https://doi.org/10.1016/j.ijfoodmicro.2010.06.028
11. Isa K, Oka K, Beauchamp N, Sato M, Wada K, Ohtani K, et al. Safety assessment of the *Clostridium butyricum* MIYAIRI 588® probiotic strain including evaluation of antimicrobial sensitivity and presence of *Clostridium* toxin genes in vitro and teratogenicity in vivo. Hum Exp Toxicol. 2016;35:818–32. https://doi.org/10.1177/0960327115607372
12. Maeda A, Ishii K, Tanaka M, Mikami Y, Arai T. KM1, a bacteriophage of *Clostridium butyricum*. Microbiology. 1986;132:2271–5. https://doi.org/10.1099/00221287-132-8-2271
13. Oka K, McCartney E, Ariyoshi T, Kudo H, Vilá B, de Jong L, et al. In vivo safety evaluation of the *Clostridium butyricum* MIYAIRI 588 strain in broilers, piglets, and turkeys. Toxicol Res Appl. 2019;3. https://doi.org/10.1177/2397847319826955
14. Hagihara M, Ariyoshi T, Kuroki Y, Eguchi S, Higashi S, Mori T, et al. *Clostridium butyricum* enhances colonization resistance against *Clostridioides difficile* by metabolic and immune modulation. Sci Rep. 2021;11:15007. https://doi.org/10.1038/s41598-021-94572-z
15. Takahashi M, Taguchi H, Yamaguchi H, Osaki T, Sakazaki R, Kamiya S. Antagonistic interaction between *Clostridium butyricum* and enterohemorrhagic *Escherichia coli* O157:H7 [in Japanese]. Kansenshogaku Zasshi. 1999;73:7–14. https://doi.org/10.11150/kansenshogakuzasshi1970.73.7
16. Seki H, Shiohara M, Matsumura T, Miyagawa N, Tanaka M, Komiyama A, et al. Prevention of antibiotic-associated diarrhea in children by *Clostridium butyricum* MIYAIRI. Pediatr Int. 2003;45:86–90. https://doi.org/10.1046/j.1442-200X.2003.01671.x
17. Muldrew KL. Rapidly fatal postlaparoscopic liver infection from the rarely isolated species *Clostridium butyricum*. Case Rep Infect Dis. 2020;2020:1839456. https://doi.org/10.1155/2020/1839456
18. Smith MF, Borriello SP, Clayden GS, Casewell MW. Clinical and bacteriological findings in necrotising enterocolitis: a controlled study. J Infect. 1980;2:23–31. https://doi.org/10.1016/S0163-4453(80)91727-2
19. Sato Y, Kujirai D, Emoto K, Yagami T, Yamada T, Izumi M, et al. Necrotizing enterocolitis associated with *Clostridium butyricum* in a Japanese man. Acute Med Surg. 2018;5:194–8. https://doi.org/10.1002/ams2.329

20. Cassir N, Benamar S, La Scola B. *Clostridium butyricum*: from beneficial to a new emerging pathogen. Clin Microbiol Infect. 2016;22:37–45. https://doi.org/10.1016/j.cmi.2015.10.014
21. Cassir N, Benamar S, Khalil JB, Croce O, Saint-Faust M, Jacquot A, et al. *Clostridium butyricum* strains and dysbiosis linked to necrotizing enterocolitis in preterm neonates. Clin Infect Dis. 2015;61:1107–15. https://doi.org/10.1093/cid/civ468
22. Shimura M, Mizuma M, Nakagawa K, Aoki S, Miura T, Takadate T, et al. Probiotic-related bacteremia after major hepatectomy for biliary cancer: a report of two cases. Surg Case Rep. 2021;7:133. https://doi.org/10.1186/s40792-021-01216-5
23. Ishikawa K, Hasegawa R, Shibutani K, Mikami Y, Kawai F, Matsuo T, et al. Probiotic-related *Clostridium butyricum* bacteremia: a case report and literature review. Anaerobe. 2023;83:102770. https://doi.org/10.1016/j.anaerobe.2023.102770
24. von Elm E, Altman DG, Egger M, Pocock SJ, Gøtzsche PC, Vandenbroucke JP; STROBE Initiative. The Strengthening the Reporting of Observational Studies in Epidemiology (STROBE) statement: guidelines for reporting observational studies. Ann Intern Med. 2007;147:573–7. https://doi.org/10.7326/0003-4819-147-8-200710160-00010
25. Sulaiman IM, Miranda N, Simpson S. MALDI-TOF mass spectrometry and 16S rRNA gene sequence analysis for the identification of foodborne *Clostridium* spp. J AOAC Int. 2021;104:1381–8. https://doi.org/10.1093/jaoacint/qsab070
26. Quan H, Li B, Couris CM, Fushimi K, Graham P, Hider P, et al. Updating and validating the Charlson Comorbidity Index and score for risk adjustment in hospital discharge abstracts using data from 6 countries. Am J Epidemiol. 2011;173:676–82. https://doi.org/10.1093/aje/kwq433
27. Wilkins T, Sequoia J. Probiotics for gastrointestinal conditions: a summary of the evidence. Am Fam Physician. 2017;96:170–8.
28. Clinical and Laboratory Standards Institute. Performance standards for antimicrobial susceptibility testing, 33rd ed (M100-ED33). Wayne (PA): The Institute; 2023.
29. Mory F, Lozniewski A, Bland S, Sedallian A, Grollier G, Girard-Pipau F, et al. Survey of anaerobic susceptibility patterns: a French multicentre study. Int J Antimicrob Agents. 1998;10:229–36. https://doi.org/10.1016/S0924-8579(98)00041-7
30. Hecht DW. Anaerobes: antibiotic resistance, clinical significance, and the role of susceptibility testing. Anaerobe. 2006;12:115–21. https://doi.org/10.1016/j.anaerobe.2005.10.004
31. Jain C, Rodriguez-R LM, Phillippy AM, Konstantinidis KT, Aluru S. High throughput ANI analysis of 90K prokaryotic genomes reveals clear species boundaries. Nat Commun. 2018;9:5114. https://doi.org/10.1038/s41467-018-07641-9
32. McKenna A, Hanna M, Banks E, Sivachenko A, Cibulskis K, Kernytsky A, et al. The Genome Analysis Toolkit: a MapReduce framework for analyzing next-generation DNA sequencing data. Genome Res. 2010;20:1297–303. https://doi.org/10.1101/gr.107524.110
33. Cingolani P, Platts A, Wang L, Coon M, Nguyen T, Wang L, et al. A program for annotating and predicting the effects of single nucleotide polymorphisms, SnpEff: SNPs in the genome of *Drosophila melanogaster* strain w1118; iso-2; iso-3. Fly (Austin). 2012;6:80–92. https://doi.org/10.4161/fly.19695
34. Tanizawa Y, Fujisawa T, Nakamura Y. DFAST: a flexible prokaryotic genome annotation pipeline for faster genome publication. Bioinformatics. 2018;34:1037–9. https://doi.org/10.1093/bioinformatics/btx713
35. Meier-Kolthoff JP, Göker M. TYGS is an automated high-throughput platform for state-of-the-art genome-based taxonomy. Nat Commun. 2019;10:2182. https://doi.org/10.1038/s41467-019-10210-3
36. Costa RL, Moreira J, Lorenzo A, Lamas CC. Infectious complications following probiotic ingestion: a potentially underestimated problem? A systematic review of reports and case series. BMC Complement Altern Med. 2018;18:329. https://doi.org/10.1186/s12906-018-2394-3
37. Linz B, Windsor HM, McGraw JJ, Hansen LM, Gajewski JP, Tomsho LP, et al. A mutation burst during the acute phase of *Helicobacter pylori* infection in humans and rhesus macaques. Nat Commun. 2014;5:4165. https://doi.org/10.1038/ncomms5165
38. Hassoun-Kheir N, Snitser O, Hussein K, Rabino G, Eluk O, Warman S, et al. Concordance between epidemiological evaluation of probability of transmission and whole genome sequence relatedness among hospitalized patients acquiring *Klebsiella pneumoniae* carbapenemase-producing *Klebsiella pneumoniae.* Clin Microbiol Infect. 2021;27:468.e1–7. https://doi.org/10.1016/j.cmi.2020.04.017
39. Goldenberg JZ, Lytvyn L, Steurich J, Parkin P, Mahant S, Johnston BC. Probiotics for the prevention of pediatric antibiotic-associated diarrhea. Cochrane Database Syst Rev. 2015;12:CD004827. https://doi.org/10.1002/14651858.CD004827.pub4
40. Goldenberg JZ, Ma SS, Saxton JD, Martzen MR, Vandvik PO, Thorlund K, et al. Probiotics for the prevention of *Clostridium difficile*-associated diarrhea in adults and children. Cochrane Database Syst Rev. 2013;5:CD006095. https://doi.org/10.1002/14651858.CD006095.pub.
41. Xu J, Ma R, Chen LF, Zhao LJ, Chen K, Zhang RB. Effects of probiotic therapy on hepatic encephalopathy in patients with liver cirrhosis: an updated meta-analysis of six randomized controlled trials. Hepatobiliary Pancreat Dis Int. 2014;13:354–60. https://doi.org/10.1016/S1499-3872(14)60280-0
42. Naidoo K, Gordon M, Fagbemi AO, Thomas AG, Akobeng AK. Probiotics for maintenance of remission in ulcerative colitis. Cochrane Database Syst Rev. 2011;12:CD007443. https://doi.org/10.1002/14651858.CD007443.pub2

Address for correspondence: Ryuichi Minoda Sada, Department of Transformative Protection to Infectious Disease, Graduate School of Medicine, Osaka University, Osaka, Japan; email: sadao@cider.osaka-u.ac.jp

Animal Exposure Model for Mapping Crimean-Congo Hemorrhagic Fever Virus Emergence Risk

Sara Baz-Flores, Débora Jiménez-Martín,[1] Alfonso Peralbo-Moreno,[1] Cesar Herraiz, David Cano-Terriza, Raúl Cuadrado-Matías, Ignacio García-Bocanegra, Francisco Ruiz-Fons

To estimate the determinants of spatial variation in Crimean-Congo hemorrhagic fever virus (CCHFV) transmission and to create a risk map as a preventive public health tool, we designed a survey of small domestic ruminants in Andalusia, Spain. To assess CCHFV exposure spatial distribution, we analyzed serum from 2,440 sheep and goats by using a double-antigen ELISA and modeled exposure probability with environmental predictors by using generalized linear mixed models. CCHFV antibodies detected in 84 samples confirmed low CCHFV prevalence in small domestic ruminants in the region. The best-fitted statistical model indicated that the most significant predictors of virus exposure risk were cattle/horse density and the normalized difference vegetation index. Model validation showed 99.7% specificity and 10.2% sensitivity for identifying CCHFV circulation areas. To map CCHFV exposure risk, we projected the model at a 1 × 1-km spatial resolution. Our study provides insight into CCHFV ecology that is useful for preventing virus transmission.

Crimean-Congo hemorrhagic fever (CCHF) is a tickborne zoonosis caused by CCHF virus (CCHFV). The World Health Organization considers CCHF one of the highest priority diseases because of its epidemic potential, its high case-fatality rate (10%–40%), and its difficult prevention and treatment (*1*). Clinical disease is restricted mainly to humans, but the virus can infect a wide range of animal species (*2*). CCHFV infections in animals are mainly asymptomatic, which complicates detection of the virus and increases the risk for human infection. Humans can become infected by the bite of a CCHFV-infected tick or through direct contact with virus-contaminated tissues or blood (*3*). Although some outbreaks are associated with high case-fatality rates, most (≈90%) human infections are asymptomatic or cause mild illness (*2*). Cases of CCHF are associated with rural areas. Veterinarians, farmers, hunters, environmental rangers, and abattoir personnel are at highest risk for infection (*4*).

CCHFV is prevalent in Africa, eastern Europe, the Middle East, and across central Asia to western China (*5*). In the 21st century, the geographic range and incidence of confirmed CCHF cases have markedly increased (*2*). Climate change and landscape transformations have affected the abundance and spatial range of CCHFV animal hosts and vectors (*6*), strongly influencing CCHFV transmission dynamics (*7*) and modifying the likelihood of disease emergence and re-emergence (*4*). Those changes are the most likely underlying reason for the emergence of CCHF in Spain.

Exposure to CCHFV on the Iberian Peninsula (mainland Spain and Portugal) was first evidenced in humans in Portugal in 1985 (*8*), but the first confirmed clinical case was reported in 2016 in Spain (*9*). Since then, 12 human cases (4 deaths) have been reported in Spain (*10*,*11*). Because no vaccine is available, humans in or near CCHFV-endemic areas are advised to take precautions when spending time in nature (or tick-prone areas), including limiting skin exposure, applying tick repellents, and thoroughly inspecting the

Author affiliations: Instituto de Investigación en Recursos Cinegéticos, Ciudad Real, Spain (S. Baz-Flores, A. Peralbo-Moreno, C. Herraiz, R. Cuadrado-Matías, F. Ruiz-Fons); Universidad de Córdoba, Córdoba, Spain (D. Jiménez-Martín, D. Cano-Terriza, I. García-Bocanegra); Instituto de Salud Carlos III, Madrid, Spain (D. Cano-Terriza, I. García-Bocanegra, F. Ruiz-Fons)

DOI: https://doi.org/10.3201/eid3004.221604

[1]These authors contributed equally to this article.

skin after field activities. Identifying spatiotemporal virus transmission hotspots may provide information for surveillance and prevention strategies to reduce exposure to CCHFV. Although the likelihood of virus exposure within the general population is low (*12*) because of a predominantly urban lifestyle, greater accuracy in risk prediction may lead to more effective preventive measures for the at-risk population (*13*).

CCHFV has been detected in several species of ticks, but the major CCHFV reservoirs and vectors are considered to be *Hyalomma* spp. ticks (*14*). Two species of *Hyalomma* ticks transmit CCHFV in the Iberian Peninsula, *H. lusitanicum* and *H. marginatum*, and both are abundant in southwestern Spain (*15*–*17*). In general, CCHFV circulates in a silent enzootic tick-vertebrate-tick cycle, the balance of which relies on a complex animal-tick-environment interplay. However, horizontal transmission (cofeeding, transstadial) and vertical transmission (transovarial) can occur within the tick population (*18*). In vertebrate animals, excluding humans, only a transient viremia (≈5 days) develops after infection, but those animals are essential hosts to *H. lusitanicum* and *H. marginatum* ticks and thus play a fundamental role in the spread of CCHFV.

Seroepidemiologic studies in animals can be useful for localizing CCHFV foci and providing information for future research efforts and prevention actions. Farm animals closely coexist with humans and have been epidemiologically linked to human CCHF cases. Therefore, those animals could be used for surveillance purposes (*19*–*21*). Small domestic ruminants (sheep and goats) are abundant in Spain. Indeed, Spain hosts the largest sheep population and the second largest goat population in the European Union (*22*). Direct or indirect interactions between those animals and wild ungulates (e.g., red deer [*Cervus elaphus*] or Eurasian wild boar [*Sus scrofa*]) may be frequent, and both species play major roles in maintaining tick populations (*16*,*17*). Thus, *H. lusitanicum* and *H. marginatum* ticks are abundant on domestic ruminants (*23*).

Because seroepidemiologic studies in animals, along with identification of CCHFV ecologic drivers, can provide insights into CCHFV transmission dynamics (*13*), resulting in better preventive strategies for the human population at risk, we designed a cross-sectional serosurvey of domestic small ruminants in a CCHFV-enzootic region of Spain, Andalusia (*17*,*24*), and statistically modeled exposure risk with environment-associated predictors to map infection risk hotspots. Our working hypothesis was that estimating ecologic drivers of CCHFV exposure risk in small domestic ruminants would reveal the spatial risk for virus transmission to humans. That information would help with the design of ad hoc public health preventive actions in CCHFV-enzootic regions (*13*,*25*,*26*).

The collection of blood samples analyzed was part of the official Animal Health Campaigns of Regional Government of Andalusia, Spain. Therefore, no ethics approval was necessary.

Materials and Methods

Study Design

To analyze the prevalence of antibodies against CCHFV in randomly selected small ruminant farms at both the animal and herd levels, during December 2015–February 2017, we conducted a cross-sectional serosurvey in Andalusia (southern Spain: 36°N–38°60′N, 1°75′W–7°25′W; Figure 1). Andalusia is the first stopover in Europe for birds annually migrating from Africa to western Europe that may carry CCHFV-infected *Hyalomma* spp. ticks. We know that CCHFV circulates enzootically in large areas of Andalusia (*13*,*25*,*26*), but we do not know the actual distribution of the virus in the region.

We randomly selected 122 farms (61 sheep farms and 61 goat farms) according to the stratified census of small ruminant farms per province. Further details on farm selection criteria have been published (*27*). We estimated the minimum number of samples per farm required to estimate antibody prevalence at the previously known circulation rates in southwestern Europe (5%) (*28*) to be 20 with a 95% CI level and an accepted 10% error by using the sample size to estimate a proportion with specified precision calculator of Epitools (https://epitools.ausvet.com.au). Subsequently, within each farm, we randomly sampled 20 small ruminants. Blood samples were obtained by jugular vein puncture and transported to the laboratory and centrifuged at 400 × *g* for 10 minutes to obtain serum that was stored at −20°C until analysis.

Serologic Analyses and Prevalence Calculations

We determined the presence of CCHFV antibodies by using a highly sensitive and specific commercial CCHF double-antigen multispecies ELISA kit (ID-Screen CCHF Double Antigen Multispecies, https://www.innovative-diagnostics.com) according to the manufacturer's instructions (*29*). We estimated the overall prevalence of antibodies from the ratio of positive samples to the total number of analyzed samples. We estimated the Clopper-Pearson exact 95% CI for any prevalence value obtained.

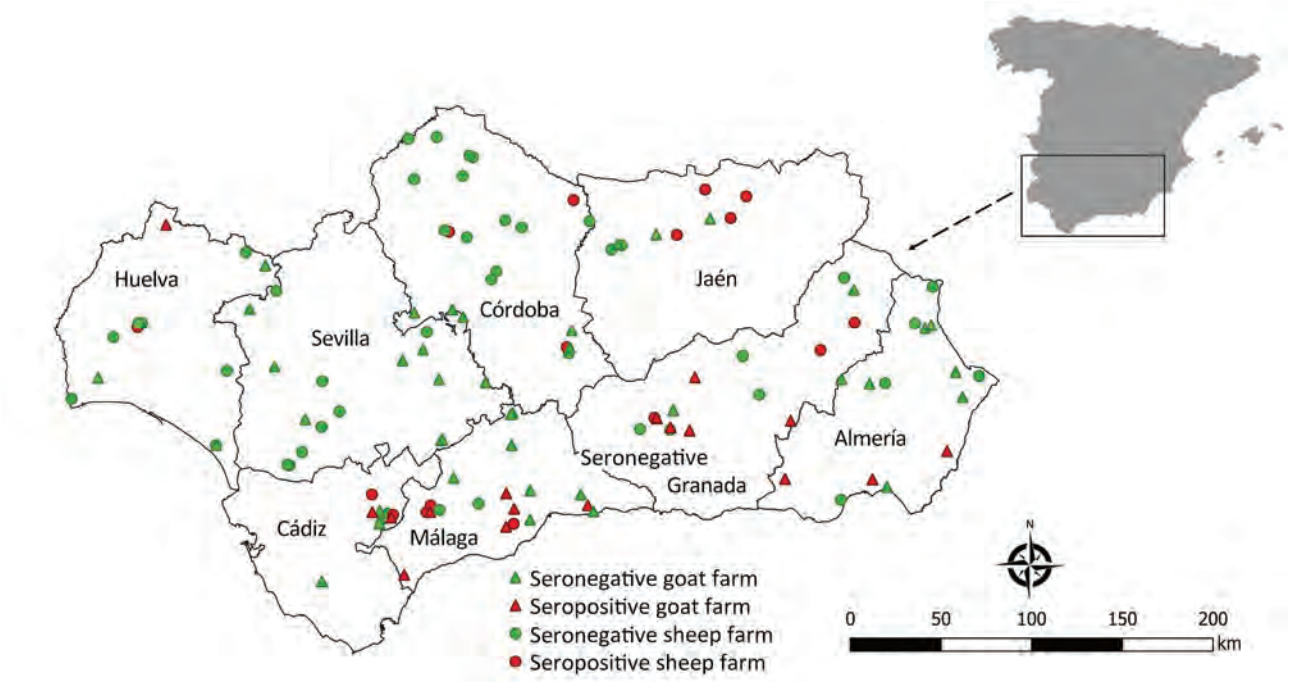

Figure 1. Location of farms in study of animal exposure model for mapping Crimean-Congo hemorrhagic fever virus emergence risk, Andalusia, Spain. Inset shows location of Andalusia within mainland Spain.

Environmental Risk Factors

We performed statistical modeling with predictors selected from environmental factors (Table 1) that characterized the vicinity of the farm. We defined a 5-km radius buffer around farm location coordinates. We selected that buffer size on the basis of the maximum expected movement distance of extensive or semiextensive herds for consumption of local resources (temporary pastures, crop stubble, natural resources). The buffer size was selected to also account for any possible indirect influence of neighboring farms or surrounding wildlife on the risk for CCHFV exposure of domestic small ruminant herds. Only a small fraction of the farms (4/122 [3.3%]) reported seasonal long-distance movements that were thus considered irrelevant for determining the buffer size. The estimated predictor values were rescaled to the spatial scale of the selected buffer by weighted averaging.

Host-Related Predictors

Wild and domestic ungulate abundance is a relevant parameter in CCHF epidemiology (*13*,*17*). We gathered domestic ruminant census data from the 2009 national census (https://www.ine.es) on a regional veterinary unit level spatial scale. We used census data for cattle, horses, and small domestic ruminants to estimate 2 predictors: small domestic ruminant density and cattle/horse density. We used hunting bag data at hunting ground level from the 2014–15 through 2020–21 hunting seasons (kindly provided by the Andalusia regional government) as a proxy of wild ungulate relative abundance (*30*). We estimated 3 predictors: relative abundance of red deer, relative abundance of wild boar, and relative abundance of other wild ungulates.

Bioclimatic Predictors

We selected 2 bioclimatic predictors from telemetry data—the land surface temperature (LST) and the normalized difference vegetation index (NDVI)—because of their potential effects on local tick abundance (*17*,*31*). Both parameters were obtained at a 1 × 1–km spatial resolution and at daily (LST) or 2-week (NDVI) temporal resolution for 2014–2016 from the MODIS website (https://modis.gsfc.nasa.gov). The NDVI is an indicator of plant photosynthetic activity that is associated with water availability and thus indicates the hydric stress that off-host ticks can experience. We estimated period average NDVI and LST and their variance for winter, summer, and the whole year. We estimated the average and variance for all 3 winters, 3 summers, and 3 years of the study and not for each year because we wanted to characterize each area, not compare between years. We selected winter and summer as the critical periods for tick survival and annual LST and NDVI as determinants of *Hyalomma* spp. tick activity (*32*).

Land Use–Related Predictors

As habitat predictors, we considered 3 land cover variables as favorable habitats for *Hyalomma* spp. (*17*,*32*) and wild ungulates (*33*): woodland, dense shrubland, and sparse shrubland cover. We obtained land-use data from the SIPNA database (https://portalrediam.cica.es/descargas). We estimated the proportion of each land cover type at the farm buffer selected scale.

Risk Analyses and Mapping

To reduce the variability in measure scales of the continuous predictors, we applied a standardization rescaling process by using the scale function of R statistical software (https://cran.r-project.org). We explored relationships among continuous predictors by building a correlation matrix (chart.correlation function of the PerformanceAnalytics R package). Thereafter, we analyzed Y~X relationships and excluded specific predictors from the set of highly correlated variables ($r \geq |0.7|$) that had the lowest power to explain the variance of the response variable (*34*). After we finished the exploratory analysis, we analyzed the association of the selected predictors with the individual risk for exposure to CCHFV (antibody positive/negative, n = 2,400) by using generalized linear mixed-effects models (*35*) with the farm as random effect factor. We built and ranked all possible models by increasing corrected Akaike Information Criterion and using the dredge function of the R MuMIn statistical package. We selected the model with the lowest Akaike Information Criterion as the best-fit model (*36*) and validated its predictive potential by means of repeated k-fold cross-validation. We divided data into 10 groups ($\kappa = 10$) and repeated the cross-validation 50 times by using the cross-validate function of the cvms R package (*37*). Subsequently, we estimated average cross-validation values to get an overall predictive capacity of the model. After we validated the model, we projected it at a 1 × 1–km spatial resolution to map predicted risk for Andalusia. For that model, we estimated selected variables for the study period at the projection spatial scale for Andalusia. We considered the first farm of the series as the reference for projection. Model projection was performed by using the predict function of the car package in the R environment.

Results

We detected antibodies against CCHFV in 84 of the 2,440 (3.4%, 95% CI 2.8%–4.2%) small ruminants tested. Exposure prevalence among sheep and goats was similar: sheep 3.0% (95% CI 2.1%–4.1%; 36/1,220) and goats 3.9% (95% CI 3.0%–5.2; 48/1,220). At least 1 seropositive animal was found in 16 of 61 (26.2%, 95% CI 16.8%–38.4%) surveyed sheep farms and in 18 of 61 (29.5%, 95% CI 19.6%-41.9%) goat farms. Overall, the number of farms with ≥1 seropositive animal was 34 of 122 (27.8%, 95% CI 20.7%–36.4%) (Figure 1).

We excluded 2 farms (1 sheep farm and 1 goat farm) and a total of 40 (seronegative) animals from the risk factor analysis because of incorrect recording of location coordinates. The best-fitted model selected 3 of the considered predictors, including cattle/horse

Table 1. Set of explanatory predictors gathered for risk factor analyses used for mapping Crimean-Congo hemorrhagic fever virus emergence risk from animal exposure model

Factor, predictor	Description, unit of measure	Average (range)
Host-related		
boveq	**Cattle and horse summed density, ind/ha**	**0.08 (0–0.45)**
peqrum	Small ruminant density, ind/ha	0.51 (0.02–1.96)
rd	Red deer density, harvested ind/ha	0.04 (0–0.48)
wb	Eurasian wild boar density, harvested ind/ha	0.05 (0–0.24)
otung	**Other wild ungulate density, harvested ind/ha**	**0.13 (0–0.45)**
Bioclimatic		
lstinv	Mean winter land surface temperature, °C	15.77 (11.92–20.76)
lstver	Mean summer land surface temperature, °C	39.61 (32.36–45.12)
lstanu	Mean annual land surface temperature, °C	29.34 (23.01–33.60)
lstvarinv	Winter land surface temperature variation, °C	25.03 (12.32–45.47)
lstvarver	Summer land surface temperature variation, °C	21.06 (9.80–30.06)
lstvaranu	Annual land surface temperature variation, °C	121.77 (64.69–185.28)
NDVIinv	Winter normalized difference vegetation index	4,563.39 (1,969.59–7,002.13)
NDVIver	Summer normalized difference vegetation index	3,053.56 (1,235.00–5,665.86)
NDVIanu	**Annual normalized difference vegetation index**	**3915.94 (1708.02–6546.01)**
NDVIvarinv	**Winter normalized difference vegetation index variation**	**473,323.50 (95,507.99–2,331,259.00)**
NDVIvarver	Summer normalized difference vegetation index variation	126,977.60 (22,445.69–1,028,808.00)
NDVIvaranu	**Variance of the annual normalized difference vegetation index**	**1,051,955.00 (207,897.60–3,747,242.00)**
Land use-related		
matdi	Proportion of sparse shrubland in the buffer, %	0.11 (0–0.55)
matde	Proportion of dense shrubland in the buffer, %	0.08 (0–0.43)
bos	**Proportion of woodland in the buffer, %**	**0.06 (0–0.41)**

*Boldface indicates variables selected for modeling after the descriptive analysis. ind/ha, individuals per hectare.

density, annual NDVI, and annual NDVI variance (Table 2). Cattle/horse density around small ruminant farms was significantly associated with exposure probability (Figure 2). A positive, albeit not statistically significant, relationship was also observed for the NDVI. In contrast, we observed a strong and statistically significant negative relationship between the annual NDVI variance and the risk for exposure of individual small domestic ruminants to CCHFV. The cross-validation analysis showed that the balanced accuracy of the model was 0.549, sensitivity was 10.2%, and specificity was 99.7%. Also, the model had good discriminatory power (area under the curve = 0.830). For a prior probability of infection of 0.05, the positive predictive value was 0.6415 and the negative predictive value was 0.9547. The spatial projection of the model showed lower predicted risk areas in central and eastern Andalusia and higher predicted risk areas north and south of the region (Figure 3).

Discussion

Although some of the human cases of CCHF in Spain could be associated with farm animals, research on domestic species is limited (*38*). Most studies in Spain have focused on wild ungulates because of their relevance to CCHFV (*24*,*25*), but even so, farm animals and their ticks may pose a risk for humans through closer contact. By selecting small domestic ruminants, we aimed to identify the areas of greatest risk for transmission to persons in contact with them and thus complement the risk maps previously obtained by using red deer (*13*). Some of the CCHF patients in Spain were animal farmers (*38*). In the absence of an effective vaccine to protect humans against CCHFV infections, the only feasible measure to protect the population at risk is prevention of tick bites. If risk for infection is higher for an animal in a territory, it is also higher for a person in that territory because the virus is transmitted mainly by tick bites to animals and humans. The factors that predispose human contact with infected ticks or animals will determine the actual risk for CCHFV infection (*12*), although risk will be greater in areas more environmentally favorable for virus transmission. Our results provide public health authorities with information about which areas of Andalusia have the highest risk for CCHFV transmission for anyone linked to small ruminant production. That information will enable design of better infection surveillance programs in the region, optimizing the resources available for those programs and improving the cost:benefit ratio of preventive actions.

Our study is based on a representative subsample of small ruminants for the study region. However, we did not include other domestic species (cattle, equids) or wild ungulates, which are relevant for CCHFV and its vectors and could improve the predictive capabilities of the model. In the future, we recommend considering the full range of species involved in CCHFV transmission to improve the accuracy of risk maps. In this study we did not corroborate that antibodies were specific for CCHFV, which should preferably be done by comparative neutralization assays in Biosafety Level 4 facilities. However, numerous positive serum samples from wild ungulates in the ELISA used were confirmed as CCHFV positive by neutralization assays against different orthonairoviruses (I. García-Bocanegra, unpub. data). The manufacturer of the multispecies double-antigen ELISA test used confirms 98.9% sensitivity and 100% specificity after testing with a multitude of animal species (*29*).

In a previous study conducted in 2 areas of Andalusia (Córdoba and Cádiz Provinces), and using the IDVet double-antigen ELISA, CCHFV seroprevalence among domestic ruminants (including cattle, sheep, and goats) was 17.9% (*38*). The inclusion of cattle samples makes it difficult to compare reported seroprevalence with our findings because cattle host higher burdens of *Hyalomma* spp. ticks than do small domestic ruminants (*39*) and may thus be more prone to CCHFV exposure. That study also found higher seroprevalence than the seroprevalence that we report for areas of northern Spain, which are less favorable areas for *Hyalomma* spp. ticks (6.8%) (*38*). The higher antibody prevalence most likely results from including cattle in the survey. Our results also contrast markedly with the high antibody prevalence (76%–87%) observed in red deer in western Andalusia (*40*). Previous studies of small domestic ruminants from Africa, Asia, and Europe showed a wide range of seroprevalence, 0.4%–74% among sheep and 2.1%–66% among goats (*28*). Our results agree with those of some studies conducted in the Mediterranean region

Table 2. Output of the generalized linear mixed-effects model used to analyze the risk for exposure to Crimean-Congo hemorrhagic fever virus*

Predictor (see Table 1)	Estimate	SE	z	p value
Intercept	−5.0337	0.4011	−12.549	<0.001
Boveq	0.6615	0.2645	2.501	<0.05
NDVIanu	0.5092	0.2831	1.799	NS
NDVIvaranu	−1.4185	0.4664	−3.041	<0.01

*NS, not significant at p<0.05; z, statistic.

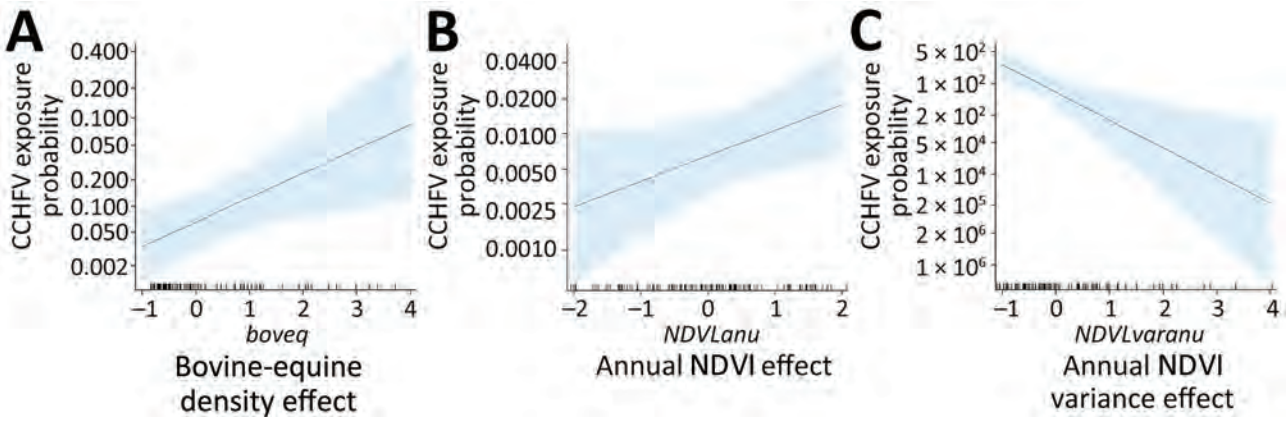

Figure 2. Model output charts displaying the effect of the best-fitted model selected variables on the risk of small ruminant exposure to Crimean-Congo hemorrhagic fever virus, Andalusia, Spain. Shaded areas indicate 95% CIs. NDVI, normalized difference vegetation index.

(*41*,*42*). The low individual seroprevalence observed for animals of both species indicates that sheep and goats are of less concern than cattle, horses, or wildlife for farmers and public health authorities.

Our selected model included horse/cattle density as a predictor of CCHFV exposure risk. The lack of association between wild ungulate abundance and CCHFV exposure risk most likely indicates a low rate of interaction with the small domestic ruminant farms selected for the study. The rate of interaction between wild ungulates and their ticks and small ruminants raised on extensive farms that are also used for large game hunting is probably higher, perhaps leading to a higher risk for exposure to CCHFV. Cattle and horses are relevant hosts for *H. marginatum* ticks (*6*,*23*,*32*,*41*) and may be more abundant than wild ungulates in the vicinity of small ruminant farms, so their association with CCHFV was not unexpected.

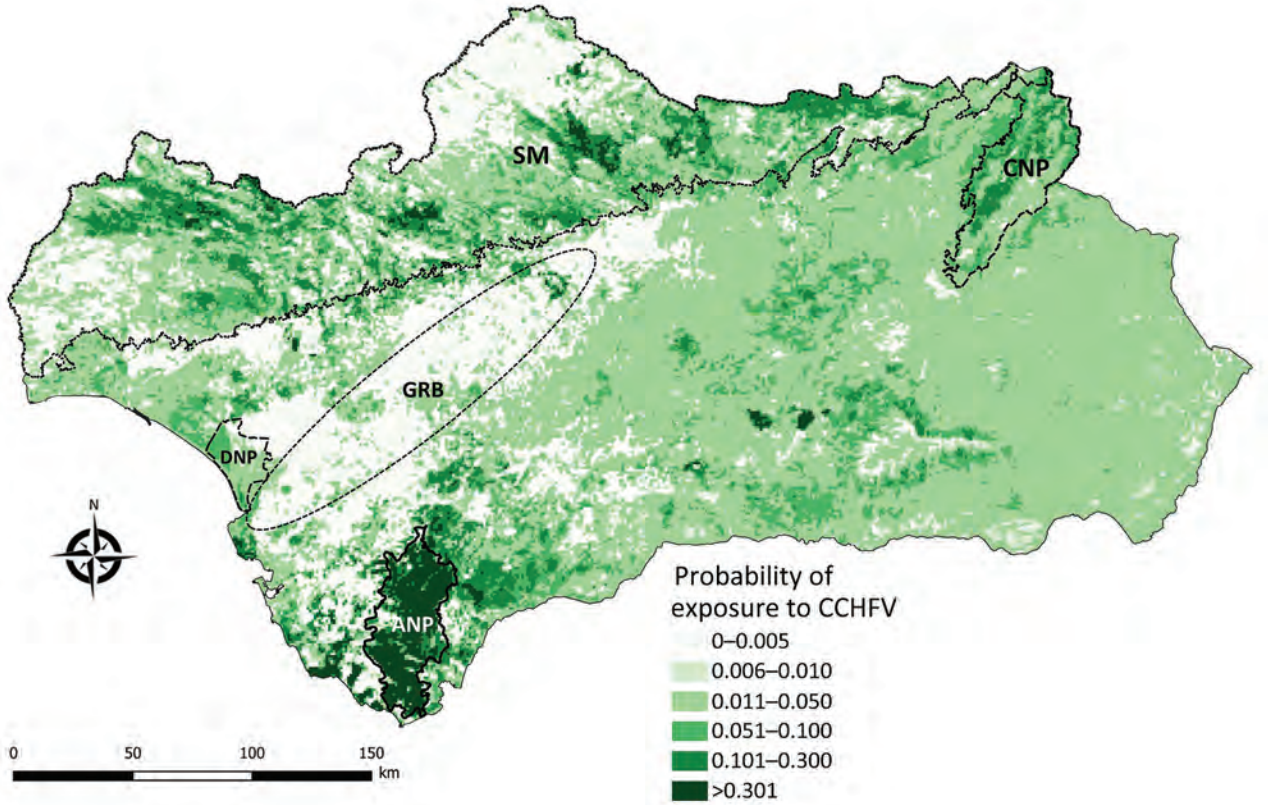

Figure 3. Spatial projection of model for risk for exposure of small ruminants to Crimean-Congo hemorrhagic fever virus in Andalusia, Spain. The model was projected at a 1 × 1–km spatial resolution. ANP, Los Alcornocales Natural Park; CNP, Sierras de Cazorla, Segura y Las Villas Natural Park; DNP, Doñana National Park; GRB, Guadalquivir River basin; SM, Sierra Morena mountain chain.

Previous studies already described the relevant role of farm animals in the risk for exposure to CCHFV (*24*,*43*). Among domestic animals, global CCHFV seroprevalence is second highest among cattle, after camels (*44*). Thus, our findings suggest that a regional strategy should perhaps be implemented to better control ticks on farm animals. For sheep and goats, increasing the frequency of acaricide application may result in more effective tick control (*41*).

The best-fitted model also included 2 abiotic predictors, NDVI and annual NDVI variance, which would probably define the environmental (climatic) niche for CCHFV vectors in southern Spain. The distribution of ticks is limited not only by host distribution but also by a combination of host presence/abundance and environmental favorability (*17*,*45*). Ticks occupy only a subset of their host range because they undergo a large part of their cycle on the ground, where abiotic factors determine tick development and survival rates (*17*,*32*). One of the limiting factors for tick survival and activity is moisture level, a determinant of tick abundance and a relevant driver of CCHFV transmission risk (*13*,*17*). The negative relationship observed between annual NDVI variance and CCHFV exposure risk may suggest that areas with substantial fluctuations in vegetation productivity (e.g., seasonal croplands) are unfavorable for CCHFV vectors, a possibility that agrees with the low predicted spatial risk in the agricultural lands of the Guadalquivir River basin.

The spatial distribution of the farms with seropositive animals was heterogeneous; most were distributed south and east of the study region. Because our model showed that this distribution was associated with some biotic and abiotic factors of the farm neighborhood, we were able to capture the environmental niche for small domestic ruminant exposure risk to CCHFV. The model projection identified that the areas of Andalusia with the highest abundance of wild ungulates (mainly red deer, wild boar, and Iberian ibex [*Capra pyrenaica*]) (*46*) had the highest risk for exposure to CCHFV. As previously observed for red deer (*13*), the predictive model not only projects the risk for small domestic ruminants but also for other hosts of CCHFV vector ticks. The model identified the areas of highest risk to be Los Alcornocales Natural Park (Cádiz and Málaga Provinces), the area surrounding the Doñana National Park (south of Huelva Province), most of the Sierra Morena mountain chain, and the Sierras de Cazorla, Segura y Las Villas Natural Park (northeastern Jaén Province). Sánchez-Seco et al. (*26*) found CCHFV-positive *Hyalomma* spp. ticks in Los Alcornocales Natural Park, whereas we detected high CCHFV prevalence among ticks and high antibody levels in the wild ungulates of Doñana National Park (*24*) and identified Los Alcornocales Natural Park, Doñana National Park, and the Sierra Morena mountain chain as high-risk areas (*13*,*25*). Recently, we found that ≈30% of wild boar in Sierras de Cazorla, Segura y Las Villas Natural Park have antibodies against CCHFV (*47*). Our risk map identifies areas of low and high risk that were identified on larger spatial resolution on a map generated for Spain from a model based on red deer (*13*). However, the limited sensitivity (10.2%) of our model to predict the risk for exposure of small domestic ruminants to CCHFV prevents us from detecting all areas where CCHFV may be circulating among small domestic ruminants in Andalusia. Therefore, in the future, it would be desirable to base estimates of CCHFV actual distribution in Andalusia on vector population dynamics and CCHFV prevalence among the vectors. Comparison of the findings of the small domestic ruminant-based model with existing evidence on the prevalence of CCHFV infection/exposure and the predictive outcome of wildlife-based risk models indicates that despite its limited predictive sensitivity and tendency to false negatives, our model can capture spatial foci of high and low CCHFV risk. Consequently, despite the observed limitations, it may constitute a useful tool for preventing cases of CCHF in humans. The high specificity of the model indicates that the identified low-risk hotspots are actually zones with low risk for exposure. We conclude that modeling of CCHFV exposure risk for small domestic ruminants, although at low rates of virus exposure, is a useful tool for mapping CCHFV transmission risk hotspots and preventing CCHF in humans, at least in the study area.

Acknowledgments

We are grateful to the Department of Agriculture, Fisheries, Water and Rural Development of the regional government of Andalusia and to the farmers for facilitating collection of animal samples and data for this study. We are also grateful to 3 anonymous reviewers and the associate editor of Emerging Infectious Diseases for their recommendations to improve our manuscript.

This study was funded by the Spanish Ministry for the Science and Innovation/Spanish Research Agency (MCIN/AEI /10.13039/501100011033/) and by the European Regional Development Fund (EU-ERDF) through projects CGL2017-89866-R and AGL2013-49159-C2-2-R. Funding support was also provided by the regional government of Castilla-La Mancha (JCCM) and the EU-European Social Fund (ESF) through project SBPLY/19/180501/000321. S.B.-F. acknowledges funding by JCCM and EU-ESF contract PREJCCM2019/11, and

C.H. acknowledges funding by JCCM and EU-ESF contract SUPLY/19/180501/000487. D.J.-M. holds a PhD contract granted by the University of Córdoba. A.P-M. was funded by the University of Castilla-La Mancha (UCLM) and EU-ERDF through contract 2019-PREDUCLM-10932. R.C.-M. received funding from MCIN, EU-ERDF, and UCLM by PRE2018-083801 contract.

About the Author

Ms. Baz-Flores is a PhD candidate who has a degree in veterinary medicine and is developing her doctoral research project at the Spanish Game and Wildlife Research Institute at the University of Castilla-La Mancha, Ciudad Real, Spain. Her research deals with the ecological determinants of CCHFV transmission at different spatiotemporal scales as a tool for improving risk prediction and preventing cases of this severe emerging human disease.

References

1. Mehand MS, Al-Shorbaji F, Millett P, Murgue B. The WHO R&D Blueprint: 2018 review of emerging infectious diseases requiring urgent research and development efforts. Antiviral Res. 2018;159:63–7. https://doi.org/10.1016/j.antiviral.2018.09.009
2. Bente DA, Forrester NL, Watts DM, McAuley AJ, Whitehouse CA, Bray M. Crimean-Congo hemorrhagic fever: history, epidemiology, pathogenesis, clinical syndrome and genetic diversity. Antiviral Res. 2013;100:159–89. https://doi.org/10.1016/j.antiviral.2013.07.006
3. Ergonul O. Crimean-Congo hemorrhagic fever virus: new outbreaks, new discoveries. Curr Opin Virol. 2012;2:215–20. https://doi.org/10.1016/j.coviro.2012.03.001
4. Spengler JR, Bergeron É, Spiropoulou CF. Crimean-Congo hemorrhagic fever and expansion from endemic regions. Curr Opin Virol. 2019;34:70–8. https://doi.org/10.1016/j.coviro.2018.12.002
5. Messina JP, Pigott DM, Golding N, Duda KA, Brownstein JS, Weiss DJ, et al. The global distribution of Crimean-Congo hemorrhagic fever. Trans R Soc Trop Med Hyg. 2015;109:503–13. https://doi.org/10.1093/trstmh/trv050
6. Bah MT, Grosbois V, Stachurski F, Muñoz F, Duhayon M, Rakotoarivony I, et al. The Crimean-Congo haemorrhagic fever tick vector *Hyalomma marginatum* in the south of France: modelling its distribution and determination of factors influencing its establishment in a newly invaded area. Transbound Emerg Dis. 2022;69:e2351–65. https://doi.org/10.1111/tbed.14578
7. Estrada-Peña A, Ayllón N, de la Fuente J. Impact of climate trends on tick-borne pathogen transmission. Front Physiol. 2012;3:64. https://doi.org/10.3389/fphys.2012.00064
8. Filipe AR, Calisher CH, Lazuick J. Antibodies to Congo-Crimean haemorrhagic fever, Dhori, Thogoto and Bhanja viruses in southern Portugal. Acta Virol. 1985;29:324–8.
9. Negredo A, de la Calle-Prieto F, Palencia-Herrejón E, Mora-Rillo M, Astray-Mochales J, Sánchez-Seco MP, et al. Crimean Congo Hemorrhagic Fever@Madrid Working Group. Autochthonous Crimean-Congo hemorrhagic fever in Spain. N Engl J Med. 2017;377:154–61. https://doi.org/10.1056/NEJMoa1615162
10. Negredo A, Sánchez-Ledesma M, Llorente F, Pérez-Olmeda M, Belhassen-García M, González-Calle D, et al. Retrospective identification of early autochthonous case of Crimean-Congo hemorrhagic fever, Spain, 2013. Emerg Infect Dis. 2021;27:1754–6. https://doi.org/10.3201/eid2706.204643
11. European Centre for Disease Prevention and Control. Communicable disease threats report. Week 32, 7–13 August 2022 [cited 2022 Sep 15]. https://www.ecdc.europa.eu/sites/default/files/documents/Communicable-disease-threats-report-13-aug-2022-all-users.pdf
12. Frías M, Cuadrado-Matías R, Del Castillo Jarilla-Fernández M, López-López P, Casades-Martí L, Madrigal E, et al. The spatial pattern of human exposure to Crimean-Congo haemorrhagic fever virus is not consistent with red deer-based risk predictions. Transbound Emerg Dis. 2022;69:e3208–14. https://doi.org/10.1111/tbed.14484
13. Cuadrado-Matías R, Cardoso B, Sas MA, García-Bocanegra I, Schuster I, González-Barrio D, et al. Red deer reveal spatial risks of Crimean-Congo haemorrhagic fever virus infection. Transbound Emerg Dis. 2022;69:e630–45. https://doi.org/10.1111/tbed.14385
14. Gargili A, Estrada-Peña A, Spengler JR, Lukashev A, Nuttall PA, Bente DA. The role of ticks in the maintenance and transmission of Crimean-Congo hemorrhagic fever virus: a review of published field and laboratory studies. Antiviral Res. 2017;144:93–119. https://doi.org/10.1016/j.antiviral.2017.05.010
15. Ruiz-Fons F, Fernández-de-Mera IG, Acevedo P, Höfle U, Vicente J, de la Fuente J, et al. Ixodid ticks parasitizing Iberian red deer (*Cervus elaphus hispanicus*) and European wild boar (*Sus scrofa*) from Spain: geographical and temporal distribution. Vet Parasitol. 2006;140:133–42. https://doi.org/10.1016/j.vetpar.2006.03.033
16. Ruiz-Fons F, Acevedo P, Sobrino R, Vicente J, Fierro Y, Fernández-de-Mera IG. Sex-biased differences in the effects of host individual, host population and environmental traits driving tick parasitism in red deer. Front Cell Infect Microbiol. 2013;3:23. https://doi.org/10.3389/fcimb.2013.00023
17. Peralbo-Moreno A, Baz-Flores S, Cuadrado-Matías R, Barroso P, Triguero-Ocaña R, Jiménez-Ruiz S, et al. Environmental factors driving fine-scale ixodid tick abundance patterns. Sci Total Environ. 2022;853:158633. https://doi.org/10.1016/j.scitotenv.2022.158633
18. Gonzalez JP, Camicas JL, Cornet JP, Faye O, Wilson ML. Sexual and transovarian transmission of Crimean-Congo haemorrhagic fever virus in *Hyalomma truncatum* ticks. Res Virol. 1992;143:23–8. https://doi.org/10.1016/S0923-2516(06)80073-7
19. Papa A, Sidira P, Kallia S, Ntouska M, Zotos N, Doumbali E, et al. Factors associated with IgG positivity to Crimean-Congo hemorrhagic fever virus in the area with the highest seroprevalence in Greece. Ticks Tick Borne Dis. 2013;4:417–20. https://doi.org/10.1016/j.ttbdis.2013.04.003
20. Spengler JR, Estrada-Peña A, Garrison AR, Schmaljohn C, Spiropoulou CF, Bergeron É, et al. A chronological review of experimental infection studies of the role of wild animals and livestock in the maintenance and transmission of Crimean-Congo hemorrhagic fever virus. Antiviral Res. 2016;135:31–47. https://doi.org/10.1016/j.antiviral.2016.09.013
21. Schuster I, Mertens M, Mrenoshki S, Staubach C, Mertens C, Brüning F, et al. Sheep and goats as indicator animals for the circulation of CCHFV in the environment. Exp Appl Acarol. 2016;68:337–46. https://doi.org/10.1007/s10493-015-9996-y

22. EUROSTAT. Livestock population in numbers [cited 2022 Jul 10]. https://ec.europa.eu/eurostat/web/products-eurostat-news/-/ddn-20200923-1
23. Castellà J, Estrada-Peña A, Almería S, Ferrer D, Gutiérrez J, Ortuño A. A survey of ticks (Acari: Ixodidae) on dairy cattle on the island of Menorca in Spain. Exp Appl Acarol. 2001;25:899–908. https://doi.org/10.1023/A:1020482017140
24. Cuadrado-Matías R, Baz-Flores S, Peralbo-Moreno A, Herrero-García G, Risalde MA, Barroso P, et al. Determinants of Crimean-Congo haemorrhagic fever virus exposure dynamics in Mediterranean environments. Transbound Emerg Dis. 2022;69:3571–81. https://doi.org/10.1111/tbed.14720
25. Moraga-Fernández A, Ruiz-Fons F, Habela MA, Royo-Hernández L, Calero-Bernal R, Gortazar C, et al. Detection of new Crimean-Congo haemorrhagic fever virus genotypes in ticks feeding on deer and wild boar, Spain. Transbound Emerg Dis. 2021;68:993–1000. https://doi.org/10.1111/tbed.13756
26. Sánchez-Seco MP, Sierra MJ, Estrada-Peña A, Valcárcel F, Molina R, de Arellano ER, et al.; Group for CCHFV Research. Widespread detection of multiple strains of Crimean-Congo hemorrhagic fever virus in ticks, Spain. Emerg Infect Dis. 2021;28:394–402. https://doi.org/10.3201/eid2802.211308
27. Jiménez-Martín D, García-Bocanegra I, Almería S, Castro-Scholten S, Dubey JP, Amaro-López MA, et al. Epidemiological surveillance of *Toxoplasma gondii* in small ruminants in southern Spain. Prev Vet Med. 2020;183:105137. https://doi.org/10.1016/j.prevetmed.2020.105137
28. Spengler JR, Bergeron É, Rollin PE. Seroepidemiological studies of Crimean-Congo hemorrhagic fever virus in domestic and wild animals. PLoS Negl Trop Dis. 2016;10:e0004210. https://doi.org/10.1371/journal.pntd.0004210
29. Sas MA, Comtet L, Donnet F, Mertens M, Vatansever Z, Tordo N, et al. A novel double-antigen sandwich ELISA for the species-independent detection of Crimean-Congo hemorrhagic fever virus-specific antibodies. Antiviral Res. 2018;151:24–6. https://doi.org/10.1016/j.antiviral.2018.01.006
30. Imperio S, Ferrante M, Grignetti A, Santini G, Focardi S. Investigating population dynamics in ungulates: do hunting statistics make up a good index of population abundance? Wildl Biol. 2010;16:205–14. https://doi.org/10.2981/08-051
31. Šumilo D, Bormane A, Asokliene L, Lucenko I, Vasilenko V, Randolph S. Tick-borne encephalitis in the Baltic States: identifying risk factors in space and time. Int J Med Microbiol. 2006;296(Suppl 40):76–9. https://doi.org/10.1016/j.ijmm.2005.12.006
32. Valcárcel F, González J, González MG, Sánchez M, Tercero JM, Elhachimi L, et al. Comparative ecology of *Hyalomma lusitanicum* and *Hyalomma marginatum* Koch, 1844 (Acarina: Ixodidae). Insects. 2020;11:303. https://doi.org/10.3390/insects11050303
33. Laguna E, Carpio AJ, Vicente J, Barasona JA, Triguero-Ocaña R, Jiménez-Ruiz S, et al. The spatial ecology of red deer under different land use and management scenarios: protected areas, mixed farms and fenced hunting estates. Sci Total Environ. 2021;786:147124. https://doi.org/10.1016/j.scitotenv.2021.147124
34. Schober P, Boer C, Schwarte LA. Correlation coefficients: appropriate use and interpretation. Anesth Analg. 2018;126:1763–8. https://doi.org/10.1213/ANE.0000000000002864
35. McCulloch CE, Searle SR, Neuhaus JM. Generalized linear, and mixed models. 2nd ed. Hoboken (NJ); John Wiley & Sons, Inc; 2011. p. 135–55.
36. Burnham KP, Anderson D. Information and likelihood theory: a basis for model selection inference. In: Barnham KP, Anderson D, editors. Model selection and multimodel inference. 2nd ed. New York (NY): Springer New York; 2002. p. 60–5.
37. Berrar D. Cross-Validation. In: Ranganathan S, Gribskov M, Nakai K, Schönbach C, editors. Encyclopedia of bioinformatics and computational biology. Amsterdam: Elsevier Inc.; 2019. p. 542–5.
38. Ministerio de Sanidad, Consumo y Bienestar Social. Situation report and risk assessment of transmission of Crimean-Congo haemorrhagic fever virus (CCHF) in Spain [cited 2024 Feb 23]. https://www.mscbs.gob.es/profesionales/saludPublica/ccayes/analisisituacion/doc/ER_FHCC.pdf
39. Camicas JL, Wilson M, Cornet JP, Digoutte J-P, Calvo MA, Adam F, et al. Ecology of ticks as potential vectors of Crimean-Congo hemorrhagic fever virus in Senegal: epidemiological implications. In: Calisher CH, editor. Hemorrhagic fever with renal syndrome, tick-and mosquito-borne viruses. New York: Springer; 1990. p. 303–22.
40. Cuadrado-Matías R, Casades-Martí L, Balseiro A, Baz-Flores S, Triguero-Ocaña R, Barroso P, et al. The spatiotemporal dynamics of Crimean-Congo haemorrhagic fever virus in enzootic Iberian scenarios. In: Abstracts of the 69th Wildlife Disease Association/14th European Wildlife Disease Association Joint Conference; Cuenca, Spain (virtual); 2021 Aug 31–Sep 2; Abstract 330 [cited 2024 Feb 23]. http://ewda.org/wp-content/uploads/2022/01/Libro_Abstracts_Cuenca_virtual_v21.pdf
41. Grech-Angelini S, Stachurski F, Lancelot R, Boissier J, Allienne JF, Marco S, et al. Ticks (Acari: Ixodidae) infesting cattle and some other domestic and wild hosts on the French Mediterranean island of Corsica. Parasit Vectors. 2016;9:582. https://doi.org/10.1186/s13071-016-1876-8
42. Schuster I, Chaintoutis SC, Dovas CI, Groschup MH, Mertens M. Detection of Crimean-Congo hemorrhagic fever virus-specific IgG antibodies in ruminants residing in central and western Macedonia, Greece. Ticks Tick Borne Dis. 2017;8:494–8. https://doi.org/10.1016/j.ttbdis.2017.02.009
43. Negredo A, Habela MA, Ramírez de Arellano E, Diez F, Lasala F, López P, et al. Survey of Crimean-Congo hemorrhagic fever enzootic focus, Spain, 2011–2015. Emerg Infect Dis. 2019;25:1177–84. https://doi.org/10.3201/eid2506.180877
44. Nasirian H. Crimean-Congo hemorrhagic fever (CCHF) seroprevalence: a systematic review and meta-analysis. Acta Trop. 2019;196:102–20. https://doi.org/10.1016/j.actatropica.2019.05.019
45. Randolph SE. Ticks and tick-borne disease systems in space and from space. Adv Parasitol. 2000;47:217–43. https://doi.org/10.1016/S0065-308X(00)47010-7
46. Palomo LJ, Gisbert J, Blanco JC. Atlas and red book of the terrestrial mammals of Spain [in Spanish]. Madrid: Organismo Autónomo de Parques Nacionales; 2007.
47. Baz-Flores S, Herraiz C, Peralbo-Moreno A, Barral M, Arnal MC, Balseiro A, et al. Mapping the risk of exposure to Crimean-Congo haemorrhagic fever virus in the Iberian Peninsula using Eurasian wild boar (*Sus scrofa*) as a model. Ticks Tick Borne Dis. 2024;15:102281.https://doi.org/10.1016/j.ttbdis.2023.102281

Address for correspondence: Francisco Ruiz-Fons, Instituto de Investigación en Recursos Cinegéticos (IREC), Ronda de Toledo 12, 13005, Ciudad Real, Spain; email: josefrancisco.ruiz@uclm.es

Geographic Disparities in Domestic Pig Population Exposure to Ebola Viruses, Guinea, 2017–2019

Solène Grayo, Alimou Camara, Bakary Doukouré, Isabelle Ellis, Cécile Troupin, Kerstin Fischer, Jessica Vanhomwegen, Michael White, Martin H. Groschup, Sandra Diederich, Noël Tordo

Although pigs are naturally susceptible to Reston virus and experimentally to Ebola virus (EBOV), their role in *Orthoebolavirus* ecology remains unknown. We tested 888 serum samples collected from pigs in Guinea during 2017–2019 (between the 2013–16 epidemic and its resurgence in 2021) by indirect ELISA against the EBOV nucleoprotein. We identified 2 hotspots of possible pig exposure by IgG titer levels: the northern coast had 48.7% of positive serum samples (37/76), and Forest Guinea, bordering Sierra Leone and Liberia, where the virus emerged and reemerged, had 50% of positive serum samples (98/196). The multitarget Luminex approach confirms ELISA results against Ebola nucleoprotein and highlights cross-reactivities to glycoprotein of EBOV, Reston virus, and Bundibugyo virus. Those results are consistent with previous observations of the circulation of *Orthoebolavirus* species in pig farming regions in Sierra Leone and Ghana, suggesting potential risk for Ebola virus disease in humans, especially in Forest Guinea.

After the original detection of Zaire Ebola virus (EBOV; species *Orthoebolavirus zairense*) in Yambuku, Democratic Republic of Congo (DRC), in 1976, an additional 5 species have been identified: *Orthoebolavirus sudanense* (Sudan virus [SUDV]) in Sudan in 1976, *Orthoebolavirus restonense* (Reston virus [RESTV]) in the United States in 1989, *Orthoebolavirus taiense* (Tai Forest virus [TAFV]) in Cote d'Ivoire in 1994, *Orthoebolavirus bundibugyoense* (Bundibugyo virus [BDBV] in Uganda in 2007, and *Orthoebolavirus bombaliense* (Bombali virus [BOMV]) in Sierra Leone in 2016 (*1*). EBOV, SUDV, TAFV, and BDBV have caused Ebola virus disease (EVD) in humans; EBOV has the highest case-fatality rates of up to 90% and is responsible for most EVD outbreaks in sub-Saharan Africa (*2*,*3*). Until 2013, EVD was thought to be confined to Central Africa (Gabon, DRC, Congo, Uganda), and epidemics were limited to hundreds of cases at the most and lasted less than a few months (*2*). In West Africa, a sporadic emergence of TAFV in chimpanzees of the Taï forest in Cote d'Ivoire caused a single nonlethal human case in 1994 (*4*,*5*); after that, the worst EBOV epidemic occurred in Guinea, Sierra Leone, and Liberia during 2013–2016 (*6*) and resurged in Guinea in 2021 (*7*). The same phenomena of expansion to West Africa can currently be observed with Marburg disease, which was detected sporadically in Guinea in 2021 (*8*), Ghana in 2022 (*9*,*10*), and, more recently, Equatorial Guinea (*11*) and Tanzania, whereas former outbreaks were limited to Central-South Africa (Angola, DRC, Kenya, South Africa, Uganda, Zimbabwe) (*12*). The spatial expansion of hemorrhagic fevers caused by filoviruses in West Africa spotlights viral adaptation to a new environment and calls into question the role of wildlife and livestock in ebolavirus ecology (*13*–*15*). On the basis of molecular and serologic traces of filovirus infection, bats are the most commonly suspected wildlife reservoirs (*16*–*22*). However, only MARV has been successfully isolated directly from Egyptian fruit bats (*Rousettus aegyptiacus*) (*23*). Other isolates from bats are still pending. Even by combining wildlife surveys and molecular screening of bat and environmental samples, no convincing evidence for a bat origin of the West Africa epidemic was confirmed (*15*).

Sporadic human Ebola infections through contact with chimpanzees, gorillas, duikers, and other wild mammals have been reported, but the role played by domestic animals and livestock as intermediate hosts in the maintenance, amplification, and transmission

Author affiliations: Institut Pasteur de Guinée, Conakry, Guinea (S. Grayo, B. Doukouré, I. Ellis, N. Tordo); Centre de Recherche en Virologie, Laboratoire des Fièvres Hémorragiques Virales de Guinée, Conakry (A. Camara); Institut Pasteur du Laos, Vientiane, Laos (C. Troupin); Friedrich-Loeffler-Institut, Standort Insel Riems, Germany (K. Fischer, M.H. Groschup, S. Diederich); Institut Pasteur, Paris, France (J. Vanhomwegen, M. White)

DOI: https://doi.org/10.3201/eid3004.231034

to humans has been poorly explored (*13*,*14*,*24*–*27*). Pigs can act as intermediate amplifying hosts for endemic or emerging viruses, leading to disease outbreaks in humans (e.g., Nipah virus in Malaysia and Singapore in the late 1990s) (*28*). After experimental infection, EBOV causes respiratory clinical symptoms in piglets and oronasal shedding and transmission to cohoused piglets and nonhuman primates (*25*,*29*). Pigs are also naturally susceptible to RESTV, as demonstrated in the Philippines in 2008 (*30*), and RESTV-specific antibodies have been found in healthy workers from pig farms, suggesting possible transmission from pigs to humans (*30*,*31*). RESTV is thus presumed not pathogenic for humans, but its pathogenicity for pigs remains unclear (*32*–*34*).

In recent years, serologic evidence of circulation of various Ebola virus species in pigs has been found in countries in West and East Africa. Studies during EVD outbreaks in Uganda (*35*), Sierra Leone (*36*), and Guinea (*37*) demonstrated some cross-reactivity against nucleoproteins (NPs) of several species, such as EBOV-NP, RESTV-NP, and SUDV-NP, suggesting possible circulation of different species. In Ghana, a country with no known EVD outbreak, 5/139 pig serum samples reacted against different glycoproteins (GPs) of EBOVs: 2 against TAFV-GP, 1 against EBOV-GP, 1 against RESTV-GP, and 1 against Lloviu virus GP (LLOV-GP) (*38*). In Guinea, which was part of the large West Africa outbreak of EVD in 2013, 19/308 pig serum samples (6.2%) collected in the Conakry area were seroreactive to EBOV-NP by ELISA. Among those 19 samples, 13 were confirmed positive by Western blot analysis against EBOV-NP, 4 cross-reacted against SUDV-NP, and 13 cross-reacted against RESTV-NP (*38*). That preliminary investigation in Conakry could be biased by the large pig trade attracting animals from other regions to the capital. This study has been extended to most pig farming areas in the different ecosystems of Guinea, in particular Forest Guinea in the southeast of the country, where the EVD outbreak started and where different species, such as BOMBV, have been detected (*39*). The study relies on 888 pig serum samples collected during 2017–2019, between the large 2013–2016 EVD outbreak and its 2021 resurgence. We screened those serum samples using a previously established in-house ELISA against EBOV-NP and also using the multiplex microsphere immunoassay (MMIA) based on the Luminex technology (Luminex, https://www.diasorin.com), which enabled evaluation of serum reactivity against several antigens of several species of *Orthoebolavirus* in parallel. Overall, this approach enabled us to estimate potential hotspots of pig exposure to multiple *Orthoebolavirus* species in different regions of Guinea.

Methods

Study Area, Ethical Approval, and Sampling

During October 2017–June 2019, we collected 888 domestic pig serum samples from different pigsties covering 7 of the 8 administrative regions of Guinea (Appendix Figure, https://wwwnc.cdc.gov/EID/article/30/4/23-1034-App1.pdf). The population of Guinea is 85% Muslim, so pig farming is mostly found in the Christian region of Forest Guinea, where we selected 2 sites: NZérékoré, a large city in Forest Guinea with suitable sanitation and access to electricity, and Koulé, a small rural village with practices of open defecation and the close proximity of pigsties and shared water resources. Other pigsties were found in the mixed population area along the Conakry-Kindia axis and on the northern seashore, where the bauxite mining industry attracts foreigners. No significant pig raising is performed in the large northeastern area.

For each site, we recorded GPS (Global Positioning System) coordinates and noted ecologic conditions of the pigsties (open air or closed), as well as the sex, age, and weight of each sampled animal. We excluded pregnant or lactating females and piglets <3 months of age from the study as specified in the protocol (no. 040/CNERS/17) agreed to by the Comité National d'Éthique pour la Recherche en Santé of Guinea. We collected blood from the precaval vein of randomly selected pigs by using sterile vacutainer tubes without anticoagulant and centrifuged at 2,000 × *g* for 20 minutes. We stored the resulting serum at −20°C in a cold container until it was transported and stored at –80°C in the Biobank of the Institut Pasteur de Guinée.

Indirect IgG ELISA based on *Escherichia coli*–Produced EBOV Nucleoprotein

We evaluated the seroreactivity of pig serum by an in-house indirect IgG ELISA assay targeting the EBOV NP produced in *Escherichia coli* (*36*,*38*). Serum samples were heat inactivated for 30 minutes at 56°C, then diluted at 1:100 and analyzed according to the ELISA protocol (*36*), including negative and positive serum controls, as well as the *E. coli* extract to evaluate nonspecific binding. We monitored the optical density (OD) at 405 nm in a Multiskan FC Microplate Photometer (ThermoFisher Scientific, https://ww.thermofisher.com). We first validated the assay to ensure the positive control serum (from a pig

immunized with EBOV-like particles) reached a predetermined OD_{405} range of 0.7–0.9. A cut-off OD_{405} value of 0.19 with an inconclusive window (0.16–0.19; i.e., <0.16 = negative; 0.16–0.19 = inconclusive; >0.19 = positive) was established as the mean value of corrected ODs plus 3 SDs, as in Fischer et al. (*38*). We tested serum samples ≥2× to provide a final conclusion in terms of reactivity against EBOV-NP (EBOV strain Mayinga, Zaire, 1976) (*36*).

Multiplex Microsphere Immunoassay with Filovirus 4-Plex

We used a previously published MMIA adapted for pig serum (*21*,*40*) to determine the presence of IgG against different antigens of orthoebolaviruses. Each of 4 color-coded magnetic bead sets (Bio-Plex ProTM Magnetic COOH Beads; Bio-Rad, https://www.bio-rad.com) was coupled at room temperature to a specific *Orthoebolavirus* antigen through carboxylate amine bonds using the Bio-Plex Amine Coupling Kit (Bio-Rad). The 4 antigens were EBOV-NP produced in *E. coli* and EBOV-GP, BDBV-GP (both Sino Biological, https://www.sinobiological.com), and RESTV-GP (IBT Bioservices, https://www.ibtbioservices.com) produced in Sf9 cells. EBOV-NP corresponds to EBOV strain Mayinga, 1976 (Gentaur, #544-MBS1206629), EBOV-GP to EBOV strain Mayinga, 1976 (Sino Biologic, #40304-V08B1), BDBV-GP to BDBV strain Uganda, 2007 (Sino Biologic, #40368-V08B), and RESTV-GP to RESTV strain Philippines, 1996 (Gentaur, #494–0504–015).

We diluted heat-inactivated serum samples at 1:400 in 50 µL of assay buffer (phosphate-buffered saline, 1% bovine serum albumin solution, 0.05% Tween-20) mixed with the antigen-coated bead sets (≈1,250 beads of each type) and placed them in the Bio-Plex Pro flat-bottom well of the MIA plate (Bio-Rad) and protected them from light. After 30 min incubation at room temperature with shaking at 700 rpm, we washed the plate 3 times with the washing solution (phosphate-buffered saline, 0.05% Tween-20). After washing, we added 50 µL of a secondary biotinylated goat antiswine IgG (Jackson ImmunoResearch, https://www.jacksonimmuno.com) at 4 µg/mL in assay buffer to each well and incubated at room temperature on an orbital shaker for 30 minutes at 700 rpm in the dark. After washing 3 times, we incubated the beads for 10 minutes at 700 rpm in the dark with 50 µL of Streptavidin-R-Phycoerythrin (ThermoFisher Scientific) diluted to 2 µg/mL in assay buffer. After 3 additional washing steps, we resuspended the beads in 100 µL of xMAP assay buffer (Bio-Rad) and agitated for 2 min at 1,100 rpm in the dark. We performed measurements using a Magpix instrument (Luminex). We measured fluorescence intensity and bead color coding by dual lasers at 2 different wavelengths: 635 nm to identify the microsphere particle and 532 nm to excite the Streptavidin-R-Phycoerythrin reporter dye. At least 100 events were read for each bead set, and binding events were displayed as mean fluorescence intensities (MFI). For each sample, we calculated MFI from ≥50 beads bearing the same antigen.

Quantitative Reverse Transcription PCR

We performed EBOV genome detection in the serum of pigs from sites with significantly higher seroreactivity. We carried out nucleic acid extraction using an ID Gene Mag Fast Extraction Kit and IDEAL 32 extraction robot (Innovative Diagnostics, https://www.innovativediagnostics.com). We performed EBOV genome detection on 10 µL of extracted RNA using the RealStar Filovirus Screen quantitative reverse transcription PCR Kit 1.0 (Altona Diagnostics, https://altona-diagnostics.com), according to manufacturer protocols. We interpreted samples with cycle threshold (Ct) ≥40 and a positive internal control as EBOV-negative and samples with Ct >0 and <40 as EBOV-positive.

Statistical Analysis

We used the Pearson χ^2 test to determine whether there was any association between EBOV serology results (i.e., number of positive pig serum samples) and 3 variables (sex, age, and sampling site) by assuming that the grouping variable and outcome are independent. Then, we estimated the strength of the association from a univariate logistic regression model using only dichotomous ELISA status of pig serum (1 = positive; 0 = negative) and excluding inconclusive serum samples from the ELISA data (n = 45). We built the generalized linear models under the form: "OD (numeric) ~ term (linear predictor for response)" ("ELISA ~ sex," or "ELISA ~ age," or "ELISA ~ sampling site") to obtain the odds ratio (OR) of positive versus negative pigs in function of sex, age, and site. The OR's interpretation of the classes is made relative to the reference (Table). In this study, the reference classes were female, 3–6 years old, and Conakry. We considered p values of <0.05 to be statistically significant, meaning the true odds ratio of the overall population was within range of the 95% CI (1 – α). We performed all data analyses using RStudio version 2022.07.2 and plotted maps using SimpleMaps (https://simplemaps.com).

Table. Seroreactivity to EBOV-NP IgG and risk factors of exposure to EBOV in domestic pig population, Guinea, 2017–2019*

			EBOV-NP IgG seroreactivity			Risk factors	
Variable	Class	Total	Positive	Negative	Inconclusive	OR (95% CI)	p value
Sex	F†	440	114 (25.91)	308 (70)	18 (4.09)	NA	NA
	M	448	109 (24.33)	312 (69.64)	27 (6.03)	0.94 (0.69–1.28)	0.712
Age, mo	3–6†	490	121 (24.69)	338 (68.98)	31 (6.33)	NA	NA
	7–12	282	83 (29.43)	188 (66.67)	11 (3.90)	1.23 (0.89–1.72)	0.215
	≥13	116	19 (16.38)	94 (81.03)	3 (2.59)	0.56 (0.33–0.96)	<0.05
Sites	Boké	29	11 (37.93)	12 (41.38)	6 (20.69)	11.23 (3.25–46.58)	<0.001
	Boffa	47	26 (55.32)	21 (44.68)	0	15.17 (5.16–56.35)	<0.001
	Dubreka	85	5 (5.88)	75 (88.24)	5 (5.88)	0.82 (0.21–3.44)	0.77
	Conakry†	53	4 (7.55)	49 (92.45)	0	NA	NA
	Coyah	169	18 (10.65)	148 (87.57)	3 (1.78)	1.49 (0.52–5.34)	0.49
	Forecariah	41	0	41 (100)	0	≈0	0.98
	Kindia	84	27 (32.14)	49 (58.33)	8 (9.52)	6.75 (2.42–24.11)	<0.001
	Dalaba	15	1 (6.67)	14 (93.33)	0	0.88 (0.04–6.53)	0.91
	Kissidougou	94	7 (7.45)	85 (90.43)	2 (2.13)	1.01 (0.29–4.01)	0.99
	Guéckédou	75	26 (34.67)	42 (56)	7 (9.33)	7.58 (2.69–27.26)	<0.001
	Koulé	43	36 (83.72)	5 (11.63)	2 (4.65)	88.20 (24.79–408.7)	<0.001
	Nzérékoré	153	62 (40.52)	79 (51.63)	12 (7.84)	9.61 (3.67–33.09)	<0.001
Total		888	223 (25.11)	620 (69.82)	45 (5.07)		

*Values are no. (%) except as indicated. EBOV, Zaire Ebola virus; NA, not applicable; OR, odds ratio.
†Indicates the reference level for 3 categorical variables (sex, age, and region).

We calculated the median MFI signal for each antigen and represented it by a thick horizontal bar in the graphs. We determined the relationship between the 2 variables by estimating the Spearman coefficient of rank correlation (ρ: number between −1 and 1; no normal distribution of variables) with a 95% CI and represented it graphically by a scatter diagram (Figure 1). A p value <0.05 means the correlation coefficient is statistically significant. We constructed graphs (Figures 1, 2) and performed statistical analyses using MedCalc Statistical Software version 20.215 for Windows (MedCalc Software, https://www.medcalc.org).

Results

In-House ELISA to Recognize EBOV-NP in Pig Serum

Of the 888 pig serum samples tested by EBOV-NP protein ELISA, a similar number were from male (n = 448) and female (n = 440) animals (Table). A total of 223 samples (25.11%) were ELISA-positive, and no significant difference was found between sexes: 114/440 (25.91%) female and 109/448 (24.33%) male (χ^2 = 1.866; p>0.05). The absence of an association with gender was supported by the estimated OR 0.94 (95% CI 0.69–1.28; p = 0.3934). The mean age of the pigs was 8 months and median was 6 months. In the 3–6-month age group, 24.69% of serum samples were reactive; 29.43% of serum samples in the 7–12-month age class were reactive, and 16.38% of serum samples in the >13 months age class were reactive. The estimated OR between age classes 3–6 months and 7–12 months was 1.2 (95% CI 0.89−1.72), which is not significant (p = 0.215).

Seroreactivity for 12 collection sites showed substantial variations, ranging from 0% to 83.7% (Table). Overall, the lower class (0%–20%) of seroreactivity included the greater Conakry area (Coyah 10.7%, Conakry 7.6%, Dubreka 5.9%, and Forecariah 0%) and 2 more distant sites, in middle Guinea (Dalaba 6.7%; only 15 serum samples collected) and Kissidougou (7.5%) in the southern part of the country (Figure 3, panel A). In that group, no site demonstrated significantly different risk for seroreactivity than Conakry (Dubreka OR = 0.82, Coyah = 0.49, Forecariah = ≈0, Dalaba = 0.88, and Kissidougou = 1.01; p>0.05). That finding was in contrast to the second class of seroreactivity (20%–40%), which included Kindia (32.1%), a main stopover for livestock drivers before the capital area, Boké (37.9%) in the northwest, and Guéckédou (34.6%) in the southeast; OR values were 6.8 (Kindria), 7.6 (Boké), and 11.2 (Guéckédou), indicating significantly higher seroreactivity than for Conakry (p<0.001). The group demonstrating the highest seroreactivity rate (>40%), corresponded to the furthest sites from Conakry: Boffa (55.32%) in the northwest part of Guinea, Nzérékoré (40.5%), and Koulé (83.7%) in the southeast part of Guinea. The estimated OR values were significant for all those sites (p<0.001), reaching 88.2 for Koulé in Forest Guinea. The geographic contrast in terms of seroreactivity was also mirrored in the distribution of OD values; the peak corresponded to southeastern sites and the trough to the Conakry area (Figure 3, panel B). The OD values were particularity high in Forest Guinea, where some pig serum samples exceeded the positive control OD value, suggesting a seroreactivity to EBOV or to

another EBOV species by cross-reactivity for the pig population in this region.

We tried to detect EBOV genome in 431 serum samples from the sites with significantly higher seroreactivity using the RealStar Filovirus Screen RT-PCR kit 1.0 (Altona Diagnostics). No positive serum was obtained from Boké (n = 29), Boffa (n = 47), Kindia (n = 84), Guéckédou (n = 75), Koulé (n = 43), or Nzérékoré (n = 153).

MMIA

We also tested pig serum samples using MMIA technology at 1:400 dilution in comparison to the ELISA technology. Under boxplot presentation, the ELISA results expressed in OD values (Figure 4, panel A) and the MMIA results expressed in MFI values distribution (Figure 4, panel B) showed the same global mean tendency across the collection sites, indicating a good correlation between the 2 technologies. Of note, we observed high reactivity in Forest Guinea, particularly in Koulé.

To better evaluate the correlation between ELISA (OD values) and MMIA (MFI values), we constructed scatter plots using the data of all testing sites in Guinea (Figure 1, panel A), those of the northern coast in

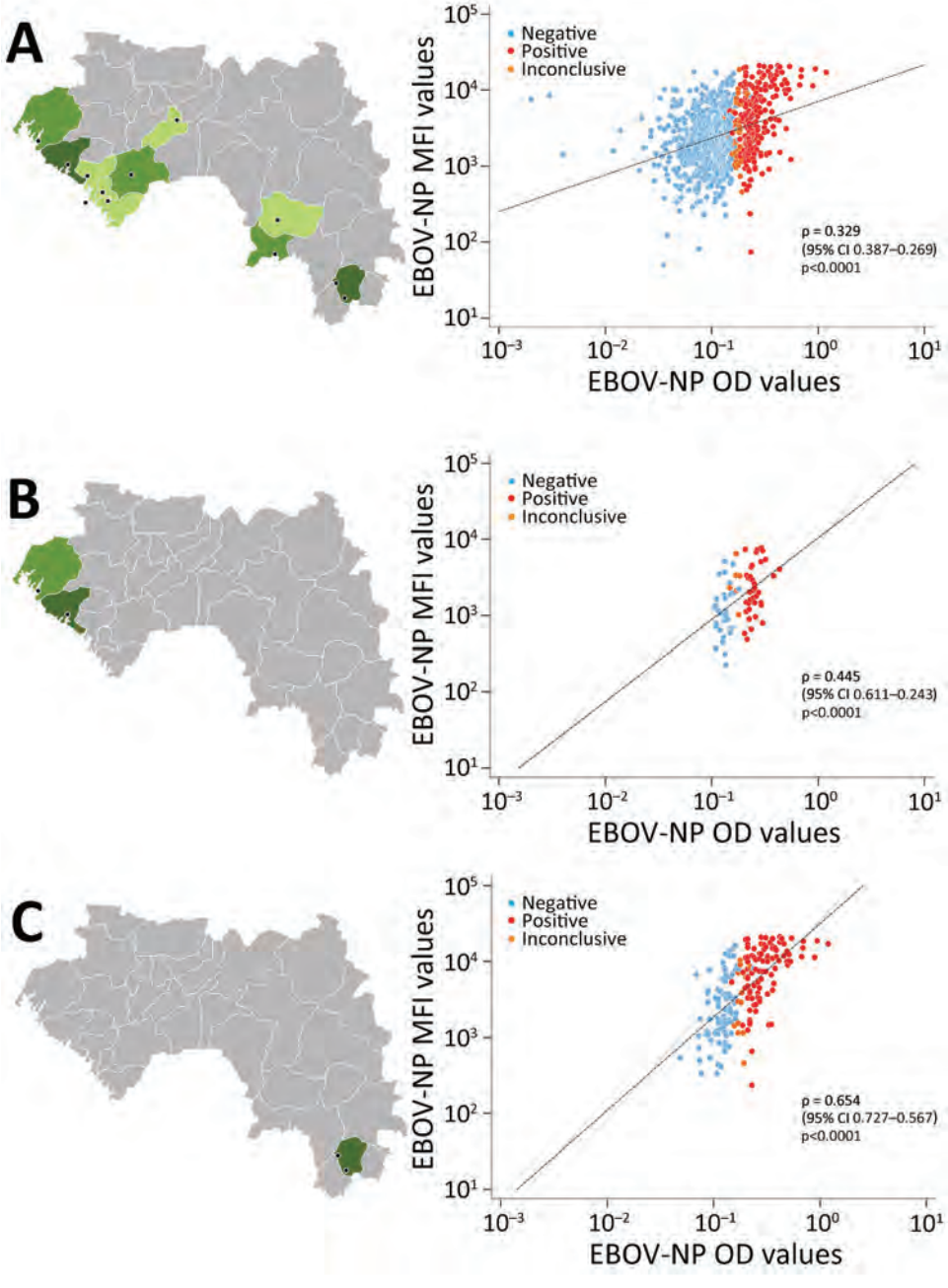

Figure 1. Correlation of indirect ELISA and multiplex microsphere immunoassay for EBOV-NP in study of geographic disparity in domestic pig population exposure to Ebola viruses, Guinea, 2017–2019. Scatter plots of MFI values obtained by multiplex microsphere immunoassay and OD values at 405 nm (OD 405) obtained by ELISA for pig serum samples are shown for all testing sites in Guinea (n = 882) (A), the northern coast (n = 75) (B), and the Forest Guinea (n = 196) (C). Black dashed lines represent reduced major axis lines; ρ indicates Spearman coefficient of rank correlation. Black dots on map indicate study location as detailed in Figure 3. EBOV, Zaire Ebola virus; MFI, mean fluorescence intensities; NP, nucleoprotein; OD, optical density.

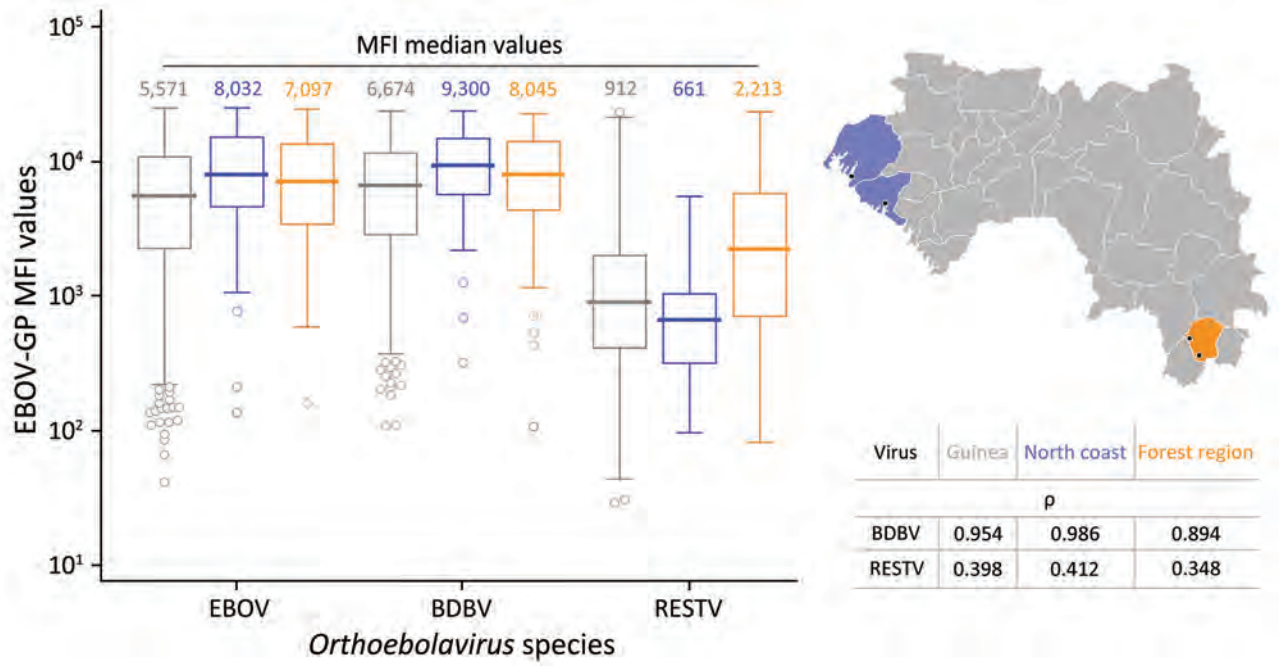

Figure 2. Pig serum samples tested by multiplex microsphere immunoassay against GP recombinant proteins of different *Orthoebolavirus* species in study of geographic disparity in domestic pig population exposure to Ebola viruses, Guinea, 2017–2019. MFI values of pig serum against EBOV, BDBV, and RESTV-GPs are shown for all testing sites in Guinea (gray), the northern coast (blue), and the Forest Guinea (orange), corresponding to locations on the map at right. Table outlines the Spearman coefficient of rank correlation (ρ) values between the species EBOV and each of the 2 species BDBV and RESTV. The associated p value was <0.0001 in all cases. Black dots on map indicate study location as detailed in Figure 3. BDBV, Bundibugyo virus; EBOV, Zaire Ebola virus; GP, glycoprotein; MFI, mean fluorescence intensities; RESTV, Reston virus.

the Maritime Guinea region (Boké, Boffa) (Figure 1, panel B), and data from Forest Guinea (Nzérékoré and Koulé) (Figure 1, panel C). When looking at all testing sites together (Figure 1, panel A), the 3 subgroups (negative, positive, and inconclusive) defined by the ELISA assay were not distinguishable by MFI values; the regression line tended to horizontal, and the global correlation coefficient was weak (n = 882, ρ = 0.329). The northern coast panel (Figure 1, panel B) showed a better correlation between both immunoassays (n = 75, ρ = 0.445). Finally, the highest correlation, at ≈2 times more than all testing sites in Guinea, was observed in Forest Guinea (n = 196, ρ = 0.654), where more positive serum samples clustered on the top right and negative serum samples clustered on the bottom left.

To further evaluate the specificity of the pig serum, we performed a multiplex analysis against the GPs of 3 *Orthoebolavirus* species: EBOV, BDBV, and RESTV. We compared the GP MFI distributions of all sites in Guinea, the northern coast, and Forest Guinea (Figure 2). Independent of the sample size or location, the median values of EBOV-GP (MFI 5,571) and BDBV-GP (MFI 6,674) were relatively close, supporting cross-reactivity between the different GPs as outlined by their amino-acid sequence identity of 70% (*41*). The median values of the RESTV-GP (MFI 913) were lower according to its amino acid sequence identity of only 58% with EBOV-GP (*41*,*42*). In addition, the reactivity against RESTV-GP of samples from Forest Guinea was clearly and significant higher (MFI 2,213) than that of samples from the northern coast (MFI 661) (p<0.0001 by Kolmogorov-Smirnov test).

Discussion

This study not only reinforces findings from previous studies regarding exposure of pigs to *Orthoebolavirus* species in Central and West Africa (*36*,*37*) but also sheds new light on the definition of potential regions at risk in Guinea. Although previous work demonstrated seroreactivity to EBOV-NP in 6.2% (19/308) of pig serum samples in pigsties around Conakry (*38*), by expanding data collection to 888 pig serum samples across Guinea, we demonstrated an overall seroreactivity of 25% (221/888) (i.e., 4× higher). Our collection from 12 different sites in Guinea covered most of the country's terrestrial ecosystems, from the ocean mangrove and swamp forest along the Atlantic littoral zone up to the evergreen and semideciduous rainforests in Forest Guinea (*43*). We only excluded the northeast part of Guinea from our investigation

because of the lower rates of pig farming in that region. We observed geographic disparities in orthoebolavirus exposure in pigs, regardless of sex and age.

The 2 hotspots of EBOV exposure for pigs were observed in pigsties with roof and outside openings in rural regions. However, the hotspots differed in ecologic conditions: 1 was in the ocean mangrove on the North Coast and 1 was in the mountain highlands of Forest Guinea where biodiversity is high. That different ecosystem might influence the exposure of pigs to orthoebolaviruses and explain the higher OD values in Koulé in Forest Guinea using either ELISA or MMIA technology.

We found a significant correlation between the 2 technologies for EBOV-NP detection, which was especially high in Forest Guinea (ρ = ≈0.7). In addition, multiplexing using the more specific GP proteins allowed us to compare 3 *Orthoebolavirus* species. The MMIA assay showed similar reaction patterns against EBOV-GP and BDBV-GP independent of the sampling location (*44*,*45*). However, reactivity to RESTV-GP was clearly higher in the southeast in Forest Guinea and less reactive in the northwest coastal region. That result is consistent with a previous study in Sierra Leone in which a pig only reacted with RESTV-NP (*36*). This similar finding between neighboring countries where pigs live in a bush habitat with probable wildlife contact suggests exposure to a different unidentified *Orthoebolavirus* species with possible zoonotic or pathogenic potential. BOMV recently discovered

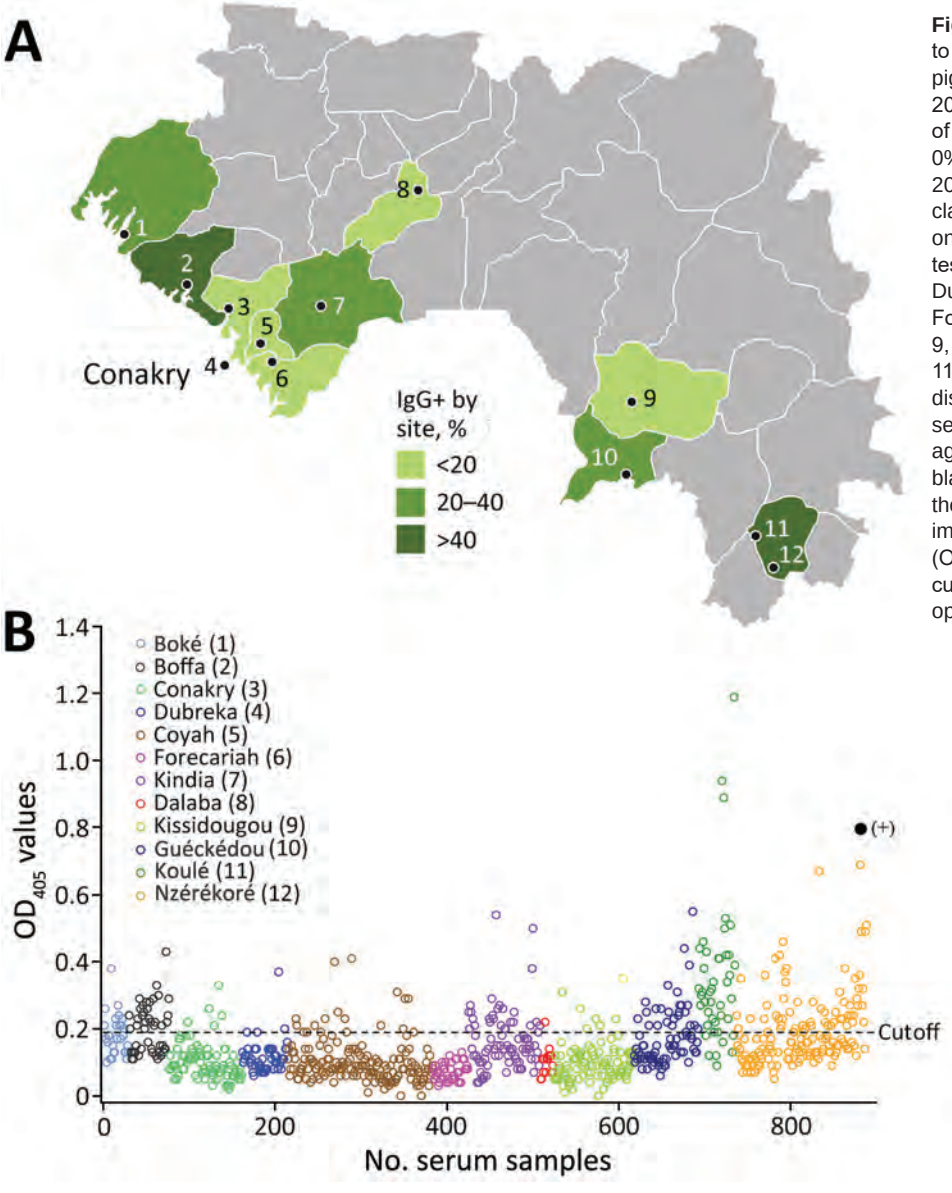

Figure 3. Disparity in seroreactivity to Zaire Ebola virus (EBOV) in pig farming regions, Guinea, 2017–2019. A) Spatial distribution of seroreactivity: lower class, 0%–20% seroreactivity; middle class, 20%–40% seroreactivity; and higher class, >40% seroreactivity. Numbers on map and in panel B key indicate testing sites: 1, Boké; 2, Boffa; 3, Dubreka; 4, Conakry; 5, Coyah; 6, Forecariah; 7, Kindia; 8, Dalaba; 9, Kissidougou; 10, Guéckédou; 11, Koulé; 12, Nzérékoré. B) Plot distribution of OD values of the 888 serum samples tested by ELISA against EBOV nucleoprotein. Solid black circle at right top represents the OD value of the serum from a pig immunized with EBOV-like particles (OD 0.8). Dashed line represents the cutoff value of the assay (0.19). OD, optical density.

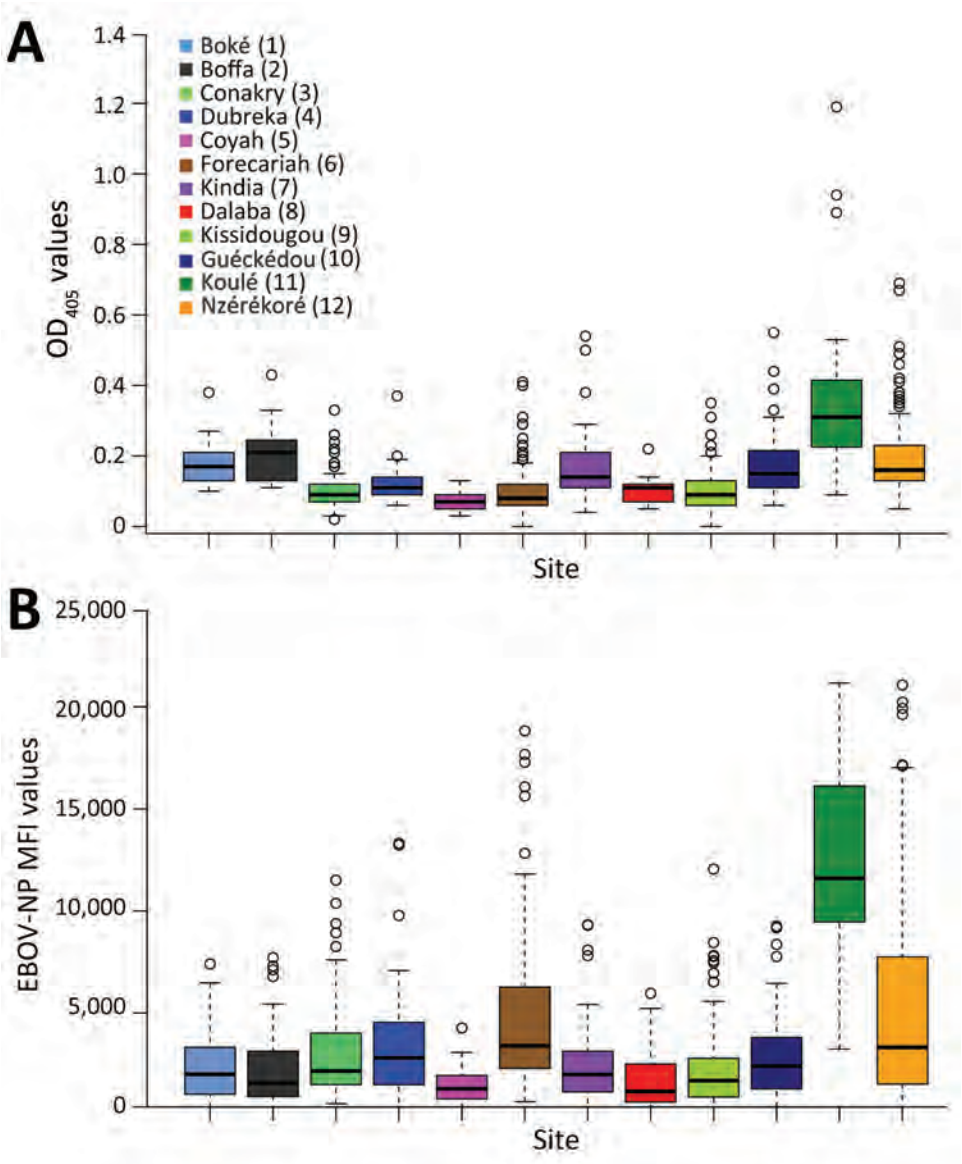

Figure 4. Comparison between results of indirect ELISA and multiplex microsphere immunoassay for EBOV-NP in study of geographic disparity in domestic pig population exposure to Ebola viruses, Guinea, 2017–2019. A) Boxplot of OD values at 405 nm (OD_{405}) obtained by ELISA by site (n = 888 pig serum samples). B) Boxplot of MFI values obtained by multiplex microsphere immunoassay (n = 882 pig serum samples). Locations in key correspond to locations on map in Figure 3. EBOV, Zaire Ebola virus; MFI, mean fluorescence intensities; NP, nucleoprotein; OD, optical density.

in insectivorous bats in both countries could be suspected to be phylogenetically positioned between RESTV and EBOV (*22*,*46*). Its detection in Nzérékoré in March 2019 occurred just before our campaign in Forest Guinea in June 2019. It should be noted that no positive pig serum was detected by RT-PCR using the RealStar Filovirus Screen RT-PCR kit 1.0, which is, however, unable to detect BOMV.

Overall, our study further emphasizes the need to deepen monitoring in areas of high seroprevalence in pigs and further evaluate filovirus pathogenicity for pigs and human. It would be key to conduct a joint investigation in humans, particularly in populations at risk (e.g., farmers, veterinarians, slaughterhouse workers), and to provide information about the risks of consuming undercooked pork products, which would be helpful for many pathogens (hepatitis E virus, Nipah virus, influenza A virus). The limitations of free-range pig husbandry and open sanitation in villages might also be considered to avoid pig exposure to EBOV from human shedding. In this study, however, a direct link with EBOV circulating in humans during the 2014–16 epidemic is highly improbable because sampling began at the end of 2017 (i.e., 1.5 years after the end of the epidemic) and most pigs tested were <1 year of age. Finally, in the One Health context, exploring the relevance of the specific ecologic surrounding of ocean mangrove or rainy forest is key. Bats have long been considered the most likely suspects, but more attention must be paid to peridomestic micromammals, such as rodents, which could serve as links between the village where they find

subsistence and wildlife in the forest. Pigs might be infected by their contaminated urine and feces. One experimental study has shown mutations associated with *Orthoebolavirus* adaptation to rodents (*47*). Investigating zoonotic *Orthoebolavirus* infection in rodents, as well as in pig populations at a local level to evaluate the potential risk of human exposure would be key.

Acknowledgments

We thank farmers who consented to participate in this study and veterinarians in Guinea for their expert collaborations during the sampling, particularly Madany Traoré. We also thank the Guinea authorities who authorized this study, especially the Ministry of Agriculture and Livestock. We would like to acknowledge Stefanie Rößler and Carolin Rüdiger for the antigen production used for the ELISA.

This study was funded by the German Federal Ministry of Food and Agriculture (EBOLA FORESIGHT project, Ref. 323–06.01–03-2815FSEBOL) and by the European Union (EBO-SURSY project, EU-FOOD/2016/379-660) piloted by World Organization for Animal Health.

About the Author

Dr. Grayo is a virologist at Institute Pasteur de Guinea. Her research interests are emerging viral infections and zoonoses. She currently focuses on viral hemorrhagic fevers and rodentborne diseases in West Africa.

References

1. Kuhn JH, Amarasinghe GK, Basler CF, Bavari S, Bukreyev A, Chandran K, et al.; Ictv Report Consortium. ICTV virus taxonomy profile: Filoviridae. J Gen Virol. 2019;100:911–2. https://doi.org/10.1099/jgv.0.001252
2. Matson MJ, Chertow DS, Munster VJ. Delayed recognition of Ebola virus disease is associated with longer and larger outbreaks. Emerg Microbes Infect. 2020;9:291–301. https://doi.org/10.1080/22221751.2020.1722036
3. Yamaoka S, Ebihara H. Pathogenicity and virulence of Ebolaviruses with species- and variant-specificity. Virulence. 2021;12:885–901. https://doi.org/10.1080/21505594.2021.1898169
4. Le Guenno B, Formenty P, Boesch C. Ebola virus outbreaks in the Ivory Coast and Liberia, 1994–1995. Curr Top Microbiol Immunol. 1999;235:77–84. https://doi.org/10.1007/978-3-642-59949-1_5
5. Stephens PR, Sundaram M, Ferreira S, Gottdenker N, Nipa KF, Schatz AM, et al. Drivers of African filovirus (Ebola and Marburg) outbreaks. Vector Borne Zoonotic Dis. 2022;22:478–90. https://doi.org/10.1089/vbz.2022.0020
6. Baize S, Pannetier D, Oestereich L, Rieger T, Koivogui L, Magassouba N, et al. Emergence of Zaire Ebola virus disease in Guinea. N Engl J Med. 2014;371:1418–25. https://doi.org/10.1056/NEJMoa1404505
7. Keita AK, Koundouno FR, Faye M, Düx A, Hinzmann J, Diallo H, et al. Resurgence of Ebola virus in 2021 in Guinea suggests a new paradigm for outbreaks. Nature. 2021;597:539–43. https://doi.org/10.1038/s41586-021-03901-9
8. Koundouno FR, Kafetzopoulou LE, Faye M, Renevey A, Soropogui B, Ifono K, et al. Detection of Marburg virus disease in Guinea. N Engl J Med. 2022;386:2528–30. https://doi.org/10.1056/NEJMc2120183
9. Wellington J, Nur A, Nicholas A, Uwishema O, Chaito H, Awosiku O, et al. Marburg virus outbreak in Ghana: an impending crisis. Ann Med Surg (Lond). 2022;81:104377. https://doi.org/10.1016/j.amsu.2022.104377
10. Hussain Z. Ghana declares its first outbreak of Marburg virus disease after two deaths. BMJ. 2022;378:o1797. https://doi.org/10.1136/bmj.o1797
11. Harris E. WHO: Marburg virus outbreak confirmed in Equatorial Guinea. JAMA. 2023;329:969. https://doi.org/10.1001/jama.2023.3199
12. Brauburger K, Hume AJ, Mühlberger E, Olejnik J. Forty-five years of Marburg virus research. Viruses. 2012;4:1878–927. https://doi.org/10.3390/v4101878
13. Kock RA, Begovoeva M, Ansumana R, Suluku R. Searching for the source of Ebola: the elusive factors driving its spillover into humans during the West African outbreak of 2013–2016. Rev Sci Tech. 2019;38:113–22. https://doi.org/10.20506/rst.38.1.2946
14. Caron A, Bourgarel M, Cappelle J, Liégeois F, De Nys HM, Roger F. Ebola virus maintenance: if not (only) bats, what else? Viruses. 2018;10:549. https://doi.org/10.3390/v10100549
15. Marí Saéz A, Weiss S, Nowak K, Lapeyre V, Zimmermann F, Düx A, et al. Investigating the zoonotic origin of the West African Ebola epidemic. EMBO Mol Med. 2015;7:17–23. https://doi.org/10.15252/emmm.201404792
16. Leroy EM, Epelboin A, Mondonge V, Pourrut X, Gonzalez JP, Muyembe-Tamfum JJ, et al. Human Ebola outbreak resulting from direct exposure to fruit bats in Luebo, Democratic Republic of Congo, 2007. Vector Borne Zoonotic Dis. 2009;9:723–8. https://doi.org/10.1089/vbz.2008.0167
17. Leroy EM, Kumulungui B, Pourrut X, Rouquet P, Hassanin A, Yaba P, et al. Fruit bats as reservoirs of Ebola virus. Nature. 2005;438:575–6. https://doi.org/10.1038/438575a
18. Pourrut X, Souris M, Towner JS, Rollin PE, Nichol ST, Gonzalez JP, et al. Large serological survey showing cocirculation of Ebola and Marburg viruses in Gabonese bat populations, and a high seroprevalence of both viruses in *Rousettus aegyptiacus*. BMC Infect Dis. 2009;9:159. https://doi.org/10.1186/1471-2334-9-159
19. Hassanin A, Nesi N, Marin J, Kadjo B, Pourrut X, Leroy É, et al. Comparative phylogeography of African fruit bats (Chiroptera, Pteropodidae) provide new insights into the outbreak of Ebola virus disease in West Africa, 2014–2016. C R Biol. 2016;339:517–28. https://doi.org/10.1016/j.crvi.2016.09.005
20. Ogawa H, Miyamoto H, Nakayama E, Yoshida R, Nakamura I, Sawa H, et al. Seroepidemiological prevalence of multiple species of Filoviruses in fruit bats (*Eidolon helvum*) migrating in Africa. J Infect Dis. 2015;212(Suppl 2):S101–8. https://doi.org/10.1093/infdis/jiv063
21. De Nys HM, Kingebeni PM, Keita AK, Butel C, Thaurignac G, Villabona-Arenas CJ, et al. Survey of Ebola viruses in frugivorous and insectivorous bats in Guinea, Cameroon, and the Democratic Republic of the Congo, 2015–2017. Emerg Infect Dis. 2018;24:2228–40. https://doi.org/10.3201/eid2412.180740
22. Goldstein T, Anthony SJ, Gbakima A, Bird BH, Bangura J, Tremeau-Bravard A, et al. The discovery of Bombali virus adds further support for bats as hosts of ebolaviruses. Nat

Microbiol. 2018;3:1084–9. https://doi.org/10.1038/s41564-018-0227-2
23. Towner JS, Pourrut X, Albariño CG, Nkogue CN, Bird BH, Grard G, et al. Marburg virus infection detected in a common African bat. PLoS One. 2007;2:e764. https://doi.org/10.1371/journal.pone.0000764
24. Weingartl HM, Nfon C, Kobinger G. Review of Ebola virus infections in domestic animals. Dev Biol (Basel). 2013;135:211–8. https://doi.org/10.1159/000178495
25. Weingartl HM, Embury-Hyatt C, Nfon C, Leung A, Smith G, Kobinger G. Transmission of Ebola virus from pigs to non-human primates. Sci Rep. 2012;2:811. https://doi.org/10.1038/srep00811
26. Boiro I, Lomonossov NN, Sotsinski VA, Constantinov OK, Tkachenko EA, Inapogui AP, et al. Clinico-epidemiologic and laboratory research on hemorrhagic fevers in Guinea [in French]. Bull Soc Pathol Exot Filiales. 1987;80:607–12.
27. Schoepp RJ, Rossi CA, Khan SH, Goba A, Fair JN. Undiagnosed acute viral febrile illnesses, Sierra Leone. Emerg Infect Dis. 2014;20:1176–82. https://doi.org/10.3201/eid2007.131265
28. McLean RK, Graham SP. The pig as an amplifying host for new and emerging zoonotic viruses. One Health. 2022;14:100384. https://doi.org/10.1016/j.onehlt.2022.100384
29. Kobinger GP, Leung A, Neufeld J, Richardson JS, Falzarano D, Smith G, et al. Replication, pathogenicity, shedding, and transmission of Zaire ebolavirus in pigs. J Infect Dis. 2011;204:200–8. https://doi.org/10.1093/infdis/jir077
30. Barrette RW, Metwally SA, Rowland JM, Xu L, Zaki SR, Nichol ST, et al. Discovery of swine as a host for the Reston ebolavirus. Science. 2009;325:204–6. https://doi.org/10.1126/science.1172705
31. Miranda ME, Miranda NL. Reston ebolavirus in humans and animals in the Philippines: a review. J Infect Dis. 2011;204(Suppl 3):S757–60. https://doi.org/10.1093/infdis/jir296
32. Pan Y, Zhang W, Cui L, Hua X, Wang M, Zeng Q. Reston virus in domestic pigs in China. Arch Virol. 2014;159:1129–32. https://doi.org/10.1007/s00705-012-1477-6
33. Marsh GA, Haining J, Robinson R, Foord A, Yamada M, Barr JA, et al. Ebola Reston virus infection of pigs: clinical significance and transmission potential. J Infect Dis. 2011;204(Suppl 3):S804–9. https://doi.org/10.1093/infdis/jir300
34. Haddock E, Saturday G, Feldmann F, Hanley PW, Okumura A, Lovaglio J, et al. Reston virus causes severe respiratory disease in young domestic pigs. Proc Natl Acad Sci U S A. 2021;118:e2015657118. https://doi.org/10.1073/pnas.2015657118
35. Atherstone C, Diederich S, Pickering B, Smith G, Casey G, Fischer K, et al. Investigation of Ebolavirus exposure in pigs presented for slaughter in Uganda. Transbound Emerg Dis. 2021;68:1521–30. https://doi.org/10.1111/tbed.13822
36. Fischer K, Jabaty J, Suluku R, Strecker T, Groseth A, Fehling SK, et al. Serological evidence for the circulation of ebolaviruses in pigs from Sierra Leone. J Infect Dis. 2018;218(suppl_5):S305–11. https://doi.org/10.1093/infdis/jiy330
37. Fischer K, Camara A, Troupin C, Fehling SK, Strecker T, Groschup MH, et al. Serological evidence of exposure to ebolaviruses in domestic pigs from Guinea. Transbound Emerg Dis. 2020;67:724–32. https://doi.org/10.1111/tbed.13391
38. Ogawa H, Ohya K, Ayizanga R, Miyamoto H, Shigeno A, Yamada M, et al. Detection of anti-ebolavirus antibodies in Ghanaian pigs. J Vet Med Sci. 2022;84:1491–4. https://doi.org/10.1292/jvms.22-0186
39. Karan LS, Makenov MT, Korneev MG, Sacko N, Boumbaly S, Yakovlev SA, et al. Bombali virus in *Mops condylurus* bats, Guinea. Emerg Infect Dis. 2019;25:1774–5. https://doi.org/10.3201/eid2509.190581
40. Vanhomwegen J, Beck C, Desprès P, Figuerola A, García R, Lecollinet S, et al. Circulation of zoonotic arboviruses in equine populations of Mallorca Island (Spain). Vector Borne Zoonotic Dis. 2017;17:340–6. https://doi.org/10.1089/vbz.2016.2042
41. Jacob ST, Crozier I, Fischer WA II, Hewlett A, Kraft CS, Vega MA, et al. Ebola virus disease. Nat Rev Dis Primers. 2020;6:13. https://doi.org/10.1038/s41572-020-0147-3
42. Kurosaki Y, Ueda MT, Nakano Y, Yasuda J, Koyanagi Y, Sato K, et al. Different effects of two mutations on the infectivity of Ebola virus glycoprotein in nine mammalian species. J Gen Virol. 2018;99:181–6. https://doi.org/10.1099/jgv.0.000999
43. Sayre RG, Comer P, Hak J, Josse C, Bow J, Warner H, et al. A new nap of standardized terrestrial ecosystems of Africa. Washington: Association of American Geographers; 2013.
44. Ayouba A, Touré A, Butel C, Keita AK, Binetruy F, Sow MS, et al. Development of a sensitive and specific serological assay based on Luminex technology for detection of antibodies to Zaire Ebola virus. J Clin Microbiol. 2016;55:165–76. https://doi.org/10.1128/JCM.01979-16
45. Manno D, Ayieko P, Ishola D, Afolabi MO, Rogers B, Baiden F, et al. Ebola virus glycoprotein IgG seroprevalence in community previously affected by Ebola, Sierra Leone. Emerg Infect Dis. 2022;28:734–8. https://doi.org/10.3201/eid2803.211496
46. Martell HJ, Masterson SG, McGreig JE, Michaelis M, Wass MN. Is the Bombali virus pathogenic in humans? Bioinformatics. 2019;35:3553–8. https://doi.org/10.1093/bioinformatics/btz267
47. Pappalardo M, Reddin IG, Cantoni D, Rossman JS, Michaelis M, Wass MN. Changes associated with Ebola virus adaptation to novel species. Bioinformatics. 2017;33:1911–5. https://doi.org/10.1093/bioinformatics/btx065

Address for correspondence: Solène Grayo, Virology Unit, Institut Pasteur de Guinée, Route de Donka, BP: 4416, Conakry, Guinea; email: solene.grayo.ext@pasteur.fr

Emergence of Poultry-Associated Human *Salmonella enterica* Serovar Abortusovis Infections, New South Wales, Australia

Michael Payne, Sarah Williamson, Qinning Wang, Xiaomei Zhang, Vitali Sintchenko, Anthony Pavic, Ruiting Lan

Salmonella enterica serovar Abortusovis is an ovine-adapted pathogen that causes spontaneous abortion. *Salmonella* Abortusovis was reported in poultry in 2009 and has since been reported in human infections in New South Wales, Australia. Phylogenomic analysis revealed a clade of 51 closely related isolates from Australia originating in 2004. That clade was genetically distinct from ovine-associated isolates. The clade was widespread in New South Wales poultry production facilities but was only responsible for sporadic human infections. Some known virulence factors associated with human infections were only found in the poultry-associated clade, some of which were acquired through prophages and plasmids. Furthermore, the ovine-associated clade showed signs of genome decay, but the poultry-associated clade did not. Those genomic changes most likely led to differences in host range and disease type. Surveillance using the newly identified genetic markers will be vital for tracking *Salmonella* Abortusovis transmission in animals and to humans and preventing future outbreaks.

Salmonella enterica serovar Abortusovis is a host-restricted pathogen of sheep that causes invasive disease and spontaneous abortion (*1*–*3*). Transmission is thought to be limited to sheep; however, early studies identified other potential carriers (*4*). Because *Salmonella* Abortusovisis is relatively rare, only a handful of studies have examined the molecular underpinning of its virulence. Other studies identified *astA*, *sodC1*, and *sseI* genes as virulence factors for invasive disease in lambs (*5*), and a mouse systemic infection model identified the *spv* toxin encoded on a plasmid as essential for virulence (*6*,*7*).

Previous examination of *Salmonella* Abortusovis epidemiology has exclusively relied on nongenomic molecular methods (*8*–*11*). Pulse-field gel electrophoresis (PFGE) and insertion sequence 200 fingerprinting have been used to identify clonal lineages in geographically distinct regions in Italy, Spain, Iran, and Switzerland (*3*,*10*–*13*). Cases and outbreaks in sheep have been described in several countries including Spain, Croatia, Switzerland, and Italy (*8*–*10*). However, the incidence of *Salmonella* Abortusovis animal infections in those and other countries is estimated to be underreported (*9*).

Salmonella Abortusovis is a reportable disease in sheep in Australia. Before 2009, the bacterium had not been reported in any animal (*14*). However, in 2009, *Salmonella* Abortusovis was detected in commercial poultry flocks in Australia (*15*) and was the second most common serovar in meat chickens in the country in 2016 (*16*). We examined the sudden emergence and proliferation of this serovar in poultry and humans in New South Wales (NSW), Australia, to investigate its evolution and implications to public health.

Author affiliations: University of New South Wales, Sydney, New South Wales, Australia (M. Payne, X. Zhang, R. Lan); Birling Laboratories, Bringelly, New South Wales, Australia (S. Williamson, A. Pavic); Institute of Clinical Pathology and Medical Research–NSW Health Pathology, Westmead Hospital, Westmead, New South Wales, Australia (Q. Wang, V. Sintchenko); University of Sydney, Sydney (V. Sintchenko)

DOI: https://doi.org/10.3201/eid3004.230958

Methods

Isolate Sources and Metadata

We analyzed genomes and metadata of 56 *Salmonella* Abortusovis isolates (Table 1; Figure 1). Of those isolates, 51 were from Australia, 47 of which we sequenced in this study. Poultry isolates from Australia were collected during 2013–2019 and were divided

Table 1. Characteristics of isolates used in a study of the emergence of poultry-associated human *Salmonella enterica* serovar Abortusovis infections, New South Wales, Australia*

Country	Bacterial source	Data source	No. isolates	Data type†
Australia	Poultry	This study	39	Illumina reads
Australia	Clinical	This study	8	Illumina reads
Australia	Clinical	NCBI	4	Assembly
Italy	Ovine	NCBI	1	Assembly
France	Unknown	NCBI	1	Illumina reads
Unknown	Unknown	NCBI	3	Illumina reads

*NCBI, National Center for Biotechnology Information (https://www.ncbi.nlm.nih.gov).
†Illumina (https://www.illumina.com).

into region A meat chickens (25 isolates), region B meat chickens (8 isolates), and egg-laying hens (6 isolates). Of the 33 isolates from regions A and B, 4 were from feed ingredients, 20 were from 10 farms in region A, and 8 were from 7 farms in region B. Multiple isolates were sampled from 5 region A farms and 1 region B farm. Human clinical isolates were collected during 2018–2020.

Sequencing and Assembly

We assembled draft genomes for all 47 isolates sequenced in this study and assembled complete genomes for 4 isolates (Table 1; Appendix 1, https://wwwnc.cdc.gov/EID/article/30/4/23-0958-App1.pdf; Appendix 2 Table 1, https://wwwnc.cdc.gov/EID/article/30/4/23-0958-App2.xlsx). We submitted all raw sequencing data to the National Center for Biotechnology Information BioProject database (no. PRJNA993380).

Phylogenetic Analyses

We used the complete genome of strain 180121-R1 as the reference because it was the earliest representative of the poultry-associated clade isolate in Australia. We used Snippy version 4.6.0 (*17*) to call single-nucleotide polymorphisms (SNPs) for both assemblies and read sets and to generate core SNP alignments. We used the core SNP alignment as an input to custom Python scripts (https://github.com/mjohnpayne/Aus_Abortusovis) to perform pairwise distance analysis. Then we used IQ-TREE versions 2.0.3 (*18*) with default settings to generate a phylogeny for all 56 genomes. We generated a multilocus sequence typing (MLST)–based phylogeny from all sequence types (STs) within 5 alleles of ST768 and visualized all phylogenies by using iTOL (*19*) (Appendix 1).

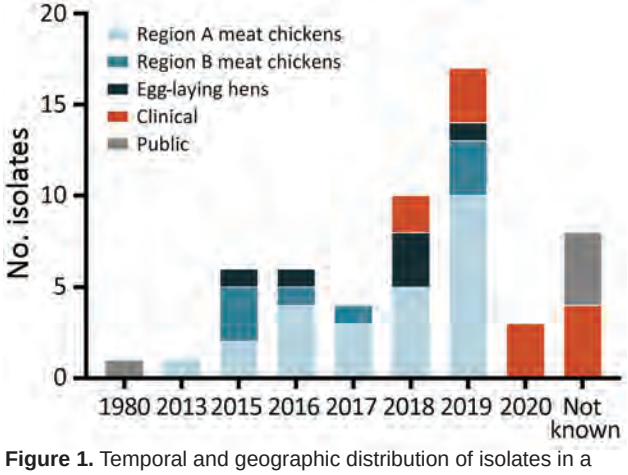

Figure 1. Temporal and geographic distribution of isolates in a study of the emergence of poultry-associated human *Salmonella enterica* serovar Abortusovis infections, New South Wales, Australia. Colors represent the region of isolation, isolates from human cases, and publicly available genomes.

Bayesian Analysis

We used BEAST version 2.6.3 (*20*) and 10,000,000 Markov chain Monte Carlo chain length to perform Bayesian phylogenetic reconstruction. A general time-reversible site model with a strict clock and coalescent constant population had the best effective sample size across 3 replicates, and we used that model to provide estimates of the most recent common ancestor (MRCA) date and evolutionary rate (Appendix 1).

Pan-Genome Analysis

We identified clade-specific genes by running roary version 3.13.0 (*21*) and default settings to define the pan-genome, and scoary version 1.6.16 (*22*) and default settings to identify clade-specific genes. We verified genes that were >80% sensitive and 100% specific for 1 clade by using KMA version 1.3.17 (*23*) and default settings to detect genes that were called absent because of assembly or annotation issues. We determined the presence of intact phages and plasmids in draft genomes by using KMA version 1.3.17 and default settings to search raw read data for phages and plasmids that were identified in complete assemblies.

Pseudogene and Genome Size Analysis

We used pseudofinder version 1.1 and default settings and a database of all uniprot protein sequences from *Salmonella* strains to detect pseudogenes (*24*). To compare genome size between the 2 *Salmonella* Abortusovis clades and exclude plasmids, we used the draft genome of isolate 405580-R1 to represent the poultry-associated clade because it lacks plasmids in the complete genome assembly. Similarly, the draft genome of ERR230420 appears to lack the pSLT-like plasmid likely found in the ovine-associated clade. We used draft genomes because the ovine-associated clade does not contain a complete genome for comparison and repetitive elements are often not assembled using Illumina (https://www.illumina.com) data. An

isolate or isolate DNA was not readily available to generate a complete genome for the ovine-associated clade for this study.

Virulence Factor Identification

We searched all assemblies by using ABRicate version 1.0.1, the virulence factor database (VFDB), and plasmidfinder gene database by using mincov and minid set to 80 (*25*–*27*). We validated ABRicate results by using KMA version 1.3.17 for raw read mapping (Appendix 1). We used PHASTEST to identify prophages in complete genomes (*28*). We used the same datasets and approach used in a previous study to identify and select *Salmonella* Abortusovis–specific gene markers (*29*) (Appendix 1).

Results

Distinct Poultry-Associated Clade

Phylogenetic analysis of the 56 isolates included in the study demonstrated that the 47 poultry and human clinical isolates from Australia represent a distinct poultry-associated clade that is at least 22,785 SNPs distant from the 9 *Salmonella* Abortusovis isolates from elsewhere, which formed an ovine-associated clade (Figure 2). The maximum pairwise SNP distance between isolates from Australia was only 42. Within the poultry-associated clade, we detected 2 subclades, 1 (subclade 1) containing 17 isolates and 1 (subclade 2) containing 34 isolates. Both subclades contained poultry isolates from regions A and B and human clinical isolates. Isolates from layer chickens were limited to a single lineage within subclade 2 and were not closely related to any human clinical isolates.

We also collected detailed source information that enabled a thorough examination of isolates at the farm level (Appendix 2 Table 2). We identified *Salmonella* Abortusovis in 2 feed ingredients, subclade 1 in canola and subclade 2 in blood meal, and in breeder hens that were progenitors of broiler chickens, suggesting possible modes of transmission. Among 17 farms, 6 had >1 isolate collected, 5 region A farms and 1 region B farm. Of note, 1 farm, A-4, contained isolates from both subclades 1 and 2, suggesting multiple introduction events (Figure 2). By contrast, all other farms contained isolates from only 1 subclade, and some were closely related across multiple years (i.e., farm B-6) suggesting long-term colonization by a single strain.

Because the poultry-associated clade was distant from other *S. enterica* Abortusovis strains, we examined the relationship of that clade to other serovars by using MLST. We located 5 additional *Salmonella* Abortusovis isolates in Enterobase (*30*). Those isolates had STs assigned but lacked genomic data, including 1 ovine isolate from Denmark (ST730) in 1920 and 1 from Italy (ST202) in 1980, plus 1 avian isolate from Australia in 2009 (ST786). We found that isolates from outside Australia that had genomic data were assigned to ST373 (6 isolates) and ST8760 (1 isolate). The ST assigned to the 2009 isolate from Australia, ST768, was also assigned to all isolates in the poultry-associated clade in this study. We identified all STs that were similar to ST768 and generated a phylogeny from MLST allele sequences. That phylogeny demonstrated that the poultry-associated clade was more closely related to the ovine-associated *Salmonella* Abortusovis clade than to any other serovars (Figure 3).

Estimation of MRCA for the Poultry-Associated Clade

Salmonella Abortusovis was observed in poultry in Australia beginning in 2009. We estimated the age of the poultry-associated clade by using temporal Bayesian analysis to determine whether that was the origin of the clade, or the clade was older. We estimated the date of the MRCA of the poultry-associated clade to be September 2004 (highest posterior density October 1998–August 2009) with a mutation rate of 2.43×10^{-7} (highest posterior density 1.55 to 3.28×10^{-7}) SNPs/site/year, equivalent to 1.19 (range 0.76–1.61) SNPs/genome/year.

Plasmids in the Poultry-Associated Clade

To characterize the plasmid complement of the poultry-associated clade, we generated complete genomes, including closed plasmid sequences for 4 isolates: 180121-R1, 401964-R1, 405987-R1, and 405580-R1 (Table 2). We found that 405580-R1 carried no plasmids, but 180121-R1 and 401964-R1 contained the same 139-kb plasmid (pSAbAus), which carried the *Yersinia* high pathogenicity island (HPI) encoding yersiniabactin, a vertebrate lysozyme inhibitor (*ivy*), and a colicin secretion protein (*cvaA*). Isolate 405987-R1 carried a 60-kb plasmid that is identical to pSAbAus with a 79-kb deletion, which included the HPI, *ivy*, and *cvaA* loci. Isolate 401964-R1 also carried an additional 33-kb plasmid that is identical to pRHB32-C15_3 (GenBank accession no. CP057236.1) apart from 12 SNPs. Plasmid pRHB32-C15_3 was isolated from an *Escherichia coli* isolate on a sheep farm in the United Kingdom in 2017. We identified plasmid Inc types in all genomes and identified IncFIB(K)_1_Kpn3 in 45 genomes and on the 139-kb and 60-kb plasmids in complete genomes.

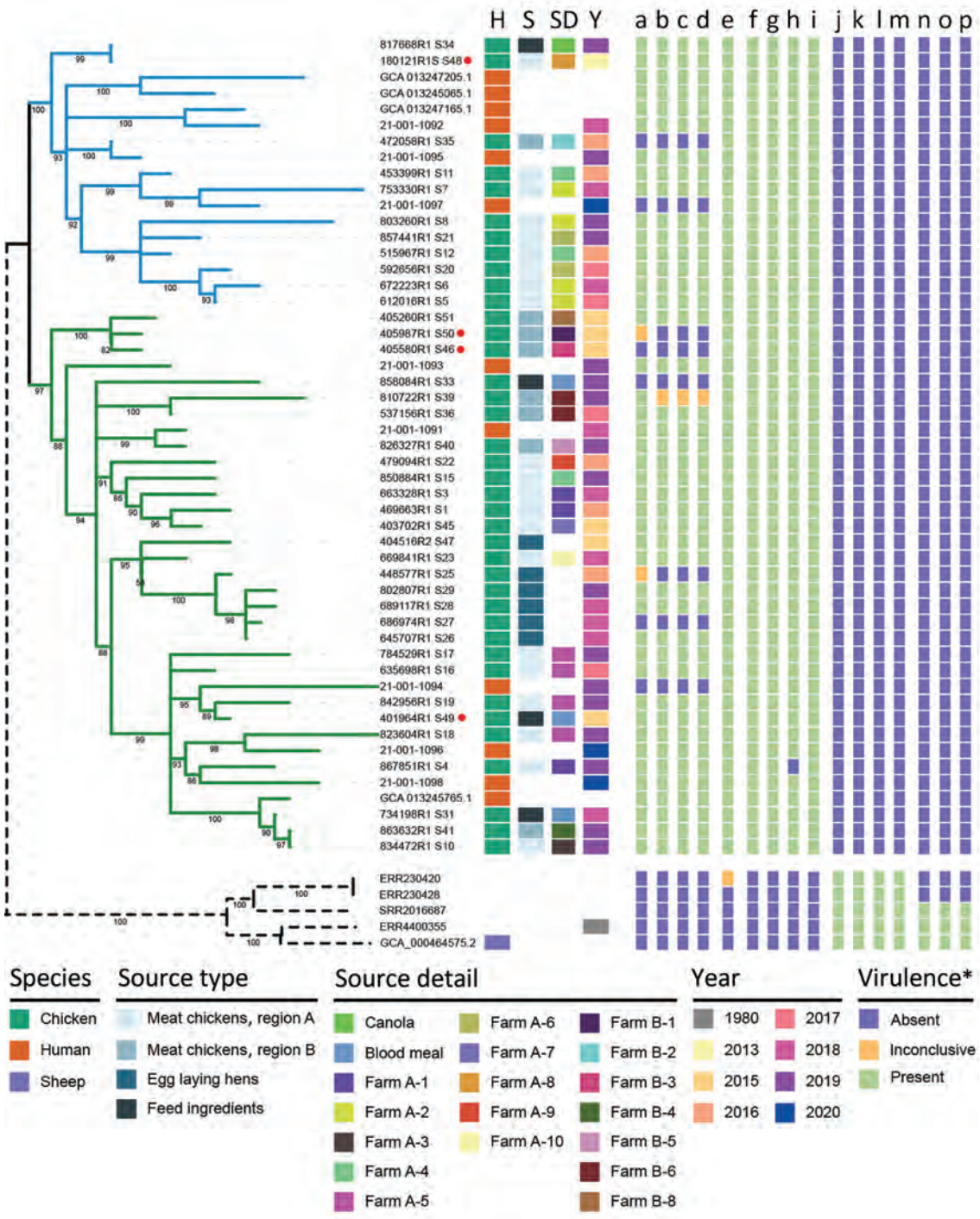

Figure 2. Phylogenetic relationships of isolates and associated metadata in a study of the emergence of poultry-associated human *Salmonella enterica* serovar Abortusovis infections, New South Wales, Australia. A maximum-likelihood phylogeny of all 56 isolates including subclade annotation and relevant metadata. Branches colors indicate subclades 1 (blue) and 2 (green) and bootstrap support values are indicated at tree nodes. Branch lengths for 5 international isolates were shortened for clarity (dashed lines). Red dots indicate complete genomes. Colors in columns indicate host species, source type, source details, year of isolation, and presence or absence of virulence genes. Virulence genes were predicted by using abricate (https://github.com/tseemann/abricate), KMA (*23*), and VFDB (*25*): a) pSAbAus; b) yersinia HPI (11 genes); c) *ivy*; d) *cvaA*; e) *cdtB*; f) *cfaB*; g) *stfF*; h) *hdeB*; i) *eutEJGHABCLKR*; j) *astA*; k) *sodCI*; l) *ompN*; m) *hcp1*; n) pSLT-like plasmid; o) *spv* toxin (3 genes); p) Fimbriae *klf/fae* (6 genes). *Some virulence genes or islands have the same presence and absence pattern in all genes; those data are collapsed into 1 column and the number of genes are indicated in parentheses in the list. Inconclusive gene presence was assigned when only KMA identified the gene and it had <20% of the normalized genome coverage. H, host species; S, source; SD, source details; Y, year.

We examined draft genomes of the remaining isolates for plasmids that we had identified in the complete genomes, and only detected pSAbAus in the poultry-associated clade. We found the complete plasmid in 42 isolates, including 2 complete genomes, and it was partially extant in 2 isolates, including 405987-R1, but was absent from 7 isolates, including 405580-R1 (Figure 2). We detected the pRHB32-C15_3 plasmid in 13 poultry-associated clade isolates (Appendix 2 Table 3).

Three genomes in the ovine-associated clade contained an IncFII(S)_1 gene and Spv toxin encoding genes *spvC*, *spvD*, and *spvR*, which are typical of *Salmonella* virulence plasmids, such as pSLT from *Salmonella* Typhimurium. Those 3 strains also contained regions 35,184–38,729 bp in length that match to the pSLT plasmid at >97% identity. Taken together, those findings show that the 3 strains likely contain a *Salmonella* virulence plasmid. However, determining the makeup of that plasmid is difficult because no complete genomes were available in the ovine-associated clade. We did not observe any evidence of a classical virulence plasmid in the other 2 strains in the ovine-associated clade or the poultry-associated clade.

Prophage Variation within the Poultry-Associated Clade

We identified prophage complements of poultry-associated clade isolates in the 4 complete genomes and identified 6 intact prophages and 1 questionable prophage (Table 3). We used the intact prophages to infer the prophage complement of isolates without complete genomes (Table 3; Appendix 2 Table 3). Of those isolates, Gifsy-2 was in all isolates from the poultry-associated clade and was the only prophage carrying a virulence factor, cytolethal distending toxin gene *cdtB* (Figure 2). All prophages were most similar to prophages in other *Salmonella* serovars, except Abortus_SfV, which was most similar to a prophage from *Shigella flexneri* (*31*).

Pan-Genome Differences between Ovine- and Poultry-Associated Clades

To identify factors that might contribute to the different host range of the poultry- and ovine-associated clades, we examined pan-genomes to identify genes associated with either clade (Figure 2). There were 433 genes unique to the poultry-associated clade, 278 of which have no known function. Among the other 155 genes, 23 are found within prophages and 55 within the pSAbAus plasmid. The 77 chromosomal genes unique to the poultry-associated clade included 2 predicted fimbrial subunit genes, *cfaB* and *stfF*; an acid resistance chaperone protein gene, *hdeB*; and 10 (*eutEJGHABCLKR*) of the 17 (*eutSPQTDMNEJGHABCLKR*) genes of the ethanolamine utilization operon (Figure 2).

The ovine-associated clade contained 130 unique genes, 62 of which have no known function. Unique genes included *astA* and *sodC1*, which have previously been identified on a Gifsy-2 phage in this clade (*5*), as well as an outer membrane porin gene, *ompN*, and *hcp1*, a type 6 secretion system gene. However, because of the lack of a complete genome in the ovine-associated clade, we could not confirm the location of those specific genes.

All isolates contained intact or nearly intact chromosomal gene sets for *Salmonella* pathogenicity islands 1, 2, 3, and 24 (also called CS54) and for the enterobactin gene cluster and 3 types of fimbriae. We also detected virulence genes *ompA* and *mig-14* in all isolates.

Ovine-Associated Clade Genomic Markers of Host Adaptation

Genome size and pseudogene number can be indicators of host restriction. Therefore, we compared those metrics between the ovine- and poultry-associated clades. A representative ovine-associated clade genome was 315 Kbp (7.1%) smaller than a representative poultry-associated clade genome (4.43 Mbp vs. 4.74 Mbp). The average ovine-associated clade genome contained 446 (range 384–667) pseudogenes, but the poultry-associated clade had 237 (range 224–248) pseudogenes (Appendix 1). That contrasting difference in the number of pseudogenes is similar in magnitude to generalist and host restricted *Salmonella* serovars. Generalist serovar Typhimurium has 201 and serovar Enteritidis has 320 pseudogenes; host-restricted serovar Typhi has 485 and serovar Gallinarium has 510 pseudogenes.

Identification and Validation of *Salmonella* Abortusovis Serovar-Specific Gene Markers

We searched for candidate-specific gene markers for the poultry-associated clade and for *Salmonella* Abortusovis in the accessory genomes of a dataset of 106 common serovars including *Salmonella* Abortusovis (Appendix 1). We identified 2 *Salmonella* Abortusovis markers and 2 poultry-associated clade markers with 100% sensitivity and 100% specificity (Table 4) and provided DNA sequences of those 4 *Salmonella* Abortusovis serovar-specific gene markers (Appendix 2 Table 1).

Discussion

Salmonella Abortusovis is an ovine-adapted serovar and not known to cause disease in humans (*3*,*6*).

The bacterium is endemic in several countries in Europe and Asia but has not been observed in the sheep population of Australia despite strong biosecurity surveillance and the serovar being notifiable (*8*–*10*,*33*). However, *Salmonella* Abortusovis was the second most frequent serovar in meat chickens in Australia in 2009 (*14*). We sequenced 47 isolates from poultry and human infections in Australia and compared those with 9 publicly available *Salmonella* Abortusovis genomes to understand the relationship

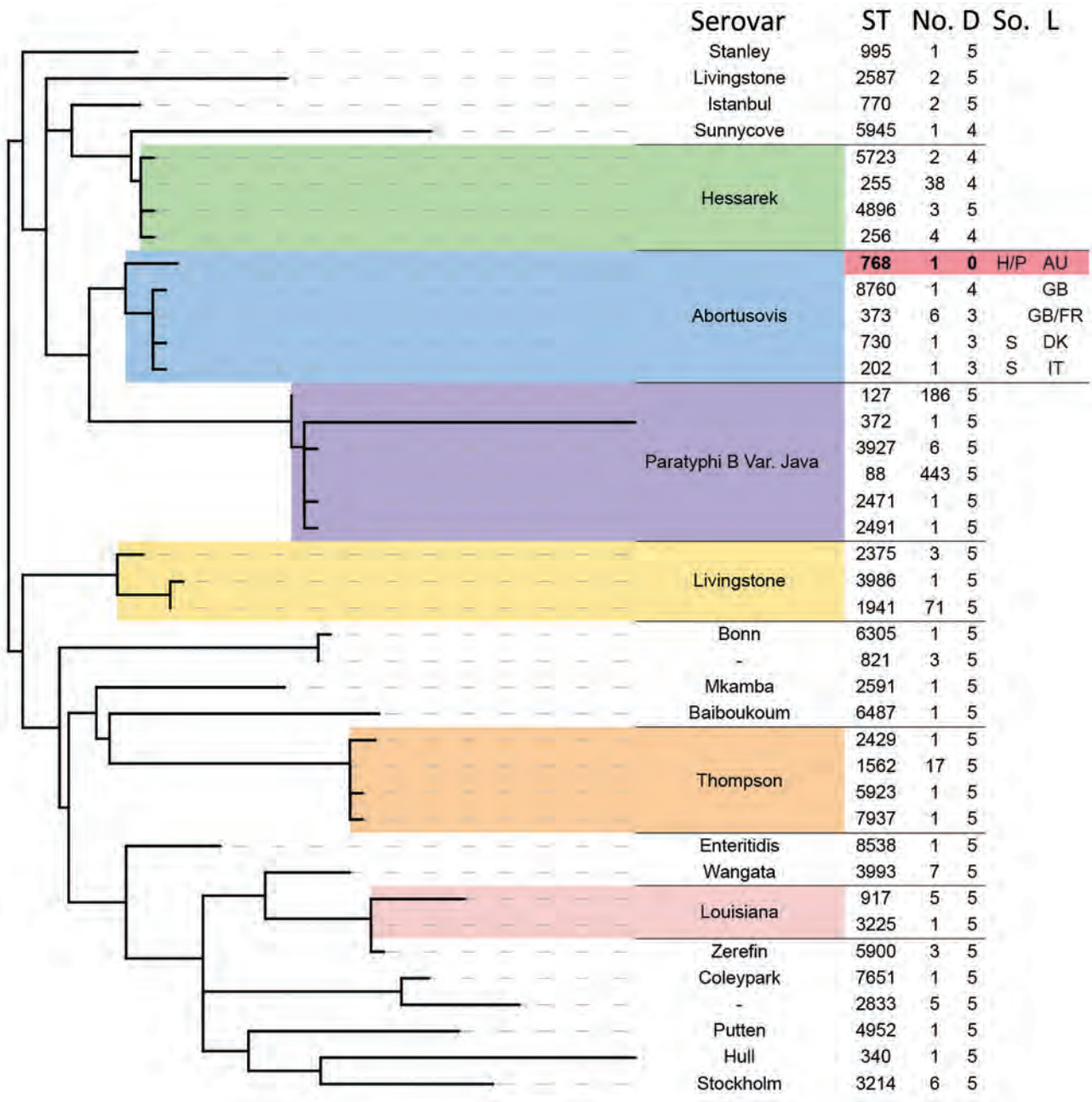

Figure 3. Phylogenetic relationship of other serovars to isolates in a study of the emergence of poultry-associated human *Salmonella enterica* serovar Abortusovis infections, New South Wales, Australia using MLST sequence data. Sequence types in the Enterobase database with five or fewer allele differences from the Australian ST768 (shaded in red) were identified and used to generate a phylogeny of related *Salmonella* isolates using maximum likelihood method. All branches with less than 50% bootstrap support were collapsed. The ST at each terminal branch is shown, as is the number of isolates in the Enterobase database assigned that ST and the number of allele differences from ST768. Available source and location data for *Salmonella* Abortusovis STs are displayed. Two letter abbreviations are used for country of origin. AU, Australia; D, allele difference from ST 768; DK, Denmark; FR, France; GB, Great Britain; H, human; IT, Italy; L, location; P, poultry; S, sheep; So., source; ST, sequence type.

Table 2. Plasmids identified in a study of the emergence of poultry-associated human *Salmonella enterica* serovar Abortusovis infections, New South Wales, Australia*

Plasmid	Genomes		Length, bp	Virulence gene carriage	Inc type
	Complete	Draft†			
pSAbAus	3, 1 partial	39, 1 partial	139,222	Yersinia HPI, *ivy*, *cvaA*	IncFIB(K)_1_Kpn3
pRHB32-C15(3)	1	12	60,178	None	IncX1_1

*HPI, high-pathogenicity island.
†Plasmid presence in draft genomes Inferred from reads.

between isolates from Australia and those from other countries and sources.

All isolates from Australia formed 1 closely related clade that is distant from the ovine-associated clade of *Salmonella* Abortusovis (Figures 1, 2). The 2004 MRCA date of the poultry-associated clade also indicates that it has existed in the NSW poultry flock for 15–20 years, a finding supported by the reported observation of *Salmonella* Abortusovis in NSW in 2009 (*15*). The relationships of the isolates sampled suggest that the serovar in poultry in Australia originated from a single introduction, however because no related isolates have been identified, the source is unknown.

Analysis of the pan genomes of all *Salmonella* Abortusovis isolates revealed substantial differences between the poultry-associated (433 unique genes) and ovine-associated clades (130 unique genes). A subset of those unique genes can be attributed to the 5 prophages and 2 plasmids only found in the poultry-associated clade and 1 putative plasmid only found in the ovine-associated clade.

Although all *Salmonella* Abortusovis isolates shared a complement of virulence factors, we noted some key differences. The poultry-associated clade carried *Yersinia* HPI, *cvaA*, and *ivy* on a plasmid, and *cdtB* on a prophage. The *Yersinia* HPI is a virulence factor in multiple human pathogens (*34*–*37*), and *cdtB* is a virulence factor in both typhoidal and nontyphoidal *Salmonella* (*38*). Other poultry-associated clade–specific genes included *hdeB*, which is known to contribute to acid resistance in *Salmonella* Enteritidis (*39*), and *ivy*, which encodes a vertebrate lysozyme inhibitor that improves survival in human saliva (*40*). Both genes could improve the chances of survival of the bacterium through the human upper gastrointestinal tract. The colicin export protein gene, *cvaA*, and the ethanolamine utilization operon, *eut*, found in 10 of 17 genes of the poultry-associated clade might contribute to infection by enabling colonization through competition with gut microbiota (*41*). Of note, ethanolamine in the host also triggers the *eutR* gene to activate SPI2 expression and increases intramacrophage survival (*42*). The fimbrial gene *cfaB* is upregulated in *Salmonella* Typhi human infection and *stfF* is upregulated in *Salmonella* Typhimurium chicken infection, but their contributions to survival and virulence are unknown (*43*,*44*).

In the ovine-associated clade, the *sodC1* gene is essential for systemic disease in lambs (*5*). The Spv toxin was essential in a murine infection model (*6*,*7*). The *spv* genes and associated pSLT-like putative plasmid were only found in 3 of 5 ovine-associated clade isolates, suggesting that virulence within that clade might vary. Indeed, the severity of *Salmonella* Abortusovis infections in sheep is known to vary greatly (*45*). Virulence genes that are specific to the ovine-associated clade include *ompN*, which is associated with survival in macrophages in *Salmonella* Typhi (*46*), and *hcp*, which is required for killing of commensal bacteria in *Salmonella* Typhimurium (*47*). The clade-specific genes and gene sets described here might explain the potential differences in host range and disease type between the ovine-associated and poultry-associated clades.

Salmonella Abortusovis was previously thought to be host restricted in sheep (*45*). Host restriction often leads to adaptations, including a reduction

Table 3. Prophages identified in a study of the emergence of poultry-associated human *Salmonella enterica* serovar Abortusovis infections, New South Wales, Australia*

Prophage†	Genomes		Length, kb	Condition§	Top PHASTEST hit	Virulence genes
	Complete	Draft‡				
Abortus_SEN8	4	43	57.2	Intact	Salmon_SEN8_NC_047753	None
Abortus_SfV	3	30	48.9	Intact	Entero_SfV_NC_003444	None
Abortus_Gifsy-2	4	43	30.1	Intact	Gifsy-2_NC_010393	*cdtB*
Abortus_Fels_1	4	43	33.2	Questionable	Salmon_Fels_1_NC_010391	None
Abortus_SPN9CC	3	18	39.1	Intact	Salmon_SPN9CC_NC_017985	None
Abortus_SPN3UB	1	22	46.7	Intact	Salmon_SPN3UB_NC_019545	None

*PHASTEST, PHAge Search Tool with Enhanced Sequence Translation (https://phastest.ca).
†Prefixed with Abortus for *Salmonella* Abortusovis.
‡Inferred from reads. 4 poultry associated clade and 1 ovine associated clade isolates could not be examined as no reads were available.
§Per PHASTEST.

Table 4. Sensitivity and specificity of serovar-specific gene markers in a study of the emergence of poultry-associated human *Salmonella enterica* serovar Abortusovis infections, New South Wales, Australia*

Specific genes	No. isolates	Length, bp	Sensitivity†	Specificity†		Protein function
				Identification, n = 2,314	Validation, n = 1,088	
Abortusovis-gene1	56	2,367	100	100	100	DUF6430
Abortusovis-gene2	56	330	100	100	100	Hypothetical
Abortusovis-AUS-gene1	51	831	100	100	100	DUF4238
Abortusovis-AUS-gene2	51	810	100	100	100	Hypothetical

*AUS, Australia; FN, false negative; TN, true negative; TP, true positive.
†We used sensitivity and specificity as described in previous studies (*29*,*32*), where sensitivity is TP/(TP+FN) and specificity is TN/(TN+FP). Per those studies, we defined FN as the genomes from *Salmonella* Abortusovis lacking any of those same gene markers; FP as the genomes from other serovars containing all those same gene markers; TN as the genomes from other serovars lacking any of those same gene markers; and TP as the genomes from *Salmonella* Abortusovis containing all specific gene markers for *Salmonella* Abortusovis.

in genome size and an increase in pseudogenization (*48*). The average number of pseudogenes in an ovine-associated clade isolate is double the average of a poultry-associated clade isolate, and the average genome was 7.1% smaller. The pseudogene count of the poultry-associated clade was also similar to those of generalist serovars, such as *Salmonella* Typhimurium and *Salmonella* Enteritidis, but the ovine-associated clade was similar to the host restricted serovars *Salmonella* Typhi and *Salmonella* Gallinarium. Those results suggest that the ovine-associated clade might be host adapted and the poultry-associated clade likely has a broader host range. That hypothesis is supported by the data in this study, namely, the ability of the poultry associated clade to infect both chickens and humans.

One of the plasmids in the poultry-associated clade is very closely related to an *E. coli* plasmid found on a sheep farm in the United Kingdom (*49*), suggesting that the poultry-associated clade was linked with sheep. However, the link is more likely to be indirect through the *E. coli* host.

The epidemiology of the isolates in this study demonstrated that the poultry-associated clade was widely distributed in NSW poultry and caused sporadic human infections. *Salmonella* Abortusovis was sampled across 8 years and was found in feed ingredients, in egg-laying hens, and in 20 different meat chicken farms from 2 regions. In addition, isolates from both region A and region B were found in each of the subclades in the phylogeny, suggesting that *Salmonella* Abortusovis has no geographic barriers. One exception was the egg layer hen population that formed a single group within subclade 2, indicating a single introduction. We also noted evidence for both long-term carriage of a single clone in 1 farm and multiple separate introductions into another farm. Isolation of *Salmonella* Abortusovis from feed ingredients suggests that transmission might have occurred through feed, but we found no identical isolates within short timespans in feed or chickens that would indicate direct transmission. Isolates from human infections were distributed across the phylogeny, suggesting that multiple separate transmission events to humans occurred; however, none caused large outbreaks. *Salmonella* Abortusovis does not efficiently transmit to humans from poultry (*50*), which might explain the low number of sporadic human cases despite the widespread detection in poultry.

The ability of the poultry-associated clade to colonize poultry and cause human disease, and the possibility that it might not cause systemic disease in lambs, make detection and differentiation of this clade from the ovine-associated clade useful. The genetic markers identified here will enable simple differentiation of the 2 *Salmonella* Abortusovis clades by using genomic data and potentially decrease root cause analysis time for detection of this novel *Salmonella* in the food industry. All markers described here could be used to produce PCR-based assays that would enable simple detection and differentiation of *Salmonella* Abortusovis clades, which is necessary because of their ability to either cause human infections or cause major losses of sheep flocks.

In conclusion, we examined the genomic epidemiology of *Salmonella* Abortusovis in poultry and human infections in NSW, Australia. The poultry-associated clade was only distantly related to existing examples of *Salmonella* Abortusovis and had key differences in virulence factors that suggest it might have differences in host range and disease type. Evidence suggests that the serotype has become endemic within the NSW poultry industry, where it can move between poultry facilities and to humans. Surveillance using the newly identified genetic markers will be vital for tracking transmission within poultry producing regions and to prevent any future outbreaks that could be caused by this serovar.

This work was supported by The National Health and Medical Research Council of the Australian Government (grant no. 1146938).

S.W. and A.P. are employed by Birling Laboratories and provided poultry isolates and metadata.

About the Author

Dr. Payne is a postdoctoral research associate at the University of New South Wales Sydney in Sydney, NSW, Australia. His research interests focus on the use of genomics to describe the population structures and evolution of bacterial pathogens.

References

1. Jack E. *Salmonella* Abortus Ovis—an atypical *Salmonella*. Vet Rec. 1968;82:558.
2. Pardon P, Sanchis R, Marly J, Lantier F, Pépin M, Popoff M. Ovine salmonellosis caused by *Salmonella* abortus ovis [in French]. Ann Rech Vet. 1988;19:221–35.
3. Belloy L, Decrausaz L, Boujon P, Hächler H, Waldvogel AS. Diagnosis by culture and PCR of *Salmonella* Abortusovis infection under clinical conditions in aborting sheep in Switzerland. Vet Microbiol. 2009;138:373–7. https://doi.org/10.1016/j.vetmic.2009.03.026
4. Vodas K, Marinov MF, Shabanov M. *Salmonella* abortus ovis carrier state in dogs and rats [in Bulgarian]. Vet Med Nauki. 1985;22:10–5.
5. Bacciu D, Falchi G, Spazziani A, Bossi L, Marogna G, Leori GS, et al. Transposition of the heat-stable toxin *astA* gene into a gifsy-2-related prophage of *Salmonella enterica* serovar Abortusovis. J Bacteriol. 2004;186:4568–74. https://doi.org/10.1128/JB.186.14.4568-4574.2004
6. Colombo MM, Leori G, Rubino S, Barbato A, Cappuccinelli P. Phenotypic features and molecular characterization of plasmids in *Salmonella abortusovis*. Microbiology. 1992; 138:725–31. https://doi.org/10.1099/00221287-138-4-725
7. Uzzau S, Gulig PA, Paglietti B, Leori G, Stocker BA, Rubino S. Role of the *Salmonella* Abortusovis virulence plasmid in the infection of BALB/c mice. FEMS Microbiol Lett. 2000;188:15–8. https://doi.org/10.1111/j.1574-6968.2000.tb09161.x
8. Habrun B, Listes E, Spicic S, Cvetnic Z, Lukacevic D, Jemersic L, et al. An outbreak of *Salmonella* Abortusovis abortions in sheep in south Croatia. J Vet Med B Infect Dis Vet Public Health. 2006;53:286–90. https://doi.org/10.1111/j.1439-0450.2006.00959.x
9. Wirz-Dittus S, Belloy L, Hüssy D, Waldvogel AS, Doherr MG. Seroprevalence survey for *Salmonella* Abortusovis infection in Swiss sheep flocks. Prev Vet Med. 2010;97:126–30. https://doi.org/10.1016/j.prevetmed. 2010.08.007
10. Valdezate S, Astorga R, Herrera-León S, Perea A, Usera MA, Huerta B, et al. Epidemiological tracing of *Salmonella enterica* serotype Abortusovis from Spanish ovine flocks by PFGE fingerprinting. Epidemiol Infect. 2007;135:695–702. https://doi.org/10.1017/S0950268806007060
11. Dionisi AM, Carattoli A, Luzzi I, Magistrali C, Pezzotti G. Molecular genotyping of *Salmonella enterica* Abortusovis by pulsed field gel electrophoresis. Vet Microbiol. 2006;116:217–23. https://doi.org/10.1016/j.vetmic.2006.03.008
12. Schiaffino A, Beuzón CR, Uzzau S, Leori G, Cappuccinelli P, Casadesús J, et al. Strain typing with IS200 fingerprints in *Salmonella* abortusovis. Appl Environ Microbiol.1996;62:2375–80. https://doi.org/10.1128/aem.62.7.2375-2380.1996
13. Nikbakht GH, Raffatellu M, Uzzau S, Tadjbakhsh H, Rubino S. IS200 fingerprinting of *Salmonella enterica* serotype Abortusovis strains isolated in Iran. Epidemiol Infect. 2002;128:333–6. https://doi.org/10.1017/S0950268801006732
14. Australian Government Department of Agriculture, Fisheries and Forestry. Animal Health Australia 2009. Canberra (ACT), Australia: The Department; 2010.
15. Heuzenroeder MW, Ross IL, Hocking H, Davos D, Young CC, Morgan G. An integrated typing service for the surveillance of *Salmonella* in chickens. Barton (ACT): Rural Industries Research and Development Corporation, Australian Government; 2013.
16. Abraham S, O'Dea M, Sahibzada S, Hewson K, Pavic A, Veltman T, et al. *Escherichia coli* and *Salmonella* spp. isolated from Australian meat chickens remain susceptible to critically important antimicrobial agents. PLoS One. 2019; 14:e0224281. https://doi.org/10.1371/journal.pone.0224281
17. Seemann T. snippy: fast bacterial variant calling from NGS reads, version 3.1 [cited 2020 Apr 19]. https://github.com/tseemann/snippy
18. Minh BQ, Schmidt HA, Chernomor O, Schrempf D, Woodhams MD, von Haeseler A, et al. IQ-TREE 2: new models and efficient methods for phylogenetic inference in the genomic era. Mol Biol Evol. 2020;37:1530–4. https://doi.org/10.1093/molbev/msaa015
19. Letunic I, Bork P. Interactive tree of life (iTOL) v3: an online tool for the display and annotation of phylogenetic and other trees. Nucleic Acids Res. 2016;44:W242–5. https://doi.org/10.1093/nar/gkw290
20. Bouckaert R, Vaughan TG, Barido-Sottani J, Duchêne S, Fourment M, Gavryushkina A, et al. BEAST 2.5: an advanced software platform for Bayesian evolutionary analysis. PLOS Comput Biol. 2019;15:e1006650. https://doi.org/10.1371/journal.pcbi.1006650
21. Page AJ, Cummins CA, Hunt M, Wong VK, Reuter S, Holden MT, et al. Roary: rapid large-scale prokaryote pan genome analysis. Bioinformatics. 2015;31:3691–3. https://doi.org/10.1093/bioinformatics/btv421
22. Brynildsrud O, Bohlin J, Scheffer L, Eldholm V. Rapid scoring of genes in microbial pan-genome-wide association studies with Scoary. Genome Biol. 2016;17:238. https://doi.org/10.1186/s13059-016-1108-8
23. Clausen PTLC, Aarestrup FM, Lund O. Rapid and precise alignment of raw reads against redundant databases with KMA. BMC Bioinformatics. 2018;19:307. https://doi.org/10.1186/s12859-018-2336-6
24. Syberg-Olsen MJ, Garber AI, Keeling PJ, McCutcheon JP, Husnik F. Pseudofinder: detection of pseudogenes in prokaryotic genomes. Mol Biol Evol. 2022;39:msac153. https://doi.org/10.1093/molbev/msac153
25. Liu B, Zheng D, Jin Q, Chen L, Yang J. VFDB 2019: a comparative pathogenomic platform with an interactive web interface. Nucleic Acids Res. 2019;47:D687–92. https://doi.org/10.1093/nar/gky1080
26. Carattoli A, Hasman H. PlasmidFinder and in silico pMLST: identification and typing of plasmid replicons in whole-genome sequencing (WGS). Methods Mol Biol. 2020;2075: 285–94. https://doi.org/10.1007/978-1-4939-9877-7_20
27. Seemann T. ABRicate, mass screening of contigs for antimicrobial resistance or virulence genes. 1.0.1 [cited 2020 Apr 19]. https://github.com/tseemann/abricate
28. Wishart DS, Han S, Saha S, Oler E, Peters H, Grant JR, et al. PHASTEST: faster than PHASTER, better than PHAST. Nucleic Acids Res. 2023;51:W443–50. https://doi.org/10.1093/nar/gkad382
29. Zhang X, Payne M, Lan R. In silico identification of serovar-specific genes for *Salmonella* serotyping. Front Microbiol. 2019;10:835. https://doi.org/10.3389/fmicb.2019.00835
30. Alikhan NF, Zhou Z, Sergeant MJ, Achtman M. A genomic overview of the population structure of *Salmonella*. PLoS Genet. 2018;14:e1007261. https://doi.org/10.1371/journal.pgen.1007261

31. Allison GE, Angeles D, Tran-Dinh N, Verma NK. Complete genomic sequence of SfV, a serotype-converting temperate bacteriophage of *Shigella flexneri*. J Bacteriol. 2002;184:1974–87. https://doi.org/10.1128/JB.184.7.1974-1987.2002
32. Zhang X, Payne M, Nguyen T, Kaur S, Lan R. Cluster-specific gene markers enhance *Shigella* and enteroinvasive *Escherichia coli* in silico serotyping. Microb Genom. 2021;7:000704. https://doi.org/10.1099/mgen.0.000704
33. Clune T, Beetson S, Besier S, Knowles G, Paskin R, Rawlin G, et al. Ovine abortion and stillbirth investigations in Australia. Aust Vet J. 2020;1:22.
34. Price SL, Vadyvaloo V, DeMarco JK, Brady A, Gray PA, Kehl-Fie TE, et al. Yersiniabactin contributes to overcoming zinc restriction during *Yersinia pestis* infection of mammalian and insect hosts. Proc Natl Acad Sci U S A. 2021;118: e2104073118. https://doi.org/10.1073/pnas.2104073118
35. Wellawa DH, Allan B, White AP, Köster W. Iron-uptake systems of chicken-associated *Salmonella* serovars and their role in colonizing the avian host. Microorganisms. 2020; 8:1203. https://doi.org/10.3390/microorganisms8081203
36. Schubert S, Picard B, Gouriou S, Heesemann J, Denamur E. *Yersinia* high-pathogenicity island contributes to virulence in *Escherichia coli* causing extraintestinal infections. Infect Immun. 2002;70:5335–7. https://doi.org/10.1128/IAI.70.9.5335-5337.2002
37. Liu D, Yang Y, Gu J, Tuo H, Li P, Xie X, et al. The *Yersinia* high-pathogenicity island (HPI) carried by a new integrative and conjugative element (ICE) in a multidrug-resistant and hypervirulent *Klebsiella pneumoniae* strain SCsl1. Vet Microbiol. 2019;239:108481. https://doi.org/10.1016/j.vetmic.2019.108481
38. Miller RA, Wiedmann M. The cytolethal distending toxin produced by nontyphoidal *Salmonella* serotypes Javiana, Montevideo, Oranienburg, and Mississippi induces DNA damage in a manner similar to that of serotype Typhi. MBio. 2016;7:e02109–16. https://doi.org/10.1128/mBio.02109-16
39. Joerger RD, Choi S. Contribution of the *hdeB*-like gene (SEN1493) to survival of *Salmonella enterica* enteritidis Nal(R) at pH 2. Foodborne Pathog Dis. 2015;12:353–9. https://doi.org/10.1089/fpd.2014.1878
40. Deckers D, Vanlint D, Callewaert L, Aertsen A, Michiels CW. Role of the lysozyme inhibitor Ivy in growth or survival of *Escherichia coli* and *Pseudomonas aeruginosa* bacteria in hen egg white and in human saliva and breast milk. Appl Environ Microbiol. 2008;74:4434–9. https://doi.org/10.1128/AEM.00589-08
41. Thiennimitr P, Winter SE, Winter MG, Xavier MN, Tolstikov V, Huseby DL, et al. Intestinal inflammation allows *Salmonella* to use ethanolamine to compete with the microbiota. Proc Natl Acad Sci U S A. 2011;108:17480–5. https://doi.org/10.1073/pnas.1107857108
42. Anderson CJ, Clark DE, Adli M, Kendall MM. Ethanolamine signaling promotes *Salmonella* niche recognition and adaptation during infection. PLoS Pathog. 2015;11:e1005278. https://doi.org/10.1371/journal.ppat.1005278
43. Harris JB, Baresch-Bernal A, Rollins SM, Alam A, LaRocque RC, Bikowski M, et al. Identification of in vivo–induced bacterial protein antigens during human infection with *Salmonella enterica* serovar Typhi. Infect Immun. 2006;74:5161–8. https://doi.org/10.1128/IAI.00488-06
44. Harvey PC, Watson M, Hulme S, Jones MA, Lovell M, Berchieri A Jr, et al. *Salmonella enterica* serovar Typhimurium colonizing the lumen of the chicken intestine grows slowly and upregulates a unique set of virulence and metabolism genes. Infect Immun. 2011;79:4105–21. https://doi.org/10.1128/IAI.01390-10
45. Hoelzer K, Moreno Switt AI, Wiedmann M. Animal contact as a source of human non-typhoidal salmonellosis. Vet Res (Faisalabad). 2011;42:34. https://doi.org/10.1186/1297-9716-42-34
46. Sabbagh SC, Lepage C, McClelland M, Daigle F. Selection of *Salmonella enterica* serovar Typhi genes involved during interaction with human macrophages by screening of a transposon mutant library. PLoS One. 2012;7:e36643. https://doi.org/10.1371/journal.pone.0036643
47. Sana TG, Flaugnatti N, Lugo KA, Lam LH, Jacobson A, Baylot V, et al. *Salmonella* Typhimurium utilizes a T6SS-mediated antibacterial weapon to establish in the host gut. Proc Natl Acad Sci U S A. 2016;113:E5044–51. https://doi.org/10.1073/pnas.1608858113
48. Langridge GC, Fookes M, Connor TR, Feltwell T, Feasey N, Parsons BN, et al. Patterns of genome evolution that have accompanied host adaptation in *Salmonella.* Proc Natl Acad Sci U S A. 2015;112:863–8. https://doi.org/10.1073/pnas.1416707112
49. AbuOun M, Jones H, Stubberfield E, Gilson D, Shaw LP, Hubbard ATM, et al.; On Behalf Of The Rehab Consortium. A genomic epidemiological study shows that prevalence of antimicrobial resistance in *Enterobacterales* is associated with the livestock host, as well as antimicrobial usage. Microb Genom. 2021;7:10–2. https://doi.org/10.1099/mgen.0.000630
50. McLure A, Shadbolt C, Desmarchelier PM, Kirk MD, Glass K. Source attribution of salmonellosis by time and geography in New South Wales, Australia. BMC Infect Dis. 2022;22:14. https://doi.org/10.1186/s12879-021-06950-7

Address for correspondence: Ruiting Lan, School of Biotechnology and Biomolecular Sciences, University of New South Wales Sydney, Sydney, NSW 2052, Australia; email: r.lan@unsw.edu.au

A One Health Perspective on *Salmonella enterica* Serovar Infantis, an Emerging Human Multidrug-Resistant Pathogen

Jennifer Mattock,[1] Marie Anne Chattaway, Hassan Hartman, Timothy J. Dallman,[2] Anthony M. Smith, Karen Keddy, Liljana Petrovska,[3] Emma J. Manners,[4] Sanelisiwe T. Duze, Shannon Smouse, Nomsa Tau, Ruth Timme, Dave J. Baker, Alison E. Mather, John Wain, Gemma C. Langridge

*Salmonell*a enterica serovar Infantis presents an ever-increasing threat to public health because of its spread throughout many countries and association with high levels of antimicrobial resistance (AMR). We analyzed whole-genome sequences of 5,284 *Salmonella* Infantis strains from 74 countries, isolated during 1989–2020 from a wide variety of human, animal, and food sources, to compare genetic phylogeny, AMR determinants, and plasmid presence. The global *Salmonella* Infantis population structure diverged into 3 clusters: a North American cluster, a European cluster, and a global cluster. The levels of AMR varied by *Salmonella* Infantis cluster and by isolation source; 73% of poultry isolates were multidrug resistant, compared with 35% of human isolates. This finding correlated with the presence of the pESI megaplasmid; 71% of poultry isolates contained pESI, compared with 32% of human isolates. This study provides key information for public health teams engaged in reducing the spread of this pathogen.

Nontyphoidal *Salmonella* infections place a large burden on public health; an estimated 79 million cases of foodborne nontyphoidal *Salmonella* infection occurred in 2010 (*1*). *Salmonella enterica* subspecies *enterica* serovar Infantis is becoming an increasingly prevalent serovar globally. A 167% increase in human infections was observed in the United States during 2001–2016 (*2*), and in European Union member states, Infantis is the predominant serovar isolated from broiler flocks and broiler meat, accounting for 56.7% of *Salmonella* isolates from broiler meat in 2018 (*3*,*4*). Higher levels have been observed in Japan, at 72.2% of isolates from ground chicken, and levels of 84% were seen in broilers in Ecuador (*5*,*6*).

Antimicrobial resistance (AMR) in *Salmonella* Infantis varies by location; in South Africa only 13.4% of 387 *Salmonella* Infantis isolates from humans had AMR (*7*). Conversely, in 2016 in European Union member states, 70% of *Salmonella* Infantis isolates from broiler meat were multidrug-resistant (MDR) (*8*). Of particular concern is the emergence of extended β-lactamases (ESBLs), such as the $bla_{\text{CTX-M-65}}$ gene, which has been reported in *Salmonella* Infantis from Ecuador, Peru, Switzerland, the United Kingdom, and the United States (*9*–*13*). The pESI megaplasmid has been found to be responsible for these high levels of AMR because it confers resistance to trimethoprim, streptomycin, sulfamethoxazole, and tetracycline; ESBLs have also been found to be carried by some pESI variants (*10*,*11*,*14*). Originally identified in Israel, pESI-like plasmids have since been reported in multiple countries (*14*–*19*).

Author affiliations: University of East Anglia, Norwich, UK (J. Mattock, E.J. Manners, A.E. Mather, J. Wain); UK Health Security Agency, London, UK (M.A. Chattaway, H. Hartman, T.J. Dallman); National Institute for Communicable Diseases, Johannesburg, South Africa (A.M. Smith, S. Smouse, N. Tau); University of Pretoria, Pretoria, South Africa (K. Keddy); Animal and Plant Health Agency, Addlestone, UK (L. Petrovska); University of the Witwatersrand, Johannesburg (S.T. Duze). US Food and Drug Administration, College Park, Maryland, USA (R. Timme); Quadram Institute Bioscience, Norwich (D.J. Baker, A.E. Mather, J. Wain, G.C. Langridge)

DOI: https://doi.org/10.3201/eid3004.231031

[1]Current affiliation: University of Edinburgh, Edinburgh, Scotland, UK.
[2]Current affiliation: Utrecht University, Utrecht, the Netherlands.
[3]Current affiliation: UK Health Security Agency, London, UK.
[4]Current affiliation: European Bioinformatics Institute, Cambridge, UK.

Salmonella Infantis has a polyphyletic population structure consisting of 2 eBurst Groups (eBG), eBG31 and eBG297, which differ by 5–7 multilocus sequence typing alleles (*16*). The dominant eBG (single locus variants around a central sequence type) globally is eBG31; eBG297 consisted of just 0.7% of *Salmonella* Infantis isolates in Enterobase on August 9, 2021 (*20*). However, higher levels (32%) of eBG297 have been reported in South Africa (*7*).

The population structure of *Salmonella* Infantis has been studied on a limited scale; whole-genome sequencing analysis of 100 *Salmonella* Infantis isolates from multiple continents and sources found no clustering by geographic location (*16*). *Salmonella* Infantis isolates were found to cluster by isolation source from human samples and chicken meat samples in Japan (*21*), by $bla_{\text{CTX-M-65}}$ presence in human and animal strains in the United States and Italy (*11*), and by pESI presence in human and poultry isolates from Switzerland (*10*).

Although MDR *Salmonella* Infantis is an emerging public health concern, no large-scale population structure study of this pathogen has been performed. Because eBG297 isolates have been analyzed in depth (*7*), our aim was to determine the global population structure of eBG31 from a One Health perspective, investigating whether population structure is associated with isolation source, location, MDR properties, or pESI presence.

Methods

Our eBG31 collection contained 5,284 isolates, sourced from the UK Health Security Agency (UKHSA), the National Institute for Communicable Diseases of South Africa, the Animal and Plant Health Agency, GenBank, and Enterobase (*20*) (Appendix 1, https://wwwnc.cdc.gov/EID/article/30/4/23-1031-App1.pdf). The collection contained strains isolated from 74 countries and spanned 4 decades and consisted of strains isolated during 1989–2020. The isolates were grouped into 8 sources: animal feed, human, environmental, food, other animals, poultry, poultry products, and unknown.

The whole-genome consensus FASTA sequences were grouped into clusters where all sequences in each cluster were <*n* single-nucleotide polymorphisms (SNPs) from another member. We generated a core SNP phylogeny of representatives of 25-SNP clusters; we identified clusters using fastbaps and used treedater to date the phylogeny (*22*–*25*). We used the ARIBA tool with the resfinder and plasmidfinder databases to screen for AMR determinants and plasmid presence; pESI was identified separately as described in Mattock et al. (*7*,*26*–*28*).

Ethical approval for the detection of gastrointestinal bacterial pathogens from fecal specimens, or the identification, characterization, and typing of cultures of gastrointestinal pathogens submitted to the Gastrointestinal Bacteria Reference Unit was not required because it is covered by UKHSA's surveillance mandate. Ethical approval for all laboratory-based surveillance and research activities was obtained from the Human Research Ethics Committee, University of the Witwatersrand, Johannesburg, South Africa (protocol reference nos. M060449 and M110499) by the Centre for Enteric Diseases, National Institute for Communicable Diseases. Ethical approval for characterization of the isolates was not required because of the surveillance mandate of Animal and Plant Health Agency.

Results

Demographics

We included isolates from a multitude of sources in the eBG31 collection. Most (60%, 3,150) of the 5,284 isolates were isolated from humans and associated with either noninvasive infections (samples from stool and urine), or invasive infection (samples from blood and cerebrospinal fluid). A further 6% (300) were from poultry and 13% (684) from poultry products, which included samples from poultry meat, eggs, and processed meals containing poultry meat. Isolates from other animals made up 6% (321) of the collection, 7% (390) were from food, 1% (74) from animal feed, and 5% (268) environmental, such as water, farm swab, and soil samples. A total of 97 isolates had no stated isolation source.

The number of isolates increased temporally until 2018; this increase was caused by isolates from public databases being included until February 2018 (Appendix 1 Figure 1). Only strains isolated by the UKHSA were included after that time. When categorized by continent, 54% (2,861) were from North America, 31% (1,642) from Europe, 6% (316) from Africa, 6% (312) from Asia, and 2% (128) from South America; origins were unknown for 0.47% (25). The United States contributed the largest number of isolates (n = 2,719) followed by the United Kingdom (n = 1,326) (Table; Figure 1).

Population Structure

At the sequence type (ST) level, most eBG31 isolates (99%, 5,205) belonged to ST32. The second most common was ST2283; 36 isolates belonged to this ST, all from Europe (17 from humans, 10 from other animals, 5 from food, and 4 from environmental samples). The

Table. Source group and country of isolates in One Health–focused analysis of *Salmonella enterica* serovar Infantis*

Country	Source group							
	Food	Environmental	Animal feed	Human	Poultry	Poultry products	Other animals	Unknown
Canada			4	21		1		
Cyprus								7
Denmark	18				1		36	11
Germany	16	7	8	1			15	1
Hungary				1				6
Japan		9		32	19	26		
Romania				2				6
South Africa		6		266				1
United Kingdom	75	52		1016	98	26	31	28
United States	234	185	57	1254	161	601	227	
Other	44	9	5	557	20	26	12	11
Unknown	3				1	4		26
Total	390	268	74	3150	300	684	321	97

*The number of isolates from each source group and the country of isolation were filtered to include countries that comprised >5% of ≥1 source group.

third most common was ST2146 with 26 isolates, all from North America (22 were from environmental samples, 3 from food, and 1 from a clinical sample). The 13 remaining STs were found in ≤3 isolates.

We identified 3 clusters of 250 SNPs; 1 contained just SRR8114924. For 50-SNP clusters, there were 408; for 25-SNP cluster, 1,288; for 10-SNP clusters, 2,876; and for 5-SNP clusters, 3,917. In a core SNP maximum-likelihood phylogeny of a member of each 25-SNP cluster, representing 5,283 eBG31 isolates (Figure 2; Appendix 1 Figure 2), Bayesian hierarchical clustering identified 3 clusters. Cluster A contained 348 sequences, representing 1,624 isolates (Figure 2, blue); cluster B had 831 sequences, representing 3,283 isolates (Figure 2, pink); and cluster C, which diverged from within cluster B, contained 109 sequences, representing 376 isolates (Figure 2, purple). When annotated by ST, the phylogeny was dominated by ST32 (Appendix 1 Figure 3); 99% (1,269/1,288) of the 25-SNP clusters were exclusively ST32. The three 25-SNP clusters containing the ST2283 isolates clustered together in cluster C, and another 3 clusters comprising the ST3815 isolates clustered in cluster A.

In contrast to previous reports, a geographic signal was visible in the clustering of isolates in the phylogeny. Cluster A mainly consisted of North American isolates (Figure 3, panel A), of which 98% (1,180/1,203) were from the United States. Cluster B also contained a large percentage of North American isolates (50%, 1,657/3,238), but higher percentages of isolates from all other continents were observed. Conversely, cluster C consisted almost exclusively of

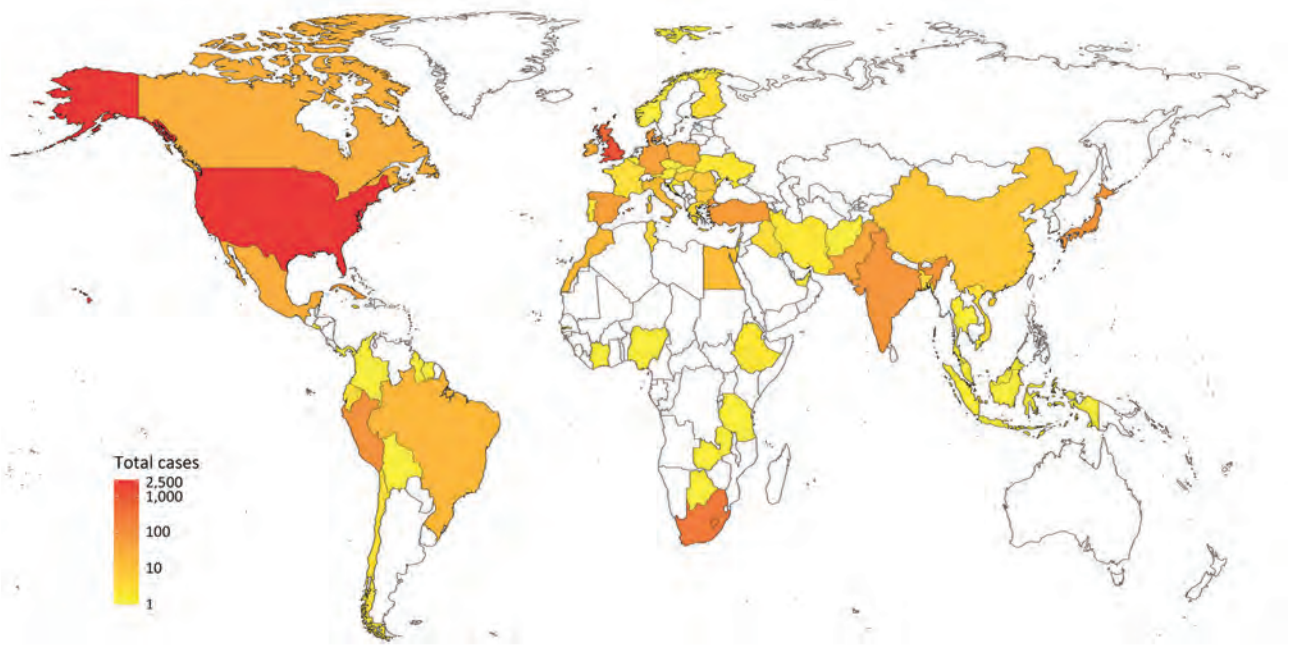

Figure 1. Heatmap indicating the number of isolates included in the dataset from each country in One Health–focused analysis.

European isolates, most of which were isolated in the United Kingdom (80%, 297/370).

The predominant isolation source in each of the clusters was humans (Figure 3, panel B). Isolates from poultry and poultry products were most often found in cluster B. However, isolates from other animals and animal feed made up a larger proportion of cluster A than the other clusters.

Minimal clustering by year was observed in the phylogeny (Appendix 1 Figure 4). The most common year range in each cluster was 2016–2020, representing 48% (785/1,624) of cluster A, 51% (1,664/3,238) of cluster B, and 67% (253/376) of cluster C. The earliest date of isolation varied; cluster B was the oldest with an isolate from 1989. Cluster A's oldest isolates were from 1996, and cluster C appeared more recently; its oldest isolate was from 2007. The time of the most recent common ancestor was calculated using relaxed clock dating of the phylogeny and estimated to be 1946; cluster A diverged in 1982 and cluster C in 1987.

We calculated the pairwise nucleotide distance between each whole-genome consensus FASTA to show the diversity within and between groups of isolates. Clusters B and C had the lowest median pairwise nucleotide distance of 191 (range 32–1,743);

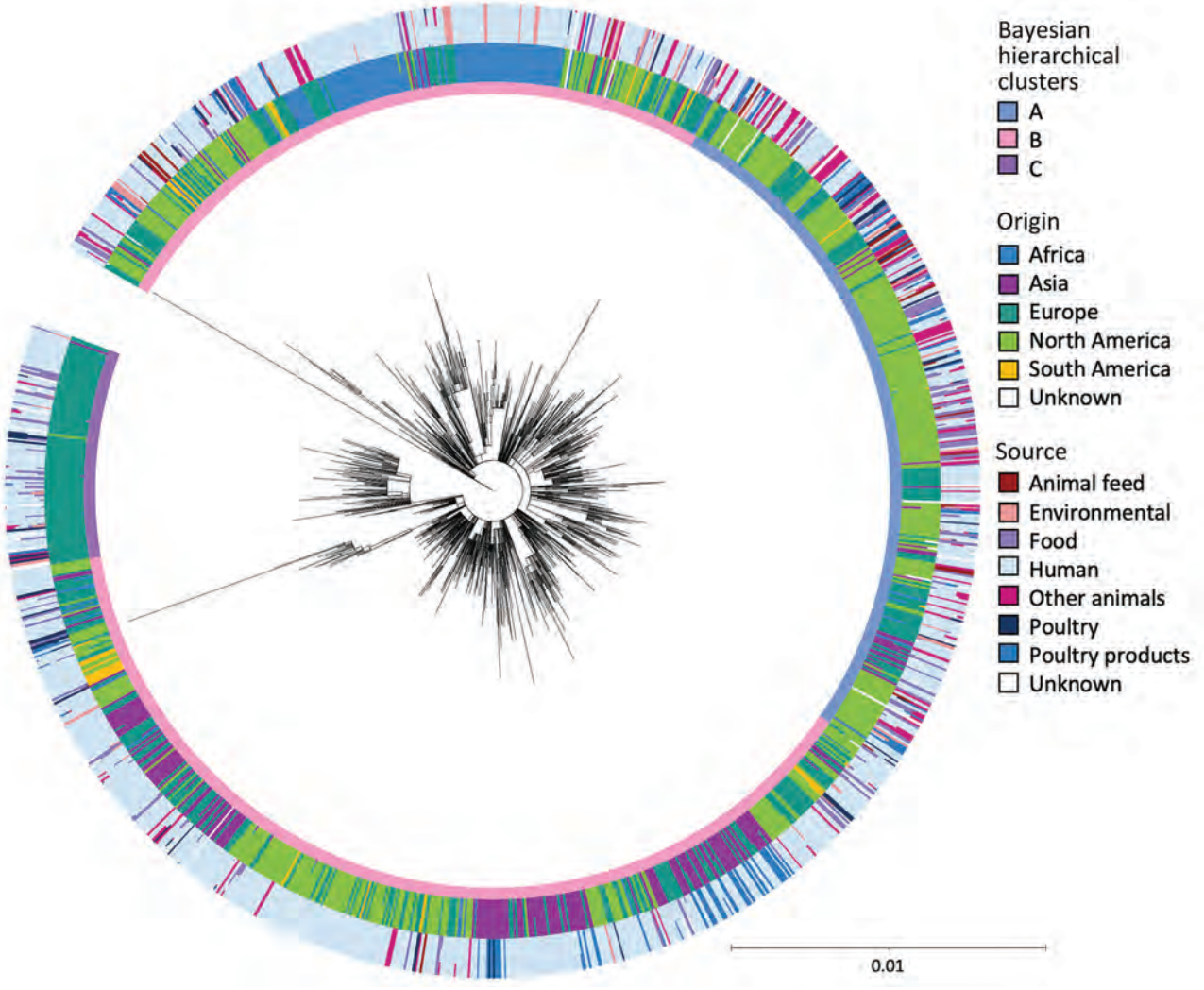

Figure 2. Core single-nucleotide polymorphism maximum-likelihood phylogeny of 1,288 representatives of 5,283 isolates in One Health–focused analysis of emerging multidrug-resistant pathogen *Salmonella enterica* serovar Infantis. The inner ring around the phylogeny is annotated with the Bayesian hierarchical clusters found by fastbaps. Cluster A consists of 348 representatives of 1,624 isolates; cluster B consists of 831 representatives of 3,283 isolates; and cluster C consists of 109 representatives of 376 isolates. The outer rings show the percentage of isolates in each 25-SNP cluster that were from each continent and source. Isolate origin was identified for Africa (n = 316), Asia (n = 312), Europe (n = 1,641), North America (n = 2,861), and South America (n = 128); the origin of the remaining isolates was unknown (n = 25). Sources were animal feed (n = 74), environmental (n = 268), food (n = 390), human (n = 3,149), other animals (n = 321), poultry (n = 300), poultry products (n = 684), and unknown (n = 97).

higher values were observed between clusters A and B (304, range 26–1,983) and clusters A and C (428, range 80–1,410). When comparing within isolation sources, strains from poultry products had the lowest median pairwise nucleotide distance at 145 (range 0–1,249) and human isolates the largest at 241 (range 0–2,060). The median pairwise nucleotide distance between human isolates and other sources ranged from 215 for environmental isolates (range 1–2,004) to 259 for poultry isolates (range 0–2,039). Poultry isolates had a similar median nucleotide distance to environmental isolates (251, range 4–1,822); a larger distance was observed between poultry isolates and those from other animals (310, range 4–1,817). The largest median pairwise nucleotide distance between source groups was poultry and animal feed at 334 (range 5–1,614). Low median pairwise nucleotide distances were observed within isolates from South America (44, range 0–920) and North America (159, range 0–1,883); the largest distance within isolates from a continent was Africa at 492 (range 0–1,885). Isolates from Africa also had the largest median pairwise nucleotide distances of all continents; distance was 395 (range 15–2,059) with North America and 422 (range 23–1,639) with South America.

AMR in *Salmonella* Infantis

In this collection, 44% (2,327/5,284) of the isolates contained ≥1 AMR gene; most of those (40%, 2,101/5,284) were MDR. Genes encoding AMR were identified in isolates throughout the phylogeny (Figure 4); 46.7% (602/1,288) of the 25-SNP clusters contained an isolate with AMR. Some 25-SNP clusters contained large numbers of isolates with AMR, such as 1 in cluster B that contained 734 isolates, of which 727 were MDR. A common resistance profile was visible in 25-SNP clusters across the phylogeny: 27.7% (357/1,288) contained an isolate with resistance to aminoglycosides, fluoroquinolones, sulphonamides, and tetracyclines (AFST). Of those, 56.9% (203/357) had an isolate with putative trimethoprim resistance, and 99.7% (356/357) contained a mutation in the quinolone-resistance determining region. The percentage of isolates with this resistance profile varied between the clusters: 1% (16/1,624) in cluster A, 43.5% (1,407/3,283) in cluster B, and 84% (316/376) in cluster C. The percentage of MDR isolates differed between the clusters; 7% (114/1,624) of isolates from cluster A were MDR, 50.5% (1,657/3,283) of isolates from cluster B were MDR, and 87.8% (330/376) from cluster C were MDR. More isolates were positive for ESBLs in cluster B (20.5%, 672/3,283) than in clusters A (0.2%, 4/1,624) and C (0%).

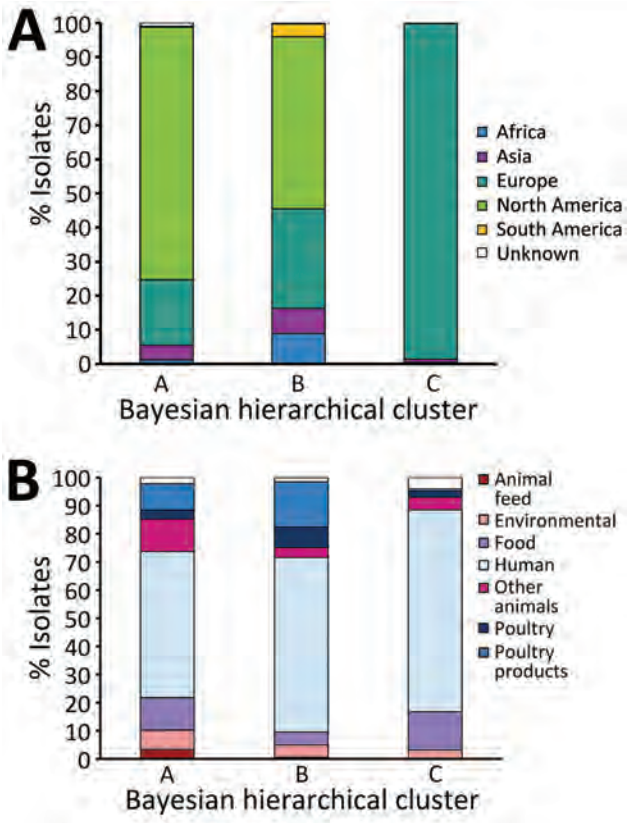

Figure 3. Source and continent composition of fastbaps clusters in study of One Health perspective of emerging multidrug-resistant pathogen *Salmonella enterica* serovar Infantis. A) Percentage of isolates from each continent in clusters A (n = 1,624), B (n = 3,283), and C (n = 376). B) Percentage of isolates from each source group in clusters A (n = 1,624), B (n = 3,283), and C (n = 376).

We observed variation in the distribution of AMR between isolation sources. Isolates from animal feed had the lowest amount of AMR; 4% (3/74) were predicted to have the AFST resistance profile. Higher levels of AMR were predicted in human isolates; 29% (913/3,150) had the AFST resistance profile, and 60% (552/913) of those also had trimethoprim resistance genes. Substantially more AMR was present in poultry and poultry product isolates: 61% (183/300) of poultry isolates and 64% (438/684) of poultry product isolates had the AFST resistance profile. β-lactam and chloramphenicol resistance was more common in poultry product isolates (43% [296/684] for β-lactam and 44% [302/684] for chloramphenicol) than in poultry isolates (21% [64/300] for β-lactam and 22% [65/300] for chloramphenicol). ESBLs were identified in 10% (312/3,150) of human isolates, 19% (58/300) of poultry isolates, and 40% (272/684) of isolates from poultry products. We observed multidrug resistance in 4% (3/74) of isolates from animal feed, 14% (38/268) of environmental isolates, 32%

(123/390) of food isolates, 35% (1,115/3,150) of human isolates, 21% (67/321) of isolates from other animals, 73% (218/300) of poultry isolates, and 73% (501/684) of poultry product isolates.

AMR profiles also varied by continent of isolation. The lowest levels of AMR were observed in isolates from Africa, of which 4% (14/316) had the AFST resistance profile, compared with 27% (763/2,861) of isolates from North America, 42% (692/1,642) of isolates from Europe, 55% (172/312) of isolates from Asia, and 76% (97/128) of isolates from South America. ESBLs were present in 0.3% (1/316) of isolates from Africa, 3% (9/312) of isolates from Asia, 4% (65/1,642) of isolates from Europe, 19% (531/2,861) of isolates from North America, and 55% (70/128) of isolates from South America. The percentage of MDR isolates was 20% (63/316) for Africa, 31% (891/2,861) for North America, 48% (793/1,642) for Europe, 80% (248/312) for Asia, and 81% (104/128) for South America.

The proportion of isolates with AMR fluctuated throughout the study period and trended upwards in the last 15 years of the collection period (Appendix 1 Figure 5). The earliest isolate in the collection (from 1989) was predicted to be resistant to 6 antimicrobial classes. AMR to aminoglycosides, sulphonamides, and tetracyclines were consistently the most common and appeared to follow a similar trend; after 2012, similar levels of AMR to fluoroquinolones were also present.

Plasmids in *Salmonella* Infantis

As observed with AMR, <50% (47%, 2502/5284) of *Salmonella* Infantis isolates contained a plasmid. Some of the most common types included IncA/C (n = 103), IncI1 (n = 251), and IncX1 (n = 65). As expected, pESI was the prevailing plasmid type, present in 36% (1,912/5,284) of *Salmonella* Infantis isolates. Low levels of IncA/C were observed in all isolation sources except animal feed; the highest level was just 4% (14/321) of other animal isolates, 2% of both human (64/3,150) and poultry product (15/684) isolates, and 0.6% (2/300) of poultry isolates. Incl1 was most

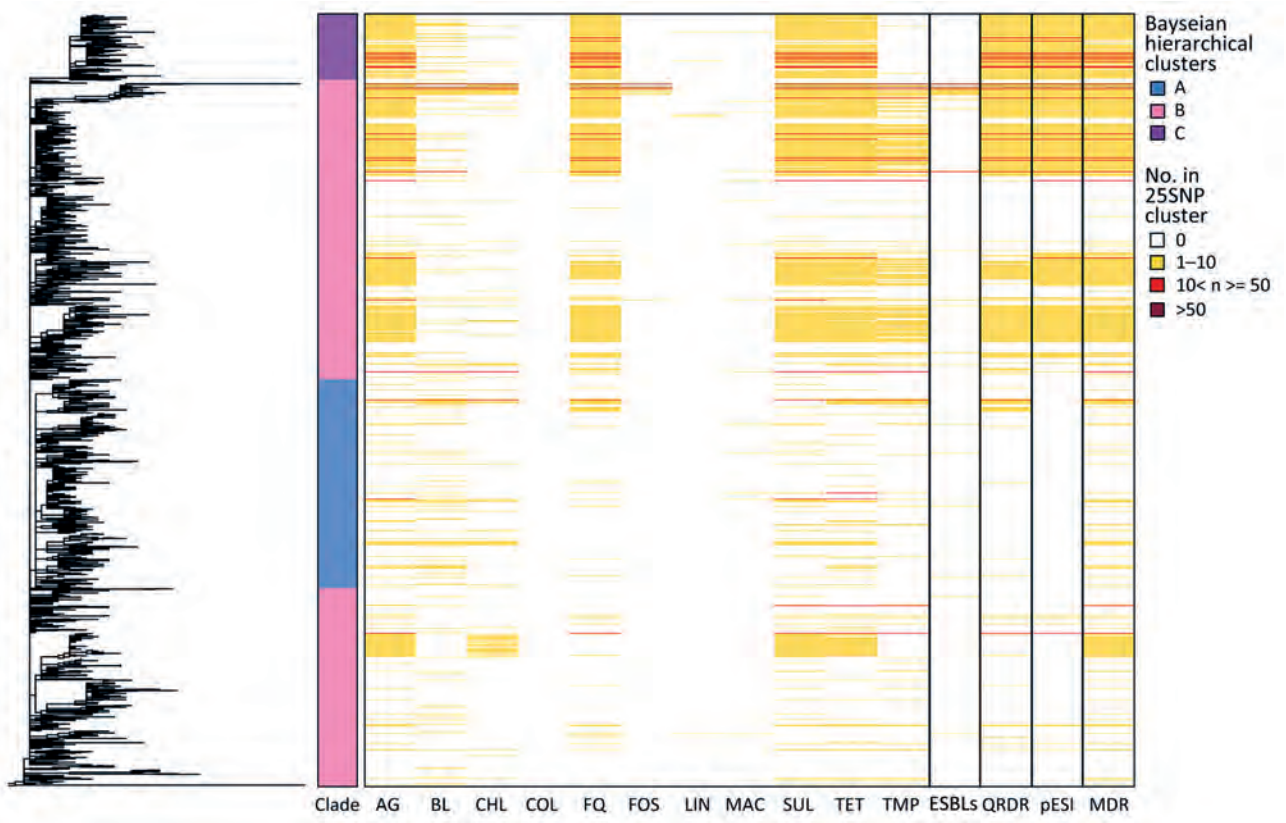

Figure 4. Phylogeny and heatmap of antimicrobial resistance and pESI in study of One Health perspective of emerging multidrug-resistant pathogen *Salmonella enterica* serovar Infantis. Heatmap shows the number of isolates in each 25 single-nucleotide polymorphism representative cluster (n = 1,288) of the eBG31 maximum-likelihood phylogeny with genes conferring resistance to antimicrobial drugs. Fastbaps clade and the number of isolates with MDR, ESBLs, mutations in the QRDR conferring resistance to fluoroquinolones and pESI presence are also shown. AG, aminoglycosides; BL, β-lactams; CHL, chloramphenicol; COL, colistin; ESBLs, extended β-lactamases; FQ, fluoroquinolones; FOS, fosfomycin; LIN, lincosamides; MAC, macrolides; MDR, multidrug-resistant; SUL, sulphonamides; TET, tetracyclines; TMP, trimethoprim.

common in other animal isolates at 9% (28/321) and IncX1 in human isolates (2%, 52/3,150). IncI1-positive isolates were found in all continents throughout the study period, mainly from humans (n = 184); IncX1 was observed in Asia, Europe, and North America.

The presence of pESI-like plasmids was observed in 71% (213/300) of poultry isolates, 71% (486/684) of isolates from poultry products, 32% (992/3,150) of human isolates, 4% (3/74) of animal feed isolates, 10% (31/321) of isolates from other animals, 31% (120/390) of food isolates, and 11% (30/268) of environmental isolates. Presence also varied by geographic location: the lowest percentage of pESI-positive isolates was from Africa at 4% (12/316), followed by North America at 28% (808/2,861), Europe at 47% (770/1,642), Asia at 71% (222/312), and South America at 77.3% (99/128). The earliest isolation of pESI in this collection was in 4 human isolates from Japan in 1999 (DRR022718, DRR022719, DRR022720, DRR022754). Although the common resistance profile AFST was distributed throughout the eBG31 phylogeny, cluster A lacked any pESI; most of cluster C contained pESI (99.7%, 375/376), and 46.8% (1,537/3,283) of cluster B contained pESI (Figure 4).

Discussion

In our large core SNP analysis of *Salmonella* Infantis, we determined that the global population structure of eBG31 consists of 3 clusters with varying isolation sources and levels of AMR. As observed previously, the dominant ST in eBG31 was ST32, comprising 99% of the isolates (*29*–*32*). The other STs were not observed in multiple continents, suggesting that those STs have emerged in specific areas but have not spread globally. A strong geographic signal was identified in the eBG31 phylogeny (Figure 2); we hypothesize that cluster B is an ancestor of the 2 other clusters, containing more genetic and geographic diversity in isolates from all continents, and we therefore designate this the global *Salmonella* Infantis cluster. Cluster A, estimated to have diverged from cluster B in 1982, mainly consisted of isolates from North America and hence is named the North American cluster. Cluster C, which diverged from cluster B in 1987, was dominated by isolates from Europe and is thus named the European cluster. This designation differs, perhaps because of our larger number of isolates, from Gymoese et al. (*16*), who found no geographic signal when examining isolates from 5 continents, and Alba et al. (*33*), who reported little clustering by location or source. Some clustering by country of isolation was described in Acar et al. (*34*); however, because that clustering was between isolates from the same region in Turkey, the contribution to global clustering was not clear. Nucleotide distances relative to the reference showed that the African eBG31 isolates were both the most diverse and the most distant to isolates from other continents; our previous work identified that an increased proportion of isolates belonged to eBG297, and this study affirms that the African *Salmonella* Infantis population differs from that observed elsewhere (*7*).

Because most eBG31 isolates were from human sources, the phylogeny was dominated by this source. Cluster C in particular contained lower numbers of environmental, poultry, and poultry product isolates; that was possibly caused by bias in data sampling because the cluster contains strains from UKHSA that were isolated after the cutoff for inclusion from Enterobase. Most of those strains were from humans, as environmental sampling tends to be performed in association with an outbreak. Although cluster C contained strains isolated as early as 2007, it contained many of the newer strains isolated during 2018–2020; this group could represent an emerging clade of *Salmonella* Infantis. The nucleotide distance between source groups, relative to the reference, identified the least diversity in the poultry product isolates and the greatest diversity between poultry/poultry products and animal feed or other animal genomes. This finding could indicate a reduction of adaptation in poultry hosts and suggest that the different niches have encouraged adaptation; the reduced distance between poultry isolates could, however, be attributed to the large number of North American poultry isolates reducing the median (e.g., 519/734 of strains in the 25-SNP cluster with the representative SRR2537092 were from poultry, and 724 isolates in that cluster were from North America).

As described in many other studies, the *Salmonella* Infantis isolates in this project were associated with high levels of putative AMR (*8*,*18*,*35*,*36*). MDR genotypes were detected in 40% of the *Salmonella* Infantis isolates; their presence was notable in isolates from poultry and poultry products, in which 73% were MDR. In comparison, just 14% of environmental isolates, 21% of isolates from other animals, 32% of food isolates, and 35% of human isolates were MDR (Appendix 2 Table 1, https://wwwnc.cdc.gov/EID/article/30/4/23-1031-App2.xlsx); this finding could indicate that the source of human infection was the nonpoultry sources with similar levels of AMR. Although that hypothesis has been suggested in Slovenia, where most broiler isolates clustered separately from human isolates (*32*), many incidences of human outbreaks associated with poultry have been reported

(*21*,*37*,*38*). Both environmental and poultry sources could be contributing to human cases, but the pESI-positive strain circulating in the poultry industry could also have a selective disadvantage to causing infection in humans, leading to less frequent observation of those strains.

Levels of AMR varied by continent; the lowest levels were observed in Africa (20% of strains were MDR) and the highest were observed in South America (81%). The higher levels in South America concurs with other reports that found all but 1 isolate tested in Ecuador were MDR and observed multiple drug resistance profiles in *Salmonella* Infantis strains from Chile (*38*,*39*). AMR fluctuated temporally, increasing in the last 15 years of the collection period. The proportion of isolates with resistance to aminoglycosides, sulphonamides, and tetracyclines followed a similar trend, joined by fluoroquinolones after 2012. This trend could be attributed to pESI, which carries resistance genes for those antimicrobial drugs. Similarly, we noted an association between pESI presence and resistance to aminoglycosides, fluoroquinolones, sulphonamides, and tetracyclines; multidrug resistance; and mutations in the quinolone-resistance determining region (Figure 4). The pESI backbone has been confirmed to carry *aadA1*, *sul1*, and *tetA* (*14*,*19*), illustrating that pESI is a strong driver of AMR in the *Salmonella* Infantis population, which supports the suggestion of Alba et al. (*33*) that pESI acquisition could be the decisive factor in the spread of the serovar throughout Europe. Of note, cluster C, the clade we suspect is an emerging dominant strain in Europe, is dominated by AMR and pESI, but cluster A, the North American cluster with relatively low levels of MDR strains (7%), lacked any pESI-positive isolates. The pESI-like plasmid was present in 808 North American isolates in this dataset, but they belonged to either cluster B or C. This finding concurs with previous research that reported 2 clades within the US *Salmonella* Infantis population, 1 with and 1 without pESI, and suggests that 2 groups of *Salmonella* Infantis are circulating in North America: 1 associated with MDR strains and pESI, and the other endemic to North America and not carrying pESI (*40*). The presence of pESI-like plasmids has recently been identified in *Salmonella* serovars Agona, Muenchen, Schwarzengrund, and Senftenberg; the increased virulence of pESI-positive isolates and transmissibility of this plasmid within the *Salmonella* Infantis global population and to other *Salmonella* serovars is a grave public health concern (*41*–*43*).

In conclusion, most *Salmonella* Infantis isolates fall within eBG31, which consists of 3 clusters: a North American cluster (cluster A), a European cluster (cluster C), and an ancestral but still extant global cluster (cluster B). Isolates from Africa were genetically more diverse and distant from isolates from the other continents, further confirming previous work that identified a distinct population structure in *Salmonella* Infantis in South Africa. Using a One Health approach, we observed high levels of AMR in poultry and poultry products, highlighting the need to reduce the levels of this pathogen in poultry production premises and encouraging the development and use of a vaccine against *Salmonella* Infantis in poultry. Finally, pESI-like plasmids were shown to be a major driver for AMR in the global *Salmonella* Infantis population, posing a major threat to public health.

This article was preprinted at https://www.biorxiv.org/content/10.1101/2023.07.28.549231v1.

Acknowledgments

We thank Anaïs Painset for help with bioinformatics training. We are grateful to Heather Carleton for sharing isolate metadata with us. All clinical *Salmonella* isolates in South Africa are collected as part of activities in the NICD GERMS-SA Laboratory Surveillance Network. We thank all participants involved in the GERMS-SA Network.

The Illumina FASTQ accessions for all the isolates are available in Appendix 2 Table 1. The ARIBA ResFinder, Plasmidfinder and gyrase results are in Appendix 2 Tables 2–4. The eBG31 reference genome can be accessed in GenBank (accession no. CP070301).

J.M. was funded by the National Institute for Health Research Health Protection Research Unit (NIHR HPRU) in Gastrointestinal Infections at University of Liverpool in partnership with Public Health England (PHE, now UKHSA), in collaboration with the University of East Anglia, University of Oxford and the Quadram Institute. E.M. was funded by the University of East Anglia. The project was part funded through the UKMRC Strategic Innovation Health Partnerships–Collaboration Research Project UK–South Africa. PI Karen Keddy. M.A.C. was supported in this study and received funding from the National Institute for Health Research (NIHR) Health Protection Research Unit in Genomics and Enabling Data (NIHR200892). The views expressed are those of the author(s) and not necessarily those of the NIHR, the Department of Health and Social Care or UKHSA. A.E.M., J.W. and G.C.L. were supported by the Biotechnology and Biological Sciences Research Council (BBSRC) Institute Strategic Programme Microbes in the Food Chain BB/R012504/1 and its constituent project BBS/E/F/000PR10348 (Theme 1, Epidemiology and Evolution of Pathogens in the Food Chain).

About the Author

Dr. Mattock is a bioinformatician at the Roslin Institute, University of Edinburgh, UK. Her research interests include the genetics, antimicrobial resistance, and epidemiology of gastrointestinal pathogens.

References

1. Havelaar AH, Kirk MD, Torgerson PR, Gibb HJ, Hald T, Lake RJ, et al.; World Health Organization Foodborne Disease Burden Epidemiology Reference Group. World Health Organization global estimates and regional comparisons of the burden of foodborne disease in 2010. PLoS Med. 2015;12:e1001923–1001923 https://doi.org/10.1371/journal.pmed.1001923
2. Centers for Disease Control and Prevention. National enteric disease surveillance: *Salmonella* annual report, 2016 [cited 2021 Aug 4]. https://www.cdc.gov/nationalsurveillance/pdfs/2016-Salmonella-report-508.pdf
3. European Food Safety Authority; European Centre for Disease Prevention and Control. The European Union One Health 2019 zoonoses report. EFSA J. 2021;19:e06406.
4. European Food Safety Authority; European Centre for Disease Prevention and Control. The European Union One Health 2018 Zoonoses Report. EFSA J. 2019;17:e05926.
5. Hara-Kudo Y, Konuma H, Kamata Y, Miyahara M, Takatori K, Onoue Y, et al. Prevalence of the main food-borne pathogens in retail food under the national food surveillance system in Japan. Food Addit Contam Part A Chem Anal Control Expo Risk Assess. 2013;30:1450–8. https://doi.org/10.1080/19440049.2012.745097
6. Vinueza-Burgos C, Cevallos M, Ron-Garrido L, Bertrand S, De Zutter L. Prevalence and diversity of *Salmonella* serotypes in Ecuadorian broilers at slaughter age. PLoS One. 2016;11:e0159567. https://doi.org/10.1371/journal.pone.0159567
7. Mattock J, Smith AM, Keddy KH, Manners EJ, Duze ST, Smouse S, et al. Genetic characterization of *Salmonella* Infantis from South Africa, 2004–2016. Access Microbiol. 2022;4:acmi000371. https://doi.org/10.1099/acmi.0.000371
8. European Food Safety Authority; European Centre for Disease Prevention and Control. The European Union summary report on antimicrobial resistance in zoonotic and indicator bacteria from humans, animals and food in 2016. EFSA J. 2018;16:e05182.
9. Granda A, Riveros M, Karen SM, Corujo A, Reyes I, Ruiz J, et al. Presence of extended-spectrum β -lactamase, CTX-M-65 in *Salmonella enterica* serovar Infantis isolated from children with diarrhea in Lima, Peru. J Pediatr Infect Dis. 2019;14:194–200. https://doi.org/10.1055/s-0039-1685502
10. Hindermann D, Gopinath G, Chase H, Negrete F, Althaus D, Zurfluh K, et al. *Salmonella enterica* serovar Infantis from food and human infections, Switzerland, 2010–2015: poultry-related multidrug resistant clones and an emerging ESBL producing clonal lineage. Front Microbiol. 2017;8:1322. https://doi.org/10.3389/fmicb.2017.01322
11. Tate H, Folster JP, Hsu C-H, Chen J, Hoffmann M, Li C, et al. Comparative analysis of extended-spectrum-β-Lactamase CTX-M-65-producing *Salmonella enterica* serovar Infantis isolates from humans, food animals, and retail chickens in the United States. Antimicrob Agents Chemother. 2017;61:e00488-17. https://doi.org/10.1128/AAC.00488-17
12. Burke L, Hopkins KL, Meunier D, de Pinna E, Fitzgerald-Hughes D, Humphreys H, et al. Resistance to third-generation cephalosporins in human non-typhoidal *Salmonella enterica* isolates from England and Wales, 2010–12. J Antimicrob Chemother. 2014;69:977–81. https://doi.org/10.1093/jac/dkt469
13. Cartelle Gestal M, Zurita J, Paz Y Mino A, Ortega-Paredes D, Alcocer I. Characterization of a small outbreak of *Salmonella enterica* serovar Infantis that harbour CTX-M-65 in Ecuador. Braz J Infect Dis. 2016;20:406–7. https://doi.org/10.1016/j.bjid.2016.03.007
14. Aviv G, Tsyba K, Steck N, Salmon-Divon M, Cornelius A, Rahav G, et al. A unique megaplasmid contributes to stress tolerance and pathogenicity of an emergent *Salmonella enterica* serovar Infantis strain. Environ Microbiol. 2014;16:977–94. https://doi.org/10.1111/1462-2920.12351
15. Franco A, Leekitcharoenphon P, Feltrin F, Alba P, Cordaro G, Iurescia M, *et al*. Emergence of a clonal lineage of multidrug-resistant ESBL-producing *Salmonella* Infantis transmitted from broilers and broiler meat to humans in Italy between 2011 and 2014. PLoS One. 2015;10:e0144802.
16. Gymoese P, Kiil K, Torpdahl M, Østerlund MT, Sørensen G, Olsen JE, et al. WGS based study of the population structure of *Salmonella enterica* serovar Infantis. BMC Genomics. 2019;20:870. https://doi.org/10.1186/s12864-019-6260-6
17. Iriarte A, Giner-Lamia J, Silva C, Betancor L, Astocondor L, Cestero JJ, et al.; SalmoIber CYTED Network. Draft genome sequence of *Salmonella enterica* subsp. *enterica* serovar Infantis strain SPE101, isolated from a chronic human infection. Genome Announc. 2017;5:e00679–17. https://doi.org/10.1128/genomeA.00679-17
18. Szmolka A, Szabó M, Kiss J, Pászti J, Adrián E, Olasz F, et al. Molecular epidemiology of the endemic multiresistance plasmid pSI54/04 of *Salmonella* Infantis in broiler and human population in Hungary. Food Microbiol. 2018;71:25–31. https://doi.org/10.1016/j.fm.2017.03.011
19. Lee WWY, Mattock J, Greig DR, Langridge GC, Baker D, Bloomfield S, *et al*. Characterization of a pESI-like plasmid and analysis of multidrug-resistant *Salmonella enterica* Infantis isolates in England and Wales. Microb Genom. 2021;7:000658.
20. Alikhan N-F, Zhou Z, Sergeant MJ, Achtman M. A genomic overview of the population structure of *Salmonella.* PLoS Genet. 2018;14:e1007261. https://doi.org/10.1371/journal.pgen.1007261
21. Yokoyama E, Murakami K, Shiwa Y, Ishige T, Ando N, Kikuchi T, et al. Phylogenetic and population genetic analysis of *Salmonella enterica* subsp. enterica serovar Infantis strains isolated in Japan using whole genome sequence data. Infect Genet Evol. 2014;27:62–8. https://doi.org/10.1016/j.meegid.2014.06.012
22. Seemann T. Snippy: rapid haploid variant calling [cited 2021 Feb 8]. https://github.com/tseemann/snippy
23. Tonkin-Hill G, Lees JA, Bentley SD, Frost SDW, Corander J. Fast hierarchical Bayesian analysis of population structure. Nucleic Acids Res. 2019;47:5539–49. https://doi.org/10.1093/nar/gkz361
24. Volz EM, Frost SDW. Scalable relaxed clock phylogenetic dating. Virus Evol. 2017;3:vex025. https://doi.org/10.1093/ve/vex025
25. Stamatakis A. RAxML version 8: a tool for phylogenetic analysis and post-analysis of large phylogenies. Bioinformatics. 2014;30(9):1312–3. https://doi.org/10.1093/bioinformatics/btu033
26. Hunt M, Mather AE, Sánchez-Busó L, Page AJ, Parkhill J, Keane JA, et al. ARIBA: rapid antimicrobial resistance genotyping directly from sequencing reads. Microb Genom. 2017;3:e000131.

27. Carattoli A, Zankari E, García-Fernández A, Voldby Larsen M, Lund O, Villa L, et al. In silico detection and typing of plasmids using PlasmidFinder and plasmid multilocus sequence typing. Antimicrob Agents Chemother. 2014;58:3895–903. https://doi.org/10.1128/AAC.02412-14
28. Zankari E, Hasman H, Cosentino S, Vestergaard M, Rasmussen S, Lund O, et al. Identification of acquired antimicrobial resistance genes. J Antimicrob Chemother. 2012;67:2640–4. https://doi.org/10.1093/jac/dks261
29. Kürekci C, Sahin S, Iwan E, Kwit R, Bomba A, Wasyl D. Whole-genome sequence analysis of *Salmonella* Infantis isolated from raw chicken meat samples and insights into pESI-like megaplasmid. Int J Food Microbiol. 2021;337:108956. https://doi.org/10.1016/j.ijfoodmicro.2020.108956
30. Mughini-Gras L, van Hoek AHAM, Cuperus T, Dam-Deisz C, van Overbeek W, van den Beld M, et al. Prevalence, risk factors and genetic traits of *Salmonella* Infantis in Dutch broiler flocks. Vet Microbiol. 2021;258:109120. https://doi.org/10.1016/j.vetmic.2021.109120
31. Vilela FP, Rodrigues DDP, Allard MW, Falcão JP. Genomic characterization and antimicrobial resistance profiles of *Salmonella enterica* serovar Infantis isolated from food, humans and veterinary-related sources in Brazil. J Appl Microbiol. 2022;132:3327–42. https://doi.org/10.1111/jam.15430
32. Papić B, Kušar D, Mićunović J, Pirš M, Ocepek M, Avberšek J. Clonal spread of pESI-positive multidrug-resistant ST32 *Salmonella enterica* serovar Infantis isolates among broilers and humans in Slovenia. Microbiol Spectr. 2022;10:e0248122. https://doi.org/10.1128/spectrum.02481-22
33. Alba P, Leekitcharoenphon P, Carfora V, Amoruso R, Cordaro G, Di Matteo P, et al. Molecular epidemiology of *Salmonella* Infantis in Europe: insights into the success of the bacterial host and its parasitic pESI-like megaplasmid. Microb Genom. 2020;6:e000365.
34. Acar S, Bulut E, Stasiewicz MJ, Soyer Y. Genome analysis of antimicrobial resistance, virulence, and plasmid presence in Turkish *Salmonella* serovar Infantis isolates. Int J Food Microbiol. 2019;307:108275. https://doi.org/10.1016/j.ijfoodmicro.2019.108275
35. Askari Badouei M, Vaezi H, Nemati A, Ghorbanyoon E, Firoozeh F, Jajarmi M, et al. High prevalence of clonally related multiple resistant *Salmonella* Infantis carrying class 1 integrons in broiler farms. Vet Ital. 2021;57.
36. Di Marcantonio L, Romantini R, Marotta F, Chiaverini A, Zilli K, Abass A, et al. The current landscape of antibiotic resistance of *Salmonella* Infantis in Italy: the expansion of extended-spectrum beta-lactamase producers on a local scale. Front Microbiol. 2022;13:812481. https://doi.org/10.3389/fmicb.2022.812481
37. Martínez-Puchol S, Riveros M, Ruidias K, Granda A, Ruiz-Roldán L, Zapata-Cachay C, et al. Dissemination of a multidrug resistant CTX-M-65 producer *Salmonella enterica* serovar Infantis clone between marketed chicken meat and children. Int J Food Microbiol. 2021;344:109109. https://doi.org/10.1016/j.ijfoodmicro.2021.109109
38. Mejía L, Medina JL, Bayas R, Salazar CS, Villavicencio F, Zapata S, et al. Genomic epidemiology of *Salmonella* Infantis in Ecuador: from poultry farms to human infections. Front Vet Sci. 2020;7:547891. https://doi.org/10.3389/fvets.2020.547891
39. Pardo-Esté C, Lorca D, Castro-Severyn J, Krüger G, Alvarez-Thon L, Zepeda P, et al. Genetic characterization of *Salmonella* Infantis with multiple drug resistance profiles isolated from a poultry-farm in Chile. Microorganisms. 2021;9:2370. https://doi.org/10.3390/microorganisms9112370
40. McMillan EA, Weinroth MD, Frye JG. Increased prevalence of *Salmonella* Infantis isolated from raw chicken and turkey products in the United States is due to a single clonal lineage carrying the pESI plasmid. Microorganisms. 2022;10:1478. https://doi.org/10.3390/microorganisms10071478
41. Drauch V, Kornschober C, Palmieri N, Hess M, Hess C. Infection dynamics of *Salmonella* Infantis strains displaying different genetic backgrounds—with or without pESI-like plasmid—vary considerably. Emerg Microbes Infect. 2021;10:1471–80. https://doi.org/10.1080/22221751.2021.1951124
42. Dos Santos AMP, Panzenhagen P, Ferrari RG, Conte-Junior CA. Large-scale genomic analysis reveals the pESI-like megaplasmid presence in *Salmonella* Agona, Muenchen, Schwarzengrund, and Senftenberg. Food Microbiol. 2022;108:104112. https://doi.org/10.1016/j.fm.2022.104112
43. Cohen E, Kriger O, Amit S, Davidovich M, Rahav G, Gal-Mor O. The emergence of a multidrug resistant *Salmonella* Muenchen in Israel is associated with horizontal acquisition of the epidemic pESI plasmid. Clin Microbiol Infect. 2022;28:1499.e7–14. https://doi.org/10.1016/j.cmi.2022.05.029

Address for correspondence: Jennifer Mattock, Roslin Institute, The University of Edinburgh, Easter Bush Campus, Midlothian, EH25 9RG, UK; email: jennifer.mattock@roslin.ed.ac.uk

Bus Riding as Amplification Mechanism for SARS-CoV-2 Transmission, Germany, 2021[1]

Meike Schöll,[2] Christoph Höhn,[2] Johannes Boucsein, Felix Moek, Jasper Plath, Maria an der Heiden, Matthew Huska, Stefan Kröger, Sofia Paraskevopoulou, Claudia Siffczyk, Udo Buchholz,[3] Raskit Lachmann[3]

To examine the risk associated with bus riding and identify transmission chains, we investigated a COVID-19 outbreak in Germany in 2021 that involved index case-patients among bus-riding students. We used routine surveillance data, performed laboratory analyses, interviewed case-patients, and conducted a cohort study. We identified 191 case-patients, 65 (34%) of whom were elementary schoolchildren. A phylogenetically unique strain and epidemiologic analyses provided a link between air travelers and cases among bus company staff, schoolchildren, other bus passengers, and their respective household members. The attack rate among bus-riding children at 1 school was ≈4 times higher than among children not taking a bus to that school. The outbreak exemplifies how an airborne agent may be transmitted effectively through (multiple) short (<20 minutes) public transport journeys and may rapidly affect many persons.

Several waves of COVID-19 have occurred in Germany (*1*). After low incidence rates in summer 2021, case numbers started to increase in late August because of the Delta variant (*2*). During the fourth COVID-19 wave in mid-September 2021 (*1*), a local public health authority (PHA) noticed an unusual increase in SARS-CoV-2 infections involving local schools in and around a city within the state of Hesse. The 7-day incidence of SARS-CoV-2 infection in this district reached 103 on September 15, compared with 99 in Hesse and 84 nationwide (Robert Koch Institute database, unpub. data). State legislation at the time prescribed mandatory use of medical masks in various settings, quarantine for persons with a positive test result (with exemptions for persons vaccinated or previously infected with SARS-CoV-2), and access bans to certain facilities for persons with COVID-19–compatible signs/symptoms (*3*). In the local elementary school, 1 case each was detected in calendar weeks (CW) 35 and 36, but in 2 subsequent days (September 14 and 15) in CW 37, test results for 18 students were positive. Because many of the students were riding a school bus, the hypothesis of the potential role of bus riding drew public attention.

On September 30, 2021, local and state PHAs invited the Robert Koch Institute (RKI), Germany's national public health institute, to jointly investigate the outbreak with the following 3 objectives: to describe the outbreak, its emergence and control; to identify potential sources and chains of transmission through a combination of epidemiologic investigations and whole-genome sequencing (WGS); and to investigate the risk, preventive factors, and modes of transmission, in particular with regard to the role of bus riding. We subsequently explored the role of bus transportation for SARS-CoV-2 transmission and the value of genomic data as a tool for identifying transmission chains.

Methods

General Outbreak Description

We defined an outbreak case-patient as anyone with a SARS-CoV-2 infection confirmed by reverse-transcription PCR (RT-PCR) who resided in the

Author affiliations: Robert Koch Institute, Berlin, Germany (M. Schöll, J. Boucsein, F. Moek, M. an der Heiden, M. Huska, S. Kröger, S. Paraskevopoulou, C. Siffczyk, U. Buchholz, R. Lachmann); European Centre for Disease Prevention and Control, Stockholm, Sweden (M. Schöll, J. Boucsein, F. Moek); Public Health Authority Main-Kinzig-Kreis, Hesse, Germany (C. Höhn, J. Plath)

DOI: https://doi.org/10.3201/eid3004.231299

[1]Preliminary results from this study were presented at the ESCAIDE conference; November 24, 2022; Stockholm, Sweden.

[2]These first authors contributed equally to this article.

[3]These senior authors contributed equally to this article.

affected district; whose symptom onset (or their test date) was from September 6 through October 15, 2021; and whose SARS-CoV-2 sample was assigned to the outbreak strain (sublineage AY.103) or who had an epidemiologic link to a case-patient with the outbreak strain. To describe the outbreak, we analyzed epidemiologic data from notified case-patients with SARS-CoV-2 infection and data from the respective laboratory samples. The principal of the most affected elementary school provided us with data on hygiene and testing routines, lists of class members and test results, and information on potential alternative exposures in the school setting.

WGS Analyses

We contacted laboratories to secure remaining specimens for WGS analysis from case-patients with potential links to the outbreak. In addition, we performed WGS on randomly selected specimens from case-patients from the greater region (*4*,*5*).

We used the complete-genome information to detect additional sequences that could belong to this outbreak cluster. For that purpose, we used the tool breakfast (https://github.com/rki-mf1/breakfast), which computes the pairwise genetic distance between multiple sequences. We assigned genomes with a genomic distance of ≤3 single-nucleotide polymorphisms from an isolate from another case-patient within the outbreak to the outbreak strain. The genomes used for the analyses were not sequenced in house but were obtained from the Germany nationwide integrated genomic surveillance of SARS-CoV-2 (*6*). Thus, sequences were assembled by the individual laboratories according to their own protocols before being submitted to the RKI as consensus sequences. Genomic surveillance of SARS-CoV-2 is based on a legal framework, which was established in the beginning of 2021. Within the molecular surveillance of SARS-CoV-2, samples were either randomly chosen (random samples) or selected according to prior defined criteria (targeted samples). From January–December 2021, >475,000 SARS-CoV-2 sequences were submitted, ≈40% of which were randomly selected. To reduce bias in the estimation of circulating virus variants and sublineage proportions, we used only random samples. To detect additional sequences within the outbreak cluster, we used all submitted sequences for similarity analysis.

Placing the Outbreak Genomes in a Phylogenetic Tree of Global SARS-CoV-2 Genomes

To identify whether the outbreak originated from a single source and whether it was effectively contained, we placed SARS-CoV-2 sequences from the outbreak case-patients in a global phylogenetic tree. The global tree contains all sequences from the GISAID (https://www.gisaid.org), GenBank, COVID-19 Genomics UK Consortium (https://www.cogconsortium.uk), and China National Center for Bioinformation (https://www.cncb.ac.cn) databases as of July 16, 2023 (>15 million sequences), and we conducted the placement by using a tool that is part of the National Center for Biotechnology Information Genome Browser (https://genome.ucsc.edu/cgi-bin/hgPhyloPlace), which relies on UShER (*7*) for placement of new sequences. Because RKI uploads all SARS-CoV-2 sequences to both GISAID and GenBank, the National Center for Biotechnology Information tree contains duplicates, which we removed manually. We then plotted the resulting deduplicated trees in R (The R Foundation for Statical Computing, https://www.r-project.org) by using the packages ggtree, treeio, ggplot2, ape, and dplyr (*8*–*12*) (Appendix Table, https://wwwnc.cdc.gov/EID/article/30/4/23-1299-App1.xlsx).

Bus-Riding Role and Associated Risk/Preventive Factors

We interviewed employees of the bus company and asked about bus schedules, hygiene, testing practices, and technical specifications of the bus. Using a computer-assisted standardized survey, we conducted phone interviews addressing households with outbreak case-patients as well as nonaffected households. The survey was designed to investigate several hypotheses regarding the COVID-19 outbreak at the elementary school, including exposure at school, during school bus rides, and during other social contacts.

To define the most likely infection setting of the case-patients, we combined information from the informal interviews, the survey, and the surveillance system. Secondary case-patients who lived in the same household as an outbreak case-patient were assigned to the infection setting "household." Only case-patients who rode the bus on days when the bus driver was assumed to be infectious were assigned to the infection setting "bus." Members of the bus company were assigned to the infection setting "workplace." Case-patients who took part in social events that were attended by outbreak case-patients were assigned to the infection setting "other." Whenever information regarding the use of the affected bus was insufficient, we conservatively assumed a different infection setting. We first conducted a cohort study of all students in grades 1–4 and defined case-patients as students having a SARS-CoV-2 infection confirmed by RT-PCR

and symptom onset (alternatively test date) during September 6–October 15, 2021. We defined all other students at this school as non–case-patients. We calculated contingency tables, attributable fractions, and risk ratios.

To calculate risk and protective factors during school bus transportation, we conducted a second cohort study of elementary school students who used the school bus ≥1 time during September 9–17, 2021. Case-patients in this cohort were defined as students with a SARS-CoV-2 infection confirmed by RT-PCR whose symptom onset (alternatively test date) was during September 14–23, 2021. Information on seating position, mask use, vaccination status, and cumulative time at risk (i.e., time spent on the bus) were compared for case-patients versus non–case-patients by using univariable logistic regression.

The outbreak investigation was conducted under the official mandate of the local PHA resulting from paragraph 25 section 1 sentence 1 German Infection Protection Act (IfSG) and was thus exempt from review ethics committee review. We followed local and RKI ethics and data protection standards.

Results

Outbreak Description

We identified 191 case-patients (median age 17.5 years; 50% female and 50% male), of which 65 (34%) were elementary schoolchildren. According to the criteria of the German Standing Committee on Vaccination, 23% of all outbreak case-patients were fully vaccinated (Table 1) (*13*).

Most (160 [84%]) case-patients were symptomatic, 5 (3%) were hospitalized, and 4 (2%) (≥60 years of age) died. We identified only 1 SARS-CoV-2 reinfection. Case numbers associated with this outbreak peaked on September 17, 2021, and the outbreak was over by October 15, 2021 (Figure 1).

Suboutbreak I among Elementary School Students

The most affected elementary school comprised 4 grade levels, each accommodating students of a similar age, with 3 to 4 classes (A, B, C, and D) per grade. Of 306 students, 70 were positive for SARS-CoV-2 during the investigation period, 65 of whom fulfilled the definition of outbreak case-patient (Table 2). Many students in classes A and B rode the school bus, and individual bus rides lasted 9–18 minutes. Students in

Table 1. Main characteristics of case-patients in COVID-19 outbreak, by age group, Hesse, Germany, 2021*

Characteristic	Age, y						Overall no. (%), n = 191
	<6, no. (%), n = 11	6–10, no. (%), n = 73	11–17, no. (%), n = 28	18–40, no. (%), n = 20	41–60, no. (%), n = 30	>60, no. (%), n = 29	
Sex							
F	5 (45.5)	32 (43.8)	14 (50.0)	14 (70.0)	13 (43.3)	18 (62.1)	96 (50.3)
M	6 (54.5)	41 (56.2)	14 (50.0)	6 (30.0)	17 (56.7)	11 (37.9)	95 (49.7)
Setting							
Household	7 (63.6)	5 (6.8)	18 (64.3)	19 (95.0)	27 (90.0)	9 (31.0)	85 (44.5)
Bus	3 (27.3)	46 (63.0)	3 (10.7)	0	1 (3.3)	6 (20.7)	59 (30.9)
School	0	19 (26.0)	1 (3.6)	0	0	0	20 (10.5)
Workplace	0	0	0	0	2 (6.7)	4 (13.8)	6 (3.1)
Travel	0	0	0	0	0	5 (17.2)	5 (2.6)
Other	1 (9.1)	0	2 (7.1)	1 (5.0)	0	4 (13.8)	8 (4.2)
Unknown	0	3 (4.1)	4 (14.3)	0	0	1 (3.4)	8 (4.2)
Prior SARS-CoV-2 infection							
Yes	0	1 (1.4)	0	0	0	0	1 (0.5)
No	11 (100)	72 (98.6)	28 (100)	20 (100)	30 (100)	29 (100)	190 (99.5)
Symptomatic infection							
Yes	7 (63.6)	62 (84.9)	23 (82.1)	20 (100)	26 (86.7)	22 (75.9)	160 (83.8)
No	4 (36.4)	11 (15.1)	5 (17.9)	0	4 (13.3)	6 (20.7)	30 (15.7)
Value missing	0	0	0	0	0	1 (3.4)	1 (0.5)
Severity of disease, most severe status selected							
No treatment	9 (81.8)	58 (79.5)	14 (50.0)	12 (60.0)	17 (56.7)	15 (51.7)	125 (65.4)
Outpatient treatment	0	6 (8.2)	0	3 (15.0)	5 (16.7)	0	14 (7.3)
Inpatient treatment	0	0	1 (3.6)	1 (5.0)	0	3 (10.3)	5 (2.6)
Treatment in ICU	0	0	0	0	2 (6.7)	0	2 (1.0)
Deceased	0	0	0	0	0	4 (13.8)	4 (2.1)
Value missing	2 (18.2)	9 (12.3)	13 (46.4)	4 (20.0)	6 (20.0)	7 (24.1)	41 (21.5)
COVID-19 vaccination status							
Fully vaccinated	0	0	0	10 (50.0)	14 (46.7)	19 (65.5)	43 (22.5)
Not or not fully vaccinated	11 (100)	73 (100)	28 (100)	10 (50.0)	16 (53.3)	10 (34.5)	148 (77.5)

*The variable on severity of disease combines information from the routine surveillance system with survey results, resulting in a high number of missing values. ICU, intensive care unit.

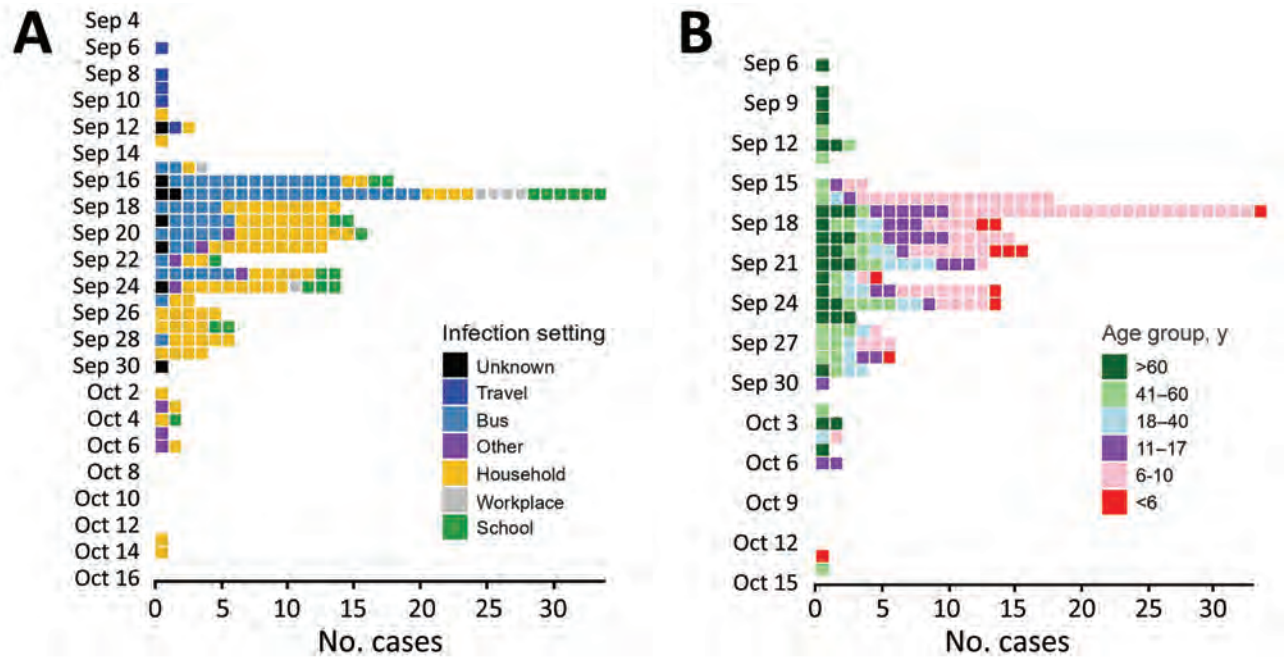

Figure 1. Epidemic curves for 191 case-patients in COVID-19 outbreak, Hesse, Germany, 2021. Dates are for symptom onset or first positive test result, whichever was earlier. A) By probable transmission setting; B) by age group.

classes C and D generally did not ride the school bus. In September 2021, students at the school were regularly tested by antigen test 3 times per week. In addition, all quarantined students (mostly from classes A and B) were tested by RT-PCR 1 time during CW 38.

Results from the first cohort study show that 65 outbreak cases at the most affected school occurred in classes with bus-riding students, resulting in a relative risk of 24 (95% CI 6–95). Because testing practices differed between quarantined and nonquarantined students, cases in classes A and B were more likely to be detected, potentially biasing that relative risk. However, when we limited our analysis to students in classes A and B, the relative risk for bus-riding students was still 4 (95% CI 3–6) times greater than for those not riding the bus. That finding suggests that an attributable proportion of case-patients among students in classes A and B (74%) were exposed to SARS-CoV-2 by bus riding. Apart from bus riding, we did not identify any other common factor (e.g., social activities, common teacher, shared meals) among case-patients at that school.

Table 2. COVID-19 attack rates by class type and grade at an elementary school, Hesse, Germany, 2021

Class type or grade	No. students	No. COVID-19 case-patients	COVID-19 attack rate, %
Class			
A	88	43	49
B	91	25	28
C	84	2	2,4
D	43	0	0
Grade			
1	91	21	23
2	68	19	28
3	81	19	24
4	66	11	17

In the second cohort study, among the 61 interviewed students who rode the school bus during September 9–17, a total of 45 students tested positive for SARS-CoV-2. Parents and care providers reported regular wearing of masks and variable seating arrangements for those children. Because the number of bus rides differed, cumulative time on the bus varied from 36 to 234 minutes. We found no statistically significant risk or protective factors among bus-riding students.

Bus Driver and Bus Properties

The school bus driver tested positive for SARS-CoV-2 on September 15. As a close contact of a SARS-CoV-2–infected person and lacking vaccination, starting September 13, he was required to be quarantined. We were told that he instead drove the public bus, the school bus, and 1 charter tour bus (with female daytrippers) until September 15. In addition, several bus passengers (or their parents) reported that the bus driver was coughing and not wearing a mask for several days until he tested positive on September 15.

The obligation to wear masks during the ride was not generally enforced on the bus. The bus

provided fresh air through air conditioning and regular air circulation; the 2 roof openings were not regularly opened in September.

Tourist Group

The school bus driver also picked up 17 air travelers returning from a trip to Georgia on September 8, 2021. He transported the group for 1 hour. In early September, 6 of the travelers tested positive for SARS-CoV-2, 5 of whom fulfilled the definition of an outbreak case-patient (Figure 1). The first documented outbreak case-patient belonged to that tourist group, and symptoms had developed on September 6, 2021, while they were still traveling abroad.

Public Passengers and Bus Company Staff

The bus driver also transported passengers on the public bus who were mostly adults and secondary school students, whereas passengers on the school bus were limited to students of 1 elementary school and 1 childcare center. We also identified subsequent case-patients among the driver's close contacts at the bus company and in all of the described passenger groups. Of the 7 members of the bus company and their respective household members who had regular and close contact with each other, 6 tested positive over the course of the outbreak.

Suboutbreak II among Day-Trippers

On September 15, 2021, the bus driver transported a group of 30 fully vaccinated female day-trippers, among which 6 became ill after the day trip. According to 1 woman's recollection, none of the passengers wore a mask during the bus ride. The bus driver joined the group during lunch time. Two of the subsequent case-patients among the day-trippers sat directly behind the bus driver during the ride; a third case-patient shared a table with the bus driver during lunch. Symptoms developed in the case-patients 4–10 days after the day trip, and they tested positive 7–17 days after the trip. Alternative exposures, other than contact with the bus driver, were not disclosed for any of the 6 case-patients.

WGS Data and Phylogenetic Sequences

We had WGS data for 39 outbreak case-patients, including a secondary case-patient in the household of a returning traveler from Georgia. On the basis of the WGS data, we identified epidemiologic links for 31 case-patients with the outbreak strain; for the remaining 8, we did not have sufficient information. The phylogenetically unique strain (novel in Germany at this time) enabled us to link the following case-patients or case groups (1 case-patient from the tourist group with a previously established epidemiologic link was later excluded on the basis of sequencing findings): schoolchildren (all 15 available sequences belonged to the outbreak strain and 7 available sequences from household members of students from this school); the tourist group (1 sequence belonging to the outbreak strain from a household member of a traveler); the female day-trippers (1 available sequence belonged to the outbreak strain); subsequent case-patients among staff of the bus company (2 available sequences of the household members of the staff of the bus company belonged to the outbreak strain); and other bus passengers (transported by the same bus company), their respective household members, or both (Figure 1, panel B; Figures 2–4).

Using the national sequencing database at RKI, we compared the outbreak sequences not only to sequences obtained from the affected district but also to all sequences available for Germany. We identified 16 additional sequences in Germany and 3 sequences in Austria and the United States clustering with the outbreak sequence. The sequences from Germany

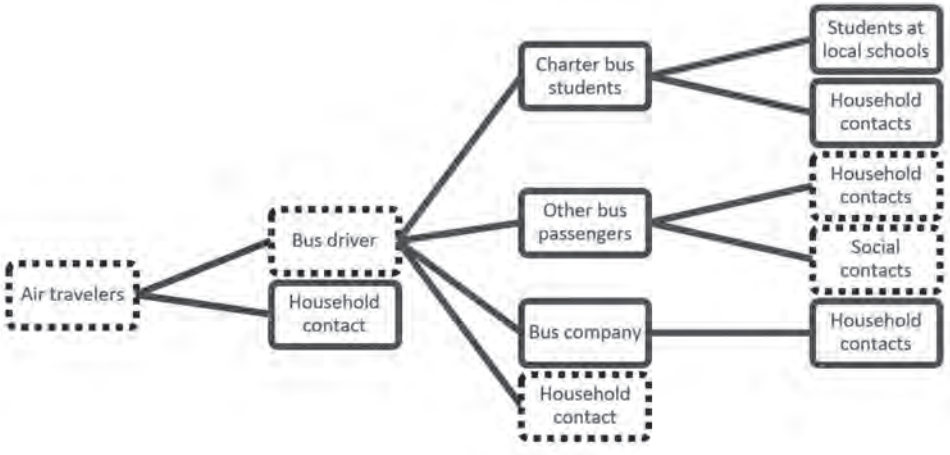

Figure 2. Plausible chains of transmission in COVID-19 outbreak in Hesse, Germany, 2021 (n = 191), Solid boxes indicate that whole-genome sequencing evidence of the outbreak strain was available for ≥1 case; dotted boxes indicate cases with no whole-genome sequencing evidence available.

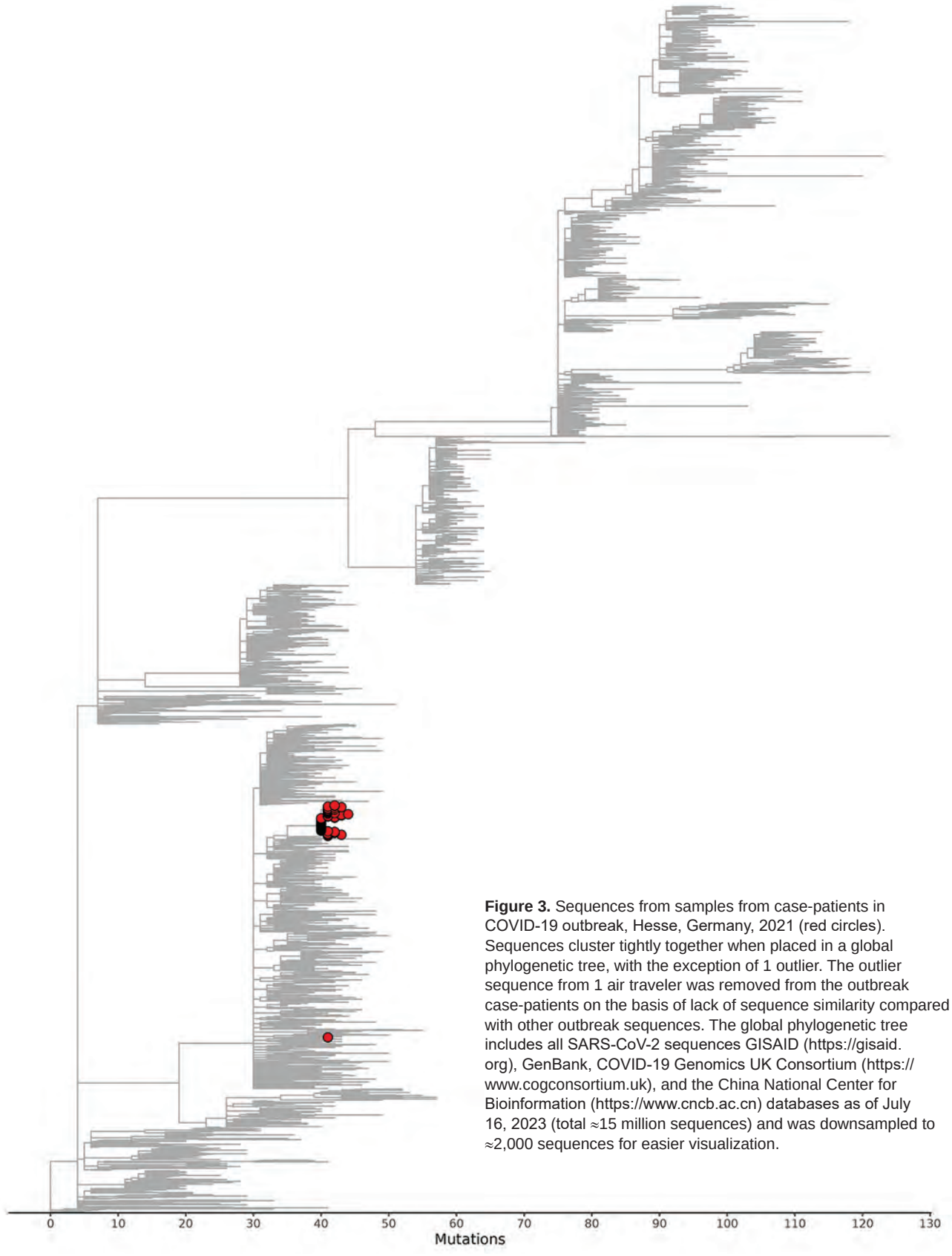

Figure 3. Sequences from samples from case-patients in COVID-19 outbreak, Hesse, Germany, 2021 (red circles). Sequences cluster tightly together when placed in a global phylogenetic tree, with the exception of 1 outlier. The outlier sequence from 1 air traveler was removed from the outbreak case-patients on the basis of lack of sequence similarity compared with other outbreak sequences. The global phylogenetic tree includes all SARS-CoV-2 sequences GISAID (https://gisaid.org), GenBank, COVID-19 Genomics UK Consortium (https://www.cogconsortium.uk), and the China National Center for Bioinformation (https://www.cncb.ac.cn) databases as of July 16, 2023 (total ≈15 million sequences) and was downsampled to ≈2,000 sequences for easier visualization.

belonged to case-patients outside of the district with symptom onset during September 21—October 12, 2021. Further epidemiologic information was available for 9 of those case-patients, all of whom could be epidemiologically linked to the outbreak; however, they were not included in the total case count because they resided outside the outbreak district.

Discussion

Using integrated epidemiologic and genomic data, we documented the introduction of a novel SARS-CoV-2 strain (AY.103) to Germany by air travelers, leading to an outbreak. Our investigation also highlights effective transmission of the SARS-CoV-2 Delta variant on a bus. Most likely, at the time of arrival in Germany, the virus spread from the air travelers to the bus driver, who during the following days may have transmitted the virus to the bus-riding schoolchildren and other passengers. The outbreak spread further within the bus company, schools, and corresponding households. To our knowledge, further transmission was prevented because of measures such as testing and quarantine implemented by the PHA after outbreak detection.

Our investigation of suboutbreak I at the elementary school suggests that although the transit time among students was only 9–18 minutes twice a day, the attributable portion of early case-patients among students explained by bus riding amounts to 74%. The actual percentage might even be greater because we considered those case-patients to have been exposed only inside the charter bus, for which we were able to verify the information in interviews.

The suboutbreak II among day trippers who were exposed to the same bus driver as the schoolchildren provides further evidence regarding transmission chains. Nevertheless, we cannot determine whether transmissions took place only during the 1-hour bus ride or also while sharing a lunch table with the bus driver.

Given the delay between the timing of the outbreak and its investigation, most samples had already been discarded. However, data from the available samples agree with our epidemiologic findings and suggest transmission as described above. The sequence lineage had not been detected in Germany before the arrival of the tourist group, suggesting that the strain was introduced by the travelers. Although it seems unlikely that a person other than the bus driver might have served as the link between all the groups with the same outbreak strain (household person of an air traveler, bus company staff, bus riding children, day trippers), we cannot exclude the possibility of an unobserved additional transmission chain.

Regarding infection of the schoolchildren, transmission could have taken place somewhere other than inside the bus. Children in every school grade were affected, and the available sequences link the respective students or their household contacts or both to the outbreak cluster. In addition, analysis of the relative risks in the school classes showed a significantly elevated relative risk for infection among bus-riding students. Those observations strongly support the hypothesis that most infections among schoolchildren were associated with bus transportation. However, because most students rode the bus twice a day, it remains unclear if transmissions happened on a single bus journey or if the cumulative exposure over several days was key.

Epidemiologic and genomic data demonstrate that contact tracing, testing, isolation, and quarantine successfully contained the outbreak. Because the outbreak strain was unique within Germany, the phylogenetic analyses prove that the outbreak strain has not spread further. As such, the effectiveness of contact tracing, isolation, and quarantine in the middle of the wave of the extremely transmissible Delta variant is convincing.

WGS was key to validating the existing epidemiologic links and identifying additional case-patients outside the cluster. Furthermore, given the specific strain and broad sequencing data for strains from the area and globally, WGS helped confirm that we did not miss other suboutbreaks. The AY.103 strain was not detected in the area after the outbreak was over, which shows that the local transmission was contained.

Our findings are relevant given that evidence of SARS-CoV-2 transmission events associated with short bus rides or public bus transportation is limited (*14*). Rather, published transmission events or outbreaks associated with bus transportation stem from longer bus rides (*15*–*18*). A large cohort study in Norway early in the pandemic (when masks were not yet routinely worn) showed a dose–response relationship between using public transport and the risk of acquiring SARS-CoV-2 (*19*). A study of US students riding school buses with infected COVID-19 passengers yielded no secondary case-patients associated with bus transport (*20*). Lack of transmission may have resulted from thorough adherence to mask wearing, lower transmissibility, and susceptibility of children to the wild virus (compared with the Delta variant), or both (*21*; O.A. Uthman, unpub. data, https://www.medrxiv.org/

content/10.1101/2022.08.26.22279248v1). Our article describes a high secondary attack rate on (multiple) short bus journeys of <20 minutes during circulation of the Delta variant.

Among the limitations of our findings, we note that because the outbreak investigation was retrospective, active case finding was limited and some cases might have gone unnoticed, particularly among

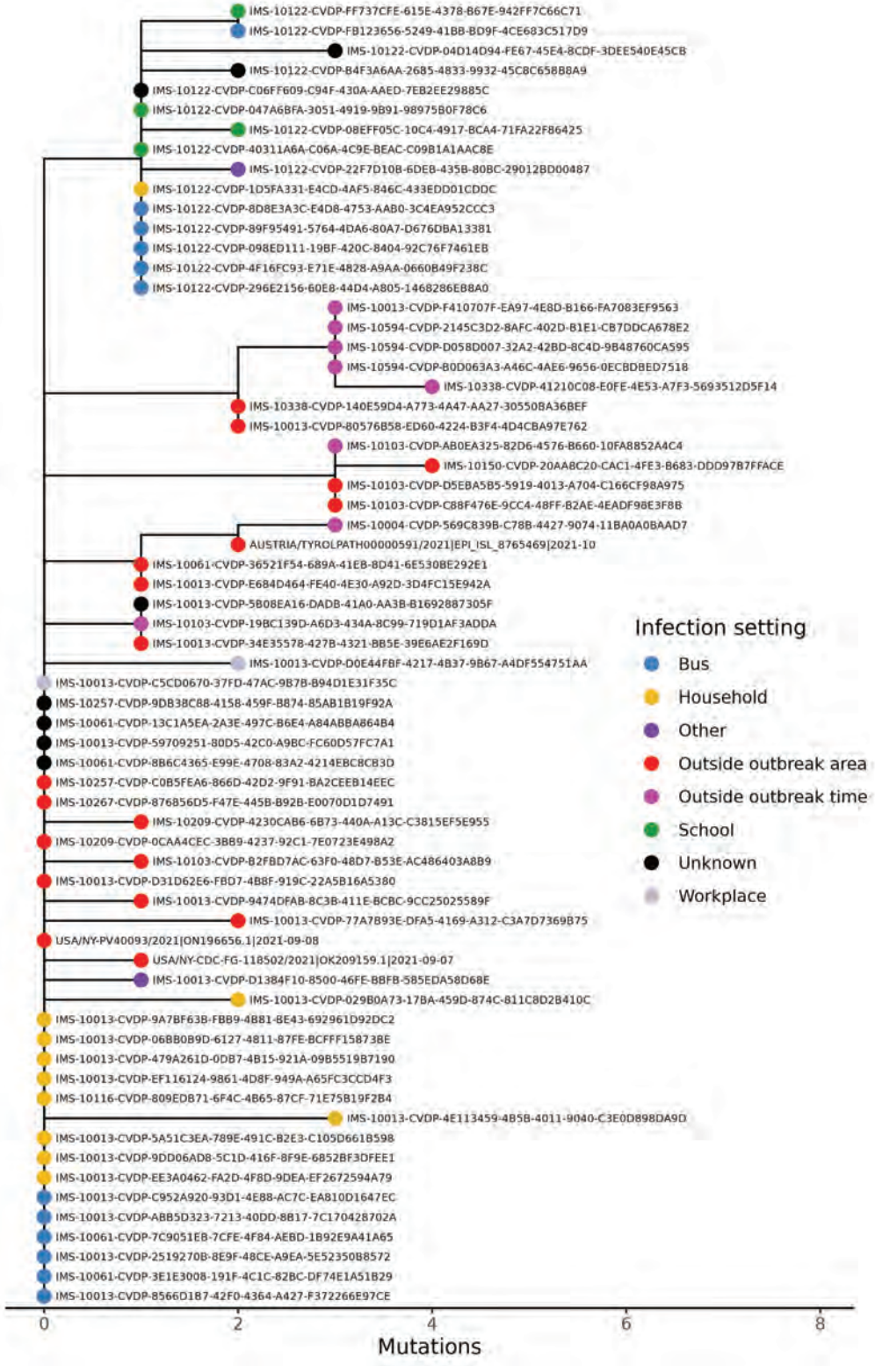

Figure 4. The subtree of the global SARS-CoV-2 phylogenetic tree in Figure 3 that contains all outbreak patient sequences contains few nonoutbreak sequences, showing that the outbreak in Hesse, Germany, 2021, was effectively contained. Three international sequences are included (2 from the United States, 1 from Austria), as well as 8 sequences that are from outside of the defined outbreak time period and 16 from outside the geographic region but still within Germany.

vaccinated household contact persons who were asymptomatic and therefore not tested. Also, outbreak case-patients and their respective links to the outbreak may have been underascertained because of lack of epidemiologic or molecular evidence.

Recall bias may have affected our identification of epidemiologic links and the data quality. Given local media coverage, the outbreak and its potential links to bus transportation were stipulated before being properly investigated. To address that limitation, we applied a conservative approach toward epidemiologic links; instead of relying on school lists for use of bus transportation, we interviewed families about actual bus use and based confirmed bus transportation on those interviews only. However, some misattribution cannot be fully excluded, and the data quality regarding mask use and seat location within the bus remains limited, given the difficulty of recall and secondhand information from parents instead of the young children themselves.

Our report showcases how local bus transportation amplified a COVID-19 outbreak. In collaboration with the affected local institutions and bus company, the local PHA rapidly identified the ongoing COVID-19 outbreak and implemented successful measures to control it. Regular testing at school enhanced early detection of SARS-CoV-2 infections, and early quarantine helped minimize subsequent transmissions at school and shows the value of quarantine measures for nonvaccinated contact persons at that time. WGS was essential for proving transmission chains.

To identify and resolve respiratory virus superspreading events, use of public transport and multiple short (<20 minutes) bus rides should be considered as potential amplification mechanisms. PHA should also consider WGS as a useful early adjunct tool for outbreak investigations. Hygiene measures, such as regular testing and mask wearing, should be implemented indoors and on public transportation during similar epidemics or pandemics.

Acknowledgments

We are grateful for the excellent and competent cooperation with the employees at the PHA in Hesse. We also thank the laboratories who provided, processed, and analyzed the samples using WGS.

All authors declare no conflicts of interest.

About the Author

Dr. Schöll is a medical doctor and political scientist. She works as an epidemiologist; her research interests are infectious disease epidemiology, crisis management, and evaluation.

References

1. Schilling J, Buda S, Tolksdorf K. Second update of the retrospective phase classification of the COVID-19 pandemic in Germany [in German]. Epidemiologisches Bulletin. 2022;10:3–5.
2. Mathieu E, Ritchie H, Rodés-Guirao L, Appel C, Giattino C, Hasell J, et al. Germany: coronavirus pandemic country profile [cited 2024 Feb 24]. https://ourworldindata.org/coronavirus/country/germany
3. Ordinance on the Protection of the Population from Infections with the Coronavirus SARS-CoV 2 [in German] [accessed 2024 Feb 27]. https://starweb.hessen.de/cache/GVBL/2021/00000.pdf
4. Ordinance on Molecular Genetic Surveillance of the Coronavirus SARS-CoV-2 [in German] [cited 2024 Feb 27]. https://www.bundesgesundheitsministerium.de/fileadmin/Dateien/3_Downloads/C/Coronavirus/Verordnungen/CorSurV_BAnz_AT_19.01.2021_V2.pdf
5. Robert Koch Institute. Guidelines for primary sequencing laboratories regarding selection of SARS-CoV-2 samples for whole-genome sequencing in the context of coronavirus surveillance regulation [in German] [cited 2024 Feb 27]. https://www.rki.de/DE/Content/InfAZ/N/Neuartiges_Coronavirus/DESH/CorSurV-Kriterien.html
6. Oh DY, Hölzer M, Paraskevopoulou S, Trofimova M, Hartkopf F, Budt M, et al.; Integrated Molecular Surveillance for SARS-CoV-2 (IMS-SC2) Laboratory Network. Advancing precision vaccinology by molecular and genomic surveillance of severe acute respiratory syndrome coronavirus 2 in Germany, 2021. Clin Infect Dis. 2022;75(Suppl 1):S110–20. https://doi.org/10.1093/cid/ciac399
7. Turakhia Y, Thornlow B, Hinrichs AS, De Maio N, Gozashti L, Lanfear R, et al. Ultrafast Sample placement on Existing tRees (USHER) enables real-time phylogenetics for the SARS-CoV-2 pandemic. Nat Genet. 2021;53:809–16. https://doi.org/10.1038/s41588-021-00862-7
8. Yu G, Smith D, Zhu H, Guan Y, Lam TT. ggtree: an R package for visualization and annotation of phylogenetic trees with their covariates and other associated data. Methods Ecol Evol. 2017;8:28–36. https://doi.org/10.1111/2041-210X.12628
9. Wang LG, Lam TT, Xu S, Dai Z, Zhou L, Feng T, et al. Treeio: an R package for phylogenetic tree input and output with richly annotated and associated data. Mol Biol Evol. 2020;37:599–603. https://doi.org/10.1093/molbev/msz240
10. Wickham H. ggplot2: elegant graphics for data analysis. New York: Springer-Verlag; 2016.
11. Paradis E, Schliep K. ape 5.0: an environment for modern phylogenetics and evolutionary analyses in R. Bioinformatics. 2019;35:526–8. https://doi.org/10.1093/bioinformatics/bty633
12. Wickham H, François R, Henry L, Müller K, Vaughan D. dplyr: a grammar of data manipulation 2023 [cited 2024 Feb 27]. https://github.com/tidyverse/dplyr
13. Vygen-Bonnet S, Koch J, Armann J, Berner R, Bogdan C, Harder T, et al.; Standing Committee on Vaccination in Germany (STIKO) for COVID-19. Decision regarding update of recommendation to vaccinate teenagers aged 12 to 17 years with mRNA-based vaccines, 9th update [in German]. Epidemiologisches Bulletin. 2021;33:3–46.
14. Heinrich J, Zhao T, Quartucci C, Herbig B, Nowak D. SARS-CoV-2 infections during travel by train and bus: a systematic review of epidemiological studies [in

German]. Gesundheitswesen. 2021;83:581–92. https://doi.org/10.1055/a-1531-5264
15. Luo K, Lei Z, Hai Z, Xiao S, Rui J, Yang H, et al. Transmission of SARS-CoV-2 in public transportation vehicles: a case study in Hunan Province, China. Open Forum Infectious Diseases. 2020;7:ofaa430.
16. Shen Y, Li C, Dong H, Wang Z, Martinez L, Sun Z, et al. Community outbreak investigation of SARS-CoV-2 transmission among bus riders in eastern China. JAMA Intern Med. 2020;180:1665–71. https://doi.org/10.1001/jamainternmed.2020.5225
17. Tsuchihashi Y, Yamagishi T, Suzuki M, Sekizuka T, Kuroda M, Itoi T, et al. High attack rate of SARS-CoV-2 infections during a bus tour in Japan. J Travel Med. 2021;28:taab111.
18 Benenson S, Ottolenghi M, Cohen MJ, Nir-Paz R, Oster Y. High attack rate of COVID-19 in an organized tour group of vaccinated travellers to Iceland. J Travel Med. 2021;28:taab157.
19. Ellingjord-Dale M, Kalleberg KT, Istre MS, Nygaard AB, Brunvoll SH, Eggesbø LM, et al. The use of public transport and contraction of SARS-CoV-2 in a large prospective cohort in Norway. BMC Infect Dis. 2022;22:252. https://doi.org/10.1186/s12879-022-07233-5
20. Ramirez DWE, Klinkhammer MD, Rowland LC. COVID-19 transmission during transportation of 1st to 12th grade students: experience of an independent school in Virginia. J Sch Health. 2021;91:678–82. https://doi.org/10.1111/josh.13058
21. Earnest R, Uddin R, Matluk N, Renzette N, Turbett SE, Siddle KJ, et al.; New England Variant Investigation Team. Comparative transmissibility of SARS-CoV-2 variants Delta and Alpha in New England, USA. Cell Rep Med. 2022;3:100583.

Address for correspondence: Raskit Lachmann, Robert Koch Institute, Seestrasse 10, 13351 Berlin, Germany; email: lachmannr@rki.de

Isolation of Diverse Simian Arteriviruses Causing Hemorrhagic Disease

Teressa M. Shaw, Samuel T. Dettle, Andres Mejia, Jennifer M. Hayes, Heather A. Simmons, Puja Basu, Jens H. Kuhn, Mitchell D. Ramuta, Cody J. Warren, Peter B. Jahrling, David H. O'Connor, Liupei Huang, Misbah Zaeem, Jiwon Seo, Igor I. Slukvin, Matthew E. Brown, Adam L. Bailey

Genetically diverse simian arteriviruses (simarteriviruses) naturally infect geographically and phylogenetically diverse monkeys, and cross-species transmission and emergence are of considerable concern. Characterization of most simarteriviruses beyond sequence analysis has not been possible because the viruses fail to propagate in the laboratory. We attempted to isolate 4 simarteriviruses, Kibale red colobus virus 1, Pebjah virus, simian hemorrhagic fever virus, and Southwest baboon virus 1, by inoculating an immortalized grivet cell line (known to replicate simian hemorrhagic fever virus), primary macaque cells, macrophages derived from macaque induced pluripotent stem cells, and mice engrafted with macaque CD34+-enriched hematopoietic stem cells. The combined effort resulted in successful virus isolation; however, no single approach was successful for all 4 simarteriviruses. We describe several approaches that might be used to isolate additional simarteriviruses for phenotypic characterization. Our results will expedite laboratory studies of simarteriviruses to elucidate virus-host interactions, assess zoonotic risk, and develop medical countermeasures.

Simarteriviruses (order Nidovirales, family Arteriviridae, subfamily Simarterivirinae) are genetically diverse viruses that naturally infect cercopithecoid monkeys throughout sub-Saharan Africa. Many divergent simarteriviruses can infect macaques, although severity of disease ranges from subclinical to highly fatal in this nonnatural host (*1*,*2*). Simarteriviruses are not known to infect humans, but the close evolutionary history of simarterivirus hosts and humans, their interhost and intrahost diversity, and various molecular characteristics suggest that those viruses might pose a zoonotic threat (*3*–*5*).

Simian hemorrhagic fever virus (SHFV), the best characterized simarterivirus, was identified as the cause of a highly fatal hemorrhagic fever epizootic at a National Institutes of Health quarantine facility in Bethesda, Maryland, USA, in 1964, affecting captive rhesus monkeys from Asia (*Macaca mulatta*), crab-eating macaques (*Macaca fascicularis*), and stump-tailed macaques (*Macaca arctoides*) (*6*–*8*). During the next 3 decades, several other epizootics in captive macaques were attributed to SHFV, but retrospective sequencing analyses indicated that other highly diverse simarteriviruses caused some of those outbreaks despite similar clinical manifestations (*9*). Healthy monkeys from Africa housed adjacent to the affected macaques from Asia were long suspected to be the natural simarterivirus hosts, but simarterivirus identification in healthy wild monkeys from Africa only began in 2011, when metagenomic sequencing was used (*10*–*14*).

Arteriviruses in general, and simarteriviruses in particular, are difficult to isolate. SHFV will only replicate to high titers in the grivet-derived cell line MA-104 and its subclones (e.g., MARC-145) (*5*,*8*,*15*–*19*). Although Kibale red colobus virus 1 (KRCV-1) can replicate in MARC-145 cells, replication is inconsistent, and virus production is low. Thus, immortalized cell lines capable of sustaining robust replication of simarteriviruses other than SHFV do not exist. If a novel simarterivirus were to emerge, threatening human or animal health, the lack of in vitro systems for virus propagation and isolation would be a major hurdle in understanding basic virology and developing medical countermeasures. We describe a

Author affiliations: University of Wisconsin, Madison, Wisconsin, USA (T.M. Shaw, S.T. Dettle, A. Mejia, M.D. Ramuta, D.H. O'Connor, L. Huang, M. Zaeem, J. Seo, I.I. Slukvin, M.E. Brown, A.L. Bailey); Wisconsin National Primate Research Center, Madison (S.T. Dettle, A. Mejia, J.M. Hayes, H.A. Simmons, P. Basu, D.H. O'Connor, I.I. Slukvin); National Institutes of Health, Fort Detrick, Frederick, Maryland, USA (J.H. Kuhn, P.B. Jahrling), The Ohio State University, Columbus, Ohio, USA (C.J. Warren)

DOI: https://doi.org/10.3201/eid3004.231457

combination of approaches resulting in successful isolation of multiple diverse simarteriviruses.

Methods

Biosafety and Ethics Statement

We obtained primary macaque tissues from the Nonhuman Primate Biologic Materials Distribution Core service at the Wisconsin National Primate Research Center in Madison, WI, USA. All experiments involving simarteriviruses were performed in a Biosafety Level 3 laboratory by trained personnel equipped with powered air purifying respirators, according to approved standard operating procedures. All experiments were approved before initiation by the institutional Biosafety Committee and Animal Care and Use Committee at the University of Wisconsin–Madison.

Virus Choices

Most simarteriviruses are uncultivable in vitro. Viruses that have been successfully used for in vivo studies are KRCV-1, SHFV, and Southwest baboon virus 1 (SWBV-1); those infections were performed in cercopithecoid nonhuman primates (NHPs). Small rodent models of simarterivirus infection would be useful to further characterize simarterivirus transmission and pathogenesis as well as to develop medical countermeasures against simarteriviruses of zoonotic concern. We chose the viruses evaluated in this study because they were previously discovered in the laboratory of David H. O'Connor at the University of Wisconsin–Madison by using unbiased deep sequencing, and we had retained residual source material from those studies. Pebjah virus (PBJV) had not been isolated, and our source material was not known to contain infectious virus. SWBV-1 had not been isolated, but we had reason to believe that our source material contained infectious virus because we had been able to productively infect NHPs with this material, as previously described (Table) (*25*).

Source Material

Low-titer MARC-145 cell culture supernatant containing KRCV-1 (*10*,*13*) was provided by Cody Warren (The Ohio State University). We obtained olive baboon plasma containing SWBV-1 RNA, cell culture supernatants containing SHFV or recombinant SHFV expressing enhanced green fluorescent protein (eGFP), and material containing PBJV RNA from previous studies (*9*,*12*,*15*,*17*,*25*). For in vitro experiments, we provide the multiplicity of infection (MOI) for SHFV in PFU, determined by plaque assay (*16*). We were unable to make similar MOI estimations for KRCV-1, PBJV, and SWBV-1 because we lacked a method for assessing virus titers; therefore, we used the same volumes of starting material for each of those viruses.

Quantification

For quantification of virus RNA in cell culture supernatants or serum samples, we extracted RNA from 20 or 50 µL of samples by using a KingFisher Flex System and MagMAX Viral and Pathogen Nucleic Acid Isolation Kit (both ThermoFisher Scientific, https://www.thermofisher.com). We eluted RNA in 50 µL water and used 8.5 µL RNA for quantitative reverse transcription PCR (qRT-PCR). We designed virus-specific TaqMan assays to detect each virus by

Table. Viruses used in study of isolation of diverse simarteriviruses causing hemorrhagic disease*

Simarterivirus	Year of discovery	Place of discovery	Natural monkey host from Africa	Disease in macaques from Asia	References
Kibale red colobus virus 1	2011	Kibale National Park, Uganda	Ugandan red colobus (*Piliocolobus tephrosceles*)	Mild (experimental exposure of crab-eating macaques)	(*10*,*17*)
Pebjah virus	1989, 2015	Primate Research Institute of New Mexico State University, Alamogordo, New Mexico, USA	Unknown	Severe/lethal (epizootic among captive crab-eating macaques)	(*9*,*20*,*21*)
Simian hemorrhagic fever virus	1964	Primate Quarantine Unit at the National Institutes of Health, Bethesda, Maryland, USA	Possible: Olive baboons (*Papio anubis*), patas monkeys (*Erythrocebus patas*)	Severe/lethal (epizootic among captive crab-eating macaques, rhesus monkeys, and stump-tailed macaques; experimental exposure of crab-eating macaques, Japanese macaques; rhesus monkeys, and stump-tailed macaques)	(*6*–*8*,*17*,*22*–*24*)
Southwest baboon virus 1	2014	Southwest National Primate Research Center, San Antonio, Texas, USA	Olive baboons (*Papio anubis*)	Subclinical (experimental exposure of rhesus monkeys)	(*12*,*22*,*25*)

*NA, not applicable.

using simarterivirus genome sequences from GenBank. We used Primer3 (https://primer3.org) for primer and probe design, and Integrated DNA Technologies (https://idtdna.com) synthesized the primers and probes according to the FAM and Zen/Iowa-Black dual-quencher system. Oligonucleotide sequences were: KRCV-1-F, 5′-ACACGGCTACCCTTACTCC-3′; KRCV-1-R, 5′-TCGAGGTTAARCGGTTGAGA-3′; KRCV-1-P, 5′-TTCTGGTCCTCTTGCGAAGGC-3′; PBJV-F, 5′-GAGGATGGTCGCCTCAACTA-3′; PBJV-R, 5′-AAGGACCCTCGTCAAATTCA-3′; PBJV-P, 5′-TGCTGTCATCACACCAGATG-3′; SHFV-F, 5′-CGACCTCCGAGTTGTTCTACCT-3′; SHFV-R, 5′-GCCTCCGTTGTCGTAGTACCT-3′; SHFV-P, 5′-CCCACCTCAGCACACATCAAACAGCT-3′; SWBV-1-F, 5′-GCTTGCTGGTAAGATTGCCA-3′; SWBV-1-R, 5′-GTCCTAGGAGCAGCTG TTGG-3′; and SWBV-1-P, 5′-TGATTAACCTGAGGAAGTATGGCTGGC-3′. We used the TaqMan RNA-to-C_T 1-Step Kit (ThermoFisher Scientific) for qRT-PCR, which we performed on a Quantstudio 6 Pro thermocycler (ThermoFisher Scientific) as follows: reverse transcription at 48°C for 15 minutes, initial denaturation at 95°C for 10 minutes, a subsequent 50 cycles at 95°C for 15 seconds, and then incubation at 60°C for 1 minute, during which signal acquisition was performed. Using a custom-designed, in vitro-transcribed RNA standard curve for SHFV, we determined that a cycle threshold (Ct) of ≈38–40 corresponded to ≈10 RNA copies/reaction and, thus, was a generalizable limit of detection in this study. We extrapolated the standard curve to a rough approximation of the copies/mL of the SHFV *N* gene, which encodes nucleoprotein: a Ct of 29 was ≈10^6 copies/mL, Ct of 22 was ≈10^8 copies/mL, and Ct of 15 was ≈10^{10} copies/mL.

MA-104 Cell Culture

MA-104 cells, derived from grivet (*Chlorocebus aethiops*) embryonic kidneys, were provided by Siyuan Ding (Washington University, St. Louis, MO, USA). We cultured the cells in Dulbecco Modified Eagle Medium containing 1% HEPES buffer, 1% sodium pyruvate, and 1% L-glutamine (GIBCO/ThermoFisher Scientific), and 10% heat-inactivated fetal calf serum (FCS; Omega Scientific, https://www.omegascientific.com).

Rhesus Monkey Peripheral Blood Mononuclear Cells

We obtained ≈15 mL of rhesus monkey whole blood in EDTA and added 15 mL of Roswell Park Memorial Institute (RPMI) 1640 medium (ThermoFisher Scientific) containing 10% FCS. We overlayed the diluted blood with 15 mL Ficoll-Paque (Cytiva, https://www.cytivalifesciences.com) and centrifuged at 800 × *g* for 30 minutes without braking. We extracted the buffy coat and treated the cells once with ACK Lysing Buffer (GIBCO/ThermoFisher Scientific), according to the manufacturer's instructions. We washed the cells 2 times with RPMI 1640 medium and then plated them for differentiation, achieved by adding bulk peripheral blood nononuclear cells (PBMCs) to flasks containing minimum essential medium α (MEM α; GIBCO/ThermoFisher Scientific), 20% heat-inactivated FCS, 1% type AB human serum (Sigma Aldrich, https://www.sigmaaldrich.com), 50 μmol/L 2-mercaptoethanol (GIBCO/ThermoFisher Scientific), 20 μg/mL human macrophage colony-stimulating factor (M-CSF; Peprotech, https://www.peprotech.com), 10 μg/mL human interleukin-1 beta (IL-1β; Peprotech), and antimicrobial/antifungal solution containing penicillin, streptomycin, and amphotericin B (GIBCO/ThermoFisher Scientific). We allowed the cells to differentiate for 6 days, changing medium every 2 days. We removed differentiated cells by using Cellstripper (Corning, https://www.corning.com) according to the manufacturer's recommendations and then plated the cells for experiments.

We inoculated cells with an SHFV MOI of 0.1 or equivalent volumes of KRCV-1, PBJV, or SWBV-1 in MEM α medium containing 2% FCS and incubated for 1 h at 37°C, gently rocking every ≈15 min. We washed monolayers 2 times with phosphate-buffered saline (PBS) and then added complete growth medium. We collected cell supernatants at different timepoints and stored them at −80°C before RNA extraction.

Rhesus Monkey Splenocytes

We obtained spleen samples from rhesus monkeys during necropsies of animals used for other studies. We mechanically dissociated 2–10 g of tissue by using scissors and a scalpel in ≈10 mL of RPMI 1640 medium containing heat-inactivated 10% FCS and antimicrobial/antimycotic solution and then passed the tissue through a 100-μm filter to obtain a single cell suspension. We treated the cells with ACK Lysing Buffer and washed 2 times with ≈20 mL RPMI medium before plating for experiments or inducing differentiation. We let bulk splenocytes adhere to tissue culture dishes for 12 hours and added nonadherent cells to a separate flask with differentiation medium prewarmed to 37°C. We maintained cells under standard tissue culture conditions (5% CO_2, 37°C) in differentiation medium for 6 days before performing experiments.

We inoculated splenocyte-derived macrophages with an SHFV MOI of 0.1 or equivalent volumes of

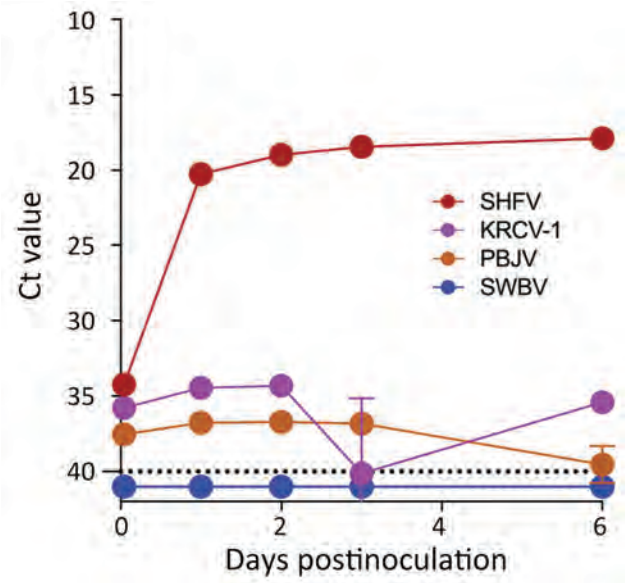

Figure 1. Simarterivirus infection of grivet embryonic kidney cell line in study of isolation of diverse simarteriviruses causing hemorrhagic disease. MA-104 cells were inoculated with SHFV at a multiplicity of infection of 1 and inoculated with KRCV-1, PBJV, or SWBV-1 by using sample volumes equivalent to that of SHFV (n = 3 experiments for each virus). Supernatants were collected at the indicated timepoints and quantitative reverse transcription PCR was used to measure simarterivirus nucleoprotein gene levels. Dashed line indicates limit of detection. Only SHFV replicated in grivet MA-104 cells. Ct, cycle threshold; KRCV-1, Kibale red colobus monkey virus 1; PBJV, Pebjah virus; SHFV, simian hemorrhagic fever virus; SWBV-1, Southwest baboon virus 1.

KRCV-1, PBJV, or SWBV-1 in MEM α containing 2% FCS for 1 hour. We washed the monolayers before adding complete growth medium and stored cell supernatants at −80°C before RNA extraction.

Flow Cytometry of Rhesus Monkey Splenocytes

We obtained a single cell suspension of rhesus monkey splenocytes and treated them with ACK Lysing Buffer as previously described. After treatment, we centrifuged the cells for 10 minutes at 300 × *g*, resuspended them in labeling buffer (PBS containing 0.5% bovine serum albumin and 2 mmol/L EDTA), and then incubated with NHP CD11b microbeads (Miltenyi Biotec, https://www.miltenyibiotec.com) for 15 min at 4°C. We washed the cells 2 times with PBS containing 0.5% bovine serum albumin and 2 mmol/L EDTA and then resuspended in 500 μL of the same buffer. We attached LS columns to a MACS manual magnetic cell separator (both Miltenyi Biotec), prepared them according to manufacturer's instructions, and added microbead-labeled cell suspensions to the columns and let unlabeled cells flow through. We washed the LS columns 3 times with buffer and, after collecting unlabeled cells, we removed the columns from the MACS separator and placed them into 15-mL conical tubes. We added 5 mL buffer to each column, recovered CD11b-enriched cells, and added differentiation medium to the labeled cells, replenishing the medium every 2 days.

Six days after initiating differentiation, we inoculated splenocyte-derived macrophages with SHFV-eGFP at an MOI of 0.1 without washing. After 24 hours, we harvested the cells by using Cellstripper and transferred them to a nontissue culture-treated 96-well V-bottom plate (Corning), which we centrifuged for 5 minutes at 500 × *g*. We rinsed the cells 2 times in fluorescence-activated cell sorter (FACS) buffer (PBS, 2% FCS, 1 mmol/L EDTA [Invitrogen/ThermoFisher Scientific]) before adding ViaDye (Cytek Biosciences, https://www.cytekbio.com) to the cells according to the manufacturer's instructions. After rinsing the cells 2 times in FACS buffer, we added Human TruStain FcX Block (Biolegend, https:;//www.biolegend.com), incubated for 10 minutes in the dark, then added human CD14 antibody (Biolegend) and incubated for an additional 20 minutes in the dark. After incubation, we washed the cells 2 times in FACS buffer before fixing for 20 minutes in 4% paraformaldehyde (Electron Microscopy Sciences, https://www.emsdiasum.com) diluted in PBS and then rinsed the cells 2 times in with FACS buffer and stored at 4°C before flow cytometric analysis on an Attune Flow Cytometer (ThermoFisher Scientific). We performed analysis by using FlowJo version 10.8 software (BD Biosciences, https://www.bdbiosciences.com).

Macrophages Derived from Induced Pluripotent Stem Cells

We generated induced pluripotent stem cells (iPSCs) from crab-eating macaques as previously described (*26*–*29*). In brief, we isolated fibroblasts from skin punches, reprogrammed them by using episomally-encoded Yamanaka factors, and maintained an undifferentiated state by passaging the cells on mouse embryonic fibroblasts every 3 days. We generated multipotent hematopoietic progenitors (MHPs) from iPSCs as described previously (*26*,*27*). In brief, we cultured iPSC aggregates on OP9 feeder cell layers for 10 days in NHP medium (MEM α, 10% Hyclone fetal bovine serum [Cytiva] that was not heat inactivated, 50 μmol/L 2-mercaptoethanol), and day-specific amounts of cytokines and chemicals (Peprotech). At differentiation day 10, we collected floating MHPs and either froze the cells in 10% vol/vol dimethyl sulfoxide/90% fetal bovine serum or used them to generate macrophages. We further differentiated MHPs to macrophages by incubating them in

ultralow-attachment 6-well plates (Corning) for 6 days in NHP medium containing 20 ng/mL of M-CSF and 10 ng/mL of IL-1β (*28*). Every 2 days, we added 2 mL NHP medium/well and additional cytokines to maintain final concentrations of 20 ng/mL M-CSF and 10 ng/mL IL-1β. We maintained the iPSC-derived macrophages in fresh NHP medium containing M-CSF and IL-1β and performed complete medium changes and replating every 6 days.

For virus exposure experiments, we plated cells ≈2.5×10^5 cells/well in 6-well ultralow attachment plates and incubated with inoculum for 1 hours at 37°C and 5% CO_2, gently rocking the plates every ≈15 min. We removed the inoculum, washed the cells 3 times with PBS, and then replenished with prewarmed medium.

Mice Engrafted with Macaque Immune Cells

Mice were prepared as previously described (*29*). In brief, we created engrafted mice by using fetal (≈100 days' gestation) tissue from rhesus monkeys obtained from the Wisconsin National Primate Research Center. We used immunodeficient NSG-SGM3 (NOD.Cg-*Prkdc*^{scid} *Il2rg*^{tm1Wjl} Tg[CMV-IL3,CSF2,KITLG]1Eav/MloySzJ) and NOG-EXL (NOD.Cg-*Prkdc*^{scid} *Il2rg*^{tm1Sug} Tg[SV40/HTLV-IL3,CSF2]10–7Jic/JicTac) transgenic mice (both from Taconic Biosciences, https://www.taconic.com) as hosts for the experiments and unengrafted NSG-SGM3 transgenic mice and background-matched wildtype NOR/LtJ mice as controls (The Jackson Laboratory, https://www.jax.org). Before the operation, we myeloablated the transgenic mice by using busulfan (*30*). We engrafted the mice surgically with 1–2 primate thymus fragments (≈1 mm^3) placed under the kidney capsule and injected 8×10^4 to 2×10^5 primate liver hematopoietic stem/progenitor cells through the tail vein; we treated the mice with 2 doses (days 0 and 7 after surgery) of 100 μg CD2 antibody via retro-orbital injection. We collected and analyzed blood samples 6–7 weeks after surgery from all mice to assess primate immune cell engraftment (NHP CD45+ cells).

Virus Exposure Studies in Mice

We analyzed 5 cohorts of laboratory mice and recorded specific genetic background, engraftment status, and virus exposure for each cohort (Appendix Table, https://wwwnc.cdc.gov/EID/article/30/4/23-1457-App1.xlsx). After engraftment and verification of graft health via flow cytometry (*29*), we transferred the mice to an animal Biosafety Level 3 laboratory and acclimated them for 4–8 days. Before virus exposure, the mice were sedated by using isoflurane gas, after which we intravenously inoculated 50 μL of virus-positive material into the retro-orbital space by using a 31-gauge needle and injected 100 μL of virus-positive material into the peritoneal cavity. We examined the mice daily and compared them with the unengrafted NSG-SGM3 and background-matched wildtype NOR/LtJ controls. We collected ≈5 drops of blood via submandibular venipuncture at 2, 6, and 12 days after virus exposure for RNA extraction and virus load measurements.

Results

Simarteriviruses in Grivet MA-104 Cells

The grivet embryonic kidney cell line, MA-104 (including several subclones, such as MARC-145), is susceptible to infection by many divergent arteriviruses. However, with the exception of SHFV, MA-104 cells do not support

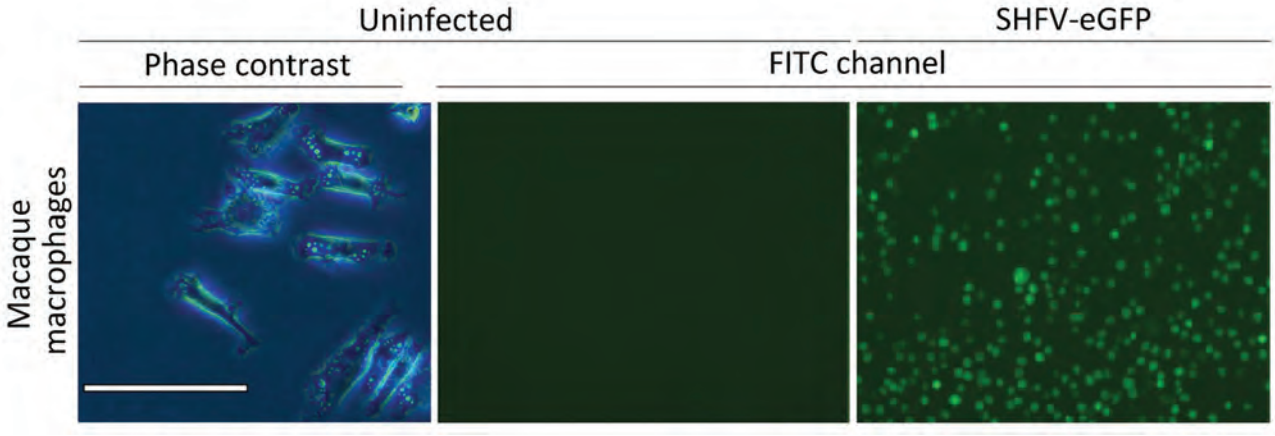

Figure 2. Primary rhesus monkey macrophages infected with simian hemorrhagic fever virus in study of diverse simarteriviruses causing hemorrhagic disease. Macrophages were isolated from spleen tissue and mock infected or infected with SHFV-eGFP. Left panel shows isolated macrophages; scale bar indicates 120 μm. Middle panel shows cells 24 hours after mock infection and right panel shows cells 24 hours after infection with SHFV-eGFP at a multiplicity of infection of 0.1; original magnification ×40. SHFV-eGFP, simian hemorrhagic fever virus–enhanced green fluorescent protein.

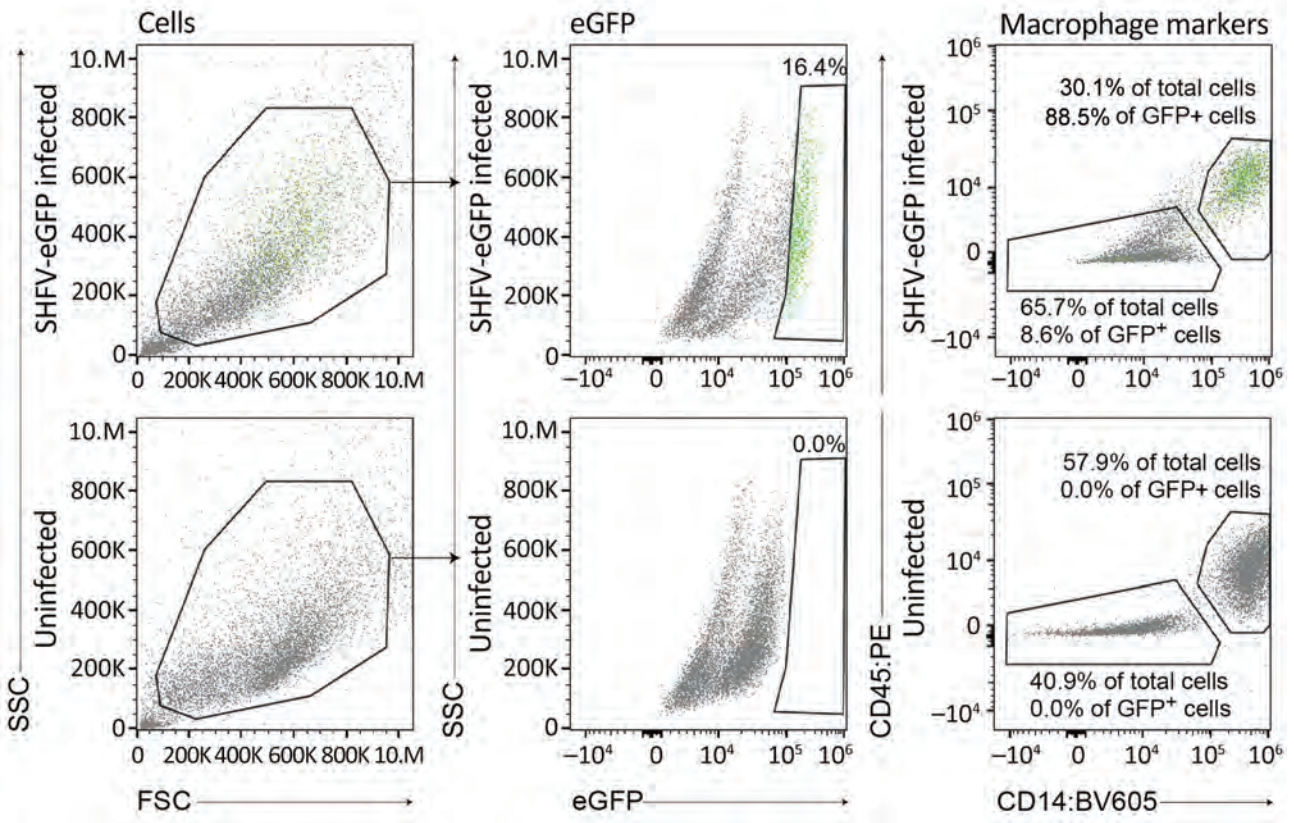

Figure 3. Flow cytometry of SHFV-eGFP–infected (top plots) and uninfected (bottom plots) splenocytes in study of isolation of diverse simarteriviruses causing hemorrhagic disease. Green dots indicate cells infected with SHFV-eGFP. BV605, brilliant violet 605 dye; eGFP, enhanced GFP; FSC, forward scatter; GFP, green fluorescent protein; PE, phycoerythrin; SHFV, simian hemorrhagic fever virus; SSC, side scatter.

robust infection with other simarteriviruses (*5*,*8*,*15*–*19*). To confirm this lack of susceptibility, we exposed MA-104 cells to residual monkey serum and other biospecimens containing KRCV-1, PBJV, SHFV, or SWBV-1. To evaluate productive infection by those viruses, we monitored cultures during ≤21 days for cytopathic effect (CPE) and used qRT-PCR targeting the virus-specific *N* gene to detect increasing concentrations of *N* RNA in cell culture supernatant; we made partial growth medium changes as needed. As expected, MA-104 cultures inoculated with SHFV displayed rapid CPE accompanied by an increase in SHFV *N* RNA levels. However, MA-104 cells inoculated with KRCV-1, PBJV, or SWBV-1 maintained normal morphologic characteristics and did not display increases in virus *N* RNA levels (Figure 1). Our results confirmed that MA-104 cells cannot be used to grow or isolate SWBV-1, KRCV-1, or PBJV.

Simarterivirus Isolation from Primary Rhesus Monkey Macrophages and Splenocytes

SHFV tropism is primarily restricted to macrophages and myeloid dendritic cells in vivo, and the virus can be propagated on primary rhesus monkey macrophages (*18*,*23*,*31*,*32*). For a second attempt to isolate KRCV-1, PBJV, SWBV-1, we obtained rhesus monkey PBMCs and splenocytes. Because of the small and variable sizes of PBMCs, we were unsure whether CPE would be discernible. Therefore, we used recombinant SHFV-eGFP (*15*) as a positive control. As expected, macrophages and splenocytes became eGFP positive within 24 h after SHFV-eGFP exposure (Figures 2, 3). Next, we exposed adherent and nonadherent PBMCs and splenocytes to wild-type SHFV or samples containing the other 3 viruses. Measuring virus-specific *N* RNA over time by qRT-PCR revealed productive infections by KRCV-1, PBJV, and SHFV, but not SWBV-1 (Figures 4, 5). We showed PBJV could be isolated in cell culture, and adherent NHP PBMCs, likely monocytes, can be used to isolate previously uncultivable simarteriviruses.

Simarterivirus Isolation from Macaque iPSCs

Phylogenetically diverse cercopithecoid monkeys are susceptible to infection by various simarteri-

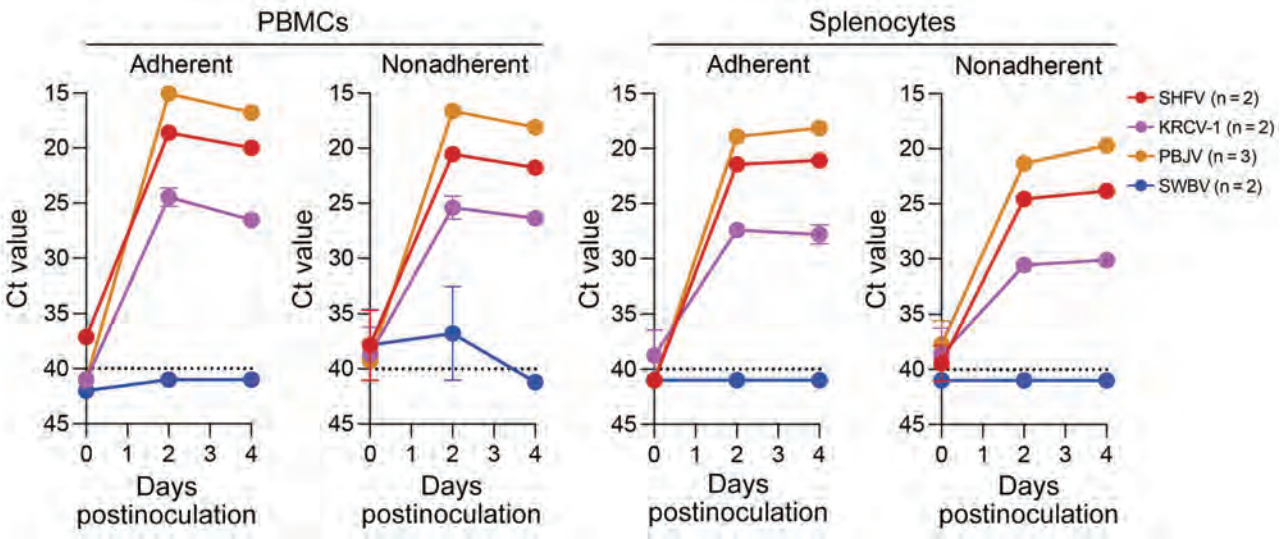

Figure 4. Ct values for virus-specific nucleoprotein RNA from rhesus monkey cells in study of diverse simarteriviruses causing hemorrhagic disease. PBMCs and splenocytes were infected with SHFV at a multiplicity of infection of 0.1 and infected with KRCV-1, PBJV, or SWBV-1 by using volumes equivalent to that of SHFV. Nucleoprotein RNA was measured by using quantitative reverse transcription PCR at different times after inoculation. Dotted lines indicate limit of detection. Numbers in parentheses indicate number of experiments performed for each virus. Error bars indicate SEMs. Ct, cycle threshold; KRCV-1, Kibale red colobus monkey virus 1; PBJV, Pebjah virus; PBMCs, peripheral blood mononuclear cells; SHFV, simian hemorrhagic fever virus; SWBV-1, Southwest baboon virus 1.

viruses (*3*); using primary macaque macrophages likely increases the chances of isolating simarteriviruses (Figure 2). However, the increasingly limited availability of macaques for biomedical research, infrastructure required for their maintenance, expertise and safety measures required to collect tissue samples, relatively small number of cells that can be purified from a tissue sample, and growing ethical concerns regarding large NHP research in general (*33*) are substantial barriers to using primary

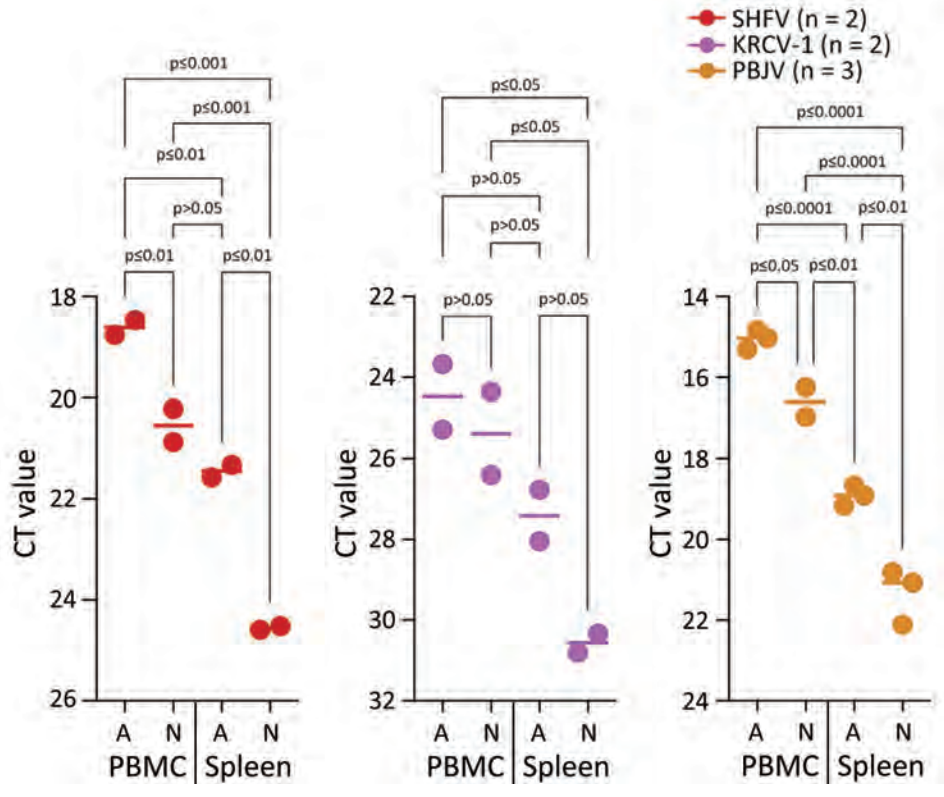

Figure 5. Comparisons of Ct values for different viruses infecting cells from rhesus monkeys in study of diverse simarteriviruses causing hemorrhagic disease. PBMCs and splenocytes were isolated from rhesus monkeys, infected with different simarteriviruses, and analyzed for infection by using quantitative reverse transcription PCR. Dots for each cell type and numbers in parentheses indicate number of experiments performed for each virus. Horizontal lines between dots indicate mean Ct values for each group. Statistical significance was determined by using 1-way analysis of variance. A, adherent; Ct, cycle threshold; KRCV-1, Kibale red colobus monkey virus 1; N, nonadherent; PBJV, Pebjah virus; PBMCs, peripheral blood mononuclear cells; SHFV, simian hemorrhagic fever virus.

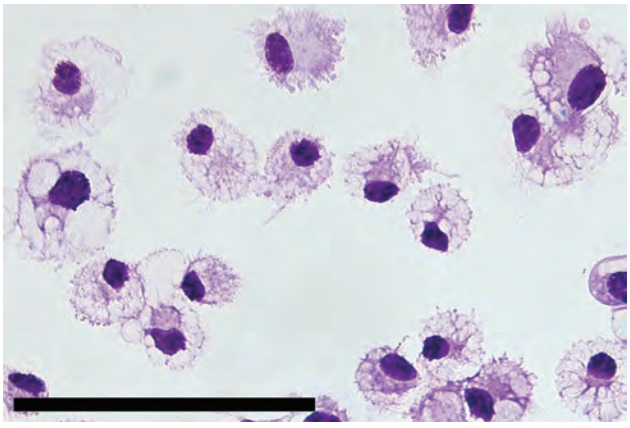

Figure 6. Induced pluripotent stem cells isolated from crab-eating macaques in study of diverse simarteriviruses causing hemorrhagic disease. Brightfield photograph shows induced pluripotent stem cell–derived macrophages stained with Wright-Giemsa dye. Scale bar indicates 100 μm.

macaque macrophages as a sustainable system for simarterivirus isolation. To overcome those potential barriers, we hypothesized that macaque iPSC-derived macrophages could be used as a reproducible and sustainable system for propagating simarteriviruses. We first differentiated iPSCs from reprogrammed crab-eating macaque fibroblasts (*26*) into CD34+ MHPs, then further differentiated the MHPs into macrophages (*28*) (Figure 6). Inoculation of the macrophages with all 4 viruses revealed productive infections by KRCV-1, PBJV, and SHFV, but not SWBV-1, measured by annihilation of cells in culture (Figure 7) and virus-specific qRT-PCR (Figure 8).

Isolation of Simarteriviruses In Vivo

We hypothesized that immunodeficient mice engrafted with fetal rhesus monkey thymus- and liver-derived CD34+-enriched hematopoietic stem and progenitor cells (*29*) would be susceptible to simarterivirus infection. Mice were inoculated simultaneously via intraperitoneal and intravenous injection to maximize the likelihood of establishing productive infections. Inoculation of simarteriviruses into unengrafted NSG-SGM3 and wildtype NOR/LtJ control mice did not result in viremia according to qRT-PCR detection of *N* RNA. However, in engrafted mice, productive infections were achieved with PBJV (all 5 mice), SHFV (4 of 6 mice), and SWBV-1 (2 of 7 mice);

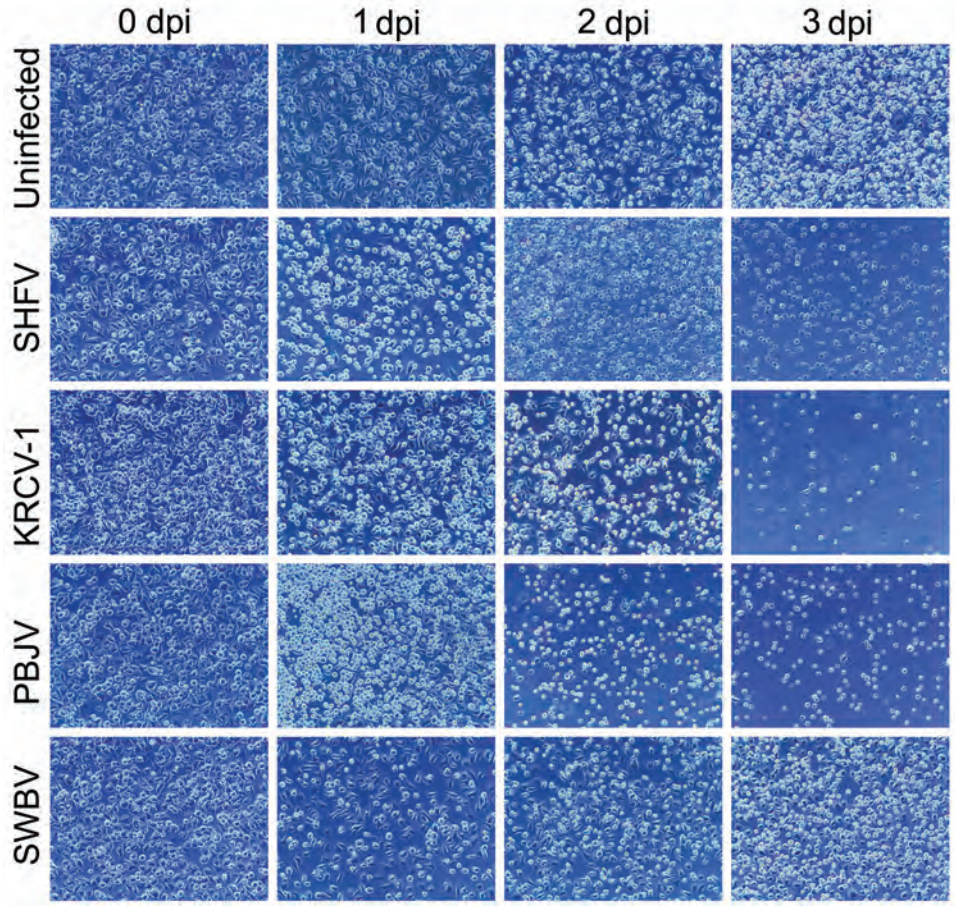

Figure 7. Cytopathic effect after infection of induced pluripotent stem cell–derived macrophages in study of diverse simarteriviruses causing hemorrhagic disease. Induced pluripotent stem cells from crab-eating macaques were differentiated into macrophages and mock infected (uninfected) or infected with different simarteriviruses. Cytopathic effect was monitored for 0–3 dpi. Original magnification ×100. dpi, days after inoculation; KRCV-1, Kibale red colobus monkey virus 1; PBJV, Pebjah virus; SHFV, simian hemorrhagic fever virus; SWBV-1, Southwest baboon virus 1.

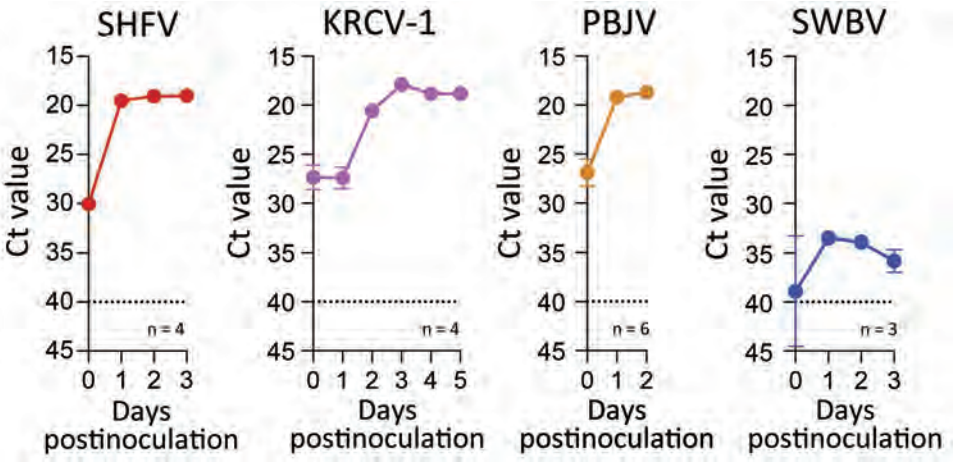

Figure 8. Ct values for virus-specific nucleoprotein RNA in macrophages infected with diverse simarteriviruses causing hemorrhagic disease. Induced pluripotent stem cell–derived macrophages from crab-eating macaques were infected with different simarteriviruses. Virus-specific nucleoprotein RNA was measured by using quantitative reverse transcription PCR on different days after inoculation. Dotted lines indicate limit of detection. Error bars indicate SEMs. Ct, cycle threshold; dpi, days after inoculation; iPSC, induced pluripotent stem cell; KRCV-1, Kibale red colobus monkey virus 1; LoD, limit of detection; PBJV, Pebjah virus; SHFV, simian hemorrhagic fever virus; SWBV-1, Southwest baboon virus 1.

1 engrafted mouse supported a brief infection with KRCV-1. Virus infections often persisted until the end of the study period (Figure 9); only 2 mice cleared virus RNA after viremia was detected.

Discussion

Simarteriviruses commonly infect cercopithecoid monkeys throughout sub-Saharan Africa. Yet, lack of simarterivirus isolates impedes in vitro and in vivo investigations partly because of an extremely limited set of tools available for working with those viruses in a laboratory setting, including the lack of in vitro systems available for simarterivirus culture. We used a combination of increasingly sophisticated approaches (an immortalized grivet cell line, primary rhesus monkey PBMCs and splenocytes, crab-eating macaque iPSC-derived macrophages, and rhesus monkey leukocyte-engrafted laboratory mice) to create a straightforward toolset for isolating simarteriviruses. The combined effort resulted in isolation of the highly virulent, epizootic PBJV and successful infection of laboratory mice with diverse simarteriviruses. However, no single host system was capable of supporting robust replication of all 4 simarteriviruses tested in this study. Only SHFV replicated in immortalized MA-104 cells (Figure 1), and, although KRCV-1 did not replicate robustly in engrafted mice, SWBV-1 only replicated in engrafted mice (Figure 9). Our findings imply fundamental differences in tissue or host tropism among simarteriviruses. Nevertheless, we reveal a path for isolating other still-uncultured simarteriviruses and

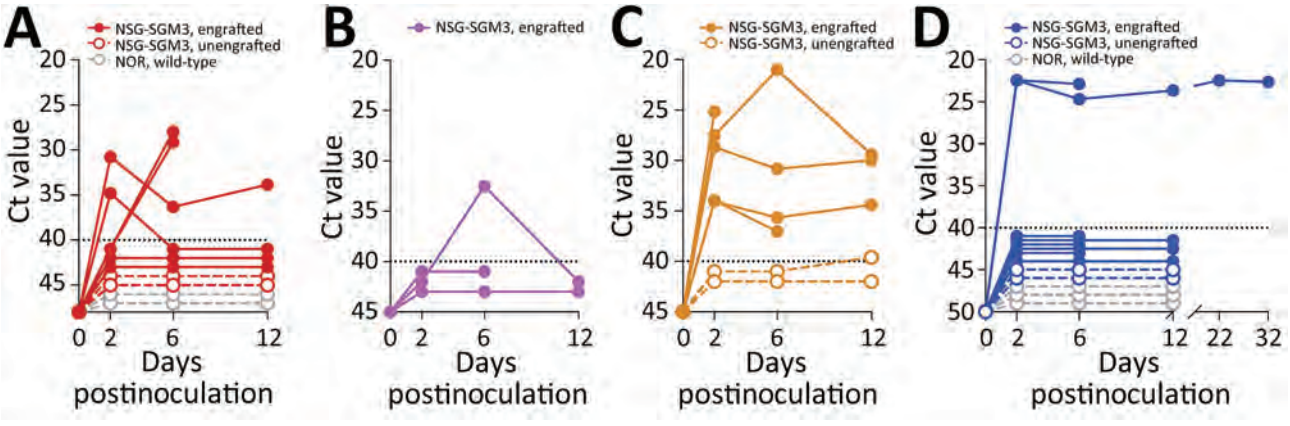

Figure 9. Ct values for virus-specific nucleoprotein RNA in mice engrafted with rhesus monkey immune cells infected with diverse simarteriviruses causing hemorrhagic disease. NSG-SGM3 (NOD.Cg-*Prkdc*^{scid} *Il2rg*^{tm1Wjl} Tg[CMV-IL3,CSF2,KITLG]1Eav/MloySzJ) mice were engrafted with fetal CD34+-enriched hematopoietic stem and progenitor cells isolated from rhesus monkeys. Engrafted and unengrafted NSG-SGM3 transgenic mice and background-matched wild-type NOR/LtJ mice were injected intraperitoneally and intravenously with 1 of 4 viruses: A) simian hemorrhagic fever virus; B) Kibale red colobus monkey virus 1; C) Pebjah virus; or D) Southwest baboon virus 1. Production of virus-specific nucleoprotein RNA in blood was measured over time by using quantitative reverse transcription PCR. Dotted lines indicates limit of detection. Ct, cycle threshold.

provide a system for evaluating medical countermeasures against simarteriviruses in vivo in highly characterized mouse models.

The 4 viruses isolated in this study are highly divergent from each other (≈50% genome identity) and represent only a portion of the known natural diversity of simarteriviruses (*11*). Functionally characterizing the many divergent simarteriviruses is critical to decipher the virus-host interactions that govern simarterivirus cross-species transmission. Although specific virus-host interactions remain largely unknown, the isolation systems developed in this study will expedite mechanistic studies of simarteriviruses in the laboratory to elucidate those interactions, to assess their zoonotic risk (*3*–*5*), and to develop candidate medical countermeasures.

Acknowledgments

We thank Stem Cell Resources at the Wisconsin National Primate Research Center (WNPRC) for providing iPSCs, the Nonhuman Primate Biological Materials Distribution Core for providing macaque samples, and Anya Crane for critically editing the manuscript.

NSG-SGM3 mice were a generous gift from Leonard Shultz at the Jackson Laboratory, Bar Harbor, ME, USA. This study utilized animals, iPSC lines, and tissues from the WNPRC.

This study was supported, in part, by National Institutes of Health (NIH), National Center for Research Resources (grant nos. P51OD011106 and P30CA014520). Part of this research was conducted at a facility constructed with support from NIH Research Facilities Improvement Program grant nos. RR15459-01 and RR020141-01. This research was also supported by pilot funding from the WNPRC and the University of Wisconsin Madison Institute for Clinical and Translational Research (NCATS CTSA grant no. Ul1TR002373), the Wisconsin Alumni Research Foundation, NIH National Institute of Allergy and Infectious Diseases (NIAID) grant no. 75N93021C00004 and NIH NHLBI grant no. U01HL134764 to M.E.B., NIH NIAID R00AI151256 to C.J.W., NIH R01 HD103443 to T.G.G., the University of Wisconsin Carbone Cancer Center support grant no. P30 CA014520, startup funds to A.L.B. from the Department of Pathology and Laboratory Medicine and the School of Medicine and Public Health at the University of Wisconsin Madison, and in part through a Laulima Government Solutions LLC prime contract with the NIH NIAID under contract no. HHSN272201800013C. J.H.K. performed this work as an employee of Tunnell Government Services, a subcontractor of Laulima Government Solutions, LLC, under contract no. HHSN272201800013C.

M.E.B. is a consultant for Taconic Biosciences.

The views and conclusions contained in this document are those of the authors and should not be interpreted as necessarily representing the official policies, either expressed or implied, of the US Department of Health and Human Services or of the institutions and companies affiliated with the authors, nor does mention of trade names, commercial products, or organizations imply endorsement by the US government.

About the Author

Ms. Shaw is a senior research specialist in the Bailey laboratory at the University of Wisconsin School of Medicine and Public Health in Madison, Wisconsin, USA. Her primary research interests focus on understanding virus-host interactions that underpin cross-species infection and disease.

References

1. Brinton MA, Gulyaeva AA, Balasuriya UBR, Dunowska M, Faaberg KS, Goldberg T, et al. ICTV virus taxonomy profile: Arteriviridae 2021. J Gen Virol. 2021;102:001632. https://doi.org/10.1099/jgv.0.001632
2. Fang Y, Snijder EJ, Balasuriya UBR. Arteriviruses. In: Howley, PM, Knipe DM, Damania BA, Cohen JI, Whelan SPJ, Freed EO, editors. Fields virology: RNA viruses, 7th ed. Philadelphia: Wolters Kluwer Health/Lippincott Williams and Wilkins; 2022. p. 104–30.
3. Bailey AL, Lauck M, Sibley SD, Friedrich TC, Kuhn JH, Freimer NB, et al. Zoonotic potential of simian arteriviruses. J Virol. 2015;90:630–5. https://doi.org/10.1128/JVI.01433-15
4. Graham BS, Sullivan NJ. Emerging viral diseases from a vaccinology perspective: preparing for the next pandemic. Nat Immunol. 2018;19:20–8. https://doi.org/10.1038/s41590-017-0007-9
5. Warren CJ, Yu S, Peters DK, Barbachano-Guerrero A, Yang Q, Burris BL, et al. Primate hemorrhagic fever-causing arteriviruses are poised for spillover to humans. Cell. 2022;185:3980–3991.e18. https://doi.org/10.1016/j.cell.2022.09.022
6. Allen AM, Palmer AE, Tauraso NM, Shelokov A. Simian hemorrhagic fever. II. Studies in pathology. Am J Trop Med Hyg. 1968;17:413–21. https://doi.org/10.4269/ajtmh.1968.17.413
7. Palmer AE, Allen AM, Tauraso NM, Shelokov A. Simian hemorrhagic fever. I. Clinical and epizootiologic aspects of an outbreak among quarantined monkeys. Am J Trop Med Hyg. 1968;17:404–12. https://doi.org/10.4269/ajtmh.1968.17.404
8. Tauraso NM, Shelokov A, Palmer AE, Allen AM. Simian hemorrhagic fever. 3. Isolation and characterization of a viral agent. Am J Trop Med Hyg. 1968;17:422–31. https://doi.org/10.4269/ajtmh.1968.17.422
9. Lauck M, Alkhovsky SV, Bào Y, Bailey AL, Shevtsova ZV, Shchetinin AM, et al. Historical outbreaks of simian hemorrhagic fever in captive macaques were caused by distinct arteriviruses. J Virol. 2015;89:8082–7. https://doi.org/10.1128/JVI.01046-15

10. Lauck M, Hyeroba D, Tumukunde A, Weny G, Lank SM, Chapman CA, et al. Novel, divergent simian hemorrhagic fever viruses in a wild Ugandan red colobus monkey discovered using direct pyrosequencing. PLoS One. 2011;6:e19056. https://doi.org/10.1371/journal.pone.0019056
11. Bailey AL, Lauck M, Ghai RR, Nelson CW, Heimbruch K, Hughes AL, et al. Arteriviruses, pegiviruses, and lentiviruses are common among wild African monkeys. J Virol. 2016;90:6724–37. https://doi.org/10.1128/JVI.00573-16
12. Bailey AL, Lauck M, Sibley SD, Pecotte J, Rice K, Weny G, et al. Two novel simian arteriviruses in captive and wild baboons (Papio spp.). J Virol. 2014;88:13231–9. https://doi.org/10.1128/JVI.02203-14
13. Bailey AL, Lauck M, Weiler A, Sibley SD, Dinis JM, Bergman Z, et al. High genetic diversity and adaptive potential of two simian hemorrhagic fever viruses in a wild primate population. PLoS One. 2014;9:e90714. https://doi.org/10.1371/journal.pone.0090714
14. Lauck M, Sibley SD, Hyeroba D, Tumukunde A, Weny G, Chapman CA, et al. Exceptional simian hemorrhagic fever virus diversity in a wild African primate community. J Virol. 2013;87:688–91. https://doi.org/10.1128/JVI.02433-12
15. Cai Y, Yu S, Fang Y, Bollinger L, Li Y, Lauck M, et al. Development and characterization of a cDNA-launch recombinant simian hemorrhagic fever virus expressing enhanced green fluorescent protein: ORF 2b' is not required for in vitro virus replication. Viruses. 2021;13:632. https://doi.org/10.3390/v13040632
16. Caì Y, Postnikova EN, Bernbaum JG, Yú SQ, Mazur S, Deiuliis NM, et al. Simian hemorrhagic fever virus cell entry is dependent on CD163 and uses a clathrin-mediated endocytosis-like pathway. J Virol. 2015;89:844–56. https://doi.org/10.1128/JVI.02697-14
17. Wahl-Jensen V, Johnson JC, Lauck M, Weinfurter JT, Moncla LH, Weiler AM, et al. Divergent simian arteriviruses cause simian hemorrhagic fever of differing severities in macaques. mBio. 2016;7:e02009-15. https://doi.org/10.1128/mBio.02009-15
18. Yú SQ, Caì Y, Lyons C, Johnson RF, Postnikova E, Mazur S, et al. Specific detection of two divergent simian arteriviruses using RNAscope in situ hybridization. PLoS One. 2016;11:e0151313. https://doi.org/10.1371/journal.pone.0151313
19. Myers MG, Vincent MM, Hensen SA, Tauraso NM. Problems in the laboratory isolation of simian hemorrhagic fever viruses and isolation of the agent responsible for the Sussex/69 epizootic. Appl Microbiol. 1972;24:62–9. https://doi.org/10.1128/am.24.1.62-69.1972
20. Renquist D. Outbreak of simian hemorrhagic fever. J Med Primatol. 1990;19:77–9. https://doi.org/10.1111/j.1600-0684.1990.tb00257.x
21. Zack PM. Simian hemorrhagic fever. In: Jones ITC, Mohr U, Hunt RD, editors. Nonhuman primates I. Berlin: Springer-Verlag; 1993. p. 118–31.
22. Cornish JP, Moore IN, Perry DL, Lara A, Minai M, Promeneur D, et al. Clinical characterization of host response to simian hemorrhagic fever virus infection in permissive and refractory hosts: a model for determining mechanisms of VHF pathogenesis. Viruses. 2019;11:67. https://doi.org/10.3390/v11010067
23. Vatter HA, Donaldson EF, Huynh J, Rawlings S, Manoharan M, Legasse A, et al. A simian hemorrhagic fever virus isolate from persistently infected baboons efficiently induces hemorrhagic fever disease in Japanese macaques. Virology. 2015;474:186–98. https://doi.org/10.1016/j.virol.2014.10.018
24. London WT. Epizootiology, transmission and approach to prevention of fatal simian haemorrhagic fever in rhesus monkeys. Nature. 1977;268:344–5. https://doi.org/10.1038/268344a0
25. Buechler C, Semler M, Baker DA, Newman C, Cornish JP, Chavez D, et al. Subclinical infection of macaques and baboons with a baboon simarterivirus. Viruses. 2018;10:701. https://doi.org/10.3390/v10120701
26. D'Souza SS, Maufort J, Kumar A, Zhang J, Smuga-Otto K, Thomson JA, et al. GSK3β inhibition promotes efficient myeloid and lymphoid hematopoiesis from non-human primate-induced pluripotent stem cells. Stem Cell Reports. 2016;6:243–56. https://doi.org/10.1016/j.stemcr.2015.12.010
27. Kumar A, D'Souza SS, Uenishi G, Park MA, Lee JH, Slukvin II. Generation of T cells from human and nonhuman primate pluripotent stem cells. Bio Protoc. 2020;10:e3675. https://doi.org/10.21769/BioProtoc.3675
28. D'Souza SS, Kumar A, Weinfurter J, Park MA, Maufort J, Tao L, et al. Generation of SIV-resistant T cells and macrophages from nonhuman primate induced pluripotent stem cells with edited CCR5 locus. Stem Cell Reports. 2022;17:953–63. https://doi.org/10.1016/j.stemcr.2022.03.003
29. Little CJ, Haynes WJ, Huang L, Daffada CM, Wolfe BK, Perrin E, et al. Robust engraftment of fetal nonhuman primate CD34-positive cells in immune-deficient mice. J Leukoc Biol. 2022;112:759–69. https://doi.org/10.1002/JLB.5TA0921-481RR
30. Poletto E, Colella P, Pimentel Vera LN, Khan S, Tomatsu S, Baldo G, et al. Improved engraftment and therapeutic efficacy by human genome-edited hematopoietic stem cells with busulfan-based myeloablation. Mol Ther Methods Clin Dev. 2022;25:392–409. PubMed https://doi.org/10.1016/j.omtm.2022.04.009
31. Johnson RF, Dodd LE, Yellayi S, Gu W, Cann JA, Jett C, et al. Simian hemorrhagic fever virus infection of rhesus macaques as a model of viral hemorrhagic fever: clinical characterization and risk factors for severe disease. Virology. 2011;421:129–40. https://doi.org/10.1016/j.virol.2011.09.016
32. Vatter HA, Brinton MA. Differential responses of disease-resistant and disease-susceptible primate macrophages and myeloid dendritic cells to simian hemorrhagic fever virus infection. J Virol. 2014;88:2095–106. https://doi.org/10.1128/JVI.02633-13
33. Ramos KS, Downey A, Yost OC, editors. Nonhuman primate models in biomedical research: state of the science and future needs. Washington, DC: The National Academies Press; 2023.

Address for correspondence: Adam L. Bailey, University of Wisconsin, 1741 WIMR Wedge, Bailey Lab, 1111 Highland Ave, Madison, WI 53705, USA; email: albailey@wisc.edu

Nephropathia Epidemica Caused by Puumala Virus in Bank Voles, Scania, Southern Sweden

Jiaxin Ling,[1] Elin Economou Lundeberg,[1] Anishia Wasberg, Inês R. Faria, Sanja Vucicevic, Bo Settergren, Åke Lundkvist

In 2018, a local case of nephropathia epidemica was reported in Scania, southern Sweden, more than 500 km south of the previously known presence of human hantavirus infections in Sweden. Another case emerged in the same area in 2020. To investigate the zoonotic origin of those cases, we trapped rodents in Ballingslöv, Norra Sandby, and Sörby in southern Sweden during 2020–2021. We found Puumala virus (PUUV) in lung tissues from 9 of 74 *Myodes glareolus* bank voles by screening tissues using a hantavirus pan–large segment reverse transcription PCR. Genetic analysis revealed that the PUUV strains were distinct from those found in northern Sweden and Denmark and belonged to the Finnish PUUV lineage. Our findings suggest an introduction of PUUV from Finland or Karelia, causing the human PUUV infections in Scania. This discovery emphasizes the need to understand the evolution, cross-species transmission, and disease outcomes of this newly found PUUV variant.

Viral zoonotic diseases give rise to most emerging or reemerging infectious diseases (*1*). Hantavirus infections are one of the most widespread rodentborne viral zoonoses. The causative agents are orthohantaviruses (hantaviruses), which constitute a family of enveloped, single-stranded, negative-sense RNA viruses belonging to the family *Hantaviridae*, order *Bunyavirales*. The hantaviral virion comprises 3 RNA segments: the small (S) encodes for the nucleocapsid protein; the medium (M) segment for the glycoprotein precursor, which later will be cleaved into Gn and Gc; and the large (L) segment for the RNA-dependent RNA polymerase.

Author affiliations: Uppsala University, Uppsala, Sweden (J. Ling, A. Wasberg, I.R. Faria, Å. Lundkvist); Central Hospital of Kristianstad, Kristianstad, Sweden (E.E. Lundeberg, S. Vucicevic, B. Settergren)

DOI: https://doi.org/10.3201/eid3004.231414

The zoonotic transmission of hantaviruses to humans occurs primarily through indirect contact, such as inhaling aerosols from virus-contaminated rodent excreta or urine (*2*). The clinical symptoms of human hantavirus infections vary from asymptomatic to fatal hemorrhagic fever with renal syndrome (HFRS) or hantavirus pulmonary syndrome (HPS). The clinical manifestations are usually associated with the hantavirus species, carried by different rodents with distinctive ecologic habitats (*2*).

In Sweden, Puumala orthohantavirus (PUUV), carried by the bank vole (*Myodes glareolus*) (*3*,*4*), causes nephropathia epidemica (NE), which is a mild form of HFRS (*3*,*5*). However, PUUV may cause a similar level of severity or fatality to that of pathogenic Murinae-associated hantaviruses such as Hantaan virus and Seoul virus (*6*). Most of the clinical cases of NE are clustered in northern Sweden; incidence rate is 20 cases/100,000 population (*7*). Antibody prevalences of human PUUV infections, up to 16%, have been reported through serologic surveys (*8*). Although bank voles are present throughout the country, field-based ecologic studies of PUUV infections in rodents have mainly been performed in northern Sweden because of the positive correlation between bank vole density and the risk for human NE cases (*9*,*10*). Sweden has 2 distinct genetic lineages of PUUV circulating in the bank vole population: the North-Scandinavian (N-SCA) variant and the South-Scandinavian variant (S-SCA) (*3*) (Figure 1). However, increasing data indicate an expansion of the distribution of hantaviruses in rodents (*4*,*11*). Several serologic studies have revealed that PUUV-infected rodents have already reached far south of the traditional endemic areas of PUUV (e.g., in the Uppsala and Stockholm areas) (*4*,*11*).

[1]These authors contributed equally to this article.

In southern Sweden, reported NE cases were travel-related until 2018, when a locally infected NE case was diagnosed in Scania, the southernmost region of Sweden (*12*). Another local NE case was diagnosed in the same geographic area in 2020. To determine the zoonotic sources of those human cases, we collected rodents close to the first patient's home to characterize potential hantaviruses circulating in southern Sweden.

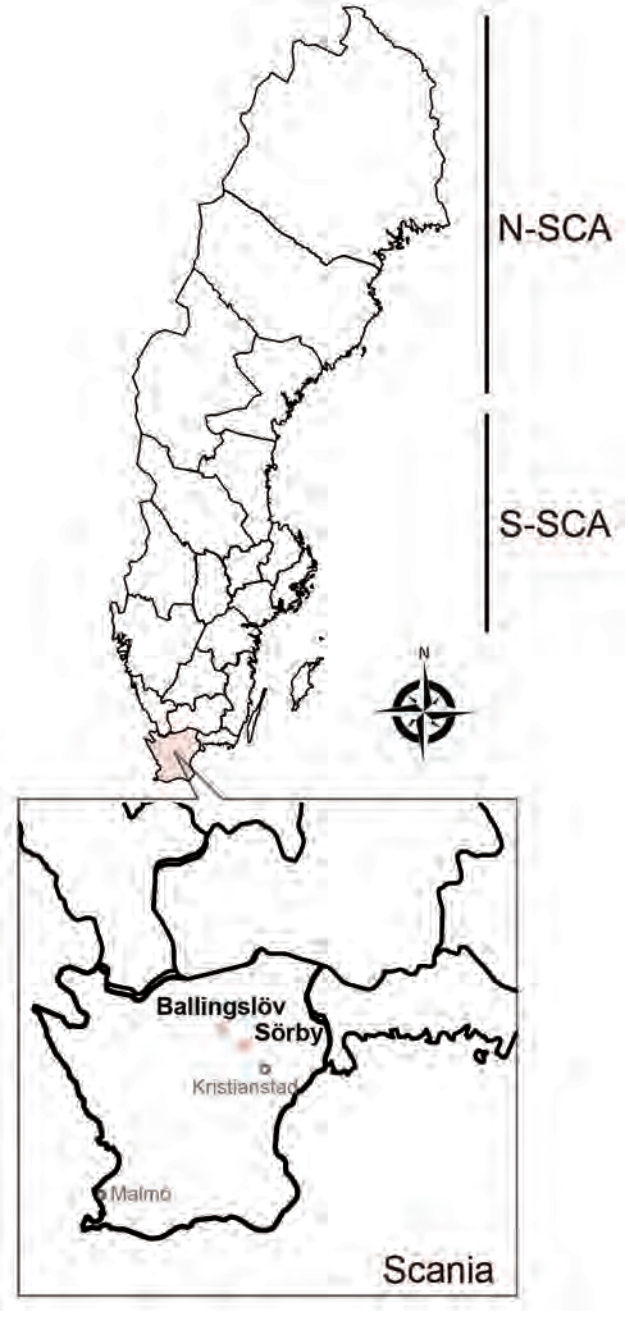

Figure 1. Rodent sampling sites for study of nephropathia epidemica caused by PUUV in *Myodes glareolus* bank voles in Scania, Sweden. New PUUV strains have been found in fields belonging to a patient with nephropathia epidemica in Scania. PUUV in Sweden belongs to the N-SCA lineage of PUUV, carried by bank voles of the Ural phylogroup, and S-SCA lineage of PUUV, carried by bank voles of the Carpathian phylogroup. Scania PUUV belongs to the Finland lineage of PUUV, carried by bank voles of the Carpathian phylogroup. N-SCA, North-Scandinavian; S-SCA, South-Scandinavian.

To capture wild rodents for this study, we attained the required permits, including approval from the Malmö/Lund Ethics Committee on Animal Testing (reference 5.8.18–02281/2020). The Department of Infectious Diseases at the Central Hospital of Kristianstad was granted permission to handle laboratory animals from the Swedish Board of Agriculture (reference 5.2.18–14256/2019). The Swedish Environmental Protection Agency granted a hunting permit (reference NV-02812–20).

Methods

Sampling

We collected rodents during September 2020, May 2021, and September 2021 at 3 geographic sites in northeastern Scania: Ballingslöv (56°22′N, 13°87′E), Norra Sandby (56°20′N, 13°93′E), and Sörby (56°15′N, 13°98′E) (Figure 1). We placed the traps at all 3 locations but captured no rodents in Norra Sandby. We used mouse snap-traps and Supercat vole traps (Swissinno, https://www.swissinno.com) with dried apples and plums for bait. We placed traps during the day and collected trapped rodents the next morning. We then placed rodents in a −25°C freezer within 2 hours of collection. We then shipped the specimens in dry ice by express postal service to the Zoonosis Science Centre (ZSC) in Uppsala, where they were stored at −80°C until analysis.

RT-PCR Screening

We dissected the rodents and harvested lung tissues for further molecular analyses. We extracted total RNA from rodent lung tissues using the QIAGEN RNeasy mini kit (QIAGEN, https://www.qiagen.com), followed by a hantavirus pan-L reverse transcription PCR (*13*). We further confirmed 9 PCR-positive samples using a PCR targeting the hantavirus S segment (*14*). We confirmed all 9 samples by partial sequences of both the PUUV S and L segments after Sanger sequencing by Macrogen Europe BV (https://dna.macrogen.com).

Amplification of Host Cytochrome b Gene

We extracted total DNA from 14 rodent lung tissues using a tissue and blood DNA extraction kit (QIAGEN), then sequencing the mitochondrial

cytochrome b (*cytB*) gene (*15*). We used the sequences for inferring the phylogeny of *M. glareolus* in Fennoscandia.

RNA Sequencing

We sent 4 RNA samples to Novogene UK (Novogene Lab, https://novogene.com) for sequencing on the basis of the initial sequencing results. After ribosomal RNA depletion, the libraries were sequenced using paired-end sequencing with 150 bp per read and ≈50 million reads by the Illumina NovaSeq 6000 sequencing platform (https://www.illumina.com). A similar data analysis pipeline was described in a previous study (*16*). In brief, the raw clean reads were quality trimmed using Trimmomatic version 0.36 (https://github.com/timflutre/trimmomatic) and then mapped to the PUUV reference sequences from GenBank (S segment, NC_005224; M segment, NC_005223; L segment, NC_005225) and a mitochondrion complete genome of *M. glareolus* (GenBank accession no. MN122864) downloaded from National Center for Biotechnology Information RefSeq database using default settings for Geneious Prime version 2019.2.1 (https://www.geneious.com).

Phylogenetic Analyses

To analyze the phylogenetic relationship of the novel viral and host sequences in comparison to other PUUV strains and rodent *cytB* sequences, we constructed phylogenetic trees using MrBayes version 3.2.6 (*17*). The reference strains and sequence information were based on earlier studies (*3*,*18*–*20*). We used MAFFT with default settings (*21*) to align global partial L-segment sequences and partial S-segment sequences; full length of S-, M- and L-segment sequence; and *cytB* sequences. We then used Aliview (*22*) for manual refinement. We determined best-fit model by jModeltest version 3.7 (*23*); we used general time-reversible plus frequencies plus invariate plus 4 matrix gamma model in all phylogenetic analyses. We used a MrBayes block for the computations with the setting including 5 million Bayesian Monte Carlo Markov chain (MCMC) generations sampling every 5,000 generations and obtained convergence (average deviation <0.01) with a 25% burn-in. We visualized all the tree results in FigTree version 1.43 (http://tree.bio.ed.ac.uk/software/Figtree) and edited them in Affinity Designer Pantone LL, 2019 (https://affinity.serif.com). We performed all computations using the UPPMAX computational cluster (https://www.uppmax.uu.se). We deposited all sequences generated in this study into GenBank (accession nos. OR602445–8, OR607515–23, OR581027–41, and OR573657–59).

Results

PUUV Variants in Scania

We collected a total of 74 rodent-like samples during 2020–2021 in the areas of the first NE patient in Scania. Morphologic identification during the dissection revealed 48 bank voles (*M. glareolus*), 25 *Apodemus* spp. mice, and 1 *Sorex* spp. shrew. After screening the lung tissues of all 74 animals, we found 9 bank voles positive by the hantavirus pan-L RT-PCR (Appendix Figure 1, https://wwwnc.cdc.gov/EID/article/30/4/23-1414-App1.pdf). We further confirmed all 9 samples for hantavirus infection by sequencing, followed by phylogenetic analyses based on global partial L-segment sequences (Appendix Figure 2). We found positive samples in 2 different geographic sites, Ballingslöv and Sörby. The phylogeny of the partial L sequences suggested that PUUV in southern Sweden has a close genetic relationship to PUUV circulating in Pallasjärvi, Finland; however, posterior probability (PP) was not supportive (PP = 0.46, which is <0.95). This finding might be explained by the short length of sequences that were used for the analyses. We further confirmed all 9 samples that were positive by the pan-L PCR with a method based on the PUUV S-segment as described previously (*14*). As expected, all 9 samples were found positive; the sequence results confirmed partial sequences of the PUUV S segment. Phylogenetic analyses based on 290 bp of the partial S sequences were in line with the tree of the partial L sequences and suggested that PUUV in southern Sweden belongs to the Finnish genetic lineage (Figure 1).

Genetic Characteristics of PUUV Variants in Scania

To obtain a higher resolution of the phylogenetic relationship between the newly found PUUV and previously known PUUV variants, we chose 4 samples, 2_Ballingslöv_2021, 3_Ballingslöv_2021, 23E_Sörby_2020, and 25R1_Sörby_2020, to represent all 9 positive samples for RNA sequencing. However, 1 sample (2_Ballingslöv_2021) was later excluded from analyses because of bad sequencing quality. After mapping using implemented Geneious RNA in Geneious Prime version 2019.2.1, we found that a total of 23,165/106,347,176 reads from 3_Ballingslöv_2021, a total of 33,899/127,526,834 reads from 23E_Sörby_2020, and a total of 4,618/87,573,296 from 25R1_Sörby_2020 can be mapped to reference genome PUUV Sotkamo. After assembling, we obtained 3 PUUV full-genome sequences.

Comparative analyses of the new PUUV strains in Scania showed that they were closely related;

diversity was 1.1%–1.8% nt and 0.2%–0.7% aa for the S segment, 3.2%–7.7% nt and 3.2%–8.1% aa for the M segment, and 2.9%–6.2% nt and 3.0%–6.3% aa for the L segment. Comparison with other PUUV strains circulating in Fennoscandia showed that all our Scania PUUV strains were more closely related to the Finnish strains. For the S segment, PUUV in Scania shared 90.0%–91.9% nt and 99.3%–100% aa sequence identities with Finnish PUUV strains (Sotkamo, Konnevesi, and Pieksamaki), 79.6%–80.1% nt and 96.5%–97.5% aa with S-SCA strains, and 79.1% nt and 96% aa with an N-SCA strain (Umeå_Human). For the M segment, they shared 90.7%–92.1% nt and 97.3%–98.6% aa sequence identities with Finnish strains (Sotkamo, Konnevesi, and Pieksamaki), 81.1%–83.4% nt and 92.0%–93.8% aa with S-SCA strains, and 81.2% nt and 92.3% aa with an N-SCA strain (Umeå_Human). For the L segment, they shared 91.4% nt and 98.3%–99.2% aa sequence identities with Finnish strains (Sotkamo, Konnevesi, and Pieksamaki) and 82.0% nt and 93.8% aa with an N-SCA strain (Umeå_Human).

We detected specific amino acid signatures in all 3 PUUV strains in Scania; they were R64K in the N protein and K798R in the glycoprotein. Of interest, 10 aa from 259–268 in the glycoprotein, located in Gn ectodomains, are missing in the 2 strains from Sörby. Sequence analyses did not find any specific amino acid signatures in the RNA-dependent RNA polymerase for those 3 strains.

Phylogenetics of PUUV in Scandinavia

We generated phylogenetic trees based on the full-length sequences of the S, M, and L segments (Appendix Figure 1). The topology of PUUV phylogenies was in agreement with other studies in which the current PUUV strains can be divided into well-supported clusters; in addition to N-SCA and S-SCA, Danish, Central European, Alpe-Adrian, Russian, Finnish, and Ukrainian lineages have been identified (*18*–*20*,*24*). In Sweden, the previously known lineages are S-SCA and N-SCA. S-SCA can be further divided into sublineages: the Mångelbo and Munga strains from Uppland; the Sollefteå, Bergsjöbo, and Fäboviken strains from Västernorrland; and the Eidosvoll strain from Norway. N-SCA can be further divided into the northern N-SCA lineage, including strains from Kiviniemi and Äijäjärvi, and the southern N-SCA lineage (*3*) (Figure 2, panel A), https://wwwnc.cdc.gov/EID/article/30/4/23-1414-F2.tif . Surprisingly, the novel PUUV strains found in Scania did not belong to the S-SCA or the Danish lineages; instead, they clustered with the Finnish PUUV strains, suggesting an Eastern phylogroup as the common ancestor.

We further examined the mitochondrial DNA of the natural hosts that carry Scania PUUV. The sequencing results obtained by conventional PCR were not sufficient for reconstructing the phylogeny of *M. glareolus*. However, we recovered the host mitochondrial DNA from the RNA sequencing data; based on the mitochondrial *cytB* gene sequences, the phylogenetic tree suggested that all 4 bank voles that tested positive for PUUV belonged to the Carpathian clade, which is different from the bank voles in Finland of the Eastern phylogroup (Appendix Figure 3).

Discussion

Our study discovered new PUUV variants in bank voles in Scania in southern Sweden, pinpointing the zoonotic source of local PUUV infection patient cases in southern Sweden. Unfortunately, we do not have access to any samples from those NE patients. However, by reviewing the diagnostic laboratory analysis of those NE cases along with our own results, we have established a genetic association between bank vole hosts in Scania and the local NE patients.

Our findings of Finnish-like PUUV variants in the bank vole population in southern Sweden raised the question of the origin of Scania PUUV. PUUV is the most common hantavirus in Europe, and its natural host, the bank vole, is widely distributed in large areas of Europe. Even though hantaviruses are thought to co-evolve with their hosts, PUUV is still absent in certain locations where bank voles are present (*25*).

In Sweden, the diversity of hantaviruses has mainly been explored in northern rodents (*3*,*4*) because most of the clinical cases of NE are clustered in the north; a likely reason is the recolonization history of bank voles in Fennoscandia. After the last ice age ended in Fennoscandia, ≈10,000 years ago, the Ural phylogroup of bank voles migrated to the north of Fennoscandia and derived mtDNA from the northern red-backed vole (*Myodes rutilus*), whereas the southern bank voles of today originate from the Carpathian phylogroup, which had multiple colonizations to western and southern Fennoscandia (*26*). In contrast, there was 1 migration route from the northeast through Finland (*26*). Our phylogeographical results of bank voles in Scania based on mtDNA data are in agreement with all previous studies; that is, they belong to the Carpathian phylogroup and not the Eastern phylogroups. Nevertheless, PUUV in bank voles in Scania belongs to the Finnish PUUV lineage; a short branch in that clade implies a recent introduction of Finnish PUUV into Sweden.

Our current data cannot resolve the mystery of this recent introduction of PUUV in southern

Sweden. One possible explanation might be that the virus, carried by bank voles, was transported from Finland or Russian Karelia (or other regions where the Finnish PUUV lineage is circulating) to Sweden and then established in bank voles there. The bank voles of the Eastern phylogroup carrying Finnish PUUV may have arrived in southern Sweden and spread the virus to Swedish bank voles but might not have been able to establish themselves as a unique phylogroup. Other less likely explanations might be an introduction via predatory birds or a reverse zoonotic transmission from humans to rodents. However, such possibilities are unlikely; only anecdotal reports on hantavirus-infected birds are available, and hantavirus transmission is known to be almost exclusively epizootic; just 1 human–human transmission has been reported, caused by Andes virus (ANDV) (*27*). Climate change or anthropic factors may have driven such cross-phylogroup transmission process, similar to what we have seen for the current distribution of Seoul hantavirus in Europe and worldwide (*28*).

We have found PUUV in the neighborhood of 1 patient in the Sörby area, which indicates further dissemination of this PUUV variant in the local bank vole population. Our sequence analysis showed that 10 amino acids are missing in the glycoprotein of the 2 PUUV strains discovered in Sörby, which could be associated with the infectivity of PUUV. Our finding of 9 PUUV-positive samples from 48 captured bank voles suggests the prevalence of this recently introduced PUUV will probably not be restricted only to this patient's fields; wider geographic distribution seems highly possible in Scania, given that the other NE patient was from northeastern Scania. However, our trapping focused on the first NE patient's neighborhood; an ethical permit allowed us to capture ≤100 rodents, which may at least partially explain the high prevalence. However, our results indicate that more studies on the surveillance of rodents in southern Sweden will contribute to the understanding of the evolutionary mechanisms of virulence and transmission for PUUV variants in rodents, which requires more rodent samplings at various ecologic sites in Scania in the future. Furthermore, investigation into whether the Scania PUUV variant is more or less infective than the N-SCA and S-SCA variants in bank voles is warranted.

Novel PUUV strains in a new geographic area might have a substantial effect on human health. Since 2018, reported NE cases have not been increasing in Scania. However, the PUUV Pieksamaki strain, the closest relative of PUUV in Scania, has already caused 1 fatal case in Finland (*19*). In Finland, the incidence of diagnosed PUUV infections is ≈31–39 cases/100,000 population, and the fatality rate is ≈0.08%–0.4% (*29*). As of January 2024, only 2 NE cases reported from Scania were known to have been local infections. The patients' symptoms included classic HFRS symptoms, such as fever, general malaise, nosebleed, and renal insufficiency, and laboratory results indicated thrombocytopenia and a moderately increased C-reactive protein. Those patients have fully recovered from their PUUV infections. We now need to understand the prevalence and pathogenicity of these new Scania PUUV strains in humans and their potential differences in virulence, compared with PUUV in N-SCA and in Finland. Future studies should isolate this new PUUV variant, and conduct larger serologic mapping surveys of rodents and febrile patients in Scania.

In conclusion, our study attempted to discover the zoonotic origin of NE cases in Scania, southern Sweden. Our identification of unique PUUV strains circulating in Scania provides critical insights into the pathogenic threats of emerging and reemerging viruses transmitted from rodents to humans.

The center of disease control in Scania (Smittskydd Skåne) funded the ethical permits for this study.

The local research fund at the Central Hospital of Kristianstad funded the sampling and transportation of rodents. J.L. is funded by the Swedish Research Council (VR 2022-03219), Åke Wibergs stiftelse (M22-0168) and Börjesson E o R stipends from Uppsala University. Funding resources were the European Union's Horizon 2020 research innovation program (grant no. 874735 [VEO]), the Swedish Research Council (VR 2017-05807), and SciLifeLab, Pandemic Laboratory Preparedness (grant no. LPP1-007 and REPLP1:005). Resources provided by the Swedish National Infrastructure for Computing at UPPMAX, partially funded by the Swedish Research Council (grant agreement no. 2018-05973), enabled computation and data handling.

About the Author

Dr. Ling is a researcher at Zoonosis Science Center, Department of Medical Biochemistry and Microbiology, Uppsala University, Sweden. Her research focuses on understanding the virulence evolution of emerging and reemerging zoonotic RNA viruses through different approaches in clinical studies, basic cell biological studies, and bioinformatics. Dr. Economou Lundeberg is an infectious disease consultant at the Central Hospital of Kristianstad in southern Sweden and a PhD candidate focusing on different aspects of tuberculosis treatment. Her previous research experience involves field studies of *Borrelia* and PUUV.

References

1. Jones KE, Patel NG, Levy MA, Storeygard A, Balk D, Gittleman JL, et al. Global trends in emerging infectious diseases. Nature. 2008;451:990–3. https://doi.org/10.1038/nature06536
2. Jonsson CB, Figueiredo LT, Vapalahti O. A global perspective on hantavirus ecology, epidemiology, and disease. Clin Microbiol Rev. 2010;23:412–41. https://doi.org/10.1128/CMR.00062-09
3. Nemirov K, Leirs H, Lundkvist A, Olsson GE. Puumala hantavirus and *Myodes glareolus* in northern Europe: no evidence of co-divergence between genetic lineages of virus and host. J Gen Virol. 2010;91:1262–74. https://doi.org/10.1099/vir.0.016618-0
4. Borg O, Wille M, Kjellander P, Bergvall UA, Lindgren PE, Chirico J, et al. Expansion of spatial and host range of Puumala virus in Sweden: an increasing threat for humans? Epidemiol Infect. 2017;145:1642–8. https://doi.org/10.1017/S0950268817000346
5. Vaheri A, Henttonen H, Voutilainen L, Mustonen J, Sironen T, Vapalahti O. Hantavirus infections in Europe and their impact on public health. Rev Med Virol. 2013;23:35–49. https://doi.org/10.1002/rmv.1722
6. Vial PA, Ferrés M, Vial C, Klingström J, Ahlm C, López R, et al. Hantavirus in humans: a review of clinical aspects and management. Lancet Infect Dis. 2023;23:e371–82. https://doi.org/10.1016/S1473-3099(23)00128-7
7. Olsson GE, Dalerum F, Hörnfeldt B, Elgh F, Palo TR, Juto P, et al. Human hantavirus infections, Sweden. Emerg Infect Dis. 2003;9:1395–401. https://doi.org/10.3201/eid0911.030275
8. Ahlm C, Linderholm M, Juto P, Stegmayr B, Settergren B. Prevalence of serum IgG antibodies to Puumala virus (haemorrhagic fever with renal syndrome) in northern Sweden. Epidemiol Infect. 1994;113:129–36. https://doi.org/10.1017/S0950268800051542
9. Olsson GE, Hjertqvist M, Lundkvist A, Hörnfeldt B. Predicting high risk for human hantavirus infections, Sweden. Emerg Infect Dis. 2009;15:104–6. https://doi.org/10.3201/eid1501.080502
10. Khalil H, Ecke F, Evander M, Bucht G, Hörnfeldt B. Population dynamics of bank voles predicts human Puumala hantavirus risk. EcoHealth. 2019;16:545–57. https://doi.org/10.1007/s10393-019-01424-4
11. Lõhmus M, Verner-Carlsson J, Borg O, Albihn A, Lundkvist Å. Hantavirus in new geographic regions, Sweden. Infect Ecol Epidemiol. 2016;6:31465. https://doi.org/10.3402/iee.v6.31465
12. Economou Lundeberg E, Frisk J. First case of nephropathia epidemica in southern Sweden [in Swedish]. Lakartidningen. 2019;5:116–118.
13. Klempa B, Fichet-Calvet E, Lecompte E, Auste B, Aniskin V, Meisel H, et al. Hantavirus in African wood mouse, Guinea. Emerg Infect Dis. 2006;12:838–40. https://doi.org/10.3201/eid1205.051487
14. Niskanen S, Jääskeläinen A, Vapalahti O, Sironen T. Evaluation of real-time RT-PCR for diagnostic use in detection of Puumala virus. Viruses. 2019;11:661. https://doi.org/10.3390/v11070661
15. Kang HJ, Arai S, Hope AG, Song JW, Cook JA, Yanagihara R. Genetic diversity and phylogeography of Seewis virus in the Eurasian common shrew in Finland and Hungary. Virol J. 2009;6:208. https://doi.org/10.1186/1743-422X-6-208
16. Wasberg A, Raghwani J, Li J, Pettersson JH, Lindahl JF, Lundkvist Å, et al. Discovery of a novel coronavirus in Swedish bank voles (*Myodes glareolus*). Viruses. 2022;14:1205. https://doi.org/10.3390/v14061205
17. Ronquist F, Huelsenbeck JP. MrBayes 3: Bayesian phylogenetic inference under mixed models. Bioinformatics. 2003;19:1572–4. https://doi.org/10.1093/bioinformatics/btg180
18. Castel G, Couteaudier M, Sauvage F, Pons JB, Murri S, Plyusnina A, et al. Complete genome and phylogeny of Puumala hantavirus isolates circulating in France. Viruses. 2015;7:5476–88. https://doi.org/10.3390/v7102884
19. Plyusnina A, Razzauti M, Sironen T, Niemimaa J, Vapalahti O, Vaheri A, et al. Analysis of complete Puumala virus genome, Finland. Emerg Infect Dis. 2012;18:2070–2. https://doi.org/10.3201/eid1811.120747
20. Williams EP, Taylor MK, Demchyshyna I, Nebogatkin I, Nesterova O, Khuda I, et al. Prevalence of hantaviruses harbored by murid rodents in northwestern Ukraine and discovery of a novel Puumala virus strain. Viruses. 2021;13:1640. https://doi.org/10.3390/v13081640
21. Katoh K, Standley DM. MAFFT multiple sequence alignment software version 7: improvements in performance and usability. Mol Biol Evol. 2013;30:772–80. https://doi.org/10.1093/molbev/mst010
22. Larsson A. AliView: a fast and lightweight alignment viewer and editor for large datasets. Bioinformatics. 2014;30:3276–8. https://doi.org/10.1093/bioinformatics/btu531
23. Posada D. jModelTest: phylogenetic model averaging. Mol Biol Evol. 2008;25:1253–6. https://doi.org/10.1093/molbev/msn083
24. Blinova E, Deviatkin A, Makenov M, Popova Y, Dzagurova T. Evolutionary formation and distribution of Puumala virus genome variants, Russia. Emerg Infect Dis. 2023;29:1420–4. https://doi.org/10.3201/eid2907.221731
25. Olsson GE, Leirs H, Henttonen H. Hantaviruses and their hosts in Europe: reservoirs here and there, but not everywhere? Vector Borne Zoonotic Dis. 2010;10:549–61. https://doi.org/10.1089/vbz.2009.0138
26. Marková S, Horníková M, Lanier HC, Henttonen H, Searle JB, Weider LJ, et al. High genomic diversity in the bank vole at the northern apex of a range expansion: the role of multiple colonizations and end-glacial refugia. Mol Ecol. 2020;29:1730–44. https://doi.org/10.1111/mec.15427
27. Martínez VP, Di Paola N, Alonso DO, Pérez-Sautu U, Bellomo CM, Iglesias AA, et al. "Super-spreaders" and person-to-person transmission of Andes virus in Argentina. N Engl J Med. 2020;383:2230–41. https://doi.org/10.1056/NEJMoa2009040
28. Lin XD, Guo WP, Wang W, Zou Y, Hao ZY, Zhou DJ, et al. Migration of Norway rats resulted in the worldwide distribution of Seoul hantavirus today. J Virol. 2012;86:972–81. https://doi.org/10.1128/JVI.00725-11
29. Vaheri A, Henttonen H, Mustonen J. Hantavirus research in Finland: highlights and perspectives. Viruses. 2021;13:1452. https://doi.org/10.3390/v13081452

Address for correspondence: Åke Lundkvist, BMC Husargatan 3, Box 582, 751 23, Uppsala, Sweden; email: ake.lundkvist@imbim.uu.se

Divergent Pathogenesis and Transmission of Highly Pathogenic Avian Influenza A(H5N1) in Swine

Bailey Arruda, Amy L. Vincent Baker, Alexandra Buckley, Tavis K. Anderson, Mia Torchetti, Nichole Hines Bergeson, Mary Lea Killian, Kristina Lantz

Highly pathogenic avian influenza (HPAI) viruses have potential to cross species barriers and cause pandemics. Since 2022, HPAI A(H5N1) belonging to the goose/Guangdong 2.3.4.4b hemagglutinin phylogenetic clade have infected poultry, wild birds, and mammals across North America. Continued circulation in birds and infection of multiple mammalian species with strains possessing adaptation mutations increase the risk for infection and subsequent reassortment with influenza A viruses endemic in swine. We assessed the susceptibility of swine to avian and mammalian HPAI H5N1 clade 2.3.4.4b strains using a pathogenesis and transmission model. All strains replicated in the lung of pigs and caused lesions consistent with influenza A infection. However, viral replication in the nasal cavity and transmission was only observed with mammalian isolates. Mammalian adaptation and reassortment may increase the risk for incursion and transmission of HPAI viruses in feral, backyard, or commercial swine.

Influenza A viruses (IAV) of avian and swine origin have caused 5 pandemics in the previous 2 centuries (*1*). Aquatic avian populations, the primary reservoir for IAV, harbor numerous virus subtypes (H1–16), to which mammals have minimal preexisting immunity (*2*). Among those subtypes, H5 avian influenza virus infections have been documented in domestic poultry, humans, marine mammals, and swine, among others (*3*–*6*).

Over the past decade, H5NX highly pathogenic avian influenza (HPAI) viruses belonging to the goose/Guangdong (Gs/GD) 2.3.4.4 hemagglutinin (HA) phylogenetic clade have caused infections in wild birds and poultry, resulting in major mortality events and spread to >84 countries, and were recognized as a panzootic (*7*,*8*). In addition, evidence exists of enzootic HPAI virus maintenance in Europe, further signifying a paradigm shift in the biology of HPAI (*9*). Since February 2022, HPAI H5N1 clade 2.3.4.4b virus originating from a trans-Atlantic incursion has caused outbreaks across North America, resulting in >77 million poultry deaths, extensive deaths in wild bird species, and unprecedented disease in wild mammals (*4*–*6*,*10*)

The transcontinental circulation of clade 2.3.4.4b viruses within bird populations continues to enable reassortment with low pathogenicity avian influenza (LPAI) viruses and resulted in the emergence of numerous genotypes of potentially different phenotypes (*11*,*12*). Furthermore, interspecies transmission between avian species and peridomestic mammals has resulted in viruses with mammalian adaptation markers that pose a public health risk should they gain efficient transmission among mammals. A subset of HPAI H5NX clade 2.3.4.4 viruses bound both α2,6-linked (human) and α2,3-linked (avian) sialic acid receptors (*13*–*16*). Furthermore, nearly half of mammal isolates of HPAI H5N1 clade 2.3.4.4b acquired mammalian adaptation markers (E627K, D701N, or T271A substitutions) in the polymerase basic (PB) 2 protein (*1*,*17*). In addition, the HPAI H5N1 viruses collected during an outbreak in farmed mink contained mutations in the neuraminidase protein that caused disruption of the second sialic acid binding site, a feature typical of human-adapted IAV (*17*). During January 2022–April 17, 2023, a total of 8 reported human cases of H5N1 influenza from clade 2.3.4.4b occurred, many severe or fatal (*4*,*18*). Those characteristics of the current clade 2.3.4.4b H5 HPAI elevate the potential for human infection and adaptation.

Author affiliations: Agriculture Research Service, Ames, Iowa, USA (B. Arruda, A.L. Vincent Baker, A. Buckley, T.K. Andersen); Animal and Plant Health Inspection Service, Ames (M. Torchetti, N. Hines Bergeson, M.L. Killian, K. Lantz)

DOI: https://doi.org/10.3201/eid3004.231141

Table 1. Virus strain accession number, genotype, constellation, and reassorted genes in study of divergent pathogenesis and transmission of highly pathogenic avian influenza A(H5N1) in swine*

Strain	GISAID accession no.†	Genotype	Constellation (PB2|PB1|PA|HA|NP|NA|M|NS)	Reassorted genes
A/turkey/Minnesota/22-010654-001/2022	16555202	B2.1	am1.2|ea1|ea1|ea1|am1.1|ea1|ea1|ea1	PB2, NP
A/bald eagle/Florida/W22-134-OP/2022	15063846	B1.1	am1.1|am1.1|ea1|ea1|am1.2|ea1|ea1|ea1	PB2, PB1, NP
A/raccoon/Washington/22-018406-002/2022	15078252	B2.1	am1.2|ea1|ea1|ea1|am1.1|ea1|ea1|ea1	PB2, NP
A/red fox/Michigan/22-018712-001/2022	15078253	B3.2	am2.1|am1.2|ea1|ea1|am1.4.1|ea1|ea1|am1.1	PB2, PB1, NP, NS

*am, American; ea, Eurasian; PB2, polymerase basic 2; PB1, polymerase basic 1; PA, polymerase acidic; HA, hemagglutinin; NP, nucleoprotein; NA, neuraminidase; M, matrix protein 1; NS, non-structural protein 1.
†GISAID, https://www.gisaid.org.

A longstanding dogma of IAV biology identified swine as a mixing vessel and vital to the emergence of human pandemic IAV by supporting reassortment that could lead to antigenic shift (*1*). However, at a receptor level, swine might be no more susceptible to infection by avian IAVs than humans (*1*). Mammalian adaption of HPAI is a multigenic trait, and the genetic changes necessary for H5N1 strains to adapt to swine and acquire efficient and sustained transmissibility are poorly understood. However, swine-adapted IAV have a propensity for evolution through polymerase errors and reassortment, followed by spread of mutated or reassorted strains through contact among densely housed commercial pigs and pig transport. If an avian IAV strain, such as H5Nx 2.3.4.4b, successfully infected domestic swine, pig-to-pig transmission, reassortment with endemic swine IAV, or acquisition of adaptive mutations that might enable an avian-to-mammalian switch could potentially occur (*1*). Continued circulation in the wild bird population

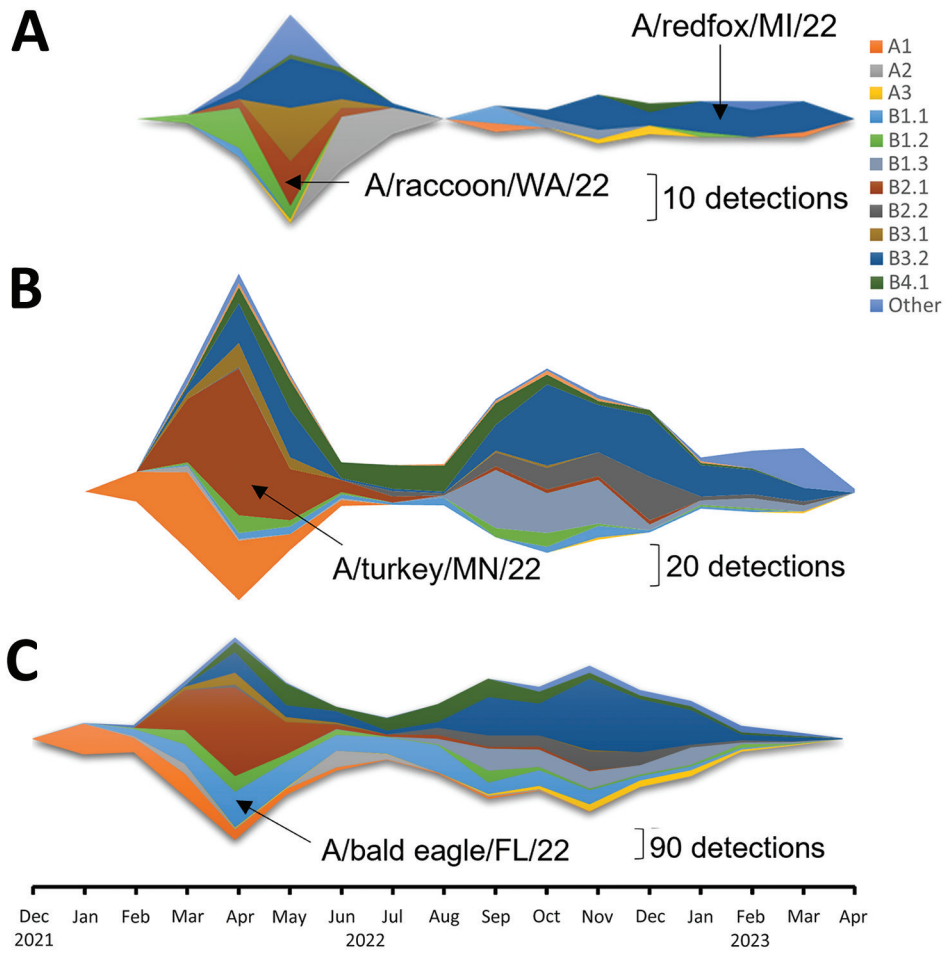

Figure 1. Detection of Eurasian lineage goose/Guangdong H5 clade 2.3.4.4b virus and identification of virus isolates used in study of divergent pathogenesis and transmission of highly pathogenic avian influenza A(H5N1) in swine, by genotype. A) Wild mammal; B) poultry; C) wild birds.

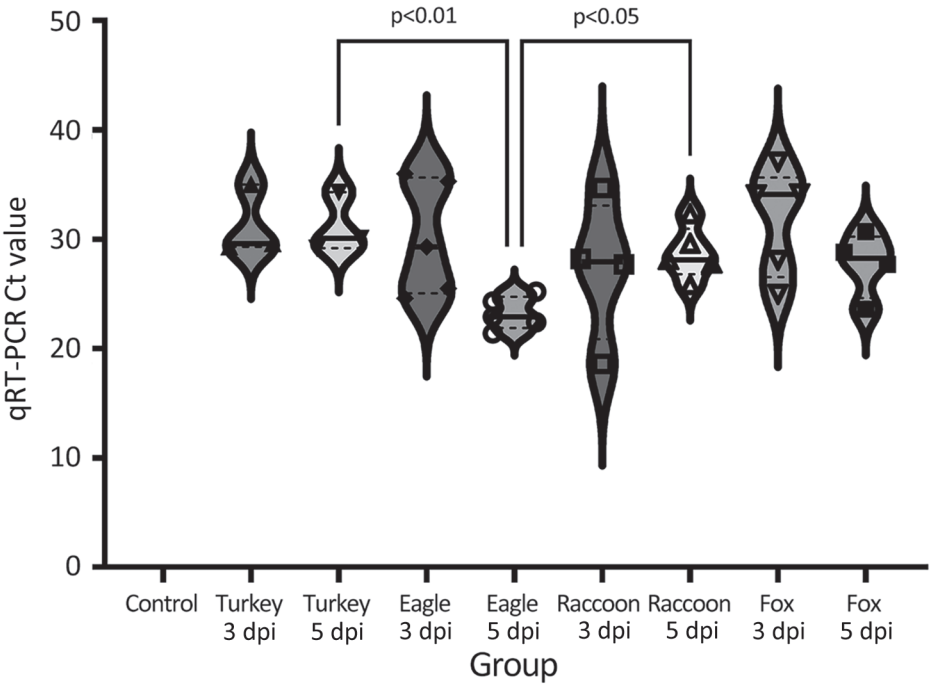

Figure 2. Violin plots showing Ct values for bronchoalveolar lavage fluid from pigs, by virus strain and dpi, in study of divergent pathogenesis and transmission of highly pathogenic avian influenza A(H5N1) in swine. Values were determined by quantitative reverse transcription PCR (ThermoFisher Scientific, https://www.thermofisher.com). All strains replicated in the lung of pigs. No statistical difference was detected between strains by dpi. Solid lines within plots indicate medians, dashed lines indicate quartiles, and symbols indicate individual pig values. dpi, days postinoculation; Eagle 3 dpi, A/bald eagle/FL/22 necropsied on 3 dpi; Eagle 5 dpi, A/bald eagle/FL/22 necropsied at 5 dpi; Fox 3 dpi, A/redfox/MI/22 necropsied at 3 dpi; Fox 5 dpi, A/redfox/MI/22 necropsied at 5 dpi; Raccoon 3 dpi, A/raccoon/WA/22 necropsied at 3 dpi; Racoon 5 dpi, A/raccoon/WA/22 necropsied at 5 dpi; Turkey 3 dpi, A/turkey/MN/22 necropsied at 3 dpi; Turkey 5 dpi, A/turkey/MN/22 necropsied at 5 dpi.

and peridomestic wild mammal infections elevate the risk for exposure of swine because of the current outbreak's wide distribution in states with large pig populations. To address concerns over susceptibility of swine to HPAI H5N1 clade 2.3.4.4b virus detected in the United States and to elucidate potential molecular mutations associated with H5N1 replication and transmission in swine, we conducted a study with 4 strains representing 3 different genotypes in a pig pathogenesis and transmission model. This information is key to building awareness and detection capabilities in the swine sector, as well as to informing risk assessments and early warning systems to safeguard human health.

Materials and Methods

Viruses

We evaluated the pathogenicity and transmission in crossbred, 4-week-old pigs of 4 strains of the 2022 spring HPAI H5N1 clade 2.3.4.4b outbreak: A/turkey/Minnesota/22–010654-001/2022 (A/turkey/MN/22), A/bald eagle/Florida/W22-134-OP/2022 (A/bald eagle/FL/22), A/raccoon/Washington/22-018406-002/2022 H5N1 (A/raccoon/WA/22) and A/redfox/Michigan/22-018712-001/2022 (A/redfox/MI/22). Those 4 strains resulted from Eurasian avian HPAI H5N1 clade 2.3.4.4b reassortment with North American LPAI lineage internal genes and represented 3 different reassortment patterns frequently detected among H5N1 strains during 2022 (Table 1; Figure 1) (Appendix 1, https://wwwnc.cdc.gov/EID/article/30/4/23-1141-App1.pdf). Both the A/raccoon/WA/22 and the A/redfox/MI/22 strains contained the PB2 E627K mammalian adaptation mutation.

Virus Propagation and Titration

We conducted the study in compliance with the Animal Care and Use Committee of the US Department of Agriculture—Agricultural Research Service National Animal Disease Center under Biosafety Level 3 guidelines, including enhancements required by the Federal Select Agent Program. We passaged virus stocks in 10-day-old embryonating chicken eggs, harvested the allantoic fluid from infected eggs, divided it into aliquots, and stored it at –70°C until use. We determined viral titers by using MDCK cells according to standard methods (*19*).

Swine Pathogenesis and Transmission Study

We blocked 88 pigs by litter and randomly allocated them into a negative control group or a group of 20 (1 group per virus strain). We inoculated 15 pigs per virus strain intranasally with 1 ml (0.5 ml per

nostril) of ≈10^5 50% tissue culture infective dose/mL using a Nasal Intranasal Mucosal Atomization Device (Teleflex, https://www.teleflex.com). We comingled 5 naive contact pigs with each of the virus-inoculated groups at 2 days postinoculation (dpi). We collected nasal swabs from inoculated pigs and contact pigs on 0, 1, 3, 5, and 7 dpi or days postcontact (dpc). We necropsied 5 inoculated pigs per group at 3, 5, and 14 or 17 dpi and the 5 contact pigs at 12 or 15 dpc. We collected bronchoalveolar lavage fluid (BALF) at necropsy on 3 and 5 dpi. We also obtained serum samples at necropsy (Appendix 1). We necropsied 8 negative control pigs from the same source herd as inoculated and contact pigs on ≈5 DPI to evaluate health status and background respiratory tract lesions.

Viral RNA Detection and Serology

We extracted viral RNA from nasal swab and BALF samples by using the MagMax Viral RNA isolation kit (ThermoFisher Scientific, https://www.thermofisher.com) and subjected it to real-time reverse transcription assays targeting multiple genes of IAV and a H5 2.3.4.4-specific HA gene (*20*). Cycle threshold (Ct) value for IAV quantitative reverse transcription PCR (qRT-PCR) interpretation was according to manufacturer's suggestion: Ct value of <38 indicated the sample was positive, Ct value of 38–40 indicated the sample was suspect; if undetected, the sample was negative. We determined seroconversion by using an IAV nucleoprotein (NP)–blocking ELISA (IDEXX, https://www.idexx.com).

Positive Sample Metagenomic Sequencing and Analyses

We amplified IAV RNA from samples as described (*10*). For each of the samples, we conducted variant calling by trimming raw FASTQ files using Trimmomatic (http://www.usadellab.org/cms/?page=trimmomatic) with a sliding window size of 5 bp and a minimum Q-score of 30, discarding reads that were trimmed to a length <100 bases. We aligned reads to reference sequences using bowtie2 version 2.3.2 (https://sourceforge.net/projects/bowtie-bio/files/bowtie2/2.3.2) and removed duplicate reads were removed using Picard (https://broadinstitute.github.io/picard). We converted the BAM files to mpileup using samtools (https://www.htslib.org) and identified within-host variants using VarScan (https://varscan.sourceforge.net). For a variant to

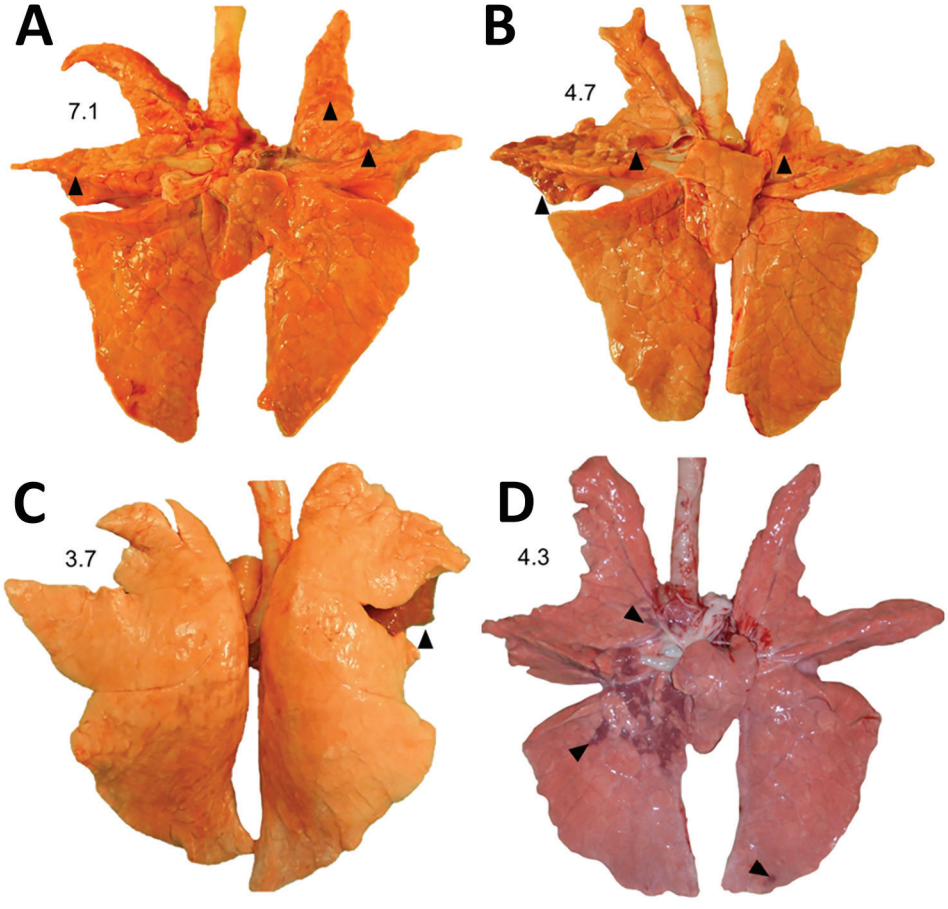

Figure 3. Macroscopic lung lesions and respective weighted macroscopic lung score of swine infected with highly pathogenic avian influenza A(H5N1) virus belonging to the goose/Guangdong 2.3.4.4b hemagglutinin phylogenetic clade. A) Multifocal pulmonary consolidation (arrowheads) in pig 777 infected with A/turkey/MN/22, necropsied at 3 days postinoculation (dpi). B) Multifocal pulmonary consolidation (arrowheads) in pig 796 infected with A/bald eagle/FL/22 necropsied on 5 dpi. C) Locally extensive pulmonary consolidation (arrowheads) in pig 58 infected with A/raccoon/WA/22 necropsied on 3 dpi. D) Multifocal pulmonary consolidation (arrowheads) of pig 78 infected with A/redfox/MI/22 necropsied on 3 dpi.

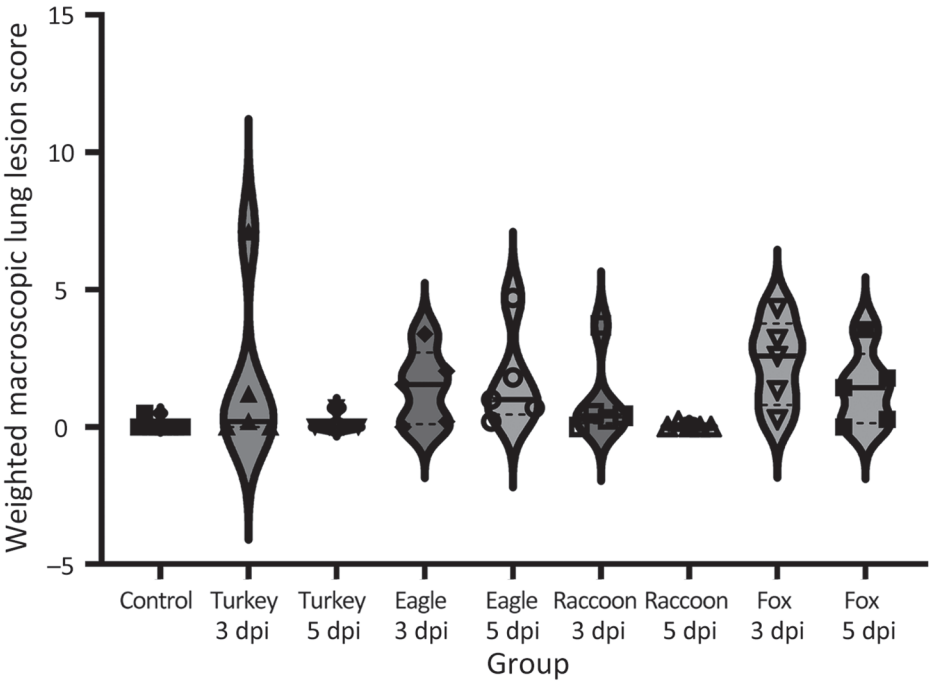

Figure 4. Violin plots of weighted macroscopic lung scores, by virus strain and dpi, of swine infected with highly pathogenic avian influenza A(H5N1) virus belonging to the goose/Guangdong 2.3.4.4b hemagglutinin phylogenetic clade. All strains caused macroscopic lesions consistent with influenza A virus infection in ≥1 pig. Solid lines within plots indicate medians, dashed lines indicate quartiles, and symbols indicate individual pig values. No statistically significant differences were detected between strains by dpiI. dpi, days postinoculation; eagle 3 dpi, A/bald eagle/FL/22 necropsied at 3 dpi; eagle 5 dpi, A/bald eagle/FL/22 necropsied at 5 dpi; fox 3 dpi, A/redfox/MI/22 necropsied at 3 dpi; fox 5 dpi, A/redfox/MI/22 necropsied at 5 dpi; raccoon 3 dpi, A/raccoon/WA/22 necropsied at 3 dpi; raccoon 5 dpi, A/raccoon/WA/22 necropsied at 5 dpi; turkey 3 dpi, A/turkey/MN/22 necropsied at 3 dpi; turkey 5 dpi, A/turkey/MN/22 necropsied at 5 dpi.

be reported, we required the sequencing depth to be 100×, PHRED quality scores to be 30, and detection frequency to be ≥1%. We compiled all reported variant calls and raw FASTQ files (https://github.com/flu-crew/datasets). We used the Sequence Feature Variant Types tool from the Influenza Research Database to download all currently available annotations for H5 HA, N1 neuraminidase, and the remaining internal genes (*21*). For each genome, we computed nucleotide diversity using the synonymous (π_S) and nonsynonymous (π_N) diversity calculations in SNPGenie (https://github.com/chasewnelson/SNPGenie) with a minimum allele frequency cutoff set to 1% (*22*) (Appendix 1).

Macroscopic and Microscopic Lesion Score

At necropsy, we recorded the percentage of affected surface area per lung lobe and used that to calculate a weighted macroscopic lung lesion score (*23*). We fixed tissue samples from the trachea and right middle or affected lung lobe in 10% buffered formalin for histologic examination and transferred to 70% ethanol after 48 hours. A veterinary pathologist blinded to treatment evaluated microscopic lesions of the lung and trachea (Appendix 1).

Immunohistochemistry

We conducted immunohistochemistry (IHC) staining manually on 5-µm–thick sections using a rabbit polyclonal anti-influenza A NP (GeneTex, https://www.genetex.com) primary antibody. We blocked slide runs by group to account for potential differences between runs and scored as previously described (Appendix 1) (*23*).

Statistical analysis

We performed all statistical analyses using GraphPad Prism 8.1.2 software (https://www.graphpad.com). We used a Kruskal-Wallis test with Dunn correction for multiple comparisons to compare the weighted macroscopic lung lesion score, microscopic pneumonia score, microscopic tracheitis score, lung IHC score of conducting airways, lung IHC score of nonconducting airways, cumulative lung IHC scores, and tracheal IHC score of virus inoculated groups by dpi. We compared the BALF qRT-PCR Ct values of positive samples using an ordinary 1-way ANOVA with a Šídák multiple comparisons test. We considered an adjusted p value of <0.05 significant in each analysis.

Results

Isolate Replication

All isolates replicated in the lungs of most inoculated pigs, although no overt clinical signs were observed (Figure 2; Appendix 1 Table 1). We detected viral RNA in BALF from 3 of the 5 inoculated pigs necropsied at both 3 and 5 dpi in the A/turkey/MN/22

group, from all inoculated pigs necropsied at both 3 and 5 dpi in the A/bald eagle/FL/22 group, 4 of the 5 inoculated pigs necropsied at both 3 and 5 dpi in the A/raccoon/WA/22 group, and all inoculated pigs necropsied at 3 dpi and 4 inoculated pigs at 5 dpi in the A/redfox/MI/22 group. The lowest group mean Ct value (23.22) was observed in the A/bald eagle/FL/22 group at 5 dpi, followed by the A/raccoon/WA/22 group at 3 dpi (Ct value 26.05) and A/redfox/MI/22 group at 5 dpi (Ct value 26.14). The lowest individual Ct value (18.16) was seen in the A/raccoon/WA/22 group at 3 dpi. We found a significant difference in mean Ct values between the A/bald eagle/FL/22 and A/turkey/MN/22 groups and the A/bald eagle/FL/22 and A/raccoon/WA/22 groups at 5 dpi ($p<0.05$) (Figure 2). We did not detect viral RNA in BALF samples from control pigs.

Macroscopic and Microscopic Lesions

Macroscopic lung lesions consistent with IAV infection developed in pigs in each of the virus-inoculated groups. Macroscopic lesions consisted of multifocal-to-locally extensive predominately cranioventral red-to-purple pulmonary consolidation (Figure 3, panels A–D). Averaging the weighted macroscopic lung lesion score at 3 and 5 dpi by group showed that the A/bald eagle/FL/22 and A/redfox/MI/22 strains caused the highest lesion scores (Figure 4). A significant difference was found between groups necropsied at 5 dpi ($p<0.05$); however, no significant difference was found in the ad hoc comparisons with only the weighted macroscopic lung lesion score of the A/bald eagle/FL/22 group compared, and the A/turkey/MN/22 at 5 dpi neared significance ($p = 0.055$).

Microscopic lung lesions consistent with IAV infection developed in inoculated pigs in each of the virus-inoculated groups; however, the number of pigs with consistent lesions and the severity of lesions varied by group. A/turkey/MN/22 caused little to no microscopic lesions; lesions consistent with IAV infection developed in only 1 of 10 inoculated pigs (Figure 5, panel A). In contrast, lung lesions consistent with IAV infection developed in most pigs in the A/bald eagle/FL/22 group (7 of 10) (Figure 5, panel B). In both the A/raccoon/WA/22 and A/redfox/MI/22 groups, lesions consistent with IAV infection

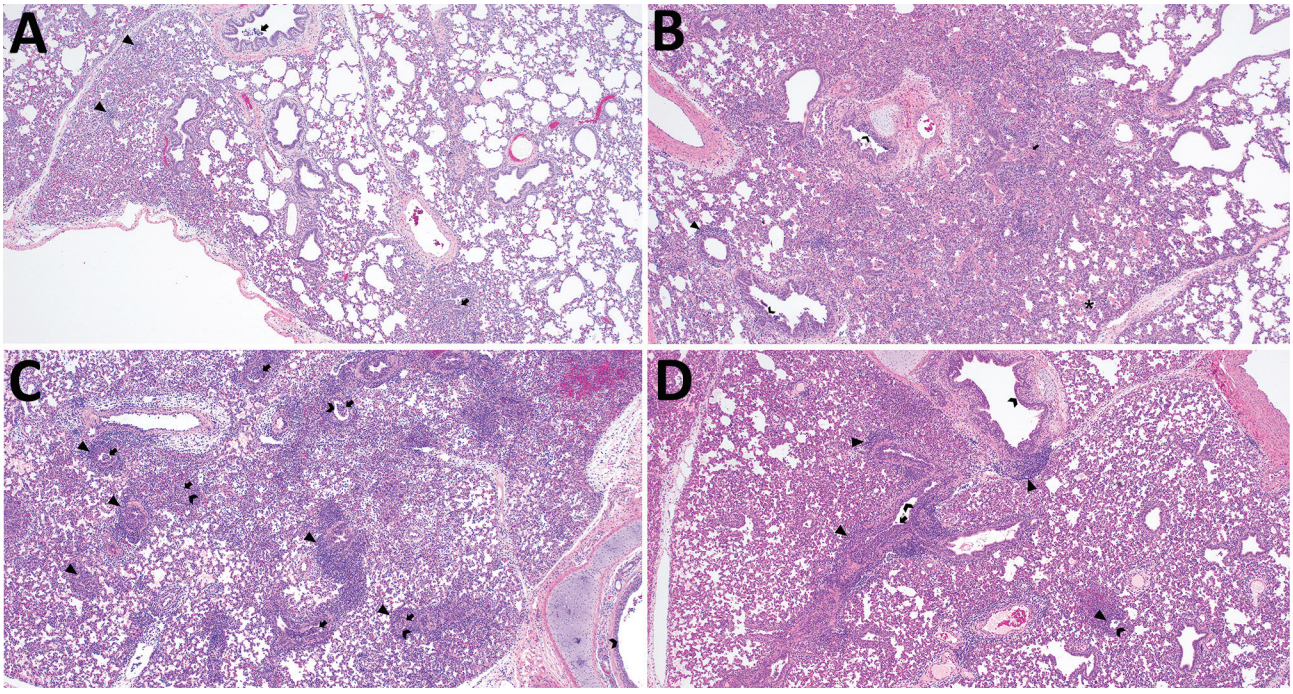

Figure 5. Microscopic lung lesions of swine infected with highly pathogenic avian influenza A(H5N1) belonging to the goose/Guangdong 2.3.4.4b hemagglutinin phylogenetic clade. A) Perivascular mononuclear inflammatory infiltrate (arrowheads) and suppurative bronchiolitis (arrows) in the lung of pig 777 infected with A/turkey/MN/22 necropsied at 3 days postinoculation (dpi). B) Peribronchiolar mononuclear inflammatory infiltrate (arrowhead), suppurative bronchiolitis (arrow), necrotizing bronchiolitis and bronchitis (chevrons), and alveolar luminal accumulation of cellular debris (asterisk) in the lung of pig 796 infected with A/bald eagle/FL/22 necropsied at 5 dpi. C) Peribronchiolar mononuclear inflammatory infiltrate (arrowheads), suppurative bronchiolitis (arrows), and necrotizing bronchiolitis and bronchitis (chevrons) in the lung of pig 58 infected with A/raccoon/WA/22 necropsied at 3 dpi. D) Peribronchiolar and peribronchial mononuclear inflammatory infiltrate (arrowheads), suppurative bronchiolitis (arrow), and necrotizing bronchiolitis and bronchitis (chevrons) in the lung of pig 78 infected with A/redfox/MI/22 necropsied at 3 dpi. Hematoxylin & eosin stain; original magnification ×40.

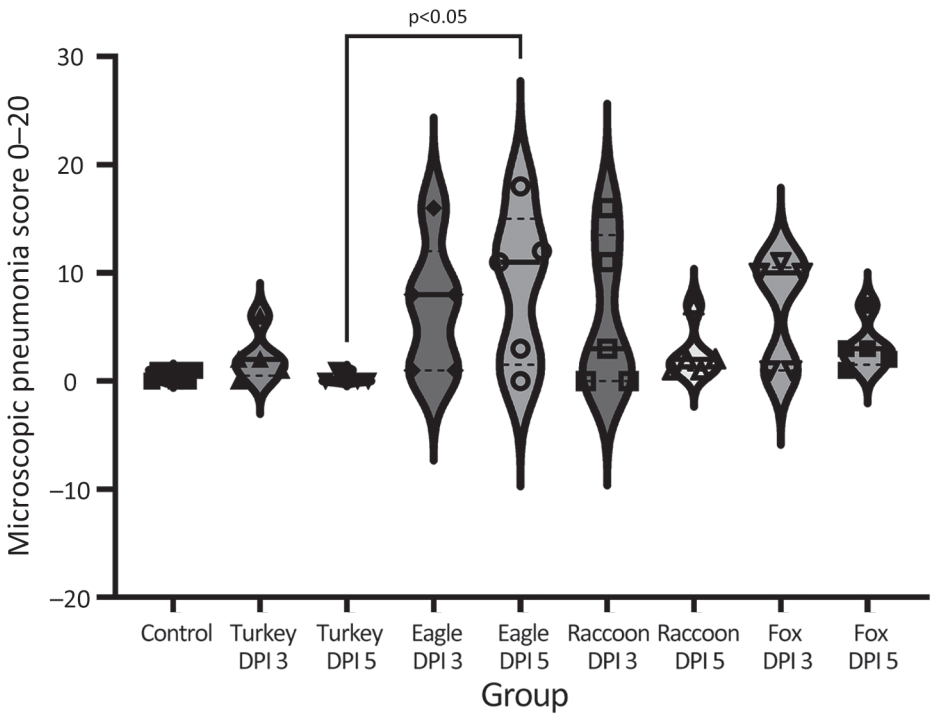

Figure 6. Violin plots of microscopic pneumonia scores, by virus strain and dpi, of swine infected with highly pathogenic avian influenza A(H5N1) virus belonging to the goose/Guangdong 2.3.4.4b hemagglutinin phylogenetic clade. Lesion severity varied by group, with the most severe lesions being observed in the A/bald eagle/FL/22 and A/red fox/MI/22 groups. Solid lines within plots indicate medians, dashed lines indicate quartiles, and symbols indicate individual pig values. dpi, days postinoculation; eagle 3 dpi, A/bald eagle/FL/22 necropsied at 3 dpi; eagle 5 dpi, A/bald eagle/FL/22 necropsied at 5 dpi; fox 3 dpi, A/redfox/MI/22 necropsied at 3 dpi; fox 5 dpi, A/redfox/MI/22 necropsied at 5 dpi; raccoon 3 dpi, A/raccoon/WA/22 necropsied at 3 dpi; raccoon 5 dpi, A/raccoon/WA/22 necropsied at 5 dpi; turkey 3 dpi, A/turkey/MN/22 necropsied at 3 dpi; turkey 5 dpi, A/turkey/MN/22 necropsied at 5 dpi.

developed in 4 of 10 inoculated pigs (Figure 5, panels C, D). A significant difference was found between the microscopic pneumonia score when comparing the A/turkey/MN/22 DPI 5 group and the A/bald eagle/FL/22 DPI 5 group ($p<0.05$) (Figure 6). Microscopic tracheitis scores were not statistically different between the virus inoculated groups (Appendix 1 Figure 1).

Alveolitis and Antigen Labeling

Divergent pathogenesis between HPAI strains was further evidenced by the extent of alveolitis and differential distribution and abundance of NP antigen by IHC. We did not detect HPAI NP antigen in any lung section from the A/turkey/MN/22 group but did detect HPAI NP antigen in the trachea of 2 pigs from this group. In contrast, we detected HPAI NP antigen in the trachea (8 of 10) and lung (7 of 10) in pigs in the A/bald eagle/FL/22 group. We also detected antigen in the respiratory epithelium of conducting airways, macrophages, pneumocytes, alveolar luminal debris, and, rarely, endothelial cells of pigs inoculated with A/bald eagle/FL/22 (Figure 7, panels A–C). In addition, the degree of alveolitis characterized by extensive widening of alveolar septa because of a mononuclear inflammatory infiltrate and luminal accumulation of edema and cellular debris, a change not typical of swine-adapted IAV, was most prominent in the A/bald eagle/FL/22 group (Figure 7, panels A, B).

We detected HPAI NP antigen in the trachea (6 of 10) or lung (2 of 10) of pigs from the A/raccoon/WA/22 group and trachea (7 of 10) or lung (5 of 10) of pigs in the A/redfox/MI/22 group. However, the distribution of antigen in those 2 groups varied compared to the A/bald eagle/FL/22 group. NP antigen was less commonly observed in macrophages, pneumocytes, and alveolar luminal debris and not observed in endothelial cells (Figure 7, panels D, E). We observed significant differences among the conducting airway (Figure 8, panel A), nonconducting airway (Figure 8, panel B), and cumulative lung IHC scores (Appendix 1 Figure 2) of the A/bald eagle/FL/22 5 dpi group and both the A/turkey/MN/22 group and A/raccoon/WA/22 5 dpi groups ($p<0.05$). We observed no significant difference for tracheal IHC score between the virus-inoculated groups (Appendix 1 Figure 3). We did not detect NP antigen in any samples from control pigs.

Mammalian Isolates

Neither A/turkey/MN/22 nor A/bald eagle/FL/22 replicated to detectable levels in the nasal cavity of inoculated pigs (0 of 15 per strain) or transmitted on the basis of seroconversion or detection of viral RNA in nasal swab samples from direct-contact pigs (0 of 5

per strain) (Table 2). In contrast, we detected A/raccoon/WA/22 in the nasal cavity of inoculated pigs (4 of 15) and transmitted to contacts (2 of 5). Similarly, we detected A/redfox/MI/22 in the nasal cavity of inoculated pigs (5 of 15) and transmitted to a single contact (Table 3). We did not detect viral RNA in any nasal swab samples from control pigs.

We identified within-host variants in PCR-positive samples across the genome for the 4 strains during infection and after transmission that were present in ≥1% of sequencing reads (Appendix 1 Table 2). Most single-nucleotide variants were present at low frequencies (Appendix 2, https://wwwnc.cdc.gov/EID/article/30/4/23-1141-App2.xlsx). Of the polymorphic amino acid sites, 41 nonsynonymous mutations occurred at sites associated with functional changes, including PB2 E627K detected as a minor variant (4.95%) in A/turkey/MN/22 at 5 dpi in a single sample

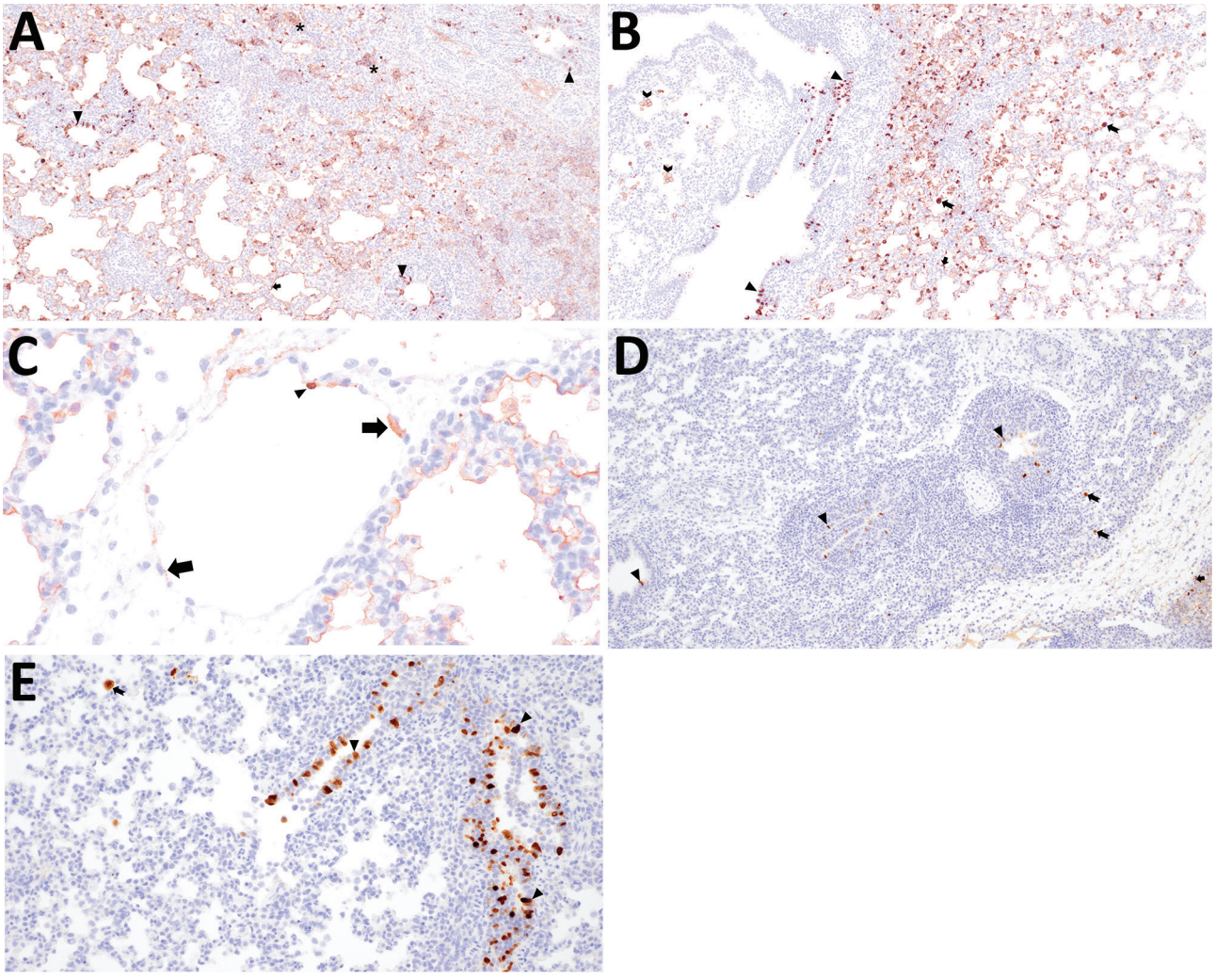

Figure 7. Immunohistochemical detection of influenza A virus nucleoprotein antigen in swine infected with H5N1 highly pathogenic avian influenza belonging to the goose/Guangdong 2.3.4.4b hemagglutinin phylogenetic clade. A) Extensive labeling of pneumocytes lining alveolar septa (arrows) and respiratory epithelium lining bronchioles (arrowheads) in the lung of pig 794 infected with A/bald eagle/FL/22 necropsied at 3 days postinoculation (dpi). Hematoxylin & eosin stain; original magnification ×40. B) Extensive labeling of pneumocytes lining alveolar septa (arrow), respiratory epithelium lining a bronchus (arrowheads), cell membrane of alveolar macrophages (chevron), and within the cytoplasm and nucleus of alveolar macrophages consistent with viral replication (notched arrow) in the lung of pig 798 infected with A/bald eagle/FL/22 necropsied on 5 dpi. Hematoxylin & eosin stain; original magnification ×40. C) Labeling in the cytoplasm (arrows) and nucleus (arrowhead) of endothelial cells in the lung of pig 791 infected with A/bald eagle/FL/22 necropsied on 3 dpi. Hematoxylin & eosin stain; original magnification ×200. D) Labeling of respiratory epithelium lining a bronchus (arrowheads), within the cytoplasm and nucleus of alveolar macrophages consistent with viral replication (notched arrow), rarely pneumocytes (arrow), in the lung of pig 58 infected with A/raccoon/WA/22 necropsied on 3 dpi. Hematoxylin & eosin stain; original magnification ×40. E) Abundant labeling of respiratory epithelium lining a bronchiole (arrowheads) and within the cytoplasm and nucleus of alveolar macrophages consistent with viral replication (notched arrow) in the lung of pig 78 infected with A/redfox/MI/22 necropsied on 3 dpi. Hematoxylin & eosin stain; original magnification ×100.

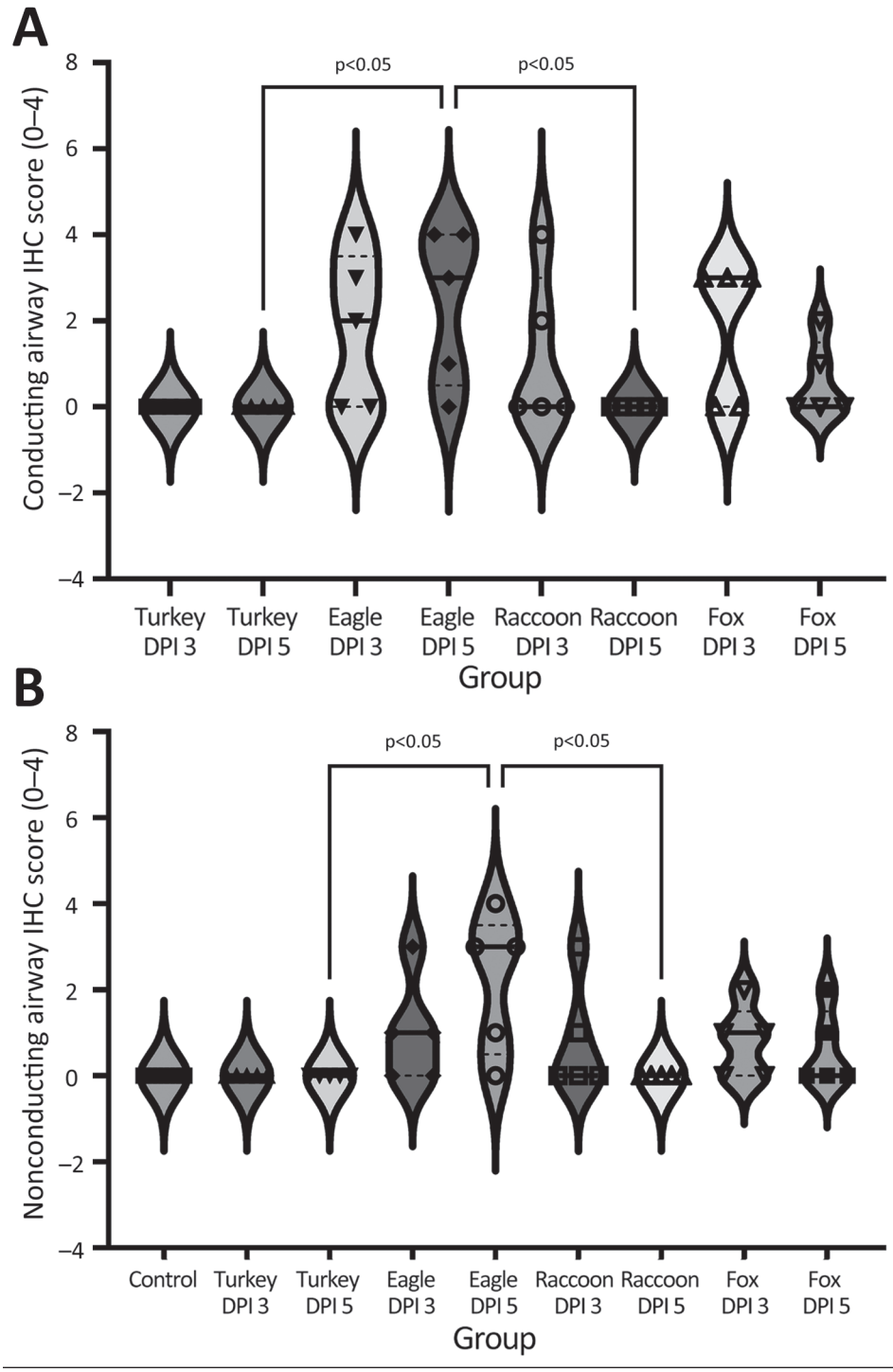

Figure 8. Violin plots of airway conducting IHC scores, by virus strain and dpi, of swine infected with highly pathogenic avian influenza A(H5N1) virus belonging to the goose/Guangdong 2.3.4.4b hemagglutinin phylogenetic clade. A) Lung conducting airway immunohistochemical scores. Influenza A virus (IAV) nucleoprotein (NP) antigen detection varied by group with the most extensive labeling (the number of positive pigs) being observed in the A/bald eagle/FL/22 and A/red fox/MI/22 groups. B) Lung nonconducting airway immunohistochemical scores. IAV NP antigen detection varied by group with the most extensive labeling being observed in the A/bald eagle/FL/22. Solid lines within plots indicate medians, dashed lines indicate quartiles, and symbols indicate individual pig values. dpi, days postinoculation; eagle 3 dpi, A/bald eagle/FL/22 necropsied at 3 dpi; eagle 5 dpi, A/bald eagle/FL/22 necropsied at 5 dpi; fox 3 dpi, A/redfox/MI/22 necropsied at 3 dpi; fox 5 dpi, A/redfox/MI/22 necropsied at 5 dpi; IHC, immunohistochemistry; raccoon 3 dpi, A/raccoon/WA/22 necropsied at 3 dpi; raccoon 5 dpi, A/raccoon/WA/22 necropsied at 5 dpi; turkey 3 dpi, A/turkey/MN/22 necropsied at 3 dpi; turkey 5 dpi, A/turkey/MN/22 necropsied at 5 dpi.

(Appendix 2). We also detected Polymorphisms at low levels in the A/bald eagle/FL/22 and A/turkey/MN/22 HA gene at position 239 (R239H and R239C). We also detected HA mutations associated with receptor binding affinity at low levels in single samples in A/redfox/MI/22 (S110N, P139L, L513S) and A/raccoon/WA/22 (S110N, M404V, E267K).

We calculated synonymous (π_S) and nonsynonymous (π_N) polymorphisms to assess selection; we considered π_N/π_S <1 suggestive of purifying selection and π_N/π_S >1 suggestive of positive selection. When we combined the diversity estimates across genes, all strains exhibited π_N/π_S <1 (A/turkey/MN/22 π_N/π_S = 0.36; A/bald eagle/FL/22 π_N/π_S = 0.40; A/redfox/

MI/22 π_N/π_S = 0.50; A/raccoon/WA/22 π_N/π_S = 0.74), suggesting that the within-host populations tended to exhibit weak purifying selection.

Discussion

We conducted a pathogenesis and transmission study to understand the susceptibility of swine to 3 genotypes of HPAI H5N1 belonging to the goose/Guangdong 2.3.4.4b HA phylogenetic clade detected within the United States. Our data demonstrated that pigs are susceptible to infection. All 4 HPAI isolates that were evaluated replicated in the lungs of pigs. In comparison to an H1N1 swine-adapted virus, the qRT-PCR Ct values in BALF of the 4 HPAI strains were lower (≈3–8 Ct), except for the A/bald eagle/FL/22 (genotype B1.1) 5 dpi group (Appendix 1 Table 3) (*24*). Replication in the nasal cavity and transmission occurred only in the A/raccoon/WA/22 (genotype B2.1) and A/redfox/MI/22 (genotype B3.2) groups containing the mammalian adaptation mutation E627K in the PB2 gene. However, the number of pigs with qRT-PCR–positive nasal swabs was considerably lower than for the swine-adapted virus; the approximate viral load was lower (≈4–6 Ct), and detection was later (1 dpi vs. 5 or 7 dpi) (Appendix 1 Table 4) (*24*). Pig 61 (relatively early detection) might have infected inoculated cohorts, and transmission to contacts at later points not captured in our study design might have occurred. The finding of replication of HPAI H5NX clade 2.3.4.4x in the lung of pigs in an experimental model has been shown, but demonstrating replication in the nasal cavity and transmission to contact pigs is novel (*25*,*26*). In addition, a recent study deemed pigs to be highly resistant to clade 2.3.4.4b infection, illustrating the need for continued assessment of genetically diverse viruses with variable phenotypes in pigs (*27*).

The effects of HPAI viruses can range from asymptomatic infections to severe disease in mammals (*28*–*31*). Multiple viral proteins contribute to the pathogenicity and transmissibility of HPAI, and a combination of adaptive mutations and reassortment are likely necessary for efficient mammal transmission (*32*). Both mammal isolates evaluated in this study contained the PB2 E627K mutation, were detected in the noses of inoculated pigs, and transmitted to ≥1 contact pig. The PB2 gene of all human seasonal viruses of the 20th century contain K627, whereas most clade 2.3.4.4b viruses detected in birds in 2022–2023 contain E627, supporting the role of that mutation in mammalian adaptation (*1*,*17*). Although we did not fully evaluate the direct effects of the E627K mutation in swine, the shedding and transmission profile shown for the 2 mammal isolates in this study indicate this adaptive mutation might have increased viral fitness through enhanced polymerase activity to enable transmission in an otherwise less susceptible host.

Whether different internal gene constellations or other genotypic differences between A/bald eagle/FL/22 (North American PB2, PB1, and NP) and A/turkey/MN/22 (North American PB2 and NP; genotype 2.1) are responsible for the pathogenic differences of those isolates in pigs is unknown. The number of North American gene segments in reassorted HPAI H5N1 clade 2.3.4.4b avian isolates and disease severity in mammals was suggested to have a positive correlation in ferret and mice models (*11*). Although we did not observe evidence of shedding or transmission, both avian isolates replicated in the lung, which is concerning because of potential reassortment with endemic swine viruses.

Viral populations were dominated by low-frequency (<5%) variation that appeared to be shaped by purifying selection. We detected a subset of mutations associated with human receptor binding and specificity (HA S110N, P139L, R239C/H, E267K, L513S) and mammalian replication (PB2 E627K). However, the detected mutations remained at low frequency, and those present early were not transmitted, did not persist, and were not consistently detected across animals. Those data are in accordance with previous studies documenting within-host evolution of H5N1 in poultry (*33*–*35*). Consequently, though adaptive mutations might occur during H5N1 infection in pigs, because of the short infection time and presence of purifying selection (π_N/π_S <1), the evolutionary potential of the strains in this study appears

Table 2. Replication and transmission data in study of divergent pathogenesis and transmission of highly pathogenic avian influenza A(H5N1) in swine*

	Inoculated pigs				Contact pigs	
Strain	NS PCR-positive	BALF PCR-positive, 3 dpi	BALF PCR-positive, 5 dpi	Seroconversion	NS PCR-positive	Seroconversion
A/turkey/MN/22	0/15	3/5	3/5	2/5	0/5	0/5
A/bald eagle/FL/22	0/15	5/5	5/5	3/5	0/5	0/5
A/raccoon/WA/22	4/15	4/5	5/5	5/5	2/5	1/5
A/red fox/MI/22	5/15	5/5	4/5	5/5	0/5	1/5

*Nasal swab samples were taken on 0, 1, 3, 5, and 7 dpi or dpc. BALF was collected at 3 and 5 dpi. Influenza A virus qRT-PCR. Seroconversion results of inoculated pigs are only on surviving pigs at ≈2 weeks dpi or dpc. BALF, bronchoalveolar lavage fluid; dpc, days postcontact; dpi, days postinoculation; NS, nasal swab; qRT-PCR, quantitative reverse transcription PCR.

limited, and the functional effects for the documented mutations require additional study.

The HA proteins of HPAI H5N1 2.3.4.4b virus preferentially bind to α2,3-linked sialic acids on the host cell (*11*), which are at low abundance in the porcine upper respiratory system (*32*). The low abundance of α2,3-linked sialic acids on epithelial cells in the pigs' nasal cavities might explain why HPAI avian isolates did not transmit. The quantity of α2,3-linked sialic acids is relatively higher in the lungs of pigs and humans and localized to pneumocytes and nonciliated bronchiolar cells (*36*–*39*). That distribution is consistent with the extent and distribution of IHC IAV NP labeling in the lung of pigs inoculated with A/bald eagle/FL/22; we noted prominent alveolitis in those pigs, in contrast to those inoculated with either A/raccoon/WA/22 or A/redfox/MI/22.

Table 3. Ct values for nasal swab samples tested for influenza A virus by qRT-PCR by pig and days postinoculation for A/raccoon/WA/22 and A/redfox/MI/22 strains

	Days postinoculation or postcontact				
Pig ID	0	1	3	5	7
A/raccoon/WA/22					
56	ND	ND	ND	NA	NA
57	ND	ND	ND	NA	NA
58	ND	ND	ND	NA	NA
59	ND	ND	ND	NA	NA
60	ND	ND	ND	NA	NA
61	ND	33.0	34.7	33.2	NA
62	ND	ND	ND	ND	NA
63	ND	ND	ND	38.8	NA
64	ND	ND	ND	ND	NA
65	ND	ND	ND	32.1	NA
66	ND	ND	ND	ND	ND
67	ND	ND	ND	ND	29.5
68	ND	ND	ND	ND	ND
69	ND	36.5	ND	36.9	35.1
70	ND	ND	ND	ND	ND
71	ND	ND	ND	ND	38.1
72	ND	ND	ND	ND	32.5
73	ND	ND	ND	ND	35.0
74	ND	ND	ND	ND	ND
75	ND	ND	ND	ND	ND
A/redfox/MI/22					
76	ND	ND	ND	NA	NA
77	ND	ND	ND	NA	NA
78	ND	ND	ND	NA	NA
79	ND	ND	ND	NA	NA
80	ND	ND	ND	NA	NA
81	ND	ND	ND	ND	NA
82	ND	ND	ND	ND	NA
83	ND	ND	ND	ND	NA
84	ND	ND	ND	ND	NA
85	ND	ND	34.8	ND	NA
86	ND	ND	28.1	39.2	37.1
87	ND	ND	ND	ND	37.9
88	ND	ND	ND	36.0	ND
89	ND	ND	ND	35.4	ND
90	ND	ND	ND	38.9	ND
91	ND	ND	ND	ND	ND
92	ND	ND	ND	ND	ND
93	ND	ND	ND	ND	ND
94	ND	ND	ND	ND	ND
95	ND	ND	ND	ND	ND

*Ct value of <38.0 indicates a positive sample, 38–40 indicates suspect sample, and ND indicates negative sample. Pigs numbered 71–75 and 91–95 are contact pigs. Ct, cycle threshold; ID, identification; NA, not available (pig previously euthanized as part of study design); ND, not detected; qRT-PCR, quantitative reverse transcription PCR.

Interspecies spillovers commonly result in dead-end infections because the virus likely requires multiple transmission events to acquire the necessary adaptive mutations (*40*). The probability of a virus acquiring a complete set of adaptive mutations in a single immunocompetent host with onward transmission is extremely low (*34*). However, continued circulation of HPAI strains that have already adapted within various mammalian species makes that possibility more likely (*1*,*34*). On-farm transmission among pigs in Indonesia of an HPAI H5N1 and identification of a purified clone with the ability to recognize α2,6 sialic acid receptors were reported (*3*). More recently, serologic evidence of infection of domestic pigs with clade 2.3.4.4b was reported (*41*). In addition, because reassortment occurred with the past 4 influenza pandemics, the propensity for reassortment in swine may increase the risk for H5N1 adaptation toward humans, particularly with the maintenance of 2009 pandemic H1N1 human seasonal virus genes in pigs (*42*). Although infrequent, incursion of LPAI into commercial swine herds in North America occurs periodically, yet the sources of incursion often remain unknown (*43*–*45*). Increased viral fitness characterized by transmission of LPAI strains after reassortment with swine-adapted IAV in pigs was demonstrated both in commercial swine herds and experimentally (*43*,*46*).

The genetic attributes that resulted in the continued circulation of the HPAI H5N1 2.3.4.4b lineage are not well understood. Repeated spillover and spillback events resulted in genotypically and phenotypically diverse reassortant viruses, some of which caused neurologic disease in mammals, a manifestation not observed in pigs (*47*). However, detection of NP antigen in endothelial cells of pigs infected with A/bald eagle/FL/22 suggests this strain might spread systemically.

The risk for reassortment of the HPAI H5N1 2.3.4.4b lineage with endemic swine IAV is a consideration on the basis of the susceptibility to this lineage demonstrated in our study, the prevalence of IAV infection and comorbidities in swine herds, and animal husbandry practices (*48*,*49*). However, the risk for incursion is likely lower in confinement operations with industry standard biosecurity than for backyard or feral pigs. Birdproofing feed and facilities, avoiding the use of untreated water, and restricting peridomestic scavenger mammals from premises are measures to increase biosecurity against HPAI H5N1 clade 2.3.4.4b virus incursion into swine herds.

Acknowledgments

We thank Nicholas Otis for his technical assistance; Randy Leon, Adam Hartfiel, Alyssa Dannen, Justin Miller, Jason Huegel, Derek Vermeer, Rebecca Cox, Kolby Stallman, and Jonathan Gardner for assistance with animal care and sample collection; and Judith Stasko and Adrienne Shircliff for preparation of histologic sections. We also gratefully acknowledge all data contributors (i.e., the authors and their originating laboratories responsible for obtaining the specimens, and their submitting laboratories for generating the genetic sequence and metadata and sharing via the GISAID Initiative [https://www.gisaid.org], on which components of this research is based). In addition, we are grateful to colleagues at the USDA ARS Southeast Poultry Research Laboratory for their contribution of the H5 2.3.4.4 assay.

This project was funded in part with Federal funds from the National Institute of Allergy and Infectious Diseases, National Institutes of Health, Department of Health and Human Services (contract no. 75N93021C00015) and the U.S. Department of Agriculture (USDA) Agricultural Research Service (contract no. 5030-32000-231-000-D). Mention of trade names or commercial products in this article is solely for the purpose of providing specific information and does not imply recommendation or endorsement by the NIH or USDA. Funding sources had no role in experimental design, data collection/analysis/interpretation, preparation of the manuscript, or decision to publish. USDA is an equal opportunity provider and employer.

About the Author

Dr. Arruda is a research veterinary medical officer and veterinary pathologist at the National Animal Disease Center. Her research focuses on intervention strategies to prevent and respond to influenza A virus infections in swine.

References

1. Long JS, Mistry B, Haslam SM, Barclay WS. Host and viral determinants of influenza A virus species specificity. Nat Rev Microbiol. 2019;17:67–81. https://doi.org/10.1038/s41579-018-0115-z
2. Belser JA, Tumpey TM. H5N1 pathogenesis studies in mammalian models. Virus Res. 2013;178:168–85. https://doi.org/10.1016/j.virusres.2013.02.003
3. Nidom CA, Takano R, Yamada S, Sakai-Tagawa Y, Daulay S, Aswadi D, et al. Influenza A (H5N1) viruses from pigs, Indonesia. Emerg Infect Dis. 2010;16:1515–23. https://doi.org/10.3201/eid1610.100508
4. Centers for Disease Control and Prevention. Technical report: highly pathogenic avian influenza A(H5N1) viruses [cited 2023 Mar 24]. https://www.cdc.gov/flu/avianflu/spotlights/2022-2023/h5n1-technical-report.htm#human-cases
5. Animal and Plant Health Inspection Office. 2022–2024 detections of highly pathogenic avian influenza in mammals [cited 2023 Dec 15]. https://www.aphis.usda.gov/aphis/ourfocus/animalhealth/animal-disease-information/avian/avian-influenza/hpai-2022/2022-hpai-mammals
6. Animal and Plant Health Inspection Office. 2022–20243 confirmations of highly pathogenic avian influenza in commercial and backyard flocks [cited 2023 Mar 24]. https://www.aphis.usda.gov/aphis/ourfocus/animalhealth/animal-disease-information/avian/avian-influenza/hpai-2022/2022-hpai-commercial-backyard-flocks
7. Lee DH, Criado MF, Swayne DE. Pathobiological origins and evolutionary history of highly pathogenic avian influenza viruses. Cold Spring Harb Perspect Med. 2021;11:a038679. https://doi.org/10.1101/cshperspect.a038679
8. Lee DH, Bertran K, Kwon JH, Swayne DE. Evolution, global spread, and pathogenicity of highly pathogenic avian influenza H5Nx clade 2.3.4.4. J Vet Sci. 2017;18(S1):269–80. https://doi.org/10.4142/jvs.2017.18.S1.269
9. Pohlmann A, King J, Fusaro A, Zecchin B, Banyard AC, Brown IH, et al. Has epizootic become enzootic? Evidence for a fundamental change in the infection dynamics of highly pathogenic avian influenza in Europe, 2021. MBio. 2022;13:e0060922. https://doi.org/10.1128/mbio.00609-22
10. Bevins SN, Shriner SA, Cumbee JC Jr, Dilione KE, Douglass KE, Ellis JW, et al. Intercontinental movement of highly pathogenic avian influenza A(H5N1) clade 2.3.4.4 virus to the United States, 2021. Emerg Infect Dis. 2022;28:1006–11. https://doi.org/10.3201/eid2805.220318
11. Kandeil A, Patton C, Jones JC, Jeevan T, Harrington WN, Trifkovic S, et al. Rapid evolution of A(H5N1) influenza viruses after intercontinental spread to North America. Nat Commun. 2023;14:3082. https://doi.org/10.1038/s41467-023-38415-7
12. Youk S, Torchetti MK, Lantz K, Lenoch JB, Killian ML, Leyson C, et al. H5N1 highly pathogenic avian influenza clade 2.3.4.4b in wild and domestic birds: introductions into the United States and reassortments, December 2021–April 2022. Virology. 2023;587:109860.
13. Sun H, Pu J, Wei Y, Sun Y, Hu J, Liu L, et al. Highly pathogenic avian influenza H5N6 viruses exhibit enhanced affinity for human type sialic acid receptor and in-contact transmission in model ferrets. J Virol. 2016;90:6235–43. https://doi.org/10.1128/JVI.00127-16
14. Yamaji R, Saad MD, Davis CT, Swayne DE, Wang D, Wong FYK, et al. Pandemic potential of highly pathogenic avian influenza clade 2.3.4.4 A(H5) viruses. Rev Med Virol. 2020;30:e2099. https://doi.org/10.1002/rmv.2099
15. Pulit-Penaloza JA, Brock N, Pappas C, Sun X, Belser JA, Zeng H, et al. Characterization of highly pathogenic avian influenza H5Nx viruses in the ferret model. Sci Rep. 2020;10:12700. https://doi.org/10.1038/s41598-020-69535-5
16. Zhao Z, Guo Z, Zhang C, Liu L, Chen L, Zhang C, et al. Avian influenza H5N6 viruses exhibit differing pathogenicities and transmissibilities in mammals. Sci Rep. 2017;7:16280. https://doi.org/10.1038/s41598-017-16139-1
17. Adlhoch C, Fusaro A, Gonzales JL, Kuiken T, Marangon S, Mirinaviciute G, et al.; European Food Safety Authority; European Centre for Disease Prevention and Control; European Union Reference Laboratory for Avian Influenza. Avian influenza overview December 2022–March 2023. EFSA J. 2023;21:e07917.
18. Centers for Disease Control and Prevention. Human infection with highly pathogenic avian influenza A(H5N1) virus in Chile [cited 2023 May 2]. https://www.cdc.gov/flu/avianflu/spotlights/2022-2023/chile-first-case-h5n1-addendum.htm

19. Vincent AL, Lager KM, Ma W, Lekcharoensuk P, Gramer MR, Loiacono C, et al. Evaluation of hemagglutinin subtype 1 swine influenza viruses from the United States. Vet Microbiol. 2006;118:212–22. https://doi.org/10.1016/j.vetmic.2006.07.017
20. Youk S, Torchetti MK, Lantz K, Lenoch JB, Killian ML, Leyson C, et al. H5N1 highly pathogenic avian influenza clade 2.3.4.4b in wild and domestic birds: introductions into the United States and reassortments, December 2021–April 2022. Virology. 2023;587:109860. https://doi.org/10.1016/j.virol.2023.109860
21. Zhang Y, Aevermann BD, Anderson TK, Burke DF, Dauphin G, Gu Z, et al. Influenza Research Database: an integrated bioinformatics resource for influenza virus research. Nucleic Acids Res. 2017;45(D1):D466–74. https://doi.org/10.1093/nar/gkw857
22. Nelson CW, Moncla LH, Hughes AL. SNPGenie: estimating evolutionary parameters to detect natural selection using pooled next-generation sequencing data. Bioinformatics. 2015;31:3709–11. https://doi.org/10.1093/bioinformatics/btv449
23. Gauger PC, Vincent AL, Loving CL, Henningson JN, Lager KM, Janke BH, et al. Kinetics of lung lesion development and pro-inflammatory cytokine response in pigs with vaccine-associated enhanced respiratory disease induced by challenge with pandemic (2009) A/H1N1 influenza virus. Vet Pathol. 2012;49:900–12. https://doi.org/10.1177/0300985812439724
24. Arruda BL, Kanefsky RA, Hau S, Janzen GM, Anderson TK, Vincent Baker AL. Mucin 4 is a cellular biomarker of necrotizing bronchiolitis in influenza A virus infection. Microbes Infect. 2023;25:105169. https://doi.org/10.1016/j.micinf.2023.105169
25. Lipatov AS, Kwon YK, Sarmento LV, Lager KM, Spackman E, Suarez DL, et al. Domestic pigs have low susceptibility to H5N1 highly pathogenic avian influenza viruses. PLoS Pathog. 2008;4:e1000102. https://doi.org/10.1371/journal.ppat.1000102
26. Kaplan BS, Torchetti MK, Lager KM, Webby RJ, Vincent AL. Absence of clinical disease and contact transmission of HPAI H5NX clade 2.3.4.4 from North America in experimentally infected pigs. Influenza Other Respir Viruses. 2017;11:464–70. https://doi.org/10.1111/irv.12463
27. Graaf A, Piesche R, Sehl-Ewert J, Grund C, Pohlmann A, Beer M, et al. Low susceptibility of pigs against experimental infection with HPAI virus H5N1 clade 2.3.4.4b. Emerg Infect Dis. 2023;29:1492–5. https://doi.org/10.3201/eid2907.230296
28. Shin DL, Siebert U, Lakemeyer J, Grilo M, Pawliczka I, Wu NH, et al. Highly pathogenic avian influenza A(H5N8) virus in gray seals, Baltic Sea. Emerg Infect Dis. 2019;25:2295–8. https://doi.org/10.3201/eid2512.181472
29. Floyd T, Banyard AC, Lean FZX, Byrne AMP, Fullick E, Whittard E, et al. Encephalitis and death in wild mammals at a rehabilitation center after infection with highly pathogenic avian influenza A(H5N8) virus, United Kingdom. Emerg Infect Dis. 2021;27:2856–63. https://doi.org/10.3201/eid2711.211225
30. Postel A, King J, Kaiser FK, Kennedy J, Lombardo MS, Reineking W, et al. Infections with highly pathogenic avian influenza A virus (HPAIV) H5N8 in harbor seals at the German North Sea coast, 2021. Emerg Microbes Infect. 2022;11:725–9. https://doi.org/10.1080/22221751.2022.2043726
31. Rijks JM, Hesselink H, Lollinga P, Wesselman R, Prins P, Weesendorp E, et al. Highly pathogenic avian influenza A(H5N1) virus in wild red foxes, the Netherlands, 2021. Emerg Infect Dis. 2021;27:2960–2. https://doi.org/10.3201/eid2711.211281
32. Neumann G. H5N1 influenza virulence, pathogenicity and transmissibility: what do we know? Future Virol. 2015;10:971–80. https://doi.org/10.2217/fvl.15.62
33. Moncla LH, Bedford T, Dussart P, Horm SV, Rith S, Buchy P, et al. Quantifying within-host diversity of H5N1 influenza viruses in humans and poultry in Cambodia. PLoS Pathog. 2020;16:e1008191. https://doi.org/10.1371/journal.ppat.1008191
34. Russell CA, Fonville JM, Brown AE, Burke DF, Smith DL, James SL, et al. The potential for respiratory droplet-transmissible A/H5N1 influenza virus to evolve in a mammalian host. Science. 2012;336:1541–7. https://doi.org/10.1126/science.1222526
35. Bordes L, Vreman S, Heutink R, Roose M, Venema S, Pritz-Verschuren SBE, et al. Highly pathogenic avian influenza H5N1 virus infections in wild red foxes (Vulpes vulpes) show neurotropism and adaptive virus mutations. Microbiol Spectr. 2023;11:e0286722. https://doi.org/10.1128/spectrum.02867-22
36. Baum LG, Paulson JC. Sialyloligosaccharides of the respiratory epithelium in the selection of human influenza virus receptor specificity. Acta Histochem Suppl. 1990;40:35–8.
37. Nicholls JM, Chan MC, Chan WY, Wong HK, Cheung CY, Kwong DL, et al. Tropism of avian influenza A (H5N1) in the upper and lower respiratory tract. Nat Med. 2007;13:147–9. https://doi.org/10.1038/nm1529
38. Shinya K, Ebina M, Yamada S, Ono M, Kasai N, Kawaoka Y. Avian flu: influenza virus receptors in the human airway. Nature. 2006;440:435–6. https://doi.org/10.1038/440435a
39. Yao L, Korteweg C, Hsueh W, Gu J. Avian influenza receptor expression in H5N1-infected and noninfected human tissues. FASEB J. 2008;22:733–40. https://doi.org/10.1096/fj.06-7880com
40. Illingworth CJ. Fitness inference from short-read data: within-host evolution of a reassortant H5N1 influenza virus. Mol Biol Evol. 2015;32:3012–26. https://doi.org/10.1093/molbev/msv171
41. Rosone F, Bonfante F, Sala MG, Maniero S, Cersini A, Ricci I, et al. Seroconversion of a swine herd in a free-range rural multi-species farm against HPAI H5N1 2.3.4.4b clade virus. Microorganisms. 2023;11:1162. https://doi.org/10.3390/microorganisms11051162
42. Neumann G, Green MA, Macken CA. Evolution of highly pathogenic avian H5N1 influenza viruses and the emergence of dominant variants. J Gen Virol. 2010;91:1984–95. https://doi.org/10.1099/vir.0.020750-0
43. Ma W, Vincent AL, Gramer MR, Brockwell CB, Lager KM, Janke BH, et al. Identification of H2N3 influenza A viruses from swine in the United States. Proc Natl Acad Sci U S A. 2007;104:20949–54. https://doi.org/10.1073/pnas.0710286104
44. Karasin AI, Brown IH, Carman S, Olsen CW. Isolation and characterization of H4N6 avian influenza viruses from pigs with pneumonia in Canada. J Virol. 2000;74:9322–7. https://doi.org/10.1128/JVI.74.19.9322-9327.2000
45. Karasin AI, West K, Carman S, Olsen CW. Characterization of avian H3N3 and H1N1 influenza A viruses isolated from pigs in Canada. J Clin Microbiol. 2004;42:4349–54. https://doi.org/10.1128/JCM.42.9.4349-4354.2004
46. Abente EJ, Kitikoon P, Lager KM, Gauger PC, Anderson TK, Vincent AL. A highly pathogenic avian-derived influenza

virus H5N1 with 2009 pandemic H1N1 internal genes demonstrates increased replication and transmission in pigs. J Gen Virol. 2017;98:18–30. https://doi.org/10.1099/jgv.0.000678
47. Kandeil A, Patton C, Jones J, Jeevan T, Harrington W, Trifkovic S, et al. Rapid evolution of A(H5N1) influenza viruses after intercontinental spread to North America. Nat Commun. 2023;14:3082.
48. Zeller MA, Anderson TK, Walia RW, Vincent AL, Gauger PC. ISU FLUture: a veterinary diagnostic laboratory web-based platform to monitor the temporal genetic patterns of Influenza A virus in swine. BMC Bioinformatics. 2018;19:397. https://doi.org/10.1186/s12859-018-2408-7
49. Trevisan G, Schwartz KJ, Burrough ER, Arruda B, Derscheid RJ, Rahe MC, et al. Visualization and application of disease diagnosis codes for population health management using porcine diseases as a model. J Vet Diagn Invest. 2021;33:428–38.

Address for correspondence: Bailey Arruda, USDA National Animal Disease Center, 1920 Dayton Ave, Ames, IA 50010, USA; email: bailey.arruda@usda.gov

Alfred Whitmore and the Discovery of Melioidosis

Jelmer Savelkoel, David A.B. Dance

We review the discovery of the tropical infectious disease melioidosis by Alfred Whitmore, a pathologist from England, and his assistant from India, C.S. Krishnaswami. We discuss how the subsequent disappearance of melioidosis from the medical literature of Burma holds parallels with the current neglect and under recognition of the disease. We urge global and national public health authorities to add melioidosis to existing neglected tropical diseases surveillance systems.

"We have, and always will have, need of both Science and Art in medical practice; they are not antagonistic principles, but are mutually helpful; there is room, enough and to spare, for the free and energetic use of both; it is ignorance alone which sees them hostile, folly indeed which seeks their division." So wrote Alfred Whitmore in 1914 (*1*). Whitmore was a remarkable man, not only in advocating what seems like a modern integration between laboratory and clinical work more than 100 years ago (*1*) but also in achieving eponymous immortality by describing a novel disease (*2*). He did this without specialist training and while working in relative isolation in his role as pathologist in Rangoon General Hospital (RGH), Burma (now Myanmar), in 1911 (*2*,*3*). Yet the way in which his findings were initially fêted and subsequently forgotten holds strong parallels with the present day under recognition and ignorance of both Whitmore and the disease he described.

The disease discovered by Whitmore and his assistant, C.S. Krishnaswami, is now known as melioidosis but is still often referred to as Whitmore's disease (*2*,*4*). The name melioidosis was only later coined by A.T. Stanton and W. Fletcher in 1921 and is derived from a Greek word meaning glanders-like disease (*5*,*6*). Over the past few years, and captivated by Whitmore's wonderful prose style, one of us has been researching his life and work (*7*–*9*). In this review, and the accompanying video, we summarize some of our more recent findings about Whitmore's career. We discuss what happened to his discovery in the years after he made it, and how that relates to melioidosis today. The information included in this review is based on the references provided and documents kindly provided by the Whitmore family.

Whitmore was born in Botcherby, in northwest England, in 1876 and grew up in Sebergham in Cumbria, where his father was rector (*10*). Among his early hobbies, Whitmore studied the process of decay of animal carcasses, which might have presaged his later career. He attended St. Bees School in Cumbria, studied medicine at Gonville and Caius College at Cambridge University, and completed his medical training at St. Mary's Hospital in London, receiving scholarships and prizes along the way (*10*). After qualifying as a doctor, he completed the Diploma in Public Health that was obligatory for entrants into the Indian Medical Service (IMS) and was commissioned as a lieutenant in January 1903 (Figure 1) (*10*,*11*). His posting to the less fashionable center of Burma might have been influenced by his finishing last in the Diploma in Public Health exam. In later life he commented, "I entered the Service with no particular ambition, chiefly perhaps because I had no money—a bad reason." His mandatory 2 years of military service were spent in India and the Andaman Islands before he arrived in Rangoon, Burma, toward the end of 1905 (*10*), little expecting that he would shortly unearth a novel infectious disease.

In the old, wooden RGH, Whitmore's initial responsibility was taking care of the dying patients on the "moribund ward," without the aid of nurses and with hygiene that left much to be desired. He even mentioned rumors of patients' feet being gnawed off by rats in a letter written to his son in January 1946, although adding that he could not "aver the truth

Author affiliations: Amsterdam UMC location University of Amsterdam, Amsterdam, the Netherlands (J. Savelkoel); Lao-Oxford-Mahosot Hospital–Wellcome Trust Research Unit, Mahosot Hospital, Vientiane, Laos (D.A.B. Dance); University of Oxford, Oxford, UK (D.A.B. Dance); London School of Hygiene & Tropical Medicine, London, UK (D.A.B. Dance)

DOI: https://doi.org/10.3201/eid3004.230693

Figure 1. Alfred Whitmore wearing his Indian Medical Service uniform, circa 1903.

of this." He thought the care that was provided was undignified for any human being. Thus, he tried to improve the lot of his patients by providing alcohol, which he described as the "best med of any that I have used," as well as cheroots (a local type of cigar) and a wheeled bath that he later found being used as a fish tank. However, his role was about to change because plans were underway to build a new hospital, albeit without a laboratory (*12*). That plan was contrary to Alfred's ideas. In a talk given in Cambridge following his return to England, he said he was "… trained to believe that there was a 'Science' as well as an 'Art' of Medicine and that the laboratory was the High Altar, as it were, of that Science." He convinced the authorities of the necessity of a laboratory, which was duly added, with Whitmore taking on the role of pathologist on condition that he would also undertake the medicolegal work in the capacity of police surgeon. He remained a passionate advocate for the integration of a laboratory within the hospital, believing that close collaboration between the clinic and laboratory were essential to good quality "Western medicine" (*1*).

Whitmore worked as pathologist and police surgeon at RGH from 1909 until 1915, during which he discovered melioidosis (*10*). Melioidosis, caused by the gram-negative bacterium *Burkholderia pseudomallei*, is now known as a disease that typically has clinical manifestations of pneumonia, sepsis, and abscess formation, predominantly in persons with underlying risk factors, details of which can be found elsewhere (*13*).

In 1911, Whitmore and Krishnaswami, who had graduated as a licentiate in medicine and surgery from Madras Medical College (*14*), undertook a postmortem examination that revealed "…a peculiar consolidation of the lungs," which they felt was consistent with glanders, a zoonotic disease of horses (*2*). The victim, however, had no history of recent animal exposure, and cultures yielded a bacterium that they recognized as different from what was then known as *Bacillus mallei* (now *Burkholderia mallei*), the cause of glanders, in its rapid luxuriant growth and motility. In 1912, they published, in the Indian Medical Gazette, their microbiological and pathological findings from 38 cases of this recently discovered disease (*2*). A more comprehensive report in the subsequent year, in which Whitmore first proposed the specific epithet pseudomallei, included additional information about each case, 31 of which were "morphine injectors" (*15*). By 1914 the term morphia injectors' septicaemia had been suggested for the disease name (*16*).

Opioid injection is not currently recognized as a risk factor for melioidosis, and the reasons for such a strong association as that reported by Whitmore are unclear (*13*). Whitmore himself initially felt the infection most likely was caused by the general debility associated with morphine injections (*15*) but later appears to have favored contamination of the injections themselves, because 46 of the 52 cases in the 1914 report also bore evidence of morphine injection (*16*). That finding would hardly have been surprising given the squalid conditions in which the drug users of the day were liable to have received their morphine (*17*).

Then along came World War I, and as a member of the IMS, Whitmore was obliged to return to military service in British India (*10*). Meanwhile, Krishnaswami continued to work on the disease until 1917, when he stated he had encountered some 200 cases (*18*), but he subsequently moved to work in what was then known as the "Lunatic Asylum" system for the rest of his career in Burma (*14*,*19*).

Whitmore spent the war at various stations in British India (*10*), frequently having brushes with authority because he did not tolerate fools, especially if they were senior officers issuing edicts from "the hill tops." On returning to Rangoon, although he had hoped to resume his job as pathologist, he was

appointed as a civil surgeon and never worked on melioidosis again (*10*). He found his role as a civil surgeon exhausting, leaving him little time for the reading he considered essential to keep up to date with the latest developments. In 1922, he moved to become superintendent of the Burma Government Medical School, a role in which he remained until he returned to England on leave in 1924, eventually retiring from the IMS in 1927 (*10*,*20*–*22*).

After a brief spell in Paignton, Devon, UK, Whitmore moved to Madingley, near Cambridge, UK, where he remained involved in education and research until his death in 1946 (Figure 2) (*23*). People thought of him as an inspirational lecturer, and his obituary in the British Medical Journal described him as "… a most lovable man with a very keen sense of humour, and all who knew him well were greatly attached to him. He seemed to radiate something buoyant and joyous, and the outlook always seemed brighter when he was about" (*23*).

Whitmore's discovery was initially celebrated by the colonial hierarchy in Burma and was specifically mentioned in the Report on the Administration of Burma for 2 consecutive years (1911–12 and 1912–13) (*24*,*25*). Lengthy debates about the appropriate form of bacteriologic support for the government in Burma had taken place, and some suggested that locating a laboratory in Rangoon would be impossible because of the climate; therefore, the authorities were doubtless keen to celebrate the success of this innovative venture (*12*,*26*). Yet, when World War I intervened, and Whitmore and Krishnaswami subsequently turned their attention to other duties, no one appears to have followed up on their findings: the next mention of melioidosis in Burma was in the 1940s (*27*). At that time, the disease appeared almost exclusively to affect the "friendless wastrels" of Rangoon, primarily persons addicted to morphine, who were unlikely ever to be economically productive and through who, through crime, might be a drain on colonial resources (*15*,*28*). In addition, up to that point, not a single case of melioidosis had been reported in a person of European heritage. Those factors must undoubtedly have been key in the apparent neglect of the disease by the colonial authorities as they struggled to restore order after the disruption of World War I.

Today, melioidosis remains a little-known disease, even within the countries where it is endemic (*29*). Melioidosis endemic regions include northern Australia, many countries in South and Southeast Asia, sub-Saharan Africa, and tropical and subtropical areas of the Americas (*30*,*31*). Melioidosis is not yet formally recognized by the World Health Organization as a neglected tropical disease (NTD), despite the growing evidence that it is widespread throughout the tropics, is estimated to cause nearly 90,000 deaths a year globally, and has a disease burden considerably greater than that of many officially recognized NTDs (*31*–*33*). However, as a disease that mainly affects lower income populations living in rural areas, another marginalized group, melioidosis remains underdiagnosed and excluded from the mandatory surveillance systems of most countries where it is endemic. A 2021 multistate outbreak in the United States from an imported aromatherapy spray and a 2022 report of isolation of *B. pseudomallei* from the environment in Mississippi, USA, for the first time, might have temporarily boosted the profile of melioidosis (*34*,*35*). Perhaps the increased attention resulting from those incidents will benefit the communities that suffer from this deadly disease.

In conclusion, global and national public health authorities should act to add melioidosis to NTD surveillance systems so that we do not again fail to follow the path initially signposted by Whitmore. We need to prevent history from repeating itself and make sure that both melioidosis, and Alfred Whitmore, are no longer forgotten.

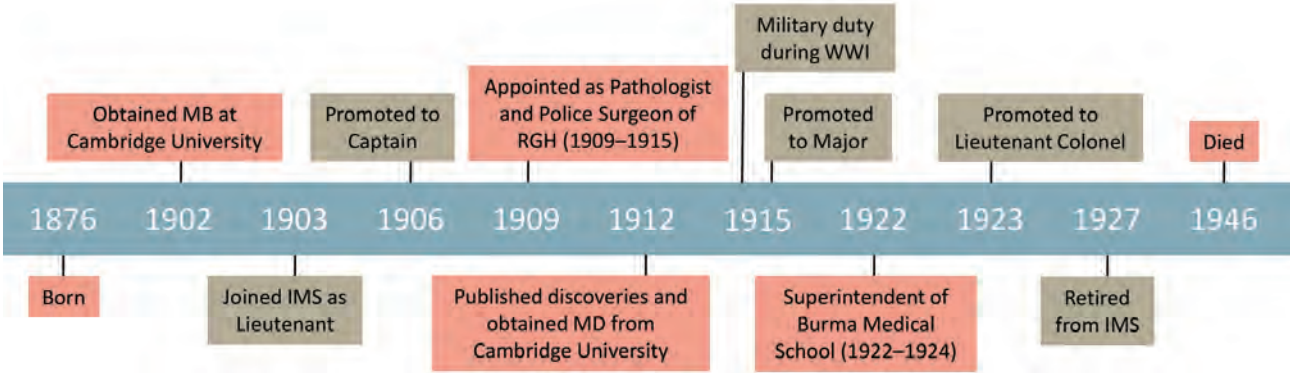

Figure 2. Timeline of the life of Alfred Whitmore and the discovery of melioidosis. The timeline highlights Whitmore's personal and military achievements. IMS, Indian Medical Service; MB, bachelor of medicine degree; RGH, Rangoon General Hospital; WWI, World War I.

Acknowledgments

We are eternally grateful to the Whitmore family, particularly Margaret Davison, Alfred Whitmore's granddaughter, for providing access to their family records; pictures from the Whitmore records used throughout the multimedia article were reproduced with her permission. We also express our gratitude to all national archives for their cooperation, and the International Melioidosis Network for their continued support.

J.S. was funded by an Amsterdam UMC PhD scholarship and a Grassroot Grant of the University of Amsterdam. D.A.B. Dance was funded by the Wellcome Trust for his work on melioidosis during 1986–2019. The funders had no role in the writing of the manuscript or the decision to submit it for publication.

D.A.B. Dance acts as a consultant to InBios International Inc. in relation to the development of diagnostic methods for melioidosis and to MerLion Pharmaceuticals GmbH and Venatorx Pharmaceuticals, Inc. in relation to the development of new therapies for melioidosis.

About the Authors

Mr. Savelkoel is a researcher at the Center for Experimental and Molecular Medicine of Amsterdam UMC, the Netherlands. His research interests include the global distribution and global health aspects of melioidosis. Prof. Dance is a retired medical microbiologist affiliated with the Lao-Oxford-Mahosot Hospital–Wellcome Trust Research Unit, Mahosot Hospital, Vientiane, Laos. He has a longstanding interest in melioidosis, previously worked in Thailand and Laos, and has been researching the life and works of Alfred Whitmore and the discovery of melioidosis.

References

1. Whitmore A. The relationship between laboratory and clinical work. Ind Med Gaz. 1914;49:178–81.
2. Whitmore A, Krishnaswami CS. An account of the discovery of a hitherto undescribed infective disease occurring among the population of Rangoon. Ind Med Gaz. 1912;47:262–7.
3. Whitmore A. On the bacteriology of an infective disease occurring in Rangoon. BMJ. 1912;2:1306–8. https://doi.org/10.1136/bmj.2.2706.1273
4. Naganathan K, Pillai SB, Kumar P, Hegde P. Whitmore's disease: an uncommon urological presentation. BMJ Case Rep. 2014;2014:bcr2013201978. https://doi.org/10.1136/bcr-2013-201978
5. Stanton AT, Fletcher W. Melioidosis, a new disease of the tropics. In: Transactions of the Fourth Congress of the Far Eastern Association of Tropical Medicine, Batavia, 1921. Weltevreden: Javasche Boekhandel en Drukkerij; 1922. p. 196–8.
6. Männikkö N. Etymologia: melioidosis. Emerg Infect Dis. 2011;17:1341. https://doi.org/10.3201/eid1707.ET1707
7. Dance DAB, White NJ. Melioidosis. In: Cox FEG, editor. The Wellcome Trust illustrated history of tropical diseases. London: The Wellcome Trust; 1996. p. 72–81.
8. Dance D. A glanders-like disease in Rangoon: Whitmore A. J Hyg 1913;13:1–34. Epidemiol Infect. 2005;133:S9–10. https://doi.org/10.1017/S095026880500422X
9. Dance DAB. Milestones in the history of melioidosis. In: Ketheesan N, editor. Melioidosis: a century of observation and research. Amsterdam: Elsevier; 2012. p. 10–17.
10. National Archives of India. Personal file of retired Indian Medical Service Officer, A. Whitmore. PR_000002799274, bundle no. 116, S no. 7.
11. Diplomas in public health. J State Med. 1903;11:113.
12. The deficiencies of the Burmah Medical Department. BMJ. 1909;2:574. https://doi.org/10.1136/bmj.2.2539.574
13. Wiersinga WJ, Virk HS, Torres AG, Currie BJ, Peacock SJ, Dance DAB, et al. Melioidosis. Nat Rev Dis Primers. 2018;4:17107. https://doi.org/10.1038/nrdp.2017.107
14. Government of Burma. Report on the lunatic asylums in Burma for the triennium 1915–17. Rangoon: Office of the Superintendent, Government Printing, Burma; 1918.
15. Whitmore A. An account of a glanders-like disease occurring in Rangoon. J Hyg. 1913;13:1–34.
16. Surgery at the Rangoon General Hospital. Ind Med Gaz. 1914;49:201–4.
17. Anderson RK. Morphia. In: Drug smuggling and taking in India and Burma. Calcutta and Simla: Thacker, Spink & Co.; 1922. p. 57–64.
18. Krishnaswami CS. Morphia injector's septicaemia. Ind Med Gaz. 1917;52:296–9.
19. Government of Burma. Report on the lunatic asylums in Burma for the triennium 1921–1923. Rangoon: Superintendent, Government Printing, Burma; 1924.
20. Government of Burma. Annual report on the working of the Burma Government Medical School Rangoon for the year 1921–22. Rangoon: Office of the Superintendent, Government Printing, Burma; 1922.
21. Government of Burma. Annual report on the working of the Burma Government Medical School Rangoon for the year 1924–25. Rangoon: Superintendent, Government Printing and Stationery, Burma; 1925.
22. Naval and Military Appointments. Indian Medical Service. BMJ. 1927;1:S187. https://doi.org/10.1136/bmj.1.3460.S165
23. Obituary: Lieut.-Col. Alfred Whitmore, M.D.Cantab. BMJ. 1946;2:68. https://doi.org/10.1136/bmj.2.4462.67-b
24. Government of Burma. Report on the Administration of Burma for the year 1911–12. Rangoon: Office of the Superintendent, Government Printing, Burma; 1913.
25. Government of Burma. Report on the Administration of Burma for the year 1912–13. Rangoon: Office of the Superintendent, Government Printing, Burma; 1914.
26. Research in tropical diseases in India. Ind Med Gaz. 1905;40:307–8.
27. Win MM, Ashley EA, Zin KN, Aung MT, Swe MMM, Ling CL, et al. Melioidosis in Myanmar. Trop Med Infect Dis. 2018;3:28. https://doi.org/10.3390/tropicalmed3010028
28. Castor RH. Drugs and drug habits in Burma. Ind Med Gaz. 1911;46:209–10.
29. Chansrichavala P, Wongsuwan N, Suddee S, Malasit M, Hongsuwan M, Wannapinij P, et al. Public awareness of melioidosis in Thailand and potential use of video clips as educational tools. PLoS One. 2015;10:e0121311. https://doi.org/10.1371/journal.pone.0121311
30. Currie BJ, Meumann EM, Kaestli M. The expanding global footprint of *Burkholderia pseudomallei* and melioidosis. Am J Trop Med Hyg. 2023;108:1081–3. https://doi.org/10.4269/ajtmh.23-0223

31. Limmathurotsakul D, Golding N, Dance DAB, Messina JP, Pigott DM, Moyes CL, et al. Predicted global distribution of *Burkholderia pseudomallei* and burden of melioidosis. Nat Microbiol. 2016;1:15008. https://doi.org/10.1038/nmicrobiol.2015.8
32. Birnie E, Virk HS, Savelkoel J, Spijker R, Bertherat E, Dance DAB, et al. Global burden of melioidosis in 2015: a systematic review and data synthesis. Lancet Infect Dis. 2019;19:892–902. https://doi.org/10.1016/S1473-3099(19)30157-4
33. Savelkoel J, Dance DAB, Currie BJ, Limmathurotsakul D, Wiersinga WJ. A call to action: time to recognise melioidosis as a neglected tropical disease. Lancet Infect Dis. 2022;22:e176–82. https://doi.org/10.1016/S1473-3099(21)00394-7
34. Gee JE, Bower WA, Kunkel A, Petras J, Gettings J, Bye M, et al. Multistate outbreak of melioidosis associated with imported aromatherapy spray. N Engl J Med. 2022;386:861–8. https://doi.org/10.1056/NEJMoa2116130
35. Centers for Disease Control and Prevention. Melioidosis locally endemic in areas of the Mississippi Gulf Coast after *Burkholderia pseudomallei* isolated in soil and water and linked to two cases—Mississippi, 2020 and 2022 [cited 2023 May 2]. https://emergency.cdc.gov/han/2022/han00470.asp

Address for correspondence: Jelmer Savelkoel, Amsterdam UMC location University of Amsterdam, Center for Experimental and Molecular Medicine, Meibergdreef 9, 1105 AZ, Rm T1.0-234, Amsterdam, the Netherlands; or David A.B. Dance; email: j.savelkoel@amsterdamumc.nl or david.d@tropmedres.ac

Effects of Shock and Vibration on Product Quality during Last-Mile Transportation of Ebola Vaccine under Refrigerated Conditions[1]

Linda Bus-Jacobs, Rute Lau, Marjolein Soethoudt, Lisa Gebbia, Edwin Janssens, Tjeerd Hermans

Analyzing vaccine stability under different storage and transportation conditions is critical to ensure that effectiveness and safety are not affected by distribution. In a simulation of the last mile in the supply chain, we found that shock and vibration had no effect on Ad26.ZEBOV/MVA-BN-Filo Ebola vaccine regimen quality under refrigerated conditions.

Ebola vaccine development has been accelerated in response to large outbreaks in West and Central Africa; those outbreaks have caused >32,000 cases and >13,500 deaths (*1*). One vaccine emerging from this effort is the heterologous Ad26.ZEBOV/MVA-BN-Filo regimen (Johnson & Johnson, https://www.jnj.com). Ad26.ZEBOV, an adenovirus serotype 26–vectored monovalent, recombinant, replication-incompetent vaccine, encodes the full-length Ebola virus Mayinga glycoprotein. MVA-BN-Filo, a recombinant, nonreplicating, modified vaccinia Ankara–vectored multivalent vaccine, encodes the glycoprotein of Ebola virus (Mayinga), Sudan virus (Gulu), and Marburg virus (Musoke) and the nucleoprotein of Taï Forest virus. Ad26.ZEBOV/MVA-BN-Filo received marketing authorization under exceptional circumstances for prophylactic use in persons ≥1 year of age in the European Union (*2*,*3*) and is on the World Health Organization's list of prequalified vaccines (*4*). This vaccine regimen has been shown to be safe and immunogenic in children and adults (*5*–*9*).

Recommended long-term storage and shipping conditions are –85°C to –55°C for the Ad26.ZEBOV component (*2*) and 25°C to –15°C for the MVA-BN-Filo component (*3*). However, infrastructure challenges may affect implementation of recommended distribution conditions, particularly in remote regions. Refrigerated (2°–8°C) liquid transport may more easily support extended vaccine distribution to rural locations than frozen conditions. Ad26.ZEBOV/MVA-BN-Filo can maintain stability at 2°–8°C (*10*). An important consideration in transporting liquid vaccines to rural areas is agitation, which can contribute to vaccine degradation and loss of potency (*11*). For our study, we subjected Ad26.ZEBOV/MVA-BN-Filo to simulated rough-road transport at 2°–8°C, conditions that are representative of the final leg or last mile in the supply chain in rural areas, to assess the effect of shock and vibration on vaccine quality.

The Study

Packaging configurations (material used and shipping and storing conditions) were representative of supplies available in Africa during large vaccination campaigns (Figure; Appendix Table 1, https://wwwnc.cdc.gov/EID/article/30/3/23-1060-App1.pdf). We conducted simulated distribution testing in 2 sequential steps at 2°–8°C to approximate last-mile transport in rural areas that included a shock test followed by a vibration test. The test simulated unpaved roads typical of rural areas, representing long-distance (100-km) travel that could occur between the distribution center and vaccination site, by using a rough-road transport simulation profile.

We dropped vials 9 times in various orientations from heights of 30.5–91.4 cm, depending on the weight of the shipping container (Appendix Table 2,

Author affiliations: Janssen Vaccines and Prevention B.V., Leiden, the Netherlands (L. Bus-Jacobs, R. Lau, M. Soethoudt, E. Janssens, T. Hermans); Janssen Research and Development LLC, Spring House, Pennsylvania, USA (L. Gebbia)

DOI: https://doi.org/10.3201/eid3004.231060

[1]Preliminary results from this study were presented at the Conference on Public Health in Africa; December 13–15, 2022; Kigali, Rwanda.

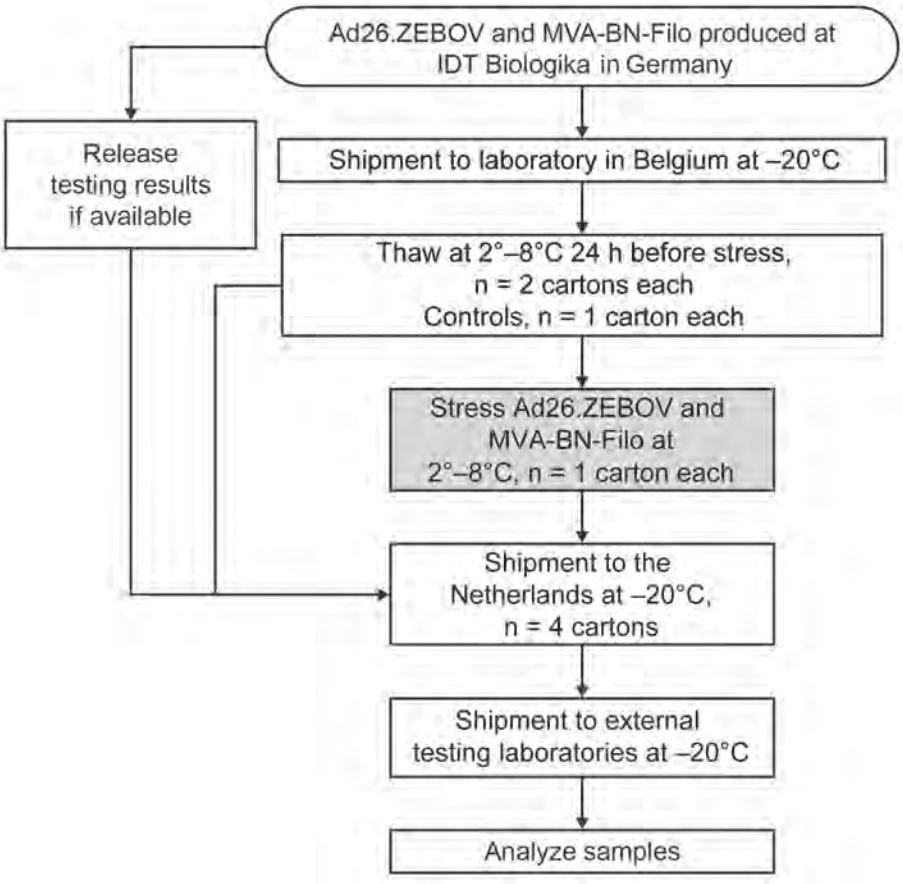

Figure. Study design to assess effects of shock and vibration on last-mile transportation of Ad26.ZEBOV/MVA-BN-Filo regimen Ebola vaccine regimen under refrigerated conditions. Ad26.ZEBOV/MVA-BN-Filo were produced and stored at –85°C to –55°C. Four paperboard cartons, each with 2 thermoformed trays containing 10 vials, were shipped to the simulation test laboratory at –20°C. The vials were thawed at 2°–8°C 24 h before testing and packed into insulated shipping containers designed to maintain an internal temperature of 2°–8°C for the duration of the study. Half of the vials (20 Ad26.ZEBOV and 20 MVA-BN-Filo) were subjected to simulated distribution testing, and half remained unstressed as controls. Control samples are non–distribution-tested samples exposed to freeze-thaw.

Figure). We determined the vibration sequence by using the International Safe Transit Association's web-based software application 4AB (https://ista.org/test_procedures.php#enhanced-simulation-section), selecting the truck profile to approximate truck transport in rural areas. During the 36-minute vibration test, vibration intensity increased and the vibration profile shape remained constant. Vials were oriented upside down to simulate a worst-case scenario.

After simulated distribution testing, we froze all 80 vials at –20°C and shipped them back to analytical laboratories, where they were stored at –85°C to –55°C before analysis. We applied assays for indicating critical quality attributes, including appearance, potency, quantity, aggregation, protein impurities, and presence of subvisible particles (Appendix Table 3). We conducted potency testing as described previously (*10*). We selected test methods and release specifications on the basis of regulatory guidance provided in the International Conference on Harmonisation Q6B and European Pharmacopoeia (*12*,*13*).

We compared assay results from the drug product vials with the control (unstressed) vials from the same batch of drug product and the release specifications, noting any deviations that occurred during the study (Appendix). The attributes evaluated did not show substantial differences between stressed and control samples of Ad26.ZEBOV (Appendix Table 4). After the simulation, the appearance of the Ad26.ZEBOV drug product was clear, without coloration or visible particulate matter. Potency, quantity of Ad26.ZEBOV viral particles, and polydispersity were within release specifications. We observed no difference in the average hydrodynamic radius of stressed (54.2 nm) and control (55.2 nm) samples. Those values exceeded the current release specification (≤53 nm), which is attributable to the method used for this study having an ≈5 nm bias versus the release method. The percentage of main hexon identified on reverse phase ultra-high performance liquid chromatograms was numerically lower in both stressed (65.06%) and control (64.42%) samples versus the reference batch (75.1%). The percentage of free hexon was similar in stressed (4.3%) samples and the reference batch (4.0%).

We observed no substantial effect on attributes of the MVA-BN-Filo drug product between stressed and control samples after the simulation (Appendix Table 4). The appearance of material in both groups

was light yellow and milky, with no visible extraneous particles; product-related particles were present in the stressed vials. Potencies of stressed and control samples were within commercial release specifications. We confirmed the transgene expression of the Zaire Ebola virus (Mayinga), Sudan virus (Gulu), and Marburg virus (Musoke) glycoproteins and the Taï Forest virus nucleoprotein encoded by MVA-BN-Filo in stressed and control samples. Genomic vaccinia DNA contents were identical between the 2 groups. Average particle sizes measured by nanoparticle tracking analysis were numerically higher in stressed (195 nm) and control (191 nm) samples versus the reference batch (157 nm). Average virus particle sizes measured by fluorescence nanoparticle tracking analysis were numerically higher in the stressed samples (453 nm) versus both the control samples (399 nm) and the reference batch (394 nm). Total subvisible particle concentrations measured by microflow imaging were numerically higher in stressed (7.82×10^6 particles/mL) versus control (4.73×10^6 particles/mL) samples, whereas mean subvisible particle sizes were numerically lower in stressed (2.49 μm) versus control (3.26 μm) samples. We identified no substantial differences between stressed and control samples from the particle size distribution graphs of the 3 methods.

Conclusions

The stability of Ebola virus vaccine drug products is critical to ensure that quality remains unaffected in conditions likely encountered during distribution. We have shown that a liquid formulation for Ad26.ZEBOV/MVA-BN-Filo is suitable for mass vaccination in resource-limited regions at risk for outbreaks (*10*). We assessed the impact of shock and vibration, simulating rough-road transport conditions at 2°–8°C, on the quality of Ad26.ZEBOV/MVA-BN-Filo.

Product stability can be demonstrated through a quantitative measure of potency, which is linked to vaccine safety and efficacy (*14*). Potency can correlate with infectious titer and transgene expression and may be negatively affected by aggregate formation (*14*). Aggregates can affect immunogenicity and subsequently compromise vaccine efficacy (*14*). We have demonstrated that Ad26.ZEBOV and MVA-BN-Filo undergoing simulated distribution contained similarly sized aggregates and viral particles similar in number and potency to the control samples, suggesting that the immunogenicity of samples exposed to simulated rough-road transport would not differ from the control samples.

One limitation of this study is that the stress that may be encountered during in-country transport was simulated. However, the simulation used in this study provides more realistic exposure to shock and vibration than can be generated by laboratory orbital shakers. Data on stability after agitation of alternative candidate Ebola virus vaccine regimens are limited in this regard (*15*).

In summary, this study shows that simulated, refrigerated (2°–8°C), rough-road truck transport, representative of the last mile of the supply chain, had no substantial effect on the quality of Ad26.ZEBOV/MVA-BN-Filo compared with the control condition. These findings confirm that refrigerated transport over rough terrain is possible and meets requirements for the challenging rural areas in the cold chain.

Medical writing support was provided by Sadie van Dyne and Courtney St. Amour, both of Lumanity Communications Inc., and was funded by Janssen Vaccines and Prevention B.V.

L.B., R.L., M.S., E.J., and T.H. are current employees of Janssen Vaccines and Prevention B.V. and may hold shares of Johnson & Johnson. L.G. is a current employee of Janssen Research and Development B.V. and may hold shares of Johnson & Johnson.

About the Author

Ms. Bus-Jacobs is Director of Chemistry, Manufacturing, and Control at Janssen Vaccines and Prevention B.V. in Leiden, the Netherlands. Her primary research interests include bioprocess technology (especially monoclonal antibodies and vaccines).

References

1. Centers for Disease Control and Prevention. History of Ebola virus disease (EVD) outbreaks. 2022 [cited 2023 Jul 7]. https://www.cdc.gov/vhf/ebola/history/chronology.html
2. European Medicines Agency. Zabdeno. 2020 Jul [cited 2023 Mar 3]. https://www.ema.europa.eu/en/medicines/human/EPAR/zabdeno
3. European Medicines Agency. Mvabea. 2020 Nov [cited 2023 Mar 3]. https://www.ema.europa.eu/en/medicines/human/EPAR/mvabea
4. World Health Organization. List of prequalified vaccines [cited 2023 May 16]. https://extranet.who.int/pqweb/vaccines/list-prequalified-vaccines
5. Barry H, Mutua G, Kibuuka H, Anywaine Z, Sirima SB, Meda N, et al.; EBL2002 Study Group. Safety and immunogenicity of 2-dose heterologous Ad26.ZEBOV, MVA-BN-Filo Ebola vaccination in healthy and HIV-infected adults: a randomised, placebo-controlled phase II clinical trial in Africa. PLoS Med. 2021;18:e1003813. https://doi.org/10.1371/journal.pmed.1003813
6. Anywaine Z, Barry H, Anzala O, Mutua G, Sirima SB, Eholie S, et al.; EBL2002 Study Group. Safety and immunogenicity of 2-dose heterologous Ad26.ZEBOV, MVA-BN-Filo Ebola vaccination in children and adolescents in Africa: a randomised, placebo-controlled, multicentre phase

II clinical trial. PLoS Med. 2022;19:e1003865. https://doi.org/10.1371/journal.pmed.1003865
7. Ishola D, Manno D, Afolabi MO, Keshinro B, Bockstal V, Rogers B, et al.; EBL3001 Study Group. Safety and long-term immunogenicity of the two-dose heterologous Ad26.ZEBOV and MVA-BN-Filo Ebola vaccine regimen in adults in Sierra Leone: a combined open-label, non-randomised stage 1, and a randomised, double-blind, controlled stage 2 trial. Lancet Infect Dis. 2022;22:97–109. https://doi.org/10.1016/S1473-3099(21)00125-0
8. Afolabi MO, Ishola D, Manno D, Keshinro B, Bockstal V, Rogers B, et al.; EBL3001 Study Group. Safety and immunogenicity of the two-dose heterologous Ad26.ZEBOV and MVA-BN-Filo Ebola vaccine regimen in children in Sierra Leone: a randomised, double-blind, controlled trial. Lancet Infect Dis. 2022;22:110–22. https://doi.org/10.1016/S1473-3099(21)00128-6
9. Kieh M, Richert L, Beavogui AH, Grund B, Leigh B, D'Ortenzio E, et al.; PREVAC Study Team. Randomized trial of vaccines for Zaire Ebola virus disease. N Engl J Med. 2022;387:2411–24. https://doi.org/10.1056/NEJMoa2200072
10. Capelle MAH, Babich L, van Deventer-Troost JPE, Salerno D, Krijgsman K, Dirmeier U, et al. Stability and suitability for storage and distribution of Ad26.ZEBOV/MVA-BN®-Filo heterologous prime-boost Ebola vaccine. Eur J Pharm Biopharm. 2018;129:215–21. https://doi.org/10.1016/j.ejpb.2018.06.001
11. Hasija M, Li L, Rahman N, Ausar SF. Forced degradation studies: an essential tool for the formulation development of vaccines. Vaccine: Development and Therapy. 2013;3:11–33. https://doi.org/10.2147/VDT.S41998
12. European Medicines Agency. ICH Q6B specifications: test procedures and acceptance criteria for biotechnological/biological products—scientific guideline [cited 2023 May 16]. https://www.ema.europa.eu/en/ich-q6b-specifications-test-procedures-acceptance-criteria-biotechnological-biological-products
13. European Directorate for the Quality of Medicines & Healthcare. European pharmacopoeia [cited 2023 May 16]. https://www.edqm.eu/en/d/99080
14. Sanyal G. Development of functionally relevant potency assays for monovalent and multivalent vaccines delivered by evolving technologies. NPJ Vaccines. 2022;7:50. https://doi.org/10.1038/s41541-022-00470-4
15. Davis H, Dow T, Isopi L, Blue JT. Examination of the effect of agitation on the potency of the Ebola Zaire vaccine rVSVΔG–ZEBOV-GP. Vaccine. 2020;38:2643–5. https://doi.org/10.1016/j.vaccine.2020.02.002

Address for correspondence: Linda Bus-Jacobs, Janssen Vaccines and Prevention B.V., Archimedesweg 6, 2333 CN Leiden, the Netherlands; email: ljacobs1@its.jnj.com

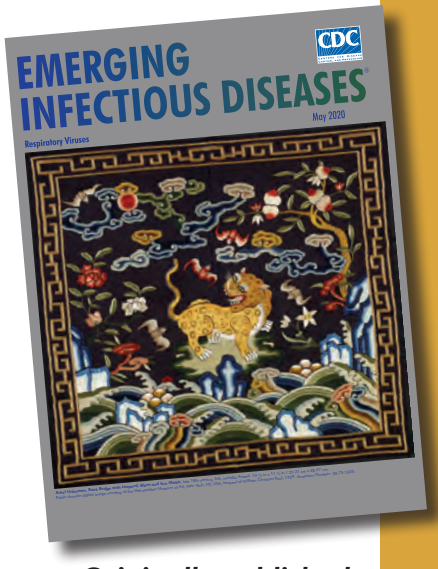

Originally published in May 2020

etymologia revisited

Coronavirus

The first coronavirus, avian infectious bronchitis virus, was discovered in 1937 by Fred Beaudette and Charles Hudson. In 1967, June Almeida and David Tyrrell performed electron microscopy on specimens from cultures of viruses known to cause colds in humans and identified particles that resembled avian infectious bronchitis virus. Almeida coined the term "coronavirus," from the Latin *corona* ("crown"), because the glycoprotein spikes of these viruses created an image similar to a solar corona. Strains that infect humans generally cause mild symptoms. However, more recently, animal coronaviruses have caused outbreaks of severe respiratory disease in humans, including severe acute respiratory syndrome (SARS), Middle East respiratory syndrome (MERS), and 2019 novel coronavirus disease (COVID-19).

References:

1. Almeida JD, Tyrrell DA. The morphology of three previously uncharacterized human respiratory viruses that grow in organ culture. J Gen Virol. 1967;1:175–8. https://doi.org/10.1099/0022-1317-1-2-175
2. Beaudette FR, Hudson CB. Cultivation of the virus of infectious bronchitis. J Am Vet Med Assoc. 1937;90:51–8.
3. Estola T. Coronaviruses, a new group of animal RNA viruses. Avian Dis. 1970;14:330–6. https://doi.org/10.2307/1588476
4. Groupe V. Demonstration of an interference phenomenon associated with infectious bronchitis virus of chickens. J Bacteriol. 1949;58:23–32. https://doi.org/10.1128/JB.58.1.23-32.1949

https://wwwnc.cdc.gov/eid/article/26/5/et-2605_article

Co-Circulating Monkeypox and Swinepox Viruses, Democratic Republic of the Congo, 2022

Thierry Kalonji, Emile Malembi, Jean Paul Matela, Toutou Likafi, Eddy Kinganda-Lusamaki, Emmanuel Hasivirwe Vakaniaki, Nicole A. Hoff, Amuri Aziza, Francisca Muyembe, Joelle Kabamba, Tine Cooreman, Béatrice Nguete, Danae Witte, Ahidjo Ayouba, Nicolas Fernandez-Nuñez, Stijn Roge, Martine Peeters, Sydney Merritt, Steve Ahuka-Mundeke, Eric Delaporte, Elisabeth Pukuta, Joachim Mariën, Eugene Bangwen, Steven Lakin, Charles Lewis, Jeffrey B. Doty, Laurens Liesenborghs, Lisa E. Hensley, Andrea McCollum, Anne W. Rimoin, Jean Jacques Muyembe-Tamfum, Robert Shongo, Didine Kaba, Placide Mbala-Kingebeni

In September 2022, deaths of pigs manifesting pox-like lesions caused by swinepox virus were reported in Tshuapa Province, Democratic Republic of the Congo. Two human mpox cases were found concurrently in the surrounding community. Specific diagnostics and robust sequencing are needed to characterize multiple poxviruses and prevent potential poxvirus transmission.

Until recently, the Democratic Republic of the Congo (DRC), located in an mpox-endemic region, has had the highest global burden of mpox (*1*). Mpox is caused by the monkeypox virus (MPXV), which belongs to the *Orthopoxvirus* genus of the Poxviridae family. Within Poxviridae, 10 other genera are known to infect animals and reptiles (*2*), including *Suipoxvirus* (*3*). The only known species of *Suipoxvirus* causes swinepox, a pox-like disease in pigs.

Two genetically distinct clades of MPXV cause disease in humans. Clade I (formerly Congo Basin clade) is endemic in Central Africa, and outbreaks are thought to result mainly from zoonotic spillover; squirrels or other small mammals are suspected reservoirs or hosts (*4*; J. Mariën et al., unpub. data, https://doi.org/10.21203/rs.3.rs-414280/v2). Clade II (formerly West African clade) is endemic in West Africa; suspected reservoirs and transmission routes are historically similar to those of clade I. In 2022, MPXV subclade IIb spread beyond West Africa, causing an unprecedented global outbreak, leading the World Health Organization to declare mpox as a Public Health Emergency of International Concern (*5*).

During 2011–2015, the incidence of MPXV cases in DRC's Tshuapa Province increased compared with the incidence during 1981–1986 in similar geographic areas (*6*). This observation is not unique, suggesting expanding spillover rates of MPXV clade I into the human population and highlighting the possibility of increasing human-to-human virus transmission (*1*,*4*).

Confirmation of suspected MPXV cases in DRC is hindered by logistical difficulties, such as complications involving sample collection and lack of

Author affiliations: Program National Lutte Contre MPX-VHF, Kinshasa, Democratic Republic of the Congo (T. Kalonji, E. Malembi, R. Shongo); Province Health Division, Tshuapa, Democratic Republic of the Congo (J.P. Matela, T. Likafi); Institute National de Recherche Biomedical, Kinshasa (E. Kinganda-Lusamaki, E.H. Vakaniaki, A. Aziza, F. Muyembe, S. Ahuka-Mundeke, E. Pukuta, J.J. Muyembe-Tamfum, P. Mbala-Kingebeni); Cliniques Universitaires de Kinshasa, Kinshasa (E. Kinganda-Lusamaki, F. Muyembe, S. Ahuka-Mundeke, J.J. Muyembe-Tamfum, P. Mbala-Kingebeni); University of Montpellier, IRD, INSERM, Montpellier, France (E. Kinganda-Lusamaki, A. Ayouba, N. Fernandez-Nuñez, M. Peeters, E. Delaporte); University of California, Los Angeles, California, USA (N.A. Hoff, S. Merritt, A.W. Rimoin); Centers for Disease Control and Prevention, Atlanta, Georgia, USA (J. Kabamba, J.B. Doty, A. McCollum); University of Antwerp, Antwerp, Belgium (T. Cooreman, J. Mariën); Kinshasa School of Public Health, Kinshasa (B. Nguete, D. Kaba); University of Florida, Gainesville, Florida, USA (D. Witte); Institute of Tropical Medicine, Antwerp (S. Roge, E. Bangwen, L. Liesenborghs); US Department of Agriculture, Manhattan, Kansas, USA (S. Lakin, C. Lewis, L.E. Hensley)

DOI: https://doi.org/10.3201/eid3004.231413

available diagnostic laboratories in remote regions (*4*). Reported increases in mpox cases without well-defined origins suggest that a One Health investigation might be a more informative strategy. As part of this approach, investigations by DRC's National Program for Mpox and Viral Hemorrhagic Fevers (PNLMPX-VHF) and its partners, including the US Centers for Disease Control and Prevention (CDC) and Belgium Institute of Tropical Medicine, have begun sampling mammals in areas with mpox cases and animals manifesting pox-like lesions (*7*). Previous sampling focused on wildlife and small animals but has recently been expanded to include domestic animals because animal husbandry is widespread throughout DRC (*8*). Yet, areas with livestock have not been regularly surveilled for health, hygiene, or suspected viruses, including MPXV. Close proximity of humans and animals provides an environment conducive to virus spillover (*9*). We report on the co-circulation of MPXV and swinepox virus in the same locality within DRC.

The Study

In early September 2022, provincial authorities in Tshuapa, a heavily forested province in northwest DRC, alerted PNLMPX-VHF regarding the deaths of

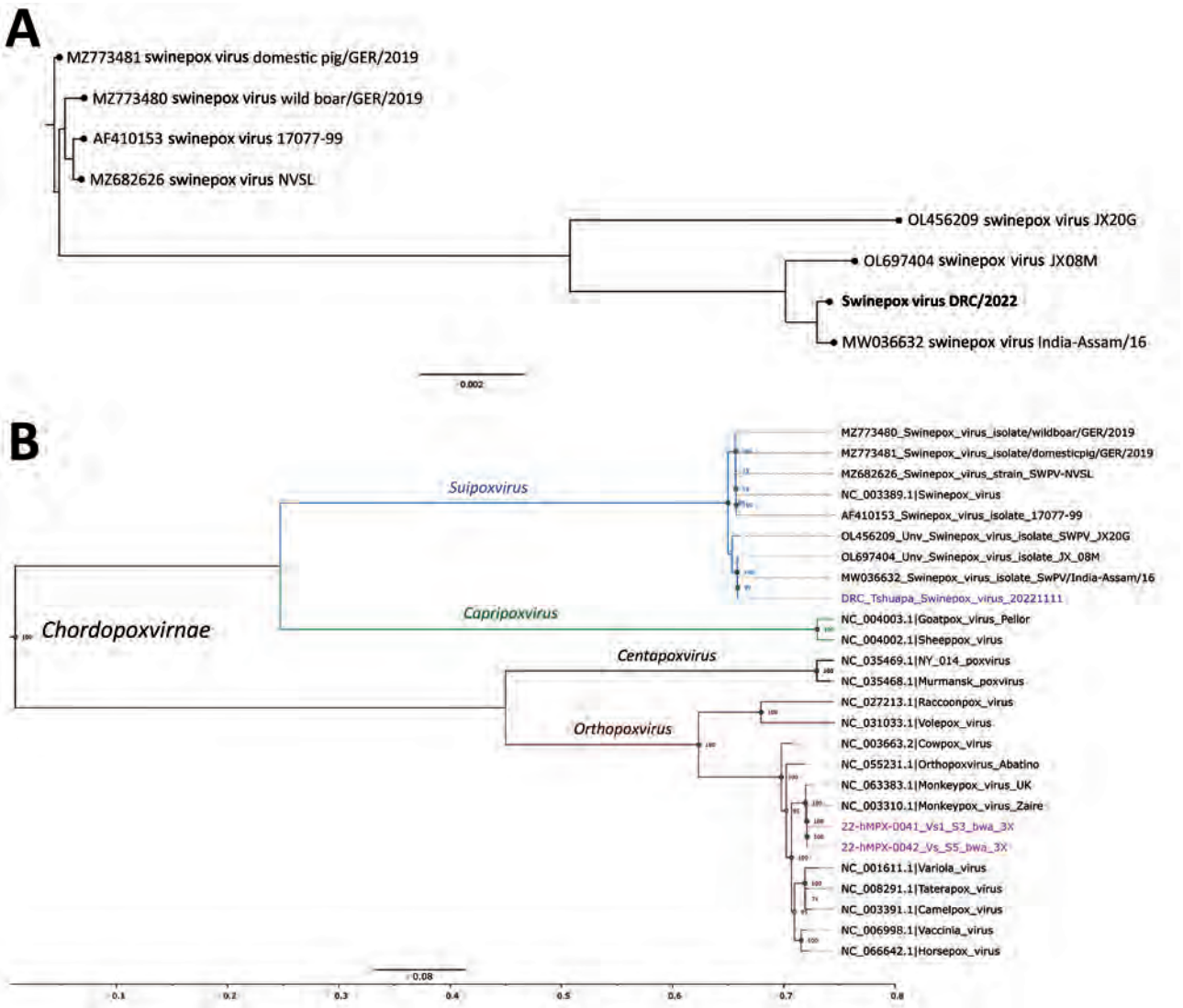

Figure 1. Phylogenetic analysis of swinepox virus (A) and monkeypox virus (B) in study of co-circulating viruses, Democratic Republic of the Congo, 2022. Poxvirus sequences for comparison were obtained from GenBank. Trees were constructed by using the maximum-likelihood method and the general time reversal substitution model with gamma distribution and proportion of invariable sites. In panel A, bold text indicates the swinepox sequence from this study; in panel B, magenta-colored text indicates monkeypox virus sequences and blue text indicates swinepox virus sequence from this study. The monkeypox virus samples belong to clade I and correspond to those previously described (*11*). Scale bars indicate nucleotide substitutions per site. DRC, Democratic Republic of the Congo.

pigs in the Boende health zone that manifested vesicular, pox-like lesions. Authorities also reported several suspected mpox cases among farm owners and residents in the area; clinical samples were not collected from those persons. Tshuapa is considered an MPXV-endemic area and has a robust surveillance program through PNLMPX-VHF, Kinshasa School of Public Health, and CDC. Through this program, suspected mpox case samples are sent to DRC's reference laboratory, the Institute National de Recherche Biomedical (INRB), for testing and, when requested, sequencing (*6*).

After the alert, during September 9–19, two pigs with pox-like lesions were identified at a domestic farm where pigs roamed freely. The first diseased pig had died on September 1; no samples had been collected. On September 10, the second pig, which had predominant umbilicated nodular dermatitis between the ears and on the face and chest, died. We collected a vesicle swab sample from the cadaver for analysis at INRB. MPXV PCR (*10*) results were negative, and we sequenced the sample by using an Illumina platform (Illumina, https://www.illumina.com) probe enrichment-based protocol and a custom-made virus research panel (Twist Biosciences, https://www.twistbioscience.com). We used the open source bioinformatics pipeline, GeVarLi (https://forge.ird.fr/transvihmi/nfernandez/GeVarLi), to clean and align sequences and assign virus lineages. We completed de novo sequence assembly by using SPAdes Genome Assembler (https://github.com/ablab/spades). Sequencing results and phylogenetic analysis indicated that the second pig had been infected with swinepox virus (Figure 1, panel A) (*11*).

After identifying a swinepox-positive pig, we launched an expanded poxvirus investigation on October 2. In the Boende health zone, we identified 16 suspected human mpox cases, all occurring within 400 m of the farm that had a confirmed swinepox case. None of the persons with suspected mpox reported having mpox vaccinations, nor did they have scars indicating past mpox or variola vaccination. We collected skin swab, oropharyngeal lesion swab, and venous blood samples from case-patients with suspected active (n = 2) and convalescent (n = 4) MPXV infections and analyzed those samples at INRB. The 2 suspected active case-patients (both children) were MPXV positive. Sequencing confirmed infection with MPXV; however, we did not detect swinepox co-infection (Figure 1, panel B). We deposited the 2 MPXV sequences in the GISAID database (https://www.gisaid.org; accession nos. EPI_ISL_18857033–4). We determined that the farm owner, not realizing his pigs were sick, permitted his 2 children to directly contact the pigs during feeding without protection. Both children exhibited mild symptoms of fever, colds, headaches, and physical asthenia and developed a rash and papules 12 days after disease onset in the first pig. Both MPXV PCR-positive children recovered without complications; in addition, the family reported that they had previously recovered from PCR-confirmed MPXV. No epidemiologic link was established between the mpox-positive children and the swinepox-positive pig.

We returned to the area to identify additional pigs with symptoms of pox-like virus infections and found 4 suspected cases, of which 3 were in a neighboring farm. All pigs with suspected infections had pox-like skin lesions on the face, mouth, or tongue and had liver pathology similar to clinical manifestations of pox-like virus infections. A third pig from the original farm died on October 24; we collected lesion

Figure 2. Animals with mpox-like lesions in study of co-circulating monkeypox and swinepox viruses, Democratic Republic of the Congo, 2022. A, B) Mpox-type lesions observed on internal tissues (A) and on the skin (B) of a pig. C) Lesion on the skin of a rodent that was found in the same geographic area as the pig.

crust, vesicle, and rectal swab samples and internal organs where vesicular lesions were noted (Figure 2, panels A, B). Small mammals found in the vicinity of the original farm and that farmer's house also showed similar skin lesions (Figure 2, panel C). We collected lung, spleen, kidney, liver, oral, and rectal swab samples from 28 small mammals (shrews and black rats [*Rattus rattus*]) for analysis at INRB; 2 rats exhibited lesions. All samples tested negative for MPXV by PCR, and no additional sequencing was performed.

Concurrently, medical staff reported periodic human outbreaks of suspected MPXV infections and wild and domesticated animal deaths in other health zones. In addition, outbreaks of pox-like disease in pigs preceded confirmed human mpox cases in the Bolomba health zone of Equateur Province in 2008 and the Masi-Manimba health zone of Kwilu Province in 2022 (*12*). Although no samples were collected from sick animals during those outbreaks, the overall frequency of reports warrants future use of One Health approaches in all investigations of pox-like diseases, regardless of the initial species in which the lesions are observed.

Conclusions

In environments endemic for zoonotic pathogens such as MPXV, the role of animal reservoirs and hosts must be considered in surveillance and outbreak control. Reports of multiple poxviruses (vaccinia virus, pseudocowpox virus, MPXV) co-circulating within a community are rare and have been primarily confined to Brazil (*2*,*13*). In addition to mpox, and now swinepox, DRC has reported cases of other poxviruses, including molluscum contagiosum and tanapox (*14*). The appearance of multiple poxviruses in the same region indicates sensitive, specific diagnostics and robust sequencing capacity are needed to characterize those agents, better understand poxvirus epidemiology, and prevent potential poxvirus transmission.

Acknowledgments

We thank the Tshuapa provincial health division staff, especially those in Boende and Mompono health zones; all health care workers involved in mpox surveillance and animal health and safety in DRC; the staff from the INRB Biorepository, including Gabriel Kabamba, Raphael Lumembe, Andre Citenga, Fiston Cikaya, Sifa Kavira, Zadoc Yungwe, and Michel Kenye; staff from the INRB Department of Epidemiology and Virology, including Guy Midingi, Sophie Gabia, Akil Prince, Chloé Muswamba, and Ola Rilia, for their valuable involvement and support; and Yu Li for review of the genetic sequences.

This work was funded by the Research Foundation-Flanders (grant no. G096222N to L.L.); US Department of Defense, Defense Threat Reduction Agency, Monkeypox Threat Reduction Network (MPX-TRN) (to A.W.R.); US CDC (to D.K.); project PANAFPOX funded and coordinated by The French National Agency for Research on AIDS and Viral Hepatitis–Maladies Infectieuses Emergentes (ANRS-MIE) and Agence Française de Développement through the AFROSCREEN project (grant agreement no. CZZ3209) in partnership with Institut Pasteur and Institute de Research pour le Developpemente (to M.P. and E.D.); and a PhD grant from the French Foreign Affairs Office (to E.K.-L.).

About the Author

Dr. Kalonji is a disease surveillance officer with the National Viral Hemorrhagic Fevers and Mpox Control Program of the DRC. His research interests include mpox, COVID-19, Ebola virus disease, cholera, and vaccine-preventable diseases.

References

1. Bunge EM, Hoet B, Chen L, Lienert F, Weidenthaler H, Baer LR, et al. The changing epidemiology of human monkeypox—a potential threat? A systematic review. PLoS Negl Trop Dis. 2022;16:e0010141. https://doi.org/10.1371/journal.pntd.0010141
2. Oliveira GP, Rodrigues RAL, Lima MT, Drumond BP, Abrahão JS. Poxvirus host range genes and virus–host spectrum: a critical review. Viruses. 2017;9:331. https://doi.org/10.3390/v9110331
3. Afonso CL, Tulman ER, Lu Z, Zsak L, Osorio FA, Balinsky C, et al. The genome of swinepox virus. J Virol. 2002;76:783–90. https://doi.org/10.1128/jvi.76.2.783-790.2002
4. Rimoin AW, Mulembakani PM, Johnston SC, Lloyd Smith JO, Kisalu NK, Kinkela TL, et al. Major increase in human monkeypox incidence 30 years after smallpox vaccination campaigns cease in the Democratic Republic of Congo. Proc Natl Acad Sci USA. 2010;107:16262–7. https://doi.org/10.1073/pnas.1005769107
5. World Health Organization. WHO Director-General's statement at the press conference following IHR Emergency Committee regarding the multicountry outbreak of monkeypox—23 July 2022 [cited 2023 Jun 20]. https://www.who.int/director-general/speeches/detail/who-director-general-s-statement-on-the-press-conference-following-IHR-emergency-committee-regarding-the-multi-country-outbreak-of-monkeypox--23-july-2022
6. Whitehouse ER, Bonwitt J, Hughes CM, Lushima RS, Likafi T, Nguete B, et al. Clinical and epidemiological findings from enhanced monkeypox surveillance in Tshuapa Province, Democratic Republic of the Congo during 2011–2015. J Infect Dis. 2021;223:1870–8. https://doi.org/10.1093/infdis/jiab133
7. Centers for Disease Control and Prevention. Mpox in animals and pets. January 4, 2023 [cited 2023 March 13]. https://www.cdc.gov/poxvirus/mpox/veterinarian/mpox-in-animals.html
8. Bosworth A, Wakerley D, Houlihan CF, Atabani SF. Monkeypox: an old foe, with new challenges. Infect Prev

Pract. 2022;4:100229. https://doi.org/10.1016/j.infpip.2022.100229
9. Vora NM, Hannah L, Walzer C, Vale MM, Lieberman S, Emerson A, et al. Interventions to reduce risk for pathogen spillover and early disease spread to prevent outbreaks, epidemics, and pandemics. Emerg Infect Dis. 2023;29:1–9. https://doi.org/10.3201/eid2903.221079
10. Li Y, Zhao H, Wilkins K, Hughes C, Damon IK. Real-time PCR assays for the specific detection of monkeypox virus West African and Congo Basin strain DNA. J Virol Methods. 2010;169:223–7. https://doi.org/10.1016/j.jviromet.2010.07.012
11. Berthet N, Descorps-Declère S, Besombes C, Curaudeau M, Nkili Meyong AA, Selekon B, et al. Genomic history of human monkey pox infections in the Central African Republic between 2001 and 2018. Sci Rep. 2021;11:13085. https://doi.org/10.1038/s41598-021-92315-8
12. World Health Organization. RD Congo: rapport de mission d'investigation et riposte à l'épidémie de monkey pox à Djoa, zone de santé de Bolomba. 2008 [cited 2023 Jun 23]. https://reliefweb.int/report/democratic-republic-congo/rd-congo-rapport-de-mission-dinvestigation-et-riposte-%C3%A0-l%C3%A9pid%C3%A9mie
13. Luques MN, Oliveira RL, Hir S, Nunes DDS, Higa LM, Mendonça AF, et al. Co-circulation of vaccinia and monkeypox viruses in rural areas of Brazil: importance of differential molecular diagnosis. Travel Med Infect Dis. 2023;53:102578. https://doi.org/10.1016/j.tmaid.2023.102578
14. Monroe BP, Nakazawa YJ, Reynolds MG, Carroll DS. Estimating the geographic distribution of human Tanapox and potential reservoirs using ecological niche modeling. Int J Health Geogr. 2014;13:34. https://doi.org/10.1186/1476-072X-13-34

Address for correspondence: Nicole Hoff, Department of Epidemiology, UCLA Fielding School of Public Health, 650 Charles E. Young Dr, CHS 41-275, Los Angeles, CA 90095, USA; email: nhoff84@ucla.edu

Case Report of Nasal Rhinosporidiosis in South Africa

Huzaifah Mayet, Denasha L. Reddy, Tika Bello Alvarez, Yahya Atiya, Nelesh P. Govender, Monica Birkhead, Tsidiso Maphanga, Sugeshnee Pather

We describe a classic case of nasal rhinosporidiosis in a woman who resided in Johannesburg, South Africa, but originated from a rural area in Eastern Cape Province. We confirmed histologic diagnosis using PCR testing and compared details with those from records on 17 other cases from South Africa.

A 24-year-old Black woman from South Africa sought care at a local primary-level clinic in Soweto, Johannesburg, South Africa, reporting a painless nasal mass of 3 years duration that caused occasional difficulty in breathing. The patient resided in Soweto but was originally from Mqunduli (31°49′S, 28°45′E), a riverside village south of Mthatha, Eastern Cape Province, South Africa. The patient reported the mass had originated in her right nostril; she disclaimed any preceding trauma and described recent onset of pain and intermittent episodes of mild, self-limiting bleeding on contact (e.g., an accidental bump) at the site of the mass. She had no rhinorrhea, and her vision was normal.

The woman was treated for sinusitis for 1 month but 2 months after initially seeking treatment was referred to the otorhinolaryngology clinic at a tertiary academic facility, where we examined her. We report details of her condition, diagnosis, treatment, and outcomes. We obtained written informed consent from the patient for publication of an account of her case including use of clinical photographs and ethics clearance from the University of the Witwatersrand Human Research Ethics Committee (M210752).

The Study

We diagnosed the patient with HIV (viral load 6,060 copies/mL, CD4+ T-cell count 570 cells/mm^3) and initiated antiretroviral therapy. She had no other underlying conditions or notable medical history and reported no international travel or contact with animals. She denied swimming in any water sources or using river or freestanding water for day-to-day purposes; she also denied interacting with any contacts, either in Soweto or Mthatha, with similar complaints or tuberculosis.

On examination, we found a nontender, 5 mm, mobile, polypoid mass in the right nostril that appeared to adhere to the anterior, superior aspect of the nasal septum near the mucocutaneous junction. Results from the remainder of her ear, nose, and throat examination, as well as examinations of her eyes and pharynx, were unremarkable. We found no cervical lymphadenopathy.

We initiated treatment with oral amoxicillin/clavulanic acid and requested a computed tomography scan of the head and neck to assess the vascularity and amenability for biopsy of the mass. The scan showed a nonenhancing, soft tissue mass in the right nasal vestibule arising from the anterior septum (Appendix Figure 1, https://wwwnc.cdc.gov/EID/article/30/4/24-0018-App1.pdf). A sample of the friable mass from the biopsy sent for histologic examination revealed multiple, variously sized, spherical subepidermal structures, the largest with thickened walls. Contents varied from a single, central acidophilic structure to numerous basophilic spheres that developed centripetally (Figure 1).

Because of postbiopsy recurrence of the mass and recent onset of pain and epistaxis, we scheduled the patient for definitive surgery to obtain a full-thickness sample. During the operation, we found a 15 mm polypoid mass in the anterior nasal cavity (Figure 2,

Author affiliations: University of the Witwatersrand, Johannesburg, South Africa (H. Mayet, D.L. Reddy, T. Bello Alvarez, Y. Atiya, N.P. Govender, S. Pather); Chris Hani Baragwanath Academic Hospital, Johannesburg (H. Mayet, D.L. Reddy, T. Bello Alvarez, Y. Atiya, S. Pather); St George's University of London, London, UK (N.P. Govender); University of Cape Town, Cape Town, South Africa (N.P. Govender); University of Exeter, Exeter, UK (N.P. Govender); National Institute for Communicable Diseases, Johannesburg (N.P. Govender, M. Birkhead, T. Maphanga); National Health Laboratory Service, Johannesburg (S. Pather)

DOI: https://doi.org/10.3201/eid3004.240018

panels A, B) attached by a stalk to the anterosuperior aspect of the septum (Figure 2, panel C). The stalk did not extend past the mucosa of the nasal septum, so the perichondrium was not macroscopically involved. We fixed the polyp for further microscopic examination (Figure 2, panels D, E; Appendix Figure 2). Examination of the rest of the patient's nasal cavities were unremarkable. Her postoperative course was uneventful, but she was not available for further follow-up.

We performed a panfungal PCR test on a section of formalin-fixed paraffin-embedded polyp from the nasal lesion. In the PCR, we amplified fungal DNA for internally transcribed spacer genes (Appendix) and confirmed 98.8% identification and 83% coverage with *Rhinosporidium* spp. (GenBank NCBI accession no. PP060009). Phylogenetically, sequences clustered with *Rhinosporidium* sp. (ex *Canis familiaris*) obtained from a dog (Appendix Figure 3).

Rhinosporidiosis is an indolent, generally benign, polypoidal infection occurring in humans and other mammals, amphibians, and aquatic birds (*1*,*2*). Host distribution reflects freshwater habitats, the environment most commonly associated with disease acquisition. Rural riverine and agricultural communities have reported the highest incidence (*3*). Other risk factors associated with human infection include contact with stagnant and silted water (typically through swimming or bathing), dust and soil, and contaminated hands or clothes; low socioeconomic status is also considered a risk factor (*3*). Highest incidence is reported in male persons <40 years of age, presumably because of increased exposure as a result of the nature and extent of their outdoor activities (*4*,*5*). The eukaryotic pathogen typically infects exposed nasal, ocular, or genitourinary tract mucosal membranes, with rare reports of cutaneous or disseminated spread in both immunocompetent and immunocompromised patients (*1*,*4*,*6*,*7*). The etiologic agent is *R. seeberi* (class: Mesomycetozoea). Mesomycetozoea comprises a unique group of microbes phylogenetically positioned between fungi and animals, presenting the taxonomic conundrum of a parasite that is neither sporozoan nor fungal, but appears to have features of both types of organism (*8*,*9*).

Rhinosporidium grows slowly in host tissues, so infection and clinical manifestations may be temporally distant. Patients with nasal or nasopharyngeal lesions manifest intermittent epistaxis, nasal obstruction, nasal mass, or nasal discharge (*3*,*4*). Clinical differential diagnoses include neoplasms, nasopharyngeal carcinomas, inverted papillomas, primary sinonasal tuberculosis, and nasal angiofibromas (*5*). Diagnosis of rhinosporidiosis is made histologically; sections show

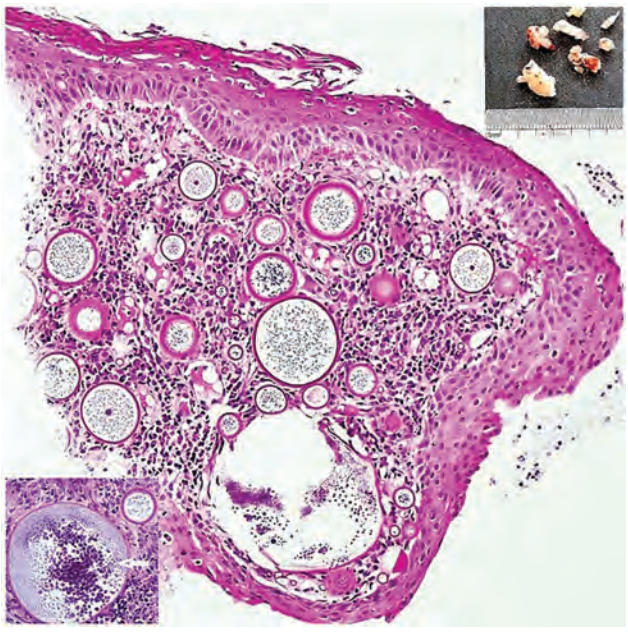

Figure 1. Results of testing in a 24-year-old Black woman with rhinosporidiosis, South Africa. Squamous mucosa with numerous thick-walled sporangia in the subepithelial region amid subacute inflammation. Hematoxylin and eosin stained section; original magnification ×100. Upper right inset shows polypoid solid fragments of tissue; lower left inset depicts sporangia enclosing endospores maturing centripetally (white arrow). Insets: original magnification ×200.

multiple sporangia, 50 to >450 μm in diameter, in various stages of maturity. During maturation, chitinous-walled sporangia contain numerous developing endospores 2–10 μm in diameter (*8*,*9*). The nucleated nature of the pathognomic structures precludes identifying the causative agent as *Microcystis*, a gram-negative, phototrophic prokaryote associated particularly with eutrophic lacustrine environments (*8*).

Treatment of rhinosporidiosis is limited to the surgical removal of polyps and electrocauterization at the attachment base; some clinicians prescribe a prolonged postoperative course of diaminodiphenyl sulfone (dapsone) alone or as part of a multidrug antimicrobial regimen (*4*–*7*). Although not curative, those adjuvants are thought to impede sporangial and endospore maturation. Refractory cases may occur because of incomplete excision, infection of the traumatized surgical sites by released endospores, or reinfection from an endospore reservoir (e.g., lymph) in disseminated cases (*4*,*5*). Recurrence, dissemination to adjacent anatomic sites, and local secondary bacterial infections are the most frequent complications (*3*). Although rhinosporidiosis is rarely fatal, diagnosis and treatment can be lifesaving when nasal infections seed to the tracheobronchial tree (*6*).

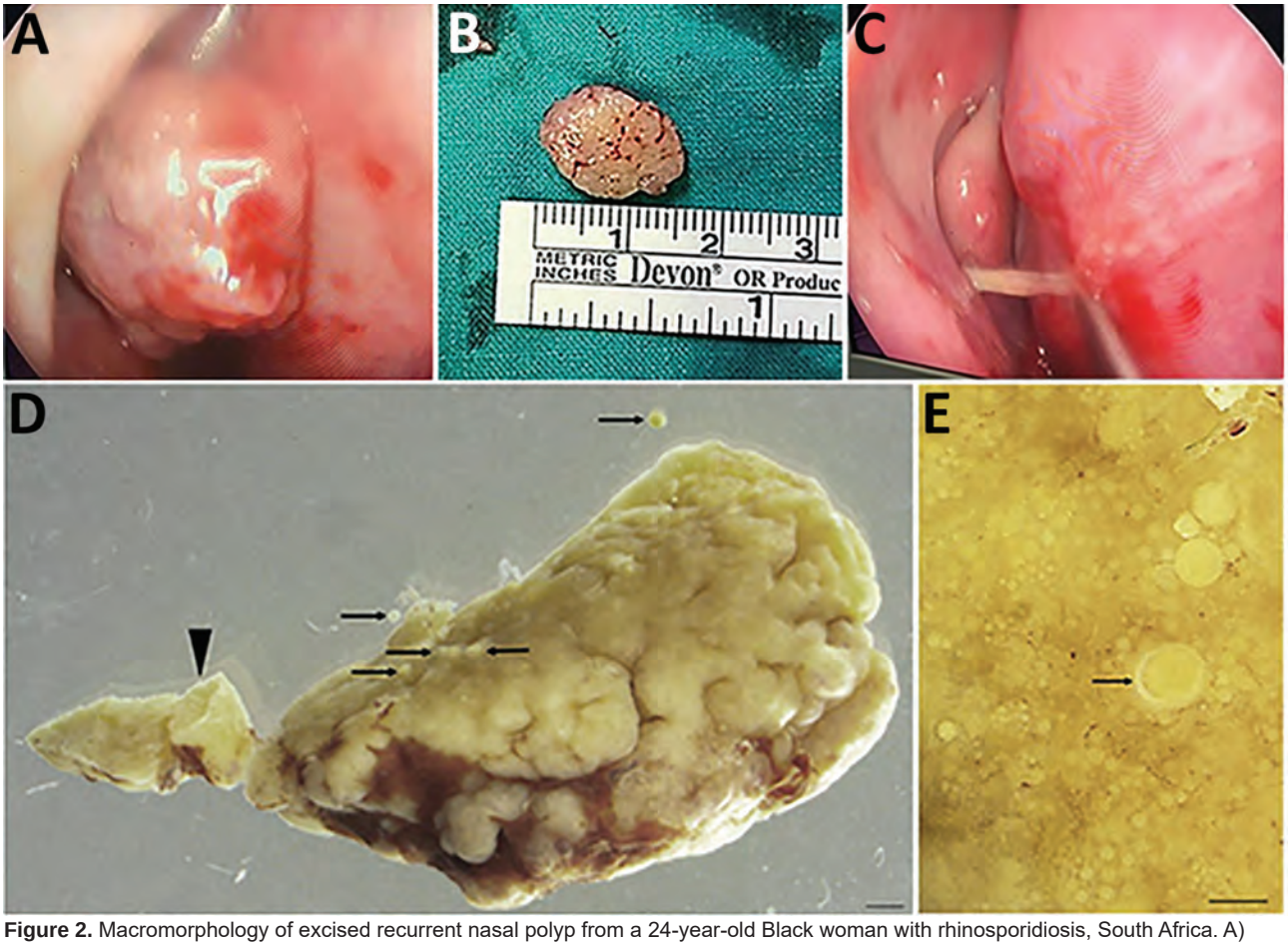

Figure 2. Macromorphology of excised recurrent nasal polyp from a 24-year-old Black woman with rhinosporidiosis, South Africa. A) Intraoperative endoscopic image of mass in right nasal cavity. B) Polypoid, oval mass measuring 15 mm. C) Stalk that attached the mass to the nasal septum. D) Portion of the pedunculated polyp (arrowhead) dotted with developing and mature sporangia (arrows). Scale bar = 1 mm. E) Surface of tissue with multiple sporangia in various stages of maturity, with the chitinous wall thickening during maturation (arrow). Scale bar = 150 μm.

The highest incidence of rhinosporidiosis has been recorded in tropical zones in India and Sri Lanka, followed by South America and Africa, but sporadic autochthonous cases have been reported from tropical and subtropical regions of all continents except Australia and Antarctica (Appendix Table). Three case series and 5 case reports document cases in South Africa (Table); the first reported case was identified by a physician with clinical experience in southern India (*10*). Most cases have been among male children and teenagers, most with conjunctival infections. Reports from several other countries in Africa, including Cameroon, Ivory Coast, Kenya, Malawi, Tanzania, Uganda, Zaire, and Zambia, are most commonly conjunctival infections. Conversely, data from Rwanda and composite global reports indicate ≈70% of infections are nasal or

Table. Case reports of rhinosporidiosis in South Africa*

Location of exposure or reporting facility†	Age, y/sex (no.)	Infection site	Date reported	Reference
Driefontein, Ladysmith, KwaZulu-Natal	12/M	Nasal	1951	(*10*)
Edendale Hospital, Pietermariztburg, KwaZulu-Natal	10/M	Ocular	1959	(*11*)
Edendale Hospital, Pietermariztburg, KwaZulu-Natal	12/M	Nasal	1977	(*12*)
Edendale Hospital, Pietermariztburg, KwaZulu-Natal	14/M	Nasal	1977	(*12*)
King Edward VIII Hospital, Durban, KwaZulu-Natal	9–15/M (4), F (2)	4 ocular, 2 nasal	1987	(*13*)
Umtata General Hospital, Mthatha, Eastern Cape	<15/M (3), F (3)	6 ocular	2005	(*14*)
Sefako Makgatho Health Sciences University, Ga-Rankuwa, Gauteng	17/M	Nasal	2017	(*15*)
Chris Hani Baragwanath Academic Hospital, Johannesburg, Gauteng	24/F	Nasal	2022	This study

*All patients were Black persons from Africa.
†Name of facility at date of publication.

nasopharyngeal infections (*5*,*9*). Misdiagnosis of nasal rhinosporidiosis in some countries in Africa could account for the predominance of reported conjunctival infection in those countries.

Despite the diagnostic simplicity of rhinosporidiosis, it is unknown if *Rhinosporidium* might have a noninfectious saprophytic developmental phase or natural hosts; how long spores are viable also remains unknown. In addition, the potential role of climate change on the epidemiology of rhinosporidiosis in South Africa is a topic for future research.

In conclusion, our study adds information about the epidemiology and diagnosis of rhinosporidiosis. Because the disease might be misdiagnosed by clinicians who are unaware of its clinical characteristics, providing education could improve rates of accurate diagnosis, leading to better disease surveillance and control efforts.

Acknowledgments

For assistance with the microbiological diagnosis of rhinosporidiosis, the authors acknowledge John Frean and Charlotte Sriruttan-Nel. For assistance with retrieving histopathology slides, the authors acknowledge members of the Histopathology Department at National Health Laboratory Services, Chris Hani Baragwanath Academic Hospital. We also thank the staff of the Electron Microscope Unit of Sefako Makgatho Health Sciences University for facilitating the scanning electron microscopy.

Author contributions: H.M., T.B.A., and D.L.R. compiled the initial manuscript, M.B. wrote all subsequent versions. H.M., T.B.A., Y.A., and D.L.R. were responsible for the clinical management of the patient. S.P. confirmed the histopathological diagnosis. T.M. and N.P.G. assisted with the panfungal PCR confirmation of the diagnosis, and T.M. performed the molecular analysis. S.P. and M.B. were responsible for the photomicrography. M.B. was responsible for the scanning electron microscopy images. All authors contributed to and approved the final manuscript.

About the Author

Dr. Mayet is a clinician currently specializing in internal medicine at the University of the Witwatersrand, Johannesburg, South Africa. His research interests include infectious diseases, but currently he is investigating lupus nephritis and its progression to chronic kidney disease.

References

1. Fredricks DN, Jolley JA, Lepp PW, Kosek JC, Relman DA. *Rhinosporidium seeberi*: a human pathogen from a novel group of aquatic protistan parasites. Emerg Infect Dis. 2000;6:273–82. https://doi.org/10.3201/eid0603.000307
2. Scheid P, Balczun C, Dehling JM, Ammon A, Sinsch U. Rhinosporidiosis in African reed frogs *Hyperolius* spp. caused by a new species of *Rhinosporidium*. Dis Aquat Organ. 2015;115:111–20. https://doi.org/10.3354/dao02888
3. Mohiuddin IM, Burud S, Harriss M. Rhinosporidiosis reinfection after 20 years—a case report from United Arab Emirates. Hamdan Med J. 2021;14:205–7. https://doi.org/10.4103/hmj.hmj_56_21
4. Arias AF, Romero SD, Garcés CG. Case report: rhinosporidiosis literature review. Am J Trop Med Hyg. 2020;104:708–11. https://doi.org/10.4269/ajtmh.20-0291
5. Ali GM, Goravey W, Al Hyassat SA, Petkar M, Al Maslamani MA, Hadi HA. Recurrent nasopharyngeal rhinosporidiosis: case report from Qatar and review of the literature. IDCases. 2020;21:e00901. https://doi.org/10.1016/j.idcr.2020.e00901
6. Pradhan S, Sirka CS, Baisakh MR. Polymorphic presentation of disseminated cutaneous rhinosporidiosis in an immunocompetent individual. Indian J Dermatol Venereol Leprol. 2018;84:614–7. https://doi.org/10.4103/ijdvl.IJDVL_52_18
7. John D, Selvin SST, Irodi A, Jacob P. Disseminated rhinosporidiosis with conjunctival involvement in an immunocompromised patient. Middle East Afr J Ophthalmol. 2017;24:51–3.
8. Vilela R, Mendoza L. The taxonomy and phylogenetics of the human and animal pathogen *Rhinosporidium seeberi*: a critical review. Rev Iberoam Micol. 2012;29:185–99. https://doi.org/10.1016/j.riam.2012.03.012
9. Izimukwiye AI, Mbarushimana D, Ndayisaba MC, Bigirimana V, Rugwizangoga B, Laga AC. Cluster of nasal rhinosporidiosis, Eastern Province, Rwanda. Emerg Infect Dis. 2019;25:1727–9. https://doi.org/10.3201/eid2509.190021
10. Dick AM. Nasal rhinosporidiosis; report of a case in Natal. S Afr Med J. 1951;25:270–1.
11. Coetzee T. Rhinosporidiosis of the conjunctiva. Br J Ophthalmol. 1959;43:309–11. https://doi.org/10.1136/bjo.43.5.309
12. Smith PL. Rhinosporidiosis: case reports. S Afr Med J. 1977;51:281.
13. Chetty R, Cooper K. Rhinosporidiosis at King Edward VIII Hospital, Durban—1976–1985. A report of 6 cases. S Afr Med J. 1987;72:217–8.
14. Salazar Campos MC, Surka J, Garcia Jardon M, Bustamante N. Ocular rhinosporidiosis. S Afr Med J. 2005;95:950–2.
15. Masilela MMJ, Selepe MS, Masilo L. Nasal rhinosporidiosis in South Africa: review of literature and report of a case. S Afr Dent J. 2017;72:420–3.

Address for correspondence: Monica Birkhead, National Institute for Communicable Diseases, Private Bag X4, Sandringham, 2192, South Africa; email: monicab@nicd.ac.za

Reemergence of Sylvatic Dengue Virus Serotype 2 in Kedougou, Senegal, 2020

Idrissa Dieng,[1] Maryam Diarra,[1] Bacary Djilocalisse Sadio, Bocar Sow, Alioune Gaye, Amadou Diallo, Martin Faye, Marie Henriette Dior Ndione, Diawo Diallo, Safietou Sankhe, Mignane Ndiaye, Fode Danfakha, Boly Diop, Amadou Alpha Sall, Gamou Fall, Oumar Faye, Cheikh Loucoubar, Ousmane Faye, Scott C. Weaver, Mawlouth Diallo, Mamadou Aliou Barry,[1] Moussa Moise Diagne[1]

In 2020, a sylvatic dengue virus serotype 2 infection outbreak resulted in 59 confirmed dengue cases in Kedougou, Senegal, suggesting those strains might not require adaptation to reemerge into urban transmission cycles. Large-scale genomic surveillance and updated molecular diagnostic tools are needed to effectively prevent dengue virus infections in Senegal.

Kedougou, Senegal's southeastern region, is a substantial arbovirus hotspot (*1*,*2*). Decades of comprehensive surveillance have existed through both a nationwide Syndromic Sentinel Surveillance Network (*3*) and passive surveillance in several public health facilities in Kedougou and Saraya districts (*2*). Whole blood samples collected from healthcare sites are routinely sent to the World Health Organization Collaborating Center for Arboviruses and Hemorrhagic Fever Viruses at Institut Pasteur de Dakar (Dakar, Senegal) for laboratory analysis of arboviruses, as previously described (*2*,*4*). We report the reemergence of sylvatic dengue virus serotype 2 (DENV-2) in Kedougou, Senegal. The study was conducted according to the guidelines of the Declaration of Helsinki and approved by the National Ethics Committee for Health Research in Senegal (protocol no. SEN20/08, approved April 6, 2020).

Author affiliations: Institut Pasteur de Dakar, Dakar, Senegal (I. Dieng, M. Diarra, B.D. Sadio, B. Sow, A. Gaye, A. Diallo, M. Faye, M.H.D. Ndione, D. Diallo, S. Sankhe, M. Ndiaye, A.A. Sall, G. Fall, Oumar Faye, C. Loucoubar, Ousmane Faye, M. Diallo, M.A. Barry, M.M. Diagne); Ministry of Health Kedougou Medical Region, Kedougou, Senegal (F. Danfakha); Ministry of Health Prevention Department, Dakar (B. Diop); University of Texas Medical Branch, Galveston, Texas, USA (S.C. Weaver)

DOI: https://doi.org/10.3201/eid3004.231301

The Study

A 27-year-old man with arbovirus infection syndrome was admitted to Military Camp in Kedougou, Senegal, in November 2020. We amplified dengue virus (DENV) RNA from serum samples by using a pan-DENV 1-step quantitative reverse transcription PCR (qRT-PCR) (*4*), which confirmed dengue virus infection. Arbovirus surveillance showed 36 additional dengue cases, 27 of which had qRT-PCR–positive samples. An investigation team from Senegal's Ministry of Health and Institut Pasteur de Dakar mobilized in December 2020 and identified 14 recently infected persons out of 42 suspected cases through retrospective tracing of health center patient records. During early December 2020 through late January 2021, a total of 4 additional qRT-PCR–positive and 4 serologically confirmed dengue cases were reported through passive surveillance.

We developed a working case definition as previously described (*5*) for suspected cases (sudden onset of fever with arbovirus symptoms) and confirmed cases (infection confirmed by laboratory methods). We conducted door-to-door case research in housing areas and collected sociodemographic and clinical data to identify infected contacts and implement effective virus spread control alongside preventive entomologic measures to eliminate mosquito breeding sites. We summarized continuous variables as means or medians and dichotomous or categorical variables as percentages with 95% CIs, as previously described (*3*). We used the Kruskal-Wallis test to compare the median ages of negative and confirmed dengue case-patients. When appropriate, we used the Pearson χ^2 or Fisher exact test to compare percentages between categories. A p value <0.05 was considered

[1]These authors contributed equally to this article.

statistically significant. We performed statistical analyses by using Stata 15 software (StataCorp LLC, https://www.stata.com).

During November 2020–February 27, 2021, we collected a total of 300 serum samples from different localities across Kedougou (Figure 1). Overall, DENV infection was found in 59 of 300 (19.6%, 95% CI 15.1%–24.2%) samples, corresponding to 32 qRT-PCR–positive and 27 IgM-positive cases. The highest number of dengue cases was recorded in Saraya health district (n = 18), followed by Bandafassi primary health center (n = 14), Kedougou health district (n = 14), and Military Camp (n = 13) (Figure 1).

Men were more affected by DENV than women; the sex ratio was 5.5:1 for confirmed cases (p = 0.005 by Pearson χ^2 test). The mean age of all patients was 25.5 (SD ±13.8) years; most (47.4%) case-patients were within the 30–45-year age group, followed by the 15–29-year (31.6%) and >45-year (1.7%) age groups. The DENV positivity rate varied significantly according to age group (p = 0.008 by Pearson χ^2 test). Among confirmed dengue cases, the most common symptoms reported were headaches (100%; p = 0.01), followed by myalgia (57.6%) and arthralgia (47.5%) (Table 1). The sylvatic nature of the epidemic, which had potential vectors mainly outside of households, increased exposure risk for young, professionally active men working in areas at the interface of the forestry sector. Early public health measures in Kedougou comprising disinfestation campaigns have substantially reduced the number of mosquitoes in homes; however, the labor force in the region is predominantly male. In numerous countries, the number of reported incident dengue cases systematically showed a male predominance, the causes (biologic, sociodemographic, and cultural) of which deserve further investigations (*6*).

Beside human investigation, we conducted entomologic surveillance during August–November 2020 at 50 sites across 5 land cover classes (forest, barren, savanna, agricultural lands, and villages). We collected 15,937 mosquitoes, encompassing >56 species within 7 genera; >50% were known sylvatic or peridomestic DENV vectors (Table 2) (*7*). No DENV was identified in monospecific mosquito pools, whereas concomitant circulation of yellow fever virus was detected, as previously reported (*2*).

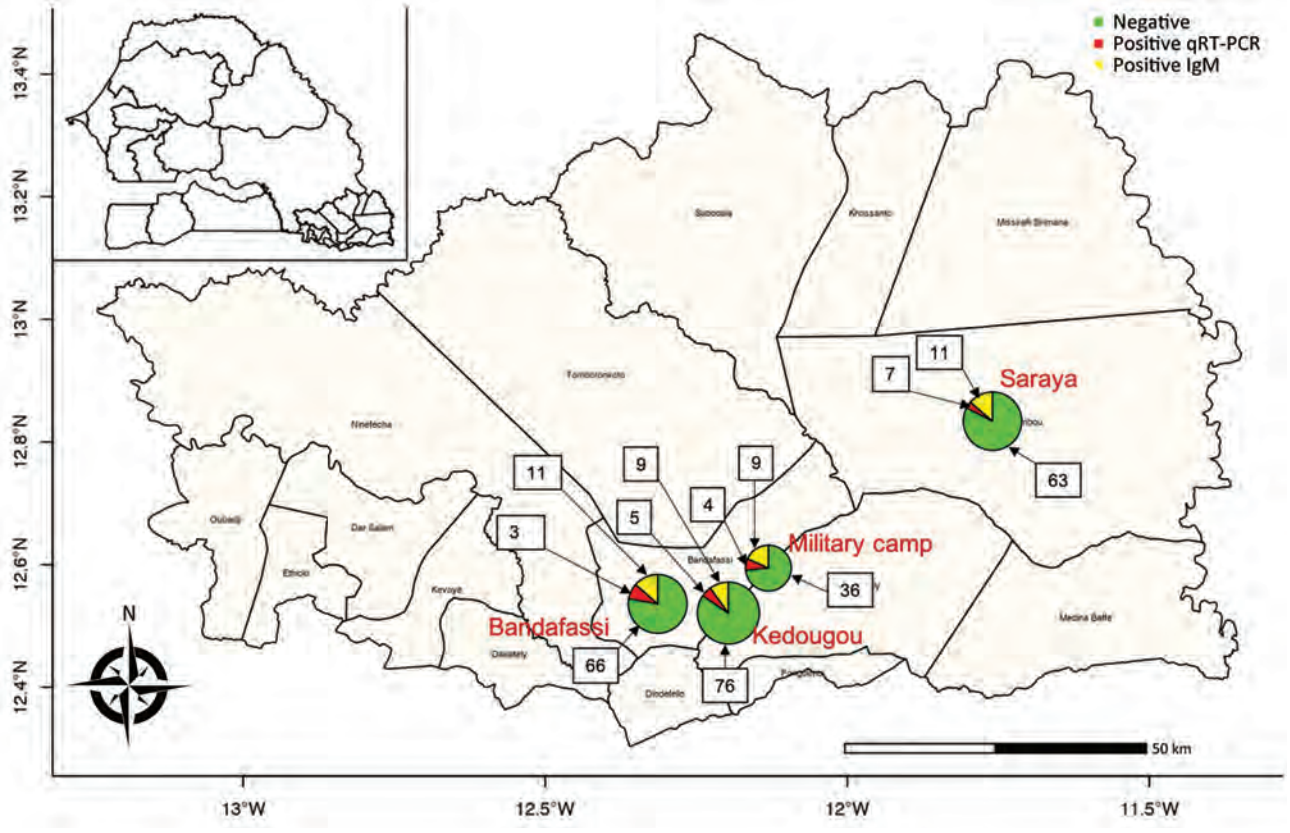

Figure 1. Distribution of reported cases within 4 healthcare centers during the sylvatic dengue outbreak in Kedougou region, Senegal, during November 2020–February 2021. Inset shows the Kedougou region in the southeastern corner of Senegal. Patient samples were positive according to qRT-PCR or dengue virus IgM assays of serum samples. Numbers in squares indicate the number of negative and positive cases. qRT-PCR, quantitative reverse transcription PCR.

Table 1. Epidemiologic and clinical characteristics of suspected and confirmed dengue fever case-patients in study of reemergence of sylvatic DENV serotype 2 in Kedougou, Senegal, 2020*

Patient characteristics	Total, n = 300	DENV negative, n = 241	DENV positive, n = 59	p value
Median age, y (IQR)	25 (14.0–35.0)	24 (14.0–34.0)	29 (18.0–33.0)	0.15†
Age group, y				0.008
<15	75 (25.5)	64 (27.0)	11 (19.3)	
15–29	107 (36.4)	89 (37.6)	18 (31.6)	
30–45	88 (29.9)	61 (25.7)	27 (47.4)	
≥45	24 (8.16)	23 (9.70)	1 (1.7)	
Unknown	6 (2.0)	4 (1.6)	2 (3.4)	
Sex				0.005
F	91 (30.3)	82 (34.0)	9 (15.2)	
M	209 (69.7)	159 (66.0)	50 (84.7)	
Headache				0.01
No	25 (8.3)	25 (10.4)	0 (0.0)	
Yes	275 (91.7)	216 (89.6)	59 (100.0)	
Myalgia				0.20
No	150 (50.0)	125 (52.0)	25 (42.4)	
Yes	150 (50.0)	116 (48.1)	34 (57.6)	
Arthralgia				0.85
No	161 (53.7)	130 (54.0)	31 (52.5)	
Yes	139 (46.3)	111 (46.0)	28 (47.5)	
Asthenia				0.16
No	252 (84.0)	206 (85.5)	46 (78.0)	
Yes	48 (16.0)	35 (14.5)	13 (22.0)	
Abdominal pain				0.82
No	262 (87.3)	211 (87.5)	51 (86.4)	
Yes	38 (12.7)	30 (12.4)	8 (13.6)	
Retroorbital pain				0.77
No	280 (93.3)	224 (93.0)	56 (95.0)	
Yes	20 (6.7)	17 (7.0)	3 (5.0)	
Vomiting				0.34
No	189 (63.0)	155 (64.3)	34 (57.6)	
Yes	111 (37.0)	86 (35.7)	25 (42.4)	
Investigated health facilities/regions				0.40
Kedougou health district	90 (30.0)	76 (31.5)	14 (23.7)	
Saraya health district	81 (27.0)	63 (26.1)	18 (30.5)	
Bandafassi PHC	80 (26.7)	66 (27.4)	14 (24.0)	
Military Camp	49 (16.3)	36 (15.0)	13 (22.0)	

*Values are no. (%) except as indicated. DENV, dengue virus; IQR, interquartile range; PHC, primary health center.
†p value was determined by using the Kruskal-Wallis test; all other p values were determined by using χ^2 or Fisher exact tests.

Even if the same mosquitoes were screened for both viruses, larger mosquito pool sizes might be used in some tests, resulting in loss of sensitivity, which could explain the absence of DENV detection in mosquitoes during the period.

We performed a molecular serotyping assay using specific oligonucleotide primers (Appendix Table 1, https://wwwnc.cdc.gov/EID/article/30/4/23-1301-App1.pdf) (*8*) for the pan-DENV qRT-PCR–positive human samples. We found no positive results, suggesting that the strains might belong to the DENV-2 sylvatic genotype, as previously described (*9*). We sequenced 8 samples that had PCR cycle threshold values <30 by using an amplicon-based approach on a MinION MK1C instrument (Oxford Nanopore Technologies, https://www.nanoporetech.com). We used 2 sylvatic DENV-2–specific primers pools to amplify the entire coding region of the genome. We prepared libraries by using the Rapid Barcoding Kit 96 (Oxford Nanopore Technologies) and loaded them onto an R9 flow cell. We performed data analysis as previously described (*8*). We obtained 3 high-quality sequences from 3 samples (Appendix Table 2) and aligned the consensus whole genomes with a dataset of 294 DENV-2 genotype sequences (Appendix Table 3) by using MAFFT (*10*). We built a maximum-likelihood phylogenetic tree by using IQ-TREE with default parameters and 1,000 bootstrap iterations (*11*). Phylogenetic analysis confirmed that sequenced strains belonged to the sylvatic

Table 2. Mosquito species collected during August–November 2020 in study of reemergence of sylvatic dengue virus serotype 2 in Kedougou, Senegal, 2020

Species	No. (%)
Aedes dalzieli	3,559 (22.3)
Aedes furcifer	2,332 (14.6)
Aedes aegypti	1,298 (8.1)
Aedes vittatus	971 (6.1)
Aedes luteocephalus	766 (4.8)
Aedes taylori	330 (2.1)
Aedes africanus	279 (1.8)
Others	6,402 (40.2)
Total	15,937 (100)

DENV-2 genotype and were closely related to a strain identified from a traveler returning from Guinea-Bissau in 2009 (*12*) (Figure 2). In 2021, a sylvatic DENV-2 infection was reported in Kolda in southern Senegal, which is near the border with Guinea-Bissau (*9*).

Conclusions

Although DENV in Senegal has multiple serotypes (*13*), we show that sylvatic strains are still circulating and can cause large outbreaks. Our results support previous research suggesting that sylvatic strains infecting

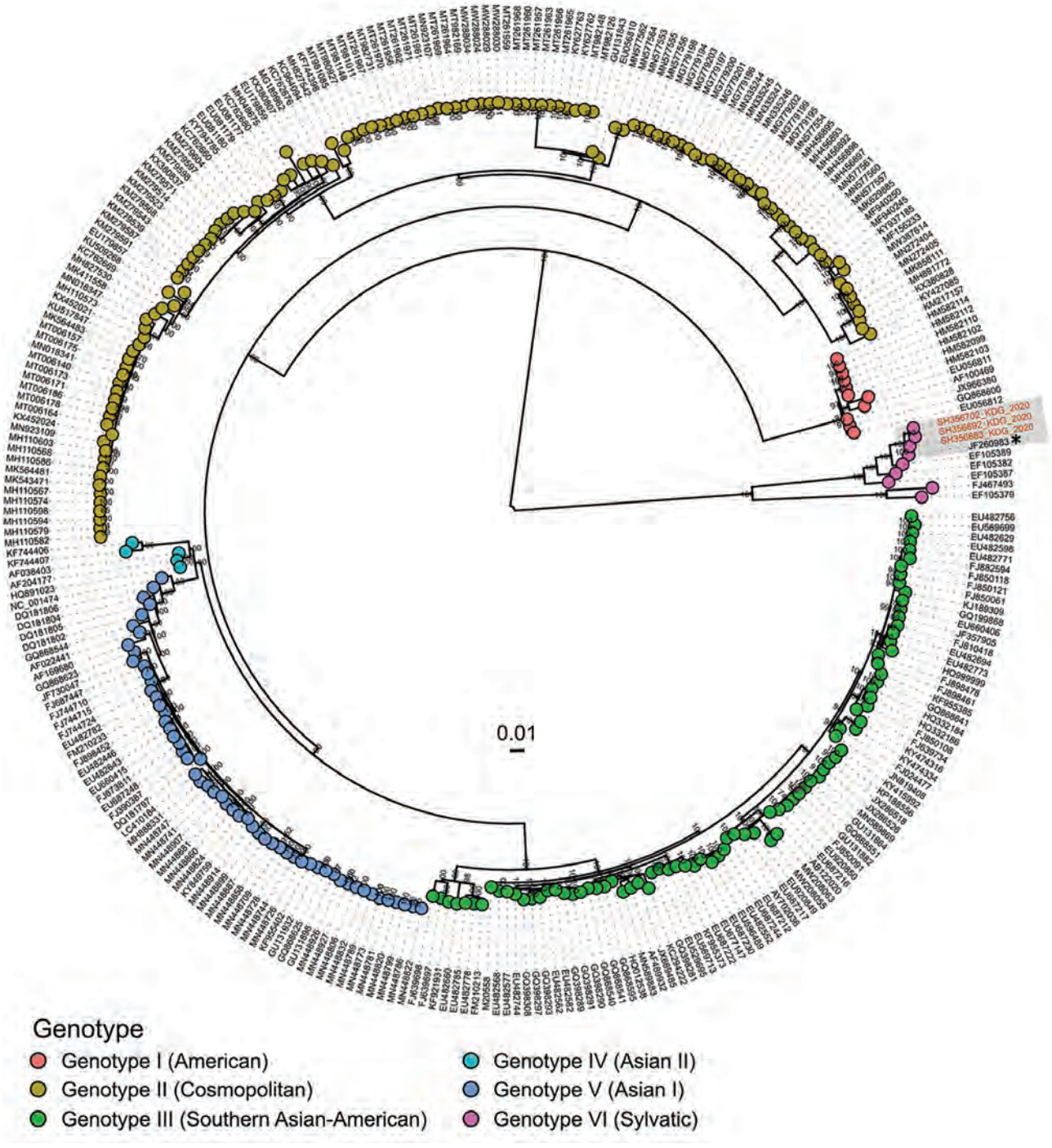

Figure 2. Phylogenetic analysis of dengue virus genomes in study of reemergence of sylvatic dengue virus serotype 2 in Kedougou, Senegal, 2020. Maximum-likelihood tree shows the relationships between sequenced dengue virus strains from the outbreak in Kedougou (red text) and sequences obtained from GenBank. Sequenced strains in this study belong to the sylvatic dengue virus serotype 2 genotype and are closely related to a sequence obtained in 2009 in Guinea-Bissau (asterisk).

humans might not require additional virus adaptation (*14*) but could reemerge in urban transmission cycles. Those strains should be considered as agents with epidemic potential, especially in areas such as Kedougou, where the ecosystem combines humans, nonhuman primates, and primatophilic mosquitoes (*7*,*15*). Large-scale genomic surveillance is needed, and molecular diagnostic tools should be updated for effective diagnosis and prevention of DENV infections.

Acknowledgments

We thank the healthcare workers from the Senegal Ministry of Health for their investment in outbreak management and the teams from different research departments within the Institut Pasteur de Dakar for their dedication and support in case investigations and diagnostics.

This work was funded by the US National Institutes of Health West African Center for Emerging Infectious Diseases (grant no. U01AI151801-01), the Pasteur International Center for Research on Emerging Infectious Diseases (grant no. U01AI151758), and the Africa Centers for Disease Control and Prevention Pathogen Genomics Initiative funds (CARES grant no. 4306-22-EIPHLSS-GENOMICS).

About the Author

Mr. Dieng is a research scientist in the Virology Department at the Institut Pasteur de Dakar. His research interests focus on arboviruses and hemorrhagic fever viruses, especially on the molecular epidemiology of dengue virus.

References

1. Sow A, Loucoubar C, Diallo D, Faye O, Ndiaye Y, Senghor CS, et al. Concurrent malaria and arbovirus infections in Kedougou, southeastern Senegal. Malar J. 2016;15:47. https://doi.org/10.1186/s12936-016-1100-5
2. Diagne MM, Ndione MHD, Gaye A, Barry MA, Diallo D, Diallo A, et al. Yellow fever outbreak in eastern Senegal, 2020–2021. Viruses. 2021;13:1475. https://doi.org/10.3390/v13081475
3. Barry MA, Arinal F, Talla C, Hedible BG, Sarr FD, Ba IO, et al. Performance of case definitions and clinical predictors for influenza surveillance among patients followed in a rural cohort in Senegal. BMC Infect Dis. 2021;21:31. https://doi.org/10.1186/s12879-020-05724-x
4. Sow A, Faye O, Diallo M, Diallo D, Chen R, Faye O, et al. Chikungunya outbreak in Kedougou, southeastern Senegal in 2009–2010. Open Forum Infect Dis. 2017;5:ofx259. https://doi.org/10.1093/ofid/ofx259
5. Dieng I, Barry MA, Talla C, Sow B, Faye O, Diagne MM, et al. Analysis of a dengue virus outbreak in Rosso, Senegal 2021. Trop Med Infect Dis. 2022;7:420. https://doi.org/10.3390/tropicalmed7120420
6. Anker, M.; Arima, Y. Male-female differences in the number of reported incident dengue fever cases in six Asian countries. Western Pac Surveill Response J. 2011;2:17–23. https://doi.org/10.5365/WPSAR.2011.2.1.002
7. Diallo M, Ba Y, Sall AA, Diop OM, Ndione JA, Mondo M, et al. Amplification of the sylvatic cycle of dengue virus type 2, Senegal, 1999–2000: entomologic findings and epidemiologic considerations. Emerg Infect Dis. 2003;9:362–7. https://doi.org/10.3201/eid0903.020219
8. Dieng I, Cunha M, Diagne MM, Sembène PM, Zanotto PMA, Faye O, et al. Origin and spread of the dengue virus type 1, genotype V in Senegal, 2015–2019. Viruses. 2021;13:57. https://doi.org/10.3390/v13010057
9. Dieng I, Sagne SN, Ndiaye M, Barry MA, Talla C, Mhamadi M, et al. Detection of human case of dengue virus 2 belonging to sylvatic genotype during routine surveillance of fever in Senegal, Kolda 2021. Front Virol. 2022;2:1050880. https://doi.org/10.3389/fviro.2022.1050880
10. Katoh K, Rozewicki J, Yamada KD. MAFFT online service: multiple sequence alignment, interactive sequence choice and visualization. Brief Bioinform. 2019;20:1160–6. https://doi.org/10.1093/bib/bbx108
11. Nguyen LT, Schmidt HA, von Haeseler A, Minh BQ. IQ-TREE: a fast and effective stochastic algorithm for estimating maximum-likelihood phylogenies. Mol Biol Evol. 2015;32:268–74. https://doi.org/10.1093/molbev/msu300
12. Franco L, Palacios G, Martinez JA, Vázquez A, Savji N, De Ory F, et al. First report of sylvatic DENV-2–associated dengue hemorrhagic fever in West Africa. PLoS Negl Trop Dis. 2011;5:e1251. https://doi.org/10.1371/journal.pntd.0001251
13. Dieng I, Ndione MHD, Fall C, Diagne MM, Diop M, Gaye A, et al. Multifoci and multiserotypes circulation of dengue virus in Senegal between 2017 and 2018. BMC Infect Dis. 2021;21:867. https://doi.org/10.1186/s12879-021-06580-z
14. Vasilakis N, Holmes EC, Fokam EB, Faye O, Diallo M, Sall AA, et al. Evolutionary processes among sylvatic dengue type 2 viruses. J Virol. 2007;81:9591–5. https://doi.org/10.1128/JVI.02776-06
15. Diallo D, Chen R, Diagne CT, Ba Y, Dia I, Sall AA, et al. Bloodfeeding patterns of sylvatic arbovirus vectors in southeastern Senegal. Trans R Soc Trop Med Hyg. 2013;107:200–3. https://doi.org/10.1093/trstmh/trs095

Address for correspondence: Moussa Moïse Diagne, Virology Department, Institut Pasteur de Dakar, 36 Avenue Pasteur, BP.220, Dakar, Senegal; email: MoussaMoise.DIAGNE@pasteur.sn

Novel Oral Poliovirus Vaccine 2 Safety Evaluation during Nationwide Supplemental Immunization Activity, Uganda, 2022

Farrell A. Tobolowsky, Fred Nsubuga, Zunera Gilani, Annet Kisakye, Helen Ndagije, Daniel Kyabayinze, Jane F. Gidudu

Given its enhanced genetic stability, novel oral poliovirus vaccine type 2 was deployed for type 2 poliovirus outbreak responses under World Health Organization Emergency Use Listing. We evaluated the safety profile of this vaccine. No safety signals were identified using a multipronged approach of passive and active surveillance.

To eliminate the risk for vaccine-related paralysis, live attenuated Sabin-strain oral poliovirus vaccine type 2 was withdrawn from routine use in a globally coordinated manner in 2016. However, because of decreased population immunity (*1*) and pathogenic reversion of vaccine virus persisting in communities or introduced during outbreak response vaccinations, circulating vaccine-derived poliovirus type 2 outbreaks have emerged across the World Health Organization (WHO) African Region, particularly during 2019–2021 (*2*–*4*). In November 2020, to reduce the risk for new type 2 emergences, WHO granted Emergency Use Listing of a more genetically stable vaccine, novel oral poliovirus vaccine type 2 (nOPV2) (BioFarma, https://www.biofarma.co.id). Initial use began in March 2021 in a limited number of qualifying countries and subsequently expanded (*3*,*5*; https://extranet.who.int/pqweb/vaccines/polio-vaccine-novel-oral-nopv-monovalent-type-2).

Author affiliations: Centers for Disease Control and Prevention, Atlanta, Georgia, USA (F.A. Tobolowsky, Z. Gilani, J.F. Gidudu); African Field Epidemiology Network, Kampala, Uganda (F. Nsubuga); Uganda National Expanded Program on Immunizations, Kampala (F. Nsubuga, D. Kyabayinze); World Health Organization, Kampala (A. Kisakye); National Drug Authority, Kampala (H. Ndagije)

DOI: https://doi.org/10.3201/eid3004.231361

Full vaccine licensure requires robust safety data and postdeployment monitoring (*6*). Although initial phase 1 and 2 clinical trials demonstrated that nOPV2 is well tolerated, those studies enrolled a small number of persons and were unlikely to detect rare adverse events; safety data were only collected actively for 7 days after vaccination (*7*,*8*). During initial use, passive and active safety surveillance implementation was not standardized, and data gaps persisted. In October 2021, after early promising safety data in large-scale use, nOPV2 rollout was expanded as recommended by the WHO Strategic Advisory Group of Experts on Immunization (*9*).

In response to 2 confirmed detections of circulating vaccine-derived poliovirus type 2 in Uganda in November 2021, a nationwide supplemental immunization activity using nOPV2 was planned for children <5 years of age. To further clarify the safety profile of nOPV2, we designed a multipronged safety evaluation using the passive surveillance system in Uganda, active hospital-based surveillance, acute flaccid paralysis (AFP) surveillance, and a cohort event monitoring system to monitor for adverse events following immunization (AEFI) and adverse events of special interest (AESI).

The Study

We conducted a safety evaluation in Uganda after the first round of the nationwide supplemental immunization activity in January 2022. We used the country's passive safety surveillance system to identify AEFI from any data source (e.g., telephone call, short messaging service, Open Data Kit, District Health Information System 2). We conducted active hospital-based surveillance for AESI in 18

sentinel sites. We included events that occurred within 42 days after vaccine administration (*10*). We defined AEFI as any untoward medical occurrence after immunization that did not necessarily have a causal relationship with the use of the vaccine (*11*). We defined AESI as prespecified medically significant events that have the potential to be causally associated with a vaccine product that needs to be carefully monitored and confirmed by further special studies (https://polioeradication.org/wp-content/uploads/2022/06/nOPV2-AESI-surveillance.pdf). AESI included anaphylaxis, aseptic meningitis or encephalitis, acute disseminated encephalomyelitis, Guillain-Barré syndrome/Fisher's syndrome, myelitis/transverse myelitis, AFP, and unexplained deaths. We used the Brighton Collaboration case definitions for validation of cases (https://brightoncollaboration.us/category/pubs-tools/case-definitions) before causality assessment by an independent national AEFI committee. We recorded vaccination status by finger marking or verbal recall for events and cases.

AFP surveillance is ongoing in Uganda through passive, active, and community-based systems. AFP was defined as limb weakness in a child <15 years of age reported during and after the nOPV2 campaign to a surveillance officer or clinician; suspected cases were investigated and adjudicated by the national polio expert committee. We included AFP cases in children <5 years of age with symptom onset ≤42 days after nOPV2 administration.

We developed a cohort event monitoring system to prospectively monitor children for any AEFI occurring after vaccine administration. We systematically selected households in designated enumeration areas to create a nationally representative sample. We offered enrollment for all eligible children in each household; eligible children were those 0–59 months of age who had been vaccinated with the first dose of nOPV2 in the supplemental immunization activity, who would reside in the selected community for ≥42 days after the initial nOPV2 vaccination, who had written informed caregiver consent, who demonstrated no acute signs or symptoms at the time of vaccination, and who had a caregiver with access to a telephone. We followed vaccinated children through telephone interviews with caregivers starting on the day of vaccine administration (day 0) and on days 3, 7, 14, 28, and 42. Caregivers reported any signs or symptoms by onset date; healthcare-seeking behavior and hospitalizations were recorded. We combined and harmonized data from all 4 surveillance systems to identify any duplication.

We defined a nonspecified serious event as an event that resulted in death, required hospitalization, or resulted in persistent or major disability (*11*). For any serious event, clinicians and healthcare workers conducted detailed investigations, and the National AEFI Causality Committee of country experts used the clinical data provided to classify each event for association into 5 categories, according to global guidelines: vaccine product–related, vaccine quality–related, immunization error–related, immunization anxiety–related, indeterminate, or coincidental (*12*). We completed descriptive data analyses using Excel (Microsoft, https://www.microsoft.com) and SAS version 9.4 (SAS Institute, Inc., https://www.sas.com). The protocol received a nonresearch determination by the Uganda AIDS Support Organization Research Ethics Committee and the Uganda National Council of Science and Technology; this activity was reviewed by the Centers for Disease Control and Prevention and was conducted consistent with applicable federal law and center policy (see e.g., 45 C.F.R. part 46.102(l)(2), 21 C.F.R. part 56; 42 U.S.C. §241(d); 5 U.S.C. §552a; 44 U.S.C. §3501 et seq.).

In the first round of the nationwide vaccination campaign in Uganda during January 14–21, 2022, a total of 9,768,697 doses of nOPV2 were administered to children <5 years of age. During January 14–March 11, 2022, an initial total of 1,159 AEFI were identified across all 4 safety surveillance systems (Table). Passive surveillance identified 43 AEFI; 2 (5%) of those events were serious. Through

Table. Adverse events identified by all surveillance systems after nOPV2 administration, Uganda, 2022*

Event	Total	Minor AEFI†	Serious AEFI
Passive surveillance	43	41	2
Acute flaccid paralysis surveillance	159‡	78§	81
AESI surveillance	5	NA	5
Cohort event monitoring	952	930	22
Total	1,159	1,049	110

*AEFI, adverse events following immunization; AESI, adverse events of special interest; nOPV2, novel oral poliovirus vaccine type 2.
†AEFI are defined as any untoward medical occurrence which follows immunization that does not necessarily have a causal relationship with the usage of the vaccine.
‡Two duplicates were identified from AFP surveillance (deduplicated total = 157) that were also identified through active hospital-based surveillance.
§After investigation, 78 AFP cases were downgraded by the National AEFI Committee to nonserious cases.

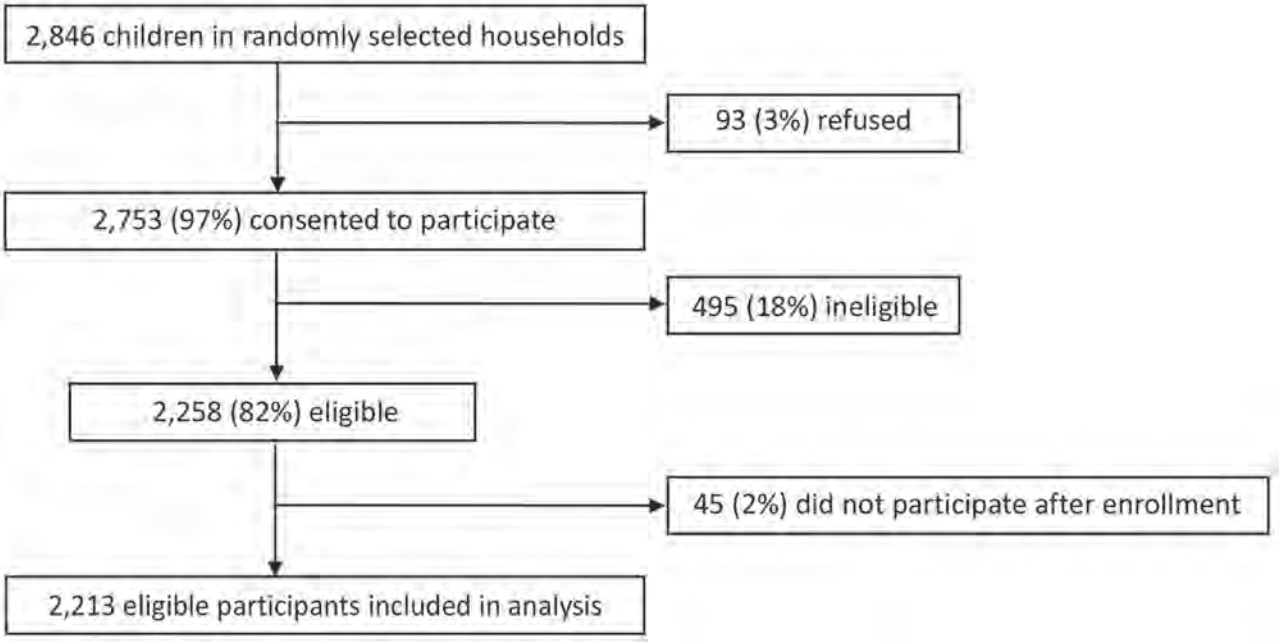

Figure. Cohort event monitoring enrollment after novel oral poliovirus vaccine type 2 administration, Uganda, 2022. Ineligible children included those who were >59 months of age, demonstrated acute signs or symptoms at the time of vaccination, were without a caretaker who had access to a phone, did not reside in the community for ≥42 days after vaccination, were without a caretaker staying with the child for ≥42 days, or did not complete enrollment, as well as any other unspecified reason.

prospective active hospital-based surveillance, 8 AESI were detected; in 5 (62.5%) of those events, patients reported that they had received nOPV2 vaccination within 42 days. Among 159 AFP cases in children <5 years of age identified through the country's active AFP surveillance, 128 (80.5%) patients reported nOPV2 receipt, and 81 (50.9%) cases were defined as serious events after investigation. Cohort event monitoring enrolled 2,213 participants (Figure); during follow-up, we found 952 AEFI, of which 22 (2%) were serious. Of the 110 conditions that were classified as serious, 6 (5.5%) were classified into the vaccine product–related reactions category, diagnosed as gastroenteritis (n = 3), acute disseminated encephalomyelitis (n = 1), encephalitis (n = 1), and acute febrile illness (n = 1).

Conclusions

Through the multipronged surveillance system, ≈6% of serious conditions were classified by the causality committee as vaccine product–related reactions; no concerning safety signals were noted. Previous data reported from countries using nOPV2 support this finding; a similar proportion (60/1529; 4%) of events were classified as vaccine product–related reactions, and no major safety concerns have been identified outside of this evaluation in phase 3 trials (*13*–*15*).

The first limitation of this evaluation is that AEFI identified through passive surveillance were likely underreported. Conversely, soliciting events through caregivers during cohort event monitoring and active AFP surveillance might have led to overreporting. Recall bias could have occurred with reported vaccination status and in cohort event monitoring, especially with later timepoints after vaccination. Last, the COVID-19 pandemic led to delays in implementation, investigations, and timely review of conditions by the causality committee.

Our evaluation adds to the growing evidence that no safety signals are associated with nOPV2 use among persons <5 years of age. With a robust multipronged approach, safety surveillance can be strengthened for vaccines with limited safety profiles that are introduced in resource-limited settings during public health emergencies, especially while awaiting full licensure.

About the Author

Dr. Tobolowsky is a Future Leaders in Infections and Global Health Threats (FLIGHT) officer and medical epidemiologist in the Global Immunization Division, Global Health Center, Centers for Disease Control and Prevention. Her primary research interests include the epidemiology of and outbreak response for communicable diseases of public health importance.

References

1. Cooper LV, Bandyopadhyay AS, Gumede N, Mach O, Mkanda P, Ndoutabé M, et al. Risk factors for the spread of vaccine-derived type 2 polioviruses after global withdrawal of trivalent oral poliovirus vaccine and the effects of outbreak responses with monovalent vaccine: a retrospective analysis of surveillance data for 51 countries in Africa. Lancet Infect Dis. 2022;22:284–94. https://doi.org/10.1016/S1473-3099(21)00453-9
2. Gray EJ, Cooper LV, Bandyopadhyay AS, Blake IM, Grassly NC. The origins and risk factors for serotype-2 vaccine-derived poliovirus (VDPV2) emergences in Africa during 2016–2019. J Infect Dis. 2023;228:80–8. https://doi.org/10.1093/infdis/jiad004
3. Alleman MM, Jorba J, Greene SA, Diop OM, Iber J, Tallis G, et al. Update on vaccine-derived poliovirus outbreaks—worldwide, July 2019–February 2020. MMWR Morb Mortal Wkly Rep. 2020;69:489–95. https://doi.org/10.15585/mmwr.mm6916a1
4. Alleman MM, Jorba J, Henderson E, Diop OM, Shaukat S, Traoré MA, et al. Update on vaccine-derived poliovirus outbreaks—worldwide, January 2020–June 2021. MMWR Morb Mortal Wkly Rep. 2021;70:1691–9. https://doi.org/10.15585/mmwr.mm7049a1
5. Bigouette JP, Henderson E, Traoré MA, Wassilak SGF, Jorba J, Mahoney F, et al. Update on vaccine-derived poliovirus outbreaks—worldwide, January 2021–December 2022. MMWR Morb Mortal Wkly Rep. 2023;72:366–71. https://doi.org/10.15585/mmwr.mm7214a3
6. Macklin GR, Peak C, Eisenhawer M, Kurji F, Mach O, Konz J, et al. Enabling accelerated vaccine roll-out for Public Health Emergencies of International Concern (PHEICs): Novel Oral Polio Vaccine type 2 (nOPV2) experience. Vaccine. 2023;41 Suppl 1:A122–A7.
7. Van Damme P, De Coster I, Bandyopadhyay AS, Revets H, Withanage K, De Smedt P, et al. The safety and immunogenicity of two novel live attenuated monovalent (serotype 2) oral poliovirus vaccines in healthy adults: a double-blind, single-centre phase 1 study. Lancet. 2019;394:148–58. https://doi.org/10.1016/S0140-6736(19)31279-6
8. Zaman K, Bandyopadhyay AS, Hoque M, Gast C, Yunus M, Jamil KM, et al. Evaluation of the safety, immunogenicity, and faecal shedding of novel oral polio vaccine type 2 in healthy newborn infants in Bangladesh: a randomised, controlled, phase 2 clinical trial. Lancet. 2023;401:131–9. https://doi.org/10.1016/S0140-6736(22)02397-2
9. Global Polio Eradication Initiative. Independent experts advise move to next use phase for novel oral polio vaccine type 2. 2021 Oct 11 [cited 2023 Mar 7]. https://polioeradication.org/news-post/independent-experts-advise-transition-to-next-use-phase-for-novel-oral-polio-vaccine-type-2-nopv2/
10. Rowhani-Rahbar A, Klein NP, Dekker CL, Edwards KM, Marchant CD, Vellozzi C, et al.; Risk Interval Working Group of the Clinical Immunization Safety Assessment Network. Biologically plausible and evidence-based risk intervals in immunization safety research. Vaccine. 2012;31:271–7. https://doi.org/10.1016/j.vaccine.2012.07.024
11. World Health Organization. Adverse events following immunization (AEFI) [cited 2023 May 26]. https://iris.who.int/bitstream/handle/10665/191391/a87773_eng.pdf
12. World Health Organization. Causality assessment of an adverse event following immunization (AEFI): user manual for the revised WHO classification, 2nd ed., 2019 update [cited 2023 Apr 10]. https://iris.who.int/bitstream/handle/10665/340802/9789241516990-eng.pdf
13. Global Polio Eradication Initiative. GACVS (Global Advisory Committee on Vaccine Safety) sub-committee on novel type 2 oral poliovirus vaccine (nOPV2) safety assessment of nOPV2 safety data. 2023 Jan 24 [cited 2023 Oct 1]. https://polioeradication.org/wp-content/uploads/2023/03/GACVS-nOPV2-committee-meeting-20230124.pdf
14. World Health Organization. Safety profile of nOPV2 vaccine [cited 2024 Jan 10]. https://www.who.int/groups/global-advisory-committee-on-vaccine-safety/topics/poliovirus-vaccines
15. Rivera Mejía L, Peña Méndez L, Bandyopadhyay AS, Gast C, Mazara S, Rodriguez K, et al. Safety and immunogenicity of shorter interval schedules of the novel oral poliovirus vaccine type 2 in infants: a phase 3, randomised, controlled, non-inferiority study in the Dominican Republic. Lancet Infect Dis. 2023;S1473-3099(23)00519-4. https://doi.org/10.1016/S1473-3099(23)00519-4

Address for correspondence: Farrell A. Tobolowsky, Centers for Disease Control and Prevention, 1600 Clifton Rd NE, Mailstop H21-6, Atlanta, GA 30329-4018, USA; email: oqk3@cdc.gov

Phylogenetic Characterization of *Orthohantavirus dobravaense* (Dobrava Virus)

Mert Erdin, Ceylan Polat, Teemu Smura, Sercan Irmak, Ortac Cetintas, Muhsin Cogal, Faruk Colak, Ahmet Karatas, Mustafa Sozen, Ferhat Matur, Olli Vapalahti, Tarja Sironen, Ibrahim Mehmet Ali Oktem

We report complete coding sequences of *Orthohantavirus dobravaense* (Dobrava virus) Igneada strains and phylogenetic characterization of all available complete coding sequences. Our analyses suggested separation of host-dependent lineages, followed by geographic clustering. Surveillance of orthohantaviruses using complete genomes would be useful for assessing public health threats from Dobrava virus.

Orthohantaviruses are globally distributed. Until now, they have been detected in rodents, insectivores, and bats. Rodentborne orthohantaviruses, which are associated with human diseases, are divided into 3 major groups, murid-borne, non–*Arvicolinae cricetidae*-borne, and *Arvicolinae*-borne viruses, according to their phylogeny and host species (*1*). Murid-borne orthohantavirus species, such as *Orthohantavirus dobravaense* (Dobrava virus; DOBV) and *O. hantanense* (Hantaan virus), which are associated with hemorrhagic fever with renal syndrome in humans, are distributed in the Old World (*1*,*2*). Non–*A. cricetidae*-borne orthohantaviruses, such as *O. bayoui* (Bayou virus) or *O. sinnombreense* (Sin Nombre virus), which cause hantavirus cardiopulmonary syndrome in human infections, are found in the Americas (*1*,*2*). *Arvicolinae*-borne orthohantaviruses, such as *O. puumalaense* (Puumala virus; PUUV) or *O. prospectense* (Prospect Hill virus), are either nonpathogenic or mildly pathogenic for humans (*1*,*2*) and are found in both the Old and New Worlds; *Arvicolinae*-borne strains are thought to serve as an evolutionary bridge between the other 2 groups.

Orthohantaviruses can be transmitted to humans through inhalation of virus-containing aerosols of rodent excreta or direct contact with reservoir hosts (*2*). In European Union/European Economic Area countries, the numbers of collective orthohantavirus case reports fluctuated between 1,647 and 4,249 cases during 2016–2020 (*3*). For instance, in 2020, PUUV virus caused 1,204 cases, Hantaan virus 14 cases, and DOBV 7 cases from the reports that confirmed laboratory information available for the causative viruses. The highest number of cases of hemorrhagic fever with renal syndrome have been detected in southeastern Europe, with 2,375 cases reported in the Balkan region during 1952–2012, most caused by PUUV or DOBV (*3*,*4*). DOBV-positive rodents have recently been found in northeastern Italy, suggesting potential geographic expansion of this clade (*5*).

Surveillance studies in rodent populations are essential for understanding the dynamics of fluctuations. Earlier studies have shown that geographic barriers might play a role in genetic diversity and clade separation among DOBV (*6*,*7*). Also, obtaining whole-genome sequences is a crucial step in understanding potential viral genetic determinants of phenotypic changes that might affect disease severity among these viruses. We report complete coding sequences of *O. dobravaense* Igneada strain and phylogenetic characterization of all available complete coding sequences of DOBV.

The Study

DOBV has caused human cases and outbreaks in the northern coastal region of Turkey (*8*–*12*). In a previous study, DOBV seropositivity and RNA positivity were discovered in rodents captured in Kirklareli Province in Eastern Thrace in Turkey, and phylogenetic analysis based on partial DOBV genomes

Author affiliations: University of Helsinki, Helsinki, Finland (M. Erdin, T. Smura, O. Vapalahti, T. Sironen); Hacettepe University, Ankara, Turkey (C. Polat); Balıkesir University, Balıkesir, Turkey (S. Irmak); Bulent Ecevit University, Zonguldak, Turkey (O. Cetintas, M. Cogal, F. Colak, M. Sozen); Ömer Halisdemir University, Niğde, Turkey (A. Karatas); Dokuz Eylul University, Izmir, Turkey (F. Matur, I.M.A. Oktem)

DOI: https://doi.org/10.3201/eid3004.230912

suggested that DOBV strains from Igneada, Turkey, are closely related to strains from Balkan countries (*13*). To understand the phyloepidemiologic distribution of DOBV, we sequenced complete coding regions of DOBV Igneada strains (GenBank accession nos. MW055917–9) from 1 archived sample that had been partially sequenced in a previous study (*13*); we compared results from the phylogenetic analyses with all available complete DOBV coding sequences in GenBank. Because of the limited number (n = 16) of complete DOBV coding sequences for all 3 segments currently available in GenBank, in addition to 55 complete small (S), 25 medium (M), and 16 large (L) sequences, we also analyzed a larger dataset of partial S-segment sequences (Appendix, https://wwwnc.cdc.gov/EID/article/30/4/23-0912-App1.pdf).

Phylogenetic analyses (Figure 1, panel A; Appendix Figure 1) and pairwise nucleotide identities (Appendix Figure 2) suggested 8 major clusters, designated by their main distribution ranges: Mediterranean, Sochi, Saaremaa, Central Europe, Germany, Rusne Island, Lithuania, and Russia. Consistent with a previous study (*13*), the DOBV Igneada strains sequenced in this study grouped together with strains from the cluster from the Mediterranean region. Of note, most human DOBV cases were from this region (*14*). The Mediterranean clade is further

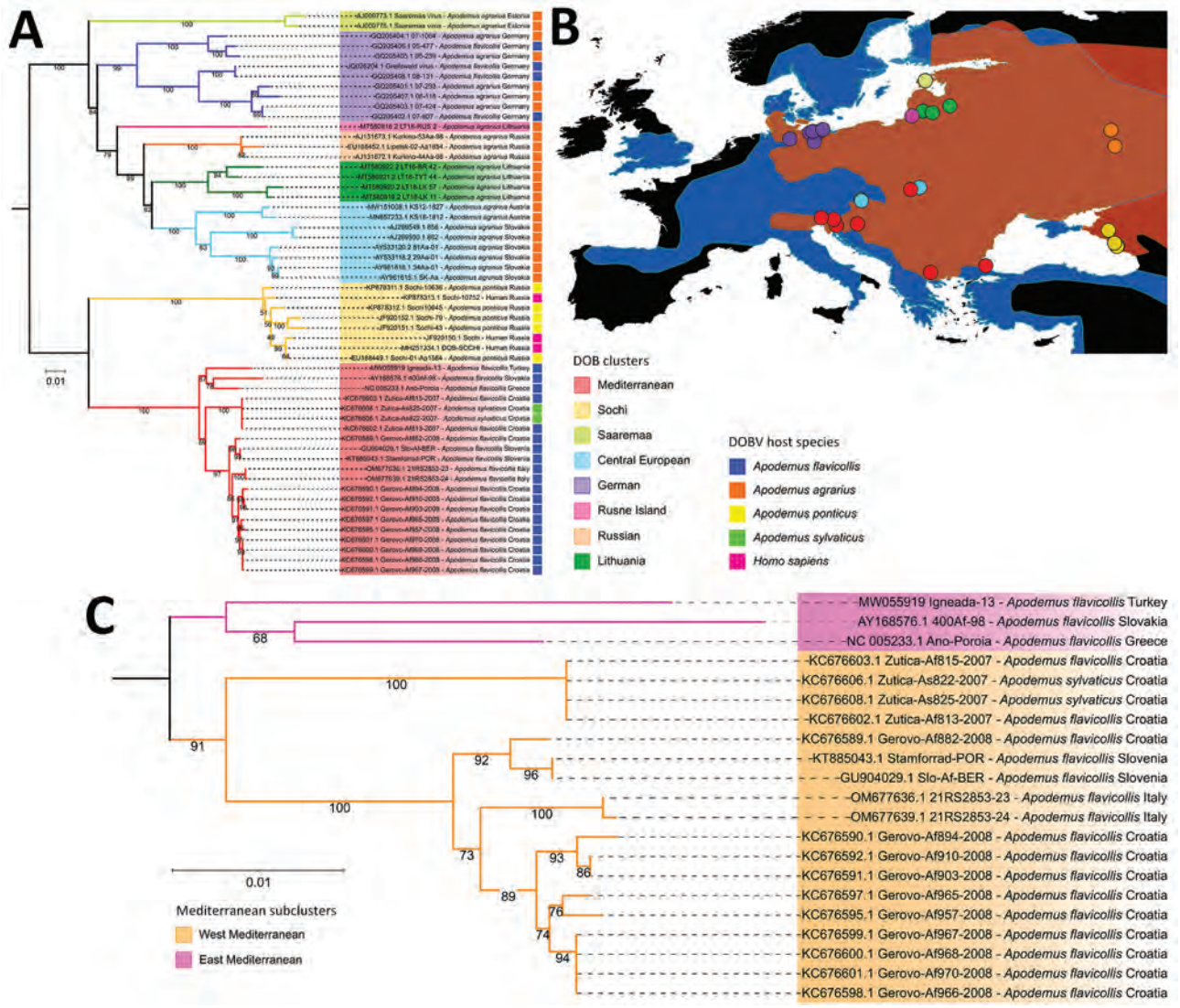

Figure 1. Phylogenetic characterization of DOBV combined with reservoir host and geographical distribution data. A) Maximum-likelihood tree based on all available complete DOBV sequences constructed using a transition plus empirical base frequencies plus gamma 4 substitution model. Colors indicate major clusters and hosts from which sequences were obtained. B) Distribution map of 2 major DOBV reservoir hosts, *Apodemus flavicollis* (blue) and *A. agrarius* (orange) mice, and their overlapping distribution zones. Solid circles indicate locations of complete sequences used in maximum-likelihood tree . C) Pruned version of the tree in panel A showing the division of the Mediterranean cluster into West and East Mediterranean subclusters. DOBV, Dobrava virus (*Orthohantavirus dobravaense*).

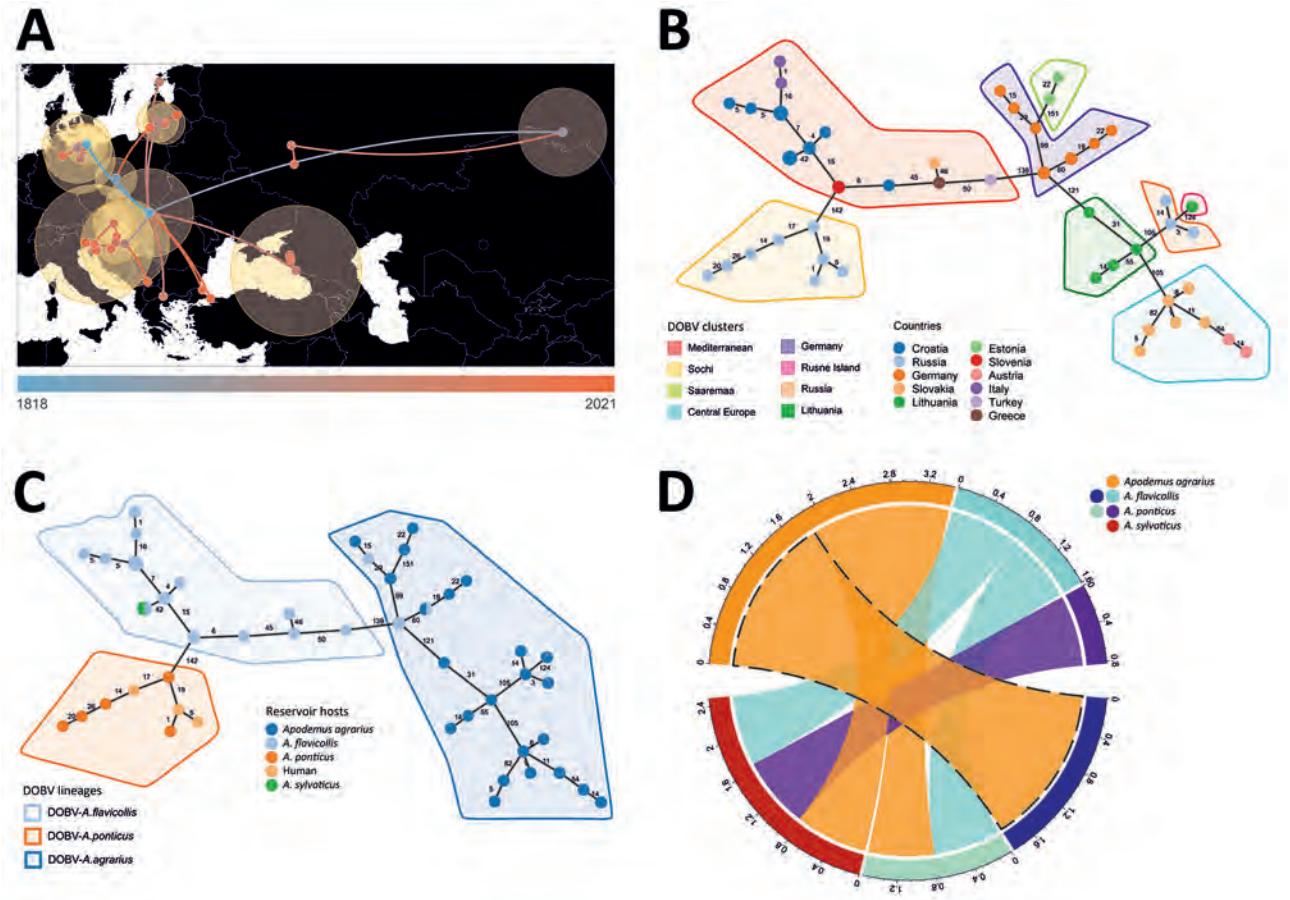

Figure 2. Host switching, phylogeographic reconstruction, and phylogenetic characterization of DOBV according to Bayesian analysis and minimum spanning tree constructions. A) Phylogeographic reconstruction of DOBV in discrete space. Each node is colored according to the estimated year of discovery, from the earliest (blue) to the latest (orange). Yellow shaded circles show the relative intensity of local viruses spread in the covered area. B) Minimum spanning tree showing the geographical cluster separation. C) Minimum spanning tree suggesting 3 major lineages according to reservoir host species. D) Chord diagram representing host switching rates of DOBV between 4 rodent species: *Apodemus flavicollis* (yellow-necked mouse), *A. agrarius* (striped field mouse), *A. ponticus* (Black Sea field mice), and *A. sylvaticus* (wood mice). DOBV, Dobrava virus (*Orthohantavirus dobravaense*).

regionally separated into West and East Mediterranean subclades (Figure 1, panel C). The West Mediterranean subclade consists of strains from Italy, Slovenia, Croatia, Hungary, and Kosovo; the East Mediterranean subclade comprises strains from Turkey, Greece, and eastern Slovakia (Appendix Figure 3).

Bayesian phylogeographic reconstruction based on all available complete and partial (>750 bases) S-segment sequences suggested that the estimated root location of DOBV is in Slovakia and Hungary in eastern Europe; from there, the virus has spread to other regions through multiple introductions, followed by local spreading (Figure 2, panel A). Minimum spanning tree phylogeny showing clear geographic clustering also supports that supposition (Figure 2, panel B). It should be noted, however, that sequence data are lacking for wide areas within the potential geographic distribution range of the main hosts of DOBV, and further studies are needed in those areas to confirm initial findings of clustering.

We derived DOBV sequences from 4 host species: *Apodemus flavicollis* (yellow-necked mice), *A. agrarius* (striped field mice), *A. sylvaticus* (wood mice), and *A. ponticus* (Black Sea field mice). Consistent with earlier studies (*15*), topology in the DOBV phylogenetic tree correlates with the geographic ranges of host species (Figure 1, panel A). Bayesian analysis suggested host-dependent lineage separation, followed by geographic clustering (Appendix Figure 3). The minimum spanning phylogenic tree correlated with the Bayesian analysis in showing clear host-dependent separation (Figure 2, panel C). In addition, our analysis suggested host-switching events between *A. flavicollis* and *A. agrarius* mice (Figure 2, panel D). The distribution ranges of *A. flavicollis* and *A. agrarius* mice overlap in eastern Europe and some parts of central Europe.

In northern Germany, there is a close phylogenetic relation of DOBV strains with those 2 reservoir hosts (Figure 1, panel B). Although probability estimates in our analysis did not support host-switching between the other host species, that lack of information might have resulted from lack of sufficient sequence data, especially on potential host-switching or spillover events between *A. flavicollis* and *A. sylvaticus* mice (Figure 1, panel A; Appendix Figure 3).

Conclusions

Tracking viral genetic changes using complete genome sequences to characterize viruses circulating in rodent populations is a crucial first step for understanding the spatiotemporal epidemiologic patterns of orthohantavirus-induced diseases and potential viral genetic determinants of virulence. Phylogenetic characterization of DOBV strains according to geographic regions within Europe and bordering countries suggests that more thorough genomic surveillance of orthohantaviruses, preferably using complete genomes, would be useful for assessing the DOBV-induced threat to public health.

This work was supported by the Federation of European Microbiological Societies, which provided a research and training grant to M.E., and by funding from Academy of Finland (grant number 339510).

About the Author

Mr. Erdin is a PhD student and doctoral researcher in University of Helsinki, Finland. His main research interests are discovery, characterization, evolution, and epidemiology of emerging and novel zoonotic viruses.

References

1. Mull N, Seifert SN, Forbes KM. A framework for understanding and predicting orthohantavirus functional traits. Trends Microbiol. 2023;31:1102–10. https://doi.org/10.1016/j.tim.2023.05.004
2. Vaheri A, Strandin T, Hepojoki J, Sironen T, Henttonen H, Mäkelä S, et al. Uncovering the mysteries of hantavirus infections. Nat Rev Microbiol. 2013;11:539–50. https://doi.org/10.1038/nrmicro3066
3. European Centre for Disease Prevention and Control. Hantavirus infection—annual epidemiological report for 2020. Stockholm: The Centre; 2023.
4. Avšič Županc T, Korva M, Markotić A. HFRS and hantaviruses in the Balkans/South-East Europe. Virus Res. 2014;187:27–33. https://doi.org/10.1016/j.virusres. 2013.12.042
5. Leopardi S, Drzewnioková P, Baggieri M, Marchi A, Bucci P, Bregoli M, et al. Identification of Dobrava-Belgrade virus in *Apodemus flavicollis* from North-Eastern Italy during enhanced mortality. Viruses. 2022;14:1241. https://doi.org/10.3390/v14061241
6. Korva M, Knap N, Rus KR, Fajs L, Grubelnik G, Bremec M, et al. Phylogeographic diversity of pathogenic and non-pathogenic hantaviruses in Slovenia. Viruses. 2013;5:3071–87. https://doi.org/10.3390/v5123071
7. Faber M, Krüger DH, Auste B, Stark K, Hofmann J, Weiss S. Molecular and epidemiological characteristics of human *Puumala* and *Dobrava-Belgrade hantavirus* infections, Germany, 2001 to 2017. Euro Surveill. 2019;24:1800675. https://doi.org/10.2807/1560-7917.ES.2019.24.32.1800675
8. Çelebi G, Öztoprak N, Öktem IMA, Heyman P, Lundkvist Å, Wahlström M, et al. Dynamics of *Puumala hantavirus* outbreak in Black Sea Region, Turkey. Zoonoses Public Health. 2019;66:783–97. https://doi.org/10.1111/zph.12625
9. Oncul O, Atalay Y, Onem Y, Turhan V, Acar A, Uyar Y, et al. Hantavirus infection in Istanbul, Turkey. Emerg Infect Dis. 2011;17:303–4. https://doi.org/10.3201/eid1702.100663
10. Kaya S, Yılmaz G, Erensoy S, Yağçı Çağlayık D, Uyar Y, Köksal I. Hantavirus infection: two case reports from a province in the Eastern Black Sea Region, Turkey [in Turkish]. Mikrobiyol Bul. 2010;44:479–87.
11. Ertek M, Buzgan T; Refik Saydam National Public Health Agency; Ministry of Health, Ankara, Turkey. An outbreak caused by hantavirus in the Black Sea region of Turkey, January–May 2009. Euro Surveill. 2009;14:19214. https://doi.org/10.2807/ese.14.20.19214-en
12. Oktem IM, Uyar Y, Dincer E, Gozalan A, Schlegel M, Babur C, et al. Dobrava-Belgrade virus in *Apodemus flavicollis* and *A. uralensis* mice, Turkey. Emerg Infect Dis. 2014;20:121–5. https://doi.org/10.3201/eid2001.121024
13. Polat C, Sironen T, Plyusnina A, Karatas A, Sozen M, Matur F, et al. *Dobrava hantavirus* variants found in *Apodemus flavicollis* mice in Kırklareli Province, Turkey. J Med Virol. 2018;90:810–8. https://doi.org/10.1002/jmv.25036
14. Avšič-Županc T, Saksida A, Korva M. Hantavirus infections. Clin Microbiol Infect. 2019;21S:e6–16. https://doi.org/10.1111/1469-0691.12291
15. Papa A. Dobrava-Belgrade virus: phylogeny, epidemiology, disease. Antiviral Res. 2012;95:104–17. https://doi.org/10.1016/j.antiviral.2012.05.011

Address for correspondence: Mert Erdin, University of Helsinki, Haartmaninkatu 3, 00290, Helsinki, Finland; email: mert.erdin@helsinki.fi

Acanthamoeba Infection and Nasal Rinsing, United States, 1994–2022

Julia C. Haston, Chelsea Serra, Erin Imada, Emalee Martin, Ibne Karim M. Ali, Jennifer R. Cope

We describe 10 patients with nonkeratitis *Acanthamoeba* infection who reported performing nasal rinsing before becoming ill. All were immunocompromised, 7 had chronic sinusitis, and many used tap water for nasal rinsing. Immunocompromised persons should be educated about safe nasal rinsing to prevent free-living ameba infections.

Acanthamoeba spp. are free-living amebae (FLA) found worldwide in soil and many types of water, including lakes, rivers, and tap water (*1*–*3*). *Acanthamoeba* amebae can cause keratitis, which is an infection of the eye that does not spread to other parts of the body. However, they can also cause a variety of severe human infections, including granulomatous amebic encephalitis (GAE), an infection of the central nervous system, as well as cutaneous disease, rhinosinusitis, pulmonary disease, osteomyelitis, and disseminated infections (*1*). *Acanthamoeba* amebae cause disease when they enter the body through the eyes, broken skin, or respiratory tract (*1*). The ameba is known to be an opportunistic pathogen, and persons at highest risk of infection include those with a history of solid organ or stem cell transplant, cancer (specifically hematologic cancers), HIV, or diabetes mellitus (*4*,*5*). Nonkeratitis *Acanthamoeba* infections are rare, affecting only 3–12 persons annually in the United States; however, 82% of cases are fatal (*5*).

Because *Acanthamoeba* amebae are ubiquitous in the environment, the source of infection is often unknown, and identifying prevention strategies is challenging. However, performing safe nasal rinsing may be one way to prevent *Acanthamoeba* infection. Nasal rinsing is the practice of irrigating the sinuses for either health or religious purposes (e.g., ritual ablution) (*6*). There are a variety of ways nasal rinsing can be performed, including through the use of a device (e.g., a neti pot or squeeze bottle) or by using cupped hands to hold water. Nasal rinsing can provide health benefits, but it can also introduce pathogens, particularly if unsterile water is used (*7*). Nasal rinsing with tap water has been associated with infections caused by FLA, including *Naegleria fowleri* and *Acanthamoeba* (*8*,*9*). A recent study showed that nearly two thirds of US adults think tap water is safe for nasal rinsing (*7*). Our case study describes clinical features and nasal rinsing behaviors of US patients with *Acanthamoeba* infections who performed nasal rinsing. Our results underscore the importance of increasing awareness about safe nasal rinsing.

The Study

We used the Centers for Disease Control and Prevention (CDC) FLA database to identify US patients with laboratory-confirmed nonkeratitis *Acanthamoeba* infections who reported nasal rinsing before the onset of symptoms. We analyzed demographic and clinical characteristics for each case. We followed the process of Haston et al. in creating the algorithm used to classify disease manifestations (*5*). Our study protocol was reviewed by CDC and our research was conducted consistent with applicable federal law and CDC policy (see, e.g., 45 C.F.R. part 46.102(l) (2), 21 C.F.R. part 56; 42 U.S.C. §241(d); 5 U.S.C. §552a; 44 U.S.C. §3501 et seq.).

Ten patients reported nasal rinsing before their *Acanthamoeba* diagnoses. Infections occurred during 1994–2022, but 9 cases occurred in the past decade. The median age of patients was 60 years (range 32–80 years) (Table 1). Seven patients were male, and 3 were female. All 10 patients had ≥1 immunocompromising condition, most commonly cancer (Table 2, https://wwwnc.cdc.gov/EID/article/30/4/23-1076-T2.htm). Four of 5 patients with cancer had chronic lymphocytic leukemia. Two patients had HIV with CD4 counts <100 cells/mm^3 at the time of *Acanthamoeba* diagnosis, meeting criteria for AIDS. Seven patients survived, which is unexpectedly high

Author affiliations: Centers for Disease Control and Prevention, Atlanta, Georgia, USA (J.C. Haston, C. Serra, E. Imada, E. Martin, I.K.M. Ali, J.R. Cope); Public Health Institute and CDC Global Health Fellowship Program, Oakland, California, USA (C. Serra)

DOI: http://doi.org/10.3201/eid3004.231076

considering the typical fatality rate for *Acanthamoeba* infection. Most patients were diagnosed by PCR, including 6 of 7 survivors.

Including both confirmed and suspected *Acanthamoeba* disease manifestations, 9 patients were diagnosed with rhinosinusitis, 6 had GAE, 6 had cutaneous disease, and 3 had osteomyelitis. Eight patients had evidence of disseminated disease, and all of those 8 patients were diagnosed with rhinosinusitis. Because at least 7 patients had a history of chronic sinusitis, there may have been a delay in identifying acute sinus symptoms, enabling dissemination to other organ systems in these patients.

Table 1. Demographic and clinical characteristics of 10 patients with *Acanthamoeba* infection who performed nasal rinsing, United States, 1994–2022

Demographic	Value
Median age (range), y	60 (32–80)
Sex	
M	7
F	3
Race	
White	5
Black	2
Asian/Pacific Islander	1
Unknown	2
Ethnicity	
Hispanic	1
Non-Hispanic	4
Unknown	5
Disease manifestation, confirmed or suspected†	
Rhinosinusitis	9
GAE	6
Cutaneous	6
Osteomyelitis	3
Pulmonary	1
Endophthalmitis	1
Diagnostic method†	
PCR	7
Histopathology	6
Immunohistochemical staining	5
Indirect immunofluorescence	2
Specimens tested†	
Skin	6
Brain	4
Sinus	4
Bone	3
Genotype	
T4	4
T1	1
Unknown	5
Underlying conditions†	
Chronic sinusitis	7
Cancer‡	5
Chronic kidney disease	5
HIV/AIDS	2
Solid organ transplant	2
Stem cell transplant	1
Microscopic Polyangiitis	1
Outcome	
Survived	7
Died	3

*Values are no. (%) patients except as indicated. GAE, granulomatous amebic encephalitis.
†Some patients may have had multiple disease manifestations, multiple diagnostic methods, or multiple comorbid conditions.
‡Four chronic lymphocytic leukemia, 1 acute myeloid leukemia.

The high percentage of patients presenting with skin or sinus manifestations may have contributed to the unusually high survival rate in this small cohort, because treatment may have been initiated at earlier stages of disease for some. Previous studies have shown that GAE is associated with poor prognosis; survival rates are <7%. In this cohort, 3 patients with confirmed or suspected GAE died and 3 survived. Of the GAE survivors, 2 developed skin lesions before central nervous system symptoms.

Seven patients reported nasal rinsing for relief of chronic sinusitis symptoms, 2 performed ritual ablution, and 1 did not report a reason for nasal rinsing. At least 4 patients reported using tap water for nasal rinsing, and 1 other patient reported using sterile water but then submerging the device in tap water. A water source was not reported for the other 5 patients. Of the 6 patients who described nasal rinsing devices, 3 used squeeze bottles, 2 used neti pots, and 1 used an electric nasal irrigator. Duration and frequency of nasal rinsing varied. One patient developed symptoms after only 2 weeks of nasal rinsing, whereas others had been nasal rinsing for years. The frequency of nasal rinsing ranged from 1 time per week to 5 times per day.

Conclusions

In these 10 case-patients with invasive *Acanthamoeba* infection, nasal rinsing may have been the transmission route. Duration and frequency of nasal rinsing behaviors varied, but most patients had been rinsing for months or even years. Whereas amebae could theoretically be introduced during any rinsing encounter, the risk of infection likely increases over time with continued exposure. At least half of the patients in this case series used tap water in their nasal rinsing practices. Even though *Acanthamoeba* and other biofilm-associated amebae have been detected in >50% of US tap water samples, a recent study reported that 33% of US adults believe that tap water is sterile, and 62% believe it to be safe for rinsing sinuses (*3*,*7*). Educating against the use of unboiled tap water for nasal rinsing may be effective in preventing invasive *Acanthamoeba* infections, particularly among immunocompromised hosts.

Most patients in this case series performed rinsing for chronic sinusitis and likely had damaged mucosal tissue because of their underlying illnesses, which may have increased the risk for infection. Furthermore, all patients were immunocompromised. Some patients demonstrated signs of acute or worsening sinusitis on initial examination, but others demonstrated only skin lesions or neurologic symptoms. Of note, the 2 patients

who performed ritual ablution did not initially have sinus symptoms, which suggests that patients with underlying sinus disease may be more likely to initially have symptoms of *Acanthamoeba* rhinosinusitis develop compared with those who do not.

The first limitation of our study is that causation cannot be determined using these data. Nasal rinsing was not definitively determined to be the route of transmission for any case. Second, survival beyond the date of report cannot be confirmed. The nature of passive case surveillance data does not allow for patient follow-up. Finally, information regarding nasal rinsing practices were limited for some cases. The small number of cases did not enable thorough assessment of practices that may be considered to increase risk for infection.

All healthcare providers caring for immunocompromised persons should educate their patients about *Acanthamoeba* infections, including how to recognize symptoms and how to practice safe nasal rinsing. CDC recommendations for performing safe nasal rinsing include using boiled, sterile, or distilled water (*6*). If tap water is used, it should be boiled for a minimum of 1 minute, or 3 minutes in elevations >1,980 meters, and cooled before use (*6*). For diagnostic support and treatment recommendations, CDC offers a 24/7 Free-Living Ameba Consultation Service. Healthcare providers can call the CDC Emergency Operations Center at (770) 488–7100 for a consultation for any confirmed or suspected *Acanthamoeba* infection.

Acknowledgments

We thank Shantanu Roy for assistance.

About the Author

Dr. Haston is a physician and medical epidemiologist in the Division of Foodborne, Waterborne, and Environmental Diseases, National Center for Emerging and Infectious Diseases, Centers for Disease Control and Prevention in Atlanta, GA. Her primary research interests are the epidemiology and prevention of free-living ameba infections.

References

1. Centers for Disease Control and Prevention. Free living amebic infections [cited 2023 Jun 5]. https://www.cdc.gov/dpdx/freeLivingAmebic
2. Carnt NA, Subedi D, Lim AW, Lee R, Mistry P, Badenoch PR, et al. Prevalence and seasonal variation of Acanthamoeba in domestic tap water in greater Sydney, Australia. Clin Exp Optom. 2020;103:782–6. https://doi.org/10.1111/cxo.13065
3. Stockman LJ, Wright CJ, Visvesvara GS, Fields BS, Beach MJ. Prevalence of *Acanthamoeba* spp. and other free-living amoebae in household water, Ohio, USA—1990–1992. Parasitol Res. 2011;108:621–7. https://doi.org/10.1007/s00436-010-2120-7
4. Centers for Disease Control and Prevention. Sources of infection and risk factors [cited 2023 Jun 5]. https://www.cdc.gov/parasites/acanthamoeba/infection-sources.html
5. Haston JC, O'Laughlin K, Matteson K, Roy S, Qvarnstrom Y, Ali IKM, Cope JR. The epidemiology and clinical features of non-keratitis *Acanthamoeba* infections in the United States, 1956–2020. Open Forum Infect Dis. 2023 Jan;10(1):ofac682. https://doi.org/10.1093/ofid/ofac682
6. Centers for Disease Control and Prevention. Sinus rinsing for health or religious practice [cited 2023 Mar 11]. https://www.cdc.gov/parasites/naegleria/sinus-rinsing.html
7. Miko S, Collier SA, Burns-Lynch CE, Andújar AA, Benedict KM, Haston JC, et al. (Mis)perception and use of unsterile water in home medical devices, PN View 360+ Survey, United States, August 2021. Emerg Infect Dis. 2023;29:397–401. https://doi.org/10.3201/eid2902.221205
8. Centers for Disease Control and Prevention. Notes from the field: primary amebic meningoencephalitis associated with ritual nasal rinsing—St. Thomas, U.S. Virgin Islands, 2012. MMWR. 2013;62:903.
9. Yoder JS, Straif-Bourgeois S, Roy SL, Moore TA, Visvesvara GS, Ratard RC, et al. Primary amebic meningoencephalitis deaths associated with sinus irrigation using contaminated tap water. Clin Infect Dis. 2012;55:e79–85. https://doi.org/10.1093/cid/cis626
10. Murakawa GJ, McCalmont T, Altman J, Telang GH, Hoffman MD, Kantor GR, et al. Disseminated acanthamebiasis in patients with AIDS. A report of five cases and a review of the literature. Arch Dermatol. 1995;131:1291–6. https://doi.org/10.1001/archderm.1995.01690230069011
11. Brondfield MN, Reid MJ, Rutishauser RL, Cope JR, Tang J, Ritter JM, et al. Disseminated Acanthamoeba infection in a heart transplant recipient treated successfully with a miltefosine-containing regimen: Case report and review of the literature. Transpl Infect Dis. 2017;19:e12661. https://doi.org/10.1111/tid.12661
12. Breland M, Beckmann N. Amebic osteomyelitis in an immunocompromised patient. Radiol Case Rep. 2016;11:207–11. https://doi.org/10.1016/j.radcr.2016.05.006
13. Winsett F, Dietert J, Tschen J, Swaby M, Bangert CA. A rare case of cutaneous acanthamoebiasis in a renal transplant patient. Dermatol Online J. 2017;23:13030/qt88s2t7wp.
14. Voshtina E, Huang H, Raj R, Atallah E. Amebic encephalitis in a patient with chronic lymphocytic leukemia on ibrutinib therapy. Case Rep Hematol. 2018;2018:6514604. https://doi.org/10.1155/2018/6514604

Address for correspondence: Julia C. Haston, Centers for Disease Control Prevention, 1600 Clifton Rd NE, Atlanta, GA 30329-4018, USA; email: qdx2@cdc.gov

Isolation of Batborne Neglected Zoonotic Agent Issyk-Kul Virus, Italy

Davide Lelli, Ana Moreno, Sabrina Canziani, Laura Soliani, Maya Carrera, Anna Castelli, Francesca Faccin, Tiziana Trogu, Enrica Sozzi, Gian Luca Cavallari, Matteo Mauri, Fabiana Ferrari, Cristian Salogni, Chiara Garbarino, Chiara Chiapponi, Marco Farioli, Antonio Lavazza

We isolated Issyk-Kul virus (ISKV) from a bat sampled from Italy in 2021 and conducted ISKV-specific surveillance in bats collected in Italy during 2017–2023. ISKV circulation among synanthropic and sedentary species of bat, such as Savi's pipistrelle bat (*Hypsugo savii*) in northern Italy, may have public health implications in this region.

Issyk-Kul virus (ISKV), family *Nairoviridae*, was first isolated in 1970 from a noctule bat (*Nyctalus noctule*) trapped near Lake Issyk-Kul, Kyrgyzstan (*1*). ISKV was subsequently detected in bats of several countries in central Asia and in *Ixodes vespertilionis* and *Argas vespertilionis* ticks (*2*). ISKV has caused sporadic outbreaks of illness in humans, characterized by fever, headaches, myalgia, and nausea (*2*,*3*). Bats and ticks are assumed to be reservoirs of ISKV; transmission to humans is associated with tick bites and exposure to bat feces and urine (*2*,*4*,*5*). Moreover, *Aedes caspius* mosquitoes, common in Europe and central Asia, may have a role as vectors, having been considered competent through experimental infection (*6*,*7*).

Portions of ISKV genome were detected in northern bats (*Eptesicus nilssonii*) in Germany (*4*) and a Brandt's bat (*Myotis brandtii*) in Sweden (*8*), suggesting that the ISKV geographic range expanded to Europe. We isolated and performed whole-genome characterization of ISKV detected in a Savi's pipistrelle bat (*Hipsugo savii*) (hereafter referred to as Savi's bat) in Italy in 2021 and present the results of ISKV-specific surveillance of 415 bats collected during 2017–2023.

Ethics review and approval were waived for this study, which did not involve animal killing or suffering. Samples were collected exclusively from animals that died in wild recovery centers in the context of the regional surveillance plans for wildlife. Therefore, we believe that it does not fall in the provisions of the national law (e.g., DLSG 4/3 2014, n. 26—Application at national level of the EU Directive 2010/63/UE), and no ethics approval or permit for animal experimentation was required.

The Study

We isolated the virus from an adult female Savi's bat that spontaneously died in a wildlife recovery center in northern Italy. The bat was originally found alive on August 17, 2021, in Bergamo Province, northern Italy, by a private citizen who brought it to the center. Clinically, the bat exhibited lethargy, inappetence, and weight loss. It died 11 days after admission to the center, and no trauma or macroscopic pathologic lesions indicative of infectious disease were observed at necropsy. DNA barcoding confirmed the species as Savi's bat. We collected organ samples (e.g., lung, heart, liver, spleen, intestine, and brain) for laboratory investigations focused mainly on virus detection.

We assessed the brains of all bats for negativity to rabies and related lyssaviruses by using real-time PCR (*9*). We isolated a virus on MARC 145 cells (fetal monkey kidney) inoculated with a pool of viscera (lung, heart, liver, spleen). Cytopathic effect was noted 5 days after inoculation during the secondary passage and was characterized by cell monolayer degeneration with isolated foci of rounded and aggregated cells (Figure 1, panels A–C). Furthermore, electron microscopy performed on cell culture supernatants

Author affiliations: University of Parma, Parma, Italy (D. Lelli); Istituto Zooprofilattico Sperimentale della Lombardia e dell' Emilia Romagna, Brescia, Italy (D. Lelli, A. Moreno, S. Canziani, L. Soliani, M. Carrera, A. Castelli, F. Faccin, T. Trogu, E. Sozzi, C. Salogni, C. Garbarino, C. Chiapponi, A. Lavazza); Wildlife Rehabilitation Center WWF of Valpredina, Cenate Sopra, Italy (G.L. Cavallari, M. Mauri); Piacenza Wildlife Rescue Centre, Piacenza, italy (F. Ferrari); DG Welfare Regione Lombardia, Milano, Italy (M. Farioli)

DOI: https://doi.org/10.3201/eid3004.231186

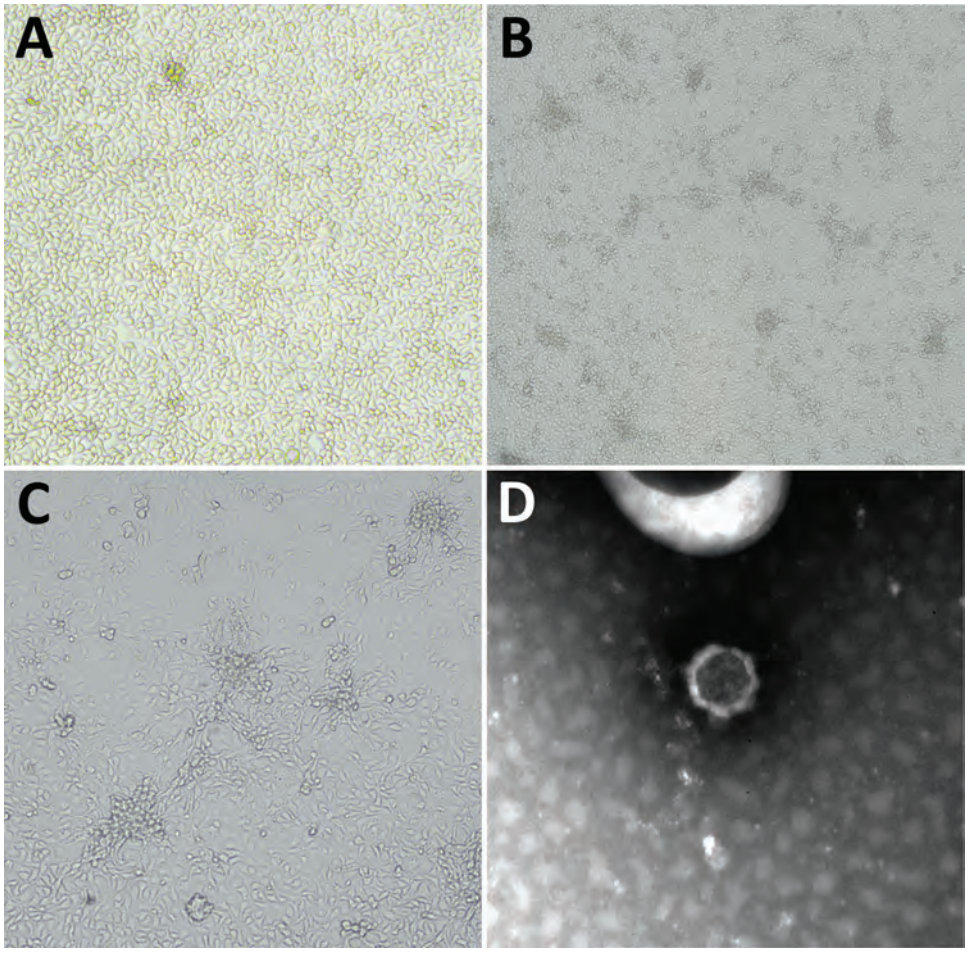

Figure 1. Microscopic appearance of Issyk-Kul virus IT-297348-34/2022, isolated from a *Hypsugo savii* bat, in study of batborne neglected zoonotic agent Issyk-Kul virus, Italy. A) Issyk-Kul–infected MARC 145 cells, mock infection; original magnification ×10. B) Issyk-Kul–infected MARC 145 cells showing cytopathic effect at 120 hours after infection; original magnification ×4. C) Issyk-Kul–infected MARC 145 cells showing cytopathic effect at 120 hours after infection; original magnification ×10. D) Negative-staining electron microscopy performed on cell supernatants (NaPT 2%), showing a viral particle of 55–60 nm morphologically referable to nairovirus; original magnification ≈x550,000

revealed distinct viral particles of 55–60 nm, morphologically referable to a nairovirus (Figure 1, panel D).

The complete genome sequence of isolated virus IT-297348–34/2022 (IT-ISKV), obtained through a standardized next-generation sequencing protocol (*10*), revealed the 3 typical nairovirus genome segments: large (L) (11,978 nt), medium (M) (4,907 nt), and small (S) (1,457 nt). The highest nucleotide identity for each gene segment was to ISKV strains detected in a Brandt's bat (*Myotis brandtii*) and bat-associated ticks in Sweden (strain Sun-2020, k99_1658, k99_589), and in northern bats (*Eptesicus nilssonii*) in Germany (strain PbGER) (Table 1). We submitted the complete genome sequences to GenBank (accession nos. OR583909–11).

The phylogenetic tree, based on the complete L genome sequences of viruses in the genus *Orthonairovirus,* assigned IT-ISKV to the Keterah genogroup. That genogroup includes the few available sequences of ISKVs detected in bats and ticks in Sweden, Germany, and central Asia, as well as other sequences of Keterah virus (detected in bats from Malaysia), Uzun Agach virus (in bats from Kazakhstan), and Gossas virus (in bats from Senegal) (Figure 1) (*11*). Phylogenetic trees constructed with complete S and M genes showed similar results with the same topology because of the small number of ISKV sequences available in the genome databases (Appendix Figures 1, 2, https://wwwnc.cdc.gov/EID/article/30/4/23-1186-App1.pdf).

After detecting IT-ISKV in the Mediterranean area, we developed and standardized ISKV-specific endpoint reverse transcription PCR targeting the L gene (Appendix) to enhance knowledge of the ISKV ecology and screen its diffusion in bat populations. We used ISKV-specific endpoint reverse transcription PCR to detect viral RNA in the necropsied tissues and to screen cultured cells. We performed Sanger sequencing of generated amplicons to confirm ISKV RNA.

During 2017–2023, we collected 415 bats representing 13 species in the Lombardy and Emilia-Romagna regions of northern Italy. The bats originated mainly from wildlife recovery centers, which usually receive rescued bats (usually near human settlements), or bats found dead during passive surveillance. Most of the bats examined were Savi's bats

Table 1. Highest nucleotide sequence identities for each protein of IT-ISKV isolated in study of batborne neglected zoonotic agent Issyk-Kul virus, Italy*

Gene	% Similarity (query cover, %)	ISKV strain	Host	Country (year)	GenBank accession no.	Reference
Large	95.44 (99)	K_k99_1658_len_12288	Bat-associated tick	Sweden (2020)	OP514654	Unpub. data
	95.34 (99)	LEZ 86–787	*Carios vespertilionis* tick	Germany (1986)	KR537441	(*11*)
	95.31 (99)	Sun-2020	*Myotis brandtii* bat	Sweden (2020)	OP380632	(*8*)
Medium	81.55 (72)	Sun-2020	*M. brandtii* bat	Sweden (2020)	OP380631	(*8*)
	81.11 (78)	k99_589	Bat-associated tick	Sweden (2020)	OP804626	Unpub. data
	81.34 (71)	LEIV-315K	*Nyctalus noctula* bat	Kyrgyzstan (1973)	KR709220	(*3*)
Small	97.51 (90)	PbGER	*Eptesicus nilssonii* bat	Germany (2008–2011)	MW275296	(*4*)
	89.11 (100)	Sun-2020	*M. brandtii* bat	Sweden (2020)	OP380630	(*8*)
	89.04 (100)	LEZ 86–787	*C. vespertilionis* tick	Germany (1986)	KR537443	(*11*)

*IT-ISKV, Issyk-Kul virus IT-297348-34/2022.

and Kuhl's bats (*Pipistrellus kuhlii*) (Appendix Table 1). We tested sampled organs (lung, heart, liver, spleen, intestine) for ISKV. We detected 8 bats positive by PCR for ISKV; 7 were Savi's bats and 1 was a whiskered bat (*Myotis mystacinus*) (Table 2), and they were recovered in 2017, 2020, 2021, 2022, and 2023 (Appendix Table 2). We constructed a phylogenetic tree based on the partial L genome sequences with all ISKVs detected in Italy (Figure 2, panel B). None of the ISKV-positive bats had ticks attached, and the ticks (*Ixodes vespertilionis*) found on the analyzed bats were ISKV negative.

Conclusions

Tickborne orthonairoviruses may be agents of human emerging infectious diseases (*13*). Crimean-Congo hemorrhagic fever virus is the most notable pathogen in the genus *Orthonairovirus* because of its public health effect with high fatality rates and widespread geographic distribution (*14*). However, several other emerging and neglected orthonairoviruses, such as ISKV, can cause clinical nonlethal diseases in humans (*15*).

Our isolation and characterization of IT-ISKV showed high L and S gene identity to the ISKV strains detected in Sweden, Germany, and central Asia (*3*,*4*,*8*). However, the level of M gene nucleotide similarity to the other known ISKV strains (80.98%–81.55%) suggests that IT-ISKV could represent a new ISKV strain from the Mediterranean area, most likely derived from an assortment with a yet unknown virus.

In that context, we conducted ISKV-specific surveillance among bats collected during 2017–2023 with the aim of determining the presence and diffusion of the virus in bat populations in northern Italy. Findings suggest that ISKV in that area seem to be associated with Savi's bats and whiskered bats, which may

Table 2. Issyk-Kul–positive bats and associated GenBank accession number assigned to the gene sequences detected in study of batborne neglected zoonotic agent Issyk-Kul virus, Italy*

Sample	Year	Bat species	Origin	Virus isolation (cell culture)	Sequence	GenBank accession no.	Nucleotide similarity (%)
251170-38/2017	2017	*Hypsugo savii*	WRC WWF Valpredina. Bergamo, Italy	No	Partial L gene	OR583901	Issyk-Kul virus LEZ 86–787 (98.79)
251170-41/2017	2017	*H. savii*	WRC WWF Valpredina. Bergamo, Italy	No	Partial L gene	OR583902	Issyk-Kul virus LEZ 86–787 (99.27)
378052-30/2020	2020	*H. savii*	WRC WWF Valpredina. Bergamo, Italy	No	Partial L gene	OR583903	Issyk-Kul virus K_k99_1658_len_12288 (99.17)
297348-34/2022	2021	*H. savii*	WRC WWF Valpredina. Bergamo, Italy	Yes	Full genome	OR583909–11, OR583905	Issyk-Kul virus/Prackenbach bat nairovirus (96.65)
297348-26/2022	2021	*H. savii*	WRC WWF Valpredina. Bergamo, Italy	No	Partial L gene	OR583904	Issyk-Kul virus LEZ 86–787 (99.42)
126482-17/2022	2022	*H. savii*	WRC Piacenza, Iataly	No	Partial L gene	OR583906	Issyk-Kul virus LEZ 86–787 (99)
356061-37/2022	2022	*H. savii*	WRC WWF Valpredina. Bergamo, Italy	No	Partial L gene	OR583907	Issyk-Kul virus/Prackenbach bat nairovirus (98.42)
24094-8/2023	2023	*Myotis mystacinus*	WRC Piacenza, Italy	No	Partial L gene	OR583908	Issyk-Kul virus LEZ 86-787 (98.91)

*L, large; WRC, wildlife recovery center; WWF, World Wildlife Fund.

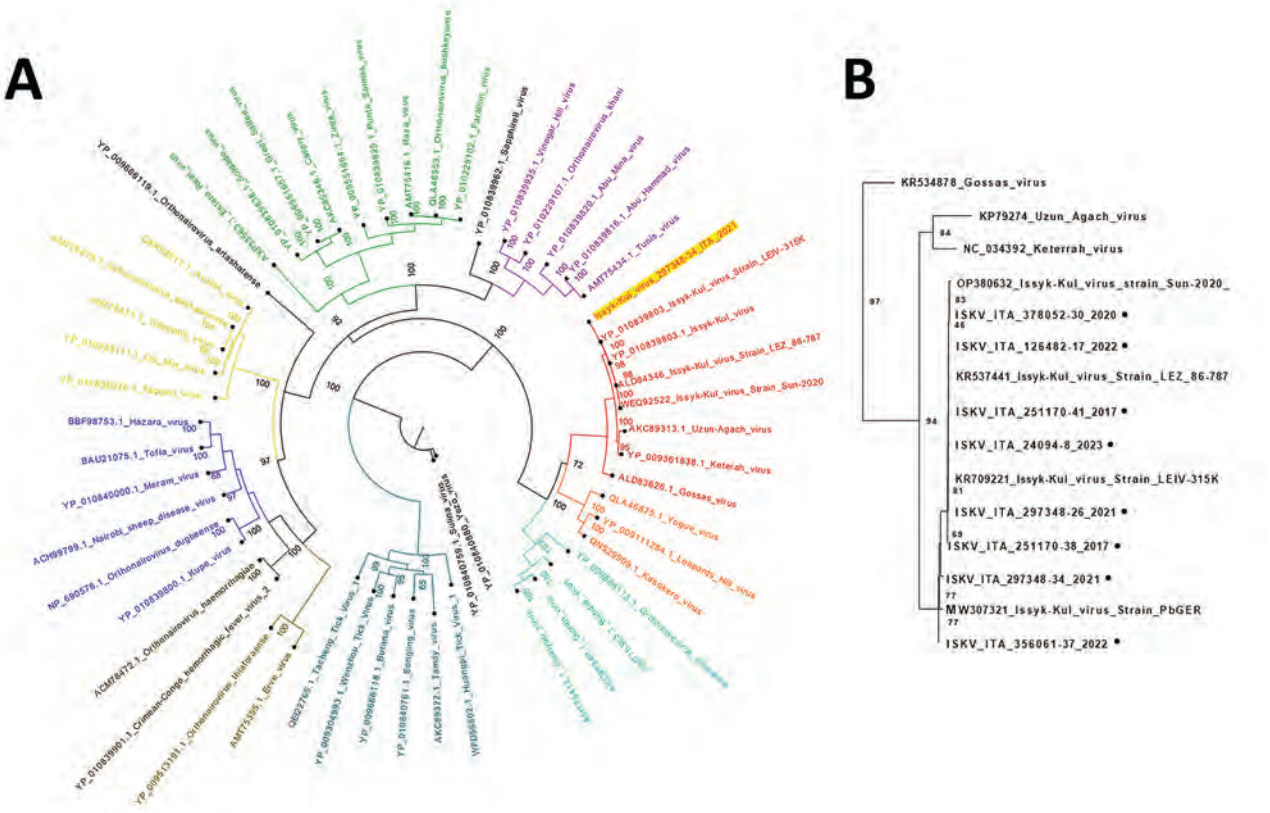

Figure 2. Phylogenetic analysis of isolates from study of batborne neglected zoonotic agent Issyk-Kul virus, Italy A) Phylogeneny nairovirus protein sequences for *Orthonairovirus* large (L) segments, including the complete sequence obtained from *Hypsugo savii* bats, highlighted in yellow. Sequence colors were based on the genogroups proposed by Ozeki et al. 2022 (*12*). B) Nucleotide alignment magnification of a short PCR-targeted region of the L segment, encompassing all sequences derived from bat surveillance conducted during 2017–2023 identified as Issyk-Kul virus IT-297348-34/2022. Numbers along branches indicate bootstrap values.

represent a previously unrecognized source for ISKV transmission to other wildlife species, ticks, and humans, as has already happened elsewhere (*2*,*3*). Savi's bats are a synanthropic and sedentary species that roost in buildings and represent the most common bat species in urban areas, suggesting possible public health implications.

ISKVs identified in bats in Italy were detected from a pool of organs, as in the previously described ISKV PbGER (*4*), which was found predominantly in the liver, spleen, and lung tissues, indicating systemic infection of bats instead of mere passaging of intestinal tick content. Future investigations may provide information about virus tissue distribution and pathogenesis by using histopathology and may define the infection prevalence in the bat populations through serologic tests.

The successful cell-culture isolation of IT-ISKV suggests the possible shedding of infectious virus particles, which represents a crucial point for assessing viral zoonotic risks that may emerge from synanthropic bats. Such results indicate the emergence of this neglected zoonotic agent in the Mediterranean area, which might have public health relevance because of its potential transmission to humans. Raising awareness of the risks deriving from this zoonosis should suggest adoption of specific surveillance and prevention programs for ISKV and other nairoviruses at the human–wild animal interface.

Acknowledgments

We thank the technicians of the IZSLER Virology section for their precious technical work.

This study was supported by the Lombardy and Emilia Romagna Wildlife Surveillance Program.

About the Author

Dr. Lelli is a senior researcher virologist at the Istituto Zooprofilattico Sperimentale della Lombardia e dell'Emilia-Romagna. His research activity involves diagnosing livestock and wildlife viral diseases. The major topics of his studies are emerging viral diseases, arthropodborne viruses, and viruses associated with bats.

References

1. Lvov DK, Karas FR, Timofeev EM, Tsyrkin YM, Vargina SG, Veselovskaya OV, et al. "Issyk-Kul" virus, a new arbovirus isolated from bats and Argas (Carios) vespertilionis (Latr., 1802) in the Kirghiz S.S.R. Arch Gesamte Virusforsch. 1973;42:207–9. https://doi.org/10.1007/BF01270841
2. L'vov DK, Kostiukov MA, Daniiarov OA, Tukhtaev TM, Sherikov BK. Outbreak of arbovirus infection in the Tadzhik SSR due to the Issyk-Kul virus (Issyk-Kul fever) [in Russian]. Vopr Virusol. 1984;29:89–92.
3. Atkinson B, Marston DA, Ellis RJ, Fooks AR, Hewson R. Complete genomic sequence of Issyk-Kul virus. Genome Announc. 2015;3:e00662–00715. 10.1128/genomeA.00662-15 https://doi.org/10.1128/genomeA.00662-15
4. Brinkmann A, Kohl C, Radonić A, Dabrowski PW, Mühldorfer K, Nitsche A, et al. First detection of bat-borne Issyk-Kul virus in Europe. Sci Rep. 2020;10:22384. 10.1038/s41598-020-79468-8 https://doi.org/10.1038/s41598-020-79468-8
5. Vargina SG, Kuchuk LA, Gershtein VI, Karas FR. Transmission of Issyk Kul virus by Argas vespertilionis ticks in experiment [in Russian]. Sborn nauch Tr Inst Virus Im Ivanov Akad Med Nauk SSSR. 1982;123–7.
6. Bulychev VP, Alekseev AN, Kostiukov MA, Gordeeva ZE, L'vov DK. Issyk-Kul virus transmission by Aedes caspius caspius Pall. mosquitoes via experimental bite [in Russian]. Med Parazitol (Mosk). 1979;48:53–6.
7. Kostiukov MA, Bulychev VP, Lapina TF. Experimental infection of Aedes caspius caspius Pall. mosquitoes on dwarf bats, Vespertilio pipistrellus, infected with the Issyk-Kul virus and its subsequent transmission to susceptible animals [in Russian]. Med Parazitol (Mosk). 1982;51:78–9.
8. Cholleti H, de Jong J, Blomström AL, Berg M. Investigation of the virome and characterization of Issyk-Kul virus from Swedish Myotis brandtii bats. Pathogens. 2022;12:12. https://doi.org/10.3390/pathogens12010012
9. Gigante CM, Dettinger L, Powell JW, Seiders M, Condori REC, Griesser R, et al. Multi-site evaluation of the LN34 pan-lyssavirus real-time RT-PCR assay for post-mortem rabies diagnostics. PLoS One. 2018;13:e0197074. https://doi.org/10.1371/journal.pone.0197074
10. Lelli D, Prosperi A, Moreno A, Chiapponi C, Gibellini AM, De Benedictis P, et al. Isolation of a novel rhabdovirus from an insectivorous bat (Pipistrellus kuhlii) in Italy. Virol J. 2018;15:37. https://doi.org/10.1186/s12985-018-0949-z
11. Walker PJ, Widen SG, Wood TG, Guzman H, Tesh RB, Vasilakis N. A global genomic characterization of nairoviruses identifies nine discrete genogroups with distinctive structural characteristics and host-vector associations. Am J Trop Med Hyg. 2016;94:1107–22. https://doi.org/10.4269/ajtmh.15-0917
12. Ozeki T, Abe H, Ushijima Y, Nze-Nkogue C, Akomo-Okoue EF, Ella GWE, et al. Identification of novel orthonairoviruses from rodents and shrews in Gabon, Central Africa. J Gen Virol. 2022;103. https://doi.org/10.1099/jgv.0.001796
13. Lv X, Liu Z, Li L, Xu W, Yuan Y, Liang X, et al. Yezo virus infection in tick-bitten patient and ticks, northeastern China. Emerg Infect Dis. 2023;29:797–800. https://doi.org/10.3201/eid2904.220885
14. Shayan S, Bokaean M, Shahrivar MR, Chinikar S. Crimean-Congo hemorrhagic fever. Lab Med. 2015;46:180–9. https://doi.org/10.1309/LMN1P2FRZ7BKZSCO
15. Sugimoto S, Suda Y, Nagata N, Fukushi S, Yoshikawa T, Kurosu T, et al. Characterization of Keterah orthonairovirus and evaluation of therapeutic candidates against Keterah orthonairovirus infectious disease. Ticks Tick Borne Dis. 2022;13:101834. https://doi.org/10.1016/j.ttbdis.2021.101834

Address for correspondence: Davide Lelli, Istituto Zooprofilattico Sperimentale della Lombardia e dell'Emilia Romagna "B. Ubertini," Via bianchi 9, Brescia 25124, Italy; email: davide.lelli@izsler.it

Melioidosis in Patients with COVID-19 Exposed to Contaminated Tap Water, Thailand, 2021

Panupong Tantirat, Yotsathon Chantarawichian, Pantila Taweewigyakarn, Somkid Kripattanapong, Charuttaporn Jitpeera, Pawinee Doungngern, Chadaporn Phiancharoen, Ratanaporn Tangwangvivat, Soawapak Hinjoy, Anupong Sujariyakul, Premjit Amornchai, Gumphol Wongsuvan, Viriya Hantakun, Vanaporn Wuthiekanun, Janjira Thaipadungpanit, Nicholas R. Thomson, David A.B. Dance, Claire Chewapreecha, Elizabeth M. Batty, Direk Limmathurotsakul

In September 2021, a total of 25 patients diagnosed with COVID-19 developed acute melioidosis after (median 7 days) admission to a COVID-19 field hospital in Thailand. Eight nonpotable tap water samples and 6 soil samples were culture-positive for *Burkholderia pseudomallei*. Genomic analysis suggested contaminated tap water as the likely cause of illness.

Melioidosis is an infectious disease caused by the gram-negative bacillus *Burkholderia pseudomallei*, which is commonly present in soil and water in tropical countries (*1*,*2*). Naturally acquired infections result from skin inoculation, inhalation, or ingestion of *B. pseudomallei* (*1*). In 2020 and 2021, multiple COVID-19 field hospitals were set up in Thailand for cases of mild and moderate COVID-19 infection. We report 25 cases of acute melioidosis among patients diagnosed with COVID-19 who were being managed at a COVID-19 field hospital in Saraburi Province, central Thailand. Our study received ethical approval from the Committee of the Faculty of Tropical Medicine, Mahidol University (TMEC 24-006).

The Study

On September 8, 2021, the Department of Disease Control, Ministry of Public Health, Thailand, was alerted to a cluster of 20 patients with culture-confirmed melioidosis (case nos. 1–20; Table, https://wwwnc.cdc.gov/EID/article/30/4/23-1476-T1.htm). The 20 patients had been admitted to a single field hospital in Saraburi Province, which had been designated a treatment facility for COVID-19, and were transferred to Kaeng Khoi Hospital, Saraburi Province, because they developed fever or pneumonia. Previously, Saraburi Province had diagnosed ≈8–12 culture-confirmed melioidosis cases per year (*2*). The outbreak investigation team suspected that nonpotable tap water (NPTW) was the source of infection because there were no other apparent sources (Appendix, https://wwwnc.cdc.gov/eid/article/30/4/23-1476-App1.pdf). The initial response included the immediate transfer of patients with diabetes and those who had received steroid therapy for COVID-19 to other hospitals, followed by re-emphasizing to staff the recommended prevention strategies for melioidosis (*3*). The recommendations included avoiding direct exposure to soil and environmental water and drinking only boiled or bottled water.

Health officials immediately planned and conducted an environmental investigation. During September 10–16, 2021, the outbreak investigation team collected samples from the field hospital, including

Author affiliations: Saraburi Hospital, Mueang Saraburi District, Saraburi, Thailand (P. Tantirat); Ministry of Public Health, Nonthaburi, Thailand (P. Tantirat, P. Taweewigyakarn, S. Kripattanapong, C. Jitpeera, P. Doungngern, C. Phiancharoen, R. Tangwangvivat, S. Hinjoy, A Sujariyakul); Kaeng Khoi Hospital, Kaeng Khoi District, Saraburi (Y. Chantarawichian); Mahidol University Mahidol-Oxford Tropical Medicine Research Unit, Bangkok, Thailand (P. Amornchai, G. Wongsuvan, V. Hantakun, V. Wuthiekanun, J. Thaipadungpanit, C. Chewapreecha, E.M. Batty, D. Limmathurotsakul); Mahidol University, Bangkok (J. Thaipadungpanit, C. Chewapreecha, D. Limmathurotsakul); Wellcome Sanger Institute, Hinxton, United Kingdom (N.R. Thomson, C. Chewapreecha); Lao-Oxford-Mahosot Hospital-Wellcome Trust Research Unit, Vientiane, Lao People's Democratic Republic (D.A.B. Dance); London School of Hygiene and Tropical Medicine, London, UK (D.A.B Dance); University of Oxford Centre for Tropical Medicine and Global Health, Oxford, UK (D.A.B. Dance, E.M. Batty, D. Limmathurotsakul)

DOI: http://doi.org/10.3201/eid3004.231476

8 commercially bottled drinking water (CBDW) samples (500 mL–1 L), 37 NPTW samples from 10 locations (1-L samples; 3–4 samples per location at different time points), and 50 soil samples (100 g per sample) (Appendix). We isolated *B. pseudomallei* from environmental samples according to previously described methods (*4*,*5*). None of the CBDW samples, 6 (12%) of 50 soil samples, and 8 (22%) of 37 NPTW samples (from 4 locations) were culture-positive for *B. pseudomallei*. The median quantitative count of *B. pseudomallei* in NPTW was 24.5 CFU/L (range 4–58 CFU/L) and in soil was 82 CFU/g (range <1–119 CFU/g). The outbreak investigation team found that the chlorination system for NPTW was not well maintained. Patients reported that they drank only CBDW and never drank NPTW, which was used for other domestic purposes, such as brushing their teeth, rinsing their mouths, and showering. The chlorination system was successfully repaired, and chlorine levels were maintained >1 ppm beginning on September 10. A further 5 melioidosis cases were identified, all of whom had been admitted before September 10. No new melioidosis cases among those who had stayed at the field hospital were reported after September 16.

Of the 25 patients diagnosed with melioidosis (Table), 12 (48%) were female and 13 (51%) male; median age was 59 (interquartile range 56–62, range 34–73) years. All patients had received a diagnosis of COVID-19, confirmed by PCR during August 16–29, 2021, and had been admitted to the field hospital in August 22–September 2, 2021. A total of 15 (60%) patients had diabetes, and all 25 (100%) patients had received steroids as part of their COVID-19 treatment. The date range of onset of symptoms attributed to melioidosis was September 1–11. The median time from admission to the field hospital to the onset of the melioidosis symptoms was 7 (interquartile range 5–9, range 4–20) days.

The most common clinical manifestations of melioidosis among patients in this cluster were secondary bacterial pneumonia (n = 22 patients [88%]) and fever (n = 15 [60%]) (Table). Clinical specimens that were culture-positive for *B. pseudomallei* were blood (n = 24 [96%]) and sputum (n = 1 [4%]). In-hospital mortality for patients we studied was 32% (8/25). Of the fatal cases, 3 patients (case nos. 2, 4, and 8) died without receiving ceftazidime or meropenem, which are recommended parenteral antibiotics for treatment of melioidosis. A total of 17 (68%) cases completed ≥10 days of parenteral ceftazidime or meropenem and subsequently received a course of oral eradicative treatment.

We confirmed the first 20 clinical isolates and all environmental isolates as *B. pseudomallei* at the Mahidol-Oxford Tropical Medicine Research Unit laboratory, Bangkok, by using a combination of colony morphology on Ashdown agar, latex agglutination test, arabinose assimilation test, and antimicrobial susceptibility tests. Testing revealed that all clinical and environmental isolates were susceptible to ceftazidime, meropenem, and trimethoprim/sulfamethoxazole. We performed whole-genome sequencing on 19 clinical isolates, 8 NPTW isolates, and 6 soil isolates (1 colony per patient or sample). We excluded 1 clinical isolate from analysis because of low sequencing depth of 7.5×. We deposited sequences in the European Nucleotide Archive (https://www.ebi.ac.uk/ena) (accession numbers in Appendix Table). We mapped isolates to the K96243 reference genome and used variant calls to construct a phylogeny after masking recombinant fragments, repetitive regions, and known *B. pseudomallei* genomic islands (*6*). We used genome assemblies to call multilocus sequence types (STs).

We categorized the isolates by both phylogenetic and multilocus sequence typing, and they clustered consistently into 4 groups. The largest cluster was ST689 and included all 19 blood and sputum samples, as well as 6 of 8 NPTW samples (Figure). The remaining soil and NPTW isolates formed 3 separate clusters (ST107, ST303, and ST315). Within the ST689 cluster, the isolates were closely related but not identical (12–98 SNP differences between isolates). The NPTW isolates were interspersed with clinical isolates in this cluster, suggesting that contaminated NPTW was a possible source of infection for these patients. Dating analysis was not feasible because of the absence of clock signals in the phylogeny.

Conclusions

Our study highlights that patients with viral infections (e.g., COVID-19) may be at risk for infection and death caused by melioidosis if exposed to NPTW contaminated by *B. pseudomallei*. Diabetes mellitus and conditions that impair innate and adaptive immune responses, particularly steroid use, are important risk factors for melioidosis (*1*). Diabetes mellitus is also a risk factor for COVID-19, and steroid treatment is recommended for patients with COVID-19 pneumonia (*7*). Therefore, unsurprisingly, co-infections with COVID-19 and *B. pseudomallei* have been reported occasionally (*8*,*9*; D. Chit Yee et al., unpub. data, https://wellcomeopenresearch.org/articles/7-160), including 1 of the 4 patients detected during the multistate outbreak of melioidosis caused by an imported aromatherapy spray in the United States (*10*), and now

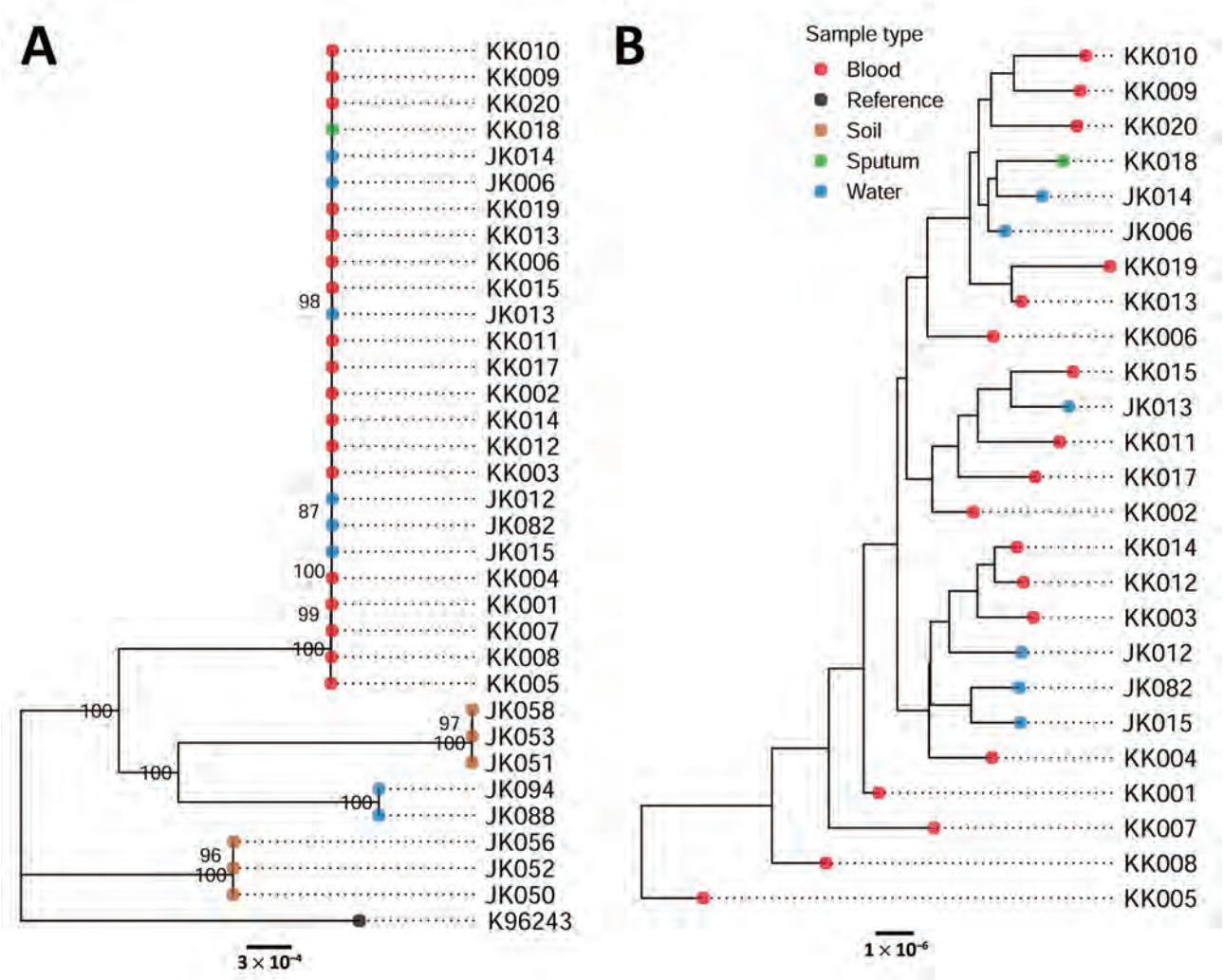

Figure. Information on 25 patients with COVID-19 who developed acute melioidosis in Saraburi Province, Thailand, 2021. A) Phylogenic tree of 19 clinical isolates and 14 environmental isolates. The K96243 reference strain is used to root the tree. B) Tree showing only the clinical and environmental isolates within the ST689 cluster. Scale bar shows number of nucleotide differences.

this cluster. Previous reports of co-infection with influenza A (*11*,*12*) or COVID-19 (*9*) and *B. pseudomallei* suggested that melioidosis could be reactivated from a latent focus following viral infection. However, the timeline of the cluster, the identified source, and genomic analysis suggest that the patients in this cluster represented recently acquired secondary infections after COVID-19. The route of infection in this cluster was probably skin exposure to contaminated NPTW at a high-infecting dose, although ingestion or inhalation are also possible.

An unknown proportion of melioidosis patients in melioidosis-endemic areas could be related to exposure to contaminated NPTW. More studies on the effects of *B. pseudomallei*-contaminated NPTW and its disinfection (*13*) in melioidosis endemic areas are required. Because general recommendations for melioidosis prevention (*3*) do not emphasize the disinfection of NPTW, those recommendations may be inadequate and should be revisited.

Acknowledgment

We thank all patients involved in providing information. We thank outbreak investigation team and all staff at Saraburi Hospital and Kaeng Khoi Hospital for their support.

This study was supported by the Department of Disease Control, Ministry of Public Health, Thailand, and the Wellcome Trust (220211/A/20/Z). This publication made use of the PubMLST website (https://pubmlst.org), developed by Keith Jolley and sited at the University of Oxford. The development of that website was funded by the Wellcome Trust. The funders had no role in the study design, data collection and analysis, decision to publish, or preparation of manuscript.

About the Author

Dr. Tantirat is assistant director of Information Technology at Saraburi Hospital and serves as the deputy director of the Bureau of Digital Health within the Office of the Permanent Secretary at the Ministry of Public Health, Thailand. His key interests include epidemiology and disease control.

References

1. Meumann EM, Limmathurotsakul D, Dunachie SJ, Wiersinga WJ, Currie BJ. *Burkholderia pseudomallei* and melioidosis. Nat Rev Microbiol. 2024;22:155-169. https://doi.org/10.1038/s41579-023-00972-5
2. Hantrakun V, Kongyu S, Klaytong P, Rongsumlee S, Day NPJ, Peacock SJ, et al. Clinical epidemiology of 7126 melioidosis patients in Thailand and the implications for a national notifiable diseases surveillance system. Open Forum Infect Dis. 2019;6:ofz498. https://doi.org/10.1093/ofid/ofz498
3. Suntornsut P, Wongsuwan N, Malasit M, Kitphati R, Michie S, Peacock SJ, et al. Barriers and recommended interventions to prevent melioidosis in northeast Thailand: A focus group study using the behaviour change wheel. PLoS Negl Trop Dis. 2016;10:e0004823. https://doi.org/10.1371/journal.pntd.0004823
4. Limmathurotsakul D, Wongsuvan G, Aanensen D, Ngamwilai S, Saiprom N, Rongkard P, et al. Melioidosis caused by *Burkholderia pseudomallei* in drinking water, Thailand, 2012. Emerg Infect Dis. 2014;20:265–8. https://doi.org/10.3201/eid2002.121891
5. Hantrakun V, Rongkard P, Oyuchua M, Amornchai P, Lim C, Wuthiekanun V, et al. Soil nutrient depletion is associated with the presence of *Burkholderia pseudomallei.* Appl Environ Microbiol. 2016;82:7086–92. https://doi.org/10.1128/AEM.02538-16
6. Croucher NJ, Page AJ, Connor TR, Delaney AJ, Keane JA, Bentley SD, et al. Rapid phylogenetic analysis of large samples of recombinant bacterial whole genome sequences using Gubbins. Nucleic Acids Res. 2015;43:e15. https://doi.org/10.1093/nar/gku1196
7. Singh AK, Majumdar S, Singh R, Misra A. Role of corticosteroid in the management of COVID-19: A systemic review and a Clinician's perspective. Diabetes Metab Syndr. 2020;14:971–8. https://doi.org/10.1016/j.dsx.2020.06.054
8. Gupta A, Siddiqui F, Purwar S, Joshi R, Mukhopadhyay C. Is it always COVID-19 in acute febrile illness in the tropics during the pandemic? PLoS Negl Trop Dis. 2022;16:e0010891. https://doi.org/10.1371/journal.pntd.0010891
9. Gulati U, Nanduri AC, Juneja P, Kaufman D, Elrod MG, Kolton CB, et al. Case Report: A fatal case of latent melioidosis activated by COVID-19. Am J Trop Med Hyg. 2022;106:1170–2. https://doi.org/10.4269/ajtmh.21-0689
10. Gee JE, Bower WA, Kunkel A, Petras J, Gettings J, Bye M, et al. Multistate outbreak of melioidosis associated with imported aromatherapy spray. N Engl J Med. 2022;386:861–8. https://doi.org/10.1056/NEJMoa2116130
11. Mackowiak PA, Smith JW. Septicemic melioidosis. Occurrence following acute influenza A six years after exposure in Vietnam. JAMA. 1978;240:764–6. https://doi.org/10.1001/jama.1978.03290080054027
12. Tan WF, Lee HG. Concurrent influenza A and pulmonary melioidosis in pregnancy. Med J Malaysia. 2021;76:245–7.
13. McRobb E, Kaestli M, Mayo M, Price EP, Sarovich DS, Godoy D, et al. Melioidosis from contaminated bore water and successful UV sterilization. Am J Trop Med Hyg. 2013;89:367–8. https://doi.org/10.4269/ajtmh.13-0101

Address for correspondence: Direk Limmathurotsakul, Mahidol-Oxford Tropical Medicine Research Unit, Faculty of Tropical Medicine, Mahidol University, 420/6 Ratchawithi Rd., Bangkok, 10400, Thailand; email: direk@tropmedres.ac

Uncommon *Salmonella* Infantis Variants with Incomplete Antigenic Formula in the Poultry Food Chain, Italy

Sara Petrin,[1] Alessia Tiengo,[1] Alessandra Longo, Maddalena Furlan, Elisa Marafin, Paola Zavagnin, Massimiliano Orsini, Carmen Losasso,[2] Lisa Barco[2]

Uncommon *Salmonella* Infantis variants displaying only flagellar antigens phenotypically showed identical incomplete antigenic formula but differed by molecular serotyping. Although most formed rough colonies, all shared antimicrobial resistances and the presence of *usg* gene with wild-type *Salmonella* Infantis. Moreover, they were undistinguishable wild-type *Salmonella* Infantis by whole-genome sequencing.

The emergence of variants posing threats to human health and animal production characterizes the epidemiology of *Salmonella* (*1*) and also *S. enterica* serovar Infantis (antigenic formula 6,7:r:1,5). Over the past few decades, this serovar has rapidly emerged along the poultry chain; as of 2023, it is the most prevalent serovar isolated from broiler chickens in the European Union and among the 4 most common serovars in humans (*2*,*3*). The European Commission identified *Salmonella* Infantis as a target serovar for which control measures must be implemented if it is isolated in breeding flocks of *Gallus gallus* chickens (*4*). Some of the mandatory control measures implemented in Italy are appropriate health measures applied at farms; eradication or slaughtering of *Salmonella*-positive birds and management of their carcasses in accordance with EC regulation no. 1069/2009; and disposal of eggs produced by *Salmonella* Infantis–positive groups and additional cleaning and disinfection procedures of the flock environment and facilities. The strict and targeted control measures implemented in case of identification of *Salmonella* Infantis–positive flocks (*5*) require standardized analytical methods (i.e., ISO 6579:1 for isolation of *Salmonella* and methods based on the Kaufmann-White scheme for serotyping or validated alternative methods) to ensure high quality of surveillance, prompt identification of positive samples, and prompt implementation of eradication measures.

Isolates with an incomplete antigenic formula that carried flagellar antigens typical of *Salmonella* Infantis (r:1,5), but lacked the somatic ones (6,7), have been increasingly isolated from poultry sources in Italy. Laboratories in charge of *Salmonella* controls and surveillance needed to quickly identify and characterize these isolates to ascertain if these atypical variants were *Salmonella* Infantis strains and consequently manage their isolation on farms for breeding *G. gallus* fowl. Our investigation also included strains showing those atypical features isolated from food matrices, to estimate their spread along the poultry chain.

The Study

We tested a total of 31 *Salmonella* strains that could be ascribed to *Salmonella* Infantis but lacked the expression of the complete antigenic formula from animals (N = 20) and food (N = 11). Those strains were isolated during 2014–2022 from samples taken in different regions of Italy (Table). We included 1 wild-type *Salmonella* Infantis strain isolated from food as a reference. We serotyped all *Salmonella* isolates by slide agglutination with *Salmonella* antiserum samples (Statens Serum Institut, Copenhagen, Denmark); we assigned antigenic formulas in accordance with ISO 6579:3. If traditional serotyping could not provide conclusive

Author affiliation: National and World Organisation for Animal Health Reference Laboratory for *Salmonella*, Istituto Zooprofilattico Sperimentale delle Venezie, Legnaro, Italy

DOI: http://doi.org/10.3201/eid3004.231074

[1]These first authors contributed equally to this article.

[2]These senior authors contributed equally to this article.

results because the complete antigenic formula was not expressed, we performed molecular serotyping by using an xMAP *Salmonella* serotyping assay (*6*). In particular, a positive match from the somatic antigen with C1 probe (*wzy* gene) is expected in case of wild-type *Salmonella* Infantis isolates. Colony morphology was investigated on agar tryptose solid medium. We assessed antimicrobial susceptibility by MIC by using the broth microdilution method with the Sensititer EUVSEC

Table. *Salmonella enterica* serovar Infantis isolates in the poultry food chain, Italy, 2014–2022*

Isolate ID	Matrix	Source	Year	Location	Antigenic formula			ST
					Seroagglutination†	Molecular serotyping‡	WGS§	
21-153004-9	Meat	Food	2014	Veneto	*S.* -: r: 1,5	*S.* Infantis (C1: r: 1,5)	O-7:r:1,5 (Infantis)	ST32
21-153004-10	Meat	Food	2014	Veneto	*S.* -: r: 1,5	*S.* Infantis (C1: r: 1,5)	O-30:r:1,5 (Gege)	ST32
21-153004-11	Meat	Food	2014	Veneto	*S.* -: r: 1,5	*S.* -: r: 1,5	O-?:r:1,5	ST32
21-153004-12	Sock sample	Animal	2014	Veneto	*S.* -: r: 1,5	*S.* Infantis (C1: r: 1,5)	O-?:r:1,5	ST32
21-153004-13	Sock sample	Animal	2016	Veneto	*S.* -: r: 1,5	*S.* -: r: 1,5	O-?:r:1,5	ST32
21-153004-14	Meat	Food	2016	Veneto	*S.* -: r: 1,5	*S.* -: r: 1,5	O-?:r:1,5	ST32
21-153004-1	Sock sample	Animal	2016	Lombardia	*S.* -: r: 1,5	*S.* Infantis (C1: r: 1,5)	O-30:r:1,5 (Gege)	ST32
21-153014-1	Sock sample	Animal	2017	Lombardia	*S.* -: r: 1,5	*S.* -: r: 1,5	O-?:r:1,5	ST32
21-153014-2	Sock sample	Animal	2017	Lombardia	*S.* -: r: 1,5	*S.* -: r: 1,5	O-?:r:1,5	ST32
21-153014-3	Sock sample	Animal	2017	Molise	*S.* -: r: 1,5	*S.* -: r: 1,5	O-?:r:1,5	ST32
21-153014-4	Sock sample	Animal	2017	Molise	*S.* -: r: 1,5	*S.* -: r: 1,5	O-?:r:1,5	ST32
21-153014-14	Sock sample	Animal	2017	Molise	*S.* -: r: 1,5	*S.* -: r: 1,5	O-?:r:1,5	ST32
21-153004-2	Meat	Food	2018	Veneto	*S.* -: r: 1,5	*S.* -: r: 1,5	O-?:r:-	ST32
21-153004-3	Carcass	Animal	2018	Veneto	*S.* -: r: 1,5	*S.* Infantis (C1: r: 1,5)	O-7:r:1,5 (Infantis)	ST32
21-153014-5	Meat	Animal	2018	Veneto	*S.* -: r: 1,5	*S.* -: r: 1,5	O-?:r:1,5	ST32
21-153014-7	Sock sample	Animal	2018	Veneto	*S.* -: r: 1,5	*S.* -: r: 1,5	O-?:r:1,5	ST32
18-1157-6	Meat	Food	2018	Veneto	*S.* -: r: 1,5	*S.* -: r: 1,5	O-?:r:1,5	ST32
21-153004-4	Sock sample	Animal	2019	Puglia	*S.* -: r: 1,5	*S.* -: r: 1,5	O-?:r:1,5	ST32
21-153004-5	Meat	Food	2019	Veneto	*S.* -: r: 1,5	*S.* -: r: 1,5	O-?:r:1,5	ST32
21-153004-6	Carcass	Animal	2019	Veneto	*S.* -: r: 1,5	*S.* Infantis (C1: r: 1,5)	O-7:r:1,5 (Infantis)	ST32
21-153014-11	Sock sample	Animal	2020	Veneto	*S.* -: r: 1,5	*S.* Infantis (C1: r: 1,5)	O-30:r:1,5 (Gege)	ST32
21-128165	Meat	Food	2021	Friuli Venezia Giulia	*S.* -: r: 1,5	*S.* -: r: 1,5	O-?:r:1,5	ST32
21SAL/2851/1	Sock sample	Animal	2021	Lazio	*S.* -: r: 1,5	*S.* -: r: 1,5	O-?:r:1,5	ST32
21-146541	Sock sample	Animal	2021	Lazio	*S.* -: r: 1,5	*S.* -: r: 1,5	O-?:r:1,5	ST32
21-21379	Sock sample	Animal	2021	Veneto	*S.* -: r: 1,5	*S.* -: r: 1,5	O-?:r:1,5	ST32
21-117758	Meat	Food	2021	Emilia Romagna	*S.* -: r: 1,5	*S.* -: r: 1,5	O-?:r:1,5	ST32
21-117759	Sock sample	Animal	2021	Umbria	*S.* -: r: 1,5	*S.* -: r: 1,5	O-?:r:1,5	ST32
22-16858-1	Meat	Food	2022	Sardegna	*S.* -: r: 1,5	*S.* -: r: 1,5	O-?:r:-	ST32
22-23625-9	Carcass	Animal	2022	Friuli Venezia Giulia	*S.* -: r: 1,5	*S.* Infantis (C1: r: 1,5)	O-30:r:1,5 (Gege)	ST32
22-39728-9	Carcass	Animal	2022	Molise	*S.* -: r: 1,5	*S.* -: r: 1,5	O-?:r:1,5	ST32
22-102991-7	Carcass	Food	2022	Veneto	*S.* -: r: 1,5	*S.* Infantis (C1: r: 1,5)	O-7:r:1,5 (Infantis)	ST5275
22-16858-3	Meat	Animal	2022	Sardegna	*S.* Infantis (6,7: r: 1,5)	*S.* Infantis (C1: r: 1,5)	O-7:r:1,5 (Infantis)	ST32

*Reference isolate showed complete antigenic formula (22-16858-3). ID, identification; ST, sequence type.
†As determined by traditional seroagglutination (ISO 6579:3).
‡As determined by molecular serotyping (xMAP *Salmonella* serotyping assay [*6*]).
§As determined by whole-genome sequencing.

panel (TREK Diagnostics System; ThermoFisher, https://www.thermofisher.com) and interpreted results in accordance with European Committee on Antibiotic Susceptibility Testing (EUCAST) epidemiologic cutoff values. We selected the *usg* gene (SIN_02055) as a marker gene specific for *Salmonella* Infantis; we used the PCR targeting this gene described by Yang et al. (*7*) as an identification marker to test whether strains belonged to *Salmonella* Infantis serovar. Finally, we performed whole-genome sequencing as described in Petrin et al. (*8*) and used a core genome multilocus sequence typing (cgMLST) scheme approach (*9*) to assess genetic relatedness among the investigated strains and with the wild-type *Salmonella* Infantis strain. We also performed in-silico serotyping as described by Costa et al. (*9*).

Thirty-one of 32 strains did not agglutinate with the somatic serum specimens for 6,7 antigens, indicating that their antigenic formula was -:r:1,5 (Table). Molecular serotyping identified a match with the C1 somatic probe in 9 strains. Of those, 3 were isolated from food and 6 from animal sources. For the remaining 22 strains, detection with the C1 somatic probe was negative. The detection of typical *Salmonella* Infantis flagellar antigens was positive for all the tested strains. In silico serotyping did not provide conclusive results on the O-antigen encoding region for 27 isolates; those results support the need for further analyses. Twenty-six strains displayed rough colony morphology (Figure 1), which in many cases contributes to increased sensitivity to immune defense, even if it remains unclear whether these strains are pathogenic (*10*). Most of the selected strains shared a similar resistance pattern to multiple antimicrobial drugs (ampicillin, ciprofloxacin, azithromycin, nalidixic acid, tetracycline, trimethoprim, and sulfamethoxazole) (Appendix Table, https://wwwnc.cdc.gov/EID/article/30/4/23-1074.App1.pdf) typical of the circulating wild-type *Salmonella* Infantis strains spread in broiler populations (*1*).

All the 31 isolates harboring incomplete antigenic formula, as well as the isolate with the complete antigenic formula, had *usg* gene present in their genomes; the presence of the gene can be considered a promising tool for rapid diagnosis of those atypical strains with incomplete expression of somatic antigens. The investigations carried out by cgMLST to establish the genetic relatedness among isolates did not enable us to identify different *Salmonella* Infantis populations on the basis of their antigenic formula, considering both traditional serotyping (Figure 2, panel A) and molecular serotyping (Figure 2, panel B).

Conclusions

Our results describe heterogeneous *Salmonella* Infantis strains widespread in the poultry food chain in Italy. This heterogeneity seems to involve the antigen-coding genetic context that probably would also affect the colony morphology (*11*). It is well known that rough morphology of *Salmonella* isolates originates from deletion or truncations of lipopolysaccharide O-antigen encoding genes (*12*). In our study, however, we could not link the rough phenotype, identified for the atypical strains, to the absence of the *wzy* gene nor to the isolation matrix and source. Further analyses at the genomic level will clarify the deletion/truncation pattern and identify the involved genes; the genetic region encoding for the O-antigen is composed of many different genes (*13*,*14*).

We found atypical strains that lacked the expres-

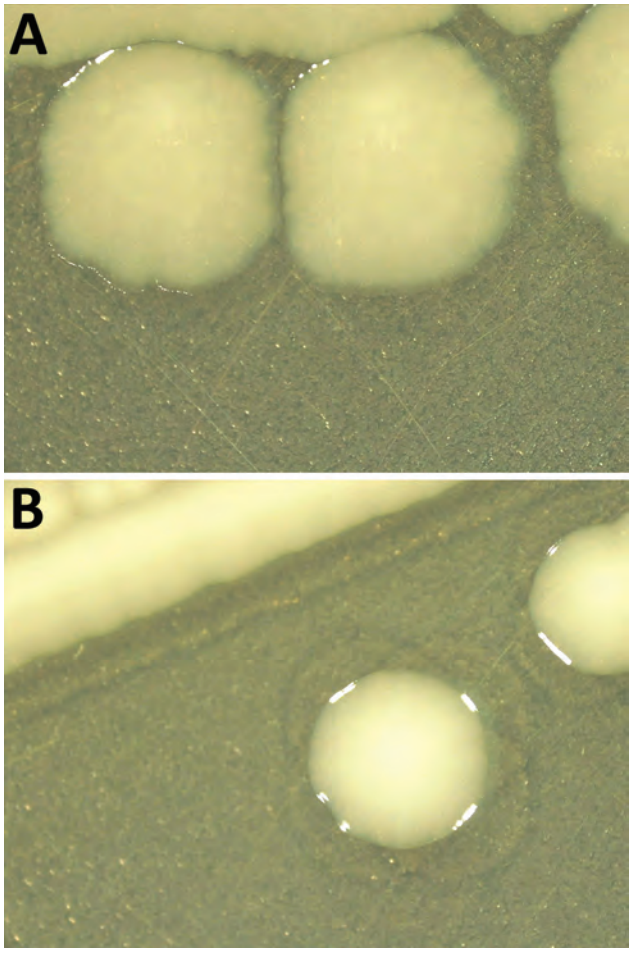

Figure 1. Comparison of colony morphology *Salmonella enterica* serovar Infantis isolates collected in Italy, 2014–2022. Isolates were grown on agar tryptose solid medium for 24 hours. A) Rough colonies from *Salmonella* Infantis atypical isolates (*S.* -:r:1,5). B) Smooth colonies from wild-type *Salmonella* Infantis isolates (*S.* 6,7:r:1,5).

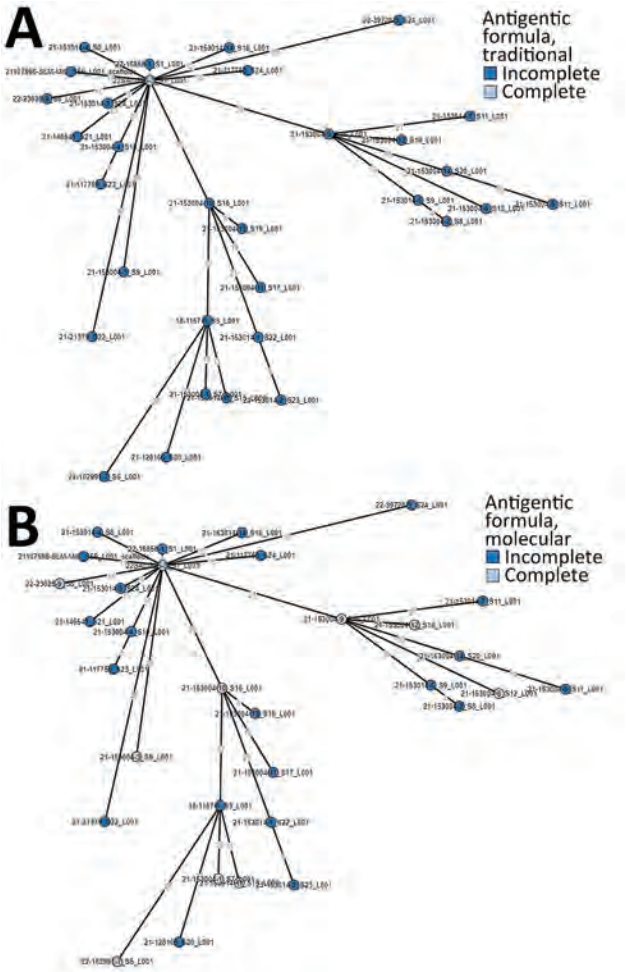

Figure 2. Minimum-spanning trees based on core genome MLST analysis of *Salmonella enterica* serovar Infantis strains collected in Italy, 2014–2022, including atypical isolates (*S.* -:r:1,5). A) Traditional serotyping. B) Molecular serotyping.

sion of the complete antigenic formula to be genetically indistinguishable from wild-type *Salmonella* Infantis. We also found a clear indication toward an antimicrobial resistance profile, shared by all the investigated atypical isolates, that provided resistance to multiple antimicrobial compounds commonly described for the wild-type circulating clones of *Salmonella* Infantis (*1*,*15*). This similarity leads to a likely closeness of those somatic variant isolates to the wild-type *Salmonella* Infantis isolates, showing a complete antigenic formula. The close relationships between *Salmonella* Infantis and variant isolates with an incomplete antigenic formula and the reasons for the lack of O-antigen expression should be further investigated. Identifying the atypical strains would pose a diagnostic issue because they would not be recognized as *Salmonella* Infantis by traditional serotyping, which remains by far the most common method used by laboratories in charge of *Salmonella* surveillance. This difficulty in identifying such atypical strains could compromise the prompt recognition of infected poultry flocks and hamper the timely implementation of the targeted control measures required by legislation, which would have serious repercussions on public health.

Acknowledgments

We thank Mario D'Incau, Elisabetta Di Giannatale, Elisa Goffredo, Maria Laura De Marchis, Alessia Zicavo, and Stefano Lollai, who contributed Salmonella strains for this study.

Raw sequence data were submitted to the European Nucleotide Archive (http://www.ebi.ac.uk/ena) under accession no. PRJEB72047.

This work was supported by the Italian Ministry of Health (grant no. RC IZS VE 02/23 Eziopatogenesi ed epidemiologia di patogeni emergenti nella filiera avicola: persistenza e adattamento di cloni emergenti di *Salmonella* Infantis e nuove strategie di biocontrollo).

About the Author

Dr. Petrin is a biotechnologist in the microbiology department of the National and WOAH Reference Laboratory for *Salmonella* in Italy. Her primary research interests are molecular epidemiology and antimicrobial drug resistance of *Salmonella*.

References

1. Franco A, Leekitcharoenphon P, Feltrin F, Alba P, Cordaro G, Iurescia M, et al. Emergence of a clonal lineage of multidrug-resistant ESBL-producing *Salmonella* Infantis transmitted from broilers and broiler meat to humans in Italy between 2011 and 2014. PLoS One. 2015;10:e0144802. https://doi.org/10.1371/journal.pone.0144802
2. European Food Safety Authority, European Centre for Disease Prevention and Control. The European Union One Health 2019 zoonoses report. EFSA J. 2021;19:6406. https://doi.org/10.2903/j.efsa.2021.6406
3. Montoro-Dasi L, Lorenzo-Rebenaque L, Marco-Fuertes A, Vega S, Marin C. Holistic strategies to control *Salmonella* Infantis: an emerging challenge in the European broiler sector. Microorganisms. 2023;11:1765. https://doi.org/10.3390/microorganisms11071765
4. Regulation (EC) No 2160/2003 of the European Parliament and of the Council of 17 November 2003 on the control of salmonella and other specified food-borne zoonotic agents. 2003 [cited 2023 Aug 8]. https://eur-lex.europa.eu/legal-content/EN/ALL/?uri=CELEX:32003R2160.
5. Commission Regulation (EU) No 200/2010 of 10 March 2010 implementing Regulation (EC) No 2160/2003 of the European Parliament and of the Council as regards a Union target for the reduction of the prevalence of *Salmonella* serotypes in adult breeding flocks of *Gallus gallus*. 2010 [cited

2023 Aug 8]. https://eur-lex.europa.eu/legal-content/en/ALL/?uri=CELEX:32010R0200
6. Fitzgerald C, Collins M, van Duyne S, Mikoleit M, Brown T, Fields P. Multiplex, bead-based suspension array for molecular determination of common *Salmonella* serogroups. J Clin Microbiol. 2007;45:3323–34. https://doi.org/10.1128/JCM.00025-07
7. Yang S-M, Baek J, Kim E, Kim HB, Ko S, Kim D, et al. Development of a genoserotyping method for *Salmonella* Infantis detection on the basis of pangenome analysis. Microorganisms. 2020;9:67. https://doi.org/10.3390/microorganisms9010067
8. Petrin S, Wijnands L, Benincà E, Mughini-Gras L, Delfgou-van Asch EHM, Villa L, et al. Assessing phenotypic virulence of *Salmonella enterica* across serovars and sources. Front Microbiol. 2023;14:1184387. https://doi.org/10.3389/fmicb.2023.1184387
9. European Food Safety Authority, Costa G, Di Piazza G, Koevoets P, Iacono G, Liebana E, et al. Guidelines for reporting whole genome sequencing-based typing data through the EFSA One Health WGS System. EFSA supporting publication. 2022;19:EN-7413. https://doi.org/10.2903/sp.efsa.2022.EN-7413
10. Lalsiamthara J, Kim JH, Lee JH. Engineering of a rough auxotrophic mutant *Salmonella* Typhimurium for effective delivery. Oncotarget. 2018;9:25441–57. https://doi.org/10.18632/oncotarget.25192
11. Jiao Y, Guo R, Tang P, Kang X, Yin J, Wu K, et al. Signature-tagged mutagenesis screening revealed a novel smooth-to-rough transition determinant of *Salmonella enterica* serovar Enteritidis. BMC Microbiol. 2017;17:48. https://doi.org/10.1186/s12866-017-0951-4
12. Park S, Won G, Kim J, Kim HB, Lee JH. Potent O-antigen-deficient (rough) mutants of salmonella Typhimurium secreting *Lawsonia intracellularis* antigens enhance immunogenicity and provide single-immunization protection against proliferative enteropathy and salmonellosis in a murine model. Vet Res (Faisalabad). 2018;49:57. https://doi.org/10.1186/s13567-018-0552-8
13. Hong Y, Reeves PR. Diversity of O-antigen repeat unit structures can account for the substantial sequence variation of Wzx translocases. J Bacteriol. 2014;196:1713–22. https://doi.org/10.1128/JB.01323-13
14. Liu B, Knirel YA, Feng L, Perepelov AV, Senchenkova SN, Reeves PR, et al. Structural diversity in *Salmonella* O antigens and its genetic basis. FEMS Microbiol Rev. 2014;38:56–89. https://doi.org/10.1111/1574-6976.12034
15. European Food Safety Authority, European Centre for Disease Prevention and Control. The European Union summary report on antimicrobial resistance in zoonotic and indicator bacteria from humans, animals and food in 2018/2019. EFSA J. 2021;19:6490. https://doi.org/10.2903/ j.efsa.2021.6490

Address for correspondence: Sara Petrin, SCS1–Microbiology Department, National and WOAH Reference Laboratory for *Salmonella*, Istituto Zooprofilattico Sperimentale delle Venezie, 31020 Legnaro (PD), Italy; email: spetrin@izsvenezie.it

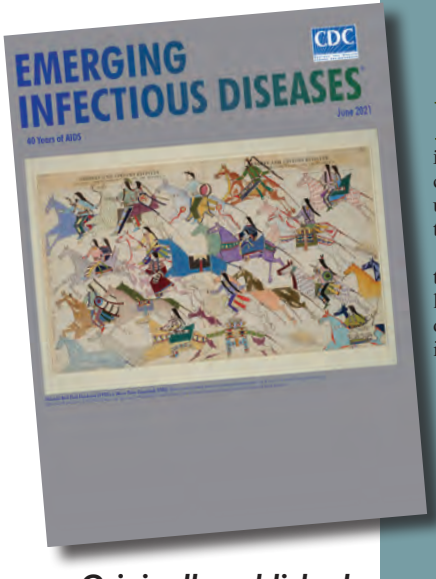

Originally published in June 2021

etymologia revisited

Enterocytozoon bieneusi

[ˈentərəˌsaitəˈʒu:ən bɪəˈnəʊsɪ]

From the Greek *enˈtĕr-ō-sīˈtōn* (intestine), *kútos* (vessel, cell), and *zōˈon* (animal), and the surname Bieneus, in memory of the first infected patient whose case was reported in Haiti during 1985. *Enterocytozoon bieneusi*, a member of the wide-ranging phylum Microsporidia, is the only species of this genus known to infect humans. Microsporidia are unicellular intracellular parasites closely related to fungi, although the nature of the relationship is not clear.

E. bieneusi, a spore-forming, obligate intracellular eukaryote, was discovered during the HIV/AIDS pandemic and is the main species responsible for intestinal microsporidiosis, a lethal disease before widespread use of antiretroviral therapies. More than 500 genotypes are described, which are divided into different host-specific or zoonotic groups. This pathogen is an emerging issue in solid organ transplantation, especially in renal transplant recipients.

Sources

1. Desportes I, Le Charpentier Y, Galian A, Bernard F, Cochand-Priollet B, Lavergne A, et al. Occurrence of a new microsporidan: *Enterocytozoon bieneusi* n.g., n. sp., in the enterocytes of a human patient with AIDS. J Protozool. 1985;32:250–4. https://doi.org/10.1111/j.1550-7408.1985.tb03046.x
2. Didier ES, Weiss LM. Microsporidiosis: not just in AIDS patients. Curr Opin Infect Dis. 2011;24:490–5. https://doi.org/10.1097/QCO.0b013e32834aa152
3. Han B, Weiss LM. Microsporidia: obligate intracellular pathogens within the fungal kingdom. Microbiol Spectr. 2017;5:97–113. https://doi.org/10.1128/microbiolspec.FUNK-0018-2016
4. Moniot M, Nourrisson C, Faure C, Delbac F, Favennec L, Dalle F, et al. Assessment of a multiplex PCR for the simultaneous diagnosis of intestinal cryptosporidiosis and microsporidiosis: epidemiologic report from a French prospective study. J Mol Diagn. 2021;23:417–23. https://doi.org/10.1016/j.jmoldx.2020.12.005

https//wwwnc.cdc.gov/eid/article/27/6/et2706_article

Ten Years of High-Consequence Pathogens—Research Gains, Readiness Gaps, and Future Goals

Jennifer H. McQuiston, Joel M. Montgomery, Christina L. Hutson

In 2014, high-consequence pathogens were described as those causing high mortality but having infrequent spillover from animals and rare human-to-human transmission (*1*). Since then, high-consequence pathogens such as ebolaviruses, monkeypox virus (MPXV), and henipaviruses have challenged that description. Unbeknownst to the authors of the 2014 article (*1*), *Orthoebolavirus zairense* (Zaire Ebola virus) was circulating at that time in Guinea, resulting in the world's largest known Ebola virus disease (EVD) outbreak. The West Africa EVD outbreak redefined our understanding of high-consequence pathogens, demonstrating their substantial potential for communicable spread; in Guinea, Liberia, and Sierra Leone, ≥28,600 persons were infected and ≥11,300 patients died. EVD cases were exported to 7 other countries by infected travelers and healthcare workers; containment took 2 years, a coordinated multinational effort, thousands of volunteers, and billions of dollars (*2*). The outbreak also drove medical progress; clinical trials tested new Ebola virus vaccines (*3*), and epidemiologic investigations showed filoviruses can persist in semen and spread through sexual contact (*4*).

During 2014–2024, eleven additional Ebola virus outbreaks have been recognized; the second largest known outbreak infected 3,470 persons in North Kivu, Democratic Republic of the Congo (DRC), during 2018–2020 (*5*). Virus sequencing data suggested that ≥3 outbreaks were most likely caused by a persistently infected survivor from a previous outbreak (*5*). Other viral hemorrhagic fevers (VHFs) also occurred. In 2019, Chapare virus caused illness in 9 patients in Bolivia, 4 of whom died; 3 healthcare workers were infected through probable nosocomial exposure, and Chapare virus was shown to persist for months in semen after acute infection (*6*). In 2022, Marburg virus was reported in Equatorial Guinea and Tanzania, infecting 24 laboratory-confirmed patients and killing 17 persons (*7*); *Orthoebolavirus sudanense* (Sudan virus) infected 164 and killed 55 persons in Uganda (*5*).

Despite achievements in Ebola virus vaccine development, similar success has lagged for medical countermeasures for other VHFs. Without vaccines or proven therapeutics, primary mitigation measures are rapid identification and isolation of case-patients, contact tracing, and strong infection control practices. Even with accessible vaccines, the response speed is key; delayed detection and response can result in larger outbreaks requiring more resources and time to control. During the 2018 DRC outbreak, regional insecurities impeded early detection and rapid response and likely contributed to the outbreak scale and complexity (*8*).

Despite successful variola virus eradication, orthopoxviruses remain high-consequence pathogens that create complex control challenges. During 2014–2024, reports of mpox caused by MPXV surged in regions where the virus is enzootic. During 2017–2022, increased reports of mpox in Nigeria initially raised little concern, even though mpox was diagnosed in occasional travelers from Nigeria who had no history of animal contact (*9*). In May 2022, MPXV clade II began circulating person-to-person globally, primarily through sexual contact among gay, bisexual, and other men who have sex with men (*10*). Thanks to smallpox preparedness work performed by the US Centers for Disease Control and Prevention and other partners, regulatory agency-approved diagnostics, the JYNNEOS vaccine (https://www.jynneos.com), and TPOXX therapeutic agent (SIGA Technologies, https://www.siga.com) were available in some countries; however, limited early supplies of the JYNNEOS vaccine and lack of licensure in some

Author affiliation: Centers for Disease Control and Prevention, Atlanta, Georgia, USA

DOI: https://doi.org/10.3201/eid3004.240160

countries meant the vaccine was not accessible to all persons at risk for MPXV exposure. Before the global mpox outbreak, no real-world efficacy data for TPOXX was available; clinical trials are ongoing. After the mpox outbreak peak in 2022, MPXV has continued to circulate at low levels through 2024; since 2022, >90,000 cases have been reported worldwide (*11*). Since 2023, similar surveillance signals have been seen in DRC with MPXV clade I (*12*), raising concerns for another global mpox outbreak caused by a more lethal virus clade.

Henipaviruses are high-consequence pathogens within the Paramyxoviridae family; >600 human infections caused by Nipah and Hendra virus have been reported in the published literature (*13*). During 2014–2024, seasonal outbreaks of Nipah virus have occurred regularly in Bangladesh and India, but the geographic range of the natural reservoir hosts, *Pteropus* spp. bats, includes Bhutan, Cambodia China, Indonesia, Madagascar, Malaysia, Maldives, Myanmar, Nepal, Pakistan, Philippines, Sri Lanka and Thailand (*14*). In Bangladesh and India, infection risk factors include date palm sap production or consumption (*15*), but person-to-person transmission has also been documented among families and close contacts; nosocomial transmission to healthcare workers remains a substantial risk factor (*13*). During a 2018 outbreak in India, Nipah virus infected 23 persons with a mortality rate >90%; of those cases, 19 were attributed to person-to-person spread among healthcare workers and patients in hospital settings (*16*). Nipah virus is considered to have substantial pandemic potential because it infects multiple mammal species, is endemic in densely human populated regions, and is an RNA virus that can have high mutation rates.

Despite a decade of ecologic studies, no definitive reservoir has been identified for Ebola virus or MPXV, making it challenging to provide clear messaging to prevent animal spillover events. Investments in early detection and response in disease-endemic countries can prevent virus spread after a spillover event. In Uganda, VHF detection rates dropped from an average of 2 weeks to only 2 days after targeted investments in diagnostic capacity were initiated (*17*). Furthermore, earlier detection translated into more rapid control measure use; the average numbers of cases per outbreak dropped from >100 before to 5 cases after those investments (*17*). However, investments are difficult to sustain and require continuous training, funding, and political will.

Since the description in 2014 (*1*), the past decade has redefined high-consequence pathogens as serious and deadly agents that pose a substantial threat to domestic and global security. Many of those pathogens are contagious, most spread from animals to humans, and some can be used as bioterrorism agents. The effects of a changing climate and increasing human–animal interactions associated with population growth and agriculture, global travel and trade, political instability, and human migration events ensure outbreaks of high-consequence pathogens will continue to pose public health threats. The 10 years since 2014 have shown how person-to-person transmission of high-consequence pathogens can fuel large, complex outbreaks, emphasizing the need for swift, effective detection and control at the earliest stages of emergence.

Recognizing the value of early detection and rapid response, a 7-1-7 framework has been proposed as a global metric for pandemic prevention (*18*): 7 days to detect emergence, 1 day to notify/mobilize a response, and 7 days to implement control measures. The framework is being piloted worldwide and has been adopted as a regional strategy in Africa. However, to meet this goal, improvements in local capacity, including specimen transport, laboratory diagnostics, trained healthcare and laboratory workers, defined reporting structures, and a robust public health workforce, are urgently needed worldwide where high-consequence pathogens continue to emerge. Investments in high-containment facilities, world-class subject matter experts, and cutting edge technologies are also critical to ensure robust public health testing capabilities at home and abroad and a more rapid resolution to outbreaks caused by high-consequence pathogens.

About the Author

Dr. McQuiston is the principal deputy director of the Division of High-Consequence Pathogens and Pathology, National Center for Emerging and Zoonotic Infectious Diseases, Centers for Disease Control and Prevention, Atlanta, Georgia, USA. Her research interests focus on preparedness and response activities related to high-consequence pathogens.

References

1. Belay ED, Monroe SS. Low-incidence, high-consequence pathogens. Emerg Infect Dis. 2014;20:319–21. https://doi.org/10.3201/eid2002.131748
2. Centers for Disease Control and Prevention. Cost of the Ebola epidemic [cited 2024 Jan 29]. https://www.cdc.gov/vhf/ebola/history/2014-2016-outbreak/cost-of-ebola.html
3. Malenfant JH, Joyce A, Choi MJ, Cossaboom CM, Whitesell AN, Harcourt BH, et al. Use of Ebola vaccine: expansion of recommendations of the Advisory Committee on Immunization Practices to include two additional populations—United States, 2021. MMWR Morb Mortal

Wkly Rep. 2022;71:290–2. https://doi.org/10.15585/mmwr.mm7108a2
4. Mate SE, Kugelman JR, Nyenswah TG, Ladner JT, Wiley MR, Cordier-Lassalle T, et al. Molecular evidence of sexual transmission of Ebola virus. N Engl J Med. 2015;373:2448–54. https://doi.org/10.1056/NEJMoa1509773
5. Centers for Disease Control and Prevention. History of Ebola disease outbreaks [cited 2024 Jan 29]. https://www.cdc.gov/vhf/ebola/history/chronology.html
6. Centers for Disease Control and Prevention. Marburg virus disease outbreaks [cited 2024 Jan 29] https://www.cdc.gov/vhf/marburg/outbreaks/chronology.html
7. Loayza Mafayle R, Morales-Betoulle ME, Romero C, Cossaboom CM, Whitmer S, Alvarez Aguilera CE, et al. Chapare hemorrhagic fever and virus detection in rodents in Bolivia in 2019. N Engl J Med. 2022;386:2283–94. https://doi.org/10.1056/NEJMoa2110339
8. Aruna A, Mbala P, Minikulu L, Mukadi D, Bulemfu D, Edidi F, et al.; CDC Ebola Response. Ebola virus disease outbreak—Democratic Republic of the Congo, August 2018–November 2019. MMWR Morb Mortal Wkly Rep. 2019;68:1162–5. https://doi.org/10.15585/mmwr.mm6850a3
9. Rao AK, Schulte J, Chen TH, Hughes CM, Davidson W, Neff JM, et al.; July 2021 Monkeypox Response Team. Monkeypox in a traveler returning from Nigeria—Dallas, Texas, July 2021. MMWR Morb Mortal Wkly Rep. 2022;71:509–16. https://doi.org/10.15585/mmwr.mm7114a1
10. McQuiston JH, Braden CR, Bowen MD, McCollum AM, McDonald R, Carnes N, et al. The CDC domestic mpox response—United States, 2022–2023. MMWR Morb Mortal Wkly Rep. 2023;72:547–52. https://doi.org/10.15585/mmwr.mm7220a2
11. Centers for Disease Control and Prevention. 2022–2023 Mpox outbreak global map [cited 2024 Jan 29]. https://www.cdc.gov/poxvirus/Mpox/response/2022/world-map.html
12. Centers for Disease Control and Prevention Health Alert Network. Mpox caused by human-to-human transmission of monkeypox virus with geographic spread in the Democratic Republic of the Congo [cited 2024 Jan 29]. https://emergency.cdc.gov/han/2023/han00501.asp
13. Hegde ST, Lee KY, Styczynski A, Jones FK, Gomes I, Das P, et al. Potential for person-to-person transmission of henipaviruses: a systemic review of the literature. J Infect Dis. 2023;Oct 31:jiad467. https://doi.org/10.1093/infdis/jiad467
14. Walsh MG. Mapping the risk of Nipah virus spillover into human populations in South and Southeast Asia. Trans R Soc Trop Med Hyg. 2015;109:563–71. https://doi.org/10.1093/trstmh/trv055
15. Islam A, McKee C, Ghosh PK, Abedin J, Epstein JH, Daszak P, et al. Seasonality of date palm sap feeding behavior by bats in Bangladesh. EcoHealth. 2021;18:359–71. https://doi.org/10.1007/s10393-021-01561-9
16. Arunkumar G, Chandni R, Mourya DT, Singh SK, Sadanandan R, Sudan P, et al.; Nipah Investigators People and Health Study Group. Outbreak investigation of Nipah virus disease in Kerala, India, 2018. J Infect Dis. 2019;219:1867–78. https://doi.org/10.1093/infdis/jiy612
17. Shoemaker TR, Balinandi S, Tumusiime A, Nyakarahuka L, Lutwama J, Mbidde E, et al. Impact of enhanced viral haemorrhagic fever surveillance on outbreak detection and response in Uganda. Lancet Infect Dis. 2018;18:373–5. https://doi.org/10.1016/S1473-3099(18)30164-6
18. Frieden TR, Lee CT, Bochner AF, Buissonnière M, McClelland A. 7-1-7: an organising principle, target, and accountability metric to make the world safer from pandemics. Lancet. 2021;398:638–40. https://doi.org/10.1016/S0140-6736(21)01250-2

Address for correspondence: Jennifer H. McQuiston, Centers for Disease Control and Prevention, 1600 Clifton Rd NE, Mailstop H24-12, Atlanta, GA 30329-4018, USA; email: jmcquiston@cdc.gov

Successful Treatment of Confirmed *Naegleria fowleri* Primary Amebic Meningoencephalitis

Ahmed Mujadid Khan Burki, Luqman Satti, Saira Mahboob, Syed Onaiz Zulfiqar Anwar, Mahwash Bizanjo, Muhammad Rafique, Najia Karim Ghanchi

Author affiliations: PNS Shifa Hospital, Karachi, Pakistan (A.M.K. Burki, L. Satti, S. Mahboob, S.O.Z. Anwar, M. Bizanjo, M. Rafique); Aga Khan University, Karachi (N.K. Ghanchi)

DOI: https://doi.org/10.3201/eid3004.230979

Primary amebic meningoencephalitis caused by *Naegleria fowleri* is a rare but nearly always fatal parasitic infection of the brain. Globally, few survivors have been reported, and the disease has no specific treatment. We report a confirmed case in Pakistan in a 22-year-old man who survived after aggressive therapy.

Naegleria fowleri amebae are thermophilic, free-living, and found in soil and fresh water, such as lakes, rivers, ponds, and untreated swimming pools. The ameba enters the brain through the nose and cribriform plate, causing primary amebic meningoencephalitis. Globally, 381 confirmed cases and only 7 (1.8%) known survivors were reported through 2018 (*1*). The Centers for Disease Control and Prevention recommends microscopic examination of fresh, unfrozen, nonrefrigerated cerebrospinal fluid (CSF) for presumptive diagnosis (*2*). If amebae are identified, the diagnosis should be confirmed through PCR. Although no specific treatment for primary amebic meningoencephalitis exists, the Centers for Disease Control and Prevention recommends combination therapy, including intravenous and intrathecal amphotericin B, azithromycin, miltefosine, rifampin, and dexamethasone (*2*).

N. fowleri ameba poses a substantial problem in Karachi, Pakistan, because of the city's hot, humid climate in the summer and its coastal location. The first case of *N. fowleri* infection in Pakistan was reported in 2008, and 146 cases were reported by October 2019 (*3*). Other than the United States (41.0%), Pakistan has reported the most *N. fowleri* infections (38.8%) (*2*).

A 22-year-old man sought care at a secondary-care hospital in Karachi on June 17, 2023, with initial symptoms of fever, drowsiness, and vomiting. He had no history of recreational water sports or swimming. His pulse rate was 105 beats/min, temperature 38.8°C, and blood pressure 121/78 mm Hg. His oxygen saturation was 95% in room air, and he had no respiratory distress. His Glasgow coma score was 11/15; he had neck rigidity, bilateral downgoing planters, and tonic-clonic seizures. Results of laboratory testing were unremarkable except an elevated leukocyte count, 19.3×10^9 cells/mL (reference range 4–10×10^9 cells/mL). We made a provisional diagnosis of acute meningoencephalitis and began empirical therapy with intravenous meropenem (2 g/12 h), intravenous vancomycin (1 g/12 h), intravenous dexamethasone (4 mg/8 h), and sodium valproate (500 mg/12 h).

On the same day, we transferred the patient to the intensive care unit of a tertiary-care hospital in Karachi for additional testing and critical care. We sent a CSF sample for microscopic examination, chemical testing, and bacterial culture. The CSF sample was slightly turbid, and test results showed high levels of protein, 950 mg/dL (reference 15–40 mg/dL); glucose, 79.2 mg/dL (reference 50–80 mg/dL); erythrocytes, 52 cells/mm^3 (reference 0 cells/mm^3); and leukocytes, 162 cells/mm^3 (reference 0–5 cells/mm^3), with 60% segmented neutrophils. A wet mount of the CSF showed trophozoite forms of an ameba (Figure). We changed the patient's treatment regimen to oral miltefosine (50 mg/6 h), intravenous amphotericin B (75 mg immediately, then 50 mg/24 h), oral rifampin (400 mg/12 h), intravenous fluconazole (400 mg/12 h), intravenous azithromycin (500 mg/24 h), intravenous sodium valproate (500 mg/8 h), and intravenous 20% man-

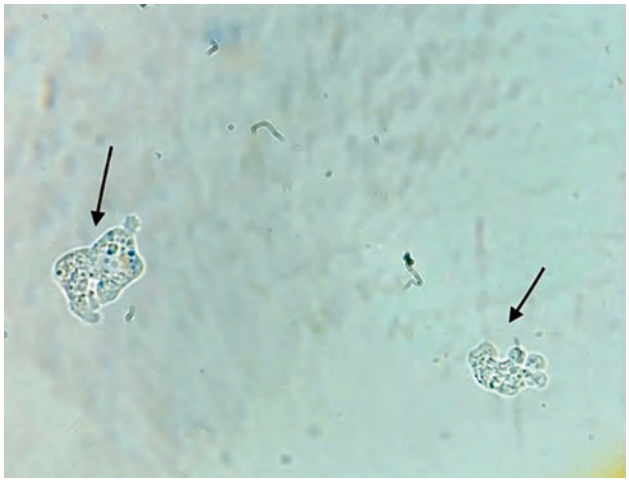

Figure. Two trophozoites with pseudopod formation identified during microscopic examination of cerebrospinal fluid from a 22-year-old man later diagnosed with *Naegleria fowleri* infection, Karachi, Pakistan, 2023. Original magnification ×40.

Table. Demographic profiles, time from symptom onset to diagnosis, and management of 8 confirmed survivors of *Naegleria fowleri* infection, 1971–2023*

Country, year of infection (reference)	Age, y/sex	Time from symptom onset to diagnosis	Therapy given	Adjuvant therapy
Australia, 1971 (*5*)	14/M	Unknown	Unknown	Unknown
United States, 1978 (*6*)	9/M	3 d	Intravenous and intrathecal amphotericin b, intravenous and intrathecal miconazole, oral rifampin, intravenous sulfisoxazole	Intravenous dexamethasone, intravenous phenytoin
Mexico, 2003 (*7*)	10/M	9 h	Intravenous amphotericin, intravenous fluconazole, intravenous dexamethasone, oral rifampin	ETT, intravenous dexamethasone
United States, 2013 (*8*)	12/F	2 d	Intravenous amphotericin, intravenous fluconazole, oral rifampin, intravenous azithromycin, oral miltefosine after 3 d, intrathecal amphotericin on second day for 10 d	Intravenous dexamethasone, extraventricular drain, intravenous 20% mannitol with hypertonic saline, hypothermia
United States, 2013 (*9*)	8/M	5 d	Intravenous amphotericin, oral rifampin, intravenous fluconazole, intravenous azithromycin, oral miltefosine	ETT, EVD, dexamethasone, mannitol
Pakistan, 2015 (*10*)	25/M	3 d	Intravenous amphotericin, oral rifampin, intravenous fluconazole	Intravenous chlorpromazine
United States, 2016 (NA)	16/M	1 d	Intravenous amphotericin, intravenous fluconazole, oral rifampin, intravenous azithromycin, oral miltefosine after 3 d, intrathecal amphotericin on second day for 10 d	Mechanical ventilation, hypothermia
Pakistan, 2023 (this case)	22/M	2 d	Intravenous amphotericin, intravenous fluconazole, oral rifampin, intravenous azithromycin, oral miltefosine, intrathecal amphotericin for 2 d	Mechanical ventilation, intravenous sodium valproate, intravenous 20% mannitol

*ETT, endotracheal tube intubation; EVD, external ventricular drain; NA, not applicable (only news reports).

nitol (200 mL/8 h). The patient's condition began to deteriorate, he had onset of seizures, and his Glasgow coma score dropped to 8/15. We placed him on mechanical ventilation 4 hours after transfer to intensive care.

We sent the CSF sample to the Aga Khan University Reference Laboratory in Karachi for PCR testing. The sample was spun down, and the cell pellet was used for DNA extraction by QIAamp DNA Extraction Kit (QIAGEN, https://www.qiagen.com), according to manufacturer protocol. Real-time PCR was performed using primers targeting the 18S rRNA gene of *Naegleria* sp., as described previously (*4*). Parallel PCRs for human RNase P gene, as assay control, and ATCC *N. fowleri* HB1 (30174D), as positive control, were performed. The PCR testing confirmed the pathogen as *N. fowleri* ameba.

On day 3, we began intrathecal amphotericin B (15 mg). The intrathecal catheter was accidently removed during nursing care, and we made the decision to discontinue the intrathecal amphotericin B. The clinical course was complicated by ventilator-associated *Acinetobacter baumannii* pneumonia that was successfully treated with intravenous and inhalational colistin. With combination therapy, the patient's condition began to improve, and on day 8, he was successfully weaned off mechanical ventilation. He completed a 3-week course of therapy, and on day 28, he was discharged. The patient has since returned to his previous state of health without any neurologic deficit.

A total of 146 cases of *N. fowleri* amoeba infections were reported in Pakistan during 2008–2019, and only 2 (1.36%) were in patients who had a history of recreational water activity (*3*). In the patient we describe, the most likely transmission could be ritual ablution with tap water, given that *N. fowleri* amebae have been isolated in the local domestic water supply (*4*). Our patient is 1 of only 8 reported laboratory-confirmed *N. fowleri* survivors worldwide (Table). The survival of our patient could be multifactorial: first, a high index of suspicion led to an early diagnosis, within 24 hours from seeking care to ICU admission; second, we used a combination of antimicrobial drugs, including miltefosine, amphotericin B, rifampin, and azithromycin, administered within 2 hours of diagnosis and ≈48 hours after onset of symptoms.

In conclusion, primary amebic meningoencephalitis caused by *N. fowleri* amoeba is a rare but fatal disease. A high index of suspicion, early diagnosis, and aggressive combination therapy can help prevent death and long-term illness.

About the Author

Dr. Burki is a consultant intensive care specialist working in the intensive care unit at PNS Shifa hospital in Karachi, Pakistan.

References:

1. Gharpure R, Bliton J, Goodman A, Ali IKM, Yoder J, Cope JR. Epidemiology and clinical characteristics of primary amebic meningoencephalitis caused by *Naegleria fowleri*: a global review. Clin Infect Dis. 2021;73:e19–27. https://doi.org/10.1093/cid/ciaa520
2. Centers for Disease Control and Prevention. *Naegleria fowleri*—primary amebic meningoencephalitis (PAM)—amebic encephalitis. Information for public health and medical professionals [cited 2023 May 3]. https://www.cdc.gov/parasites/naegleria/health_professionals.html
3. Ali M, Jamal SB, Farhat SM. *Naegleria fowleri* in Pakistan. Lancet Infect Dis. 2020;20:27–8. https://doi.org/10.1016/S1473-3099(19)30675-9
4. Ghanchi NK, Khan E, Khan A, Muhammad W, Malik FR, Zafar A. *Naegleria fowleri* meningoencephalitis associated with public water supply, Pakistan, 2014. Emerg Infect Dis. 2016;22:1835–7. https://doi.org/10.3201/eid2210.151236
5. Anderson K, Jamieson A. Primary amoebic meningoencephalitis. Lancet. 1972;2:379. https://doi.org/10.1016/S0140-6736(72)91763-1
6. Seidel JS, Harmatz P, Visvesvera GS. Successful treatment of PAM. N Engl J Med. 1982;306:346–8. https://doi.org/10.1056/NEJM198202113060607
7. Vargas-Zepeda J, Gómez-Alcalá AV, Vásquez-Morales JA, Licea-Amaya L, De Jonckheere JF, Lares-Villa F. Successful treatment of *Naegleria fowleri* meningoencephalitis by using intravenous amphotericin B, fluconazole and rifampicin. Arch Med Res. 2005;36:83–6. https://doi.org/10.1016/j.arcmed.2004.11.003
8. Linam WM, Ahmed M, Cope JR, Chu C, Visvesvara GS, da Silva AJ, et al. Successful treatment of an adolescent with *Naegleria fowleri* primary amebic meningoencephalitis. Pediatrics. 2015;135:e744–8. https://doi.org/10.1542/peds.2014-2292
9. Cope JR, Conrad DA, Cohen N, Cotilla M, DaSilva A, Jackson J, et al. Use of the novel therapeutic agent miltefosine for the treatment of primary amebic meningoencephalitis: report of 1 fatal and 1 surviving case. Clin Infect Dis. 2016;62:774–6. https://doi.org/10.1093/cid/civ1021
10. Ghanchi NK, Jamil B, Khan E, Ansar Z, Samreen A, Zafar A, et al. Case series of *Naegleria fowleri* primary ameobic meningoencephalitis from Karachi, Pakistan. Am J Trop Med Hyg. 2017;97:1600–2. https://doi.org/10.4269/ajtmh.17-0110

Address for correspondence: Luqman Satti, Department of Medical Microbiology, Clinical Pathology Laboratory. National University of Medical Sciences Rawalpindi, Pakistan; email: luqmansatti@hotmail.com

Case Management of Imported Crimean-Congo Hemorrhagic Fever, Senegal, July 2023

Youssou Bamar Gueye, Yoro Sall, Jerlie Loko Roka, Ibra Diagne, Kalidou Djibril Sow, Alseyni Diallo, Pape Samba Dièye, Jean Pierre Diallo, Boly Diop, Omer Pasi

Author affiliations: Ministry of Health and Social Action, Dakar, Senegal (Y.B. Gueye, Y. Sall, I. Diagne, K.D. Sow, A. Diallo, P.S. Dièye, J.P. Diallo, B. Diop); Centers for Disease Control and Prevention, Atlanta, Georgia, USA (J. Loko Roka, O. Pasi)

DOI: https://doi.org/10.3201/eid3004.231492

We report an imported Crimean-Congo hemorrhagic fever case in Senegal. The patient received PCR confirmation of virus infection 10 days after symptom onset. We identified 46 patient contacts in Senegal; 87.7% were healthcare professionals. Strengthening border crossing and community surveillance systems can help reduce the risks of infectious disease transmission.

Crimean-Congo hemorrhagic fever (CCHF), a severe form of hemorrhagic fever primarily transmitted to humans and animals through tick bites, is caused by CCHF virus (CCHFV). In addition, direct human contact with blood or infected tissues from viremic animals and contact with blood or secretions of an infected person have been described as transmission routes (*1*,*2*). In Senegal, the circulation of CCHFV has been reported in humans, livestock, and ticks in different areas of the country (*3*,*4*). During March–September 2023, Senegal declared a CCHF outbreak that had 8 cases distributed across 5 regions of the country (*5*). During July 2023, CCHF was diagnosed in a Senegal hospital for the 4th patient, who resided in another country. We report on the management of this imported CCHF case in Senegal.

The patient was a man in his 50s who was a trader residing in the capital of a country neighboring Senegal. He might have come into close contact with animals through his work or at home. He experienced fever, headache, and abdominal pain 2 days after returning to his rural home on July 16, 2023. The symptoms led to a consultation at a private healthcare facility in his home country, where treatment was initiated without improvement. The persistence of clinical symptoms prompted a consultation at a referral hospital in his country of residence, after which the patient's health further deteriorated 2 days later.

He had petechiae, and an abdominal ultrasound revealed hepatopathy, which prompted a family decision to seek better care in Senegal.

In Senegal, a fibroscopy and biologic tests were conducted, and results showed severe thrombocytopenia at 2,000 platelets/μL (reference range 150,000–450,000/μL). The patient was transferred to a healthcare facility that managed severe clinical cases. Because of a worsening clinical condition, including hyperglycemia and hematemesis, the patient was then transferred to the National Hospital of Pikine, Dakar, and admitted to the intensive care unit. On the 3rd day of intensive care hospitalization, the health district team collected blood samples for biologic analysis. PCR testing was positive for CCHFV 10 days after disease onset, but the patient died from multiorgan failure on the same day that PCR results were obtained.

During the case study, the investigation team identified 38 contacts in the patient's home country; 46 contacts were identified in Senegal, most (87.7%) healthcare personnel, including doctors, nurses, and laboratory staff. No bloodborne pathogen exposure incidents were reported during patient care or while handling the patient's samples. However, the level of infection prevention and control (IPC) was relatively low. We assessed the IPC level by using a structured assessment that had questions regarding the availability and usage of personal protective equipment, material sterilization, waste management, and the healthcare personnel's IPC training.

We observed a delay in diagnosis for this patient despite seeking medical attention at the onset of symptoms. The time between the onset of symptoms and diagnosis was 10 days. In India, a study involving 4 CCHF cases reported an average delay of 5.75 days from symptom onset to diagnosis (*6*). However, in northern Senegal, a CCHF case was diagnosed within 3 days of symptom onset because the 4S surveillance network, a Senegal surveillance sentinel sites system (*4*), was deployed. The 4S surveillance system encompasses 25 sentinel sites distributed across the country; ≥1 site exists in each of the country's 14 regions.

Healthcare personnel accounted for 87.7% of this patient's contacts in Senegal. According to reports in the literature, healthcare professionals are one of the socioprofessional categories most affected by secondary CCHF infection (*7*,*8*). One study showed that 49% of laboratory-confirmed secondary CCHF cases were among healthcare personnel; needlestick injuries were the primary mode of exposure in 62.7% of those cases (*8*). In addition, that study identified 21 CCHF cases associated with travel (*8*). The case we report indicates that countries should adhere to Annex 1 of the World Health Organization's International Health Regulations that defines the core capacity requirements for detecting ill travelers (*9*). During management of this CCHF case, we found no documented incidents of blood exposure, and no secondary CCHF cases were reported at the end of the 14-day contact follow-up, despite the relatively low IPC level.

In conclusion, we believe the delay in diagnosing this CCHF case resulted from the patient seeking care at multiple healthcare facilities. The healthcare personnel exposure that we identified highlights the necessity of systematically adhering to standard IPC precautions. Establishing a system for detecting potential epidemic diseases at border crossings, coupled with strengthening community surveillance, can help reduce the risks of infectious disease transmission.

Acknowledgments

We thank all of the medical teams across the country for their invaluable commitment to providing health care to their patients.

About the Author

Dr. Gueye is the operation unit chief at the Senegal National Emergency Operation Center within the Ministry of Health and Social Action. His research interests focus on viral infectious diseases transmissible by blood, sickle cell disease, and hemophilia.

References

1. Abudurexiti A, Adkins S, Alioto D, Alkhovsky SV, Avšič-Županc T, Ballinger MJ, et al. Taxonomy of the order Bunyavirales: update 2019. Arch Virol. 2019;164:1949–65. https://doi.org/10.1007/s00705-019-04253-6
2. Hawman DW, Feldmann H. Crimean-Congo haemorrhagic fever virus. Nat Rev Microbiol. 2023;21:463–77. https://doi.org/10.1038/s41579-023-00871-9
3. Mhamadi M, Badji A, Dieng I, Gaye A, Ndiaye EH, Ndiaye M, et al. Crimean-Congo hemorrhagic fever virus survey in humans, ticks, and livestock in Agnam (northeastern Senegal) from February 2021 to March 2022. Trop Med Infect Dis. 2022;7:324. https://doi.org/10.3390/tropicalmed7100324
4. Dieng I, Barry MA, Diagne MM, Diop B, Ndiaye M, Faye M, et al. Detection of Crimean Congo haemorrhagic fever virus in north-eastern Senegal, Bokidiawé 2019. Emerg Microbes Infect. 2020;9:2485–7. https://doi.org/10.1080/22221751.2020.1847605
5. World Health Organization African Region. Weekly bulletin on outbreaks and other emergencies, week 42, October 16–22, 2023 [cited 2024 Feb 15]. https://iris.who.int/bitstream/handle/10665/373912/OEW42-1622102023.pdf
6. Tripathi S, Bhati R, Gopalakrishnan M, Bohra GK, Tiwari S, Panda S, et al. Clinical profile and outcome of patients with Crimean Congo haemorrhagic fever: a hospital based observational study from Rajasthan, India. Trans R Soc Trop Med Hyg. 2020;114:643–9. https://doi.org/10.1093/trstmh/traa014

7. Maltezou HC, Papa A, Ventouri S, Tseki C, Pervanidou D, Pavli A, et al. A case of Crimean-Congo haemorrhagic fever imported in Greece: contact tracing and management of exposed healthcare workers. J Infect Prev. 2019;20:171–8. https://doi.org/10.1177/1757177419852666
8. Leblebicioglu H, Sunbul M, Guner R, Bodur H, Bulut C, Duygu F, et al. Healthcare-associated Crimean-Congo haemorrhagic fever in Turkey, 2002–2014: a multicentre retrospective cross-sectional study. Clin Microbiol Infect. 2016;22:387.e1–4. https://doi.org/10.1016/j.cmi.2015.11.024
9. World Health Organization. International health regulations (2005), 3rd edition [cited 2023 Aug 24]. https://www.who.int/publications/i/item/9789241580496

Address for correspondence: Jerlie Loko Roka, Centers for Disease Control and Prevention, Senegal office, B.P. 49, Rte des Almadies, Dakar, Senegal; email: myu3@cdc.gov

Potential Sexual Transmission of Antifungal-Resistant *Trichophyton indotineae*

Stephanie Spivack, Jeremy A.W. Gold, Shawn R. Lockhart, Priyanka Anand, Laura A.S. Quilter, Dallas J. Smith, Briana Bowen, Jane M. Gould, Ahmed Eltokhy, Ahmed Gamal, Mauricio Retuerto, Thomas S. McCormick, Mahmoud A. Ghannoum

Author affiliations: Temple University Hospital Section of Infectious Diseases, Philadelphia, Pennsylvania, USA (S. Spivack); Centers for Disease Control and Prevention, Atlanta, Georgia, USA (J.A.W. Gold, S.R. Lockhart, P. Anand, L.A.S. Quilter, D.J. Smith); Department of Public Health, Philadelphia (B. Bowen, J.M. Gould); Center for Medical Mycology, Case Western Reserve University and University Hospitals Cleveland Medical Center, Cleveland, Ohio, USA (A. Eltokhy, A. Gamal, M. Retuerto, T.S. McCormick, M.A. Ghannoum)

DOI: https://doi.org/10.3201/eid3004.240115

We describe a case of tinea genitalis in an immunocompetent woman in Pennsylvania, USA. Infection was caused by *Trichophyton indotineae* potentially acquired through sexual contact. The fungus was resistant to terbinafine (first-line antifungal) but improved with itraconazole. Clinicians should be aware of *T. indotineae* as a potential cause of antifungal-resistant genital lesions.

Dermatophytosis, also called ringworm or tinea, is a common superficial fungal skin infection most often caused by *Trichophyton*, *Microsporum*, or *Epidermophyton* fungi and often treated using over-the-counter topical antifungal agents (*1*). Oral terbinafine is a first-line antifungal treatment for extensive skin infections, which typically occur in immunocompromised or older persons (*1*). Outbreaks of extensive, recalcitrant, and frequently terbinafine-resistant dermatophytosis in immunocompetent persons are ongoing in southern Asia because of the recently emerged dermatophyte *Trichophyton indotineae* (formerly *Trichophyton mentagrophytes* genotype VIII). *T. indotineae* typically causes tinea faciei, corporis, or cruris; easily spreads person-to-person; and has been reported globally, including in multiple US states (*2*–*4*). Laboratory identification requires advanced molecular techniques because culture-based methods cannot distinguish *T. indotineae* from other *Trichophyton* species (*2*).

Previous reports describe sexual transmission of genital dermatophytosis (*5*,*6*), including cases caused by *T. mentagrophytes* genotype VII, a dermatophyte closely related to *T. indotineae* but not associated with terbinafine resistance (*7*,*8*). We report a case of tinea genitalis in an immunocompetent woman in Pennsylvania, USA, that was caused by an antifungal-resistant *T. indotineae* strain potentially acquired through sexual contact. Our study was reviewed by the Centers for Disease Control and Prevention (CDC) and conducted consistent with applicable federal laws and CDC policy.

During winter 2022, a healthy young cisgender woman traveled to South Asia. While there, she had vaginal intercourse with a man who had purple genital and buttocks lesions. Subsequently, she experienced similar lesions, beginning on her inner thigh, then spreading to her genitals and buttocks. In spring 2022, she returned to the United States and sought care from a primary care provider and dermatologist. She received mometasone 0.1% ointment (topical medium-potency corticosteroid) for suspected contact dermatitis, econazole 1% (topical antifungal) cream, a prednisone taper pack, and diphenhydramine. The reported lesions did not resolve, and corticosteroids worsened the condition. The result of a thigh skin-punch biopsy was positive for hyphae by periodic acid-Schiff stain, consistent with dermatophytosis. The patient subsequently received multiple antifungal courses including topical ketoconazole, oral terbinafine (250 mg/d for 2 weeks), and fluconazole (150 mg/wk to 200 mg/d for >20 cumulative weeks), all without lesion resolution.

In spring 2023, physical examination by an infectious disease physician revealed an annular, scaling, hyperpigmented eruption on the patient's buttocks involving the intergluteal cleft and 3 small hyperpigmented areas on the mons pubis. She reported having a new male sexual partner in the United States who developed similar lesions on his genitals after they had sexual intercourse. Given clinical suspicion for *T. indotineae* infection, she was prescribed a 1-week course of itraconazole. On telephone follow-up 4 days later, she reported decreasing rash size and pruritis. She missed a follow-up visit but was present for a telemedicine visit 6 weeks later, when she reported resumption of pruritis and 2 new small pruritic patches on her right buttock and labia. She was prescribed an additional 2-week course of itraconazole (200 mg 2×/d). Her pruritis resolved, and she reported no recurrence at 3-months follow-up. The rash on the patient's sexual partner resolved, but we are unaware of the treatment he received.

The infectious disease physician sent a skin scraping from the gluteal region for fungal culture and advanced mycologic testing at the Center for Medical Mycology of the University Hospitals Cleveland Medical Center (Cleveland, OH, USA). Macroscopic and microscopic morphology and broth microdilution antifungal susceptibility testing (Figure) demonstrated MICs of 16 μg/mL for terbinafine, 16 μg/mL for fluconazole, 0.016 μg/mL for itraconazole, and ≤0.031 μg/mL for efinaconazole (Clinical and Laboratory Standards Institute, https://clsi.org/standards/products/microbiology/documents/m38). Although breakpoints do not exist for dermatophytes, MIC ≥0.5 μg/mL for terbinafine has been correlated with resistance-conferring gene mutations (*4*). On the basis of

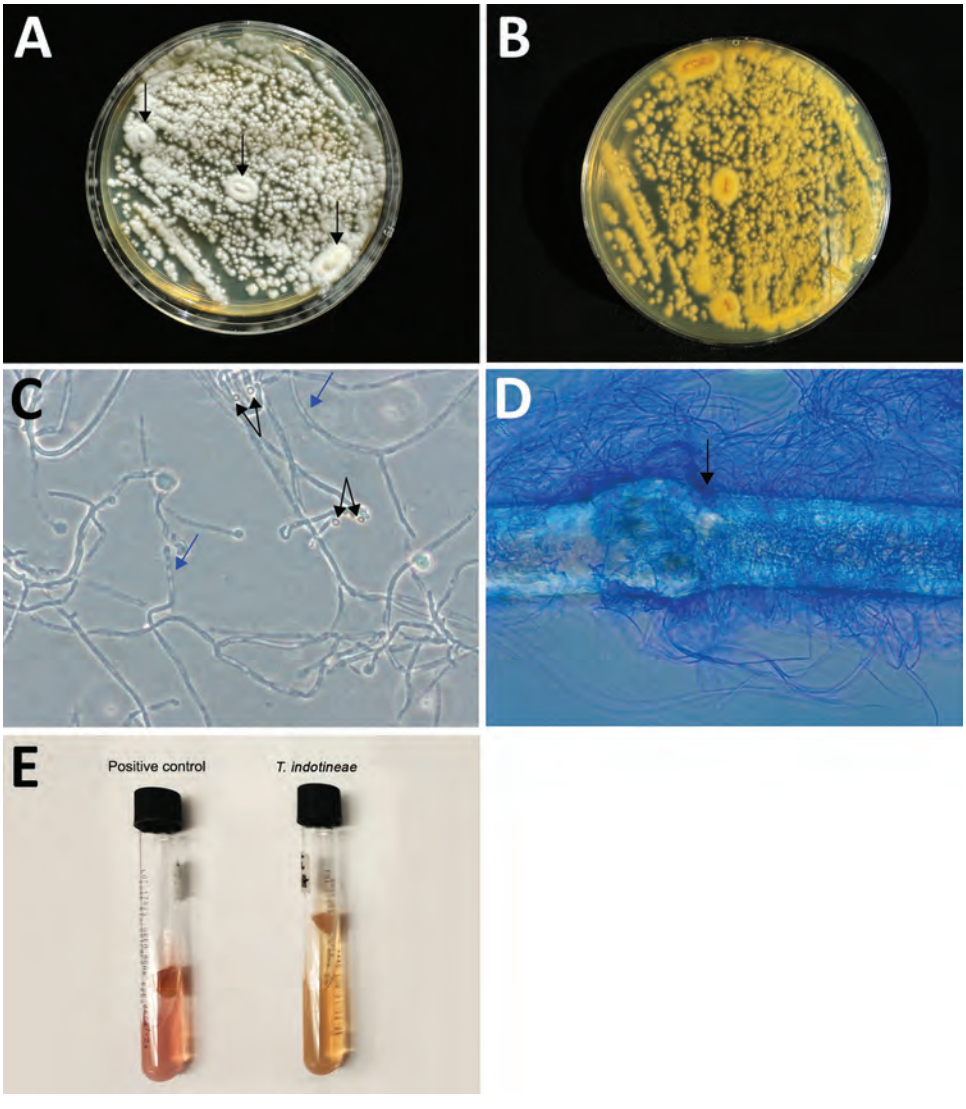

Figure. Results of gross and microscopic morphology and microbiological laboratory testing to identify *Trichophyton indotineae* in a woman in Pennsylvania, USA. A, B) Colonies were velvety white, flat, and had a raised center (arrow) (A) and a light yellow pigment on reverse (B). C) Numerous microconidia showed the pyriform and clavate forms (black arrow) and fungal hyphae with septation (blue arrows). Original magnification ×40. D) In vitro hair perforation test was positive (arrow). Original magnification ×100. E) *T. indotineae* had a negative urease test (yellowish color), while the positive control, *Trichophyton tonsurans*, was pinkish.

internal transcribed spacer sequencing, we initially identified the isolate as *T. interdigitale*. Given concern for *T. indotineae* infection, we performed a BLAST search (https://blast.ncbi.nlm.nih.gov), which identified the isolate as *T. indotineae* (GenBank accession no. PP336547).

Our report highlights the emergence of antifungal-resistant *T. indotineae* as a cause of genital lesions and possible acquisition and transmission through sexual contact. Clinicians should be aware that visual inspection without diagnostic testing cannot reliably distinguish dermatophytosis from other causes of inflammatory skin conditions (e.g., contact dermatitis) (*9*). Subsequent inappropriate use of corticosteroids can exacerbate dermatophytosis. Diagnostic testing (e.g., with potassium hydroxide preparation) is essential to correctly diagnose and appropriately treat fungal skin infections (*1*,*9*). Increasing clinician awareness of dermatophytosis as a potential cause of genital lesions might prevent diagnostic delays (*7*). Itraconazole is often effective against *T. indotineae* infections, but there are challenges related to absorption, interactions between medications, insurance coverage, and possible need for prolonged therapy (sometimes requiring >3 months) and higher dosages of itraconazole (e.g., 200 mg 2×/d) (*2*,*10*). Strong inflammatory reactions that have been reported after initiation of antifungal treatment should not be confused with therapeutic failure (*6*). In conclusion, our report underscores the need for clinical vigilance, increased surveillance such as through sexual health provider networks to identify emerging trends in severe and antifungal-resistant dermatophytosis, studies to understand *T. indotineae* transmission dynamics, and laboratory capacity to identify dermatophyte species and test for antifungal susceptibility.

About the Author

Dr. Spivack is an infectious disease physician and assistant professor of clinical medicine at the Lewis Katz School of Medicine at Temple University in Philadelphia, Pennsylvania. Dr. Spivack's primary research interests include harm reduction, HIV, hepatitis C, and bioethics.

References

1. Ely JW, Rosenfeld S, Seabury Stone M. Diagnosis and management of tinea infections. Am Fam Physician. 2014;90:702–10.
2. Caplan AS, Chaturvedi S, Zhu Y, Todd GC, Yin L, Lopez A, et al. Notes from the field: first reported US cases of tinea caused by *Trichophyton indotineae*—New York City, December 2021–March 2023. MMWR Morb Mortal Wkly Rep. 2023;72:536–7. https://doi.org/10.15585/mmwr.mm7219a4
3. Uhrlaß S, Verma SB, Gräser Y, Rezaei-Matehkolaei A, Hatami M, Schaller M, et al. *Trichophyton indotineae*—an emerging pathogen causing recalcitrant dermatophytoses in India and worldwide: a multidimensional perspective. J Fungi (Basel). 2022;8:757. https://doi.org/10.3390/jof8070757
4. Cañete-Gibas CF, Mele J, Patterson HP, Sanders CJ, Ferrer D, Garcia V, et al. Terbinafine-resistant dermatophytes and the presence of *Trichophyton indotineae* in North America. J Clin Microbiol. 2023;61:e0056223. https://doi.org/10.1128/jcm.00562-23
5. Chromy D, Osmers A-M, Bauer WM, Touzeau-Roemer V, Borst C, Esser S, et al. Sexually transmitted dermatophytes can cause severe infection among men who have sex with men as tinea genitalis. Open Forum Infect Dis. 2023;10:ofad519.
6. Luchsinger I, Bosshard PP, Kasper RS, Reinhardt D, Lautenschlager S. Tinea genitalis: a new entity of sexually transmitted infection? Case series and review of the literature. Sex Transm Infect. 2015;91:493–6. https://doi.org/10.1136/sextrans-2015-052036
7. Jabet A, Dellière S, Seang S, Chermak A, Schneider L, Chiarabini T, et al. Sexually transmitted *Trichophyton mentagrophytes* genotype VII infection among men who have sex with men. Emerg Infect Dis. 2023;29:1411–4. https://doi.org/10.3201/eid2907.230025
8. Nenoff P, Wendrock-Shiga G, Mechtel D, Schubert K, Jarsumbeck R, Lusmöller E, et al. *Trichophyton mentagrophytes* ITS genotype VII from Thailand. In: Bouchara J-P, Nenoff P, Gupta AK, Chaturvedi V, editors. Dermatophytes and dermatophytoses. Cham, Switzerland: Springer International Publishing; 2021. p. 231–56.
9. Yadgar RJ, Bhatia N, Friedman A. Cutaneous fungal infections are commonly misdiagnosed: a survey-based study. J Am Acad Dermatol. 2017;76:562–3. https://doi.org/10.1016/j.jaad.2016.09.041
10. Khurana A, Agarwal A, Agrawal D, Panesar S, Ghadlinge M, Sardana K, et al. Effect of different itraconazole dosing regimens on cure rates, treatment duration, safety, and relapse rates in adult patients with tinea corporis/cruris: a randomized clinical trial. JAMA Dermatol. 2022;158:1269–78. https://doi.org/10.1001/jamadermatol.2022.3745

Address for correspondence: Mahmoud A. Ghannoum, 10900 Euclid Ave, Case Western Reserve University and University Hospitals Cleveland Medical Center, Cleveland, OH 44106, USA; email: mahmoud.ghannoum@case.edu

Chlamydia pneumoniae Upsurge at Tertiary Hospital, Lausanne, Switzerland

Florian Tagini, Onya Opota, Gilbert Greub

Author affiliation: Institute of Microbiology, Lausanne University Hospital, Lausanne, Switzerland

DOI: https://doi.org/10.3201/eid3004.231610

Chlamydia pneumoniae infection cases have usually accounted for <1.5% of community-acquired respiratory tract infections. Currently, Lausanne, Switzerland is experiencing a notable upsurge in cases, with 28 reported within a span of a few months. This upsurge in cases highlights the need for heightened awareness among clinicians.

The intracellular bacterium *Chlamydia pneumoniae* is a recognized cause of community-acquired pneumonia (*1*). High-frequency estimates were initially derived from serologic studies, but the advent of molecular techniques has revealed rates that are generally <1.5% among patients with respiratory tract infections, although epidemiological change between initial and current rate estimates cannot be ruled out (*2*,*3*). Sporadic outbreaks have been documented, such as a 2014 prison outbreak in Texas (*4*) and a 2016 community-acquired pneumonia outbreak in South Korea (*5*). In recent years, studies have also linked *C. pneumoniae* bacteria to bronchitis and asthma (*6*). *C. pneumoniae* bacteria has also been documented in patients with cystic fibrosis (*7*). Of note, infections occur at higher rates in children than in adults (*2*).

At the height of the SARS-CoV-2 pandemic, *C. pneumoniae* bacteria detection rates were low, paralleling the near-extinction state observed for *Mycoplasma pneumoniae* bacteria in Europe (*8*). However, a current rebound of *M. pneumoniae* infections is occurring (*9*). We report a similar increase in PCR-positive *C. pneumoniae* bacteria detection rates at a tertiary hospital in Switzerland. As the case series and the analysis thereof derive from the pathogen surveillance to which our institute is legally bound by the health authorities, Swiss legislation on human research is not applicable and the consent of the patients concerned is not required. This publication complies with the applicable data protection legislation and institutional guidelines.

During routine epidemiologic surveillance at Lausanne University Hospital in Lausanne, Switzerland, positive *C. pneumoniae* bacteria PCR rates surged to 3.61% during October–December 2023, peaking at 6.66% in October, contrasting with the usual 0%–0.75% range reported over the past decade (Figure 1, panel A, B). The PCR method we used for testing has been previously described in Opota et al. (*10*). In this most recent outbreak, we documented *C. pneumoniae* bacteria in 28 patients in 2023; of those, 20 were children (mean age 8 years) and 8 were adults (mean age 43 years). Patients with *C. pneumoniae* bacteria sometimes reported wheezing as a major clinical complaint. We tested bacterial loads in patients positive for *C. pneumoniae* bacteria and found that the mean bacterial load was 1,534,821 DNA copies/mL (range 200–11,998,897 DNA copies/mL). We collected nasopharyngeal swabs most frequently (n = 24), whereas we collected sputum samples (n = 5) and nasal swab samples (nostril only, n = 1) less frequently. Of note, bacterial loads were not higher in the analyzed sputa

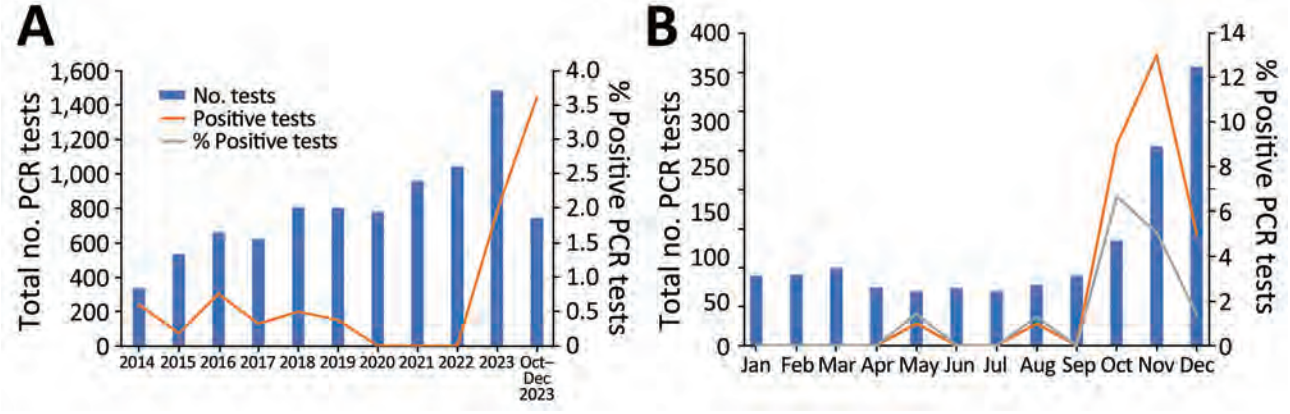

Figure 1. Positivity rate of *Chlamydia pneumoniae* PCRs in a tertiary care hospital, Lausanne, Switzerland. A) Yearly number of *C. pneumoniae* PCR tests conducted during 2014-2023. The final bar shows the last quarter of 2023, when the positivity rate exhibited a notable increase to 3.61%. B) Monthly numbers of *C. pneumoniae* PCR tests performed in 2023, showcasing positive tests and corresponding positivity rates. The data reveal a peak in the percentage of positivity of 6.66% in October.

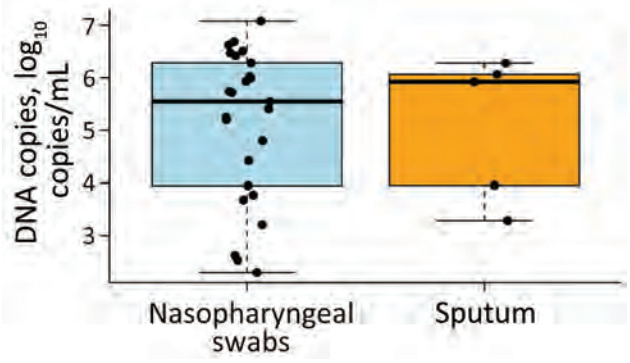

Figure 2. Boxplot of the quantifications of the *Chlamydia pneumoniae*–positive PCRs, by sample type, in a tertiary care hospital, Lausanne, Switzerland. In total, 24 nasopharyngeal swab and 5 sputum samples were available. For 2 patients, data were paired, with 1 nasopharyngeal swab and 1 sputum sample available for each. Black dots indicate individual samples; horizontal lines within boxes indicate medians; box tops and bottoms indicate interquartile range; and error bars indicate 1.5 times the value of the interquartile ranges. The nostril swab was omitted from the analysis. We observed no statistically significant difference between the groups (Wilcoxon rank-sum test).

than in the nasopharyngeal swabs (p = 1 by Wilcoxon rank-sum test) (Figure 2).

The results of this analysis should be interpreted with caution in the absence of a larger number of paired samples. This analysis includes only 2 paired samples exhibiting <1 logarithm (decimal) of difference in DNA copies per milliliter.

To explain this sudden surge of *C. pneumoniae* bacterial infection, we suspect 2 primary factors. First, decreased immunity may have developed because of fewer circulating strains in the population over the past 3 years, related to SARS-CoV-2 transmission prevention measures. Second, recently relaxed hygiene standards after the SARS-CoV-2 pandemic may have increased the risk for infection.

Clinical suspicion of *C. pneumoniae* infection is particularly warranted when patients' clinical manifestations include a persistent dry cough or wheezing. Molecular testing, if available, should be the first-line diagnostic tool with nasopharyngeal swabs as an acceptable sample collection method. We do not recommend serologic testing in such cases because of the need to collect convalescent serum and the late appearance of antibodies. Antibodies generally develop 2–3 weeks after symptom onset for IgM and 4–8 weeks for IgG, which is rather late for diagnostic and therapeutic purposes. Furthermore, because *C. pneumoniae* bacterial infection can be treated by macrolides, doxycycline, or fluoroquinolones, current increases in both *C. pneumoniae* and *M. pneumoniae* bacteria lead us to recommend PCR testing for both bacteria in symptomatic patients, instead of testing only for respiratory viruses. Although co-infection with *M. pneumoniae* bacteria occurred in only 1 patient (*M. pneumoniae* PCR was tested on all samples) in our cohort, viral co-infections are not uncommon. Many multiplexed PCR respiratory panels are available and could help monitor the trend of *C. pneumoniae* bacterial infections on a larger scale.

In conclusion, we outline an upsurge of *C. pneumoniae* bacterial infections in the Lausanne region of Switzerland, especially in the pediatric population, raising concerns for other settings and regions. We found no clear epidemiologic link between patients, which suggests that we are detecting a minority of cases and that infections may occur at higher rates in the community than we have documented. This local finding highlights the importance of considering this intracellular bacterium as a causative agent, along with other fastidious organisms such as *M. pneumoniae* bacteria, which are also on the rise (*9*).

About the Author

Dr. Tagini is a trainee in clinical microbiology and infectious diseases at the Lausanne University Hospital. His research interests are focused mainly on intracellular bacteria and bacterial genomics.

References

1. Grayston JT, Campbell LA, Kuo CC, Mordhorst CH, Saikku P, Thom DH, et al. A new respiratory tract pathogen: *Chlamydia pneumoniae* strain TWAR. J Infect Dis. 1990;161:618–25. https://doi.org/10.1093/infdis/161.4.618
2. Kumar S, Hammerschlag MR. Acute respiratory infection due to *Chlamydia pneumoniae*: current status of diagnostic methods. Clin Infect Dis. 2007;44:568–76. https://doi.org/10.1086/511076
3. Senn L, Jaton K, Fitting JW, Greub G. Does respiratory infection due to *Chlamydia pneumoniae* still exist? Clin Infect Dis. 2011;53:847–8. https://doi.org/10.1093/cid/cir515
4. Conklin L, Adjemian J, Loo J, Mandal S, Davis C, Parks S, et al. Investigation of a *Chlamydia pneumoniae* outbreak in a federal correctional facility in Texas. Clin Infect Dis. 2013;57:639–47. https://doi.org/10.1093/cid/cit357
5. Han HY, Moon JU, Rhim JW, Kang HM, Lee SJ, Yang EA. Surge of *Chlamydia pneumoniae* pneumonia in children hospitalized with community-acquired pneumonia at a single center in Korea in 2016. J Infect Chemother. 2023;29:453–7. https://doi.org/10.1016/j.jiac.2023.01.012
6. Hahn DL, Schure A, Patel K, Childs T, Drizik E, Webley W. *Chlamydia pneumoniae*–specific IgE is prevalent in asthma and is associated with disease severity. PLoS One. 2012;7:e35945. https://doi.org/10.1371/journal.pone.0035945
7. Pittet LF, Bertelli C, Scherz V, Rochat I, Mardegan C, Brouillet R, et al. *Chlamydia pneumoniae* and *Mycoplasma pneumoniae* in children with cystic fibrosis: impact on bacterial respiratory microbiota diversity. Pathog Dis. 2021;79:ftaa074.

8. Meyer Sauteur PM, Beeton ML, Pereyre S, Bébéar C, Gardette M, Hénin N, et al.; ESGMAC the ESGMAC MAPS study group. *Mycoplasma pneumoniae*: gone forever? Lancet Microbe. 2023;4:e763. https://doi.org/10.1016/S2666-5247(23)00182-9
9. Meyer Sauteur PM, Beeton ML, Pereyre S, Bébéar C, Gardette M, Hénin N, et al. European Society of Clinical Microbiology and Infectious Diseases (ESCMID) Study Group for Mycoplasma and Chlamydia Infections (ESGMAC), and the ESGMAC *Mycoplasma pneumoniae* Surveillance (MAPS) Study Group. *Mycoplasma pneumoniae*: delayed re-emergence after COVID-19 pandemic restrictions. Lancet Microbe. 2024;5:e100–1. https://doi.org/10.1016/S2666-5247(23)00344-0
10. Opota O, Brouillet R, Greub G, Jaton K. Methods for real-time PCR-based diagnosis of *Chlamydia pneumoniae*, *Chlamydia psittaci*, and *Chlamydia abortus* infections in an opened molecular diagnostic platform. Methods Mol Biol. 2017;1616:171–81. https://doi.org/10.1007/978-1-4939-7037-7_11

Address for correspondence: Gilbert Greub, Institute of Microbiology, Department of Laboratory Medicine and Pathology, Lausanne University Hospital and University of Lausanne, Bugnon 48, CH-1011 Lausanne, Switzerland; email: gilbert.greub@chuv.ch

Highly Pathogenic Avian Influenza A(H5N1) Viruses from Multispecies Outbreak, Argentina, August 2023

Agustina Rimondi, Ralph E.T. Vanstreels, Valeria Olivera, Agustina Donini, Martina Miqueo Lauriente, Marcela M. Uhart

Author affiliations: Robert Koch Institute, Berlin, Germany (A. Rimondi); Instituto Nacional de Tecnología Agropecuaria Instituto de Virología e Innovaciones Tecnológicas, Buenos Aires, Argentina (A. Rimondi, V. Olivera); University of California School of Veterinary Medicine, Davis, California, USA (R.E.T. Vanstreels, M.M. Uhart); Southern Right Whale Health Monitoring Program, Puerto Madryn, Argentina (A. Donini, M.M. Uhart); Secretaria de Ambiente y Cambio Climático de Provincia de Río Negro, Viedma, Argentina (M. Miqueo Lauriente)

DOI: https://doi.org/10.3201/eid3004.231725

We report full-genome characterization of highly pathogenic avian influenza A(H5N1) clade 2.3.4.4b virus from an outbreak among sea lions (August 2023) in Argentina and possible spillover to fur seals and terns. Mammalian adaptation mutations in virus isolated from marine mammals and a human in Chile were detected in mammalian and avian hosts.

In February 2023, the first case of highly pathogenic avian influenza (HPAI) A(H5N1) in Argentina was detected in a wild goose near the border with Bolivia and Chile (Appendix Figure 1, https://wwwnc.cdc.gov/EID/article/30/4/23-1725-App1.pdf) (*1*). In contrast with Peru and Chile, where extensive mortality of seabirds and marine mammals had been attributed to the virus in the preceding months (*2*,*3*), the initial spread of HPAI H5N1 in Argentina was largely limited to backyard and industrial poultry (94 outbreaks), causing the death or disposal of 2.2 million birds. Argentina declared itself free from the disease in poultry on August 8, 2023; before then, HPAI H5N1 detections in wildlife in Argentina had been scarce (7 events during February–April) and limited to aquatic birds (Anatidae, Laridae, and Rallidae) (*1*,*4*). However, soon thereafter, the national animal health services confirmed HPAI H5N1 in South American sea lions (*Otaria byronia*) from Río Grande, southernmost Argentina. Over subsequent weeks, the virus was detected in sea lions northward along the Argentina coast, and sporadic cases also occurred in South American fur seals (*Arctocephalus australis*). The most affected site was Punta Bermeja (Appendix Figure 1), the largest sea lion colony in Argentina, where an estimated 811 sea lions died over 2 months; minimal numbers (<5) of fur seals and terns were also affected (*1*,*4*).

In collaboration with provincial authorities and park rangers, we collected swab samples (oronasal, rectal, tracheal, lung, and brain) from 16 deceased sea lions, 1 fur seal, 1 great grebe (*Podiceps major*), and 1 South American tern (*Sterna hirundinacea*) discovered at Punta Bermeja on August 26, 2023. A sampled adult male sea lion was seen alive showing clinical signs consistent with HPAI infection (inability to stand or walk, muscular tremors and spasms, difficulty breathing, and abundant oral mucus). We tested the samples by real-time reverse transcription PCR targeting influenza A virus (*5*) and confirmed that all were positive. On the basis of viral RNA yields, we selected brain samples from 4 sea lions, 1 fur seal, and 1 tern for full-genome sequencing (Appendix Figure 2). We used maximum-likelihood tree phylogenetic analysis (*6*) and mutational analysis

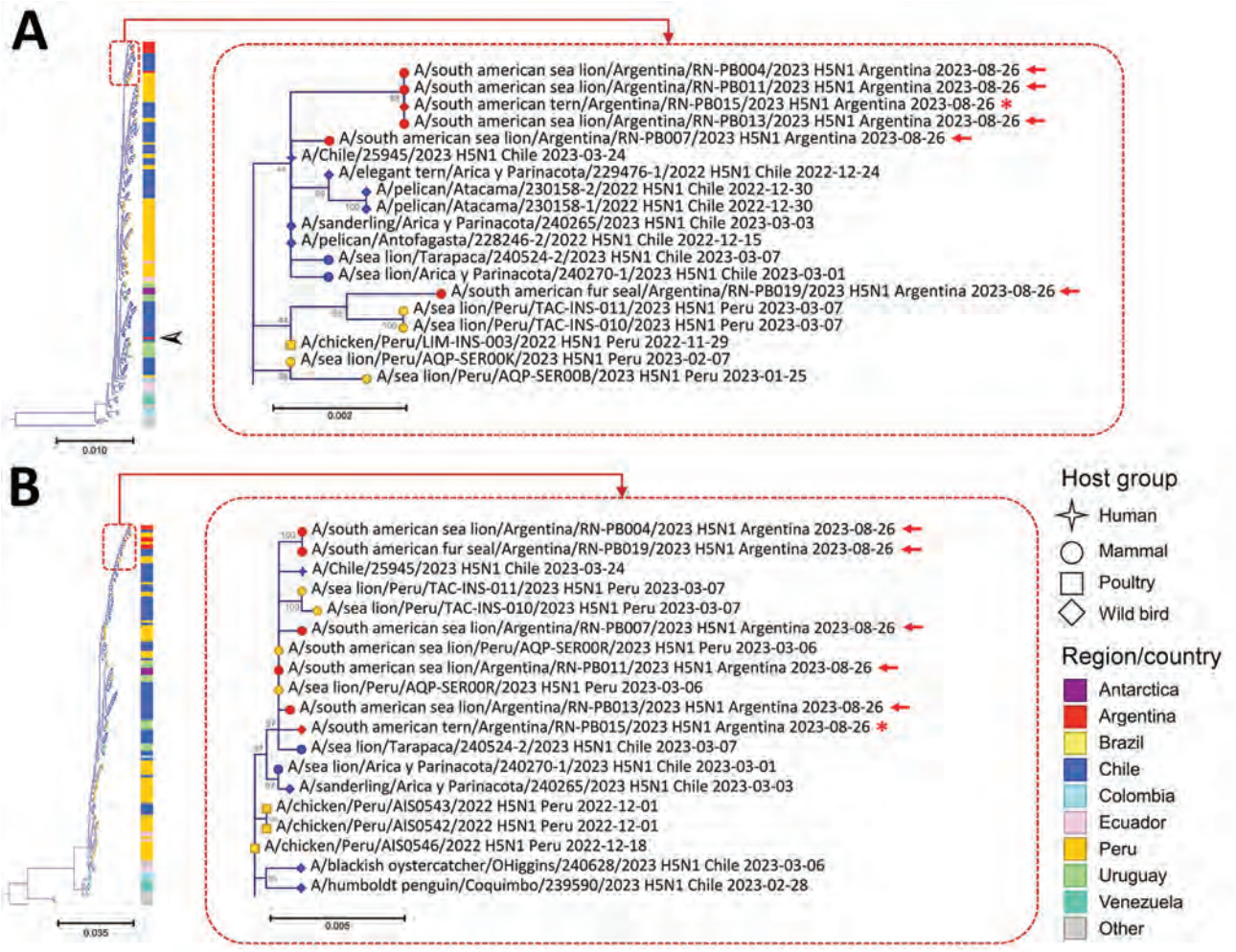

Figure. Maximum-likelihood trees for hemagglutinin (A) and polymerase basic 2 (B) gene segments evaluated in study of highly pathogenic avian influenza A(H5N1) in Argentina compared with reference strains from other countries in South America. Tree areas have been enlarged at right to show detail. Red arrows indicate virus from marine mammals in Argentina; red asterisk indicates virus from a tern in Argentina. Black arrowhead along full tree in panel A indicates the hemagglutinin sequence from the first detection of HPAI H5N1 in a wild goose in Argentina. Node shape represents host group, and node color (and bars adjacent to trees) represents the region/country. Branch lengths are drawn proportionally to the extent of changes. Values adjacent to nodes represent bootstrap support ≥40. Scale bars indicate nucleotide substitutions per site.

to compare the sequences (GenBank accession nos. OR987081–128) with representative HPAI H5N1 strains from South America.

Phylogenetic trees (Figure; Appendix Figure 2) showed that the viruses we identified belong to HPAI H5N1 clade 2.3.4.4b and are closely related to H5N1 viruses that circulated in South America during 2022–2023. Our finding supports the hypothesis that, after introduction from North America into Peru in November 2022, HPAI H5N1 viruses continued spreading across the continent and into Argentina. Of note, the viruses from Punta Bermeja did not cluster with the hemagglutinin and neuraminidase sequences available from HPAI H5N1 first detected in a wild goose in Argentina. Instead, all gene segments from the viruses were closely related to virus sequences from sea lions in Chile and Peru (*2*; C. Pardo Roa, unpub. data, https://www.biorxiv.org/content/10.1101/2023.06.30.547205v); 6 gene segments (all except polymerase basic protein 1 and nucleocapsid protein) also clustered with the virus isolated from a human in Chile (*7*). That finding suggests that viruses from Punta Bermeja may have been derived from a separate HPAI H5N1 introduction into Argentina. Because of the lack of genomic data for HPAI H5N1 viruses circulating in Argentina during February–July 2023, the finer scale pathways (local geographic routes and host species involved) of how these viruses arrived at Punta Bermeja remain unclear. Even so, the viruses

that we report did not cluster with those from birds in Uruguay, Brazil, or Bird Island (Antarctica), possibly suggesting separate pathways of virus spread.

On the basis of previous comparisons with HPAI H5N1 isolates from other countries in South America, we identified 9 mutations already present in viruses infecting sea lions in Peru and Chile but not in the goose/Guangdong reference strain or in viruses from birds and mammals from North America in 2022 (Table, https://wwwnc.cdc.gov/eid/article/30/4/23-1725-t1). Specifically, we found Q591K and D701N mutations in polymerase basic 2 associated with increased pathogenicity to mammals (*8*). The virus we detected in the South American tern also has those mutations, but they were absent from previously reported HPAI H5N1 viruses from avian hosts in South America (except for A/sanderling/Arica y Parinacota/240265/2023, which has the D701N mutation). That finding further supports the hypothesis that HPAI H5N1 viruses from sea lions from Peru and Chile acquired mammalian adaptation mutations that improved their ability to infect pinnipeds while possibly retaining the ability to infect avian hosts. Given the rapid and widespread dissemination of the viruses among pinnipeds in South America and the substantial associated mortalities (*3*,*9*), it seems likely that pinniped-to-pinniped transmission played a role in the spread of the mammal-adapted HPAI H5N1 viruses in the region. It is alarming that the HPAI H5N1 viruses infecting pinnipeds and seabirds in Argentina share the same mammalian adaptation mutations as the virus from the affected human in Chile, which highlights the potential threat posed by these viruses to public health.

Acknowledgments

We gratefully acknowledge all data contributors (i.e., the authors and their originating laboratories responsible for obtaining the specimens, and their submitting laboratories for generating the genetic sequence and metadata and sharing via the GISAID Initiative [https://www.gisaid.org], on which this research is based). We thank the Secretaría de Ambiente y Cambio Climático de la Provincia de Río Negro, especially Dina Migani and Federico Hollman, and Sebastián Ortega from Área Natural Protegida Bahía de San Antonio.

M.M.U. and A.R. designed the study and contributed funding; R.E.T.V., A.D., and M.M.L. collected samples; M.M.L. contributed surveillance data; V.O. performed the laboratory analyses; A.R. and R.E.T.V. performed the bioinformatic analyses; A.R., R.E.T.V., and M.M.U. wrote the manuscript. All authors have read, revised, and approved the manuscript.

About the Author

Dr. Rimondi is a scientist at the National Institute of Agricultural Technology in Argentina and a postdoctoral fellow from Alexander von Humboldt Foundation from Germany working on HPAI H5N1 at the Robert Koch Institute. Her primary research interests focus on molecular epidemiology and host–pathogen interactions of avian influenza viruses.

References

1. Servicio Nacional de Sanidad y Calidad Agroalimentaria. State of the epidemiological situation in Argentina [in Spanish] [cited 2023 Dec 12]. https://www.argentina.gob.ar/senasa/estado-de-la-situacion-epidemiologica-en-la-argentina
2. Leguia M, Garcia-Glaessner A, Muñoz-Saavedra B, Juarez D, Barrera P, Calvo-Mac C, et al. Highly pathogenic avian influenza A (H5N1) in marine mammals and seabirds in Peru. Nat Commun. 2023;14:5489. https://doi.org/10.1038/s41467-023-41182-0
3. Ulloa M, Fernández A, Ariyama N, Colom-Rivero A, Rivera C, Nuñez P, et al. Mass mortality event in South American sea lions (*Otaria flavescens*) correlated to highly pathogenic avian influenza (HPAI) H5N1 outbreak in Chile. Vet Q. 2023;43:1–10. https://doi.org/10.1080/01652176.2023.2265173
4. World Organisation for Animal Health. WAHIS: World Animal Health Information System [cited 2023 Dec 12]. https://wahis.woah.org
5. Pan American Health Organization. CDC protocol for real-time RT-PCR for the new subtype of influenza A(H1N1) virus [in Spanish] [cited 2023 Dec 12]. https://www.paho.org/es/node/36933
6. Nguyen LT, Schmidt HA, von Haeseler A, Minh BQ. IQ-TREE: a fast and effective stochastic algorithm for estimating maximum-likelihood phylogenies. Mol Biol Evol. 2015;32:268–74. https://doi.org/10.1093/molbev/msu300
7. Castillo A, Fasce R, Parra B, Andrade W, Covarrubias P, Hueche A, et al. The first case of human infection with H5N1 avian Influenza A virus in Chile. J Travel Med. 2023;30(5):taad083. https://doi.org/10.1093/jtm/taad083
8. Lee CY, An SH, Choi JG, Lee YJ, Kim JH, Kwon HJ. Rank orders of mammalian pathogenicity-related PB2 mutations of avian influenza A viruses. Sci Rep. 2020;10:5359. https://doi.org/10.1038/s41598-020-62036-5
9. Campagna C, Uhart M, Falabella V, Campagna J, Zavattieri V, Vanstreels RET, et al. Catastrophic mortality of southern elephant seals caused by H5N1 avian influenza. Mar Mamm Sci. 2024;40:322–5. https://doi.org/10.1111/mms.13101

Address for correspondence: Agustina Rimondi, Robert Koch Institute, Holländerstrasse 102, 13407, Berlin, Germany; email: rimondia@rki.de or rimondi.agustina@inta.gob.ar

Link between Monkeypox Virus Genomes from Museum Specimens and 1965 Zoo Outbreak

Michelle Hämmerle, Aigerim Rymbekova, Pere Gelabert, Susanna Sawyer, Olivia Cheronet, Paolo Bernardi, Sébastien Calvignac-Spencer, Martin Kuhlwilm,[1] Meriam Guellil,[1] Ron Pinhasi[1]

Author affiliations: University of Vienna, Vienna, Austria (M. Hämmerle, A. Rymbekova, P. Gelabert, S. Sawyer, O. Cheronet, P. Bernardi, M. Kuhlwilm, M. Guellil, R. Pinhasi); Helmholtz Centre for Infection Research, Greifswald, Germany (S. Calvignac-Spencer); University of Greifswald, Greifswald (S. Calvignac-Spencer)

DOI: https://doi.org/10.3201/eid3004.231546

We used pathogen genomics to test orangutan specimens from a museum in Bonn, Germany, to identify the origin of the animals and the circumstances of their death. We found monkeypox virus genomes in the samples and determined that they represent cases from a 1965 outbreak at Rotterdam Zoo in Rotterdam, the Netherlands.

Monkeypox virus (MPXV) (*Orthopoxvirus* genus, *Poxviridae* family), which causes mpox, is a large double-stranded DNA zoonotic virus first identified in 1958 in macaque primates (*1*). The first human case was reported in 1970, and recent outbreaks have attracted worldwide public attention (*1*). The 2022 outbreak has been one of the largest documented and affected numerous countries around the globe (*1*).

MPXV is known to infect chimpanzees, one of the nonhuman great ape species (*2*). The past 3 decades that great ape–infecting viruses have been studied has provided insight into the coevolution of these viruses and their hosts, and sometimes the origins of other important human pathogens, such as herpes simplex virus 2 (*3*). Museomics, which uses DNA from museum specimens for genomic studies, complements the study of contemporary wild populations because viral DNA has been detected in museum (*4*) and archeological specimens (*5*).

We report findings related to 4 orangutan (*Pongo* sp.) specimens that came to the zoologic research museum Alexander Koenig in Bonn, Germany, in 1965 and that were originally reported to be from wild animals from Sumatra. We extracted DNA from the orangutan teeth, built genomic libraries (Appendix Figure 1, https://wwwnc.cdc.gov/EID/article/30/4/23-1546-App1.pdf), performed shotgun sequencing, and used a hybridization capture bait set targeting various DNA viruses.

Two of the specimens showed sufficient endogenous DNA content to validate their taxonomic assignment to Sumatran orangutans (*Pongo abelii*) genomically (Appendix Figure 2). Our analysis found low levels of human contamination (0.7%–1.1%) and short insert sizes consistent with degraded DNA but no deamination patterns typical for ancient DNA (Appendix). We conducted taxonomic classification of the captured data by using Kraken2 (https://github.com/DerrickWood/kraken2), which revealed the presence of MPXV.

MPXV is likely bound to reservoir species normally distributed throughout Africa (*6*). Because this virus has occasionally spread out of Africa, we further investigated the origin and history of the MPXV-positive orangutans. We requested, and the museum provided, a letter from the wildlife trader in the Netherlands who sold the specimens to the museum in 1965. The letter stated that the specimens originated from captive zoo animals from 1964, rather than from wild animals from Sumatra. The letter did not specify from which zoo the animals were obtained.

We then mapped the reads to a MPXV genome (GenBank accession no. KJ642614) (Appendix Figures 3, 4) from a 1965 outbreak in the Rotterdam Zoo, Rotterdam, the Netherlands. This genome was the best match and very close in age to the animals we tested. Sample MAM1965–0547 yielded the best results, showing 19.12 mean depth of coverage (Table). For the 3 other specimens, we obtained 9.57-fold, 0.03-fold, and 2.81-fold mean genome coverage.

MPXVs were first identified from outbreaks in facilities housing nonhuman primates in the 1950s and 1960s. Genomes of isolates derived from those outbreaks have since been sequenced by other researchers, enabling us to investigate the potential ties of our specimens to specific outbreaks by using phylogenetic analyses. The MPXV genomes from the museum orangutans fall into clade IIa and were closely related to the genome derived from the 1965 Rotterdam Zoo outbreak (Figure; Appendix Figure 5); only 2 mutations were identified between the genomes sequenced in this study and the ones from 1965 (Appendix). The Rotterdam Zoo outbreak severely affected orangutans kept at the facility, and 6 of 10 infected animals died (*7*). Those orangutans were possibly infected by an animal that had previously been in contact with other MPXV-infected monkeys (*6*). Given the concordance of the dates and circumstances, combined with

[1]These authors contributed equally to this article.

Table. Relevant mapping statistics of MPXV genomes from the museum orangutan specimens from Europe when mapped to the genome responsible for the MPXV zoo outbreak in Rotterdam, the Netherlands, 1965

Sample	No. sequenced reads	Mapped reads no. duplicates, MQ>30	Mean mapping quality	Mean fragment length, bp	Mean coverage depth, ± SD	% Coverage			Frequency first base	
						1×	5×	10×	C to G	G to A
MAM1965-547	3,139,078	27,482	36.39	125.6	19.12 ± 10.60	98.73	96.8	81.85	0.023	0
MAM1965-545	1,492,386	12,963	36.6	135.68	9.57 ± 5.11	98.56	84.73	38.83	0.024	0
MAM1965-544	151,272	67	34.35	64.36	0.03 ± 0.24	1.812	0	0	0.143	0
MAM1965-546	270,634	4,616	36.28	108.89	2.81 ± 2.62	78.78	21.48	1.54	0.014	0

*MPXV, monkeypox virus; MQ, mapping quality.

the genetic evidence, we are confident that we identified some of those animals within our museum specimens. This case is unusual because we were able to tie nonhuman great ape museum specimens to a specific outbreak. The genome isolated in 1965 and the ones obtained from dry specimens stored for >50 years are almost identical.

Our work linking the MPXV infection of those orangutans to a specific outbreak further highlights the importance of museum specimens to the study of virus diversity and evolution. Several human viruses were first discovered in captive nonhuman primates. Human respiratory syncytial virus was first identified in 1956 in captive chimpanzees (*8*,*9*). If natural history collections

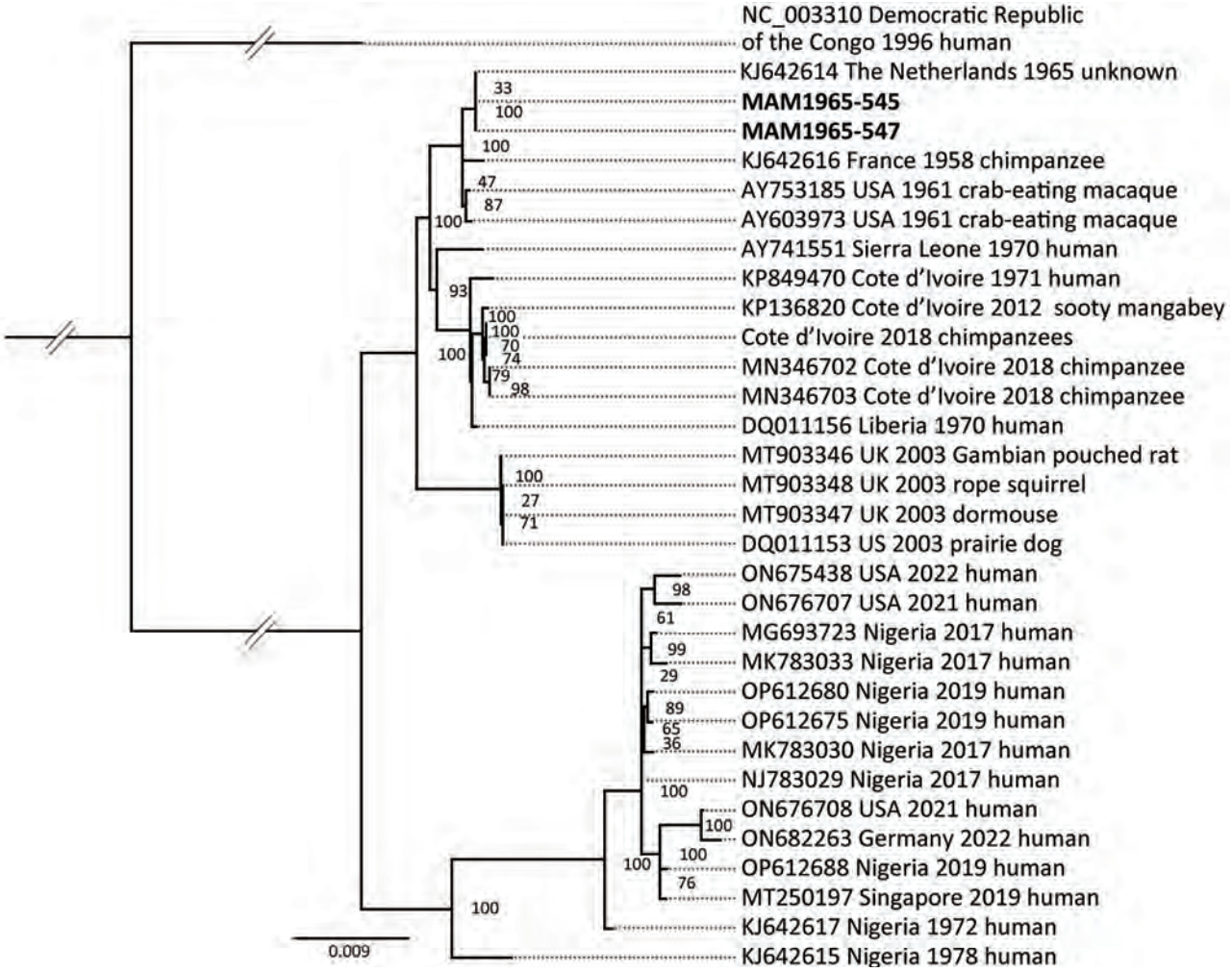

Figure. Maximum-likelihood phylogeny tree showing the close relation between MPXV genomes from museum orangutan samples from Germany (bold text), which fall into clade IIa, to the genome derived from the MPXV zoo outbreak in Rotterdam, the Netherlands, 1965. The phylogeny tree is rooted on the outgroup genome (GenBank accession no. NC_003310) from clade I with the museum orangutan genomes MAM1965–545 and MAM1965–547. The consensus sequences for the ancient sequences are based on a mapping to the Rotterdam genome. The final single-nucleotide polymorphisms alignment length was 138,240 bp. The collapsed node contains genomes from *Pan troglodytes verus* from Cote d'Ivoire (GenBank accession nos. MN346690, MN346692, MN346694–8, MN346700–1).

have regularly acquired specimens from such outbreaks and we can identify them in their records, such specimens could represent not only a treasure trove of biodiversity (*10*) but also an alternative source of pathologic specimens and infectious agent genomic material.

Acknowledgments

We are grateful to the Zoologisches Forschungsmuseum A. Koenig, Leibniz-Institut zur Analyse des Biodiversitätswandels in Bonn, in particular Eva Bärmann, Jan Decher, and Christian Montermann at the Section Theriology.

The computational results of this work have been achieved by using the Life Science Compute Cluster of the University of Vienna (Vienna, Austria). Data from this study are available in the European Nucleotide Archive: sequencing reads, accession no. PRJEB67701; capture data, ERR12141761, accession nos. ERR12141763, ERR12141765, and ERR12141766; and shotgun data, accession nos. ERR1214809–811 and ERR1214826.

This project was funded by the Vienna Science and Technology Fund (grant no. 10.47379/VRG20001) and by the Austrian Science Fund (grant no. FW547002 awarded to M.K.), Austrian Science Fund (grant no. M3108-G to S.S., grant no. P–36433 to P.G., and grant no. FW547001 ESP162-B to M.G.).

About the Author

Miss Hämmerle is a PhD student at the Department of Evolutionary Anthropology at the University of Vienna. Her research interests focus on ancient host and pathogen DNA in great apes and humans.

Reference

1. Titanji BK, Tegomoh B, Nematollahi S, Konomos M, Kulkarni PA. Monkeypox: a contemporary review for healthcare professionals. Open Forum Infect Dis. 2022; 9:ofac310.
2. Patrono LV, Pléh K, Samuni L, Ulrich M, Röthemeier C, Sachse A, et al. Monkeypox virus emergence in wild chimpanzees reveals distinct clinical outcomes and viral diversity. Nat Microbiol. 2020;5:955–65. https://doi.org/10.1038/s41564-020-0706-0
3. Calvignac-Spencer S, Düx A, Gogarten JF, Leendertz FH, Patrono LV. A great ape perspective on the origins and evolution of human viruses. Adv Virus Res. 2021;110:1–26. https://doi.org/10.1016/bs.aivir.2021.06.001
4. Calvignac S, Terme J-M, Hensley SM, Jalinot P, Greenwood AD, Hänni C. Ancient DNA identification of early 20th century simian T-cell leukemia virus type 1. Mol Biol Evol. 2008;25:1093–8. https://doi.org/10.1093/molbev/msn054
5. de-Dios T, Scheib CL, Houldcroft CJ. An adagio for viruses, played out on ancient DNA. Genome Biol Evol. 2023;15:evad047.
6. Parker S, Buller RM. A review of experimental and natural infections of animals with monkeypox virus between 1958 and 2012. Future Virol. 2013;8:129–57. https://doi.org/10.2217/fvl.12.130
7. Peters JC. An epizootic of monkey pox at Rotterdam Zoo. Int Zoo Yearb. 1966;6:274–5. https://doi.org/10.1111/j.1748-1090.1966.tb01794.x
8. Bem RA, Domachowske JB, Rosenberg HF. Animal models of human respiratory syncytial virus disease. Am J Physiol Lung Cell Mol Physiol. 2011;301:L148–56. https://doi.org/10.1152/ajplung.00065.2011
9. Morris JA, Blount RE, Savage RE. Recovery of cytopathogenic agent from chimpanzees with coryza. Exp Biol Med. 1956;92:544–9. https://doi.org/10.3181/00379727-92-22538
10. Card DC, Shapiro B, Giribet G, Moritz C, Edwards SV. Museum genomics. Annu Rev Genet. 2021;55:633–59. https://doi.org/10.1146/annurev-genet-071719-020506

Address for correspondence: Michelle Hämmerle or Ron Pinhasi, University of Vienna, Djerassiplatz 1, 1030 Vienna, Austria; email: michelle.haemmerle@univie.ac.at or ron.pinhasi@univie.ac.at

Case of Human Orthohantavirus Infection, Michigan, USA, 2021

Samuel M. Goodfellow, Robert A. Nofchissey, Dustin Arsnoe, Chunyan Ye, Seonghyeon Lee, Jieun Park, Won-Keun Kim, Kartik Chandran, Shannon L.M. Whitmer, John D. Klena, Jonathan W. Dyal, Trevor Shoemaker, Diana Riner, Mary Grace Stobierski, Kimberly Signs, Steven B. Bradfute

Author affiliations: University of New Mexico Health Sciences Center, Albuquerque, New Mexico, USA (S.M. Goodfellow, R.A. Nofchissey, C. Ye, S.B. Bradfute); US Department of Agriculture Animal and Plant Health Inspection Service Wildlife Services–Michigan Program, Okemos, Michigan, USA (D. Arsnoe); Hallym University College of Medicine, Chuncheon, South Korea (S. Lee, J. Park, W.-K. Kim); Albert Einstein College of Medicine, Bronx, New York, USA (K. Chandran); Centers for Disease Control and Prevention, Atlanta, Georgia, USA (S.L.M. Whitmer, J.D. Klena, J.W. Dyal, T. Shoemaker); Michigan Department of Health and Human Services, Lansing, Michigan, USA (D. Riner, M.G. Stobierski, K. Signs)

DOI: http://doi.org/10.3201/eid3004.231138

Orthohantaviruses cause hantavirus cardiopulmonary syndrome; most cases occur in the southwest region of the United States. We discuss a clinical case of orthohantavirus infection in a 65-year-old woman in Michigan and the phylogeographic link of partial viral fragments from the patient and rodents captured near the presumed site of infection.

Orthohantaviruses are negative-sense, enveloped RNA viruses that are transmitted by host reservoirs, such as rodents, to humans. Human infection occurs through inhalation of aerosolized viral particles from host excreta, such as urine or feces, often in enclosed spaces during infestations. New World orthohantavirus infection results in hantavirus cardiopulmonary syndrome (HCPS), which consists of febrile illness with edema and respiratory failure (*1*). In the United States, most HCPS cases occur in the Southwest and have a ≈35% mortality rate (*2*).

The dominant orthohantavirus that causes HCPS in the United States is Sin Nombre virus (SNV), which is thought to be carried and transmitted by the western deer mouse (*Peromyscus sonoriensis*). New York virus (NYV) is another pathogenic variant of orthohantavirus that is found in white-footed deer mice (*Peromyscus leucopus*); cases occur primarily in the Northeast region of the country (*3*). Although multiple host reservoirs for orthohantaviruses are distributed throughout the United States, most human cases are caused by SNV (*4*,*5*).

In early May 2021, a previously healthy 65-year-old woman visited an emergency department in Washtenaw County, Michigan, USA, with febrile prodrome of 3–6 days, thrombocytopenia, mild transaminase elevation, and acute hypoxic respiratory failure of unclear etiology requiring intubation. An extensive infectious disease workup was conducted, and physicians initially ruled out such pulmonary pathogens as SARS-CoV-2, common respiratory viruses, fungal agents, and *Legionella* spp. The family was interviewed to obtain a travel and animal exposure history, which revealed that the patient had not traveled outside of Michigan in the previous year. The interview also confirmed that the patient had not consumed unpasteurized dairy or undercooked meat, had a mostly indoor dog, lived near a natural area but used trails/sidewalks, and had no known rodent infestation in the home. However, the spouse reported that the patient had spent time recently cleaning out a relative's home that had been uninhabited for 2 years and was infested with mice.

Table. Measurements, location, and quantitative PCR results from captured rodents at likely site of patient orthohantavirus exposure, Michigan, USA, 2021*

Sample ID	Species (common name)	Weight, g	Total length, mm	Tail length, mm	Hind foot length, mm	Ear size, mm	Age/sex	Location of capture	PCR+ tissue (Ct values)
YR-01	*Peromyscus leucopus* (white-footed mouse)	13.2	152	75	19.5	16.5	Subadult/M	Garage right front corner	Kidney (33, 33), BAF (35, 35)
YR-02	*Blarina brevicauda* (Northern short-tailed shrew)	18	115	27	15	2.5	Adult/F	Backyard	NA
YR-03	*P. leucopus*	21	174	86	20.5	17.5	Adult/F	Backyard	Kidney (39, 39), liver (38, 34)
YR-04	*Tamias striatus* (Eastern chipmunk)	84.5	221	75	33.5	18	Adult/F	Backyard	NA
YR-05	*T. striatus*	73.5	222	85	36.5	18	Adult/M	Backyard	NA
YR-06	*P. leucopus*	17	159	73	20.5	17	Subadult/M	Porch right back corner	NA
YR-07	*T. striatus*	90	225	83	35	14.5	Adult/F	Neighbor backyard, right side	NA
YR-08	*T. striatus*	91	224	83	35	19	Adult/F	Neighbor backyard, right side	NA
YR-09	*T. striatus*	88	227	93	34	15	Adult/F	Neighbor backyard, right side	NA
YR-10	*T. striatus*	94	202†	48†	36	18	Adult/M	Backyard	Lung (35, 35)
YR-11	*T. striatus*	58	214	85	36	14	Subadult/M	Backyard	NA
YR-12	*T. striatus*	49	196	72	37	17	Subadult/M	Backyard	Lung (39, 39)

*BAF, brown adipose fat; Ct, cycle threshold; ID, identification; PCR+, positive result determined by quantitative reverse transcription PCR.
†Bobbed tail.

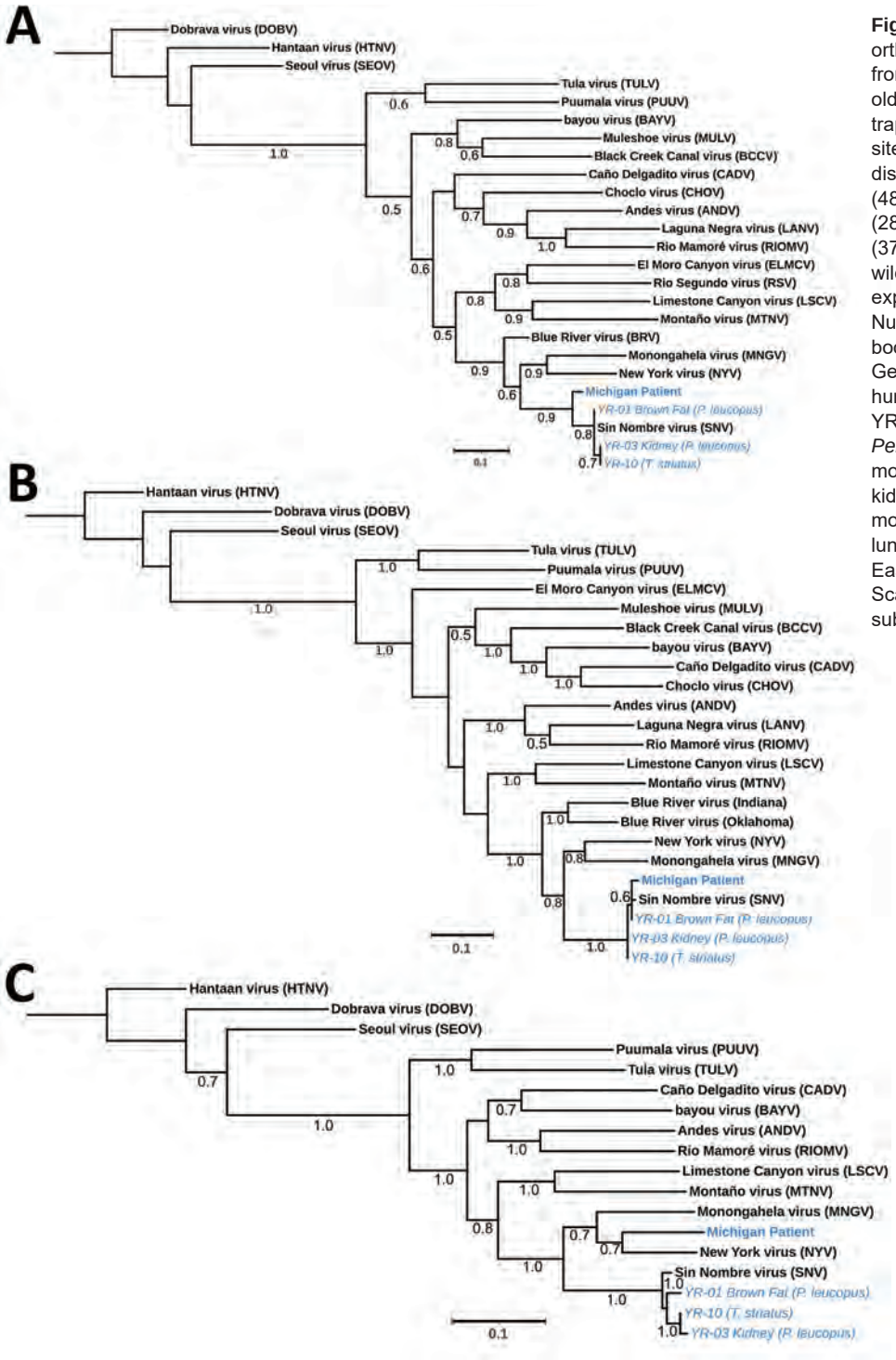

Figure. Phylogenetic analysis of orthohantavirus sequence fragments from samples taken from a 65-year-old woman in Michigan, USA, and trapped rodents from the likely site of exposure (blue text). Trees displaying the patient small fragment (481 bp) (A), medium fragment (283 bp) (B), and large fragment (377 bp) (C) were aligned against wild-caught rodents near site of exposure and reference sequences. Numbers along branches indicate bootstrap values of 500 replicates. GenBank accession numbers: human patient, OR428177–9; YR-01, brown adipose fat from a *Peromyscus leucopus* white-footed mouse, OR428180–2; YR-03, kidney tissue from a *P. leucopus* mouse, OR428183–5; and YR-10, lung tissue from a *Tamias striatus* Eastern chipmunk, OR428186–8. Scale bars indicate number of substitutions per site.

Results of a tickborne disease panel were negative, but hantavirus antibody testing performed at a commercial lab showed positive results for both IgM and IgG. The treating hospital notified the Michigan Department of Health and Human Services of a case of HCPS. Confirmatory hantavirus testing was arranged and confirmed with the Centers for Disease Control and Prevention, using serum samples collected from hospitalization.

Trapping was performed in and around the suspected site of exposure (relative's home) using Sherman folding traps (https://shermantraps.com;

94 trap nights), resulting in 12 rodents captured (12.8% trap success) under an approved animal-use protocol (*6*). Trapping was conducted 12 days after the patient was released from the hospital. Researchers observed signs of previous trapping efforts; 5 unusable *Peromyscus* mouse carcasses were found in snap traps in the residential basement. Signs of infestation were evident. Of the 12 trapped rodents, 3 (25%) were *P. leucopus* mice, 1 (8%) was a Northern short-tailed shrew (*Blarina brevicauda*), and 8 (67%) were Eastern chipmunks (*Tamias striatus*) (Table). The surrounding flora consisted of lawns, shrubs, and an evergreen windbreak near a public trail.

Using quantitative reverse transcription PCR, we screened lung, liver, brown fat, or kidney tissue from captured rodents and from a plasma sample of the patient obtained during hospitalization (*6*). Brown fat and kidney tissue from 2 *P. leucopus* mice and lung tissue from 2 *T. striatus* chipmunks tested positive for SNV. Three fragments were obtained from the patient sample, 1 for the short segment (480 bp), 1 for the medium segment (283 bp), and 1 for the large segment (377 bp). Similar fragments were also generated from 3 of the 4 infected rodents; all sequences are publicly available in GenBank (accession nos. OR428177–88). We compared fragments by using phylogenetic analysis against several known orthohantavirus reference sequences to determine potential identification. The partial sequences of SNV short and medium segments from the patient formed a phylogenetic lineage with SNV sequences from the rodents collected in or near the suspected site of exposure in Michigan. However, the patient's large fragment formed a lineage with NYV, suggesting that this species may be an SNV or NYV variant (Figure).

Previously, we identified the likely site of rodent-to-human SNV transmission in a patient case study (*6*). Here, we attempted a similar approach but were only able to generate partial sequences for the patient sample, which we compared with captured rodents. Orthohantavirus incubation periods can be up to several weeks after exposure (*7*), which may impact the timeliness of trapping efforts. We found infected *P. leucopus* mice and *T. striatus* chipmunks at the site of exposure, both of which have been reported to carry NYV or SNV; *P. leucopus* mice are susceptible and capable vessels for SNV replication after laboratory infection (*6*,*8*–*10*). This finding suggests that orthohantaviruses may not be as species host–restricted as previously thought. Further studies are warranted to clarify (or define) orthohantavirus species in Michigan to anticipate the risk for patient infection. Increasing surveillance and diagnostic efforts can enable prospective detection of circulating viruses.

Acknowledgments

We thank Michigan's Department of Health and Human Services and Washtenaw County Health Department for collaboration, along with the Centers for Disease Control and Prevention Epidemiology and Ecology teams that participated in this response.

This work was supported in part by a University of New Mexico School of Medicine Research Allocation Committee (UNM SOM RAC) grant (S.B.B.) and an NIH/NIAID grant (AI-I7-042 U19, K.C.). S.M.G. was supported by UNM HSC Infectious Disease and Inflammation Program NIH grant T32AI007.

About the Author

Dr. Goodfellow is a recent graduate from the University of New Mexico Health Sciences Center. His primary research interests are emerging and re-emerging infectious diseases, surveillance efforts, and science policy.

References

1. Nichol ST, Spiropoulou CF, Morzunov S, Rollin PE, Ksiazek TG, Feldmann H, et al. Genetic identification of a hantavirus associated with an outbreak of acute respiratory illness. Science. 1993;262:914–7. https://doi.org/10.1126/science.8235615
2. Akram SM, Mangat R, Huang B. Hantavirus cardiopulmonary syndrome. In: StatPearls [Internet]. Treasure Island (FL): StatPearls Publishing; 2024.
3. Hjelle B, Lee SW, Song W, Torrez-Martinez N, Song JW, Yanagihara R, et al. Molecular linkage of hantavirus pulmonary syndrome to the white-footed mouse, *Peromyscus leucopus*: genetic characterization of the M genome of New York virus. J Virol. 1995;69:8137–41. https://doi.org/10.1128/jvi.69.12.8137-8141.1995
4. Rollin PE, Ksiazek TG, Elliott LH, Ravkov EV, Martin ML, Morzunov S, et al. Isolation of black creek canal virus, a new hantavirus from *Sigmodon hispidus* in Florida. J Medical Virology. 1995;46: 35–39. https://doi.org/10.1002/jmv.1890460108
5. Ksiazek TG, Martin ML, Groves MG, Nichol ST, Peters CJ, Monroe MC, et al. Isolation, genetic diversity, and geographic distribution of Bayou virus (Bunyaviridae: hantavirus). Am J Trop Med Hyg. 1997;57:445–8. https://doi.org/10.4269/ajtmh.1997.57.445
6. Goodfellow SM, Nofchissey RA, Schwalm KC, Cook JA, Dunnum JL, Guo Y, et al. Tracing transmission of Sin Nombre virus and discovery of infection in multiple rodent species. J Virol. 2021;95:e0153421. https://doi.org/10.1128/JVI.01534-21
7. Vial PA, Valdivieso F, Mertz G, Castillo C, Belmar E, Delgado I, et al. Incubation period of hantavirus cardiopulmonary syndrome. Emerg Infect Dis. 2006;12:1271–3. https://doi.org/10.3201/eid1208.051127

8. Mills JN, Ksiazek TG, Ellis BA, Rollin PE, Nichol ST, Yates TL, et al. Patterns of association with host and habitat: antibody reactive with Sin Nombre virus in small mammals in the major biotic communities of the southwestern United States. Am J Trop Med Hyg. 1997;56:273–84. https://doi.org/10.4269/ajtmh.1997.56.273
9. Childs JE, Ksiazek TG, Spiropoulou CF, Krebs JW, Morzunov S, Maupin GO, et al. Serologic and genetic identification of *Peromyscus maniculatus* as the primary rodent reservoir for a new hantavirus in the southwestern United States. J Infect Dis. 1994;169:1271–80. https://doi.org/10.1093/infdis/169.6.1271
10. Quizon K, Holloway K, Iranpour M, Warner BM, Deschambault Y, Soule G, et al. Experimental infection of peromyscus species rodents with Sin Nombre virus. Emerg Infect Dis. 2022;28:1882–5. https://doi.org/10.3201/eid2809.220509

Address for correspondence: Steven B. Bradfute, University of New Mexico, 915 Camino de Salud NE, 3190 IDTC Bldg 0289, Albuquerque, NM 87131, USA; email: sbradfute@salud.unm.edu

Autochthonous Ascariasis, Mississippi, USA

Charlotte V. Hobbs,[1] James Matthew Rhinewalt,[1] Irene Arguello, Lacy Malloch, Lora Martin, William M. Poston, Paul Byers, Richard S. Bradbury

Author affiliations: University of Alabama at Birmingham/Childrens of Alabama, Birmingham, Alabama, USA (C.V. Hobbs); Children's of Mississippi/University of Mississippi Medical Center, Jackson, Mississippi, USA (C.V. Hobbs, I. Arguello, L. Malloch, L. Martin); Internal Medicine and Pediatric Clinic, New Albany, Mississippi, USA (J.M. Rhinewalt); Baptist Hospital Systems, New Albany (W.M. Poston); Mississippi State Department of Health, Jackson (P. Byers); James Cook University, Townsville, Queensland, Australia (R.S. Bradbury)

DOI: https://doi.org/10.3201/eid3004.240176

We describe a case of a 2-year-old child who expelled a single adult female *Ascaris lumbricoides* worm. The patient is from a rural county in Mississippi, USA, with no reported travel outside of the United States. The caregivers in the home practice good sanitation. Exposure to domestic pigs is the likely source of infection.

[1]These authors are co–first authors.

A reported increase of hookworm and strongyloidiasis transmission in rural Alabama, USA, in 2017 (*1*) has led to more interest in isolated cases of autochthonous transmission of soil-transmitted helminths in the southeastern United States. This increased transmission and interest led to several small- and large-scale surveys of soil-transmitted helminths and other parasitic diseases in Mississippi (*2*–*4*), Alabama (*5*), and Texas (*6*). No cases of ascariasis were identified in those surveys. However, highly endemic porcine ascariasis is present in some farmed pigs in the United States (*7*). Sporadic reports have been documented of autochthonous ascariasis cases and case clusters in northeastern states (*8*), and *Ascaris lumbricoides* roundworm–mediated Löffler syndrome (eosinophilic pneumonitis) has been reported in Louisiana over the past decade (*9*). Those autochthonous ascariasis cases represented spillover infections to humans from pigs. We describe a case of zoonotic ascariasis from New Albany in Union County, Mississippi.

A previously healthy 2-year-old girl was brought to her local pediatrician with complaints of abdominal cramping for 2 weeks, loose stools (without blood or mucous), and a decreased appetite. The family was originally from Mexico but had lived in the United States for 13 years. Neither the patient nor her twin sister had been outside of the United States. The family lived on a farm with pigs, and both children reportedly ate dirt from the house plants. The mother found a motile worm in the patient's diaper, filmed the worm, and then discarded the diaper and worm.

We identified the helminth from the video (Video, https://wwwnc.cdc.gov/EID/article/30/4/24-0176-V1.htm) as an adult female *A. lumbricoides* worm because of the characteristic size, shape, reddish-orange color, and a pointed rather than recurved tail. The patient was treated by her pediatrician with ivermectin (1 dose of a 3 mg tablet) because albendazole was not available and mebendazole was not covered by the patient's insurance. We performed automated complete blood counts by using an in-office hematology analyzer (without eosinophil count capacity). The patient was not anemic (hemoglobin 11.8 g/dL [reference range, for age 11–13.7 g/dL]; mean corpuscular volume 80.4 fL [reference range for age 75–86 fL]). We treated the family members as a precautionary measure. We obtained stool samples from the patient within 24 hours of treatment but detected no eggs on Kato–Katz microscopic smear. The patient did not expel any additional worms. We followed

the patient clinically with complete blood counts, and her symptoms resolved without complication.

The Mississippi State Department of Health conducted field visits to the patient's home, but the family's pigs had been sent to slaughter. The family has 2 flush toilets in their home used for all defecation and disposal of feces. The Mississippi State Department of Health counselled all family members on handwashing, especially after contact with soil where pigs had defecated.

This case represents an autochthonous acquisition of ascariasis in the southeast United States. Only 1 worm was expelled by the patient, even after treatment, and the absence of eggs when treatment occurred suggests that this patient harbored a single adult worm infection. The lifespan of adult *A. lumbricoides* worms within human hosts is up to 2 years, and eggs may remain viable in soil for up to 10 years (*10*). The patient's family had been living in the United States for 13 years, and no promiscuous defecation was occurring in the child's environment. However, the child lived near domestic pigs, which is a common zoonotic origin for this infection.

Ascariasis is often asymptomatic or subclinical, although abdominal pain, distension, and wasting may occur (*7*–*10*). Adult worms migrating in the intestinal tract may obstruct the bile or pancreatic ducts, leading to cholecystitis or pancreatitis (*10*). Occasionally, migrating adult worms may be expelled through the rectum or emerge from the nose or mouth. In patients with heavy worm infections, bowel obstruction, intussusception, volvulus, and small bowel perforation may occur (*10*). Heavy infections may also cause malabsorption and stunting with consequent vitamin deficiencies, growth retardation, altered immunity, and impaired cognition (*7*,*10*). A larva migrans syndrome may be observed, caused by immune-mediated responses to the visceral migration of *A. lumbricoides* worm larvae through the lungs and appearing as Löffler syndrome (*9*).

Confusion exists over the taxonomic status of *Ascaris* helminths in pigs and humans. The genus *Ascaris* was once split into 2 species, *A. suum* and *A. lumbricoides*, but modern genotyping methods have determined that the 2 categories are instead separate genotypes of the same species, *A. lumbricoides* (*7*). Genotypic surveillance of adult *A. lumbricoides* worms from farmed pigs in Iowa found 10 haplotypes present, including those belonging to *A. lumbricoides* (human), *A. suum* (pig), and hybrid genotypes (*7*).

In summary, we describe a case of likely zoonotic autochthonous human ascariasis acquired in rural northern Mississippi. Sporadic ascariasis cases in the United States are most often zoonotic in origin, with exposure to pigs, or soil contaminated with pig feces, as the primary risk factor.

Acknowledgments

We thank the DPDx group in the Division of Parasitic Diseases and Malaria, Centers for Disease Control and Prevention, for their confirmation of the identity of the *A. lumbricoides* worm. We also thank Cathy Gordon for her review of clinical laboratory values.

About the Author

Dr. Hobbs is a professor of pediatric infectious disease and attending physician at Children's of Alabama, University of Alabama Medical Center, Birmingham, Alabama, USA. Her research interests include parasitic diseases in children in resource-limited settings and congenital infections.

References

1. McKenna ML, McAtee S, Bryan PE, Jeun R, Ward T, Kraus J, et al. Human intestinal parasite burden and poor sanitation in rural Alabama. Am J Trop Med Hyg. 2017;97:1623–8. https://doi.org/10.4269/ajtmh.17-0396
2. Bradbury RS, Lane M, Arguello I, Handali S, Cooley G, Pilotte N, et al. Parasitic disease surveillance, Mississippi, USA. Emerg Infect Dis. 2021;27:2201–4. https://doi.org/10.3201/eid2708.204318
3. Bradbury RS, Arguello I, Lane M, Cooley G, Handali S, Dimitrova SD, et al. Parasitic infection surveillance in Mississippi Delta children. Am J Trop Med Hyg. 2020;103:1150–3. https://doi.org/10.4269/ajtmh.20-0026
4. Bradbury RS, Martin L, Malloch L, Martin M, Williams JM, Patterson K, et al. Surveillance for soil-transmitted helminths in high-risk county, Mississippi, USA. Emerg Infect Dis. 2023;29:2533–7. https://doi.org/10.3201/eid2912.230709
5. Poole C, Barker T, Bradbury R, Capone D, Chatham AH, Handali S, et al. Cross-sectional study of soil-transmitted helminthiases in Black Belt Region of Alabama, USA. Emerg Infect Dis. 2023;29:2461–70. https://doi.org/10.3201/eid2912.230751
6. Singer R, Xu TH, Herrera LNS, Villar MJ, Faust KM, Hotez PJ, et al. Prevalence of intestinal parasites in a low-income Texas community. Am J Trop Med Hyg. 2020;102:1386–95. https://doi.org/10.4269/ajtmh.19-0915
7. Jesudoss Chelladurai J, Murphy K, Snobl T, Bader C, West C, Thompson K, et al. Molecular epidemiology of *Ascaris* infecting pigs in Iowa, USA. J Infect Dis. 2017;215:131–8. https://doi.org/10.1093/infdis/jiw507
8. Miller LA, Colby K, Manning SE, Hoenig D, McEvoy E, Montgomery S, et al. Ascariasis in humans and pigs on small-scale farms, Maine, USA, 2010–2013. Emerg Infect Dis. 2015;21:332–4. https://doi.org/10.3201/eid2102.140048
9. Gipson K, Avery R, Shah H, Pepiak D, Bégué RE, Malone J, et al. Löffler syndrome on a Louisiana pig farm. Respir Med Case Rep. 2016;19:128–31. https://doi.org/10.1016/j.rmcr.2016.09.003

10. Lynn MK, Morrissey JA, Conserve DF. Soil-transmitted helminths in the USA: a review of five common parasites and future directions for avenues of enhanced epidemiologic inquiry. Curr Trop Med Rep. 2021;8:32–42. https://doi.org/10.1007/s40475-020-00221-2

Address for correspondence: Charlotte Hobbs, University of Alabama at Birmingham/Children's of Alabama, 1600 7th Ave S, Birmingham, AL 35233, USA; email: charlottehobbs@uabmc.edu

Detection of Rat Hepatitis E Virus in Pigs, Spain, 2023

Lucia Rios-Muñoz, Moisés Gonzálvez, Javier Caballero-Gomez, Sabrina Castro-Scholten, María Casares-Jimenez, Irene Agulló-Ros, Diana Corona-Mata, Ignacio García-Bocanegra, Pedro Lopez-Lopez, Tomás Fajardo, João R. Mesquita, María A. Risalde, Antonio Rivero-Juarez, Antonio Rivero

Author affiliations: Universidad de Córdoba, Córdoba, Spain (L. Rios-Muñoz, M. Gonzálvez, J. Caballero-Gomez, S. Castro-Scholten, I. Agulló-Ros, I. García-Bocanegra, T. Fajardo, M.A. Risalde); Instituto Maimónides de Investigación Biomédica de Córdoba, Hospital Universitario Reina Sofía, Córdoba (L. Rios-Muñoz, J. Caballero-Gomez, M. Casares-Jimenez, D. Corona-Mata, P. Lopez-Lopez, A. Rivero-Juarez, A. Rivero); Universidad de Murcia, Murcia, Spain (M. Gonzálvez); Instituto de Salud Carlos III, Madrid, Spain (J. Caballero-Gomez, M. Casares-Jimenez, D. Corona-Mata, I. García-Bocanegra, P. Lopez-Lopez, M.A. Risalde, A. Rivero-Juarez, A. Rivero); Universidade do Porto and Laboratório para a Investigação Integrativa e Translacional em Saúde Populacional, Porto, Portugal (J.R. Mesquita)

DOI: https://doi.org/10.3201/eid3004.231629

We identified rat hepatitis E virus (HEV) RNA in farmed pigs from Spain. Our results indicate that pigs might be susceptible to rat HEV and could serve as viral intermediaries between rodents and humans. Europe should evaluate the prevalence of rat HEV in farmed pigs to assess the risk to public health.

Hepatitis E virus (HEV) is a major cause of acute viral hepatitis in Europe. HEV is classified into 8 major genotypes, but zoonotic genotype 3 is the most prevalent on the continent (*1*). HEV was considered the only zoonotic species in the Hepeviridae family until rat HEV (*Rocahepevirus ratti*) was identified. Rat HEV was the causal agent of chronic hepatitis in a transplant recipient from Hong Kong in 2018 (*2*). Since that discovery, nearly 30 cases of chronic and acute hepatitis have been reported in America, Asia, and Europe (*3*–*6*), affecting both immunosuppressed and immunocompetent persons. Those cases highlight the zoonotic potential of rat HEV, emphasizing its growing concern to public health.

Rodents are the main host of rat HEV, but its transmission routes remain unclear. Although direct and indirect contact with rodents have been suggested as potential transmission routes, only 1 registered case has involved such contact (*6*). Thus, alternative sources of infection seem possible, potentially from an alternate host with which humans have more contact (*7*). Because domestic pigs (*Sus scrofa domestica*) are highly susceptible to HEV and constitute the main natural viral reservoir, they could also be susceptible to rat HEV and potentially serve as hosts. Confirming that hypothesis could have major implications for public health. We aimed to assess the presence of rat HEV in a population of farmed pigs in Spain.

During May–June 2023, we randomly selected and prospectively sampled domestic pigs from 5 intensive breeding system farms in Cordoba, southern Spain. We collected rectal fecal samples from each pig and stored samples at −80°C until RNA extraction (Appendix, https://wwwnc.cdc.gov/EID/article/30/4/23-1629-App1.pdf).

We included a total of 387 pigs in the study and found rat HEV in 44 pigs, an individual prevalence of 11.4% (95% CI 8.6%–14.9%) (Table). Sequencing confirmed the identity as rat HEV (species *R. ratti)* (GenBank accession nos. OR977681–7 and OR977689–7711) (Appendix Figures 1, 2). Among the 5 farms, 2 (40%) had ≥1 rat HEV–positive pig. Of note, 93.2% (41/44) of positive animals were from the same farm (Figure; Appendix Table 3). HEV RNA was detected in 6 pigs, indicating a prevalence of 1.6% (95% CI 0.6%–3.4%). All HEV-positive pigs were from the same farm and had sequences consistent with HEV genotype 3f (GenBank accession nos. OR818554–60), but rat HEV was not detected in that farm.

The hypothesis that pigs are not susceptible to rat HEV was formed on the basis of experimental in vivo studies (*8*). Because animals in that study were not infected after challenge with rat HEV strains (*8*), it

Table. Demographic data of pigs and characteristics of farms in a study of detection of rat HEV in pigs, Spain, 2023*

Characteristics	No. (%), n = 387
Age range	
Adult	188 (48.6)
Subadult	169 (43.7)
Unknown	30 (7.8)
Breed	
Iberian	159 (41.1)
White	148 (38.2)
Iberian cross	80 (20.7)
Aptitude	
Reproductive	188 (48.6)
Fattening	199 (51.4)
Farm HEV status	
Rat HEV–positive	44 (11.4)
HEV-positive	6 (1.6)

*HEV, hepatitis E virus.

appeared that pigs were resistant to rat HEV infection. However, our study detected rat HEV RNA in pigs, suggesting the possible role of pigs in rat HEV epidemiology. That finding increases the range of species susceptible to rat HEV, suggesting that its transmission might not be restricted to rodents. The number of positive animals we found suggests that rat HEV is widespread among pig populations in the study area. That observation might be linked to the elevated positivity rate (55%) discovered in rodents from the same region (*9*), implying that the lack of rodent control measures might increase the risk for rat HEV transmission.

The presence of rat HEV in farmed pigs is of public health concern, especially considering global pork consumption. Our study highlights the possibility that pigs intended for human consumption could contribute to rat HEV transmission. The European Food Safety Authority (EFSA) recommends monitoring HEV in pigs to identify alterations in virus distribution and prevent its spread to new farms, aiming to reduce human cases (*10*). Our results suggest that a preliminary evaluation of rat HEV in farmed pigs should be also conducted in Europe, which could confirm our results and increase our understanding of virus transmission.

The first limitation of our study is that because of its exploratory nature, the sampling area was restricted to a single region, but our findings underscore the need to extend the evaluation of rat HEV to determine its magnitude. Second, because no serologic assays

Figure. Geographic locations of farms included in a study of rat hepatitis E virus in pigs, Spain, 2023. Triangles indicate farms with ≥1 pig positive for rat HEV RNA are marked, circles farms with no positive pigs. Inset shows shaded area in Spain where the sampling occurred.

are available for detecting rat HEV antibodies in pigs, our analysis was limited to molecular testing on fecal samples; thus, we cannot confirm rat HEV infection. However, our study justifies the design of new studies to evaluate the presence of rat HEV in blood and tissues samples. Finally, implementation of serologic analysis on rat HEV might enhance our comprehension of the pathogenesis of both HEV and rat HEV and assist in future investigations into risk factors.

In conclusion, our study shows the possibility that pigs are susceptible to rat HEV infection, challenging previous assumptions. Further studies are warranted to determine the role of pigs in rat HEV epidemiology and to assess the risk for direct or indirect zoonotic transmission from pigs. In addition, Europe should conduct an evaluation of rat HEV in farmed pigs to assess the overall risk to public health.

Acknowledgment

We gratefully acknowledge Laura Ruiz Torres and Ismael Zafra Soto for their technical support in sample processing and analysis.

This work was supported by the Andalusian General Secretariat for Research, Development, and Innovation in Health (grant no. PI-0287-2019), the Spanish Ministry of Health (grant no. RD12/0017/0012), co-financed by European Regional Development Fund (ERDF), and the Carlos III Health Institute (grant nos. PI21/00793 and PI22/01098). Projects PI21/00793 and PI22/01098 were funded by Carlos III Health Institute (ISCIII) and co-funded by the European Union.

A.R.-J. is the recipient of a Miguel Servet Research Contract by the Spanish Ministry of Sciences (contract no. CP18/00111). J.C.-G. is supported by the CIBERINFEC (grant no. CB21/13/00083), Carlos III Health Institute, Spanish Ministry of Science and NextGenerationEU. L.R.-M. is the recipient of a INVESTIGO research program grant funded by the European Union NextGenerationEU Plan. M.C.-J. is the recipient of a PFIS predoctoral grant (grant no. FI22/00180) from the Carlos III Health Institute and co-funded by the European Union. D.C.-M. is the recipient of a Rio-Hortega grant (grant no. CM22/00176) from the Carlos III Health Institute and co-funded by the European Union. M.G. was supported by postdoctoral contract Margarita Salas from the University of Murcia, and P.L.-L. was supported by postdoctoral contract Margarita Salas from the University of Córdoba from the Program of Requalification of the Spanish University System (Spanish Ministry of Universities) financed by the European Union-NextGenerationEU. S.C.-S. and I.A.-R. hold an FPU grants from the Spanish Ministry of Universities (grant no. FPU19/06026 to S.C.-S. and grant no. FPU19/03969 to I.A.-R.). The funders did not play any role in the design, conclusions, interpretation of the study, or decision to publish.

Author contributions: L.R.-M., A.R.-J., and A.R. were involved in the study design and conception, interpretation of the data, drafting of the manuscript, study supervision, and funding obtention. M.G., S.C.-S., T.F., and I.A.-R. were involved in sampling design, collection and storage. L.R.-M., P.L.-L., M.C.-J., and J.C.-G. performed RNA extraction and molecular determinations, phylogenetic analysis and GenBank submission. All authors have revised the manuscript and approved its publication.

About the Author

Ms. Ríos-Muñoz is a researcher specializing in infectious zoonotic diseases and a PhD candidate at Universidad de Córdoba, Córdoba, Spain. Her research interests focus on hepatitis E virus and rat hepatitis E virus.

References

1. Adlhoch C, Avellon A, Baylis SA, Ciccaglione AR, Couturier E, de Sousa R, et al. Hepatitis E virus: assessment of the epidemiological situation in humans in Europe, 2014/15. J Clin Virol. 2016;82:9–16. https://doi.org/10.1016/j.jcv.2016.06.010
2. Sridhar S, Yip CCY, Wu S, Cai J, Zhang AJX, Leung KH, et al. Rat hepatitis E virus as cause of persistent hepatitis after liver transplant. Emerg Infect Dis. 2018;24:2241–50. https://doi.org/10.3201/eid2412.180937
3. Rivero-Juarez A, Frias M, Perez AB, Pineda JA, Reina G, Fuentes-Lopez A, et al.; HEPAVIR and GEHEP-014 Study Groups. Orthohepevirus C infection as an emerging cause of acute hepatitis in Spain: first report in Europe. J Hepatol. 2022;77:326–31. https://doi.org/10.1016/j.jhep.2022.01.028
4. Rodriguez C, Marchand S, Sessa A, Cappy P, Pawlotsky JM. Orthohepevirus C hepatitis, an underdiagnosed disease? J Hepatol. 2023;79:e39–41. https://doi.org/10.1016/j.jhep.2023.02.008
5. Andonov A, Robbins M, Borlang J, Cao J, Hatchette T, Stueck A, et al. Rat hepatitis E virus linked to severe acute hepatitis in an immunocompetent patient. J Infect Dis. 2019;220:951–5. https://doi.org/10.1093/infdis/jiz025
6. Sridhar S, Yip CCY, Lo KHY, Wu S, Situ J, Chew NFS, et al. Hepatitis E virus species C infection in humans, Hong Kong. Clin Infect Dis. 2022;75:288–96. https://doi.org/10.1093/cid/ciab919
7. Reuter G, Boros Á, Pankovics P. Review of hepatitis E virus in rats: evident risk of species *Orthohepevirus* C to human zoonotic infection and disease. Viruses. 2020;12:1148. https://doi.org/10.3390/v12101148
8. Cossaboom CM, Córdoba L, Sanford BJ, Piñeyro P, Kenney SP, Dryman BA, et al. Cross-species infection of pigs with a novel rabbit, but not rat, strain of hepatitis E virus isolated in the United States. J Gen Virol. 2012;93:1687–95. https://doi.org/10.1099/vir.0.041509-0
9. Casares-Jimenez M, Garcia-Garcia T, Suárez-Cárdenas JM, Perez-Jimenez AB, Martín MA, Caballero-Gómez J, et al. Correlation of hepatitis E and rat hepatitis E viruses urban

wastewater monitoring and clinical cases. Sci Total Environ. 2024;908:168203. https://doi.org/10.1016/j.scitotenv.2023.168203
10. Nigsch A. Surveillance plan proposal for early detection of zoonotic pathogens in pigs and poultry. EFSA Supporting Publications. 2023; 20:1–32. https://doi.org/10.2903/sp.efsa.2023.EN-7855

Address for correspondence: Antonio Rivero-Juarez, Virología Clínica y Zoonosis, Instituto Maimonides de Investigación Biomédica de Córdoba (IMIBIC), Avenida Menedez Pidal, s/n. 14004, Córdoba, Spain; email: arjvet@gmail.com

Seroprevalence of Avian Influenza A(H5N6) Virus Infection, Guangdong Province, China, 2022

Yang Wang,[1] Chunguang Yang,[1] Yong Liu,[1] Jiawei Zhang, Wei Qu, Jingyi Liang, Chuanmeizi Tu, Qianyi Mai, Kailin Mai, Pei Feng, Wenjing Huang, Zhengshi Lin, Chitin Hon, Zifeng Yang, Weiqi Pan

Author affiliations: The First Affiliated Hospital of Guangzhou Medical University, Guangzhou, China (Y. Wang, C. Yang, J. Zhang, W. Qu, J. Liang, C. Tu, Q. Mai, K. Mai, W. Huang, Z. Lin, Z. Yang, W. Pan); Guangzhou National Laboratory, Guangzhou (Y. Wang, C. Yang, C. Hon, Z. Yang); Guangzhou Kingmed Center for Clinical Laboratory Co., Ltd., Guangzhou (Y. Liu); Macau University of Science and Technology, Macau, China (P. Feng, C. Hon, Z. Yang, W. Pan)

DOI: https://doi.org/10.3201/eid3004.231226

In 2022, we assessed avian influenza A virus subtype H5N6 seroprevalence among the general population in Guangdong Province, China, amid rising numbers of human infections. Among the tested samples, we found 1 to be seropositive, suggesting that the virus poses a low but present risk to the general population.

The highly pathogenic avian influenza A virus subtype H5, identified in Guangdong Province, China, in 1996, has evolved into multiple distinct phylogenetic clades and undergone reassortment events (*1*). In 2014, a new clade (2.3.4.4) that included influenza A(H5N6) virus emerged in Asia and has caused both epizootic and zoonotic cases worldwide (*2*). As of August 1, 2023, a total of 86 human cases of H5N6 infection have been reported globally; 40 (46.5%) have resulted in death (*3*). Most cases were reported in China, and 1 case was reported in Laos (*3*). An increase in the number of H5N6 human infections during 2021 and 2022 has been observed, reaching a total of 55 cases, exceeding the cumulative total number of the reported H5N6 human infections in the preceding years (Figure 1, panel A). This sudden upsurge has consequently raised concerns over a higher risk for H5N6 transmission.

Previous studies have indicated a higher prevalence of human infections with H5 viruses, according to serologic evidence, compared with the number of World Health Organization–confirmed cases (*4*). A shortage of serologic surveillance studies focusing on human H5N6 infections in the general population exists (*5*,*6*). To better assess the risk for H5N6 infections during the 2021–22 wave, we conducted a cross-sectional serologic study during January–March 2022 (Figure 1, panel A) in Dongguan and Huizhou cities in Guangdong Province. The cities were the epicenters of human H5N6 infections in 2021 (Figure 1, panel B). Given the unclear seroprevalence of H5N6 virus in the general population, we used an estimated H5N1 seropositivity rate of 1.2% (*4*) for our sample size calculation, targeting a 95% CI and a precision of 0.006. Assuming a dropout rate of 15%, we calculated that a sample size of 6,012 in the general population would be required. This study was approved by the ethics committee of the First Affiliated Hospital of Guangzhou Medical University (ethics approval no. 2016-78).

We excluded poultry workers and patients with oncologic diseases, hematologic malignancies, or immunocompromising conditions from our study. The patients who reported respiratory symptoms or diseases were not excluded and represented a small fraction of the sample pool (46 [0.72%]). We collected serum samples from 6,363 participants at 72 local hospitals and physical examination centers across Dongguan and Huizhou cities, ensuring a broad regional representation. Of the participants, most were outpatients (4,284 [67.33%]); the remaining participants were hospitalized patients (699 [10.99%]) or persons undergoing routine physical examinations (1,380 [21.69]). The median age of participants was 41 years (25th–75th percentile 29–55 years). Of the 6,363 samples, 42.2% (2,685) were from men and 57.8% (3,678) from women; 53.4% (3,401) of samples were from Huizhou (Table). We screened the residual serum samples by using a hemagglutination inhibition (HI) assay against a recombinant H5N6 virus

[1]These authors contributed equally to this article.

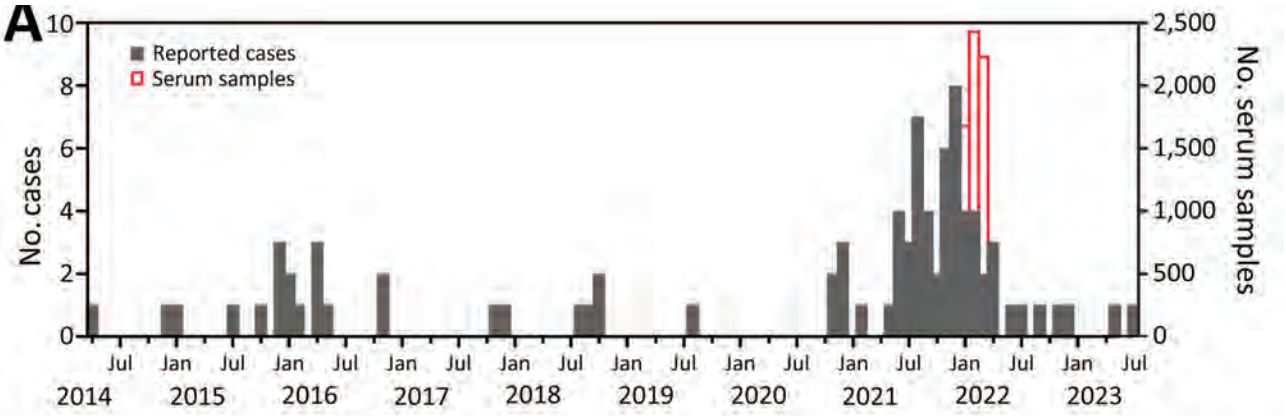

B

	Southern China												Northern China	
Year	GX	**GD**	HN	SC	JS	CQ	JX	YN	AH	FJ	ZJ	HB	GZ	HA	BJ
2014		1		1											
2015		3					1	2							
2016	1	3	3						1			1			
2017	1									1					
2018	2	1			1										
2019															1
2020			1		1	1			1				1		
2021	11	**5**	9	8		2					1				
2022	5	1	1	3	3		2			1	1			1	
2023	1			1											
Total	21	14	14	13	5	3	3	2	2	2	2	1	1	1	1

Figure. Collection timepoints and locations of 6,363 persons from whom residual serum samples were collected in Huizhou and Dongguan cities, Guangdong Province, China, plotted against the temporal and spatial distribution of human infection with influenza A virus subtype H5N6 in China as a whole. A) Temporal distribution of 85 human infections with H5N6 in China during 2014–2023 and collection timepoints of 6,363 residual serum samples. Scales for the y-axes differ substantially to underscore patterns but do not permit direct comparisons. B) Geographic distribution of 85 human H5N6 infections in China by province, municipality, or autonomous region, as of August 1, 2023. The numbers represent the confirmed cases of infection in each area. Guangdong Province (boldface), the site of the seroprevalence study, reported all 5 local H5N6 cases in 2021 within Dongguan (n = 2) and Huizhou (n = 3) cities, where the residual serum samples were collected. AH, Anhui; BJ, Beijing; CQ, Chongqing; FJ, Fujian; GD, Guangdong; GX, Guangxi; GZ, Guizhou; HA, Henan; HB, Hubei; HN, Hunan; JS, Jiangsu; JX, Jiangxi; SC, Sichuan; YN, Yunnan; ZJ, Zhejiang.

derived from A/Huizhou/1/2021(H5N6) (2.3.4.4b subclade), according to previously published studies (*7*). We confirmed 15 serum samples with an HI titer ≥10 by microneutralization assay, as described previously (*7*). We defined a seropositive result for H5N6 as having both HI and microneutraliza-

Table. Demographic characteristics of 6,363 persons from whom serum samples were collected for influenza A virus subtype H5N6 titer testing, Huizhou and Dongguan, Guangdong Province, China, January–March 2022*

Demographic characteristic	Value
Age group, y	
0–14	566 (8.9)
15–24	531 (8.3)
25–54	3633 (57.1)
55–64	768 (12.1)
>65	865 (13.6)
Median age, y (25th–75th percentile)	41 (29–55)
Sex	
M	2,685 (42.2)
F	3,678 (57.8)
Location	
Huizhou	3,401 (53.4)
Dongguan	2,962 (46.6)

*Values are no. (%) except as indicated.

tion titers ≥20 (*6*). Among those samples, we identified 1 confirmed seropositive specimen, collected on March 15, 2022, from a 22-year-old woman with an HI titer of 1:20 and an microneutralization titer of 1:80. We also identified 1 suspicious specimen, collected on March 1, 2022, from a 3-year-old boy with an HI titer of an 1:10 and an microneutralization titer of 1:40 (Appendix Table, https://wwwnc.cdc.gov/EID/article/30/4/23-1226-App1.pdf). Neither participant had a reported history of influenza-like illness before serum collection. All other samples were seronegative.

The seroprevalence of H5N6 infection in humans varies across different regions and time (*5*,*6*). In this cross-sectional study, we identified 1 seropositive serum sample among 6,363 residual serum samples collected from the general population in Huizhou and Dongguan, China, during January–March 2022. The seroprevalence in the general population was lower than that among poultry workers, which can reach up to 2.0% (*6*). This difference in seroprevalence suggests a lower risk factor for H5N6 infection in the general population compared with poultry workers, consistent with the poultry-to-human transmission route of H5N6 virus (*8*). Of note, the participant with a seropositivity against H5N6 virus did not report a history of influenza-like illness, indicating that the virus can also cause mild or asymptomatic infections. Our findings underscore the necessity of enhancing surveillance for H5N6 virus, especially in poultry workers or persons with poultry contact history, because of their higher risk for exposure.

One limitation of our study is that the exclusion of poultry workers and the lack of poultry contact history information limited our capacity to assess risk for these specific groups. In addition, our focus on Guangdong Province may not reflect other regions' epidemiologic profiles. We used cross-sectional residual serum samples instead of paired serum samples collected before and after the 2021–22 A(H5N6) wave. The paired serum sample approach, although more challenging, could better identify recent infections by tracking antibody titer changes.

This work was supported by the National Multidisciplinary Innovation Team Project of Traditional Chinese Medicine (ZYYCXTU-D-202206), National Natural Science Foundation of China (grant nos. 31970884, 82361168672, and 82174053), Major Project of Guangzhou National Laboratory (grant nos. GZNL2023A01001), and Open Project of State Key Laboratory of Respiratory Disease (grant nos. SKLRD-OP-202209).

About the Author

Dr. Wang is an associate professor at the Guangzhou National Laboratory. His research interests are surveillance, vaccine development, and pathogenesis of respiratory viruses.

References

1. Smith GJ, Donis RO; World Health Organization/World Organisation for Animal Health/Food and Agriculture Organization (WHO/OIE/FAO) H5 Evolution Working Group. Nomenclature updates resulting from the evolution of avian influenza A(H5) virus clades 2.1.3.2a, 2.2.1, and 2.3.4 during 2013–2014. Influenza Other Respir Viruses. 2015;9:271–6. https://doi.org/10.1111/irv.12324
2. Jeong S, Otgontogtokh N, Lee DH, Davganyam B, Lee SH, Cho AY, et al. Highly pathogenic avian influenza clade 2.3.4.4 subtype H5N6 viruses isolated from wild whooper swans, Mongolia, 2020. Emerg Infect Dis. 2021;27:1181–3. https://doi.org/10.3201/eid2704.203859
3. Center for Health Protection. Avian influenza report, volume 19, number 30. 2023 Aug 1 [cited 2023 Aug 1]. https://www.chp.gov.hk/files/pdf/2023_avian_influenza_report_vol19_wk30.pdf
4. Wang TT, Parides MK, Palese P. Seroevidence for H5N1 influenza infections in humans: meta-analysis. Science. 2012;335:1463. https://doi.org/10.1126/science.1218888
5. Ma MJ, Zhao T, Chen SH, Xia X, Yang XX, Wang GL, et al. Avian influenza A virus infection among workers at live poultry markets, China, 2013–2016. Emerg Infect Dis. 2018;24:1246–56. https://doi.org/10.3201/eid2407.172059
6. Quan C, Wang Q, Zhang J, Zhao M, Dai Q, Huang T, et al. Avian influenza A viruses among occupationally exposed populations, China, 2014–2016. Emerg Infect Dis. 2019;25:2215–25. https://doi.org/10.3201/eid2512.190261
7. Guan W, Qu R, Shen L, Mai K, Pan W, Lin Z, et al. Baloxavir marboxil use for critical human infection of avian influenza A H5N6 virus. Med. 2023;5:32-41.e5.
8. Zhu W, Li X, Dong J, Bo H, Liu J, Yang J, et al. Epidemiologic, clinical, and genetic characteristics of human infections with influenza A(H5N6) viruses, China. Emerg Infect Dis. 2022;28:1332–44. https://doi.org/10.3201/eid2807.212482

Address for correspondence: Weiqi Pan or Zifeng Yang, The First Affiliated Hospital of Guangzhou Medical University, 151 Yanjiang Rd, Guangzhou, Guangdong, 510120, China; email: panweiqi@gird.cn or jeffyah@163.com; Chitin Hon, Macau University of Science and Technology, Avenida Wai Long, Taipa, Macau, China; email: cthon@must.edu.mo

Ocular Dirofilariasis in Migrant from Sri Lanka to Australia

Elliott D. Cope, Nishant Gupta, Anson V. Koehler, Robin B. Gasser, Amy Crowe

Author affiliations: Royal Victorian Eye and Ear Hospital, East Melbourne, Victoria, Australia (E.D. Cope, N. Gupta); The University of Melbourne, Parkville, Victoria, Australia (A.V. Koehler, R.B. Gasser); St Vincents Hospital, Fitzroy, Victoria, Australia (A. Crowe)

DOI: https://doi.org/10.3201/eid3004.240125

We describe a case of imported ocular dirofilariasis in Australia, linked to the Hong Kong genotype of *Dirofilaria* sp., in a migrant from Sri Lanka. Surgical extraction and mitochondrial sequences analyses confirmed this filarioid nematode as the causative agent and a *Dirofilaria* sp. not previously reported in Australia.

Human dirofilariasis, caused by nematodes such as *Dirofilaria repens* or *D. immitis*, is a zoonotic disease transmitted through the bite of various mosquito species (*1*). The definitive hosts of *Dirofilaria* sp. nematodes are canine and feline populations. Clinical manifestations of human infections, including the development of nodules in multiple anatomic locations, result from the migration or dwelling of worms in subcutaneous tissues (*1*). Human dirofilariasis is typically species-specific depending on the geographic area; *D. repens* nematode infections are found in Europe and Asia and *D. immitis* nematode infections in the Americas (*1*). Recently, a new genotype, called *Dirofilaria* sp. *hongkongensis* in the literature and referred to in this article as *Dirofilaria* sp. Hong Kong genotype (*2*), is proposed as a causative agent of subcutaneous or subconjunctival dirofilariosis in humans with a likely reservoir in canines. *Dirofilaria* sp. Hong Kong genotype is considered a nomen nudum within the scientific community because a proper morphologic description is missing (*3*). In Australia, only 21 human cases of dirofilariasis have been reported (*1*). Four documented cases of orbital dirofilariasis have been linked to suspected *Drofilaria* infection (*1*).

Dirofilaria nematode infection is usually transmitted by mosquitoes (including those of the *Aedes*, *Anopheles*, and *Culex* genera) from carnivores. Mosquitoes play a crucial role in transmission by injecting the microfilaria into the accidental human host, which enables the transmitted larvae to develop further, but the nematodes do not typically reach full maturity in the human host, and they are usually sequestered in tissue. In rare instances, the adult stages of *Dirofilaria* nematodes are found in humans, usually in the lungs or in the cutaneous or subconjunctival areas (*1*).

In Australia, estimated prevalence of the *D. immitis* nematode in the canine population is 20% in some areas of the east coast, home to many species and genera of mosquitoes (e.g., *Aedes*, *Anopheles*, and *Culex*) (*4*,*5*,*6*). Of the 21 human dirofilariasis cases reported from mainland Australia in the past 40 years, most are linked to *D. immitis* nematode infection, and others are linked to *D. repens* nematode infection in returned travelers (*1*,*4*). We describe an imported case of human dirofilariasis of the Hong Kong genotype in Australia.

A 77-year-old man with a history of heart disease and diabetes was referred to the emergency department of the Royal Victorian Eye and Ear Hospital in Melbourne, Victoria, Australia, by an ophthalmologist because of concerns about a possible worm in the subconjunctiva. The patient had redness and pain in his left eye for 1 month but reported no visual impairment. He had immigrated from Sri Lanka to Melbourne 18 months earlier, and he had no history of recent travel, pet ownership, freshwater swimming, or gardening. Our examination of his left eye revealed normal visual acuity (6/6) and intraocular pressures (14 mm Hg). During the examination, we observed a mobile, whitish, curled, translucent, and elongated foreign body in the subconjunctiva positioned at approximately 4 o'clock, adjacent to the limbus, with an overlying mild conjunctival injection. Our posterior segment assessment of the eye (dilated pupil) was un-

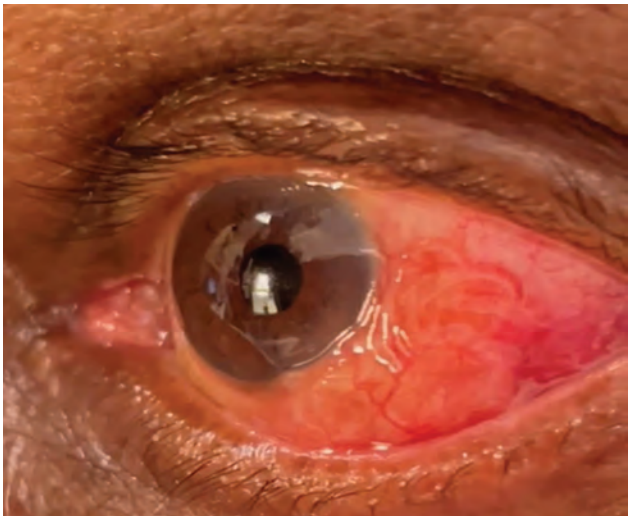

Figure 1. Left eye of a patient who recently migrated to Australia and originated from Sri Lanka, showing a subconjunctival infection that was identified as *Dirofilaria* sp. Hong Kong genotype nematode. The nematode can be seen at 3–5 o'clock, adjacent to the limbus of the eye.

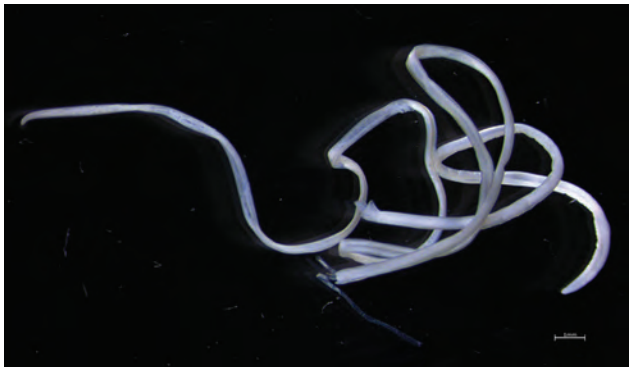

Figure 2. Macroscopic view of a *Dirofilaria* sp. Hong Kong genotype nematode after surgical extraction from the left eye of a patient who recently migrated from Sri Lanka to Australia. The nematode was 12 cm long. Scale bar indicates 1 mm.

remarkable (Figure 1). We surgically removed the foreign body, which was a 12-cm-long worm (Figure 2), after a limited peritomy (Appendix Figure, https://wwwnc.cdc.gov/EID/article/30 /4/ 24-0125-App1.pdf). We then suspended the worm in physiologic saline and submitted it for macroscopic and genetic analysis. The patient was discharged the next day and returned for a follow-up examination 1 week later.

Our microscopic examination of the surgically removed worm confirmed that it was a female worm with a thick, nonridged cuticle and a complete alimentary tract and reproductive system. We found no larvae in the uterus. We genetically characterized the worm by using PCR-based sequencing of a portion of the mitochondrial cytochrome c oxidase 1 (941 bp) gene and of the 12S nuclear ribosomal RNA gene (610 bp) (*7*). The sequences we obtained (GenBank accession nos. OR755977 and OR768484) were almost identical (940/941 bp for mitochondrial cytochrome c oxidase 1; 610/611 bp for 12S) to those representing the Hong Kong genotype of the *Dirofilaria* nematode (GenBank accession no. KX265050).

We presume that the patient acquired the *Dirofilaria* nematode infection in Sri Lanka, where prevalence of dirofilariasis is high (30%–69%) in feline and canine populations and some cases are linked to the Hong Kong genotype (*8*). Of the 173 reported cases of human dirofilariasis caused by *D. repens* nematodes reported during 1965–2020, a total of 40 cases were in patients with subconjunctival infections (*9*). We are concerned that some of those infections might have been misidentified as *D. repens* because molecular methods were not used for genetic analysis and identification (*8*).

This study emphasizes the importance of using molecular tools for the accurate diagnosis of filariases and the need for heightened clinical suspicions of rare zoonotic infections. This emphasis is particularly important for patients who have a travel history from countries endemic for neglected tropical diseases.

Acknowledgments

We thank Carmel Crock for assistance and the patient for providing us permission to publish the findings.

This study was partially supported through a grant from the Australian Research Council.

About the Author

Dr. Cope is a senior emergency registrar at the Royal Victorian Eye and Ear Hospital, Melbourne. He has an interest in ocular infections and diseases.

References

1. Simón F, Siles-Lucas M, Morchón R, González-Miguel J, Mellado I, Carretón E, et al. Human and animal dirofilariasis: the emergence of a zoonotic mosaic. Clin Microbiol Rev. 2012;25:507–44. https://doi.org/10.1128/CMR.00012-12
2. To KK, Wong SS, Poon RW, Trendell-Smith NJ, Ngan AH, Lam JW, et al. A novel *Dirofilaria* species causing human and canine infections in Hong Kong. J Clin Microbiol. 2012;50:3534–41. https://doi.org/10.1128/JCM.01590-12
3. Perles L, Dantas-Torres F, Krücken J, Morchón R, Walochnik J, Otranto D. Zoonotic dirofilariases: one, no one, or more than one parasite. Trends Parasitol. 2024;S1471-4922(23)00312-4. https://doi.org/10.1016/j.pt.2023.12.007
4. Theodore SG, Sawkins HJ, Mathew M, Yadav S, Norton R. Human pulmonary dirofilariasis: an unexpected differential diagnosis for a solitary lung lesion. Med J Aust. 2023;219:455–6. https://doi.org/10.5694/mja2.52115
5. Constantinoiu C, Croton C, Paterson MBA, Knott L, Henning J, Mallyon J, et al. Prevalence of canine heartworm infection in Queensland, Australia: comparison of diagnostic methods and investigation of factors associated with reduction in antigen detection. Parasit Vectors. 2023;16:63. https://doi.org/10.1186/s13071-022-05633-9
6. Ong OTW, Skinner EB, Johnson BJ, Old JM. Mosquito-borne viruses and non-human vertebrates in Australia: a review. Viruses. 2021;13:265. https://doi.org/10.3390/v13020265
7. Lefoulon E, Bain O, Bourret J, Junker K, Guerrero R, Cañizales I, et al. Shaking the tree: multi-locus sequence typing usurps current onchocercid (filarial nematode) phylogeny. PLoS Negl Trop Dis. 2015;9(11):e0004233.
8. Atapattu U, Koehler AV, Huggins LG, Wiethoelter A, Traub RJ, Colella V. Dogs are reservoir hosts of the zoonotic *Dirofilaria* sp. '*hongkongensis*' and potentially of *Brugia* sp. Sri Lanka genotype in Sri Lanka. One Health. 2023;17:100625. https://doi.org/10.1016/j.onehlt.2023.100625
9. Iddawela D, Ehambaram K, Wickramasinghe S. Human ocular dirofilariasis due to *Dirofilaria repens* in Sri Lanka. Asian Pac J Trop Med. 2015;8:1022–6. https://doi.org/10.1016/j.apjtm.2015.11.010

Address for correspondence: Elliott Cope, The Royal Victorian Eye and Ear Hospital, 32 Gisborne St, East Melbourne, Victoria, Australia; email: elliott.d.cope@gmail.com

Drug-Resistant Tuberculosis, Georgia, Kazakhstan, Kyrgyzstan, Moldova, and Ukraine, 2017–2022

Victor Naestholt Dahl, Tetiana Butova, Alex Rosenthal, Alina Grinev, Andrei Gabrielian, Sergo Vashakidze, Natalia Shubladze, Bekzat Toxanbayeva, Lyailya Chingissova, Valeriu Crudu, Dumitru Chesov, Gulmira Kalmambetova, Gulbarchyn Saparova, Christian Morberg Wejse, Dmytro Butov; Ukraine TB-Portal Study Group

Author affiliations: Aarhus University Hospital, Aarhus, Denmark (V.N. Dahl, C.M. Wejse); Merefa Central District Hospital, Merefra, Ukraine (T. Butova); National Institutes of Health, Bethesda, Maryland, USA (A. Rosenthal, A. Grinev, A. Gabrielian); National Center for Tuberculosis and Lung Diseases, Tbilisi, Georgia (S. Vashakidze, N. Shubladze); National Scientific Center of Phthisiopulmonology, Almaty, Kazakhstan (B. Toxanbayeva, L. Chingissova); Institute of Phthisiopneumology, Chisinau, Moldova (V. Crudu); State University of Medicine and Pharmacy, Chisinua (D. Chesov); National TB Program, Bishkek, Kyrgyzstan (G. Kalmambetova, G. Saparova); Kharkiv National Medical University, Kharkiv, Ukraine (D. Butov)

DOI: https://doi.org/10.3201/eid3004.231732

In 2021, the World Health Organization recommended new extensively drug-resistant (XDR) and pre-XDR tuberculosis (TB) definitions. In a recent cohort of TB patients in Eastern Europe, we show that XDR TB as currently defined is associated with exceptionally poor treatment outcomes, considerably worse than for the former definition (31% vs. 54% treatment success).

In early 2021, the World Health Organization (WHO) recommended new definitions of extensively drug resistant (XDR) and pre-XDR tuberculosis (TB) (*1*,*2*). Previously, pre-XDR TB was informally defined as TB caused by *Mycobacterium tuberculosis* strains with resistance to rifampin and isoniazid plus resistance to either a fluoroquinolone or a second-line injectable, but not both (*1*–*3*). Now, pre-XDR TB is officially defined as strains with resistance to rifampin, isoniazid, and a fluoroquinolone (levofloxacin or moxifloxacin), whereas XDR TB is now defined as additional resistance to ≥1 group A drug (bedaquiline or linezolid), replacing the second-line injectables used in the former definitions (*1*–*3*).

Treatment outcomes of patients with XDR TB as currently defined have been sparsely reported. A study from France with 93 patients fulfilling the new pre-XDR TB and XDR TB definitions, including 9 patients with XDR TB, found a combined treatment success of 68% (n = 63), comparable to that of multidrug-resistant (MDR) TB (*4*). Another study following 9 XDR TB patients from Georgia documented a treatment success of only 22% (n = 2/9) (*5*). We describe MDR TB, pre-XDR TB, and XDR TB treatment outcomes in Georgia, Kazakhstan, Kyrgyzstan, Moldova, and Ukraine during 2017–2022 in patients with drug susceptibility tests available for fluroquinolones, second-line injectables, bedaquiline, and linezolid.

Using prospectively collected data from the National Institute of Allergy and Infectious Diseases TB Portals Program, as described elsewhere (*6*), we included 1,960 patients with MDR TB, pre-XDR TB, and XDR TB in the analysis. Median age was 43 (interquartile range 35–51) years; 78% (1,535) were men and 22% (425) women; 63% (1,235) were smokers, and 18% 350) were persons with HIV. Most patients were from Ukraine (n = 1,455), Moldova (n = 289), and Georgia (n = 160), whereas only a few were from Kazakhstan (n = 39) and Kyrgyzstan (n = 17).

Of the 1,960 patients, 36% (698) were classified in a different category using the current definitions than for the previous definitions; XDR TB accounted for a much smaller percentage (2.7%, 95% CI 2.0%–3.5%) of patients than under the previous definition (18.5%, 95% CI 16.8%–20.3%). Using WHO treatment outcomes (*6*,*7*), our results showed that the current XDR TB definition was associated with low treatment success (sum of treatment completed and cured), only 31% (95% CI 19%–45%), compared with 54% (95% CI 49%–59%) using the former definition (p = 0.002 by χ^2 test) (Figure). That finding was mainly driven by a higher percentage of failure using the current definition (33%, 95% CI 21%–47%) than when using the former (15%, 95% CI 11%–19%; p = 0.001) and a lower percentage of cured (25% [95% CI 14%–39%] vs. 46% [95% CI 41%–51%]; p = 0.004). Although a history of TB among patients with XDR TB was associated with a notably lower percentage of successful outcomes (23%, 95% CI 11%–41%) compared with the percentage of successful outcomes in persons without a history of TB (47%, 95% CI 24%–71%), this difference did not reach statistical significance (p = 0.076). MDR TB and pre-XDR TB treatment outcomes were comparable for both definitions.

Our study showed that XDR TB by the current definition is associated with exceptionally poor treatment outcomes, considerably worse than XDR TB by the former definition. The new XDR TB definition is applicable to fewer patients than the former definition,

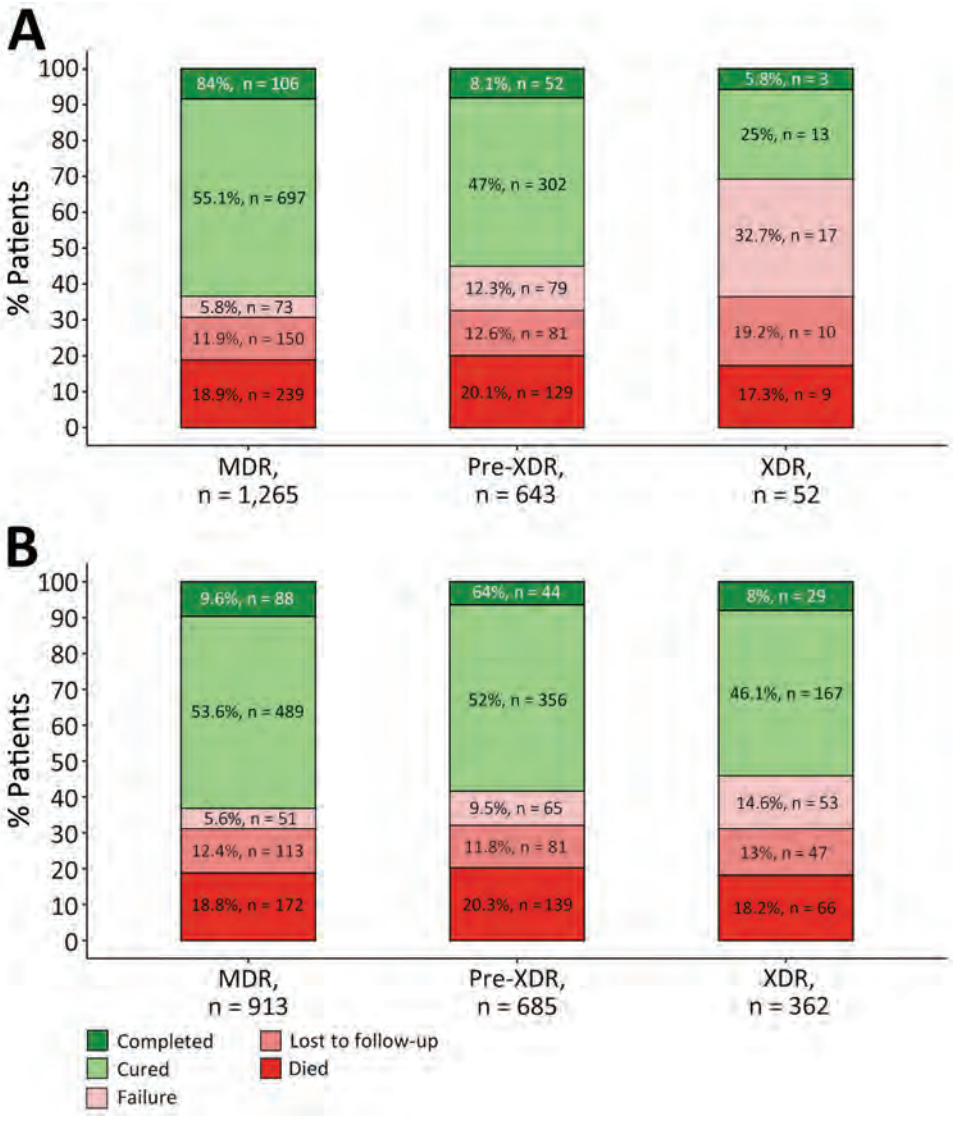

Figure. Treatment outcomes for patients with MDR, pre-XDR, and XDR tuberculosis (TB) in Georgia, Kazakhstan, Kyrgyzstan, Moldova, and Ukraine during 2017–2022 by current (A) and former (B) definitions of drug resistance. We excluded 9 patients with an unevaluated outcome and 15 patients without outcome data. TB treatment outcomes were defined according to WHO recommendations (*6*,*7*). MDR TB was defined as TB caused by *Mycobacterium tuberculosis* strains resistant to at least both rifampin and isoniazid (*1*). We used the current definition of pre-XDR TB from 2021 as TB caused by *M. tuberculosis* strains fulfilling the definition of MDR TB but including resistance to any fluoroquinolone (levofloxacin or moxifloxacin), whereas XDR TB was defined as additional resistance to ≥1 group A drug (bedaquiline or linezolid) (A). The previous, informal definition of pre-XDR TB was MDR TB plus additional resistance to any fluoroquinolone, or any second-line injectable, but not both, whereas the definition of XDR TB from 2006 was TB resistant to any fluoroquinolone and to ≥1 of 3 second-line injectable drugs (capreomycin, kanamycin, and amikacin), in addition to MDR TB. MDR, multidrug-resistant; XDR, extensively drug-resistant.

and treatment options are more limited. Veziris et al. (*8*) also observed a decrease in XDR TB patients using the revised definitions. Still, as use of bedaquiline and linezolid increases globally, resistance to those drugs will undoubtly increase, resulting in a higher number of XDR TB patients in the future. Better treatment outcomes for MDR TB have been associated with the use of bedaquiline, linezolid, and fluoroquinolones (*2*,*9*), and studies have shown worse outcomes for patients with bedaquiline resistance (*10*). Previous exposure to those drugs (i.e., bedaquiline, linezolid, fluoroquinolones) has been associated with worse patient outcomes compared with patients without previous exposure (*5*). Altogether, those factors explain the treatment success of only 31% for XDR TB, even lower than that recently found in a meta-analysis involving 10,223 XDR TB patients (94 studies, 26 countries) using the former definition, which together showed a pooled successful treatment outcome of 44% (95% CI 38%–50%) (*3*). That review found a XDR TB treatment success of 6% and 25% in 2 studies from Ukraine (n = 126).

The current definitions of pre-XDR TB and XDR TB, recommended since early 2021, are undoubtly more relevant than the former definitions, given they take into account WHO-recommended treatment regimens containing bedaquiline, pretomanid, linezolid, and moxifloxacin. Worryingly, but not surprisingly, the new definitions are associated with exceptionally poor outcomes for XDR TB, indicating loss of effective drugs. Upscaling of drug susceptibility testing, assessment of acquired drug resistance, and availability of diagnostic tools and drugs are crucial to avoid a future increase in patients with very limited treatment options. Treatment strategies should be assesed

under programmatic conditions to improve understanding of the recommended treatment regimens, their implementation, and the effects on TB management globally.

This research was supported by the grants from the National Institute of Allergy and Infectious Diseases/ US Civilian Research & Development Foundation, CRDF Global (DAA9-19-66199) and the Ministry of Health of Ukraine (#0123100178). The study funders had no role in the study design, data collection, data analysis, data interpretation, or writing of the report.

About the Author

Dr. Dahl is a medical doctor and PhD student at the Department of Infectious Diseases, Aarhus University Hospital, Aarhus, Denmark. He is interested in complicated respiratory infections such as tuberculosis and nontuberculous mycobacteria and mainly works with clinical epidemiology and systematic reviews.

References

1. World Health Organization. Meeting report of the WHO expert consultation on the definition of extensively drug-resistant tuberculosis [cited 2023 Dec 6]. https://www.who.int/publications/i/item/9789240018662
2. Roelens M, Battista Migliori G, Rozanova L, Estill J, Campbell JR, Cegielski JP, et al. Evidence-based definition for extensively drug-resistant tuberculosis. Am J Respir Crit Care Med. 2021;204:713–22. https://doi.org/10.1164/rccm.202009-3527OC
3. Pedersen OS, Holmgaard FB, Mikkelsen MKD, Lange C, Sotgiu G, Lillebaek T, et al. Global treatment outcomes of extensively drug-resistant tuberculosis in adults: A systematic review and meta-analysis. J Infect. 2023;87:177–89. https://doi.org/10.1016/j.jinf.2023.06.014
4. Kherabi Y, Fréchet-Jachym M, Rioux C, Yazdanpanah Y, Méchaï F, Pourcher V, et al.; MDR-TB Management Group. Revised definitions of tuberculosis resistance and treatment outcomes, France, 2006–2019. Emerg Infect Dis. 2022;28:1796–804. https://doi.org/10.3201/eid2809.220458
5. Mikiashvili L, Kempker RR, Chakhaia T, Bablishvili N, Avaliani Z, Lomtadze N, et al. Impact of prior TB treatment with new/companion drugs on clinical outcomes in patients receiving concomitant bedaquiline and delamanid for MDR/RR-TB. Clin Infect Dis. 2023 Nov 14 [Epub ahead of print]. https://doi.org/10.1093/cid/ciad694
6. Pedersen OS, Butova T, Kapustnyk V, Miasoiedov V, Kuzhko M, Hryshchuk L, et al. Treatment outcomes and risk factors for an unsuccessful outcome among patients with highly drug-resistant tuberculosis in Ukraine. Clin Microbiol Infect. 2024;30:360–7. https://doi.org/10.1016/j.cmi.2023.12.001
7. World Health Organization. Definitions and reporting framework for tuberculosis—2013 revision: updated December 2014 and January 2020 [cited 2023 Dec 6]. https://www.who.int/publications/i/item/9789241505345
8. Veziris N, Bonnet I, Morel F, Guglielmetti L, Maitre T, Fournier Le Ray L, et al.; CNR MyRMA; Members of the CNR-MyRMA (French National Reference Center for Mycobacteria). Impact of the revised definition of extensively drug-resistant tuberculosis. Eur Respir J. 2021;58:2100641 https://doi.org/10.1183/13993003.00641-2021
9. Collaborative Group for the Meta-Analysis of Individual Patient Data in MDR-TB treatment–2017; Ahmad N, Ahuja SD, Akkerman OW, et al. Treatment correlates of successful outcomes in pulmonary multidrug-resistant tuberculosis: an individual patient data meta-analysis. Lancet. 2018;392:821–34. https://doi.org/10.1016/S0140-6736(18)31644-
10. Ismail NA, Omar SV, Moultrie H, Bhyat Z, Conradie F, Enwerem M, et al. Assessment of epidemiological and genetic characteristics and clinical outcomes of resistance to bedaquiline in patients treated for rifampicin-resistant tuberculosis: a cross-sectional and longitudinal study. Lancet Infect Dis. 2022;22:496–506. https://doi.org/10.1016/S1473-3099(21)00470-9

Address for correspondence: Victor Næstholt Dahl, Department of Infectious Diseases, Aarhus University Hospital, Palle Juul-Jensens Blvd 99, Aarhus, Denmark, DK-8200; email: vicmat@rm.dk

Opportunistic *Elizabethkingia miricola* Infections in Intensive Care Unit, Spain

Eva Soler-Iborte, Mario Rivera-Izquierdo, Carmen Valero-Ubierna

Author affiliations: Hospital Universitario San Cecilio, Granada, Spain (E. Soler-Iborte, M. Rivera-Izquierdo, C. Valero-Ubierna); Instituto biosanitario de Granada, Granada, (M. Rivera-Izquierdo); Ciber de Epidemiología y Salud Pública, Madrid, Spain (M. Rivera-Izquierdo)

DOI: https://doi.org/10.3201/eid3004.231491

In 2021, we identified a cluster of *Elizabethkingia miricola* cases in an intensive care unit in Spain. Because *E. miricola* is not considered a special surveillance agent in Spain, whole-genome sequencing was not performed. The bacterial source was not identified. All *Elizabethkingia* species should be listed as special surveillance bacteria.

The *Elizabethkingia* genus is formed by a group of gram-negative, aerobic, and nonfermenting bacteria widely distributed in nature and environments, such as water and hospital taps (*1*). In 2003, a new a

bacterial species was identified in the condensation water obtained from the Mir space station in 1997 and was assigned as *Chryseobacterium miricola* (*2*). That new species was later transferred to the *Elizabethkingia* genus and renamed *Elizabethkingia miricola* (*3*). This species is considered as an uncommon low-pathogenic agent in clinical samples, acting as an opportunistic pathogen, but since 2008, it has become an emerging bacterium of increasing relevance (*4*). *E. miricola* has not been fully epidemiologically characterized but is considered intrinsically resistant to multiple drugs (*5*).

We describe a cluster of *E. miricola* in the intensive care unit (ICU) of the Hospital Universitario San Cecilio in Granada, Spain. The index case corresponded to a 66-year-old man hospitalized for COVID-19. The microbiology service identified *E. miricola* isolates from a bronchial aspirate sample by using matrix-assisted laser desorption/ionization time-of-flight mass spectrometry and informed the ICU of a positive result on March 19, 2021. Two days later, a 70-year-old man hospitalized in the same unit for COVID-19 also tested positive for *E. miricola* in a bronchial aspirate sample sent for a previous diagnosis with tracheobronchitis associated with *Stenotrophomonas maltophilia.*

Throughout 2021, we found 13 more cases of *E. miricola* in the same ICU. Given the identification of the same species, and for clinical and epidemiologic criteria, the outbreak was considered nosocomial. However, although isolates were retained for potential future research, no whole-genome sequencing could be performed because the species is not included as special surveillance agent for the Andalusian Health System because of resource limitations. The reason for admission in 11 (73.3%) patients was COVID-19. Of the 15 case-patients, 11 (73.3%) were men and 4 (26.7%) women, 6 (40.0%) had tracheobronchitis diagnoses, 3 (20.0%) had

Table. Characteristics of case-patients in an outbreak opportunistic *Elizabethkingia miricola* infections in an intensive care unit, Spain*

Age, y/sex	Isolation sample	ICU stay, d	Diagnosis†	Diagnosis date, 2021	Death	Reason for admission	Antimicrobial drug resistance‡
66/M	BAS	40	Isolation	Mar 17	N	COVID-19	Carbapenems, ceftazidime, cefepime, aztreonam
70/M	BAS	63	Isolation	Mar 19	N	COVID-19	Carbapenems, ceftazidime, cefepime, aztreonam
46/F	BAS	12	Isolation	Mar 27	Y	Carcinosis	Carbapenems, ceftazidime, cefepime, aztreonam, aminoglycosides
64/M	BAS	61	Tracheobronchitis	Apr 22	N	COVID-19	Carbapenems, ceftazidime, cefepime, aztreonam, piperacillin/tazobactam
57/F	BAS, catheter	20	Bacteriemia	Apr 27	Y	COVID-19	Carbapenems, ceftazidime, cefepime, aztreonam, piperacillin/tazobactam, aminoglycosides, trimethoprim/sulfamethoxazole
50/M	BAS	58	Tracheobronchitis	May 19	Y	COVID-19	Carbapenems, ceftazidime, amikacin
52/M	BAS	37	Tracheobronchitis	May 20	N	COVID-19	Carbapenems, ceftazidime, amikacin
56/M	BAS	43	Ventilator-associated pneumonia	May 22	Y	COVID-19	Amikacin
58/F	BAS	80	Tracheobronchitis	May 29	N	COVID-19	Amikacin
58/M	BAS	30	Isolation	Jul 7	Y	Fever	Piperacillin/tazobactam, linezolid
37/F	BAS	51	Isolation	Aug 20	Y	COVID-19	Piperacillin/tazobactam, linezolid
32/M	BAS	93	Tracheobronchitis	Sep 18	Y	COVID-19	Piperacillin/tazobactam, linezolid
74/M	BAS	27	Tracheobronchitis	Sep 28	Y	Epileptic seizures	Piperacillin/tazobactam, linezolid
61/M	BAS	27	Ventilator-associated pneumonia	Oct 27	N	Septic shock	Piperacillin/tazobactam, linezolid, vancomycin,
73/M	BAS	15	Ventilator-associated pneumonia	Dec 30	N	COVID-19	Piperacillin/tazobactam, linezolid, levofloxacin

*BAS, bronchoaspiration; ICU, intensive care unit.
†Isolation means that no other clinical pathology was reported by the responsible physician in the ICU. Therefore, *E. miricola* identification was considered as asymptomatic colonization.
‡Antibiograms were compatible with the same agent, but development of new resistances was identified during the 9-mo outbreak. Trimethoprim/sulfamethoxazole showed the best antibiogram sensitivity: 10 patients showed sensitivity, 4 intermediate sensitivity, and only 1 showed resistance. Sensitivity to levofloxacin was observed for 7 (46.7%) patients; 4 more showed intermediate sensitivity.

ventilator-associated pneumonia, and 1 (6.7%) had catheter-related bacteremia; 8 (53.3%) patients died (Table).

All patients received steroid treatment during their ICU stays. All case-patients were intubated during their hospitalization. The average length of ICU stay was 43.8 days, and the length between admission and identification of the agent was long, a mean of 26.4 days.

Because 290 days elapsed from identification of the index case (March 19) to identification of the last case (December 30), we assumed persistence of the agent in the ICU environment. Nevertheless, despite a search of environmental and surface samples, the definitive focus of persistence was not identified. Because of possible cross-transmission in a unit with such vulnerable patients, we notified the Service of Preventive Medicine and Public Health, which initiated prevention measures. Because of the lack of available knowledge related to *E. miricola* and closely related species, we reinforced standard precautions and established contact precautions. Finally, by December 2021, we conducted a thorough disinfection of all surfaces in the ICU, after which no more cases were identified.

In other countries, cases of multidrug resistance were identified in the context of antimicrobial drug pressure and cases of sepsis and pneumonia were diagnosed among immunosuppressed patients (*5*). In our hospital, 8 (53.3%) patients died. The average time from bacterial isolation to death was 18.2 (range 2–65) days.

Elisabethkingia isolates are usually resistant to multiple antibiotics. In analyses of different isolates collected in South Korea and Taiwan (*5*), all *E. miricola* isolates were resistant to cephalosporins, aminoglycosides, and carbapenems. Those data are similar to results obtained in our hospital (Table). A study conducted in Switzerland found genes encoding metallo-β-lactamases in a multidrug-resistant *E. miricola* isolated from the urine of a 2-year-old boy (*6*). Those genes provide resistance to penicillin-β-lactamase inhibitor combinations, carbapenems, cefotaxime, and cefoxitin. Trimethoprim/sulfamethoxazole showed the best antibiogram sensitivity in our outbreak, only 1 of 15 patients showed resistance (Table).

In summary, our study underlines the need to find *Elizabethkingia* spp. bacteria in ICUs. In addition, all species in the *Elizabethkingia* genus should be listed as special surveillance bacteria due to their capacity to cause major illness and death in vulnerable patients. Future studies analyzing differences in the outcomes between patients with *E. miricola* and other patients admitted to ICU, including patient characteristics and treatments, could expand on the information provided in this study. Finally, to enable early detection of outbreaks of intrinsically antimicrobial-resistant bacteria, modify patient treatment, and save lives, whole-genome sequencing needs to be instituted when rare agents not previously considered for special surveillance are identified.

E.S.-I. and C.V.-U. participated in the treatment and preventive measures for controlling the outbreak. M.R.-I. supervised the work. All authors participated in writing and revising the manuscript for intellectual content.

About the Author

Dr. Soler-Iborte is a preventive medicine and public health resident at Hospital Universitario San Cecilio, Granada, Spain. Her research interests include nosocomial infections, vaccines, epidemiology and infectious disease prevention in the hospital setting.

References

1. Zdziarski P, Paściak M, Rogala K, Korzeniowska-Kowal A, Gamian A. *Elizabethkingia miricola* as an opportunistic oral pathogen associated with superinfectious complications in humoral immunodeficiency: a case report. BMC Infect Dis. 2017;17:763. https://doi.org/10.1186/s12879-017-2886-7
2. Li Y, Kawamura Y, Fujiwara N, Naka T, Liu H, Huang X, et al. *Chryseobacterium miricola* sp. nov., a novel species isolated from condensation water of space station Mir. Syst Appl Microbiol. 2003;26:523–8. https://doi.org/10.1078/072320203770865828
3. Kim KK, Kim MK, Lim JH, Park HY, Lee ST. Transfer of *Chryseobacterium meningosepticum* and *Chryseobacterium miricola* to *Elizabethkingia* gen. nov. as *Elizabethkingia meningoseptica* comb. nov. and *Elizabethkingia miricola* comb. nov. Int J Syst Evol Microbiol. 2005;55:1287–93. https://doi.org/10.1099/ijs.0.63541-0
4. Gupta P, Zaman K, Mohan B, Taneja N. *Elizabethkingia miricola*: A rare non-fermenter causing urinary tract infection. World J Clin Cases. 2017;5:187–90. https://doi.org/10.12998/wjcc.v5.i5.187
5. Lin JN, Lai CH, Yang CH, Huang YH. *Elizabethkingia* infections in humans: from genomics to clinics. Microorganisms. 2019;7:295. https://doi.org/10.3390/microorganisms7090295
6. Colapietro M, Endimiani A, Sabatini A, Marcoccia F, Celenza G, Segatore B, et al. BlaB-15, a new BlaB metallo-β-lactamase variant found in an *Elizabethkingia miricola* clinical isolate. Diagn Microbiol Infect Dis. 2016;85:195–7. https://doi.org/10.1016/j.diagmicrobio.2015.11.016

Address for correspondence. Eva Soler-Iborte, Service of Preventive Medicine and Public Health, Hospital Universitario San Cecilio, Avenida del Conocimiento s/n 18016, Granada, Spain; email: eva.soler.sspa@juntadeandalucia.es

Crimean-Congo Hemorrhagic Fever Virus Seroprevalence in Human and Livestock Populations, Northern Tanzania

Ellen C. Hughes, William de Glanville, Tito Kibona, Blandina Theophil Mmbaga, Melinda K. Rostal, Emanuel S. Swai, Sarah Cleaveland, Felix Lankester, Brian J. Willett, Kathryn J. Allan

Author affiliations: University of Liverpool Institute of Infection Veterinary and Ecological Sciences, Liverpool, UK (E.C. Hughes); University of Glasgow College of Medical Veterinary and Life Sciences, Glasgow, Scotland, UK (E.C. Hughes, W. de Glanville, S. Cleaveland, K.J. Allan); Washington State University, Pullman, Washington, USA (E.C. Hughes, F. Lankester); Nelson Mandela African Institute of Science and Technology, Arusha, Tanzania (T. Kibona); Global Animal Health Tanzania, Arusha, Tanzania (T. Kibona, F. Lankester); Kilimanjaro Christian Medical University College, Kilimanjaro, Tanzania (B.T. Mmbaga); EcoHealth Alliance, New York, New York, USA (M.K. Rostal); Ministry of Livestock and Fisheries, Dodoma, Tanzania (E.S. Swai); MRC-University of Glasgow Centre for Virus Research, Glasgow, UK (B.J. Willet)

DOI: https://doi.org/10.3201/eid3004.231204

We conducted a cross-sectional study of Crimean-Congo hemorrhagic fever virus (CCHFV) in northern Tanzania. CCHFV seroprevalence in humans and ruminant livestock was high, as were spatial heterogeneity levels. CCHFV could represent an unrecognized human health risk in this region and should be included as a differential diagnosis for febrile illness.

Crimean-Congo hemorrhagic fever virus (CCHFV) is a tickborne orthonairovirus with potential to cause severe Crimean-Congo hemorrhagic fever (CCHF) disease in humans, which can lead to human-to-human transmission (*1*). CCHFV is a World Health Organization priority pathogen for research and development (*2*). Although a wide range of wild and domestic animals can be infected (*3*), CCHFV does not typically cause clinical disease in nonhuman species (*1*). In eastern Africa, intermittent outbreaks of CCHF disease in humans have occurred in Uganda since 2013 (*4*), but the epidemiology of CCHFV remains poorly understood. Northern Tanzania, neighboring Uganda, has been identified as an area likely to be at high risk for human disease caused by CCHFV, because competent tick vectors and suitable environmental conditions exist in the region (*5*), but no clinical CCHF cases have yet been reported in the country.

To investigate CCHFV exposure in northern Tanzania, we performed serologic testing on human and ruminant livestock serum samples collected in 2016 during an investigation of several zoonotic pathogens (*6*) (Appendix, https://wwwnc.cdc.gov/EID/article/30/4/23-1204-App1.pdf). The study used a multilevel sampling frame of 351 humans and 7,456 randomly selected livestock in linked households in Arusha and Manyara Regions (Figure). We tested serum samples by using the ID Screen CCHF Double Antigen Multi-species ELISA (IDvet, https://www.innovative-diagnostics.com) (Appendix). We estimated seroprevalence by using the Survey package in R (The R Foundation for Statistical Computing, https://www.r-project.org) (*7*). We assessed species-level differences in seroprevalence by using a mixed-effects model with household and village as random effects. We investigated patterns of spatial autocorrelation in village-level seroprevalence by using the Moran *I* statistic and assessed correlation of village-level seroprevalence between species pairs by using the Pearson correlation coefficient (ρ) (Appendix).

Overall, seroprevalence was high in all livestock species: cattle 49.6% (95% CI 40.0%–59.2%), goats 33.8% (95% CI 21.7%–47.5%), sheep 27.8% (95% CI 17.0%–40.6%) (Table; Figure). Sheep and goats had significantly lower odds of exposure than cattle: sheep OR was 0.32 (95% CI 0.27–0.37, $p \leq 0.001$) and goats OR 0.45 (95% CI 0.39–0.51; $p \leq 0.001$). Village-level seroprevalence ranged widely in all species but values were consistent with those reported elsewhere in East Africa (*3*) (Table). The finding of higher seroprevalence in cattle than in sheep and goats is also consistent with other settings in Africa (*3*) and might reflect differences in host feeding preferences of *Hyalomma* spp. ticks, considered chief vectors of CCHFV (*1*). However, further work is required to understand the relative contribution of different host species to viral maintenance, and their relationship to human infection risk.

Overall, human seroprevalence was 15.1% (95% CI 11.7%–19.2%), but village-level seroprevalence varied widely between study sites (Table). Seroprevalence was similar to that reported in health-care-seeking patients in Kenya in 2012 (*8*), but higher than the 1.2% seroprevalence reported in community participants elsewhere in Tanzania (*9*). However, interpretation of those regional comparisons is challenging in light of the substantial observed between-village variation in our study (Table).

Assessment of spatial autocorrelation via Moran *I* statistic showed no evidence of village-level spatial

Table. Seroprevalence of Crimean-Congo hemorrhagic fever virus in human and livestock populations, northern Tanzania*

Species	No. tested	Overall seroprevalence (95% CI)	Seroprevalence range per village (95% CI)		Moran *I* statistic (p value)
			Low	High	
Cattle	3,015	49.6 (40.0–59.2)	5.3 (1.2–9.4)	76.6 (70.3–82.8)	−0.09 (0.60)
Sheep	2,059	27.8 (17.0–40.6)	0.0 (0–3.9)	70.3 (55.5–85.0)	−0.09 (0.57)
Goats	2,382	33.8 (21.7–47.5)	0.0 (0–5.8)	79.6 (68.3–90.8)	−0.10 (0.61)
Human	351	15.1 (8.5–23.8)	0.0 (0.0–16.1)	50 (30.7–69.2)	0.43 (0.001)

*Serum samples were collected in northern in 2016 and tested for antibodies to Crimean-Congo hemorrhagic fever virus. Moran I statistic and associated p value are shown for the village level (Appendix).

autocorrelation in livestock (Table), suggesting that although context-specific drivers, such as husbandry practices and local agroecology are likely involved, drivers of exposure were not observable at this scale. In contrast, we observed significant positive spatial autocorrelation in the village-level human seroprevalence (Moran *I* statistic 0.43; p≤0.001) and clustering of higher seroprevalence villages in the western part of Manyara (Figure). In addition, species-pair correlations showed that village-level human and livestock seroprevalence were not well correlated (cattle, ρ = 0.34, p = 0.142; sheep, ρ = 0.35, p = 0.13; goats, ρ = 0.42, p = 0.062), and we saw high human seroprevalence in some low livestock seroprevalence locations and vice versa (Appendix). That heterogeneity, combined with differences in spatial distribution, could suggest different drivers of exposure in livestock and human populations. However, discrepancies in sample size could exaggerate those differences, so further linked investigation into human and livestock exposure and patterns of tick infection are required. Further exploration of specific risk factors is ongoing and could provide clarity on drivers of exposure.

The high human exposure levels to CCHFV implies that clinical CCHF is a potentially serious, underdiagnosed health risk in this population and suggests that CCHF should be included as a differential diagnosis for undifferentiated febrile illness in northern Tanzania. However, evidence of human seropositivity in the absence of clinical cases is common, even where health professionals are familiar with CCHF diagnosis (*8*,*10*). The causes of disease emergence in such populations are poorly understood, and further research into regions like northern Tanzania, where the virus is endemic but human disease has not been reported, is critical to understanding human disease risk.

In conclusion, we found that CCHFV is circulating widely in livestock across northern Tanzania. CCHFV seroprevalence in the region shows high

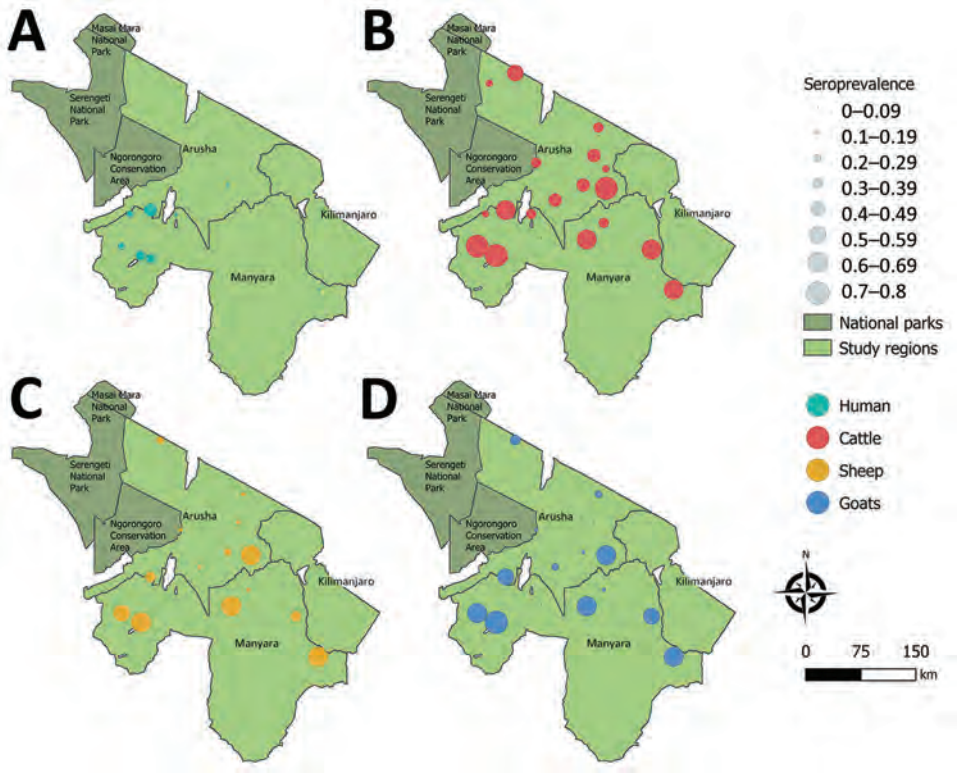

Figure. Sampling area for study of seroprevalence of Crimean-Congo hemorrhagic fever virus in human and livestock populations, northern Tanzania. Circles indicates seroprevalence rates for humans (A), cattle (B), sheep (C), and goats (D). The pictured region is near Uganda, where human Crimean-Congo hemorrhagic fever cases have been documented (*4*).

spatial heterogeneity and further investigations are needed to understand drivers of exposure. In addition, high human seroprevalence demonstrates widespread exposure of the population to CCHFV and suggests that CCHF should be included as a differential diagnosis for febrile illness in this region.

This article was preprinted at https://www.medrxiv.org/content/10.1101/2023.08.31.23294720v1.

Acknowledgments

We thank the livestock keepers, as well as village, ward, district, and regional authorities, who participated in this study. We are grateful to Kunda Mnzava, Tauta Maapi, Rigobert Tarimo, Fadhili Mshana, Zanuni Kweka, Euphrasia Mariki, Ephrasia Hugho, Nelson Amani, Victor Mosha, and Elizabeth Kasagama for their contribution to field and laboratory work.

This research was supported by the Supporting Evidence Based Interventions project, University of Edinburgh (grant no. R83537) and the Zoonoses and Emerging Livestock Systems program (funded through BBSRC, DfID, ESRC, MRC, NERC and DSTL) (project no. BB/L018926/1). E.C.H. was supported by the University of Glasgow, College of Medicine, Veterinary and Life Sciences Doctoral Training Programme.

About the Author

Dr. Hughes is a veterinarian and post-doctoral researcher who works for the Global Burden of Animal Diseases Programme at the University of Liverpool, Liverpool, UK. Her research interests include emerging and endemic zoonoses, disease burden estimation, and One Health approaches to animal and human health.

References

1. Bente DA, Forrester NL, Watts DM, McAuley AJ, Whitehouse CA, Bray M. Crimean-Congo hemorrhagic fever: history, epidemiology, pathogenesis, clinical syndrome and genetic diversity. Antiviral Res. 2013;100:159–89. https://doi.org/10.1016/j.antiviral.2013.07.006
2. World Health Organization. Prioritizing diseases for research and development in emergency contexts [cited 2022 Feb 26]. https://www.who.int/activities/prioritizing-diseases-for-research-and-development-in-emergency-contexts
3. Spengler JR, Bergeron É, Rollin PE. Seroepidemiological studies of Crimean-Congo hemorrhagic fever virus in domestic and wild animals. PLoS Negl Trop Dis. 2016;10:e0004210. https://doi.org/10.1371/journal.pntd.0004210
4. Balinandi S, von Brömssen C, Tumusiime A, Kyondo J, Kwon H, Monteil VM, et al. Serological and molecular study of Crimean-Congo hemorrhagic fever virus in cattle from selected districts in Uganda. J Virol Methods. 2021;290:114075–114075. https://doi.org/10.1016/j.jviromet.2021.114075
5. Messina JP, Pigott DM, Golding N, Duda KA, Brownstein JS, Weiss DJ, et al. The global distribution of Crimean-Congo hemorrhagic fever. Trans R Soc Trop Med Hyg. 2015;109:503–13. https://doi.org/10.1093/trstmh/trv050
6. Herzog CM, de Glanville WA, Willett BJ, Kibona TJ, Cattadori IM, Kapur V, et al. Pastoral production is associated with increased peste des petits ruminants seroprevalence in northern Tanzania across sheep, goats and cattle. Epidemiol Infect. 2019;147:e242. https://doi.org/10.1017/S0950268819001262
7. Lumley T. Analysis of complex survey samples. J Stat Softw. 2004;9:1–19. https://doi.org/10.18637/jss.v009.i08
8. Christova I, Panayotova E, Groschup MH, Trifonova I, Tchakarova S, Sas MA. High seroprevalence for Crimean-Congo haemorrhagic fever virus in ruminants in the absence of reported human cases in many regions of Bulgaria. Exp Appl Acarol. 2018;75:227–34. https://doi.org/10.1007/s10493-018-0258-7
9. Rugarabamu S, Mwanyika GO, Rumisha SF, Sindato C, Lim HY, Misinzo G, et al. Seroprevalence and associated risk factors of selected zoonotic viral hemorrhagic fevers in Tanzania. Int J Infect Dis. 2021;109:174–81. https://doi.org/10.1016/j.ijid.2021.07.006
10. Hoogstraal H. The pidemiology of tick-borne CCHF in Asia Europe and Africa. J Med Entomol. 1979;15:307–417. https://doi.org/10.1093/jmedent/15.4.307

Address for correspondence: Ellen C. Hughes, c/o Prof. Brian Willett, MRC-University of Glasgow Centre for Virus Research, Garscube Campus, 464 Bearsden Rd, Glasgow, Scotland G61 1QH, UK; email: ellen.hughes@liverpool.ac.uk

Breaking Through: My Life in Science

Katalin Karikó; Crown Publishing Group, New York, NY, USA, 2023; ISBN: 9780593443163; Pages: 330; Price: $21.99 (hardcover), $13.99 (ebook)

In Breaking Through: My Life in Science, Dr. Katalin Karikó describes her fascinating, sometimes frustrating, and always inspiring journey from life in post–World War II communist Hungary to finally being recognized for her contributions toward successfully developing mitochondrial RNA (mRNA) technology that was used, among other things, to develop the Pfizer-BioNTech SARS-CoV-2 vaccine. Karikó's autobiography was published just a week after she and her long-term collaborator, Dr. Drew Weissman, were awarded the 2023 Nobel Prize in physiology and medicine. The story takes us chronologically from growing up in rural 1950–1960s Hungary, through working as a researcher in academic medical centers in Philadelphia, Pennsylvania, USA, raising a two-time Olympic gold medalist rower, and finally to her current roles as a biochemist and researcher and senior vice-president at BioNTech company in Mainz, Germany.

Although Karikó cautions readers that scientists can be notoriously bad at explaining things to nonscientists, she herself writes in an engagingly clear and simple style. Readers will be inspired by her description of growing up in a rural Hungarian town in an adobe hut with no indoor plumbing, limited electricity, and very little heat. Her mother was a bookkeeper and her father a butcher who sometimes got in trouble with local Communist Party leadership. What I found most moving was the persistence Karikó displayed in studying so hard in primary school that she placed nationally in biology competitions. Karikó notes that she received one of several spots in an extremely competitive university biology program in Hungary held specifically for students from less advantaged backgrounds. Karikó's university educational experience and later scientific contributions illustrate the potential value of programs to assist academically qualified but economically challenged students (*1*,*2*).

Upon arriving in the United States as a non–tenure track laboratory researcher at Temple University, Karikó entered an environment in which she faced seemingly insurmountable resistance. The male principal investigator at times screamed and threw objects at her. When she attempted to leave, he threatened to have her deported and blackballed. Karikó describes her decades of meticulous work researching mRNA during which time she applied for grants and submitted articles reporting her work to prestigious scientific journals, only to have those manuscripts rejected. Department heads reminded her continuously about her need to bring in funds. Karikó remained in nontenured positions until one day in 2013 she arrived at her laboratory at the University of Pennsylvania to find her equipment being moved out. She moved to the BioNTech company to continue her research and just 10 years later, she had won the Nobel Prize for scientific work that led directly to saving millions of lives. One wonders how much grants and promotion systems that reward creativity, meticulousness, and perseverance, not just rapid success and publication, could lead to more breakthroughs.

Dr. Kariko's story recounts her persistence over many obstacles in pursuit of goals springing from her love for science. Scientists, clinicians, and lay readers will all find this story a compelling read.

References

1. US Supreme Court. Students for Fair Admissions, Inc. *v* President and Fellows of Harvard College. No. 20-1199. Argued October 31, 2022. Decided June 29, 2023 [cited 2023 Dec 12]. https://www.supremecourt.gov/opinions/22pdf/20-1199_hgdj.pdf
2. Chetty R, Deming DJ, Friedman JN. Diversifying society's leaders? The determinants and causal effects of admission to highly selective private colleges. Working paper 31492. National Bureau of Economic Research Working Paper Series. 2023 Jul. https://doi.org/10.3386/w31492

Sara C. Keller

Author affiliation: Johns Hopkins University School of Medicine, Baltimore, Maryland, USA

DOI: https://doi.org/10.3201/eid3004.231656

Address for correspondence: Sara C. Keller, Johns Hopkins University School of Medicine, 550 N Broadway St, Ste 405, Baltimore, MD 21287, USA; email: skeller9@jhmi.edu

Rembrandt van Rijn (1606–1669), *The Night Watch* (detail) (1642). Oil on canvas, 149 in × 171 in/379.5 cm × 453.5 cm. Digital image courtesy of Rijksmuseum, Amsterdam, the Netherlands.

Standing Ready to Respond

Byron Breedlove

"Shine, shine, the light of good works shine.
The watch before the city gates, depicted in their prime.
The golden light all grimy now,
300 years have passed.
The worthy Captain and his squad of troopers standing fast."

—King Crimson, "The Night Watch"

During a career spanning nearly five decades, Dutch artist Rembrandt van Rijn created approximately 350 paintings, 300 etchings, and 100 drawings. Rembrandt's favorite subject was, apparently, himself. According to The National Gallery of Art, Washington, DC, USA, "nearly 80 self-portraits—paintings, drawings, and prints—are attributed to him." Although those portraits chronicle his changing appearance as he aged, many other details of his life are lost. In her 2011 essay, "Much have I travel'd in the

Author affiliation: Centers for Disease Control and Prevention, Atlanta, Georgia, USA

DOI: https://doi.org/10.3201/eid3004.240257

realms of gold," Polyxeni Potter notes "Rembrandt's life has been shrouded in mystery, largely because no written records exist beyond the usual certificates of birth, baptism, marriage, and death. He left no journal, and seven surviving letters from his hand concern routine transactions."

That paucity of biographical details has not diminished Rembrandt's reputation. The Rijksmuseum states that Rembrandt "is regarded as the greatest painter ever to have lived in the Netherlands. Paintings by him are currently valued at tens or even hundreds of millions of euros. The most famous of them all, *The Night Watch,* is estimated to be worth more than €500 million." The title, however, is a misnomer. Art historians Zuzanna Stanska and Nicole Ganbold note, "For hundreds of years, the painting was coated with a dark varnish and dirt, which misled scholars into thinking that it depicted a nocturnal scene, hence its common title. In fact, throughout the centuries the layer of varnish grew so thick that it protected the canvas from a knife attack in 1911. The varnish was eventually removed in the 1940s, but the title remained."

The actual title, *Officers and Other Civic Guardsmen of District II in Amsterdam, Under the Command of Captain Frans Banninck Cocq and Lieutenant Willem van Ruytenburch*, seems too mundane for this nearly life-sized painting that has inspired several movies, the second movement of Gustav Mahler's Symphony No. 7, a song titled *The Night Watch* by the band King Crimson, and a 2014 live reenactment by actors in a shopping mall in the Netherlands.

Rembrandt completed the painting in 1642, the year his wife Saskia died after a lengthy illness. The Rijksmuseum states that "Rembrandt's largest and most famous painting was made for one of the three headquarters of Amsterdam's civic guard. These groups of civilian soldiers defended the city from attack. Rembrandt was the first to paint all of the figures in a civic guard piece in action." Yvette Hoitink, a professional genealogist, noted that such voluntary citizen militia, or *schutterij*, existed throughout the Netherlands from at least the 1500s until 1901 and could be summoned to quell riots and unrest, help control fires, and defend municipalities during war.

Rembrandt's *The Night Watch* contrasts with static depictions of *schutterij* from the 1600s that show militia members standing in a row or seated around a banquet table. Art critic Fisun Güner wrote, "In this richly hued, tenebrous masterpiece, where light is used to lend the scene an ethereal quality amid the commonplace bustle of movement and action, we detect a certain strangeness, a certain unreality to the scene—even though it's a painting full of noise."

Appearing in the background before the city gates, shadowed figures are gesturing, conversing, and handling weapons; a standard bearer hoists a flag; and a drummer prepares to add his cadence. In this painting, Rembrandt shows, according to Güner, that "he is interested in creating a drama and bringing it to life with emotional force, mixing a sense of the solemn (or at least of attempted solemnity) and the comic. So here we have a ragtaggle crowd not quite managing to fall into step behind the figure of the captain as he gestures for his men to march out."

In the foreground, Captain Banninck Cocq, garbed in black save a white frilled collar and red sash, issues orders. His lieutenant, Willem van Ruytenburch, listens to his captain, his luminous yellow-gold attire contrasting with the painting's dark background. Near the center, the illuminated figure of a young girl seems out of context, but Stanska and Ganbold explain her role: "Attached to her dress we can see a dead chicken with its claws raised to the sky, a bag of gunpowder and firearms—all symbols of the guild. Rembrandt thought of her as an imaginary mascot of the civic militia." The girl's resemblance to the artist's wife, Saskia, has also been noted. Rembrandt's favorite subject also makes a guest appearance. Between the standard bearer and a helmeted militiaman, just behind the captain's right shoulder, careful inspection reveals half the face of a man wearing a beret, identified by many as being Rembrandt.

The notion of a "night guard" to respond to situations that endanger the public resonates in other realms, including public health agencies that must be prepared to respond to an array of disease outbreaks and health threats. One priority is the more than 70 high-consequence pathogens: emerging and unknown bacteria, viruses, and prions, that can be easily transmitted from person to person, are associated with high mortality rates, and can potentially cause major public health outbreaks and trigger public fear.

Currently, the World Health Organization is "a leading a proactive approach to bolster global readiness and response to potential future epidemics and pandemics, the Research and Development (R&D) Blueprint maintains its commitment to expediting research on emerging disease threats." That response includes the initiative dubbed "Disease X," which the World Health Organization describes as a disease that could emerge and cause an international epidemic or the next global pandemic.

An effective, modern public health surveillance system to monitor disease outbreaks, collect information, and share findings is crucial. As Alexander Langmuir, the epidemiologist who started the Centers for Disease Control and Prevention Epidemic Intelligence Service, noted in his 1962 Cutter Lecture on Preventive Health, "Good surveillance does not necessarily ensure the making of the right decisions, but it reduces the chances of wrong ones."

Planning for an outbreak from an as-yet unrecognized pathogen could help public health authorities respond more effectively with regard to detecting pathogen emergence; developing vaccines, treatments, and countermeasures; and recommending sound policies. Instead of starting from scratch, surveillance and planning would enable public health responders to be better prepared to venture forth, like the iconic figures immortalized in Rembrandt's *Night Watch*, to ensure public health and safety.

Bibliography

1. Belay ED, Monroe SS. Low-incidence, high-consequence pathogens. Emerg Infect Dis. 2014;20:319–21. https://doi.org/10.3201/eid2002.131748
2. Centers for Disease Control and Prevention. Division of High-Consequence Pathogens and Pathology. Division diseases and specialty areas [cited 2024 Feb 20]. https://www.cdc.gov/ncezid/dhcpp/diseases-specialty-areas.html
3. Fripp R, Richard Palmer-James R, Wetton J. King Crimson, The Night Watch. Starless and Bible Black, EG Music Inc., 1974. Partial transcript of lyrics.
4. Güner F. Why Rembrandt's The Night Watch is still a mystery [cited 2024 Feb 15]. https://www.bbc.com/culture/article/20190214-does-rembrandts-the-night-watch-reveal-a-murder-plot
5. Hoitink Y. Dutch genealogy. Dutch term—Schutterij [cited 2024 Feb 8]. https://www.dutchgenealogy.nl/schutterij
6. Langmuir AD. The surveillance of communicable diseases of national importance. N Engl J Med. 1963;268:182–92. https://doi.org/10.1056/NEJM196301242680405
7. National Gallery of Art. Self-portrait: Rembrandt van Rijn [cited 2024 Feb 8]. https://www.nga.gov/collection/highlights/rembrandt-self-portrait.html
8. National Institute of Allergy and Infectious Diseases. NIAID Emerging Infectious Diseases/Pathogens [cited 2024 Feb 20]. https://www.niaid.nih.gov/research/emerging-infectious-diseases-pathogens
9. Potter P. Much have I travel'd in the realms of gold. Emerg Infect Dis. 2011;17:1985–6. https://doi.org/10.3201/eid1710.AC1710
10. Rijksmuseum. The Night Watch, Rembrandt van Rijn, 1642 [cited 2024 Feb 4]. https://www.rijksmuseum.nl/en/collection/SK-C-5
11. Savevska S. The Night Watch by Rembrandt [cited 2024 Feb 4]. https://medium.com/@sofijasavevska/the-night-watch-by-rembrandt-d525a771fab
12. Stanska Z, Nicole Ganbold N. 15 things you didn't know about the Night Watch by Rembrandt [cited 2024 Feb 20]. https://www.dailyartmagazine.com/15-things-you-may-not-know-about-the-night-watch-by-rembrandt
13. World Health Organization. A scientific framework for epidemic and pandemic research preparedness [cited 2024 Feb 20]. https://www.who.int/news-room/events/detail/2024/01/09/default-calendar/a-scientific-framework-for-epidemic-and-pandemic-research-preparedness
14. World Health Organization. Global research and innovation for health emergencies, 2023 [cited 2024 Feb 20]. https://cdn.who.int/media/docs/default-source/documents/r-d-blueprint-meetings/global-research-and-innovation-for-health-emergencies_report-2023.pdf

Address for correspondence: Byron Breedlove, EID Journal, Centers for Disease Control and Prevention, 1600 Clifton Rd NE, Mailstop H16-2, Atlanta, GA 30329-4018, USA; email: wbb1@cdc.gov

Corrections

Vol. 17, No. 10

The name of author Anwar Benabdellah was omitted in Diagnosis of Rickettsioses from Eschar Swab Samples, Algeria (N. Mouffok et al.). The article has been corrected online (https://wwwnc.cdc.gov/eid/article/17/10/11-0332_article).

Vol. 30, No. 3

The author list was incorrect in Larone's Medically Important Fungi: A Guide to Identification, 7th Edition (M.M. Azar). The article has been corrected online (https://wwwnc.cdc.gov/eid/article/30/3/23-1623_article).

EMERGING INFECTIOUS DISEASES®

Upcoming Issue • May 2024
Crimean-Congo Hemorrhagic Fever

- Crimean-Congo Hemorrhagic Fever Virus for Clinicians—Diagnosis, Clinical Management, and Therapeutics
- Crimean Congo Hemorrhagic Fever Virus for Clinicians—Epidemiology, Clinical Manifestations, and Prevention
- Case Series of Jamestown Canyon Virus Infections with Neurologic Outcomes, Canada
- SARS-CoV-2 Transmission in Alberta, British Columbia, and Ontario, Canada, January 2020–January 2022
- Cross-Sectional Study of Q Fever Seroprevalence among Blood Donors, Israel
- Interventional Study of Nonpharmaceutical Measures to Prevent COVID-19 onboard Cruise Ships
- Mpox Diagnosis, Behavioral Risk Modification, and Vaccination Uptake among Gay, Bisexual, and Other Men Who Have Sex with Men, United Kingdom, 2022
- Antigenic Characterization of Novel Human Norovirus GII.4 Variants, San Francisco, 2017 and Hong Kong, 2019
- Protective Efficacy of Lyophilized Vesicular Stomatitis Virus–Based Vaccines in Animal Models
- *Paranannizziopsis* spp. Infection in Wild Vipers, Europe
- Identifying Contact Time Required for Secondary Transmission of *Clostridioides difficile* Infections via Real-Time Locating System
- *Sphingobium yanoikuyae* Bacteremia, Japan

Complete list of articles in the May issue at https://wwwnc.cdc.gov/eid/#issue-308

Earning CME Credit

To obtain credit, you should first read the journal article. After reading the article, you should be able to answer the following, related, multiple-choice questions. To complete the questions (with a minimum 75% passing score) and earn continuing medical education (CME) credit, please go to https://www.medscape.org/qna/processor/71268?showStandAlone=true&src=prt_jcme_eid_mscpedu. Credit cannot be obtained for tests completed on paper, although you may use the worksheet below to keep a record of your answers.

You must be a registered user on http://www.medscape.org. If you are not registered on http://www.medscape.org, please click on the "Register" link on the right hand side of the website.

Only one answer is correct for each question. Once you successfully answer all post-test questions, you will be able to view and/or print your certificate. For questions regarding this activity, contact the accredited provider, CME@medscape.net. For technical assistance, contact CME@medscape.net. American Medical Association's Physician's Recognition Award (AMA PRA) credits are accepted in the US as evidence of participation in CME activities. For further information on this award, please go to https://www.ama-assn.org. The AMA has determined that physicians not licensed in the US who participate in this CME activity are eligible for *AMA PRA Category 1 Credits*™. Through agreements that the AMA has made with agencies in some countries, AMA PRA credit may be acceptable as evidence of participation in CME activities. If you are not licensed in the US, please complete the questions online, print the AMA PRA CME credit certificate, and present it to your national medical association for review..

Article Title

Concurrent Outbreaks of Hepatitis A, Invasive Meningococcal Disease, and Mpox, Florida, USA, 2021–2022

CME Questions

1. Which of the following statements regarding the hepatitis A virus (HAV) outbreak in the current study is most accurate?

A. Nearly half of all cases of HAV infection during the examination period met the outbreak case definition
B. 90% of nonoutbreak cases of HAV infection had a risk factor for HAV
C. <10% of nonoutbreak cases of HAV infection were related to international travel
D. Approximately one-third of persons who met criteria for HAV outbreak infection were men who have sex with men (MSM)

2. Which of the following statements regarding the invasive meningococcal disease (IMD) outbreak in the current study is most accurate?

A. 90% of all cases of IMD during the reporting period were outbreak-associated
B. 38% of cases of outbreak-associated IMD were among MSM
C. 20% of cases of outbreak-associated IMD were fatal
D. The clinical presentation of outbreak-associated IMD with the highest fatality rate was meningitis

3. Which of the following statements regarding the mpox outbreak in the current study is most accurate?

A. Half of the cases were associated with travel out of state
B. 98% of cases occurred among male persons
C. 40% of cases occurred among MSM
D. The rate of hospitalization associated with mpox was 45%

4. Which of the following trends did the current study note regarding outbreaks of mpox, IMD, and HAV?

A. The prevalence of all 3 infection types increased gradually throughout 2022
B. As the number of mpox cases increased during summer 2022, the rate of HAV infection fell, whereas rates of IMD continued to increase
C. 10 adults acquired both HAV infection and IMD
D. HIV infection was most common among persons with mpox infection vs IMD or HAV infection

Earning CME Credit

To obtain credit, you should first read the journal article. After reading the article, you should be able to answer the following, related, multiple-choice questions. To complete the questions (with a minimum 75% passing score) and earn continuing medical education (CME) credit, please go to https://www.medscape.org/qna/processor/71283?showStandAlone=true&src=prt_jcme_eid_mscpedu. Credit cannot be obtained for tests completed on paper, although you may use the worksheet below to keep a record of your answers.

You must be a registered user on http://www.medscape.org. If you are not registered on http://www.medscape.org, please click on the "Register" link on the right hand side of the website.

Only one answer is correct for each question. Once you successfully answer all post-test questions, you will be able to view and/or print your certificate. For questions regarding this activity, contact the accredited provider, CME@medscape.net. For technical assistance, contact CME@medscape.net. American Medical Association's Physician's Recognition Award (AMA PRA) credits are accepted in the US as evidence of participation in CME activities. For further information on this award, please go to https://www.ama-assn.org. The AMA has determined that physicians not licensed in the US who participate in this CME activity are eligible for *AMA PRA Category 1 Credits*™. Through agreements that the AMA has made with agencies in some countries, AMA PRA credit may be acceptable as evidence of participation in CME activities. If you are not licensed in the US, please complete the questions online, print the AMA PRA CME credit certificate, and present it to your national medical association for review.

Article Title

Deaths Associated with Pediatric Hepatitis of Unknown Etiology, United States, October 2021–June 2023

CME Questions

1. Which of the following statements regarding the outbreak of pediatric acute hepatitis of unknown etiology between 2021 and 2023 is most accurate?

A. > 4000 children were affected in the United States by 2023
B. > 30,000 children were affected globally by 2022
C. The main pathogen identified in the outbreak has been adenovirus species F, type 41
D. Before the outbreak, < 15% of cases of pediatric acute liver failure were found to be idiopathic

2. In the current study, which of the following statements regarding the demographics and past medical history of children who died after a diagnosis of acute hepatitis is most accurate?

A. All cases were concentrated in the southern United States
B. The median age of cases was 7 months
C. The majority of cases were among Hispanic or Latino children
D. 75% of cases had a history of immunocompromise

3. Which of the following statements regarding the clinical characteristics of children included in the current study is most accurate?

A. Three-quarters of cases had respiratory symptoms
B. The median duration of symptoms before presentation at the hospital was 2 days
C. The median alanine aminotransferase level at presentation was approximately 400 U/L
D. The median international normalized ratio level at presentation was normal

4. What was the rate of positive polymerase chain reaction testing for adenovirus in the hospital among children included in the current study?

A. 25%
B. 50%
C. 75%
D. 100%

Emerging Infectious Diseases

Spotlight Topics

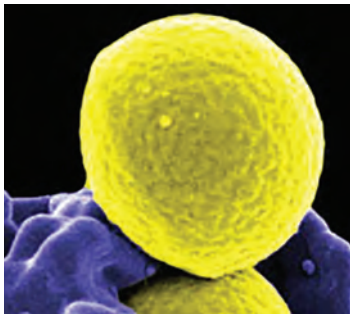

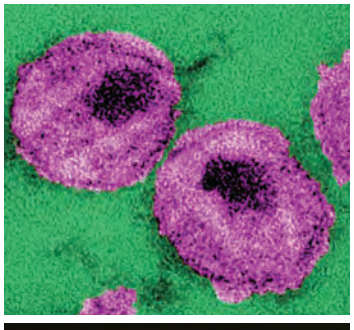

Antimicrobial resistance
Ebola • Etymologia
Food safety • HIV-AIDS
Influenza • Lyme disease
Malaria • MERS • Pneumonia •
Rabies • Ticks • Tuberculosis
Coronavirus • Zika • mpox

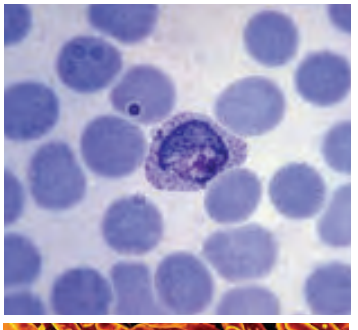

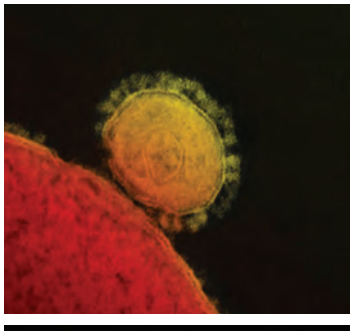

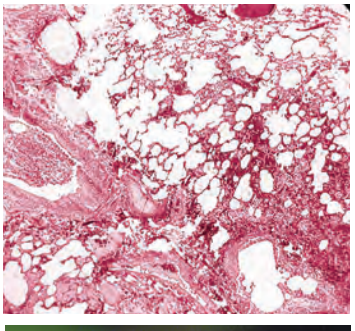

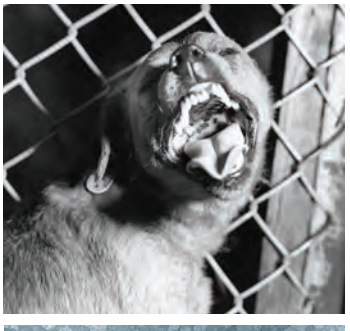

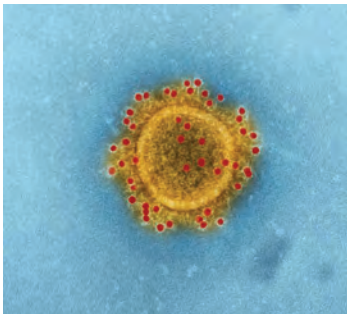

EID's spotlight topics highlight the latest articles and information on emerging infectious disease topics in our global community

https://wwwnc.cdc.gov/eid/page/spotlight-topics